RADIOLOGY AND ONCOLOGY

vol.57 no.2
june 2023

RADIOLOGY AND ONCOLOGY

June 2023
Vol. 57 No. 2
Pages 141-278
ISSN 1318-2099
UDC 616-006
CODEN: RONCEM

Publisher
Association of Radiology and Oncology

Aims and Scope
Radiology and Oncology is a multidisciplinary journal devoted to the publishing original and high-quality scientific papers and review articles, pertinent to oncologic imaging, interventional radiology, nuclear medicine, radiotherapy, clinical and experimental oncology, radiobiology, medical physics, and radiation protection. Papers on more general aspects of interest to the radiologists and oncologists are also published (no case reports).

Editorial office

Radiology and Oncology
Zaloška cesta 2
P. O. Box 2217
SI-1000 Ljubljana
Slovenia
Phone: +386 1 5879 369
Phone/Fax: +386 1 5879 434
E-mail: gsersa@onko-i.si

Reader for English
Vida Kološa

Secretary
Mira Klemenčič, Zvezdana Vukmirović, Vijoleta Kaluža, Uroš Kuhar

Design
Monika Fink-Serša, Samo Rovan, Ivana Ljubanović

Layout
Matjaž Lužar

Printed by
Tiskarna Ozimek, Slovenia

Published quarterly in 400 copies

Beneficiary name: DRUŠTVO RADIOLOGIJE IN ONKOLOGIJE
Zaloška cesta 2
1000 Ljubljana
Slovenia

Beneficiary bank account number: SI56 02010-0090006751
IBAN: SI56 0201 0009 0006 751
Our bank name: Nova Ljubljanska banka, d.d.,
Ljubljana, Trg republike 2,
1520 Ljubljana; Slovenia

SWIFT: LJBASI2X

Subscription fee for institutions EUR 100, individuals EUR 50

The publication of this journal is subsidized by the Slovenian Research Agency.

Indexed and abstracted by:

- *Baidu Scholar*
- *Case*
- *Chemical Abstracts Service (CAS) - CAplus*
- *Chemical Abstracts Service (CAS) - SciFinder*
- *CNKI Scholar (China National Knowledge Infrastructure)*
- *CNPIEC - cnpLINKer*
- *Dimensions*
- *DOAJ (Directory of Open Access Journals)*
- *EBSCO (relevant databases)*
- *EBSCO Discovery Service*
- *Embase*
- *Genamics JournalSeek*
- *Google Scholar*
- *Japan Science and Technology Agency (JST)*
- *J-Gate*
- *Journal Citation Reports/Science Edition*
- *JournalGuide*
- *JournalTOCs*
- *KESLI-NDSL (Korean National Discovery for Science Leaders)*
- *Medline*
- *Meta*
- *Microsoft Academic*
- *Naviga (Softweco)*
- *Primo Central (ExLibris)*
- *ProQuest (relevant databases)*
- *Publons*
- *PubMed*
- *PubMed Central*
- *PubsHub*
- *QOAM (Quality Open Access Market)*
- *ReadCube*
- *Reaxys*
- *SCImago (SJR)*
- *SCOPUS*
- *Sherpa/RoMEO*
- *Summon (Serials Solutions/ProQuest)*
- *TDNet*
- *Ulrich's Periodicals Directory/ulrichsweb*
- *WanFang Data*
- *Web of Science - Current Contents/Clinical Medicine*
- *Web of Science - Science Citation Index Expanded*
- *WorldCat (OCLC)*

This journal is printed on acid- free paper

On the web: ISSN 1581-3207
https://content.sciendo.com/raon
http://www.radioloncol.com

contents

review

Bleomycin electrosclerotherapy (BEST) for the treatment of vascular malformations. An International Network for Sharing Practices on Electrochemotherapy (InspECT) study group report

Tobian Muir[1], Giulia Bertino[2], Ales Groselj[3,4], Lakshmi Ratnam[5], Erika Kis[6], Joy Odili[7], Ian McCafferty[8], Walter A Wohlgemuth[9], Maja Cemazar[10,11], Aljosa Krt[11], Masa Bosnjak[10], Alessandro Zanasi[13], Michela Battista[13], Francesca de Terlizzi[13], Luca G Campana[14], Gregor Sersa[10,15]

[1] Department of Reconstructive Plastic Surgery, James Cook University Hospital, Middlesbrough, United Kingdom
[2] Department of Otolaryngology Head Neck Surgery, University of Pavia, Istituto di Ricovero e Cura a Carattere Scientifico (IRCCS) Policlinico San Matteo Foundation, Pavia, Italy,
[3] Department of Otorhinolaryngology and Cervicofacial Surgery, University Medical Centre Ljubljana, Ljubljana, Slovenia
[4] Faculty of Medicine, University of Ljubljana, Ljubljana, Slovenia
[5] Department of Interventional Radiology, St George's University Hospitals NHS Foundation Trust, London, United Kingdom
[6] Department of Dermatology and Allergology, University of Szeged, Szeged, Hungary
[7] Department of Plastic Surgery, St. Georges University Hospitals NHS Trust, London, United Kingdom
[8] Birmingham Women's and Children's Hospital NHS Foundation Trust, Birmingham, United Kingdom
[9] Universitätsklinik und Poliklinik für Radiologie, Universitätsmedizin Halle, Halle, Germany
[10] Department of Experimental Oncology, Institute of Oncology Ljubljana, Ljubljana, Slovenia
[11] Faculty of Health Sciences, University of Primorska, Slovenia
[12] Department of Otorhinolaryngology, Izola General Hospital, Izola, Slovenia
[13] IGEA S.p.A., Clinical Biophysics Lab. Carpi, Modena, Italy
[14] Department of Surgery, Manchester University NHS Foundation Trust, Manchester, United Kingdom
[15] Faculty of Health Sciences, University of Ljubljana, Ljubljana, Slovenia

Radiol Oncol 2023; 57(2): 141-149.

Received 26 May 2023
Accepted 3 June 2023

Correspondence to: Mr. Tobian Muir, Department of Reconstructive Plastic Surgery, James Cook University Hospital, Middlesbrough, United Kingdom. E-mail: tobian.muir@nhs.net and Prof. Gregor Sersa, Department of Experimental Oncology, Institute of Oncology Ljubljana, Zaloska 2, SI-1000 Ljubljana, Slovenia. E-mail: gsersa@onko-i.si

Disclosure: No potential conflicts of interest were disclosed.

Background. Biomedical applications of electroporation are expanding out of the field of oncology into vaccination, treatment of arrhythmias and now in the treatment of vascular malformations. Bleomycin is a widely used sclerosing agent in the treatment of various vascular malformations. The application of electric pulses in addition to bleomycin enhances the effectiveness of the drug, as demonstrated by electrochemotherapy, which utilizes bleomycin in the treatment of tumors. The same principle is used in bleomycin electrosclerotherapy (BEST). The approach seems to be effective in the treatment of low-flow (venous and lymphatic) and, potentially, even high-flow (arteriovenous) malformations. Although there are only a few published reports to date, the surgical community is interested, and an increasing number of centers are applying BEST in the treatment of vascular malformations. Within the International Network for Sharing Practices on Electrochemotherapy (InspECT) consortium, a dedicated working group has been constituted to develop standard operating procedures for BEST and foster clinical trials.

Conclusions. By treatment standardization and successful completion of clinical trials demonstrating the effectiveness and safety of the approach, higher quality data and better clinical outcomes may be achieved.

Key words: vascular malformations; bleomycin electrosclerotherapy; bleomycin; electrochemotherapy

Classification of vascular malformations

Vascular malformations are a rare condition caused by abnormally developed blood vessels. They can occur anywhere in the body and range from simple and benign to complex conditions, with an incidence of around 1.5% in the general population.

The latest and most used categorization is the International Society for the Study of Vascular Anomalies (ISSVA) classification (Table 1).[1] This classification divides vascular anomalies into two main categories: tumors (true proliferative neoplasms) and malformations (morphogenetic defects). These two categories are further subcategorized: tumors are divided into benign, locally aggressive/borderline and malignant, whereas malformations are subdivided into simple, combined or associated with other anomalies. Clinically, vascular anomalies can also be divided into low-flow and high-flow malformations.[2]

Treatment of vascular malformations

Current approaches vary depending on the type and anatomical location of the vascular malformation. Treatment options include observation, sclerotherapy, laser therapy, embolization, and surgery.[3,4] Observation is recommended for asymptomatic superficial or low-flow malformations that pose no immediate risk to the patient and are stable in size. Sclerotherapy involves the injection of sclerosing agents, such as bleomycin, or other agents (pingyangmycin, absolute ethanol, ethanolamine oleate, polidocanol, doxycycline, cyanoacrylate, sodium morrhuate and sodium tetradecyl sulfate (STS)).[5,6] Laser therapy is used to treat superficial vascular malformations and involves the use of a laser to heat the affected area and reduce vessel size. Embolization is a minimally invasive procedure in which small particles, metal coils, or solidifying liquid agents are injected into the malformation to block the flow of blood and reduce its size. This treatment is typically used for high-flow malformations. Surgery may be necessary for high-flow malformations that are difficult to treat with the other methods mentioned. Depending on the size and anatomical location, the surgeon may only remove part of the lesion.[7]

The use of bleomycin combined with electroporation (electrochemotherapy) in oncology

There are several **biomedical applications of electroporation**. Reversible and irreversible electroporation are distinguished by the amplitude, timing and number of electric pulse applications. Irreversible electroporation is based on irreversible disruption of the cell membrane causing destabilization of cell physiology to the extent that cells die either by apoptosis, necrosis or even immunogenic cell death.[8] In contrast, reversible electroporation does not cause cell death but temporarily disrupts the cell membrane in such a way that it becomes permeable for molecules that have hampered transport through the membrane.[9–12] This

TABLE 1. International Society for the Study of Vascular Anomalies (ISSVA) classification for vascular anomalies 2018

VASCULAR TUMORS			VASCULAR MALFORMATIONS	
Benign	**Locally aggressive**	**Malignant**	**Simple**	**Combined**
Infantile hemangioma	Kaposiform hemangioendothelioma	Epithelioid hemangioendothelioma Angiosarcoma	Capillary malformation (CM)	CVM, CLM
Congenital hemangioma	Retiform hemangioendothelioma		Lymphatic malformation (LM)	LVM. CLVM
Tufted hemangioma	PILA. Dabska tumor		Venous malformation (VM)	CAVM
Spindle-cell hemangioma	Composite hemangioendothelioma		Arteriovenous malformation (AVM)	
Epithelioid hemangioma	Kaposi sarcoma			CLAVM
Pyogenic granuloma			Arteriovenous fistula	

AVM = arteriovenous malformation; CAVM = capillary arteriovenous malformation; CLAVM = capillary lymphatic arteriovenous malformation; CLM = capillary lymphatic malformations; CLVM = capillary lymphatic venous malformation; CM = capillary malformation; CVM = capillary venous malformations; LM = lymphatic malformation; LVM = lymphatic venous malformation; PILA – papillary intralymphatic angioendothelioma; VM - venous malformation

phenomenon can be exploited for enhanced drug, DNA or RNA delivery into cells. If we deliver nucleic acids, it is called gene electrotransfer, which can be used for cancer immune-gene therapy; for example, if introduced, DNA or mRNA encodes immunomodulatory molecules. It can also be used for vaccination purposes.[13,14] The biomedical applications of gene electrotransfer can be used in the treatment of cancer, as well as other diseases, including vaccination for infectious diseases such as SARS CoV-2 virus.[15] In the case of electrochemotherapy, electroporation is used to enhance the delivery of cytotoxic molecules for cancer treatment. The principle is to inject cytotoxic drugs such as bleomycin or cisplatin into the cancer patient and apply electric pulses at the site of the tumor, where enhanced drug uptake is desired.[16] Therefore, electrochemotherapy is a local treatment since drug cytotoxicity is enhanced only at the site of electric pulse applications. This approach is being used widely in the treatment of either cutaneous tumors or deep-seated tumors in internal organs, such as liver and pancreas.[16] Several electrodes were designed that are best suited for the delivery of electric pulses to specific anatomical locations. Due to its simple principle, i.e., the use of highly cytotoxic drugs and the application of electric pulses for its enhanced cytotoxicity, electrochemotherapy is effective on tumors of different histological origins. Its objective response rate ranges between 70-80%.[17] Electrochemotherapy is listed in many national and international guidelines as a local ablative therapy and is applied in more than 200 centers across Europe.[16]

Electrochemotherapy mechanisms of action

There are three underlying **mechanisms of electrochemotherapy**. The first is enhanced drug delivery to tumor cells, which die due to the cytotoxicity of the drugs, either by apoptosis or necrosis. This is predominantly related to the drug used and its mode of action. Bleomycin, for example, induces mitotic cell death, which induces slow resolution of the tumor mass. Experimental data on tumors in mice demonstrate that the drug concentration in tumor cells after electroporation is increased 10 times or more, depending on the tumor type, in the case of bleomycin electrochemotherapy.[18]

The second mechanism is the induction of the immune response due to immunogenic tumor cell death induced by the drug. It is well known that certain ablative therapies induce immunogenic cell death that can attract and boost the immune response of the organism. This mechanism has been described in radiation therapy, thermal ablative techniques, and electrochemotherapy.[10,12,19] Several groups have investigated the role of immunogenic cell death in the effectiveness of electrochemotherapy. Now, the experimental data indicate that the response of the tumors varies depending on the immunogenicity of the tumors; more immunogenic tumors respond better to electrochemotherapy than less immunogenic tumors, which was linked to more pronounced immunogenic cell death after electrochemotherapy.[10,12,20] Additionally, clinical data on the treatment of melanoma demonstrate that local treatment of cutaneous metastases can boost or interact with treatment using immune checkpoint inhibitors, such as pembrolizumab.[21] Patients treated with both electrochemotherapy and immune checkpoint inhibitors had lower disease progression rates and longer survival than those who received pembrolizumab only.

The third mechanism is the vascular disrupting effect of electrochemotherapy. In early preclinical research, it was established that the application of electric pulses only temporarily abrogates blood flow within tumors. This phenomenon was termed vascular lock and lasts less than an hour.[22,23] Furthermore, the effect is enhanced when the drug is present during application of the electric pulses. Investigations have shown that it results in vascular disruption that occurs within hours in tumors. Endothelial cells start to die, blood flow is obstructed, and secondary tumor cell death is induced within days due to induced tumor hypoxia.[24–27] The phenomenon is predominantly confined to the tumor vasculature, sparing the normal vasculature around the tumors. The reason for this is because of the high proliferation rate of endothelial cells in tumors compared to the vasculature in normal tissues, where the endothelial proliferation rate is very slow. The vascular disrupting effect of electrochemotherapy is not fully understood. To date, we do not know in what proportion this vascular disrupting effect contributes to the overall effectiveness of electrochemotherapy in specific tumor types. We know that it is dependent on the distribution and extent of tumor vascularization, and better vascularized tumors respond better to electrochemotherapy.[28,29] Preclinical data also indicate that tumor perfusion influences the effectiveness of the treatment, with well perfused tumors showing an improved response.[30]

FIGURE 1. Treatment of vascularized melanoma metastasis by electrochemotherapy. **(A)** Highly vascularized tumor before treatment. **(B)** Bleeding due to electrode insertion after application of electric pulses to the tumor. **(C)** Bleeding stopped immediately after electric pulse application.

Combination of bleomycin with reversible electroporation for treatment of vascular malformations

Electrochemotherapy is safely applied to palliate bleeding cutaneous metastases and treat vascular tumors e.g., Kaposi sarcoma, superficial angiosarcoma[31-34] and highly vascularized liver metastases.[35,36] Bleeding after the insertion of needle electrodes quickly stops due to vascular lock.[37] Additionally, both superficial and liver tumors themselves also do not bleed after electrochemotherapy due to the vascular disrupting effect. These observations indicate that electrochemotherapy indeed exerts vascular effects, the abovementioned vascular lock and the vascular disrupting effect. Furthermore, several reports indicate that electrochemotherapy can be safely applied to control or treat bleeding tumors.[37] Of note, bleeding stops almost immediately after the application of electric pulses; therefore, treatment of bleeding tumors is also one of the indications for electrochemotherapy (Figure 1).

These data support the potential advantage of bleomycin electrosclerotherapy in the treatment of vascular malformations. Bleomycin is already one of the most frequently used sclerotherapy agents in the treatment of these lesions.[5,6] Therefore, the combination with electric pulses may only add to the effectiveness of bleomycin since it would increase the uptake of the drug into the endothelial lining of the affected blood vessels. In many cases, blood vessels are abnormal and endothelial cell proliferation is higher than that in normal blood vessels.[38] Therefore, the vasculature in vascular malformations is impaired as it is in tumors, and electrochemotherapy is supposed to be effective in both.

Histological evidence from liver biopsies indicates that venules are more sensitive to electrochemotherapy than arterioles in normal liver parenchyma.[39] This would indicate that venous malformations would have been more susceptible to BEST.

We recently performed a study on pigs investigating vascular changes in large blood vessels such as the portal vein, inferior vena cava, and lineal vein. In this study, the vessels were directly exposed to electroporation and electrochemotherapy by the application of electric pulses using plate electrodes that embraced the vessels. Electrochemotherapy may temporarily disrupt the endothelial lining and disrupt the vasa vasorum of the vessels (unpublished data). This effect may, however, be a desired one in the treatment of all vascular malformations, specifically because we have not observed thrombi formation in the treated vessels in the pig model.

All this evidence supports the use of bleomycin electroporation in the treatment of vascular malformations, also called bleomycin electrosclerotherapy (BEST). In principle, BEST could be a safe and effective approach for the treatment of vascular malformations; however, more clinical data are needed to confirm this approach. To date, there are only a handful of clinical reports on the treatment of vascular malformations with BEST. Finally, and importantly, the technique needs to be standardized through the development of dedicated standard operating procedures.

Overview of current clinical BEST reports

Publications on BEST are still limited in number. Table 2 summarizes the clinical studies and case reports published thus far.[40–45] In summary, different types of vascular malformations have been treated, with favorable clinical outcomes. Most of the studies used intralesional bleomycin, either diluted or mixed with lidocaine. Bleomycin dosage varied between studies, but in most reports, it was lower than in traditional sclerotherapy. In addition, the number of treatments required was much lower when BEST was used than when bleomycin was used alone. Drug dosage, the number of treatments needed, and route of drug administration are all aspects that need to be explored to develop recommendations for the future use of BEST.

Another relevant aspect of BEST is the application of electric pulses. Due to the blood accumulated in the malformation, the electrical conductivity of the treated tissue is high. Therefore, it is assumed that the coverage of the target lesion with electric pulses does not need to be so strict as in electrochemotherapy. In this regard, some clinicians who perform BEST on patients report that fewer applications of electric pulses to the lesions are needed. This aspect that requires clarification in future studies.

Studies on BEST should also report the number and amplitudes of pulse applications and the electrical parameters (current). The predominantly used generator is from one producer, and varying electrodes specific to this generator are used. Usually, in each electric pulse application 8 pulses of 1000–1300 V/cm in frequency 5 kHz are applied. Since different electrodes are used for different clinical situations, the reports should describe which electrodes were used. Furthermore, when standard operating procedures for BEST will be prepared, recommendations for the use of specific types of electrodes should also be prepared.

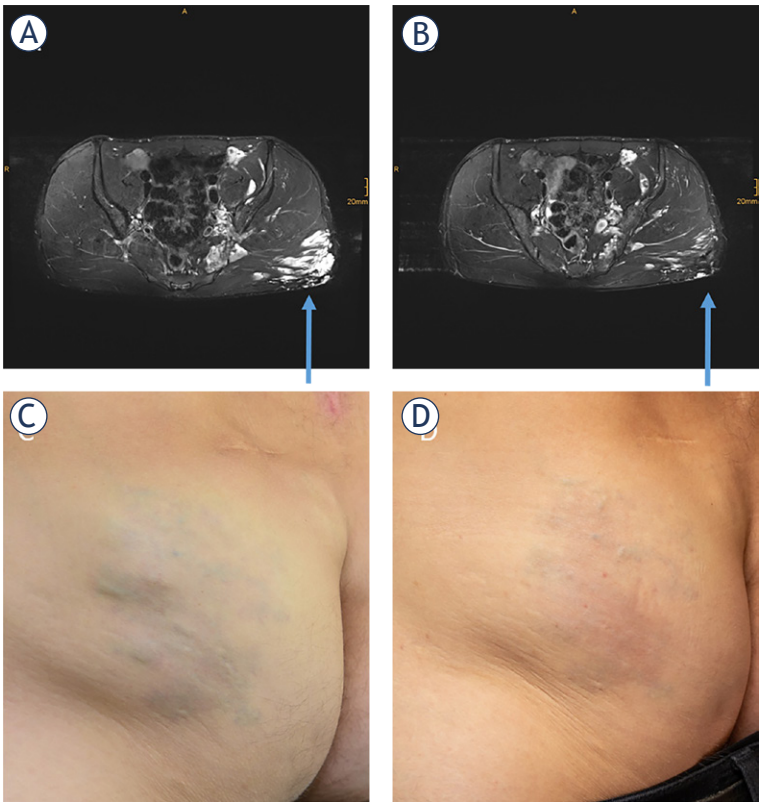

FIGURE 2. Patient treated by BEST. Axial T2-weighted, fat-saturated MRI with hyperintense (arrow) gluteal venous malformation before treatment **(A)**. Axial T2-weighted, fat-saturated MRI of the same region 4 months after treatment. The main part of the venous malformation is occluded **(B)**. Photography before **(C)** and after the treatment **(D)**.

BEST standardization

To date, there are no standardized guidelines for BEST. As a result, each center applies the treatment according to local protocols and clinical experience. Therefore, standardization of some procedural aspects is needed.

The spread of a new technology depends on its **safety**. Safety aspects have already been corroborated, since there are already some reports of significant morbidity with bleomycin only, but not with BEST treatment.[46] We must be aware that cytotoxic drugs are used for the treatment of benign disease, that can be spilled and are sometimes also used in very young patients. This safety aspect is also related to the experience in image-guided bleomycin and electric pulse application (Figure 2).

Currently, BEST must be practiced in the framework of clinical studies, where **patient referral and suitability for BEST treatment need to be defined**. The patients need to be informed about other treatment options and their suitability for the treatment evaluated by a multidisciplinary team (MDT).

It is expected that in the early stage of development, BEST will be considered in recurrences after previous treatments, whereas subsequently more precise indications for specific types of vascular malformations will be individuated.

TABLE 2. Clinical studies and case reports using bleomycin electrosclerotherapy[40–45]

Reference	Type of malformation	N of pts	Bleomycin dose and concentration	Electrodes used	N of pulse applications	Response	Comment
McMorrow *et al.*, Br J Oral and Maxillofacial Surg 2017[44]	Venous malformation	1	Reduced dose: 1/3 of the standard dose	Not reported	Not reported	Considerable improvement after 6 unsuccessful sessions with bleomycin	Case report with poor respiratory function
Horbach *et al.*, Dermatologic Surgery 2020[45]	Hypertrophic capillary malformations	5 pts. (out of 20 planned)	0.25 mg or units/cm^3	Plate & needle	Not reported	7-8 weeks DEROI (changes in colorimetry) Flux in ROI (in Perfusion Units)	Randomized controlled pilot trial
Dalmady *et al.*, Pediatrics 2020[43]	Lymphatic malformation	1	0.5 mg/kg (5.4 mg)	Needle	1st session: 68 applications 2nd session: 74 applications	63% growth-corrected volume decrease. No recurrence at 18 months Follow up	Case report
Wohlgemuth *et al.*, Journal of Vascular Surgery 2021[40]	Venous malformations	17 pts. (20 lesions)	Calculated based on the size of the lesion. C = 0.25 mg/mL Intralesional injection (25% concentration of standard bleomycin sclerotherapy)	Needle & finger	Not reported	3-month post-therapy Changes in volume MRI: Volume reduction,%: > 90% 9 lesions > 70% in < 90% 6 lesions > 50% in < 70% 2 lesions < 35% 2 lesions No response 1 lesion	Retrospective observational case study
Kostusiak *et al.*, Dermatologic Surgery 2022[42]	Various vascular malformations	30 pts. VM: 17 AVM: 3 CVM LM: 2 Mixed: 2	Calculated based on the size of the lesion. Bleomycin mixed with 1 mL plain 1% lidocaine Dose not reported	Needle & finger	Not reported	17 Complete Response 7: significant improvement 1: moderate improvement 1: minor response 1: no response 3: active follow up	Prospective observational case study Electrosclerotherapy offered to non-responding patients to standard bleomycin
Krt *et al.*, Front Oncol 2022[41]	Arteriovenous malformation	1	750 IU BLM intralesional	Plate	15	CR 18 months after BEST	Case report

AVM = arteriovenous malformation; BLM = bleomycin; CVM = capillary venous malformations; VM - venous malformation; LM = lymphatic malformation;

Other relevant procedural aspects that need to be clarified include drug injection, questions of dosage, the need for general anesthesia, electrode placement and delivery of electric pulses.

Exclusion criteria need to be defined as well, such as pregnancy, lactation and allergy or hypersensitivity to bleomycin, or abnormal respiratory parameters.

The application of electric pulses, especially with needle electrodes, is painful. Therefore, **local or general anesthesia is needed.** In this regard, the experience accumulated with electrochemotherapy can be informative. Generally, the choice of the type of anesthesia is at the discretion of each center. However, there is a recent report that continuous intravenous sedation is also an option that requires less anesthetic and is much shorter in time.[47]

Another important issue is the **route of bleomycin injection**. In electrochemotherapy, the preferred route is intravenous injection; however, in BEST treatment, this is a limited option since intravenous sclerotherapy with bleomycin is not the standard of care. Instead, direct injection is preferred, possibly under image guidance and potentially with a lower dose to avoid systemic toxicity.

In electrochemotherapy, the **bleomycin dose** in intravenous or intratumoral administration is defined.[48] In elderly patients older than 65 years or with renal impairment, the intravenously administered dose can be decreased by 1/3.[48] In BEST treatment, the dose can be substantially decreased. The lowest effective dose of bleomycin for BEST treatment still needs to be established. The concentration of bleomycin in the solution needs to be standardized.

Another peculiar aspect is that the **volume of the drug solution** is dependent on the type and volume of the malformation. Furthermore, it depends on whether bleomycin is diluted either with foam, lidocaine or contrast agent and whether there is drainage from the malformation that needs to be stopped, either by compression or intravascular techniques. By all means, the concentration and volume of the drug injected needs to be recorded and reported. The dose and route of administration may also differ in the case of fast or slow flow malformations. The treatment can be repeated up to a cumulative dose for bleomycin of 400 000 IU.[48]

The **interval between the intralesional bleomycin injection and the application of electric**

pulses needs to be short, while the drug is present in the treated tissue. The one-minute interval would be enough. A similar situation is also observed in electrochemotherapy, where the time interval is different when bleomycin is injected either intratumorally or intravenously. In the case of intravenous injection, the time interval is 8 minutes, and after intratumoral injection, the time interval is just 1-3 minutes.[48] The **choice of the electrodes** used is dependent on many factors. The type, location and size of the malformation are the most important factors. Needle electrodes with shorter or longer needles in fixed geometry are available. Some centers have concerns about so-called hexagonal electrodes since they deliver many electric pulses between the needles with a high risk of skin hyperpigmentation at the puncture sites. Some malformations require so-called variable geometry electrodes. These are single long needle electrodes that can be placed separately and can cover deeper mostly subfascial malformations.

Vascular malformations **do not need to be covered entirely with electric pulses,** in contrast to electrochemotherapy. In the case of BEST, damage to the endothelium and vessels needs to be done throughout the malformation but not necessarily with dense and complete coverage of the whole lesion, since the goal is to improve the symptoms more than eradicating the lesion. In this way, the risk of tissue swelling and mucosal ulceration could be reduced.

BEST treatment can be performed as a day case procedure unless pain, bleeding or swelling is anticipated. Generally, follow-up is recommended at approximately three-month intervals.

These are recommendations and considerations for BEST treatment according to the experiences gained by the authors of this manuscript. The members of this working group will continue to share experiences and discuss results to identify the procedural aspects associated with the best results. When a more formal consensus is reached, we will propose our best practice in the form of standard operating procedures (SOPs).

Role of InspECT in BEST applications

InspECT is an international network of 42 clinical centers using electrochemotherapy for the treatment of cancer. This is the largest group of experts on electroporation-based treatments. Some of them are acquainted with BEST and report a positive experience as other external centers. Together, these centers form a network that can promote BEST worldwide. A dedicated working group for vascular malformations has been formed within InspECT. This group will promote clinical studies with BEST and seek collaboration with other centers. This paper aims to raise interest and awareness in the treatment of vascular malformations with BEST and provide an overview of the current status of development of this approach.

Future directions and conclusions

The number of clinicians using BEST to treat vascular malformations is growing. Due to the first and positive experiences in various vascular malformations, BEST application is being practiced in an increasing number of centers throughout Europe and the UK. This article summarizes the rationale and underlying mechanisms of BEST, along with the initial clinical experiences. Additionally, it highlights the main controversial procedural aspects and the need for dedicated SOPs.

Acknowledgments

The authors acknowledge the financial support from the state budget by the Slovenian Research Agency, program no. P3-0003.

References

1. Classification International Society for the Study of Vascular Anomalies. [Internet]. [cited 2023 May 16]. Available at: https://www.issva.org/classification
2. Wu IC, Orbach DB. Neurointerventional management of high-flow vascular malformations of the head and neck. *Neuroimaging Clin N Am* 2009; **19:** 219-40. doi: 10.1016/j.nic.2009.01.005.
3. Sadick M, Wohlgemuth WA, Huelse R, Lange B, Henzler T, Schoenberg SO, et al. Interdisciplinary management of head and neck vascular anomalies: clinical presentation, diagnostic findings and minimalinvasive therapies. *Eur J Radiol Open* 2017; **4:** 63-8. doi: 10.1016/j.ejro.2017.05.001
4. Hage AN, Beecham Chick JF, Srinivasa RN, Bundy JJ, Chauhan NR, Acord M, et al. Treatment of venous malformations: the data, where we are, and how it is done. *Tech Vasc Interv Radiol* 2018; **21:** 45-54. doi: 10.1053/j.tvir.2018.03.001
5. Horbach SER, Lokhorst MM, Saeed P, de Goüyon Matignon de Pontouraude CMF, Rothová A, Van Der Horst CMAM. Sclerotherapy for low-flow vascular malformations of the head and neck: a systematic review of sclerosing agents. *J Plast Reconstr Aesthet Surg* 2016; **69:** 295-304. doi: 10.1016/j.bjps.2015.10.045
6. Maria L De, Sanctis P De, Balakrishnan K, Tollefson M, Brinjikji W. Sclerotherapy for venous malformations of head and neck: systematic review and meta-analysis. *Neurointervention* 2020; **15:** 4. doi: 10.5469/neuroint.2019.00213

7. Johnson AB, Richter GT. Surgical considerations in vascular malformations. *Tech Vasc Interv Radiol* 2019; **22:** 100635. doi: 10.1016/j.tvir.2019.100635

8. Wang YJ, Fletcher R, Yu J, Zhang L. Immunogenic effects of chemotherapy-induced tumor cell death. *Genes Dis* 2018; **5:** 194. doi: 10.1016/j.gendis.2018.05.003

9. Sersa G, Ursic K, Cemazar M, Heller R, Bosnjak M, Campana LG. Biological factors of the tumour response to electrochemotherapy: review of the evidence and a research roadmap. *Eur J Surg Oncol* 2021; **47:** 1836-1846. doi: 10.1016/j.ejso.2021.03.229

10. Ursic K, Kos S, Kamensek U, Cemazar M, Miceska S, Markelc B, et al. Potentiation of electrochemotherapy effectiveness by immunostimulation with IL-12 gene electrotransfer in mice is dependent on tumor immune status. *J Control Release* 2021; **332**: 623-35. doi: 10.1016/j.jconrel.2021.03.009

11. Yarmush ML, Golberg A, Sersa G, Kotnik T, Miklavcic D. Electroporation-based technologies for medicine: principles, applications, and challenges. *Annu Rev Biomed Eng* 2014; **16:** 295-320. doi: 10.1146/annurev-bioeng-071813-104622

12. Kesar U, Markelc B, Jesenko T, Valentinuzzi KU, Cemazar M, Strojan P, et al. Effects of electrochemotherapy on immunologically important modifications in tumor cells. *Vaccines* 2023; **11:** 925. doi: 10.3390/vaccines11050925

13. Sersa G, Teissie J, Cemazar M, Signori E, Kamensek U, Marshall G, et al. Electrochemotherapy of tumors as in situ vaccination boosted by immunogene electrotransfer. *Cancer Immunol Immunother* 2015; **64:** 1315-27. doi: 10.1007/s00262-015-1724-2

14. Groselj A, Bosnjak M, Jesenko T, Cemazar M, Markelc B, Strojan P, et al. Treatment of skin tumors with intratumoral interleukin 12 gene electrotransfer in the head and neck region: a first-in-human clinical trial protocol. *Radiol Oncol* 2022; **56:** 398-408. doi: 10.2478/raon-2022-0021

15. Conforti A, Marra E, Palombo F, Roscilli G, Ravà M, Fumagalli V, et al. COVID-eVax, an electroporated DNA vaccine candidate encoding the SARS-CoV-2 RBD, elicits protective responses in animal models. *Mol Ther* 2022; **30:** 311-26. doi: 10.1016/j.ymthe.2021.09.011

16. Campana LG, Edhemovic I, Soden D, Perrone AM, Scarpa M, Campanacci L, et al. Electrochemotherapy – emerging applications technical advances, new indications, combined approaches, and multi-institutional collaboration. *Eur J Surg Oncol* 2019; **45:** 92-102. doi: 10.1016/j.ejso.2018.11.023

17. Clover AJP, de Terlizzi F, Bertino G, Curatolo P, Odili J, Campana LG, et al. Electrochemotherapy in the treatment of cutaneous malignancy: outcomes and subgroup analysis from the cumulative results from the pan-European International Network for Sharing Practice in Electrochemotherapy database for 2482 lesions in 987 patients (2008–2019). *Eur J Cancer 2020*; **138:** 30-40. doi: 10.1016/j.ejca.2020.06.020

18. Mir LM, Orlowski S, Belehradek J, Paoletti C. Electrochemotherapy potentiation of antitumour effect of bleomycin by local electric pulses. *Eur J Cancer* 1991; **27:** 68-72. doi: 10.1016/0277-5379(91)90064-K

19. Wang M, Duan Y, Yang M, Guo Y, Li F, Wang J, et al. The analysis of immunogenic cell death induced by ablation at different temperatures in hepatocellular carcinoma cells. *Front Cell Dev Biol* 2023; **11:** 1146195**.** doi: 10.3389/fcell.2023.1146195

20. Polajzer T, Jarm T, Miklavcic D. Analysis of damage-associated molecular pattern molecules due to electroporation of cells in vitro. *Radiol Oncol* 2020; **54:** 317-328. doi: 10.2478/raon-2020-0047

21. Campana LG, Peric B, Mascherini M, Spina R, Kunte C, Kis E, et al. Combination of pembrolizumab with electrochemotherapy in cutaneous metastases from melanoma: a comparative retrospective study from the inspect and slovenian cancer registry. *Cancers* 2021; **13:** 4289. doi: 10.3390/cancers13174289

22. Sersa G, Cemazar M, Parkins CS, Chaplin DJ. Tumour blood flow changes induced by application of electric pulses. *Eur J Cancer* 1999; **35:** 672-7. doi: 10.1016/S0959-8049(98)00426-2

23. Gehl J, Skovsgaard T, Mir LM. Vascular reactions to in vivo electroporation: characterization and consequences for drug and gene delivery. *Biochim Biophys Acta Gen Subj* 2002; **1569:** 51-8. doi: 10.1016/S0304-4165(01)00233-1

24. Jarm T, Cemazar M, Miklavcic D, Sersa G. Antivascular effects of electrochemotherapy: implications in treatment of bleeding metastases. *Expert Rev Anticancer Ther* 2010; **10:** 729-46. doi: 10.1586/era.10.43.

25. Markelc B, Sersa G, Cemazar M. Differential mechanisms associated with vascular disrupting action of electrochemotherapy: intravital microscopy on the level of single normal and tumor blood vessels. *PLoS One* 2013; **8:** e59557 doi: 10.1371/journal.pone.0059557

26. Markelc B, Bellard E, Sersa G, Jesenko T, Pelofy S, Teissié J, et al. Increased permeability of blood vessels after reversible electroporation is facilitated by alterations in endothelial cell-to-cell junctions. *J Control Release* 2018; **276:** 30-41. doi: 10.1016/j.jconrel.2018.02.032

27. Sersa G, Jarm T, Kotnik T, Coer A, Podkrajsek M, Sentjurc M, et al. Vascular disrupting action of electroporation and electrochemotherapy with bleomycin in murine sarcoma. *Br J Cancer* 2008; **98:** 388-98. doi: 10.1038/sj.bjc.6604168

28. Djokic M, Cemazar M, Popovic P, Kos B, Dezman R, Bosnjak M, et al. Electrochemotherapy as treatment option for hepatocellular carcinoma, a prospective pilot study. *Eur J Surg Oncol* 2018; **44:** 651-657. doi: 10.1016/j.ejso.2018.01.090

29. Edhemovic I, Brecelj E, Cemazar M, Boc N, Trotovsek B, Djokic M, et al. Intraoperative electrochemotherapy of colorectal liver metastases: a prospective phase II study. *Eur J Surg Oncl* 2020; **46:** 1628-1633. doi: 10.1016/j.ejso.2020.04.037

30. Groselj A, Kranjc S, Bosnjak M, Krzan M, Kosjek T, Prevc A, et al. Vascularization of the tumours affects the pharmacokinetics of bleomycin and the effectiveness of electrochemotherapy. *Basic Clin Pharmacol Toxicol* 2018; **123:** 247-256. doi: 10.1111/bcpt.13012

31. Curatolo P, Careri R, Simioni A, Campana LG. Cryotherapy, imiquimod, and electrochemotherapy are effective options for kaposi sarcoma: a call for standardization to allow for comparisons and informed decisions. *J Cutan Med Surg* 2020; **24:** 218-9. doi: 10.1177/1203475419893302

32. Lalanda R, Bartolo J, Carvalhal S, Abecasis N, Farricha V, Sofia R, et al. Cutaneous and subcutaneous Kaposi's sarcoma lesions treated with electrochemotherapy. *Int J Dermatol* 2023; **62:** 115-119. doi: 10.1111/ijd.16261

33. Guida M, Campana LG, Curatolo P, Strippoli S, Bonadies A, Grilz G, et al. Local treatment with electrochemotherapy of superficial angiosarcomas: efficacy and safety results from a multi-institutional retrospective study. *J Surg Oncol* 2016; **114:** 246-53. doi: 10.1002/jso.24287

34. Campana LG, Kis E, Bottyán K, Orlando A, de Terlizzi F, Mitsala G, et al. Electrochemotherapy for advanced cutaneous angiosarcoma: a European register-based cohort study from the International Network for Sharing Practices of Electrochemotherapy (InspECT). *Int J Surg* 2019; **72:** 34-42. doi: 10.1016/J.IJSU.2019.10.013

35. Djokic M, Cemazar M, Bosnjak M, Dezman R, Badovinac D, Miklavcic D, et al. A Prospective phase II study evaluating intraoperative electrochemotherapy of hepatocellular carcinoma. *Cancers* 2020; **12:** 3778. doi: 10.3390/cancers12123778

36. Spiliotis AE, Holländer S, Rudzitis-Auth J, Wagenpfeil G, Eisele R, Nika S, et al. Evaluation of electrochemotherapy with bleomycin in the treatment of colorectal hepatic metastases in a rat model. *Cancers* 2023; **15:** 1598. doi: 10.3390/cancers15051598

37. Gehl J, Geertsen PF. Palliation of haemorrhaging and ulcerated cutaneous tumours using electrochemotherapy. *Eur J Cancer Supp* 2006; **4:** 35-7. doi: 10.1016/j.ejcsup.2006.07.007

38. Lampejo AO, Ghavimi SAA, Hägerling R, Agarwal S, Murfee WL. Lymphatic/blood vessel plasticity: motivation for a future research area based on present and past observations. *Am J Physiol Heart Circ Physiol* 2023; **324:** H109-21. doi: 10.1152/ajpheart.00612.2022

39. Gasljevic G, Edhemovic I, Cemazar M, Brecelj E, Gadzijev EM, Music MM, et al. Histopathological findings in colorectal liver metastases after electrochemotherapy. *PLoS One* 2017; **12:** e0180709. doi: 10.1371/journal.pone.0180709

40. Wohlgemuth WA, Müller-Wille R, Meyer L, Wildgruber M, Guntau M, Heydt S von der, et al. Bleomycin electrosclerotherapy in therapy-resistant venous malformations of the body. *J Vasc Surg Venous Lymphat Disord* 2021; **9:** 731-9. doi: 10.1016/J.JVSV.2020.09.009

41. Krt A, Cemazar M, Lovric D, Sersa G, Jamsek C, Groselj A. Combining superselective catheterization and electrochemotherapy: a new technological approach to the treatment of high-flow head and neck vascular malformations. *Front Oncol* 2022; **12:** 1025270. doi: 10.3389/FONC.2022.1025270

42. Kostusiak M, Murugan S, Muir T. Bleomycin electrosclerotherapy treatment in the management of vascular malformations. *Dermatol Surg* 2022; **48:** 67-71. doi: 10.1097/DSS.0000000000003220

43. Dalmády S, Csoma Z, Besenyi Z, Bottyán K, Oláh J, Kemény L, et al. New treatment option for capillary lymphangioma: bleomycin-based electrochemotherapy of an infant. *Pediatrics* 2020; **146:** e20200566. doi: 10.1542/PEDS.2020-0566

44. McMorrow L, Shaikh M, Kessell G, Muir T. Bleomycin electrosclerotherapy: new treatment to manage vascular malformations. *Br J Oral Maxillofac Surg* 2017; **55**: 977-9. doi: 10.1016/J.BJOMS.2017.10.002

45. Horbach SER, Wolkerstorfer A, Jolink F, Bloemen PR, van der Horst CMAM. Electrosclerotherapy as a novel treatment option for hypertrophic capillary malformations: a randomized controlled pilot trial. *Dermatol Surg* 2020; **46:** 491-8. doi: 10.1097/DSS.0000000000002191

46. Ge V, Banakh I, Tiruvoipati R, Haji K. Bleomycin-induced pulmonary toxicity and treatment with infliximab: a case report. *Clin Case Rep* 2018; **6:** 2011-4. doi: 10.1002/CCR3.1790

47. Benedik J, Ogorevc B, Brezar SK, Cemazar M, Sersa G, Groselj A. Comparison of general anesthesia and continuous intravenous sedation for electrochemotherapy of head and neck skin lesions. *Front Oncol* 2022; **12:** 1011721. doi: 10.3389/FONC.2022.1011721

48. Gehl J, Sersa G, Matthiessen LW, Muir T, Soden D, Occhini A, et al. Updated standard operating procedures for electrochemotherapy of cutaneous tumours and skin metastases. *Acta Oncol* 2018; **57:** 874-82. doi: 10.1080/0284186X.2018.1454602

research article

Correlation of mean apparent diffusion coefficient (ADC) and maximal standard uptake value (SUVmax) evaluated by diffusion-weighted MRI and 18F-FDG-PET/CT in children with Hodgkin lymphoma: a feasibility study

Nicolas Rosbach[1], Sebastian Fischer[1], Vitali Koch[1], Thomas J. Vogl[1], Konrad Bochennek[2], Thomas Lehrnbecher[2], Scherwin Mahmoudi[1], Leon Grünewald[1], Frank Grünwald[3], Simon Bernatz[1]

[1] Department of Diagnostic and Interventional Radiology, University Hospital Frankfurt, Goethe University, Frankfurt am Main, Germany

[2] Division of Paediatric Haematology and Oncology, Hospital for Children and Adolescents, University Hospital Frankfurt, Goethe University, Frankfurt am Main, Germany

[3] Department of Nuclear Medicine, University Hospital Frankfurt, Goethe University, Frankfurt am Main, Germany

Radiol Oncol 2023; 57(2): 150-157.

Received 02 February 2023
Accepted 27 March 2023

Correspondence to: Dr. Nicolas Rosbach, Institute for Diagnostic and Interventional Radiology, University Hospital Frankfurt, Theodor-Stern-Kai 7, 60590 Frankfurt am Main, Germany. E-mail: nicolas.rosbach@kgu.de

Disclosure: No potential conflicts of interest were disclosed.

Background. The objective was to analyse if magnetic resonance imaging (MRI) can act as a non-radiation exposure surrogate for (18)F-Fluorodeoxyglucose (FDG) positron emission tomography/computed tomography (PET/CT) in children with histologically confirmed Hodgkin lymphoma (HL) before treatment. This was done by analysing a potential correlation between apparent diffusion coefficient (ADC) in MRI and the maximum standardized uptake value (SUVmax) in FDG-PET/CT.

Patients and methods. Seventeen patients (six female, eleven male, median age: 16 years, range: 12–20 years) with histologically confirmed HL were retrospectively analysed. The patients underwent both MRI and (18)F-FDG PET/CT before the start of treatment. (18)F-FDG PET/CT data and correlating ADC maps in MRI were collected. For each HL-lesion two readers independently evaluated the SUVmax and correlating meanADC.

Results. The seventeen patients had a total of 72 evaluable lesions of HL and there was no significant difference in the number of lesions between male and female patients (median male: 15, range: 12–19 years, median female: 17 range: 12–18 years, $p = 0.021$). The mean duration between MRI and PET/CT was 5.9 ± 5.3 days. The inter-reader agreement as assessed by the intraclass correlation coefficient (ICC) was excellent (ICC = 0.98, 95% CI: 0.97–0.99). The correlated SUVmax and meanADC of all 17 patients (ROIs n = 72) showed a strong negative correlation of -0.75 (95% CI: -0.84, – -0.63, $p = 0.001$). Analysis revealed a difference in the correlations of the examination fields. The correlated SUVmax and meanADC showed a strong correlation at neck and thoracal examinations (neck: -0.83, 95% CI: -0.93, – -0.63, $p < 0.0001$, thoracal: -0.82, 95% CI: -0.91, – -0.64, $p < 0.0001$) and a fair correlation at abdominal examinations of -0.62 (95% CI: -0.83, – -0.28, $p = 0.001$).

Conclusions. SUVmax and meanADC showed a strong negative correlation in paediatric HL lesions. The assessment seemed robust according to inter-reader agreements. Our results suggest that ADC maps and meanADC have the potential to replace PET/CT in the analysis of disease activity in paediatric Hodgkin lymphoma patients. This may help reduce the number of PET/CT examinations and decrease radiation exposure to children.

Key words: Hodgkin lymphoma; diffusion weighted imaging; apparent diffusion coefficient; MRI; PET/CT

Introduction

Hodgkin lymphoma (HL) accounts for approximately 6% of all paediatric cancers. It has an incidence rate of 12 cases per million per year in the age group 0–14 with a male predominance.[1,2] Clinical trials and advances in therapy lead to an improvement of the 5-year survival rate for children newly diagnosed with HL.[3,4] The current National Comprehensive Cancer Network (NCCN) guidelines do not address HL in paediatric patients.[5] Therefore, initial radiological staging examinations depend on study protocols. Most patients with HL receive (18)F-Fluorodeoxyglucose (FDG) positron emission tomography/computed tomography (PET/CT) scans as initial staging and during follow-up to assess early response and to identify responders or non-responders to chemotherapy.[6-8] Over 95% of children with HL will become long-time survivors.[4] Currently the Deauville five-point scale is recommended for FDG-PET/CT-based response assessment in patients with lymphoma. It is a visual scale using mediastinal and liver blood pool FDG-uptake as reference points.[9] The therapeutic improvements lead to increasing live expectancy and increasing number of dose-intense follow-up examinations with PET/CT. Several studies examined methods to reduce the radiation exposure for paediatric patients in whole body PET/CTs, but FDG-PET/CT is still the preferred examination to evaluate the treatment response of HL patients.[10] Magnetic resonance imaging (MRI) plays an important role in a wide field of paediatric specialities, ranging from acute trauma to oncology.[11-14] In HL patients MRI is used to evaluate soft tissue lesions. In contrast to PET/CT imaging there is no radiation exposure in MRI examinations, which is especially beneficial in paediatric patients. In MRI with diffusion weighted imaging (DWI) apparent diffusion coefficient maps can be calculated. Apparent diffusion coefficient (ADC) maps have been utilized in different setting such as ischemic stroke, heart imaging and differentiation between several types of cancer and cancer detection.[15-18] The potential of MRI-derived apparent diffusion coefficient measurements as radiation free surrogate for SUVmax has not yet been evaluated. In the present study, we retrospectively evaluated the correlation between ADC and SUVmax in paediatric patients with HL.

Patients and methods

This retrospective study was approved by the institutional review board (IRB) of the University Hospital Frankfurt (IRB; 2022-603).

Inclusion criteria were (I) histologically confirmed Hodgkin lymphoma with (II) pretherapeutic MRI and (III) (18)F-FDG PET/CT on the same MRI or PET/CT in (IV) patients < 18 years with a (V) maximum duration between MRI and PET/CT of 30 days.

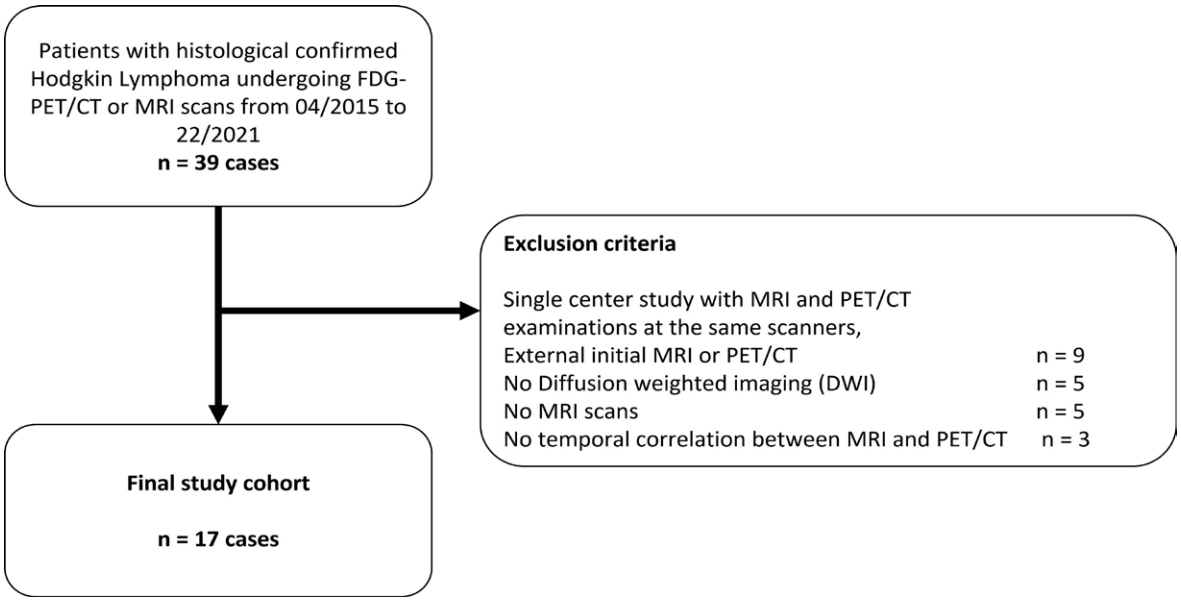

FIGURE 1. Flowchart for recruitment of study subjects according to the Standards for Reporting of Diagnostic Accuracy (STARD) studies.

TABLE 1. Magnetic resonance imaging sequences

Sequence	Orientation	Body part
T2w-TIRM in transversal orientation	transversal	neck
T1w-TSE (fat suppressed, +/- contrast media)	transversal	neck
T1w-TSE (no fat suppression, with substraction, +/- contrast media)	coronal	neck
DWI (b-values: 50, 200, 800)	transversal	neck, body
T2w-HASTE	coronal, sagittal and transversal	body
T1w-VIBE (with fat suppression) without breath-hold-imaging +/- contrast media	transversal	body

DWI = diffusion-weighted magnetic resonance imaging; HASTE = T2-weighted half-Fourier acquisition single-shot turbo spin-echo; T1w = T1-weighted; T2w = T2-weighted; TIRM = turbo inversion recovery magnitude; TSE = turbo spin echo; VIBE = T1-weighted volumetric interpolated breath-hold examination

Exclusion criteria were (I) missing ADC assessment, (II) duration between MRI and PET/CT > 30 days, (III) imaging artifacts (Figure 1).

MR imaging acquisition and examination

Examinations of this retrospective single centre study took place at University Hospital Frankfurt am Main/Germany at a single 1.5-T MRI Scanner in clinical routine using a standard 18-channel body-coil (Magnetom Aera; Siemens Healthineers, Forchheim/Germany) and at a single PET/CT Scanner (Biograph 6; Siemens Healthineers, Forchheim/Germany).

Neck MRI examinations were performed using the following sequences: (a) T2-weighted (T2w) Turbo inversion recovery magnitude (TIRM) in transversal orientation, (b) T1-weighted (T1w) turbo spin echo (TSE) in transversal (with fat suppression) and coronal orientation (without fat suppression, substraction images were calculated) with and without contrast media, and diffusion-weighted magnetic resonance imaging (DWI) (b-values: 50, 200, 800).

Body MRI examinations were performed using the following sequences: (a) T2-weighted half-Fourier acquisition single-shot turbo spin-echo (HASTE) in coronal, sagittal and transversal orientation, (b) diffusion-weighted magnetic resonance imaging (b-values: 50, 200, 800), and (c) T1-weighted volumetric interpolated breath-hold examination (VIBE) dixon (with fat suppression) in transversal orientation without breath-hold-imaging, without and with contrast media (Table 1).

In PET/CT examinations the mean computed tomography dose index (CTDI) was 2.2 ± 0.8 Milli-Gray (mGy). The mean dose length product (DLP) was 215.1 ± 92.1 mGy*cm (Table 2).

Image evaluation

Image evaluation was performed by using a conventional picture archiving and communication system station (PACS-station, Centricity Universal Viewer, Version 7.0). MRI examinations and (18) F-FDG PET/CT examinations with temporal correlation (both examinations within one month) were paired (Figure 2). At MRI, the Hodgkin le-

TABLE 2. Radiation exposure and examination time

Modality	CTDI [mGy]		DLP [mGy*cm]		Examination time [min]	
	Mean (SD)	Range	Mean (SD)	Range	Mean (SD)	Range
FDG-PET/CT	2.2 (0.8)	1.2–4.1	215.1 (92.1)	93.9–410.2	28 (8:26)[1]	20–49
MRI						
Neck					19:45 (3:41)	17:21–24:47
Thorax					09:23 (2:12)	08:01–10:29
Abdomen					09:23 (2:59)	07:32–12:21

CTDI = computed tomography dose index; DLP = dose length product; mGy = milligray; min = minutes; [1] FDG has to distribute for 1h after application. Time given in the table is the scanning time after application

TABLE 3. Patient characteristics and classifications

Variable	Retrospective cohort of patients diagnosed with Hodgkin lymphoma; baseline features
No. of patients	17
Median age (SD), years	15.8 (2.2)
Sex	
Male	11 (65%)
Female	6 (35%)
Lugano classification	
1	3 (18%)
2	6 (35%)
3	4 (23%)
4	4 (23%)
Hodgkin lymphoma subtypes (WHO classification)	
Nodular sclerosis	9 (52%)
Mixed cellularity	5 (29%)
Lymphocyte rich	2 (12%)
Lymphocyte depleted	1 (6%)

Unless otherwise indicated, data are the number of patients.
WHO = World Health Organization

FIGURE 2. MRI and FDG-PET/CT imaging of two Hodgkin lymphoma (HL) patients. Left side **(A, B)**: 12yo patient with newly diagnosed HL, **(A)** MRI examination with thoracal apparent diffusion coefficient (ADC) map. **(B)** correlating FDG-PET/CT examination with a HL lesion and calculated SUVmax. right side **(C, D)**: 9yo patient with newly diagnosed HL, **(C)** MRI examination with neck ADC map. **(D)** correlating FDG-PET/CT examination with a HL lesion and calculated SUVmax.

sions were identified on DWI and ADC. For each Hodgkin lesion in (18)F-FDG PET/CT with measured SUV two readers (N.R, board-certified radiologist with six years of experience and S.B., radiology resident with four years of experience) defined a 2D-ROI in the correlating MRI lesion in ADC maps covering the entire HL lesion and the mean ADC was evaluated. In total 72 ROIs with correlating SUVmax lesions were evaluated. After an initial analysis the 72 ROIs were subdivided into the three different examination areas. 22 ROIs were selected at neck imaging, 28 ROIs at thoracal imaging and 22 ROIs at abdominal imaging. Image quality and noise were evaluated by using a 5-point Likert scales (1, unacceptable; 5, excellent).

Statistical analysis

Statistical analyses were performed using RStudio 2021.09.2 (Posit PBC). The nonparametric Kolmogorov-Smirnov test was applied to assess the normality of the data. Variables were expressed as means ± standard deviation and analyzed with the Wilcoxon test. A $p < .05$ (two-tailed) was considered statistically significant. Correlation between SUVmax and meanADC was calculated using the Pearson's Product Moment Correlation Coefficient. The difference between the correlations of neck, thoracal and abdominal meanADC was calculated using the Fisher Z-Transformation with Z Test statistic (Z-Score) and probability (p).[19,20] According to Landis and Koch, weighted κ statistics was used evaluating the interrater agreement.[21]

Results

Between April 2015 and November 2021 39 pediatric patients underwent treatment for Hodgkin lymphoma at the University Hospital Frankfurt am Main and received as part of routine diagnostics a PET/CT examination. Out of these, seventeen patients (median age: 16 years, range: 12–20 years; six females [median age: 17 range: 12–18 years] and

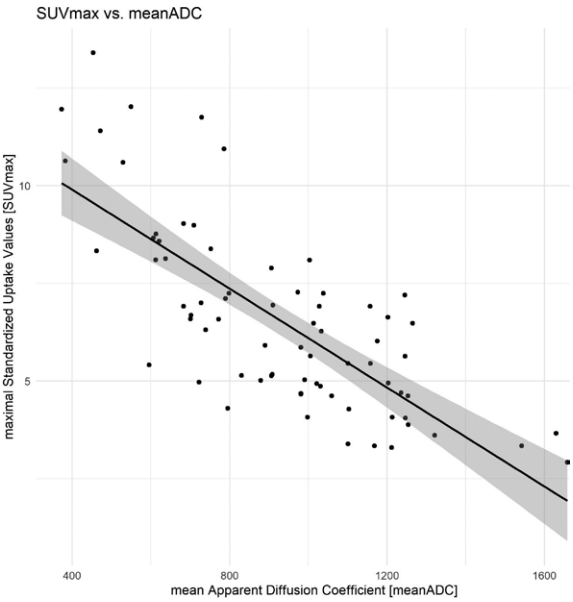

FIGURE 3. Correlation of SUVmax and mean apparent diffusion coefficient (ADC). The calculated meanADC of the MRI examinations show a strong inverse correlation with the correlating SUVmax of the FDG-PET/CT examinations.

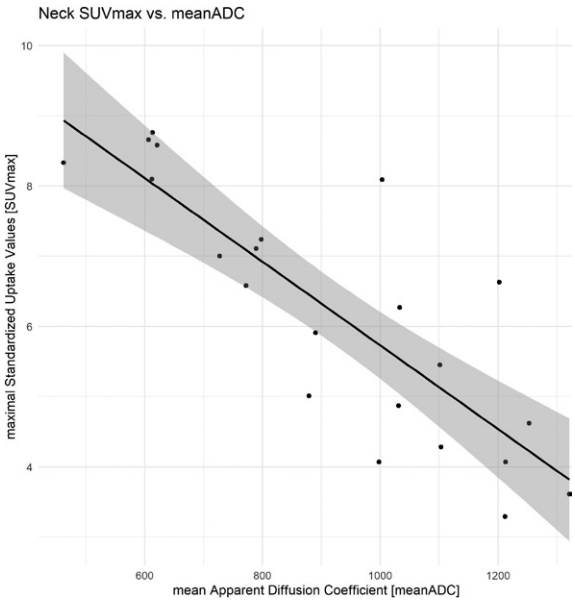

FIGURE 4. Neck imaging: correlation of SUVmax and mean apparent diffusion coefficient (ADC). The calculated meanADC of the MRI examinations show a strong inverse correlation with the correlating SUVmax of the FDG-PET/CT examinations.

eleven males [median age: 15, range: 12–19 years]) met the inclusion criteria (Table 3).

One ROI was defined in each of the 72 evaluable lesions in MRI examinations of 17 patients (Figure 2).

Pretherapeutic mean ADC was 931.17 x 10–3 mm^2/s ± 282.39 x 10–3 mm^2/s (minimum: 373 x 10–3 mm^2/s, maximum: 1658 x 10–3 mm^2/s). Pretherapeutic mean SUVmax was 6.53 ± 2.37 (minimum: 2.92, maximum: 13.4). The meanADC lesions of MRI showed a high inverse correlation of -0.75 (95% CI: -0.84 – -0.63, p = 0.001) with the matched SUVmax (Figure 3) of all 72 ROIs. The intraclass correlation coefficient (ICC) for the evaluation of the mean ADC was 0.98 (95% CI: 0.97–0.99).

The 72 ROIs were then subdivided into 22 neck, 28 thoracal and 22 abdominal lesions.

At the neck lesions, pretherapeutic meanADC was 919.95 x 10–3 mm^2/s ± 243.77 x 10–3 mm^2/s (minimum: 462 x 10–3 mm^2/s, maximum: 1321 x 10–3 mm^2/s). Pretherapeutic mean SUVmax was 4.26 ± 0.93 (minimum: 2.85, maximum: 6.04). The meanADC lesions of neck MRI showed a high inverse correlation of -0.83 (95% CI: -0.92 – -0.63, p < 0.001) with the matched SUVmax (Figure 4) of the 22 ROIs. The intraclass correlation coefficient for the evaluation of the neck mean ADC was 0.98 (95% CI: 0.95–0.99).

At the thoracal lesions, pretherapeutic meanADC was 976.22 x 10–3 mm^2/s ± 355.34 x 10–3 mm^2/s (minimum: 373 x 10–3 mm^2/s, maximum: 1630 x 10–3 mm^2/s). Pretherapeutic mean SUVmax was 4.70 ± 1.30 (minimum: 2.82, maximum: 6.94). The meanADC lesions of thoracal MRI showed a high inverse correlation of -0.82 (95% CI: -0.91 – -0.64, p < 0.001) with the matched SUVmax (Figure 5) of the 28 ROIs. The intraclass correlation coefficient for the evaluation of the thoracal mean ADC was 0.99 (95% CI: 0.98–1.00).

At the abdominal lesions, pretherapeutic meanADC was 931.68 x 10–3 mm^2/s ± 244.72 x 10–3 mm^2/s (minimum: 529 x 10–3 mm^2/s, maximum: 1658 x 10–3 mm^2/s). Pretherapeutic mean SUVmax was 4.66 ± 1.27 (minimum: 2.69, maximum: 7.44). The meanADC lesions of abdominal MRI showed an inverse correlation of -0.62 (95% CI: -0.83 – -0.28, p = 0.001) with the matched SUVmax (Figure 6) of the 22 ROIs. The intraclass correlation coefficient for the evaluation of the abdominal mean ADC was 0.97 (95% CI: 0.95–0.99).

The correlations of neck and thoracal imaging differed not significantly (Z-Score = 0.10, p = 0.92). There is no significant difference of the correlations of neck and abdominal (Z-Score = 1.42, p = 0.15) and of thoracal and abdominal imaging (Z-Score = 1.42, p = 0.16).

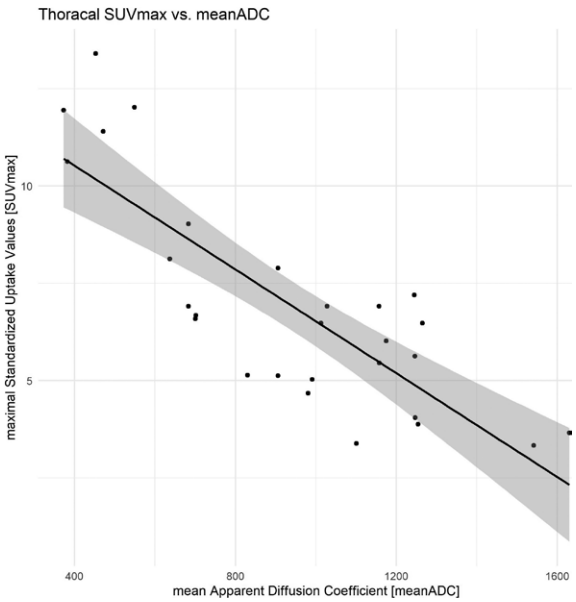

FIGURE 5. Thoracal imaging: correlation of SUVmax and mean apparent diffusion coefficient (ADC). The calculated meanADC of the MRI examinations show a strong inverse correlation with the correlating SUVmax of the FDG-PET/CT examinations.

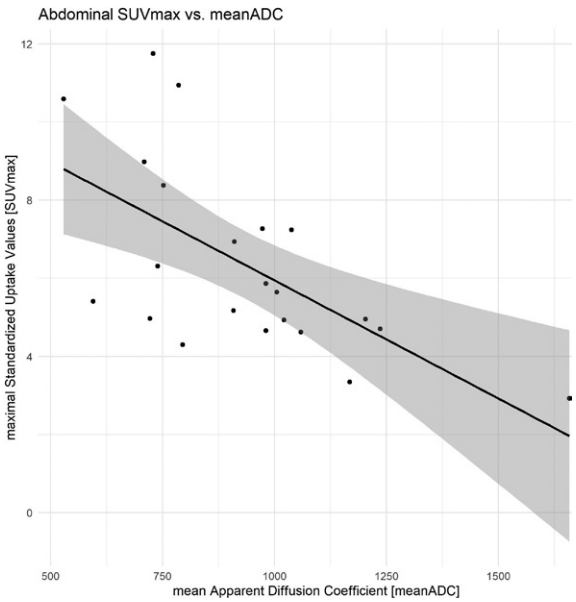

FIGURE 6. Abdominal imaging: correlation of SUVmax and meanADC. The calculated meanADC of the MRI examinations show a fair inverse correlation with the correlating SUVmax of the FDG-PET/CT examinations.

Image ratings

ADC maps were evaluated regarding image noise and image quality. Image noise was rated with mean scores of 4.6 ± 0.7. Image quality was rated with mean scores of 4.4 ± 0.9. The interrater agreement was good for image quality ($\kappa = 0.7 \pm 0.14$) and image noise ($\kappa = 0.64 \pm 0.21$) ($p < 0.0001$).

Discussion

Currently study protocols for HL patients contain PET/CT and MRI for initial staging, early assessment, and treatment response. Several studies demonstrated the important role of FDG-PET/CT scans as initial staging and during follow-up in HL patients.[22-24] Children are radiation sensitive because of the high cell division rate. Radiation dose induced damages in children are closely examined in several studies.[25] The increasing number of examinations with X-rays in patients leads to a lifelong increased risk of radiation induced cancer.[26] Paediatric radiology societies point out the necessity of the ALARA (as low as reasonably achievable) principle in radiation exposure at children.[27] On the other hand, assessment of the activity by PET/CT might reduce radiation exposure, as patients with negative PET/CT assessed early point during therapy might not receive radiotherapy. MRI might be beneficial in paediatric patients as there is no radiation exposure. Whole-body MRI (WB-MRI) examinations can play an important role as initial staging and follow-up examination in HL patients.[28,29] Spijkers *et al.* demonstrated a high correlation between WB-MRI with DWI and FDG-PET/CT scans in staging of adult HL patients.[30] The results of our feasibility study support that the results of Spijkers *et al.* also hold in paediatric patients, as ADC maps and FDG-PET/CT examinations showed a strong inverse correlation.

Our preliminary results in pre-therapeutic imaging suggests that pretherapeutic MRI ADC maps and meanADC demonstrated a strong inverse correlation with SUVmax of FDG-PET/CT neck and thoracal examinations in paediatric HL patients. However, data must be confirmed in the assessment of therapy response.

At abdominal imaging the correlation between meanADC and SUVmax decreased with no significant difference to neck and thoracal imaging. The inter reader agreement at abdominal MRI meanADC was excellent. Noise and image quality did not influence the evaluation of mean ADC. Pediatric MRI examinations were performed without breath-hold imaging. There may be an influ-

ence of breathing artifacts on the acquisition of abdominal DWI sequences. Further examinations in breath-hold imaging are necessary to exclude a potential breathing influence.

With this study we shed light on the potential application of MRI instead of PET/CT to assess paediatric patients with HL to reduce radiation exposure.

In this study only pretherapeutic FDG-PET/CT and MRI scans were selected to exclude a potential bias due to treatment. MRI scans with ADC maps may play an important role in follow-up examinations and assessment of treatment response of HL patients. To evaluate a post therapeutic correlation of meanADC and SUVmax further studies are necessary.

The examinations of our study were performed with a single MRI scanner, and one single DWI sequence was used at all patients. This is important as Kivrak *et al*. and Hoang-Dinh *et al*. demonstrated a statistically significant difference in the calculated ADC maps of different MRI scanners from different vendors.[31,32] The difference in calculated ACD maps may be caused by different DWI sequence settings. Sadinski *et al*. demonstrated a high reproducibility of ADC maps at a single scanner and Newitt *et al*. demonstrated a high reproducibility of ADC maps at different scanners from different vendors with the same DWI settings.[33,34] The evaluation of the robustness of the pretherapeutic correlation between meanADC and SUVmax in different scanners was beyond the scope of our analysis and requires further studies.

This study has limitations beyond its retrospective design. Missing MRI, missing pretherapeutic MRI and PET/CT examinations and missing temporal correlation between MRI and PET/CT reduced the number of eligible patients, which might has resulted in a selection bias. To exclude inter-scanner noise, we only included examinations from the same scanner. This homogenized the signals, but at the same time, limited the number of eligible patients and might limit the generalizability of the results.

References

1. The Lancet Haematology. New guidelines for paediatric Hodgkin lymphoma. *Lancet Haematol* 2020; **7:** e851. doi: 10.1016/S2352-3026(20)30371-9
2. Nagpal P, Akl MR, Ayoub NM, Tomiyama T, Cousins T, Tai B, et al. Pediatric Hodgkin lymphoma: biomarkers, drugs, and clinical trials for transla-tional science and medicine. *Oncotarget* 2016; **7:** 67551-73. doi: 10.18632/oncotarget.11509
3. Ansell SM. Hodgkin lymphoma: diagnosis and treatment. *Mayo Clin Proc* 2015; **90:** 1574-83. doi: 10.1016/j.mayocp.2015.07.005
4. Ehrhardt MJ, Flerlage JE, Armenian SH, Castellino SM, Hodgson DC, Hudson MM. Integration of pediatric Hodgkin lymphoma treatment and late effects guidelines: seeing the forest beyond the trees. *J Natl Compr Canc Netw* 2021; **19:** 755-64. doi: 10.6004/jnccn.2021.7042
5. Hoppe RT, Advani RH, Ai WZ, Ambinder RF, Armand P, Bello CM, et al. Hodgkin lymphoma, Version 2.2020, NCCN Clinical Practice Guidelines in Oncology. *J Natl Compr Canc Netw* 2020; **18:** p. 755-81. doi: 10.6004/jnccn.2020.0026
6. Kluge R, Kurch L, Georgi T, Metzger M. Current role of FDG-PET in pediatric Hodgkin's lymphoma. *Semin Nucl Med* 2017; **47:** 242-57. doi: 10.1053/j.semnuclmed.2017.01.001
7. Cheson BD, Fisher RI, Barrington SF, Cavalli F, Schwartz LH, Zucca E, et al. Recommendations for initial evaluation, staging, and response assessment of Hodgkin and non-Hodgkin lymphoma: the Lugano classification. *J Clin Oncol* 2014; **32:** 3059-68. doi: 10.1200/JCO.2013.54.8800
8. Zaucha JM, Chauvie S, Zaucha R, Biggii A, Gallamini A. The role of PET/CT in the modern treatment of Hodgkin lymphoma. *Cancer Treat Rev* 2019; **77:** 44-56. doi: 10.1016/j.ctrv.2019.06.002
9. El-Galaly TC, Villa D, Gormsen LC, Baech J, Lo A, Cheah CY. FDG-PET/CT in the management of lymphomas: current status and future directions. *J Intern Med* 2018; **284:** 358-76. doi: 10.1111/joim.12813
10. Kertész H, Beyer T, London K, Saleh H, Chung D, Rausch I, et al. Reducing radiation exposure to paediatric patients undergoing [18F]FDG-PET/CT imaging. *Mol Imaging Biol* 2021; **23:** 775-86. doi: 10.1007/s11307-021-01601-4
11. Banka P, Geva T. Advances in pediatric cardiac MRI. *Curr Opin Pediatr* 2016; **28:** 575-83. doi: 10.1097/MOP.0000000000000400
12. Daneman A. Special issue: Pediatric imaging. *Acta Radiol* 2013; **54:** 982. doi: 10.1258/ar.2012.12a008
13. Davis JT, Kwatra N, Schooler GR. Pediatric whole-body MRI: a review of current imaging techniques and clinical applications. *J Magn Reson Imaging* 2016; **44:** 783-93. doi: 10.1002/jmri.25259
14. Shapira-Zaltsberg G, Wilson N, Trejo Perez E, Abbott L, Dinning S, Kapoor C, et al. Whole-body diffusion-weighted MRI compared to (18 F)FDG PET/CT in initial staging and therapy response assessment of Hodgkin lymphoma in pediatric patients. *Can Assoc Radiol J* 2020; **71:** 217-25. doi: 10.1177/0846537119888380
15. Bozdağ M, Er A, Çinkooğlu A. Histogram Analysis of ADC Maps for differentiating brain metastases from different histological types of lung cancers. *Can Assoc Radiol J* 2021; **72:** 271-8. doi: 10.1177/0846537120933837
16. Juan CJ, Lin SC, Li YH, Chang CC, Jeng YH, Peng HH, et al. Improving interobserver agreement and performance of deep learning models for segmenting acute ischemic stroke by combining DWI with optimized ADC thresholds. *Eur Radiol* 2022; **32:** 5371-81. doi: 10.1007/s00330-022-08633-6
17. Lee SM, Lee KW, Kim MA, Song YS, Goo JM, Park CM. Serial texture analyses on ADC maps for evaluation of antiangiogenic therapy in rat breast cancer. *Anticancer Res* 2019; **39:** 1875-82. doi: 10.21873/anticanres.13295
18. Manetta R, Palumbo P, Gianneramo C, Bruno F, Arrigoni F, Natella R, et al. Correlation between ADC values and Gleason score in evaluation of prostate cancer: multicentre experience and review of the literature. *Gland Surg* 2019; **8(Suppl 3):** S216-22. doi: 10.21037/gs.2019.05.02
19. Schober P, Boer C, Schwarte LA. Correlation Coefficients: appropriate use and interpre-tation. *Anesth Analg* 2018; **126:** 1763-8. doi: 10.1213/ANE.0000000000002864
20. Schober P, Mascha EJ, Vetter TR. Statistics from A (Agreement) to Z (z Score): a guide to interpreting common measures of association, agreement, diagnostic accuracy, effect size, heter-ogeneity, and reliability in medical research. *Anesth Analg* 2021; **133:** 1633-41. doi: 10.1213/ANE.0000000000005773
21. Landis JR, Koch GG. Koch, The measurement of observer agreement for categorical data. *Biometrics* 1977; **33:** 159-74. PMID: 843571
22. Kamal NM, Elsaban K. Role of 18f-fdg-pet/ct in assessment of pediatric Hodgkin's lymphoma. *Q J Nucl Med Mol Imaging* 2021; **65:** 376-85. doi: 10.23736/S1824-4785.16.02695-9
23. Qiu L, Chen Y, Wu J. The role of 18F-FDG PET and 18F-FDG PET/CT in the evaluation of pediatric Hodgkin's lymphoma and non-Hodgkin's lymphoma. *Hell J Nucl Med* 2013; **16:** 230-6. doi: 10.1967/s0024499100091

24. Verhagen MV, Menezes LJ, Neriman D, Watson TA, Punwani S, Taylor SA, et al. (18)F-FDG PET/MRI for staging and interim response assessment in pediatric and adolescent Hodgkin lymphoma: a prospective study with (18) F-FDG PET/CT as the reference standard. *J Nucl Med* 2021; **62:** 1524-30. doi: 10.2967/jnumed.120.260059

25. Chu C, Gao Y, Lan X, Lin J, Thomas AM, Li S. Stem-cell therapy as a potential strategy for radiation-induced brain injury. *Stem Cell Rev Rep* 2020; **16:** 639-49. doi: 10.1007/s12015-020-09984-7

26. Linet MS, Slovis TL, Miller DL, Kleinerman R, Lee C, Rajaraman P, et al. Cancer risks associated with external radiation from diagnostic imaging procedures. *CA Cancer J Clin* 2012; **62:** 75-100. doi: 10.3322/caac.21132

27. Kollmann C, Jenderka KV, Moran CM, Draghi F, Jimenez Diaz JF, Sande R. EFSUMB clinical safety statement for diagnostic ultrasound - (2019 revision). *Ultraschall Med* 2020; **41:** 387-9. doi: 10.1055/a-1010-6018

28. Albano D, Bruno A, Patti C, Micci G, Midiri M, Tarella C, et al. Whole-body magnetic resonance imaging (WB-MRI) in lymphoma: state of the art. *Hematol Oncol* 2020; **38:** 12-21. doi: 10.1002/hon.2676

29. Galia M, Albano D, Tarella C, Patti C, Sconfienza LM, Mulè A, et al. Whole-body magnetic resonance in indolent lymphomas under watchful waiting: the time is now. *Eur Radiol* 2018; **28:** 1187-93. doi: 10.1007/s00330-017-5071-x

30. Spijkers S, Littooij AS, Kwee TC, Tolboom N, Beishuizen A, Bruin MCA, et al. Whole-body MRI versus an FDG-PET/CT-based reference standard for staging of paediatric Hodgkin lymphoma: a prospective multicentre study. *Eur Radiol* 2021; **31:** 1494-504. doi: 10.1007/s00330-020-07182-0

31. Kıvrak AS, Paksoy Y, Erol C, Koplay M, Özbek S, Kara F. Comparison of apparent diffusion coefficient values among different MRI platforms: a multicenter phantom study. *Diagn Interv Radiol* 2013; **19:** 433-7. doi: 10.5152/dir.2013.13034

32. Hoang-Dinh A, Nguyen-Quang T, Bui-Van L, Gonindard-Melodelima C, Souchon R, Rouvière O. Reproducibility of apparent diffusion coefficient measurement in normal prostate peripheral zone at 1.5T MRI. *Diagn Interv Imaging* 2022; **103:** 545-54. doi: 10.1016/j.diii.2022.06.001

33. Newitt DC, Zhang Z, Gibbs JE, Partridge SC, Chenevert TL, Rosen MA, et al. Test-retest repeatability and reproducibility of ADC measures by breast DWI: results from the ACRIN 6698 trial. *J Magn Reson Imaging* 2019; **49:** 1617-28. doi: 10.1002/jmri.26539

34. Sadinski M, Medved M, Karademir I, Wang S, Peng Y, Jiang, et al. Short-term reproducibility of apparent diffusion coefficient estimated from diffusion-weighted MRI of the prostate. *Abdom Imaging* 2015; **40:** 2523-8. doi: 10.1007/s00261-015-0396-x

research article

CT-guided biopsies of unspecified suspect intrahepatic lesions: pre-procedure Lipiodol-marking improves the biopsy success rate

Marcel Christian Langenbach[1,2], Thomas Joseph Vogl[1], Amelie Buchinger[1], Katrin Eichler[1], Jan-Erik Scholtz[1], Renate Hammerstingl[1], Tatjana Gruber-Rouh[1]

[1] Institute for Diagnostic and Interventional Radiology, University Hospital Frankfurt, Goethe University Frankfurt, Frankfurt, Germany

[2] Cardiovascular Imaging Research Center, Department of Radiology, Massachusetts General Hospital, Harvard Medical School, Boston, MA, USA

Radiol Oncol 2023; 57(2): 158-167.

Received 17 February 2023
Accepted 20 April 2023

Correspondence to: Prof. Tatjana Gruber-Rouh, Goethe University Frankfurt, University Hospital Frankfurt, Institute for Diagnostic and Interventional Radiology, Theodor-Stern-Kai 7, 60590 Frankfurt, Germany, E mail: tatjana.gruber-rouh@kgu.de

Disclosure: No potential conflicts of interest were disclosed.

Background. While computed tomography (CT)-guided liver biopsies are commonly performed using unenhanced images, contrast-enhanced images are beneficial for challenging puncture pathways and lesion locations. This study aimed to evaluate the accuracy of CT-guided biopsies for intrahepatic lesions using unenhanced, intravenous (IV)-enhanced, or intra-arterial Lipiodol-marked CT for lesion marking.

Patients and methods. Six-hundred-seven patients (men: 358 [59.0%], mean age 61 years; SD ±12.04) with suspect hepatic lesions and CT-guided liver biopsies were retrospectively evaluated. Successful biopsies were histopathological findings other than typical liver tissue or non-specific findings. Data was ascertained regarding the use of contrast medium for the biopsy-planning CT, unenhanced (group 1) *vs.* Lipiodol (group 2) *vs.* IV contrast (group 3). Technical success and influencing factors were insulated. Complications were noted. The results were analyzed using the Wilcoxon-Man-Whitney t-test, Chi-square test, and Spearman-Rho.

Results. Overall lesion hitting rate was 73.1%, with significantly better rates using Lipiodol-marked lesions (79.3%) compared to group 1 (73.8%) and group 3 (65.2%) ($p = 0.037$). Smaller lesions (<20 mm diameter) benefited significantly from Lipiodol-marking with 71.2% successful biopsy rate compared to group 1 (65.5%) and group 3 (47.7%) ($p = 0.021$). Liver cirrhosis ($p = 0.94$) and entity of parenchymal lesions ($p = 0.78$) had no impact on the hitting rate between the groups. No major complications occurred during the interventions.

Conclusions. Pre-biopsy Lipiodol marking of suspect hepatic lesions significantly increases the lesion-hitting rate and is especially beneficial for biopsy of smaller targets below 20 mm diameter. Further, Lipiodol marking is superior to IV contrast for non-visible lesions in unenhanced CT. Target lesion entity has no impact on the hitting rate.

Key words: ethiodized oil; liver; biopsy; X-ray computed tomography

Introduction

Suspicious hepatic lesions are often detected incidentally or during staging and remain suspect despite the use of various diagnostic imaging methods. However, accurate diagnosis is crucial in the majority of suspect cases, especially in patients with known or suspected malignant disease.[1,2] Thus, biopsies of suspicious intrahepatic lesions are an established procedure commonly performed in the clinical routine, with several options for image guidance available.

Therefore, various guiding procedures have been established for liver biopsies with good success rates providing reliable histopathological results. Ultrasound-guided biopsy is the primary option for all hepatic lesions, widely available, and allows for a biopsy performed under continuous dynamic guidance.[3,4] However, the applicability of ultrasound is limited by the location of the lesion (*e.g.*, infra-diaphragmatic, deep in the liver) and interference with other structures, especially ribs or intestinal gas. In challenging cases with uncertain identification of the target lesions by ultrasound, magnetic resonance imaging (MRI)- or computed tomography (CT)-guidance may be beneficial for a safe and reliable biopsy.[5-7]

MRI guidance is technically feasible but uncommon for biopsy hepatic lesions due to high cost, time-consuming, restricted availability, and motion artifacts. The clinical applicability is commonly limited to other, more steady regions like the prostate or breast.[8]

In addition to ultrasound-guided biopsy, CT-guided biopsy is an integral part of routine clinical diagnostics. In most cases, the target liver lesions are visible in unenhanced CT images, commonly acquired for biopsy planning. Especially with the knowledge of a previous contrast-enhanced CT or MRI in which the lesions were identified and stated as suspect.[9] Nevertheless, some hepatic lesions are challenging to delaminate in an unenhanced CT, particularly in altered liver parenchyma like hepatic cirrhosis. Also, lesions with a deep parenchymal position or with small size are challenging to detect.[10,11] Contrast-enhanced CT images are commonly used to overcome this limitation with two options available; application of intravenous (IV) contrast medium during the examination or a previous lesion marking using Lipiodol as a contrast agent.[12-14] Intravenous contrast is promptly washed out of the lesion and liver parenchyma and may not allow sufficient differentiation during the entire examination.[15,16] In comparison, Lipiodol is interventionally administered intra-arterial during angiography and provides a long-lasting uptake (Lipiodol washout half-life 29 to 55 days[17]) in the lesion or perilesional altered tissue during the complete intervention.[12,18]

A novel approach uses fusion imaging, ultrasound, or real-time fluoroscopy synchronized with previously acquired contrast-enhanced CT or MRI images to delineate the lesion during the intervention. This technique requires the newest equipment accompanied by high costs and is limited to a few centers only.[19]

This study aimed to evaluate the interventional performance of CT-guided biopsies of suspicious intrahepatic lesions performed using unenhanced CT, intravenous contrast agent, or prior interventional lesion marking with Lipiodol for image guidance by analysis of the accuracy and potential influencing factors.

Patients and methods

Patient series and study setting

The institutional review board (IRB) approved this retrospective cohort study with a waiver for written informed consent. Inclusion criteria were as follows: unclear and suspect hepatic lesion, CT-guided biopsy of the hepatic lesion, unenhanced, IV contrast or previous Lipiodol-angiography for lesion marking, age 18 and above. All patients who met the inclusion criteria (Figure 1) were included. We excluded all patients with a time interval between CT-guided biopsy and Lipiodol-angiography of more than two months (n = 18) or an abort of the CT intervention during the examination due to lack of lesion visibility or sufficient biopsy window (n = 23).

CT-guided biopsy

Data were evaluated for the whole study population, and a comparison of the three groups, unenhanced (group 1), Lipiodol enhanced (group 2), and IV contrast medium enhanced (group 3) was performed. Only patients who were not eligible for an ultrasound-guided biopsy or after an unsuccessful ultrasound-guided biopsy were referred to the radiology department for a CT-guided intervention. The interdisciplinary tumor board made the decision to biopsy. The enhancement protocol was selected at the time of the decision for biopsy based on several parameters and experience. Patients with lesions expected to be displayed well in unenhanced CT, either by size, location, or based on previous imaging, were planned for an unenhanced biopsy. A contrast protocol was determined in patients with lesions that might be more challenging to display in unenhanced CT. The decision for contrast protocol, Lipiodol (Example given in Figure 2) *vs.* IV contrast medium (*e.g.*, Figure 3), was also based on the lesions' location and parameters (*e.g.*, size, architecture with visible changes in the liver parenchyma). Small lesions and lesions with a challenging location were more likely marked with Lipiodol due to a more long-

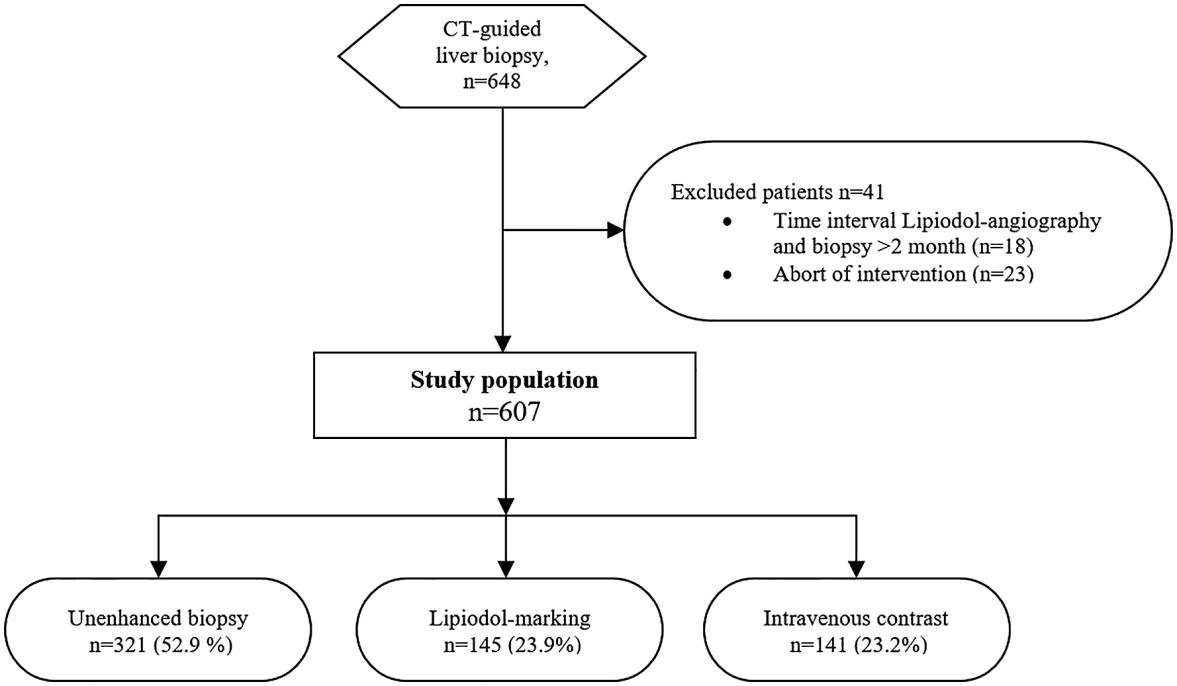

FIGURE 1. The Standards for the Reporting of Diagnostic Accuracy studies (STARD) flow diagram for a study of 607 patients undergoing CT-guided liver biopsy.

lasting uptake which enables a secure identification during the whole examination, while IV contrast might have been washed out. In clinical practice, more intravenous contrast applications were performed in the early years of the study period. In the last years, more patients were examined using a previous intra-arterial enhancement by Lipiodol based on good local experience. The study population and the three groups were subdivided by lesion size and occurrence of liver cirrhosis.

All patients received a transcutaneous CT-guided biopsy of the hepatic lesion using the same 128-multislice CT scanner [SOMATOM Definition AS, Siemens Healthineers] for image acquisition. The interventions were performed by interventional radiologists with more than five years of experience in CT-guided interventions. The obtained core biopsies were histopathologically analyzed by the local Institute for Pathology. Successful biopsy was defined as histopathological findings other than typical liver tissue or non-specific findings. Based on our experience, Lipiodol does not affect the analysis of the specimen.

Before the examination, the coagulation profile was checked. Patients who were planned for an application of IV contrast medium were screened for contraindications, *e.g.*, reduced renal function or hyperthyroidism. The use of oral anticoagulants was prohibited based on national guidelines. No changes to institutional guidelines (standard operating procedures) were made. If patients were planned for IV contrast, 60 ml of contrast agent [Imeron® 350, Bracco] were administered with an application rate of 3-5 mL/s. We used a fixed delay of 60 s until the first planning scan was initiated.

After the patients received the first planning scan, the access path was planned using a standard 3D-CT workstation [syngo.via, Siemens Healthineers] without software modifications. In the case of multiple lesions with a similar suspect appearance, the lesion with the best reachability was defined as the target. Based on the biopsy planning, the cutaneous entry point was marked. After introducing the coaxial needle, the lesion approach was performed under image guidance. A coaxial approach was used for CT-guided intervention. This approach is characterized by combining two needles: a puncture sheath [17 G, Puncture Sheath, Somatex® Medical Technologies, Germany] and a biopsy handy [18 G, Biopsy Handy, Somatex® Medical Technologies, Germany]. The sheath - a thicker, shorter needle (5cm, 10 cm, or 15 cm) is inserted down to the anterior edge of the lesion. Then, the biopsy handy - a thinner, longer needle (10 cm, 15 cm, or 20 cm) is introduced through the sheath. Finally, the biopsy needle is inserted 2 cm into the edge of the lesion for tissue sampling. Three or four samples can be

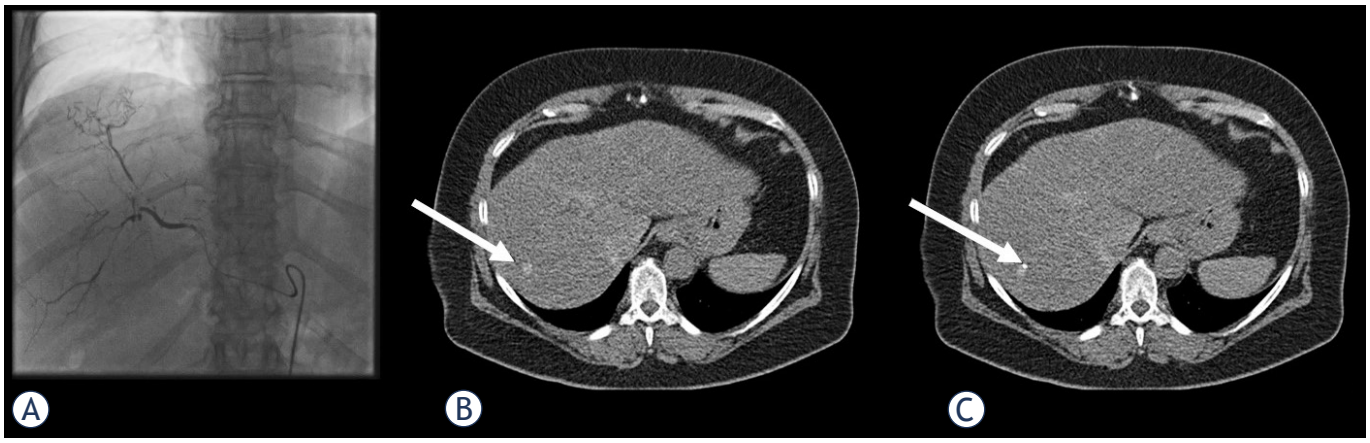

FIGURE 2. The decision for a biopsy of the suspicious hepatic lesion was made for the same male patient. Because of the small lesion size and isodensity in the unenhanced CT, a prior intra-arterial Lipiodol-marking **(A)** was performed. Directly after the intervention **(B)** and during the CT intervention **(C)** (white arrow) was well displayable, and the biopsy was successful, revealing a hepatocellular carcinoma.

taken using the thinner biopsy needle. After the examination, additional CT single shots were performed to rule out immediate complications like bleeding or pneumothorax. Afterward, the patients had bed rest for 2 hours, a laboratory check of the blood parameters, and an ultrasound follow-up after 6 hours to rule out potential complications such as capsular hematoma or any other signs of bleeding.

Angiography

In patients with a prior Lipiodol-marking, the angiography was performed at a minimum interval of 12 hours before the biopsy. The angiographic approach was according to our standard procedure for hepatic interventions (Figure 2A).[12] The same team of interventional radiologists with over five years of experience conducted all interventions. The angiographic approach was through the femoral artery in all cases. After the introduction of the catheter [Boston Scientific], contrast medium iomeprol [Imeron®, Bracco] was used to display the abdominal and hepatic vessels. Following this, an overview angiography was performed. The superior mesenteric artery and celiac trunk were selectively catheterized, including an indirect portography to demonstrate vascular anatomy, ensure the portal vein's patency, and rule out portal vein thrombosis. Then, super-selective catheterization of the segmental and subsegmental hepatic branches was performed using a microcatheter [Progreat®, Terumo] for approach and precise placement. Lipiodol [Lipiodol Ultra-Fluid®, Guerbet] was administered as a tumor visualizer and transient embolic agent until stasis with a maximum amount of 15 ml. After the procedure, all patients were transferred to our ward for a minimum of 24-hour surveillance.

Data analysis

Patient data were retrieved from the electronic patient record (Orbis, Dedalus Healthcare), imaging data from the local radiology information system (RIS, GE Healthcare), and picture archiving and communication system (PACS, GE Healthcare). We included patients who matched the inclusion criteria and received a CT-guided biopsy between 01/2010 and 12/2018.

Demographic data, underlying hepatic diseases, and liver cirrhosis were analyzed. Based on the CT images, lesion diameter, number of lesions, and lesion localization were noted. In patients with a prior Lipiodol angiography, the Lipiodol enhancement of the lesions was evaluated (visible or non-visible). During the CT-guided intervention, the puncture path (lateral-intercostal, anterolateral, anterior-subcostal, dorsolateral), length cutis-to-lesion, and liver capsule-to-lesion were measured. Dose-length-product (DLP) and the number of images of the entire examination, which includes the planning scan and the post-procedure scan, as well as for puncture sequence, including scans for needle placement, positioning, and sample acquisition, were noted and compared. This differentiation was made to achieve optimal comparability, as the differences in radiation exposure are caused

TABLE 1. Overview of patient characteristics. P-values based on the Chi-square test indicate only a difference in the distribution of liver cirrhosis in comparison of the three enhancement groups

Characteristic	Overall	Unenhanced biopsy	Lipiodol-enhanced	i.v. contrast-enhanced	p-value
Age, y (SD)	61.0 ± 12.0	61.9 ± 11.95	60.4 ± 11.12	59.6 ± 13.04	0.228
Gender, n (%)					
Male	358 (59.0)	177 (55.1)	108 (74.5)	73 (51.8)	0.134
Female	249 (41.0)	144 (44.9)	37 (25.5)	68 (48.2)	
Hepatic disease, n (%)					
HCV	101 (16.6)	34 (10.6)	53 (36.6)	14 (9.9)	
HBV	28 (4.6)	6 (1.9)	17 (11.7)	5 (3.5)	
HCV+HBV	8 (1.3)	3 (0.9)	3 (2.1)	2 (1.4)	0.354
NASH	34 (5.6)	12 (3.7)	17 (11.7)	5 (3.5)	
Toxic damage	48 (7.9)	20 (6.2)	16 (11.0)	12 (8.5)	
Others	53 (8.7)	26 (8.1)	19 (13.1)	8 (5.7)	
No disease	335 (55.2)	220 (68.5)	20 (13.8)	95 (67.4)	
Cirrhosis	188 (33.0)	59 (19.2)	100 (71.9)	29 (3.6)	0.013
Intrahepatic lesions, n (%)					
1 lesion	297 (48.9)	164 (51.1)	68 (46.9)	65 (46.1)	0.541
2 lesions	116 (19.1)	45 (14.0)	37 (25.5)	34 (24.1)	
3 or more lesions	194 (32.0)	112 (34.9)	40 (27.6)	42 (29.8)	
Lesion size, mm (SD)	29.3 ± 18.0	30.1 ± 18.1	25.9 ± 17.4	29.8 ± 18.7	0.182

Results are presented as mean and standard deviation or number (%)

HBV = Hepatitis-B-Virus; HCV = Hepatitis-C-Virus; i.v. – intravenous; NASH – Non-alcoholic steato hepatitis; SD = Standard deviation

by the required placement and positioning scans. For the angiography, the dose-area-product (DAB) was noted. The major endpoint of this study was the evaluation of the hitting rate, defined by histopathological findings other than healthy liver tissue. Successful biopsy findings were defined as follows: hemangioma, focal nodular hyperplasia, regenerative nodule, granuloma, adenoma, necrosis, and all types of malignancies. Unsuccessful biopsies were defined as healthy liver tissue, steatosis, inflammatory disease, fibrosis, and toxic damage.

Statistics

IBM SPSS statistics version 24 (IBM) was used for statistical analysis. For continuous data, median, mean, standard deviation, minimum, maximum, and range were calculated. For all continuous data, results were calculated for the whole study group and the three cohorts. The Chi-square test was used to test for differences in the successful biopsies between the three cohorts. In the first step, the whole study population was analyzed. In the second step, different subgroups (*e.g.*, lesions < 20 mm, liver cirrhosis) were compared in detail.

Further, the Chi-square test was used to check for differences in the distribution of attributes within the groups. Correlations were calculated according to Spearman-Rho. P-values less than 0.05 was considered statistically significant. A logistic regression analysis was performed to screen for potential factors within the demographic factors influencing the lesion hitting rate.

Complications

Patient records were also screened for complications, during the intervention or within the 24-hour surveillance. Complications were rated according to the severity score based on SIR's latest classification: 0 = no complications, 1 = mild adverse events (no/non-substantial therapy required), 2 = moderate adverse event (substantial treatment required), 3 = severe adverse events (escalation of care), 4 = life-threatening or disabling event, 5 = patient death. Complication score was evaluated for the whole study population and the subgroups.[20]

Results

Study population

Six hundred-seven patients, 358 men (59%) and 249 women (41%) (mean age 61 years; SD ± 12.04; range 22–86 years) with unclear suspect liver lesions, were retrospectively evaluated. In 321 patients (52.9%), the biopsy was obtained with unenhanced imaging, 145 lesions were prior marked with Lipiodol (23.9%), and 141 patients received IV contrast for the intervention (23.2%) (Figure 1).

Liver cirrhosis was histopathologically diagnosed in 188 patients (33.0%). Patient characteristics are displayed in detail in Table 1.

Most patients had a known hepatic disease (n = 310, 51.1%). The most common disease was hepatitis C in 101 cases (16.6%). Other more frequent pre-existing hepatic diseases were toxic liver damage (n = 48, 7.9%), non-alcoholic steatohepatitis (NASH) (n = 34, 5.6%), and hepatitis B infection (n = 28, 4.6%). No pre-existing hepatic disease was reported in 297 patients (48.9%).

Lesion characteristics

Based on patient medical records and the planning CT scan for the biopsy, 297 patients (48.9%) had a solitary suspect hepatic lesion, while 310 (51.1%) had two or more lesions. The target lesions were localized in all liver segments, with the majority found in liver segments 4 and 6 (each n = 112, 18.5%), and no differences according to the Chi-square test were seen between the three groups (p = 0.052). The mean lesion size was 29 ± 18 mm (range 4–116 mm). Target lesion smaller than 20 mm was seen in 229 patients (31.5%), and lesion smaller than 10 mm was seen in 38 patients (6.3%) (Table 1).

Biopsy

Access path was in 335 cases (55.2%) from lateral-intercostal, in 224 patients (36.9%) from anterior-subcostal, in 44 cases (7.2%) from anterior-lateral subcostal and in 4 cases (0.7%) from dorsal-lateral intercostal. The mean access path length from cutis to the lesion was 83 mm (± 26 mm), and within the liver from capsule to lesion, 43 mm (± 26 mm). Per patient, 2.6 probes were obtained in mean (± 1.3), equal across all groups assessed by the Chi-square test (p = 0.307) (Table 2). Regarding the visual aspect, all lesions previously marked in the angiography were seen in the biopsy-CT, either by lesion enhancement or circular enhancement of the surrounding tissue.

Lesion hitting rate

The target lesion was successfully biopsied in 444 patients (73.1%). In 163 patients (26.9%), the biopsy probe revealed healthy liver tissue defined as non-hitting of the target lesion. For group 1 with unenhanced CT, the biopsy was successful in 73.8% (n = 232). Group 2, with a prior Lipiodol-marking of the target lesion, showed the significantly highest hitting rate with 79.3% (n = 115) (Figure 2). The lowest hitting rate was seen in group 3 with IV contrast medium with 65.2% (n = 92) (Figure 3). The difference between all three groups was stated as significant (p = 0.037). In patients with liver target lesions smaller than 20 mm, the successful hitting rate was significantly higher after Lipiodol-marking compared to unenhanced or intravenous contrast-enhanced images (71.2%, 65.5%, and 47.7%, respectively) (p = 0.021). The location within the liver based on the liver segment model had no impact on the lesion hitting rate (p = 0.107) (Figure 4).

The presence of liver cirrhosis showed no significant impact on the overall success of liver biopsy in all three groups (p = 0.94). In the subset of patients without liver cirrhosis, a successful biopsy was highest in the Lipiodol group, 74.4%, compared to 71.5% in the unenhanced group and 58.5% using IV contrast (p = 0.049).

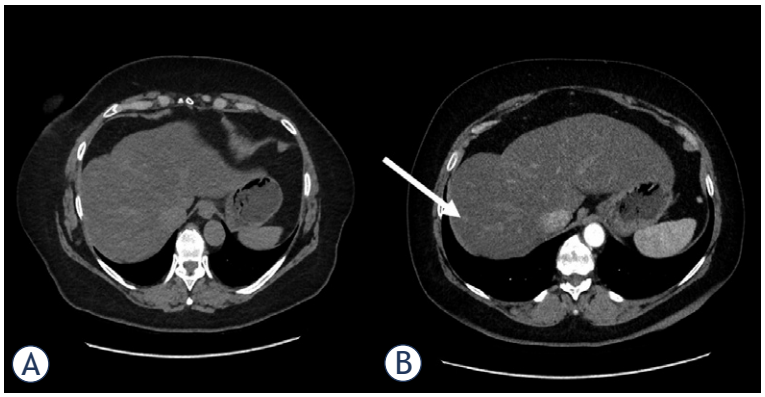

FIGURE 3. A male patient with a suspect and unclear hepatic lesion with 6 mm in segment 7. While not visible in the unenhanced CT **(A)**, the lesion impressed arterial hypervascularized after intravenous contrast medium application **(B)** (white arrow).

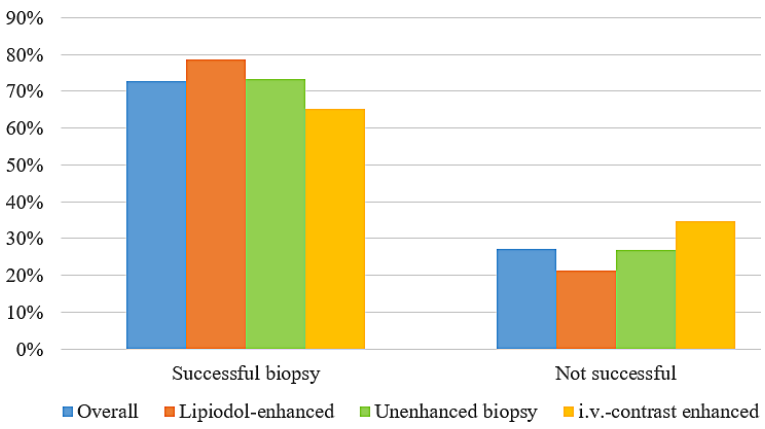

FIGURE 4. Presentation of histopathologically correlated puncture successes for the overall cohort and individual groups individually.

TABLE 2. Biopsy characteristics overall and for the three enhancement groups. A Chi-square test was performed to test for differences between the groups. Significance is indicated in bold

Characteristic	Overall	Unenhanced biopsy	Lipiodol-enhanced	i.v. contrast-enhanced	p-value
Biopsy access path					
Lateral-intercostal	335 (55.2)	162 (50.5)	94 (64.8)	79 (56.0)	
Anterior-subcostal	224 (36.9)	25 (7.8)	9 (6.2)	10 (7.1)	0.718
Anterior-lateral	44 (7.2)	132 (41.1)	42 (29.0)	50 (35.5)	
Dorsal-lateral	4 (0.7)	2 (0.6)	0	2 (1.4)	
Segment localization					
1	6 (1.0)	2 (0.6)	2 (1.4)	2 (1.4)	
2	54 (8.9)	29 (9.0)	14 (9.7)	11 (7.8)	
3	41 (6.8)	23 (7.2)	8 (5.5)	10 (7.1)	
4	112 (18.5)	66 (20.6)	23 (15.9)	23 (16.3)	0.052
5	95 (15.7)	57 (17.8)	21 (14.5)	17 (12.1)	
6	112 (18.5)	69 (21.5)	21 (14.5)	22 (15.6)	
7	82 (13.5)	31 (9.7)	22 (15.2)	29 (20.6)	
8	105 (17.3)	44 (13.7)	34 (23.4)	27 (19.1)	
Access path length [mm] (SD)					
Cutis to lesion	83 ±26	82 ±27	85 ±27	83 ±26	0.527
Liver capsule to lesion	43 ±26	44 ±21	41 ±21	43 ±21	0.473
Obtained probes (SD)	2.6 ±1.3	2.7 ±1.5	2.5 ±0.9	2.4 ±0.9	0.158
Radiation exposure (SD)					
Whole examination [mGycm²]	498.3 ±429.5	361.0 ±166.6	411.3 ±517.9	900.3 ±495.6	**0.019**
Biopsy scans [mGycm²]	80.1 ±58.0	79.7 ±60.0	88.2 ±56.3	72.6 ±56.4	0.053
Intervention *(i)-images [n]*	34.4 ±24.0	34.6 ±23.8	37.7 ±23.4	30.6 ±24.7	0.182
Complications					
Sub-capsular liver bleeding	3 (0.5)	1 (0.3)	1 (0.7)	1 (0.7)	
Fluid edge around liver	2 (0.3)	1 (0.3)	0	1 (0.7)	0.870
Bleeding along the access path	1 (0.2)	0	1 (0.7)	0	
Circulatory problems	1 (0.2)	1 (0.3)	0	0	

Values are mean and standard deviation or number (%)

i.v. = – intravenous; SD = Standard deviation

Patients with a known malignant disease also showed a significant difference comparing the three procedures. A successful biopsy was possible in 83.0% (n = 39) using Lipiodol-marking, in 68.2% (n=131) unenhanced, and in 58.3% (n = 35) with IV contrast medium (p = 0.024). The entity of the biopsied lesion did not impact the hitting rate by showing no significant difference between the protocols.

Based on the performed logistic regression analysis, the lesion diameter (regression coefficient 0.023, p = 0.048) and the number of obtained probes (r = 0.199, p = 0.047) significantly impacted the hitting rate. Age and length of the puncture path, from cutis or liver capsule to lesion, revealed no significant impact.

Histopathological results

Histopathological results revealed that the major malignant disease was HCC in 155 cases (25.5%). Inflammatory changes in the liver tissue were found to lead the non-malignant changes in 134 patients (22.1%). Appendix 1 shows the high variability of the diagnosed diseases.

Radiation exposure

Overall DLP was 498.31 mGycm² in mean (± 429.53 mGycm²) for the complete examination, including control and post-procedure scan. In the unenhanced group 1, 361.00 mGycm² (± 166.55 mGycm²), in the Lipiodol-marking group 2, 411.27 mGycm² (± 517.87 mGycm²), and in the IV contrast-medium group 3 900.27 mGycm² (± 495.55 mGycm²), reaching a significant difference with higher exposure in group 3 (p = 0.019).

Only counting the applied radiation during the biopsy scans, which contain the scans for needle placement, positioning, and sample acquisition, overall DLP was 80.07 mGycm² in mean (± 57.97 mGycm²), in group 1 with 79.69 mGycm² in mean (± 59.98 mGycm²), in group 2 with 88.19 mGycm² in mean (± 56.33 mGycm²) and group 3 with 72.59 mGycm² in mean (± 56.37 mGycm²), showing no significant differences (p = 0.053). The total amount of the intervention (i)-sequences was n = 34.4 (± 24.0), in group 1 n = 34.6 (± 23.8), in group 2 n = 37.7 (± 23.4), and in group 3 n = 30.6 (± 24.7) equal across all groups (p = 0.182) (Table 2).

For the previously performed angiography in group 2 to mark the lesion with Lipiodol, an overall DAP of 10421 cGycm² in mean (± 10277 cGycm²) was noted.

Complications

In 599 patients, no treatment-related complication was stated in the patient's medical record. Eight patients presented with a grade 1 complication: 3 patients with sub-capsular bleeding (0.5%), minimal hemorrhagic fluid edge surrounding the liver in 2 patients (0.3%), bleeding in the access path (1 patient, 0.2%), bleeding in the tumor (1 patient, 0.2%), and circulatory problems due to orthostatic problems (1 patient, 0.2%). No complications of grade 2 or higher were seen related to the intervention. No significant differences in the occurrence of complications were reported (p = 0.870). Details are given in Table 2.

Discussion

This study's purpose was to compare three different enhancement protocols, unenhanced, with a prior Lipiodol marking and application of IV contrast, for CT-guided biopsies of unspecified suspect intrahepatic lesions.

CT-guided biopsies of suspect and unclear hepatic lesions are an established procedure in the diagnostic cascade with high reliability and a detection rate based on the study of Haage *et al.* of 90.5%.[21] Several technical adaptions to increase the safety and success rate are possible, for example, variation of the access path or the needle thickness.[22] The histopathological reliability of the obtained tissue is very good, as various studies showed with an accuracy between 80% and 97%.[23,24]

A previous study by Gerhards *et al*. investigated the use of Lipiodol for biopsy of HCC-suspect or proven HCC lesions in a very small and selected patient cohort. The lesion hitting rates showed comparable results to our study, with a benefit of Lipiodol confirming our presented results. This study goes beyond the results of Gerhards *et al*. by investigating various lesion entities, different biopsy groups, with and without contrast enhancement, and a larger study cohort.[25]

The detectability of HCC lesions by the additional use of Lipiodol compared to conventional contrast medium was proven by Rizvi *et al*. With prior Lipiodol-marking, the detection rate of HCC lesions was perfect (sensitivity 1.0, specificity 0.6, accuracy 0.91), while conventional contrast medium (sensitivity 0.65, specificity 1.0, accuracy 0.68) showed benefits in discriminating the lesion entity.[26] Setting this fact in context to our study, only a reliable lesion marking is essential for a successful CT-guided biopsy. This is the case in most lesions and is supported by our results with a favorable lesion hitting rate due to the usage of Lipiodol. A clear delineation and diagnosis of the lesion entity are optional, as it will be diagnosed based on the histopathological probe. Nevertheless, Lipiodol distribution within the suspected lesion can unveil HCCs, which may direct the patient directly into therapy, avoiding a biopsy.[12,17]

We also investigated the impact of existing liver cirrhosis on the biopsy results. Cirrhotic liver might have been a potential influencing factor making a successful biopsy more difficult as the lesion is camouflaged by reticular liver tissue. This was refuted by the results of our study showing no difference between the three study groups. Possible reasons for the results are the stronger tissue response during the intervention allowing for a bit easier needle control or the better visibility of the lesions in unenhanced imaging based on the altered tissue type, even in reticular liver tissue.

Another important point is the impact of lesion size on technical success. Smaller lesions are much more difficult for a secure biopsy.[27,28] With a previous Lipiodol marking, especially lesions below 20 mm were easier to detect securely and to puncture successfully. Previous studies mainly investigated only HCC lesions with this question, but our study showed a benefit across all entities. Further, small lesions are defined as very variable in the literature with a size below 20 to 50 mm making the existing data inconclusive and problematic to compare with our results. The sensitivity of Lipiodol-CT for this small lesion ranged between 58% and 98% based on previous studies.[29-32] For example, our results should be considered in clinical practice for patients with a small unclear lesion in MRI imaging, which will be difficultly detectable in unenhanced CT. These patients benefit the most from a prior marking, with Lipiodol offering the best reliable biopsy method.

Interestingly, the patient group with an intravenous contrast medium application during the intervention showed the lowest lesion hitting rate. We identified two potential biases causing these results. First, these patients were primarily scheduled for interventions without contrast medium. In the CT scan directly before the examination

for the biopsy planning, the lesion was not detectable. Reasons for this might have been a small size or a challenging access path. Then the decision to administer IV contrast to visualize the lesion was reached. Second, the time of visibility is limited, and especially small lesions are challenging to detect after wash-out of the contrast medium. Compared to the unenhanced group, the IV contrast group might contain more technically complex patients. Patients presenting small lesions or a challenging access path in pre-interventional imaging might benefit from a prior Lipiodol-marking of the target lesion. Especially lesions that may be isodense in unenhanced, enhanced CT and obscured in delayed phase CT should be marked before the intervention.

As mentioned, most studies investigate the role of Lipiodol in the context of HCC, and it is known that the best and strongest enhancement is seen for hypervascularized lesions. But based on previous studies on TACE, it is known that Lipiodol shows an enhancement also in a wide variability of other tumors, *e.g.*, breast cancer or colorectal carcinoma, which are often hypo vascularized. Although not all lesions enhance strong and homogeneity, the wall area or the area of altered liver tissue around the lesions shows a typical enhancement that can be used for biopsy guidance. This underlines the potential for clinical use even if the entity of the lesion is not known before the intervention.

Besides CT, CEUS (Contrast-enhanced ultrasound) and cone beam CT (CBCT) with intra-arterial contrast application are useful other imaging modalities to assess suspicious intrahepatic lesions interventionally.[33] These techniques also allow for the accurate detection and localization of hepatic lesions. However, both modalities may not be widely available in all medical facilities, limiting their accessibility for some patients. Additionally, CEUS requires highly skilled operators with specific training and expertise. The quality and accuracy of the results may depend on the operator's skill and experience. CBCT fusion imaging with ultrasound for transcutaneous hepatic interventions is a new approach with promising first results, but it still requires further investigation.[34]

The overall complication rate was very low, with no major complications. This is according to the prevalence of complications reported in other studies[21-23], stating that a CT-guided biopsy is an approved and secure intervention well established in the clinical practice. The contrast medium did not influence the complication rate, even in challenging lesion locations.

Besides all benefits of the biopsy, the application of Lipiodol is an interventional procedure with the potential occurrence of complications and increased radiation exposure. Although a transarterial embolization is established in the clinical routine, the rate of major complications is low at under 0.9%.[35] Additionally, the increased radiation exposure comes with the risk of stochastic radiation damage and radiation-related late effects. Consequently, the application should be reserved for patients who benefit the most. Based on the results, prior Lipiodol-marking can be beneficial in patients with a lesion below 20 mm or a potentially challenging access path.

We acknowledge that this retrospective study had several limitations. This study intended to compare different enhancement protocols for CT-guided biopsies of various intrahepatic lesions. Therefore, we used a retrospective design and a relatively small cohort in a few tumor entities. A study including a prospective design and multiple centers, probably with a closer look at selected lesion entities, is required to prove the results. The histopathological results are problematic in a few cases as the pathologists described several patterns—further, the decision process for the enhancement protocol needed to be randomized. The multidisciplinary tumor board made the decision based on several parameters. This was based on pre-interventional imaging, lesion characteristics, age, or the patient's individual preference. This decision might have led to a selection bias. Also, IV enhancement was favored in the early years, while Lipiodol enhancement was performed based on convincing local experience in the later years. For lesions with the pathological finding of necrosis, this might also have been caused by a diffuse necrotic area, which might be considered as a non-successful biopsy. From the pathological results, no differentiation is possible.

In conclusion, the use of Lipiodol as a contrast agent and pre-puncture marking in angiography increases the lesion-hitting rate in CT-guided biopsies of suspect and unclear hepatic lesions significantly, especially for small suspect liver lesions with a diameter below 20 mm and might be used as an alternative to unenhanced imaging or IV contrast enhancement. For lesions that cannot be seen in unenhanced CT, Lipiodol marking is superior to IV marking and should be preferred.

Acknowledgment

The present study was founded receiving a research grant by Guerbet. The authors declare no relationships with any companies whose products or services may be related to the subject matter of the article. The funding sources were not involved in study design, data collection or analysis, manuscript preparation, or the decision to submit the manuscript.

References

1. Bravo AA, Sheth SG, Chopra S. Liver biopsy. *N Engl J Med* 2001; **344:** 495-500. doi: 10.1056/NEJM200102153440706
2. Rockey DC, Caldwell SH, Goodman ZD, Nelson RC, Smith AD. Liver biopsy. *Hepatology* 2009; **49:** 1017-44. doi: 10.1002/hep.22742
3. Gazelle GS, Haaga JR. Guided percutaneous biopsy of intraabdominal lesions. *AJR Am J Roentgenol* 1989; **153:** 929-35. doi: 10.2214/ajr.153.5.929
4. Otto R. Interventional ultrasound. *Eur Radiol* 2002; **12:** 283-7. doi: 10.1007/s00330-001-1272-3
5. Di Tommaso L, Spadaccini M, Donadon M, Personeni N, Elamin A, Aghemo A, et al. Role of liver biopsy in hepatocellular carcinoma. *World J Gastroenterol* 2019; **25:** 6041-52. doi: 10.3748/wjg.v25.i40.6041
6. Al Knawy B, Shiffman M. Percutaneous liver biopsy in clinical practice. *Liver Int* 2007; **27:** 1166-73. doi: 10.1111/j.1478-3231.2007.01592.x
7. Karamshi M. Performing a percutaneous liver biopsy in parenchymal liver diseases. *Br J Nurs* 2008; **17:** 746-52. doi: 10.12968/bjon.2008.17.12.30303
8. Lipnik AJ, Brown DB. Image-guided percutaneous abdominal mass biopsy: technical and clinical considerations. *Radiol Clin North Am* 2015; **53:** 1049-59. doi: 10.1016/j.rcl.2015.05.007
9. Ha HK, Sachs PB, Haaga JR, Abdul-Karim F. CT-guided liver biopsy: an update. *Clin Imaging* 1991; **15:** 99-104. doi: 10.1016/0899-7071(91)90155-o
10. Schullian P, Widmann G, Lang TB, Knoflach M, Bale R. Accuracy and diagnostic yield of CT-guided stereotactic liver biopsy of primary and secondary liver tumors. *Comput Aided Surg* 2011; **16:** 181-7. doi: 10.3109/10929088.2011.578367
11. Haaga JR, Reich NE, Havrilla TR, Alfidi RJ, Meaney TF. CT guided biopsy. *Cleve Clin Q* 1977; **44:** 27-33. doi: 10.3949/ccjm.44.1.27
12. Langenbach MC, Vogl TJ, von den Driesch I, Kaltenbach B, Scholtz J-E, Hammerstingl RM, et al. Analysis of Lipiodol uptake in angiography and computed tomography for the diagnosis of malignant versus benign hepatocellular nodules in cirrhotic liver. *Eur Radiol* 2019; **29:** 6539-49. doi: 10.1007/s00330-019-06297-3
13. Sainani NI, Schlett CL, Hahn PF, Gervais DA, Mueller PR, Arellano RS. Computed tomography-guided percutaneous biopsy of isoattenuating focal liver lesions. *Abdom Imaging* 2014; **39:** 633-44. doi: 10.1007/s00261-014-0089-x
14. Willatt JM, Francis IR, Novelli PM, Vellody R, Pandya A, Krishnamurthy VN. Interventional therapies for hepatocellular carcinoma. *Cancer Imaging* 2012; **12:** 79-88. doi: 10.1102/1470-7330.2012.0011
15. Sun JH, Zhou GH, Zhang YL, Nie CH, Zhou TY, Ai J, et al. Chemoembolization of liver cancer with drug-loading microsphere 50-100μm. *Oncotarget* 2017; **8:** 5392-9. doi: 10.1097/RCT.0000000000000659
16. Martino CR, Haaga JR, Bryan PJ, LiPuma JP, El Yousef SJ, Alfidi RJ. CT-guided liver biopsies: eight years' experience. Work in progress. *Radiology* 1984; **152:** 755-7. doi: 10.1148/radiology.152.3.6463257
17. Nezami N, VAN Breugel JMM, Konstantinidis M, Chapiro J, Savic LJ, Miszczuk MA, et al. Lipiodol deposition and washout in primary and metastatic liver tumors after chemoembolization. *In Vivo* 2021; **35:** 3261-70. doi: 10.21873/invivo.12621
18. Chan MKH, Lee V, Chiang CL, Lee FAS, Law G, Sin NY, et al. Lipiodol versus diaphragm in 4D-CBCT-guided stereotactic radiotherapy of hepatocellular carcinomas. *Strahlenther Onkol* 2016; **192:** 92-101. doi: 10.1007/s00066-015-0929-9
19. Ahn SJ, Lee JM, Chang W, Lee SM, Kang H-J, Yang H-K, et al. Clinical utility of real-time ultrasound-multimodality fusion guidance for percutaneous biopsy of focal liver lesions. *Eur J Radiol* 2018; **103:** 76-83. doi: 10.1016/j.ejrad.2018.04.002
20. Khalilzadeh O, Baerlocher MO, Shyn PB, Connolly BL, Devane AM, Morris CS, et al. Proposal of a new adverse event classification by the Society of Interventional Radiology Standards of Practice Committee. *J Vasc Interv Radiol* 2017; **28:** 1432-7.e3. doi: 10.1016/j.jvir.2017.06.019
21. Haage P, Piroth W, Staatz G, Adam G, Günther RW. [CT-guided percutaneous biopsies for the classification of focal liver lesions: a comparison between 14 G and 18 G puncture biopsy needles]. [German]. *Rofo* 1999; **171:** 44-8. doi: 10.1055/s-1999-9895
22. Pagani JJ. Biopsy of focal hepatic lesions. Comparison of 18 and 22 gauge needles. *Radiology* 1983; **147:** 673-5. doi: 10.1148/radiology.147.3.6844603
23. Lüning M, Schmeisser B, Wolff H, Schöpke W, Hoppe E, Meyer R. [Analysis of the results of 96 CT-guided fine needle biopsies of liver masses]. [German]. *Rofo* 1984; **141:** 267-75. doi: 10.1055/s-2008-1053132
24. Knöpfle E, Bohndorf K, Wagner T. [Does the core biopsy of solid liver lesions permit an exact histological classification? Results of a prospective study under routine clinical conditions]. [German]. *Rofo* 1997; **167:** 406-11. doi: 10.1055/s-2007-1015552
25. Gerhards A, Mildenberger P, Herber S, Lehr HA, Thelen M. [Prospective benefit and effect of lipiodol marking in hepatocellular carcinoma]. [German]. *Rofo* 2005; **177:** 1380-6. doi: 10.1055/s-2005-858565
26. Rizvi S, Camci C, Yong Y, Parker G, Shrago S, Stokes K, et al. Is post-Lipiodol CT better than *i.v.* contrast CT scan for early detection of HCC? A single liver transplant center experience. *Transplant Proc* 2006; **38:** 2993-5. doi: 10.1016/j.transproceed.2006.08.125
27. Frazer C. Imaging of hepatocellular carcinoma. *J Gastroenterol Hepatol* 1999; **14:** 750-6. doi: 10.1046/j.1440-1746.1999.01946.x
28. Schaudt A, Kriener S, Schwarz W, Wullstein C, Zangos S, Vogl T, et al. Role of transarterial chemoembolization for hepatocellular carcinoma before liver transplantation with special consideration of tumor necrosis. *Clin Transplant* 2009; **23(Suppl 21):** 61-7. doi: 10.1111/j.1399-0012.2009.01111.x
29. Choi BI, Park JH, Kim BH, Kim SH, Han MC, Kim CW. Small hepatocellular carcinoma: detection with sonography, computed tomography (CT), angiography and Lipiodol-CT. *Br J Radiol* 1989; **62:** 897-903. doi: 10.1259/0007-1285-62-742-897
30. Taourel PG, Pageaux GP, Coste V, Fabre JM, Pradel JA, Ramos J, et al. Small hepatocellular carcinoma in patients undergoing liver transplantation: detection with CT after injection of iodized oil. *Radiology* 1995; **197:** 377-80. doi: 10.1148/radiology.197.2.7480680
31. Takayasu K, Moriyama N, Muramatsu Y, Makuuchi M, Hasegawa H, Okazaki N, et al. The diagnosis of small hepatocellular carcinomas: efficacy of various imaging procedures in 100 patients. *AJR Am J Roentgenol* 1990; **155:** 49-54. doi: 10.2214/ajr.155.1.1693808
32. Spreafico C, Marchianò A, Mazzaferro V, Frigerio LF, Regalia E, Lanocita R, et al. Hepatocellular carcinoma in patients who undergo liver transplantation: sensitivity of CT with iodized oil. *Radiology* 1997; **203:** 457-60. doi: 10.1148/radiology.203.2.9114104
33. Wilsen CB, Patel MK, Douek ML, Masamed R, Dittmar KM, Lu DSK, et al. Contrast-enhanced ultrasound for abdominal image-guided procedures. *Abdom Radiol (NY)* 2023; **48:** 1438-53. doi: 10.1007/s00261-023-03804-5
34. Monfardini L, Orsi F, Caserta R, Sallemi C, Della Vigna P, Bonomo G, et al. Ultrasound and cone beam CT fusion for liver ablation: technical note. *Int J Hyperthermia* 2018; **35:** 500-4. doi: 10.1080/02656736.2018.1509237
35. Tu J, Jia Z, Ying X, Zhang D, Li S, Tian F, et al. The incidence and outcome of major complication following conventional TAE/TACE for hepatocellular carcinoma. *Medicine* 2016; **95:** e5606. doi: 10.1097/MD.0000000000005606

research article

Radiological assessment of skeletal muscle index and myosteatosis and their impact postoperative outcomes after liver transplantation

Miha Petric[1,2], Taja Jordan[3], Popuri Karteek[4], Sabina Licen[5], Blaz Trotovsek[1,2], Ales Tomazic[1,2]

[1] Department of Abdominal Surgery, University Medical Centre Ljubljana, Ljubljana, Slovenia
[2] Faculty of Medicine, University of Ljubljana, Ljubljana, Slovenia
[3] Institute of Radiology, University Medical Centre Ljubljana, Ljubljana, Slovenia
[4] Department of Computer Science, Memorial University of Newfoundland, St. John's, NL, Canada
[5] Faculty of Health Sciences, University of Primorska, Izola, Slovenia

Radiol Oncol 2023; 57(2): 168-177.

Received 12 March 2023
Accepted 16 May 2023

Correspondence to: Miha Petrič; Department of Abdominal Surgery, University Medical Centre Ljubljana, Zaloška cesta 7, SI-1000 Ljubljana, Slovenia. E mail: miha.petric@kclj.si

Disclosure: No potential conflicts of interest were disclosed.

Background. Liver transplantation offers curative treatment to patients with acute and chronic end-stage liver disease. The impact of nutritional status on postoperative outcomes after liver transplantation remains poorly understood. The present study investigated the predictive value of radiologically assessed skeletal muscle index (SMI) and myosteatosis (MI) on postoperative outcomes.

Patients and methods. Data of 138 adult patients who underwent their first orthotopic liver transplantation were retrospectively analysed. SMI and MI in computer tomography (CT) scan at the third lumbar vertebra level were calculated. Results were analyzed for the length of hospitalisation and postoperative outcomes.

Results. In 63% of male and 28.9% of female recipients, low SMI was found. High MI was found in 45(32.6%) patients. Male patients with high SMI had longer intensive care unit (ICU) stay ($P < 0.025$). Low SMI had no influence on ICU stay in female patients ($P = 0.544$), length of hospitalisation (male, $P > 0.05$; female, $P = 0.843$), postoperative complication rates (males, $P = 0.883$; females, $P = 0.113$), infection rate (males, $P = 0.293$, females, $P = 0.285$) and graft rejection (males, $P = 0.875$; females, $P = 0.135$). The presence of MI did not influence ICU stay ($P = 0.161$), hospitalization ($P = 0.771$), postoperative complication rates ($P = 0.467$), infection rate ($P = 0.173$) or graft rejection rate ($P = 0.173$).

Conclusions. In our study, changes in body composition of liver transplant recipients observed with SMI and MI had no impact on postoperative course after liver transplantation. CT body composition analysis of recipients and uniformly accepted cut-off points are crucial to producing reliable data in the future.

Key words: muscle mass; liver transplantation; myosteatosis; skeletal muscle index; GLIM score

Introduction

Since 1963 when the first liver transplantation (LT) was performed by Starzl[1], it has become a standard treatment modality for patients with acute liver failure and chronic liver disease.[2] Ninety percent 5-year survival rate and better quality of life are the two most important outcomes of LT.[2] Most liver transplant centres use the Model for End-stage Liver Disease (MELD) score for organ allocation.[3] Patients with MELD score 15 or more, patients with poor quality of life due to chronic liver disease

symptoms (diuretic-intractable ascites, variceal bleeding, pruritus, cachexia), and patients with acute liver failure are those who benefit most from LT.[3] MELD score can underestimate the severity of liver disease in specific groups of patients (acute on chronic liver disease, presence of sarcopenia, chronic kidney disease, etc.).[3] Several modifications of the MELD score have been introduced, but none offers a more reliable and accurate scoring system. Albumin-bilirubin (ALBI) score is mainly used as an objective method to assess liver function and predict postoperative complications, particularly after hepatectomy in patients with hepatocellular carcinoma (HCC).[4] Its role in determining post-LT outcomes is not yet determined. Two main objective parameters of nutritional status are sarcopenia and myosteatosis (MI). The European Working Group on Sarcopenia defines sarcopenia as the presence of low muscle mass (under the 5th percentile) and low muscle function (strength or performance) in patients with advanced age, cancer, or other diseases.[5,6] Myosteatosis is defined as the abnormal fatty transformation of skeletal muscle. It negatively affects muscle strength and is common in advanced age[7,8], diabetes[7,8], obesity[9,10], chronic[9], and malignant diseases.[11,12] Overview of the literature shows large number of different methods used for body composition assessment in patients with liver cirrhosis.[13] There is still no consensus on the best tools for each body component in patients with liver cirrhosis. Most frequently used are computed tomography (CT), bioimpedance analysis (BIA), dual-energy X-ray absorptiometry (DXA) and anthropometry.[13] Some of them BIA, DXA and body mass index (BMI)) are not applicable in patients with end-stage liver disease due to frequent water retention.[14,15] In the last decade, computed tomography with automated or semiautomated body composition analysis at the third lumbar vertebra has emerged as an objective method of defining the nutritional status of patients with chronic liver disease.[15,16] Nutritional assessment with CT is not affected by water retention or presence of ascites. Skeletal muscle volume and myosteatosis can be measured from CT images obtained as a part of routine pre-transplant evaluation.[14] Skeletal muscle mass index (SMI) is calculated as muscle mass area divided by the square of the height. The Global Leadership Initiative on Malnutrition (GLIM)[16] score was introduced as a potential nutritional assessment tool in recent years. It was shown to have good predictive value as a risk assessment tool for postoperative morbidity and mortality in patients after colorectal surgery.[17] However, its role as a predictive factor in LT is not yet established.

This study aimed to investigate feasibility of radiological assessment of a nutritional status of a patient and the predictive value of SMI and MI on postoperative complications, length of hospitalization, liver graft rejection, and mortality. We further compared the predictive value of SMI and MI with MELD, ALBI, and GLIM scores.

Patients and methods

We retrospectively analyzed 138 adult patients who had first orthotropic LT from brain dead donors between 1.1.2012 and 1.1.2020 in our institution. We excluded patients who had re-LT procedure and those whose abdominal CT scan could not be obtained from data base or received reduced size and liver graft from donation after cardiac death (DCD) donor. From the medical database, we collected recipient age, gender, body mass index, underlying liver disease, presence of ascites, hepatocellular carcinoma (HCC), and laboratory parameters (serum levels of sodium, creatinine, albumin, protein, bilirubin, and International normalized ratio (INR)). We calculated MELD and ALBI scores from laboratory parameters. Among GLIM criteria, we used chronic liver failure and end-stage liver disease as etiologic and SMI or MI as phenotypic criteria. Length of intensive care unit (ICU) stay, hospitalization, postoperative complications according to Clavien-Dindo classification[18], infections, and 90-day mortality were collected from the database of liver recipients and analyzed. Diagnosis of liver rejections was confirmed with laboratory tests and histological examination of all liver graft specimens obtained by ultrasound-guided biopsy. Acute rejection was defined with 6 points or more according to the liver allograft fibrosis score.[19]

The Slovenian National Medical Ethics Committee approved our study design (approval number 0120–230/2018–10) and waived the need to obtain informed consent from participants.

CT-body composition analysis

Abdominal CT scans were obtained from the hospital database system. In case of multiple CT scans, we used last CT scan before LT procedure. A single slice of each patient at the level of the 3rd lumbar vertebrae was selected for automatic segmentation. CT scans were analysed using the "Automated Body Composition Analyzer using Computed to-

TABLE 1. Laboratory and clinical data of patients

Variable	Min	Max	IQR	SD	95% CI	
					Lower	Upper
BMI	15	38	6	4.775	25.13	26.74
Waiting time for liver transplantation (days)	1	691	166	151.311	108.44	159.38
Sodium	121	147	6	4.701	136.09	137.68
Creatinine	41	696	46	67.082	85.91	108.49
Albumin	10	62	10	7.674	31.28	33.86
Protein	23	89	12	11.494	65.80	69.74
Bilirubin	2	687	56	107.535	51.83	88.04
INR	1	4	1	.502	1.44	1.61
MELD score	7	46	9	6.700	14.30	16.56
ALBI score	-4	0	1.13	0.802	-1.87	-1.60

ALBI score = albumin-bilirubin score; BMI = body mass index; INR = international normalized ratio; IQR = Interquartile range; MELD score = model for end-stage liver disease score

TABLE 2. Aetiology of liver disease and incidence of myosteatosis

Variable		Myosteatosis	
		no	yes
Liver failure	Alcohol-related	32	28
	Virus-related	14	3
	Other	47	14
$\chi 2$	9.717		
Degrees of freedom (Df)	2		
p	*0.008*		

mography image Segmentation" (ABACS)[20] software, which uses predefined Hounsfield units (HU) values to recognize different tissues. ABACS uses HU values from −29 to +150 HU to assess and calculate the total cross-sectional area for muscular tissue (SMA – skeletal muscle area). The L3 skeletal muscles included the psoas muscle, the lumbar muscles, the erector spinae, the transversus abdominis muscle, the internal and external oblique muscles, and the rectus abdominis. SMI was calculated using the following formula: SMI = SMA (cm^2) / height2 (m^2)[9,21] and patients were divided into a group with lower SMI (men < 52.4 cm^2/m^2, women < 38 cm^2/m^2)[9,21] and another with normal SMI. MI was determined by the medium value of HU in a skeletal muscle area. We used recently defined threshold parameters for MI in a patient with a chronic liver disease (< 33 HU in patients with a BMI ≥ 25 kg/m^2 and < 41 HU in those with a BMI < 25).[22-24] Based on previous literature findings and conclusions no adjustment for sex was made for MI.[23,24]

Statistical analysis

Data were analysed using SPSS for macOS, 26th edition. Descriptive statistics such as frequencies, percentages, mean/median, and standard deviations were used for description and summary. Because the data were not normally distributed, patient characteristics were compared between groups using the Kruskal-Wallis test and the Mann-Whitney U test. In addition, Spearman rank-order correlation and multiple linear regression were used to determine the relationship between variables and predict patient outcomes based on their characteristics and condition, as well as the chi-square independence test. A P-value ≤ 0.05 was considered statistically significant.

Results

Patients characteristics

Between 1.1.2012 and 1.1.2020, 138 patients (100 men and 38 women) met the criteria for inclusion in the study. The median age was 57.5 years (22 to 69 years). Table 1 provides general data on the population laboratory and clinical variables.

Sixty-one (61, 44.2%) patients had LT due to inherited or metabolic liver disease, 60 patients had alcoholic liver disease (43.5%), and 17 patients had virus-related liver disease (12.3%). At the time of LT, 80 (58%) patients had ascites, and 27 patients had HCC (19.4%).

Incidence of low SMI and MI

In our study group, 63% of male and 28.9% of female patients had low SMI. MI was present in 45 (32.6%) patients. We found no statistical significance between the aetiology of underlying liver disease and SMI ($P = 0.214$). The aetiology of liver disease had a statistically significant influence on the incidence of MI. Patients with alcoholic aetiology had more fatty infiltrated muscles than patients with other liver disease aetiologies ($P = 0.008$) (Table 2).

A Spearman's rank-order correlation was run to determine the relationship between the MI and BMI. There was a moderate, negative correlation between MI and BMI, which was statistically significant ($rs = -0.597$, $p < 0.000$).

Eighty patients (57.9%) had decompensated liver cirrhosis with the presence of ascites at the time of CT scan. The Mann-Whitney U test indicates that ascites significantly impacted patients' SMI. The presence of ascites correlated with low SMI ($P < 0.05$, Figure 1) and had no impact on the incidence of MI ($P = 0.244$).

Presence of HCC in patients with liver disease (27 patients, 19.6%) had no influence on SMI ($P = 0.546$) or MI ($P = 0.174$).

Influence of low SMI on hospitalization

The Mann-Whitney U test indicates that male patients with normal or high SMI (> 52.4 $cm^2/m^{2)}$ had a longer ICU length of stay ($P < 0.025$). Linear regression was calculated to predict ICU length of stay based on SMI. A significant regression equation was found ($F(1.96) = 6.823$, $P = 0.010$) (Figure 2), with R^2 of 0.066. SMI was found to significantly predict length of ICU stay ($\beta = 0.258$; 95% CI 0.026, 0.189; $P = 0.010$). The predicted length of stay equals -1.117+0.107 (SMI) days when SMI is measured in cm^2/m^2. The ICU length of stay increased by 0.107 days for each cm^2/m^2 of SMI in the male population.

A Spearman's rank-order correlation showed no difference in hospitalization time between males with low or normal SMI. Mann-Whitney U test indicates statistically significant differences between low or normal SMI ($P < 0.05$) in more extended hospitalization in male patients with normal SMI. In addition, the linear regression analysis was performed to predict the length of hospital stay based on SMI in male patients; however, no statistically significant regression equation was found ($\beta = -0.031$; 95% CI -0.656, 0.480; $P > 0.05$). In the female population, we found no statistically significant influence of SMI on ICU length of stay ($\beta = -0.123$; 95% CI -0.741, 0.463; $P = 0.544$) and hospitalization time ($\beta = 0.013$; 95% CI 0.075, 0.941; $P = 0.843$).

Influence of MI on hospitalisation

The Mann-Whitney U test indicates that there were no differences among the groups (MI and no-MI) regarding the ICU length of stay ($P = 0.161$) or hospitalization ($P = 0.771$).

Influence of SMI and MI on postoperative complications

Postoperative complications of stage 2 or more by Clavien-Dindo classification[19] were present in 79 patients (57.2%). Infection occurred in 59 patients (42.8%), most commonly as intra-abdominal infection (50.8%), respiratory tract infection (23.7%) and urosepsis (6.8%). 5 (3.6%) patients developed critical illness myopathy. Surgical intervention was needed in 38% of patients with postoperative complications.

There was no statistically significant difference in the frequency of postoperative complications between males ($P = 0.883$) and females ($P = 0.113$) with low or normal SMI. The postoperative infection rate was similar in males ($P = 0.293$) and females ($P = 0.285$) with low or normal SMI. MI did not show significant influence on postoperative complications ($P = 0.839$) and infection rate ($P = 0.703$).

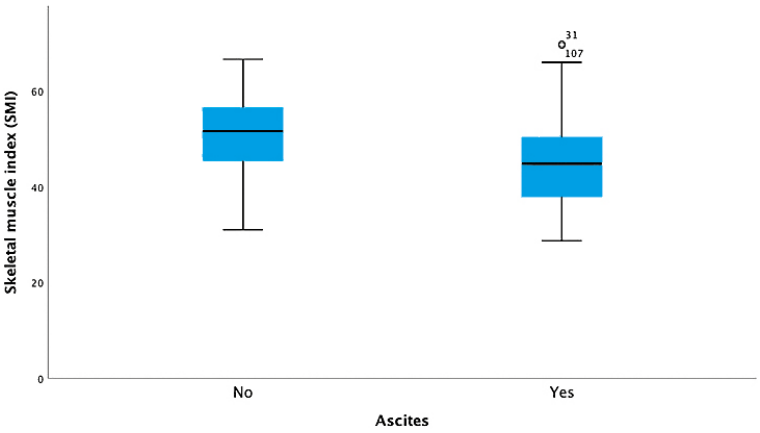

FIGURE 1. Correlation between ascites and skeletal muscle index.

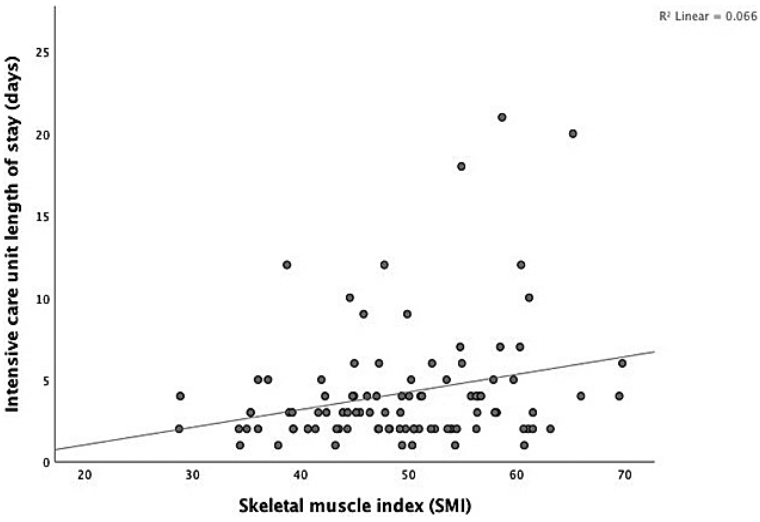

FIGURE 2. Scatter diagram showing a positive correlation between the intensive care unit length of stay (days) and skeletal muscle index.

Influence of SMI and MI on liver graft rejection

Rejection was diagnosed in 22 patients (16.1%), 20 in male and 2 in female patients. We found no statistically significant influence of SMI (males, P = 0.875; females, P = 0.135) and MI (P = 0.449) on liver graft rejection.

Influence of MELD and ALBI score on postoperative outcomes

The median MELD score was 14 (7 – 46). A Spearman's rank-order correlation was run to determine the relationship between the MELD score and ICU length of stay (days). There was a weak, positive correlation between the MELD score and ICU length of stay, which was statistically significant (r_s = 0.261, P < 0.002). There was no significant relationship between the MELD score and complication rate or length of hospitalization (P > 0.05).

There is a week, positive correlation between the ALBI score and ICU length of stay and hospitalisation time, which was statistically significant (r_s = 0.279, P < 0.001; r_s = 0.197; P = 0.022). There is no correlation between the ALBI score and postoperative complications.

GLIM score

GLIM score using skeletal muscle index as a phenotypic factor

We analyzed differences between patients who meets criteria for positive GLIM score (acute or chronic liver disease as etiological factor and skeletal muscle index as a phenotypic factor) and those with negative GLIM score regarding ICU length of stay, postoperative complications, rate of infections, graft rejections and mortality.

Based on the chi-square independence test, no association was found between the groups in postoperative complications (χ2(1) = 0.600; P = 0.438), rate of infections (χ2(1) = 0.918; P = 0.338), graft rejection (χ2(1) = 1.205; P = 0.272), and mortality (χ2(1) = 0.232; P = 0.630). In addition, there were no statistically significant differences in ICU length of stay between groups (χ2(14) = 15.125; P = 0.370), based on the Mann-Whitney test.

GLIM score using myosteatosis as a phenotypic factor

We analyzed differences between patient who meets criteria for positive GLIM score (acute or chronic liver disease as etiological factor and myosteatosis as a phenotypic factor) and those with negative GLIM score regarding ICU length of stay, postoperative complications, rate of infections, graft rejections and mortality.

Based on the chi-square independence test, there was no association between the groups in terms of postoperative complications (χ2(1) = 1.378; P = 0.242), infection rate (χ2(1) = 2.921; P = 0.089), graft rejection (χ2(1) = 0.873; P = 0.352), and mortality (χ2(1) = 0.010; P = 0.922). In addition, there were no statistically significant differences in ICU length of stay between groups (χ2(14) = 16.271; P = 0.297), based on the Mann-Whitney test.

Multiple linear regression analysis

Multiple linear regression was calculated to predict ICU length of stay on SMI and infection. A significant regression equation was found (F (2. 95) = 11.192, P < 0.000), with R^2 of 0.191. SMI was found to significantly predict length of ICU stay (β = 0.292; 95% CI 0.045, 0.199; P = 0.002). The length of ICU stays increased by 0.122 days per cm^2/m^2 SMI in male patients with infection.

Mortality

In our study group, 5 (3.6%) patients died in the first 90 days after liver transplantation. Two patients died immediately after the procedure due to irreversible haemorrhagic shock with disseminated intravascular thrombosis and abdominal organ ischemia. The cause of death in three patients was sepsis with multiorgan failure in one patient (day 66), and severe postoperative bleeding, intraabdominal infection with liver abscess, and multiorgan failure in two patients (34 and 53 days). One year survival rate was 95%. Due to the small number of patients, statistical analysis was not performed.

Discussion

Malnutrition with skeletal muscle mass loss is a frequent complication in patients with chronic or end-stage liver disease.[25] The aetiology of malnutrition is multifactorial.[23] Insufficient calorie intake (early satiety, loss of appetite, alcohol consumption, diet restriction), metabolic abnormalities, catabolic state of metabolism, and malabsorption are the main contributors to muscle loss.[25,26] It affects from 30 to 70%[27,28] of patients with end-stage liver disease and up to 80%[27] of patients with alcohol-re-

lated liver disease. Myosteatosis affects more than half of patients with chronic liver disease.[9] In our patient population, we used selected parameters for low SMI (men < 52.4 cm^2/m^2, women < 38 cm^2/m^2)[9,21] and MI (< 33 HU in patients with a BMI ≥ 25 kg/m^2 and < 41 HU in those with a BMI < 25).[22-24] These cut-off values were determined specifically for patients on LT waiting list are the most widely used in literature.[22-24] Low SMI was present in 63% of males and 28.9% of females. More than one-third of the patients (32.6%) had fatty infiltration of the skeletal muscle. Patients with alcoholic aetiology had more fat-infiltrated muscles than other aetiologies for end-stage liver disease (P < 0.008). Alterations in the metabolism of fatty acids, eating habits, and alcohol consumption probably result in fatty infiltration of skeletal muscle fibres. However, due to the small numbers of patients (3 patients) with non-alcoholic steatohepatitis (NASH) or non-alcoholic fatty liver disease (NAFLD) in our study group, we cannot properly assess the relationship between the aetiology of underlying liver disease and the degree of MI.

Several studies have shown that sarcopenia and myosteatosis are associated with a higher incidence of postoperative complications, infection rate, duration of hospitalization, and mortality in a wide range of gastrointestinal cancers, including tumours of the hepatopancreatobiliary system.[29-32] Lack of a strictly defined patient population, different methods of measurement of muscle mass and function, and the absence of uniformly accepted cut-off points for patients with chronic or end-stage liver disease are the leading causes for wide ranges of sarcopenia incidence reported in the literature.[14,21,33] Therefore, the selected cut-off points for patients with cancer are used for evaluation, which may affect the quality of results.

Sarcopenia is associated with poorer outcomes in patients with chronic liver disease on the waitlist or after LT.[34,35] Patients with end-stage liver disease and sarcopenia have shorter survival than non-sarcopenic patients (22 ± 3 *vs*. 95 ± 22-month, P < 0.001).[9,36] The main cause of death in patients with end-stage liver disease is sepsis.[37] Incidence of sepsis as a cause of death is even higher in presence of sarcopenia (36% *vs*. 16%, P < 0.001) or myosteatosis (32% *vs*. 19%, P = 0.020).[9] Lower muscle mass is also associated with a higher incidence of hepatic encephalopathy in patients with end-stage liver disease.[38,39] On the other hand, a group from USA[40] showed that sarcopenic patients had a higher tendency for pulmonary complications than the non-sarcopenic group (38% *vs*. 18%, P = 0.100); however, there was no significant difference in morbidity and mortality.

CT imaging is considered as the gold standard for body composition assessment. SMI calculated on the level of third lumbar vertebra is superior since it correlates best with the actual quantity of the muscles in the body.[41] It is not affected by ascites and is part of preoperative evaluation in patients with hepatocellular carcinoma or the complications of portal hypertension. The value of SMI as a predicting factor for postoperative morbidity and mortality is yet to be determined. However, it has been shown in several reports that it has a negative impact on postoperative outcomes. Lower values of SMI are associated with more significant postoperative mortality, higher infection risk, and postoperative complications, more extended intensive care unit stay, ventilator dependency, and higher waitlist mortality rates in patients with end-stage liver disease.[33,42,43] SMI as a predicting factor for higher mortality rate in patients with end-stage liver disease was superior to other nutritional assessment indicators, such as BMI, upper arm muscle circumference, and triceps skinfold thickness.[44] However, some other reports showed contrasting findings. Using SMI for prespecified definitions of sarcopenia had no impact on mortality or delisting from the transplant waitlist between patients with and without sarcopenia.[45] Length of hospitalization following LT, days of hospitalization during the first year post-LT, survival at one year, or overall survival was not different between sarcopenic and nonsarcopenic patients.[46] Low SMI alone was not associated with graft and patient survival (P = 0.273 and P = 0.278) after LT.[47] These conflicting results are probably due to heterogeneity of used specific cut-off points (sex, age, race) and lack of strictly defined parameters representative uniquely for patients with chronic liver disease. We found a negative correlation between BMI and SMI, probably due to high-volume ascites in the patient population This confirms findings that BMI is not suitable for body assessment in patients with end-stage liver disease. In our study, the presence of ascites was associated with significantly lower SMI (P < 0.05) in patients with end-stage liver disease but did not influence MI. There is a weak, positive correlation between SMI and ICU length of stay in male patients, which was statistically significant (rs = 0.226, P < 0.025). We speculate that the main reason is a more pronounced systemic inflammatory reaction to surgical stress in patients with preserved muscle mass. It is known that muscle mass is mandatory for the normal function of the

immune system.[48] Experience from Japan[49] shows a connection between low SMI and decreased incidence of graft rejection in living-donor liver transplantation. Analysis of our results shows no statistically significant difference in postoperative complications, rate of postoperative infection, and liver graft rejection rate between males and females with low or normal SMI ($P > 0.05$). BIA is commonly used technique in body composition analysis in every day clinical practice.[50] Its key parameters are resistance, reactance and phase angle (PA). PA is found to be associated with outcomes in different diseases and has been found to be useful for monitoring fluid changes and response to interventions.[50] The main limitation is the complexity of the determinants that requires its adjustment to the individual phenotypic diagnosis of each patient. Results can be affected by altered water and electrolyte balance, fluid retention and diuretic therapy.[50] DXA allows for the quantification of three body compartments (bone mass, fat mass, and bone fat-free mass (or lean mass)) based upon the differential tissue attenuation of X-ray photons.[51] However, it can be affected by presence of ascites.[52] Even though DXA can be modified to exclude influence of ascites or tissue oedema the correlation between the lean mass index and SMI was weaker ($\gamma = 0.29$, $p = 0.035$) and falsely high in patients with ascites before liver transplantation.[53] Main disadvantages of DXA compared to CT is inability to assess muscle mass quality (myosteatosis).[51]

Myosteatosis is a more clearly defined factor, and its influence is more uniformly established in literature.[54] However, there are many different cut off points (HU < 25 to HU < 39) reported in literature in patients with malignant disease.[55] Majority of reports uses a Martin cut-off point (< 33 HU in patients with a BMI ≥ 25 kg/m^2 and < 41 HU in those with a BMI < 25)[56] for determining presence of myosteatosis. Martin cut-off point is also recently defined threshold parameters for MI in a patient with a chronic liver disease.[22-24] It has been shown that severely ill patients with myosteatosis have a lower survival rate than those without fatty infiltration in muscles.[57] Myosteatosis negatively impacts the survival of patients with end-stage liver disease (28 ± 5 *vs*. 95 ± 22-month, $P < 0.001$)[9,36] and is associated with longer hospitalization and higher morbidity.[43] Patients with myosteatosis showed a higher mortality rate, most commonly due to respiratory and septic complication.[47] Myosteatosis had no influence on ICU length of stay ($P = 0.161$), hospitalisation ($P = 0.771$), postoperative complications ($P = 0.839$), infection rate ($P = 0.703$) and graft rejection ($P= 0.449$) in our patient population.

The nutritional status on the waitlist for LT as a possible risk factor is overlooked with the MELD score.[58] Another important limiting factor of the MELD score is using serum creatinine levels for score calculation.[3] Serum creatinine level may vary significantly and is influenced by chronic kidney disease, ascites, paracentesis, and the influence of gender and liver disease on skeletal muscle mass.[59] Variation of serum creatinine levels may affect the MELD score and underestimate the severity of liver disease.[58] Thus, several modifications of the MELD score were developed to incorporate the nutritional parameters. Body composition MELD (BC-MELD)[60] has a better predictive value for waiting list mortality than MELD score. MELD-sarcopenia score showed a positive predictive value in patients with a lower score (< 15) on the postoperative course; however, it was not useful in patients with MELD above 15.[61,62] Combining SMI in MELD in multivariate analysis (AUROC= 0.812) is significantly better than MELD alone (AUROC = 0.787) for predicting 5-year mortality ($P < 0.001$).[44] We found a weak, positive correlation between the MELD score and ICU length of stay ($rs = 0.261$, $P < 0.002$). ALBI score showed promising results in more accurate prediction of liver disease severity and mortality on waitlist compared to the Child-Pugh score; however, its predictive value was inferior to the MELD score.[63] Patients with pre-transplant ALBI grade 3 liver disease had increased mortality after LT.[64] We found a weak, positive correlation between the ALBI score and ICU length of stay and hospitalization time, which was statistically significant ($rs = 0.279$, $P < 0.001$; $rs = 0.197$; $P = 0.022$). We found no correlation between the ALBI score and postoperative complications. The GLIM score[16] was established as a potential assessment tool for evaluating patient nutritional status in recent years. Our results showed no difference between the patients who met GLIM criteria and those who did not, regarding ICU stay, length of hospitalization, postoperative complications, infection, and mortality.

We believe that nutritional status in a patient with end-stage liver disease is an essential aspect of pre-transplant workup. However, its precise role is not yet determined. LT is a complex surgical procedure influenced by numerous factors. In the early phase of LT, donor characteristics and comorbidities, quality of liver graft retrieval, liver graft quality, cold preservation duration, ischemic damage to the liver graft during static cold storage,

recipient medical conditions and comorbidities, surgical procedure, and early postoperative therapy are by our opinion the most essential factors. However, muscle mass status, muscle function and myosteatosis are crucial factors in a period of rehabilitation.[65]

Patient with cachexia or with high-risk (< 18.5 kg/m^2, Child-Pough C)[66] to lose muscle mass should be screened and involved in intensive but personalized nutritional support therapy. Nutritional requirements in end stage liver disease are 35 kcal/kg per day in non-obese patients (BMI 30 kg/m^2) and 1,2g/kg per day intake of proteins.[66] It is safe to calculate requirements based on the dry weight of a patients.[66] In presence of hepatic encephalopathy (HE), animal protein should be substituted with vegetable protein origin. Randomized control study[67] showed that substitution of animal protein with vegetable protein for a period of six months (30–35 kcal/kg/d,1.0–1.5 g/kg/d protein) improved neuropsychiatric performance in patients with minimal HE and decrease their risk of developing overt HE compared to no intervention. It is unreal to expect to gain muscle mass in cirrhotic patients, but muscle mass preservation should be focus of such nutritional interventions. There are several strategies to prevent muscle mass loss in patients with end stage liver disease. First strategy is nutritional supplementations. Patients should have frequent small meals to avoid prolong fasting period (> 6 h).[66,68,69] Enteral supplements with side branched amino acids should be administered.[66,68,69] Snacks rich in carbohydrates should be taken as a late-night snack.[66,68,69] Second, physical activity in a form of resistance and endurance exercise, is probably appropriate and beneficial.[70] Micronutrition, especially administration of fat-soluble vitamins[71] and ammonia lowering therapy[72] is also important. Role of immunonutrition in patient with end stage liver disease is not yet established.[66,73] Post-transplant screening is advised in all patients after liver transplantation.[66,73]

There are several drawbacks to our study. The two most important are the retrospective nature of data collection and the lack of functional assessment of recipients' muscles. Another factor that may influence results is the relatively small number of cases that may affect some results or may not produce statistical significance due to the complexity of the treatment and numerous factors that determine its outcome.

In conclusion radiological assessment of a patient's nutritional status at the third lumbar vertebra represents an objective and reproducible method. It should become a standard screening tool in patients with acute or chronic end-stage liver disease. Due to complexity of liver transplant procedure, liver graft and liver recipients' factors, it is difficult to established impact of a skeletal muscle index and myosteatosis on postoperative outcomes. However, nutritional interventions and physical activity should be part of the clinical pathway in patients with end-stage liver disease waiting for liver transplantation. Prospective randomized controlled studies are not possible due to ethical considerations; hence, standardization and uniformity in definitions, methods, and cut-off points are crucial to producing reliable data in the future.

Acknowledgments

Authors would like to acknowledge all participants in liver transplant programme in our institution for their dedicated work.

References

1. Starzl TE, Marchioro TL, Vonkaulla KN, Hermann G, Brittain RS, Waddell WR. Homotransplantation of the liver in humans. *Surg Gynecol Obstet* 1963; **117:** 659-76. PMID: 14100514
2. Song AT, Avelino-Silva VI, Pecora RA, Pugliese V, D'Albuquerque LA, Abdala E. Liver transplantation: fifty years of experience. *World J Gastroenterol* 2014; **20:** 5363-74. doi: 10.3748/wjg.v20.i18.5363
3. Polyak A, Kuo A, Sundaram V. Evolution of liver transplant organ allocation policy: current limitations and future directions. *World J Hepatol* 2021; **13:** 830-9. doi: 10.4254/with.v13.i8.830
4. Deng M, Ng SWY, Cheung ST, Chong CCN. Clinical application of Albumin-Bilirubin (ALBI) scores: the current status. *Surgeon* 2020; **18:** 178-86. doi: 10.1016/j.surge.2019.09.002
5. Cruz-Jentoft AJ, Bahat G, Bauer J, Boirie Y, Bruyère O, Cederholm T, et al. Sarcopenia: revised European consensus on definition and diagnosis. *Age Ageing* 2019; **48:** 16-31. doi: 10.1093/ageing/afy169
6. Reginster JY, Beaudart C, Al-Daghri N, Avouac B, Bauer J, Bere N, et al. Update on the ESCEO recommendation for the conduct of clinical trials for drugs aiming at the treatment of sarcopenia in older adults. *Aging Clin Exp Res* 2021; **33:** 3-17. doi: 10.1007/s40520-020-01663-4
7. Delmonico MJ, Harris TB, Visser M, Park SW, Conroy MB, Velasquez-Mieyer P, et al. Health, aging, and body. Longitudinal study of muscle strength, quality, and adipose tissue infiltration. *Am J Clin Nutr* 2009; **90:** 1579-85. doi: 10.3945/ajcn.2009.28047
8. Miljkovic I, Kuipers AL, Cvejkus R, Bunker CH, Patrick AL, Gordon CL, el al. Myosteatosis increases with aging and is associated with incident diabetes in African ancestry men. *Obesity* 2016; **24:** 476-82. doi: 10.1002/oby.21328
9. Montano-Loza AJ, Angulo P, Meza-Junco J, Prado CM, Sawyer MB, Beaumont C, et al. Sarcopenic obesity and myosteatosis are associated with higher mortality in patients with cirrhosis. *J Cachexia Sarcopenia Muscle* 2015; **7:** 126-35. doi: 10.1002/jcsm.12039
10. Goodpaster BH, Theriault R, Watkins SC, Kelley DE. Intramuscular lipid content is increased in obesity and decreased by weight loss. *Metabolism* 2000; **49:** 467-72. doi: 10.1016/s0026-0495(00)80010-4

11. Lee CM, Kang J. Prognostic impact of myosteatosis in patients with colorectal cancer: a systematic review and meta-analysis. *J Cachexia Sarcopenia Muscle* 2020; **11:** 1270-82. doi: 10.1002/jcsm.12575

12. Srpcic M, Jordan T, Popuri K, Sok M. Sarcopenia and myosteatosis at presentation adversely affect survival after esophagectomy for esophageal cancer. *Radiol Oncol* 2020; **54:** 237-46. doi: 10.2478/raon-2020-0016

13. Espinosa-Flores AJ, Guzman-Ortiz E, Melendez-Mier G, Ternovoy SK, Bueno-Hernandez N, Roldan-Valadez E. A scoping review of the methods used in patients with liver cirrhosis to assess body composition and their nutritional findings. [Ahead of print]. *Eur J Clin Nutr* 2023. doi:10.1038/s41430-023-01287-7

14. Lee CM, Kang BK, Kim M. Radiologic definition of sarcopenia in chronic liver disease. *Life (Basel)* 2021; **11:** 86. doi: 10.3390/life11020086

15. Kjønigsen LJ, Harneshaug M, Fløtten AM, Karterud LK, Petterson K, Skjolde G, et al. Reproducibility of semiautomated body composition segmentation of abdominal computed tomography: a multiobserver study. *Eur Radiol Exp* 2019; **3:** 42. doi: 10.1186/s41747-019-0122-5

16. Jensen GL, Cederholm T, Correia MITD, Gonzalez MC, Fukushima R, Higashiguchi T, et al. GLIM criteria for the diagnosis of malnutrition: a consensus report from the global clinical nutrition community. *JPEN J Parenter Enteral Nutr* 2019; **43:** 32-40. doi: 10.1002/jpen.1440

17. Song HN, Wang WB, Luo X, Huang DD, Ruan XJ, Xing CG, et al. Effect of GLIM-defined malnutrition on postoperative clinical outcomes in patients with colorectal cancer. *Jpn J Clin Oncol* 2022; **52:** 466-74. doi: 10.1093/jjco/hyab215.

18. Dindo D, Demartines N, Clavien PA. Classification of surgical complications: a new proposal with evaluation in a cohort of 6336 patients and results of a survey. *Ann Surg* 2004; **240:** 205-13. doi: 10.1097/01.sla.0000133083.54934.ae

19. Venturi C, Sempoux C, Bueno J, Ferreres Pinas JC, Bourdeaux C, Abarca-Quinones J, et al. Novel histologic scoring system for long-term allograft fibrosis after liver transplantation in children. *Am J Transplant* 2012; **12:** 2986-96. doi: 10.1111/j.1600-6143.2012.04210.x

20. Popuri K, Cobzas D, Esfandiari N, Baracos V, Jagersand M. Body composition assessment in axial CT images using FEM-based automatic segmentation of skeletal muscle. *IEEE Trans Med Imaging* 2016; **35:** 512-20. doi: 10.1109/TMI.2015.2479252

21. van Vugt JL, Levolger S, de Bruin RW, van Rosmalen J, Metselaar HJ, IJzermans JN. Systematic review and meta-analysis of the impact of computed tomography-assessed skeletal muscle mass on outcome in patients awaiting or undergoing liver transplantation. *Am J Transplant* 2016; **16:** 2277-92. doi: 10.1111/ajt.13732

22. Ebadi M, Tsien C, Bhanji RA, Dunichand-Hoedl AR, Rider E, Motamedrad M, et al. Myosteatosis in cirrhosis: a review of diagnosis, pathophysiological mechanisms and potential interventions. *Cells* 2022; **11:** 1216. doi: 10.3390/cells11071216

23. Eslamparast T, Montano-Loza AJ, Raman M, Tandon P. Sarcopenic obesity in cirrhosis – the confluence of 2 prognostic titans. *Liver Int* 2018; **38:** 1706-17. doi: 10.1111/liv.13876

24. Czigany Z, Kramp W, Bednarsch J, van der Kroft G, Boecker J, Strnad P, et al. Myosteatosis to predict inferior perioperative outcome in patients undergoing orthotopic liver transplantation. *Am J Transplant* 2020; **20:** 493-503. doi: 10.1111/ajt.15577

25. Dasarathy S, Merli M. Sarcopenia from mechanism to diagnosis and treatment in liver disease. *J Hepatol* 2016; **65:** 1232-44. doi: 10.1016/j.jhep.2016.07.040

26. Ebadi M, Bhanji RA, Mazurak VC, Montano-Loza AJ. Sarcopenia in cirrhosis: from pathogenesis to interventions. J *Gastroenterol* 2019; **54:** 845-59. doi:10.1007/s00535-019-01605-6

27. Montano-Loza AJ. Skeletal muscle abnormalities and outcomes after liver transplantation. *Liver Transpl* 2014; **20:** 1293-95. doi: 10.1002/lt.23995

28. Kim HY, Jang JW. Sarcopenia in the prognosis of cirrhosis: going beyond the MELD score. *World J Gastroenterol* 2015; **21:** 7637-47. doi: 10.3748/wjg.v21.i25.7637

29. Levolger S, van Vugt JLA, de Bruin RWF, IJzermans JNM. Systematic review of sarcopenia in patients operated on for gastrointestinal and hepatopancreatobiliary malignancies. *Br J Surg* 2015, **102:** 1448-58. doi: 10.1002/bjs.9893

30. Cao Q, Xiong Y, Zhong Z, Ye Q. Computed tomography-assessed sarcopenia indexes predict major complications following surgery for hepatopancreatobiliary malignancy: a meta-analysis. *Ann Nutr Metab* 2019; **74:** 24-34. doi: 10.1159/000494887

31. Kaibori M, Ishizaki M, Iida H, Matsui K, Sakaguchi T, Inoue K, et al. Effect of intramuscular adipose tissue content on prognosis in patients undergoing hepatocellular carcinoma resection. *J Gastrointest Surg* 2015; **19:** 1315-23. doi: 10.1007/s11605-015-2838-8

32. Ooi PH, Hager A, Mazurak VC, Dajani K, Bhargava R, Gilmour SM, et al. Sarcopenia in chronic liver disease: impact on outcomes. *Liver Transpl* 2019; **25:** 1422-38. doi: 10.1002/lt.25591

33. Weerink LBM, van der Hoorn A, van Leeuwen BL, de Bock GH. Low skeletal muscle mass and postoperative morbidity in surgical oncology: a systematic review and meta-analysis. *J Cachexia Sarcopenia Muscle* 2020; **11:** 636-49. doi: 10.1002/jcsm.12529

34. Hsu CS, Kao JH. Sarcopenia and chronic liver diseases. *Expert Rev Gastroenterol Hepatol* 2018; **12:** 1229-44. doi: 10.1080/17474124.2018.1534586

35. Pinto Dos Santos D, Kloeckner R, Koch S, Hoppe-Lotichius M, Zöller D, Toenges G, et al. Sarcopenia as prognostic factor for survival after orthotopic liver transplantation. *Eur J Gastroenterol Hepatol* 2020; **32:** 626-34. doi: 10.1097/MEG.0000000000001552

36. Montano-Loza AJ, Meza-Junco J, Prado CM, Lieffers JR, Baracos VE, Bain VG, et al. Muscle wasting is associated with mortality in patients with cirrhosis. *Clin Gastroenterol Hepatol* 2012; **10:** 166-73, 173.e1. doi: 10.1016/j.cgh.2011.08.028

37. Lucidi C, Lattanzi B, Di Gregorio V, Incicco S, D'Ambrosio D, Venditti M, et al. A low muscle mass increases mortality in compensated cirrhotic patients with sepsis. *Liver Int* 2018; **38:** 851-7. doi: 10.1111/liv.13691

38. Chang KV, Chen JD, Wu WT, Huang KC, Lin HY, Han DS. Is sarcopenia associated with hepatic encephalopathy in liver cirrhosis? A systematic review and meta-analysis. *J Formos Med Assoc* 2019; **118:** 833-42. doi: 10.1016/j.jfma.2018.09.011

39. Lattanzi B, D'Ambrosio D, Merli M. Hepatic encephalopathy and sarcopenia: two faces of the same metabolic alteration. *J Clin Exp Hepatol* 2019; **9:** 125-13. doi: 10.1016/j.jceh.2018.04.007

40. Dhaliwal A, Larson D, Hiat M, Muinov LM, Harrison WL, Sayles H, et al. Impact of sarcopenia on mortality in patients undergoing liver re-transplantation. *World J Hepatol* 2020; **12:** 807-15. doi: 10.4254/wjh.v12.i10.807

41. Lee CM, Kang BK, Kim M. Radiologic definition of sarcopenia in chronic liver disease. *Life* 2021; **11:** 86. doi: 10.3390/life11020086

42. Meeks AC, Madill J. Sarcopenia in liver transplantation: a review. *Clin Nutr ESPEN* 2017; **22:** 76-80. doi: 10.1016/j.clnesp.2017.08.005

43. van Vugt JL, Levolger S, de Bruin RW, van Rosmalen J, Metselaar HJ, IJzermans JN. Systematic review and meta-analysis of the impact of computed tomography-assessed skeletal muscle mass on outcome in patients awaiting or undergoing liver transplantation. *Am J Transplant* 2016; **16:** 2277-92. doi: 10.1111/ajt.13732

44. Yao J, Zhou X, Yuan L, Niu LY, Zhang A, Shi H, et al. Prognostic value of the third lumbar skeletal muscle mass index in patients with liver cirrhosis and ascites. *Clin Nutr* 2020; **39:** 1908-13. doi: 10.1016/j.clnu.2019.08.006

45. Kappus MR, Wegermann K, Bozdogan E, Patel YA, Janas G, Shropshire E, et al. Use of skeletal muscle index as a predictor of wait-list mortality in patients with end-stage liver disease. *Liver Transpl* 2020; **26:** 1090-9. doi: 10.1002/lt.25802

46. Aby ES, Lee E, Saggi SS, Viramontes MR, Grotts JF, Agopian VG, et al. Pretransplant sarcopenia in patients with NASH cirrhosis does not impact rehospitalization or mortality. *J Clin Gastroenterol* 2019; **53:** 680-5. doi: 10.1097/MCG.0000000000001109

47. Czigany Z, Kramp W, Lurje I, Miller H, Bednarsch J, Lang SA, et al. The role of recipient myosteatosis in graft and patient survival after deceased donor liver transplantation. *J Cachexia Sarcopenia Muscle* 2021; **12:** 358-67. doi: 10.1002/jcsm.12669

48. Nelke C, Dziewas R, Minnerup J, Meuth SG, Ruck T. Skeletal muscle as potential central link between sarcopenia and immune senescence. *EBioMedicine* 2019; **49:** 381-8. doi: 10.1016/j.ebiom.2019.10.034

49. Wakabayashi T, Shinoda M, Obara H, Kitago M, Yagi H, Abe Y, et al. Decreased incidence of acute cellular rejection in low-muscle-mass recipients after living-donor liver transplantation. *Transplant Proc* 2018; **50:** 3626-34. doi: 10.1016/j.transproceed.2018.06.028

50. Bellido D, García-García C, Talluri A, Lukaski HC, García-Almeida JM. Future lines of research on phase angle: strengths and limitations. *Rev Endocr Metab Disord* 2023; **24:** 563-83. doi: 10.1007/s11154-023-09803-7

51. Lee CM, Kang BK, Kim M. Radiologic definition of sarcopenia in chronic liver disease. *Life* 2021; **11:** 86. doi: 10.3390/life11020086

52. Kallwitz ER. Sarcopenia and liver transplant: the relevance of too little muscle mass. *World J Gastroenterol* 2015; **21:** 10982-93. doi: 10.3748/wjg.v21.i39.10982

53. Lindqvist C, Brismar TB, Majeed A, Wahlin S. Assessment of muscle mass depletion in chronic liver disease: dual-energy x-ray absorptiometry compared with computed tomography. *Nutrition* 2019; **61:** 93-8. doi: 10.1016/j.nut.2018.10.031

54. Shenvi SD, Taber DJ, Hardie AD, Botstein JO, McGillicuddy JW. Assessment of magnetic resonance imaging derived fat fraction as a sensitive and reliable predictor of myosteatosis in liver transplant recipients. *HPB (Oxford)* 2020; **22:** 102-8. doi: 10.1016/j.hpb.2019.06.006

55. Ahn H, Kim DW, Ko Y, Ha J, Shin YB, Lee J, et al. Updated systematic review and meta-analysis on diagnostic issues and the prognostic impact of myosteatosis: a new paradigm beyond sarcopenia. *Ageing Res Rev* 2021; **70:** 101398. doi: 10.1016/j.arr.2021.101398

56. Martin L, Birdsell L, Macdonald N, Reiman T, Clandinin MT, McCargar LJ, et al. Cancer cachexia in the age of obesity: skeletal muscle depletion is a powerful prognostic factor, independent of body mass index. *J Clin Oncol* 2013; **31:**1539-47. doi: 10.1200/JCO.2012.45.2722

57. Loosen SH, Schulze-Hagen M, Püngel T, Bündgens L, Wirtz T, Kather JN, et al. Skeletal muscle composition predicts outcome in critically Ill patients. *Crit Care Explor* 2020; **2:** e0171. doi: 10.1097/CCE.0000000000000171

58. Kim HY, Jang JW. Sarcopenia in the prognosis of cirrhosis: going beyond the MELD score. *World J Gastroenterol* 2015; **21:** 7637-47. doi: 10.3748/wjg.v21.i25.7637

59. Francoz C, Prié D, Abdelrazek W, Moreau R, Mandot A, Belghiti J, et al. Inaccuracies of creatinine and creatinine-based equations in candidates for liver transplantation with low creatinine: impact on the model for end-stage liver disease score. *Liver Transpl* 2010; **16:** 1169-77. doi: 10.1002/lt.22128

60. Hamaguchi Y, Kaido T, Okumura S, Kobayashi A, Shirai H, Yao S, et al. Including body composition in MELD scores improves mortality prediction among patients awaiting liver transplantation. *Clin Nutr* 2020; **39:** 1885-92. doi: 10.1016/j.clnu.2019.08.012

61. Montano-Loza AJ, Duarte-Rojo A, Meza-Junco J, Baracos VE, Sawyer MB, Pang JX, et al. Inclusion of sarcopenia within MELD (MELD-Sarcopenia) and the prediction of mortality in patients with cirrhosis. *Clin Transl Gastroenterol* 2015; **6:** e102. doi: 10.1038/ctg.2015.31

62. van Vugt JLA, Alferink LJM, Buettner S, Gaspersz MP, Bot D, Darwish Murad S, et al. A model including sarcopenia surpasses the MELD score in predicting waiting list mortality in cirrhotic liver transplant candidates: a competing risk analysis in a national cohort. *J Hepatol* 2018; **68:** 707-14. doi: 10.1016/j.jhep.2017.11.030

63. Chedid MF, Picon RV, Chedid AD. ALBI and PALBI: novel scores for outcome prediction of cirrhotic outpatients awaiting liver transplantation. *Ann Hepatol* 2018; **17:** 906-7. doi: 10.5604/01.3001.0012.7190

64. Bernardi N, Chedid MF, Grezzana-Filho TJM, Chedid AD, Pinto MA, Leipnitz I, et al. Pre-transplant ALBI grade 3 is associated with increased mortality after liver transplantation. *Dig Dis Sci* 2019**; 64:** 1695-704. doi: 10.1007/s10620-019-5456-6

65. Miarka M, Gibiński K, Janik MK, Główczyńska R, Zając K, Pacho R, et al. Sarcopenia-the impact on physical capacity of liver transplant patients. *Life* 2021; **11:** 740. doi: 10.3390/life11080740.

66. European Association for the Study of the Liver. EASL Clinical Practice Guidelines on nutrition in chronic liver disease. *J Hepatol* 2019; **70:** 172-93. doi: 10.1016/j.jhep.2018.06.024

67. Maharshi S, Sharma BC, Sachdeva S, Srivastava S, Sharma P. Efficacy of nutritional therapy for patients with cirrhosis and minimal hepatic encephalopathy in a randomized trial. *Clin Gastroenterol Hepatol* 2016; **14:** 454-60. e453. doi: 10.1016/j.cgh.2015.09.028

68. Ebadi M, Bhanji RA, Mazurak VC, Montano-Loza AJ. Sarcopenia in cirrhosis: from pathogenesis to interventions. *J Gastroenterol* 2019; **54:** 845-59. doi: 10.1007/s00535-019-01605-6

69. Dasarathy S, Merli M. Sarcopenia from mechanism to diagnosis and treatment in liver disease. *J Hepatol* 2016; **65:** 1232-44. doi: 10.1016/j.jhep.2016.07.040

70. Berzigotti A, Albillos A, Villanueva C, Genesca J, Ardevol A, Augustin S, et al. Effects of an intensive lifestyle intervention program on portal hypertension in patients with cirrhosis and obesity: the SportDiet study. *Hepatology* 2017; **65:** 1293-305. doi: 10.1002/hep.28992

71. Stokes CS, Volmer DA, Grunhage F, Lammert F. Vitamin D in chronic liver disease. *Liver Int* 2013; **33:** 338-52. doi: 10.1111/liv.12106

72. Miarka M, Gibiński K, Janik MK, Główczyńska R, Zając K, Pacho R, et al. Sarcopenia-the Impact on physical capacity of liver transplant patients. *Life* 2021**; 11:** 740. doi: 10.3390/life11080740

73. Lei Q, Wang X, Zheng H, Bi J, Tan S, Li N. Peri-operative immunonutrition in patients undergoing liver transplantation: a meta-analysis of randomized controlled trials. *Asia Pac J Clin Nutr* 2015; **24:** 583-90. doi: 10.6133/apjcn.2015.24.4.20.

research article

ADC values as a biomarker of fetal brain maturation

Lucija Kobal[1], Katarina Surlan Popovic[2], Jernej Avsenik[2], Tina Vipotnik Vesnaver[2]

[1] Faculty of Medicine, University of Ljubljana, Ljubljana, Slovenia
[2] Clinical Institute of Radiology, University Medical Centre Ljubljana, Ljubljana, Slovenia

Radiol Oncol 2023; 57(2): 178-183.

Received 3 February 2023
Accepted 17 April 2023

Correspondence to: Dr. Tina Vipotnik Vesnaver, Institute of Radiology, University Medical Centre Ljubljana, Zaloška 7, SI-1000 Ljubljana, Slovenija. E-mail: tina.vipotnikvesnaver@kclj.si

Disclosure: No potential conflicts of interest were disclosed.

Background. During the period of fetal development, myelination plays a key role and follows specific time and spatial sequences. The water content in the brain is inversely proportional to myelination – the more myelinated the brain, the lower the water content in it. The diffusion of water molecules can be quantitatively assessed using the apparent diffusion coefficient (ADC). We were interested in whether, by determining the ADC values, we could quantitatively evaluate the development of the fetal brain.

Patients and methods. The study included 42 fetuses with gestational age 25 to 35 weeks. We manually selected 13 regions on diffusion-weighted images. Statistically significant differences between ADC values were checked using one-way analysis of variance and Tukey's post hoc test. The relationship between the ADC values and the gestational age of the fetuses was then assessed using linear regression.

Results. The average gestational age of the fetuses was 29.8 ± 2.4 weeks. ADC values in the thalami, pons and cerebellum differed significantly among each other and from the ADC values in other brain regions. In the thalami, pons and cerebellum, linear regression showed a significant decrease in ADC values with increasing gestational age.

Conclusions. ADC values change with the increasing gestational age of the fetus and differ among different brain regions. In the pons, cerebellum and thalami, the ADC coefficient could be used as a biomarker of fetal brain maturation since ADC values decrease linearly with increasing gestational age.

Key words: myelination; fetal brain maturation; ADC; biomarker; diffusion-weighted imaging; diffusion

Introduction

Human brain development is a complex process that begins in the third gestational week and continues well after birth, even into adulthood.[1] In our study, we were interested in the process of myelination and how it can affect apparent diffusion coefficient (ADC) values.

Myelination is the final stage in the development of the white matter of the brain. It begins in the second half of pregnancy, after the proliferation and maturation of oligodendrocyte cells. It also has a characteristic course, from caudal to rostral regions of the brain, from the center outwards, and from dorsal to ventral regions of the brain.[2,3] As early as around the 20th week of gestation, microscopic amounts of myelin can be observed, especially in the medulla oblongata and pons. The brainstem is completely myelinated at 29 weeks.[4] Between the 37th and 40th gestational week, mature myelin is present in the cerebellum and the internal capsule.[4,5] Sensory pathways are myelinated earlier than motor pathways, and occipital areas are myelinated earlier than parietal, temporal and frontal areas. Myelination of the brain also takes place in the postnatal period – it is completed only after the age of 20 when the areas of the corpus callosum and prefrontal brain become fully myelinated.[6-9]

Knowing the exact course of myelination is crucial for detecting pathological changes that affect myelination. In premature infants, hypomyelination may be a predictive factor for motor and cognitive impairments. Myelination can also be affected by many genetic and autoimmune diseases and infections.[10-12]

As the brain matures, the water content changes over time. The amount of water in the brain is inversely proportional to myelination - the more myelinated the brain, the less water it contains. The decrease in water content can be attributed to the accumulation of lipids and proteins and changes in the electrolytic composition of tissues. The reduction in the proportion of water continues even after birth. In addition to the water content, the movement of water molecules in the brain is also affected by the number of cells and the amount of myelin, both of which limit the movement of molecules.[13-17]

With the development of MRI, especially with the advance of diffusion-weighted magnetic resonance imaging (DWI), an opportunity has appeared for the non-invasive assessment of myelination in fetuses. Furthermore, the diffusion of water molecules can now be quantitatively evaluated using the ADC values.

DWI is an extremely useful technique for detecting hyperacute hypoxic-ischemic changes, it can be helpful in other disease processes that affect the movement of water molecules in tissues, *e.g.*, abscesses, tumours etc. and it can also be used to monitor the normal development of the fetal brain.[18-23] This technique is already a part of the standard protocol in fetal MR imaging to diagnose anomalies of the central nervous system but, despite previous studies that have addressed this issue, it is still not completely clear whether a quantitative evaluation of fetal brain development using ADC values can be used in clinical practice. We do not yet have reference ADC values that would allow us to compare healthy fetuses with fetuses suspected of developing anomalies of the central nervous system.[24-30] Research is therefore increasingly focused on studying ADC values in different areas of the fetal brain.

In our study, we observed how ADC values change during the process of fetal brain maturation. We postulated that the values would depend on the gestational age of the fetus and also on the areas of the brain. The determined ADC values could serve as reference values in daily clinical work. They would be useful in assessing the level of fetal brain maturity and early detection of pathological changes.

The purpose of our research was to determine how ADC values change with the gestational age of the fetus. We were interested in how ADC values differ among different brain areas. We also wanted to discover whether the ADC could be used as a biomarker of fetal brain maturation.

Our hypotheses were:

1. ADC is a useful biomarker of fetal brain maturation.
2. ADC values depend on the age of the fetus and the area of the brain.

Patients and methods

The retrospective study was conducted at the Clinical Institute of Radiology of the University Medical Center Ljubljana. The National Medical Ethics Committee of the Republic of Slovenia judged that the research was ethically acceptable and gave consent for its implementation (No. 0120-56/2022/3).

Patients

We initially selected 59 fetuses that had had an MRI done between 18. 1. 2015 and 4. 3. 2021. Of these, the MRI images of 17 fetuses were excluded since their DWI images had artefacts due to fetal movement. We therefore performed the measurements on MRI images of 42 fetuses. We included fetuses that have been referred for MRI due to suspicious US changes in the central nervous system (CNS), face or neck (wider cisterna magna, suspected agenesis of the corpus callosum, ranula etc.) but in which we did not confirm CNS anomalies with MRI. All included pregnant women underwent amniocentesis, which excluded chromosomal abnormalities and infections. After birth, no signs indicating abnormal development of the central nervous system were found in our group. The gestational age of the fetuses was from 25 to 35 weeks (mean 29.8 ± 2.4 weeks).

Magnetic resonance imaging

Examinations were performed on a Siemens Aera 1.5 T MR device. The pregnant women did not eat or drink for four hours before the examination and, during the examination, they were in a supine or left decubitus position. They did not receive any medication before the procedure. An abdominal coil with a small, 24 cm field of view and a 192 ×

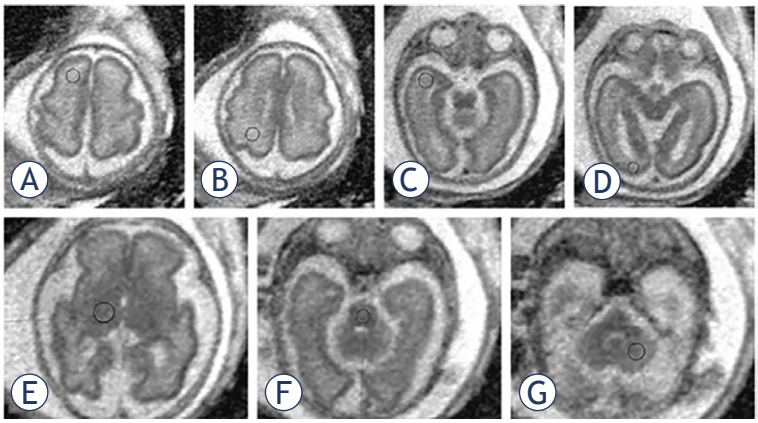

FIGURE 1. Position of the ROI in the brain of a fetus with a gestational age of 29 weeks. Region of interests (ROIs) were placed in each brain region bilaterally. Markings are visible only on one side. **(A)** Frontal white matter, **(B)** parietal white matter, **(C)** temporal white matter, **(D)** occipital white matter, **(E)** thalamus, **(F)** pons, **(G)** hemisphere of the cerebellum.

TABLE 1. Intraclass correlation coefficient (ICC) for different regions of interest (ROIs)

ROI	ICC
FWM	0.91
PWM	0.90
TWM	0.75
OWM	0.78
Thalami	0.85
Pons	0.81
Cerebellum	0.92

FWM = frontal white matter; OWM = occipital white matter; PWM = parietal white matter; TWM = temporal white matter

160 matrix was used. A 3D scout sequence was performed to assess the fetal position. Scout sequence is an ultrafast T2-weighted sequence, with slice thicknesses of 6–8 mm, gaps of 1–2 mm, and a large field of view. Our protocol consisted of ultrafast T2-weighted sequences in three planes (axial, coronary, sagittal) with slice thicknesses of 3 and 4 mm and intermediate intervals of 0.3 mm, T1- and T2-gradient sequences in the axial plane (the former with slice thickness 4.5 mm and intermediate intervals 0.5 mm, the latter with slice thickness 3 mm and intermediate intervals 0.3 mm) and DWI-sequence in the axial plane (slice thickness 5 mm with intermediate intervals 2 mm). Diffusion was measured in three directions at values of b = 0 s/mm^2, b = 500 s/mm^2, and b = 1000 s/mm^2.

ADC value measurements

ADC measurements were performed by two researchers (L.K., T.V.V.). On ADC maps, we manually selected 13 areas (region of interest, ROI) using a Syngo. via program (Siemens Medical Solutions USA, Inc. ©2022): bilaterally in the frontal white matter (FWM), parietal white matter (PWM), temporal white matter (TWM) and occipital white matter (OWM), bilaterally in the white matter of the cerebellum, in both thalami and the central part of the pons. The surface area of the ROI was adapted to the age of the fetus and the anatomical area, with values between 15 and 65 mm^2.

Statistical data analysis

Statistical data analysis and graph production were performed using IBM SPSS Statistics (IBM SPSS Statistics for Windows, version 25.0; IBM Corp., Armonk, NY). Interrater reliability was assessed using the intraclass correlation coefficient (ICC) with a two-way mixed model for the average of the measurements.

ICC values below 0.5 indicate low, between 0.5 and 0.75 moderate, between 0.75 and 0.9 good, and above 0.9 excellent reliability. Since the ICC was 0.75 or higher in all measured brain areas, we averaged the measurements of the two researchers. Statistically significant differences between ADC values for different areas of the brain were checked using one-way analysis of variance (ANOVA). Statistically significant differences between ADC values in individual groups were searched for with Tukey's post hoc test. Before the one-way analysis of variance, we checked the homogeneity of the variances with Levene's test, whereby we rejected the null hypothesis that the variances are homogeneous or homoscedastic. The association between the ADC values of the brain regions and the gestational age of the fetuses was then evaluated using linear regression. Before the statistical data analysis, we determined the p-value 0.05 as the threshold.

Results

ICC values by individual brain areas are shown in Table 1.

The average ADC values for different ROIs are shown in Figure 2. Using one-way analysis of variance, we found that there was a statistically significant difference between the ADC values for dif-

ferent brain areas. The ADC values in the thalami, pons and cerebellum differed significantly from each other and from the ADC values in all other brain areas. There were no significant differences between ADC values in FWM, PWM, TWM and OWM.

In the thalami, pons and cerebellum, linear regression showed a statistically significant decrease in ADC values with increasing gestational age (Figure 3). ADC values also decreased with increasing gestational age in PWM and OWM, but the results were not statistically significant. ADC values increased in FWM and TWM, but the increase in values in these areas was also not statistically significant.

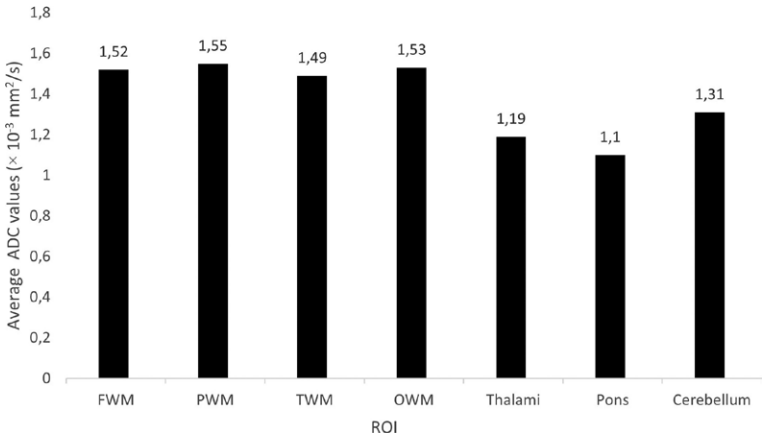

FIGURE 2. Average apparent diffusion coefficient (ADC) values for different regions of interest (ROIs).

Discussion

Our study confirmed that the average ADC values in fetuses differ among different brain areas. As shown in Figure 2, the lowest values were measured in the pons, thalami and cerebellum, and the highest in the FWM, PWM, TWM and OWM. These differences can be attributed to the characteristic course of myelination and the number of neurons in individual areas. The amount of neurons in the thalami is greater than in the white matter, so the diffusion of water is more limited. Since myelination proceeds from the caudal to the rostral regions of the brain, from the central regions to the periphery, and from the dorsal to the ventral regions, the pons, thalami and cerebellum are myelinated earlier than the white matter of the cerebral hemispheres, where the myelination process still takes place in the postnatal period. ADC values in fetuses, therefore cannot be compared with values in newborns and children, nor with values in preterm infants of the same gestational age, since large changes in the amount and distribution of water in the brain occur after birth.[2,3]

ADC values in the pons, thalami and cerebellum were much lower than in the white matter of the cerebral hemispheres, which is consistent with previous research. The average values in these areas were comparable with previous studies, while the average ADC values for FWM, PWM, TWM and OWM were slightly lower in our study. The largest deviations can be seen for the FWM area, where in our research we measured an average ADC value of 1.52 × 10^{-3} mm²/s. Han *et al.* (1.8 × 10^{-3} mm²/s), Schneider *et al.* (1.8 × 10^{-3} mm²/s), Hoffmann *et al.* (1.8 × 10^{-3} mm²/s) and Righini *et al.* (2.9 × 10^{-3} mm²/s) all recorded higher values.[25,27-31] These differences could be attributed to the slightly lower average age of the fetuses in our study and the possible non-linear changing of ADC values, as described below.

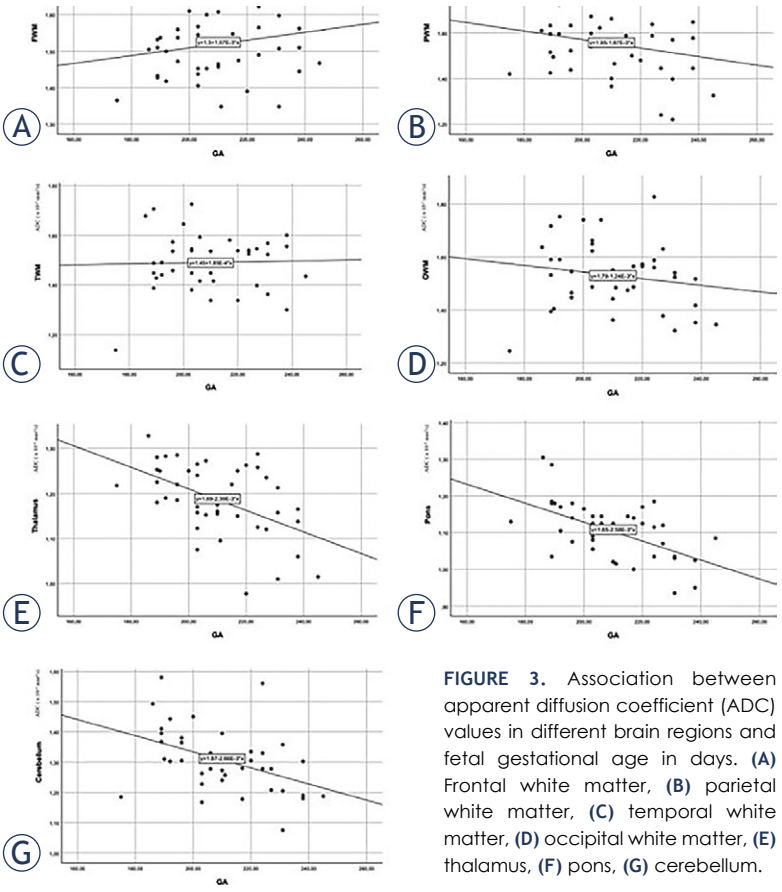

FIGURE 3. Association between apparent diffusion coefficient (ADC) values in different brain regions and fetal gestational age in days. **(A)** Frontal white matter, **(B)** parietal white matter, **(C)** temporal white matter, **(D)** occipital white matter, **(E)** thalamus, **(F)** pons, **(G)** cerebellum.

OWM is known to be myelinated earlier than PWM, TWM and FWM.[8] We were unable to confirm this with our research. The results of our research showed that ADC values did not differ

statistically significantly among these areas. We attribute these results to the fact that the occipital part of the brain in fetuses is thinner than in the rest of the cerebral hemispheres. The ROIs were therefore placed closer to the cerebrospinal fluid than in other areas, which may have resulted in partial coverage of the cerebrospinal fluid signal in the ROI. As a result, measurements may be affected by averaging the values of cerebrospinal fluid and brain parenchyma. This may also explain why the ICCs between the researchers differed predominantly in the areas of OWM and TWM, where the cerebral mantle is also thinner.

In the thalami, pons and cerebellum, linear regression showed a statistically significant decrease in ADC values with increasing gestational age (Figure 3). ADC values also decreased with increasing gestational age in PWM and OWM, but the results were not statistically significant. In FWM and TWM, ADC values increased in our study, but the increase in values was not statistically significant in these areas either. The FWM is the last of all brain areas to be myelinated, the amount of water there being the highest for the longest time, which could be the reason for the measured values in our research.

All the studies published so far have confirmed the decline in ADC values with increasing gestational age in the areas of the cerebellum, thalami and pons.[25,27-31] The results indicate that in these areas of the brain, the amount of water decreases with age, which affects the reduction of ADC values. In our study, ADC values also declined most rapidly in the cerebellum, pons and thalami, which suggests earlier maturation of these regions and is consistent with other studies.

Differences among studies occurred in other brain areas. A decrease in ADC values in PWM and OWM was demonstrated by Han *et al.*, Hoffmann *et al.* and Righini *et al.*, while Cannie *et al.* detected an increase in ADC values in OWM.[27-30] Similar to our study, some other researchers have also detected an increase in ADC values with gestational age in FWM.[48,50,53] Schneider *et al*, on the other hand, measured increasing ADC values in FWM, PWM, TWM and OWM until the 30th gestational week, but thereafter the ADC values began to decrease.[31]

The results of Schneider *et al.* are consistent with the course of fetal brain development. During development, the brain consists of several layers - above the ventricular layer, there is an intermediate layer, a subplate and a cortical layer. Wide extracellular spaces are present in the intermediate layer and subplate, which allow nerve cells to migrate. In these spaces, water molecules can move freely, which could explain the rise in ADC values. Schneider *et al.* explained the repeated decline in ADC value by a combination of different factors that begin to dominate after the 30th week: the subplate and the intermediate layer slowly disappear, the total amount of water decreases and, at the same time, the number of lipids and macromolecules in the intracellular spaces increases. We therefore allow the possibility that the change in ADC values in FWM, PWM, TWM and OWM with increasing gestational age is not linear, but may be better explained by more complex models, for example using a quadratic polynomial curve, which means that the values initially increase and then decrease.[31]

The multilayered structure of the brain is visible on T2-weighted sequences in fetuses of the gestational age of 20–28 weeks but, with increasing gestational age, the boundaries between the layers are blurred. Due to the poor image resolution of the ADC maps, it is very difficult to distinguish the layers from each other, even in younger fetuses. When manually placing the ROIs, due to the poor resolution on the ADC maps we may also capture areas of the subplate, which later develop into the cerebral cortex, and not the white matter, which could affect the results of the measurements.

The downside of our research was the relatively small number of subjects. A disadvantage is also the probability of measurement errors due to the movement of the fetus during the examination, which was reduced by preparing the mothers for the MRI examination and eliminating poor-quality images. In fetal MRI, measurements are also affected by the small size of the structures, which may result in the capture of the cerebrospinal fluid or subplate in selected cases. ROI drawing may also be challenging due to the poor resolution of the brain layers on the ADC maps.

Another thing to consider before comparing results from different studies is variability in measured ADC values due to the use of different MRI equipment and sequence selections.

Conclusions

We conclude that ADC values are a reliable indicator of brain maturation in the areas of the pons, cerebellum and thalami. The results of our research are concordant with previous research, which has shown that the values in these areas decrease linearly with increasing gestational age. We also

confirmed that the ADC values are higher in the FWM, PWM, TWM, and OWM regions than in the pons, cerebellum and thalami. However, it is still unknown how ADC values in FWM, PWM, TWM and OWM change with gestational age, since results vary among studies. Further research is needed to define more precisely the variation of ADC values in these areas, which would help us to set reference values. Nevertheless, we confirmed our second hypothesis that ADC values in different brain areas differ from each other and also change over time.

References

1. Stiles J, Jernigan TL. The basics of brain development. *Neuropsychol Rev* 2010; **20:** 327-48. doi: 10.1007/s11065-010-9148-4
2. Gilles FH. Myelination in the neonatal brain. *Hum Pathol* 1976; **7:** 244-8. doi: 10.1016/s0046-8177(76)80035-4
3. Keene MF. Some observations on myelination in the human central nervous system. *J Anat* 1931; **66:** 1-13. PMID: 17104349
4. Huppi PS, Inder TE. Magnetic resonance techniques in the evaluation of the perinatal brain: recent advances and future directions. *Semin Neonatol* 2001; **6:** 195-210. doi: 10.1053/siny.2001.0039
5. Baumann N, Pham-Dinh D. Biology of oligodendrocyte and myelin in the mammalian central nervous system. *Physiol Rev* 2001; **81:** 871-927. doi: 10.1152/physrev.2001.81.2.871
6. Kinney HC, Brody BA, Kloman AS, Gilles FH. Sequence of central nervous system myelination in human infancy: II. patterns of myelination in autopsied infants. *J Neuropathol Exp Neurol* 1988; **47:** 217-34. doi: 10.1097/00005072-198805000-00003
7. Joseph VJ. *Neurology of the newborn.* Philadelphia: Saunders/Elsevier; 2008.
8. Deoni SCL, Mercure E, Blasi A, Gasston D, Thomson A, Johnson M, et al. Mapping infant brain myelination with magnetic resonance imaging. *J Neurosci* 2011; **31:** 784-91. doi: 10.1523/JNEUROSCI.2106-10.2011
9. Bregant T. [Development, growth and maturation of the brain]. [Slovenian]. *Psihološka obzorja* 2012; **21:** 51-60. doi: 10.20419/2012.21.363
10. Woodward LJ, Anderson PJ, Austin NC, Howard K, Inder TE. Neonatal MRI to predict neurodevelopmental outcomes in preterm infants. *N Engl J Med* 2006; **355:** 685-94. doi: 10.1056/NEJMoa053792
11. Valk J, van der Knaap MS. The significance of MRI in myelin disorders. *MAGMA 2* 1994; 191-201. doi: 10.1007/BF01705240
12. Duncan ID, Radcliff AB. Inherited and acquired disorders of myelin: the underlying myelin pathology. *Exp Neurol* 2016; **283:** 452-75. doi: 10.1016/j.expneurol.2016.04.002
13. Matsumae M, Kurita D, Atsumi H, Haida M, Sato O, Tsugane R. Sequential changes in MR water proton relaxation time detect the process of rat brain myelination during maturation. *Mech Ageing Dev* 2001; **122:** 1281-91. doi: 10.1016/s0047-6374(01)00265-2
14. McArdle CB, Richardson CJ, Nicholas DA, Mirfakhraee M, Hayden CK, Amparo EK. Developmental features of the neonatal brain: MR imaging. Part I. Gray-white matter differentiation and myelination. *Radiology* 1987; **162:** 223-9. doi: 10.1148/radiology.162.1.3786767
15. Lorenzo AV, Keasley W, Conner S, Black P, Dorval V. Change in the water and electrolyte pattern of the brain and of the intracranial pressure during development in rabbits. *Z Kinderchir* 1981; **34:** 410-15. doi: 10.1055/s-2008-1063384
16. Donaldson HH. On the percentage of water in the brain and in the spinal cord of the albino rat. *J Comp Neurol Psychol* 2004; **20:** 119-44. doi: 10.1002/cne.920200203
17. Agrawal HC, Davis MJ, Himwich WA. Developmental changes in mouse brain: weight, water content and free amino acids. *J Neurochem* 1968; **15:** 917-23. doi: 10.1111/j.1471-4159.1968.tb11633.x
18. Cowan FM, Pennock JM, Hanrahan JD, Manji KP, Edwards AD. Early detection of cerebral infarction and hypoxic isehemic encephalopathy in neonates using diffusion-weighted magnetic resonance imaging. *Neuropediatr* 1994; **25:** 172-5. doi: 10.1055/s-2008-1073018
19. Johnson AJ, Lee BCP, Lin W. Echoplanar diffusion-weighted imaging in neonates and infants with suspected hypoxic-ishemic injury: correlation with patient outcome. *AJR Am J Roenrgenol* 1999; **172:** 219-26. doi: 10.2214/ajr.172.1.9888771
20. Robertson RL, Ben-Sira L, Barnes PD, Mulkern RV, Robson CD, Maier SE. MR Line-scan diffusion-weighted imaging of term neonates with perinatal brain ischemia. *AJNR Am J Neuroradiol* 1999; **20:** 1658-70. PMID: 10543637
21. Janet SS, Richard LR, Tzika AA, du Plessis AJ, Volpe JJ. Time course of changes in diffusion-weighted magnetic resonance imaging in a case of neonatal encephalopathy with defined onset and duration of hypoxic-ishemic insult. *Pediatrics* 2015; **108:** 1211-14. doi: 10.1542/peds.108.5.1211
22. Toft PB, Leth H, Peitersen B, Lou HC, Thomsen C. The apparent diffusion coefficient of water in gray and white matter of the infant brain. *J Comput Assist Tomogr* 1996; **20:** 1006-11. doi: 10.1097/00004728-199611000-00029
23. Forbes KPN, Pipe JG, Bird CR. Changes in brain water diffusion during the 1st year of life. *Radiol* 2002; **222:** 405-9. doi: 10.1148/radiol.2222010179
24. Ouyang M, Dubois J, Yu Q, Mukherjee P, Huang H. Delineation of early brain development from fetuses to infants with diffusion MRI and beyond. *Neuroimage* 2019; **185:** 836-50. doi: 10.1016/j.neuroimage.2018.04.017
25. Schneider MM, Berman JI, Baumer FM, Glass HC, Jeng S, Jeremy RJ, et al. Normative apparent diffusion coefficient values in the developing fetal brain. *Am J Neuroradiol* 2009; **30:** 1799-803. doi: 10.3174/ajnr.A1661
26. Di Trani MG, Manganaro L, Antonelli A, Guerreri M, De Feo R, Catalano C, et al. Apparent diffusion coefficient assessment of brain development in normal fetuses and ventriculomegaly. *Front Physics* 2019; **7:** 1-9. doi: 10.3389/fphy.2019.00160
27. Cannie M, de Keyzer F, Meersschaert J, Jani J, Lewi L, Deprest J, et al. A diffusion-weighted template for gestational age-related apparent diffusion coefficient values in the developing fetal brain. *Ultrasound Ob Gyn* 2007; **30:** 318-24. doi: 0.1002/uog.4078
28. Righini A, Bianchini E, Parazzini C, Gementi P, Ramenghi L, Baldoli C, et al. Apparent diffusion coefficient determination in normal fetal brain: a prenatal MR imaging study. *Am J Neuroradiol* 2003; **24:** 799-804.
29. Han R, Huang L, Sun Z, Zhang D, Chen X, Yang X, et al. Assessment of apparent diffusion coefficient of normal fetal brain development from gestational age week 24 up to term age: a preliminary study. *Fetal Diagnosis Therapy* 2014; **37:** 102-7. doi: 10.1159/000363650
30. Hoffmann C, Weisz B, Lipitz S, Yaniv G, Katorza E, Bergmann D, et al. Regional apparent diffusion coefficient values in 3rd trimester fetal brain. *Neuroradiol* 2014; **56:** 561-7. doi: 10.1007/s00234-014-1359-6
31. Schneider JF, Confort-Gouny S, le Fur Y, Viout P, Bennathan B, Chapon F, et al. Diffusion-weighted imaging in normal fetal brain maturation. *European Radiol* 2007; **17:** 2422-9. doi: 10.1007/s00330-007-0634-x

research article

Longitudinal monitoring of Apparent Diffusion Coefficient (ADC) in patients with prostate cancer undergoing MR-guided radiotherapy on an MR-Linac at 1.5 T: a prospective feasibility study

Haidara Almansour[1], Fritz Schick[2], Marcel Nachbar[3,4], Saif Afat[1], Victor Fritz[2], Daniela Thorwarth[4,5], Daniel Zips[3,5,6], Felix Bertram[6], Arndt-Christian Müller[6,7], Konstantin Nikolaou[1,8], Ahmed E Othman[1,9], Daniel Wegener[6]

[1] Department of Diagnostic and Interventional Radiology, Eberhard-Karls University, Tuebingen, Germany
[2] Section for Experimental Radiology, Department of Radiology, Eberhard-Karls University, Tuebingen, Germany
[3] Department of Radiation Oncology, Charité University Medicine Berlin, Berlin, Germany
[4] Section for Biomedical Physics, Department of Radiation Oncology, Eberhard-Karls University, Tuebingen, Germany
[5] German Cancer Consortium (DKTK), Partner Site Tuebingen and German Cancer Research Center (DKFZ), Heidelberg, Germany
[6] Department of Radiation Oncology, Eberhard-Karls University, Tuebingen, Germany
[7] Department of Radiation Oncology, RKH Klinikum Ludwigsburg, Ludwigsburg, Germany
[8] Cluster of Excellence iFIT (EXC 2180) "Image Guided and Functionally Instructed Tumor Therapies", University of Tuebingen, Tuebingen, Germany
[9] Department of Neuroradiology, University Medical Center Mainz, Mainz, Germany

Radiol Oncol 2023; 57(2): 184-190.

Received 20 January 2023
Accepted 30 March 2023

Correspondence to: Ahmed E. Othman, Professor and Consultant Radiologist, Department of Neuroradiology, University Medical Center Mainz, 55131 Mainz, Germany. E-mail: ahmed.e.othman@googlemail.com

Disclosure: The authors` institution operates a Linac Unity (Elekta, Sweden). The Department of Radiation Oncology Tübingen receives financial and technical support by Elekta, Philips, Siemens, Dr. Sennewald Medizintechnik, Kaiku Health, TheraPanacea, PTW and ITV in the context of research cooperation's. The aforementioned entities had no role in the design of the study; in the collection, analyses, or interpretation of data; in the writing of the manuscript, or in the decision to publish the results. The authors declare no further conflicts of interest.

Background. Hybrid MRI linear accelerators (MR-Linac) might enable individualized online adaptation of radiotherapy using quantitative MRI sequences as diffusion-weighted imaging (DWI). The purpose of this study was to investigate the dynamics of lesion apparent diffusion coefficient (ADC) in patients with prostate cancer undergoing MR-guided radiation therapy (MRgRT) on a 1.5T MR-Linac. The ADC values at a diagnostic 3T MRI scanner were used as the reference standard.

Patients and and methods. In this prospective single-center study, patients with biopsy-confirmed prostate cancer who underwent both an MRI exam at a 3T scanner (MRI_{3T}) and an exam at a 1.5T MR-Linac (MRL) at baseline and during radiotherapy were included. Lesion ADC values were measured by a radiologist and a radiation oncologist on the slice with the largest lesion. ADC values were compared before *vs.* during radiotherapy (during the second week) on both systems via paired t-tests. Furthermore, Pearson correlation coefficient and inter-reader agreement were computed.

Results. A total of nine male patients aged 67 ± 6 years [range 60 – 67 years] were included. In seven patients, the cancerous lesion was in the peripheral zone, and in two patients the lesion was in the transition zone. Inter-reader reliability regarding lesion ADC measurement was excellent with an intraclass correlation coefficient of (ICC) > 0.90 both at baseline and during radiotherapy. Thus, the results of the first reader will be reported. In both systems, there was a

statistically significant elevation of lesion ADC during radiotherapy (mean MRL-ADC at baseline was 0.97 ± 0.18 x 10^{-3} mm^2/s vs. mean MRL-ADC during radiotherapy 1.38 ± 0.3 x 10^{-3} mm^2/s, yielding a mean lesion ADC elevation of 0.41 ± 0.20 x 10^{-3} mm^2/s, $p < 0.001$). Mean MRI_{3T}-ADC at baseline was 0.78 ± 0.165 x 10^{-3} mm^2/s vs. mean MRI_{3T}-ADC during radiotherapy 0.99 ± 0.175 x 10^{-3} mm^2/s, yielding a mean lesion ADC elevation of 0.21 ± 0.96 x 10^{-3} mm^2/s $p < 0.001$). The absolute ADC values from MRL were consistently significantly higher than those from MRI_{3T} at baseline and during radiotherapy ($p < = 0.001$). However, there was a strong positive correlation between MRL-ADC and MRI_{3T}-ADC at baseline ($r = 0.798$, $p = 0.01$) and during radiotherapy ($r = 0.863$, $p = 0.003$).

Conclusions. Lesion ADC as measured on MRL increased significantly during radiotherapy and ADC measurements of lesions on both systems showed similar dynamics. This indicates that lesion ADC as measured on the MRL may be used as a biomarker for evaluation of treatment response. In contrast, absolute ADC values as calculated by the algorithm of the manufacturer of the MRL showed systematic deviations from values obtained on a diagnostic 3T MRI system. These preliminary findings are promising but need large-scale validation. Once validated, lesion ADC on MRL might be used for real-time assessment of tumor response in patients with prostate cancer undergoing MR-guided radiation therapy.

Key words: prostate carcinoma; MRI; adaptive radiotherapy; image guidance; MR-Linac; ADC

Introduction

Radiotherapy (RT) is a curative treatment option for patients with localized prostate cancer.[1] MR-guided radiotherapy (MRgRT) enables improved soft tissue contrast and enhances accuracy of treatment planning.[2] In this context, the hybrid magnetic resonance 1.5T scanner with a linear accelerator MR-Linac (MRL) is currently being used in centers around the world to perform high-precision MRgRT with daily plan adaptations based on anatomical MR sequences.[3,4] Furthermore, functional MRI sequences such as diffusion weighted imaging (DWI) are being additionally taken into account for radiotherapy planning, as they provide valuable "real-time" functional information.[5] The apparent diffusion coefficient (ADC) of a tumor lesion has been shown to function as a biomarker for prostate cancer on diagnostic scanners.[6] MRL presents a novel opportunity to integrate ADC-values of a tumor lesion into daily plan adaptations and individualize radiotherapy.[7] A prerequisite is the clinical translatability of ADC-measurements on MRL to a "gold standard" 3T diagnostic scanner (MRI_{3T}).

In a previous study, it was demonstrated that ADC measurements of a region of interest in intraprostatic tumor lesions on MRL correlated with corresponding measurements on a diagnostic 3T MRI scanner (MRI_{3T}).[8] In that analysis, the MRIs on both scanners were performed prior to treatment initiation. However, as an initial step to evaluate, whether ADC measurements on an MRL might function as a biomarker enabling response assessment under RT, the longitudinal stability of ADC data gained on an MRL should be examined.

The purpose of this study is to longitudinally investigate the dynamics of lesion ADC in patients with prostate cancer undergoing MR-guided radiation therapy on an MR-Linac using the ADC values at a 3T MRI scanner as a reference standard.

Patients and methods

Participant sample, study design and MRI technique

All patients included in this prospective study were recruited in the M-base Pro 1.0[9] or M-base HyPro 2.0 at our institution (ClinicalTrials.gov Identifiers: NCT02724670; NCT03880851). The study was conducted according to the guidelines of the Declaration of Helsinki, and approved by the Institutional Review Board of the medical faculty of Tuebingen University (No. 022/2016BO1, 14.03.2016 and No. 920/2018BO1, 10.07.2019). Informed consent was obtained from all subjects involved in the study. All patients consented to prospectively undergo multiple MRIs on an MRL and additionally on a MRI_{3T} at several points prior to and during RT. The aforementioned studies each examine a novel MR-adaptive concept for radiotherapy of primary localized prostate cancer. Between February 2019 and October 2021, 9 patients with biopsy-confirmed prostate cancer and available MRL and MRI_{3T} data sets prior to RT and under RT were included. All patients were treated daily on a 1.5T MRL (Elekta Unity™, Philips, Stockholm, Sweden).[10] All patients were treated according to national guidelines with either 39 x 2 Gy per fraction over eight weeks (M-base 1.0 study, n = 3 patients) or 20 x 3 Gy per fraction over four weeks (M-base Hypro 2.0

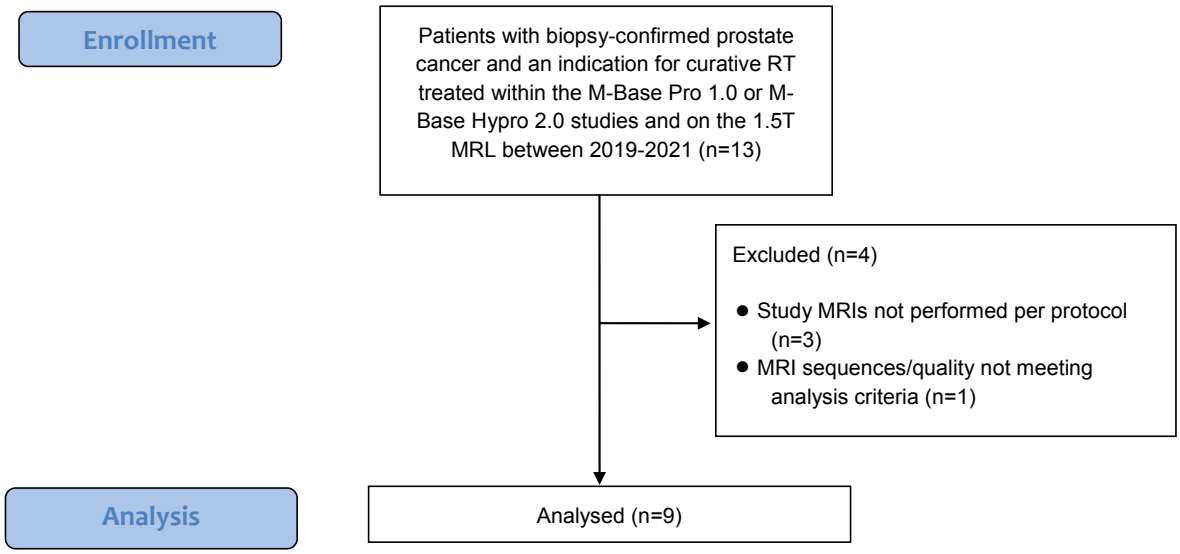

RT = radiotherapy; MRL = 1.5 T MR-Linac Unity.

FIGURE 1. Flow diagram illustrating the inclusion/ exclusion process.

study, n = 6 patients) and additional neoadjuvant androgen deprivation therapy (ADT) of six months for intermediate risk patients and 24-36 months for high risk patients.[11] The time point of the MRL and MRI_{3T} was during week 2 of RT in both treatment protocols. MRI technique, specifications and acquisition parameters of the examinations on both systems have been previously described.[8] Most study participants in this study were used in the prior publication[8], but only examinations prior to RT were analyzed. No lesion ADC dynamics during RT were reported in the previous study.[8]

Lesion ADC evaluation

The ADC maps for MRL and MRI_{3T} for each patient, prior to and during radiotherapy, were independently presented to two readers (reader 1, a board certified radiation oncologist with 8 years of experience reader 2, a radiology resident with 4 years of experience). Both readers placed an elliptic region-of-interest (ROI) within the lesions for each patient in MRL and MRI_{3T} image sets. A dedicated workstation (GE Healthcare Centricity™ PACS RA1000, Milwaukee WI, USA) was utilized for image analysis using a dedicated software (syngo.via, Siemens Healthcare, Erlangen, Germany).

Statistical analysis

Continuous variables were reported as mean and standard deviation. Paired t-tests were used for pair-wise pre- *vs*. during-treatment comparisons, as well as MRL *vs*. MRI-3T. Intraclass correlation coefficient (ICC, two-way, absolute agreement) was used to compute inter-reader agreement. An ICC of less than 0.4 signalizes poor agreement, of 0.40 to 0.59 indicates fair agreement, of 0.60 to 0.74 good agreement, and an ICC of 0.75 to 1.00 signalizes excellent agreement.[12] Pearson Correlation coefficient was used to compare lesion ADC between MRL and MRI_{3T}. Level of significance was set at 0.05. Statistical analyses were performed using SPSS (v26.0, IBM-Corp, Armonk, NY, USA).

Results

A total of nine patients were included. Figure 1 delineates the the inclusion/exclusion process.

Table 1 summarizes patients' characteristics. For each patient, the two imaging examinations prior to and during RT were successfully performed and evaluated.

The mean elapsed time between the baseline MRL exam and the MRL exam during radiotherapy was 26 days ± 14 days. The mean time difference between MRI_{3T} and MRL examinations at baseline was 1.7 days ± 1.7 days. Similarly, the mean time difference between MRI_{3T} and MRL examinations during radiotherapy was was 1.7 days ± 1.3 days.

Inter-reader reliability regarding lesion ADC measurement was excellent with ICC > 0.90 both at baseline and during radiotherapy (ICC for MRL

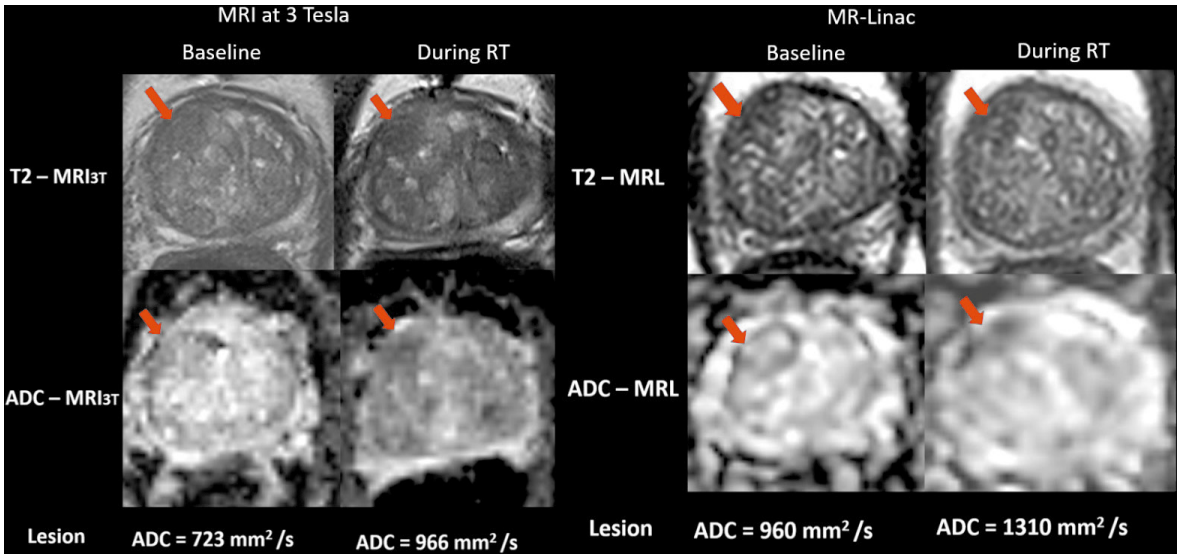

FIGURE 2. T2-weighted MR images (scan time: 2 minutes) and apparent diffusion coefficient (ADC) maps of a 66-year-old male patient with prostate cancer in the antero-apical region of the transition zone (red arrows) at baseline (left column) and during radiotherapy (right column) as recorded on MR-Linac (MRL) and on standard MRI at 3T (MRI3T). The figure shows similar dynamics of lesion ADC elevation during radiotherapy.

at baseline was 0.927 and during radiotherapy was 0.976; ICC for MRI_{3T} at baseline was 0.978 and during radiotherapy was 0.998).

For reader 1, in both systems, there was a statistically significant elevation of lesion ADC during radiotherapy (Figure 2). Mean MRL-ADC at baseline was 0.97 ± 0.18 mm^2/s *vs.* mean MRL-ADC during radiotherapy 1.38 ± 0.3 mm^2/s, yielding a mean lesion ADC elevation of 0.41 ± 0.20 mm^2/s, p <0.001. Mean MRI_{3T}-ADC at baseline was 0.78 ± 0.165 mm^2/s *vs.* mean MRI_{3T}-ADC during radiotherapy 0.99 ± 0.175 mm^2/s, yielding a mean lesion ADC elevation of 0.21 ± 0.96 mm^2/s p <0.001.

The ADC values at MRL were consistently significantly higher than MRI_{3T} at baseline and during radiotherapy (p < 0.01). However, there was a strong positive correlation between MRL-ADC and MRI_{3T}-ADC at baseline (r = 0.798, p = 0.01) and during radiotherapy (r = 0.863, p = 0.003) (Figure 3).

Similarly, for reader 2, in both systems, there was a statistically significant elevation of lesion ADC during radiotherapy (mean MRL-ADC at baseline was 1.0 ± 0.23 x 10^{-3} mm^2/s *vs.* mean MRL-ADC during radiotherapy 1.36 ± 0.30 x 10^{-3} mm^2/s, yielding a mean lesion ADC elevation of 0.36 ± 0.17 x 10^{-3} mm^2/s, p <0.001). Mean MRI_{3T}-ADC at baseline was 0.78 ± 0.17 x 10^{-3} mm2/s *vs.* mean MRI_{3T}-ADC during radiotherapy 1.0 ± 0.183 x 10^{-3} mm^2/s, yielding a mean lesion ADC elevation of 0.22 ± 0.129 x 10^{-3} mm^2/s p <0.001).

The ADC values at MRL were consistently significantly higher than MRI_{3T} at baseline and during radiotherapy (p < 0.001). However, there was a strong positive correlation between MRL-ADC and MRI_{3T}-ADC at baseline (r = 0.872, p = 0.002) and during radiotherapy (r = 0.788, p = 0.012).

Discussion

This prospective study compared lesion ADC values in patients with prostate carcinoma undergoing MR-guided radiotherapy on an MRL at 1.5 T to a diagnostic scanner at 3T. Absolute values of lesion ADC measurements differed while dynamics in the context of radiation therapy were comparable between the scanners. In both systems, there was a statistically significant elevation of lesion ADC during radiotherapy with a strong positive correlation of lesion ADC between the scanners.

ADC changes during radiotherapy

ADC changes of the intraprostatic tumor are to be expected both during radiotherapy and during ADT and the correlation between ADC and prostate cancer aggressiveness has been shown before on diagnostic scanners.[17,18] The mean ADC-values calculated in this study on both scanners are similar to values found in the literature: Tamada

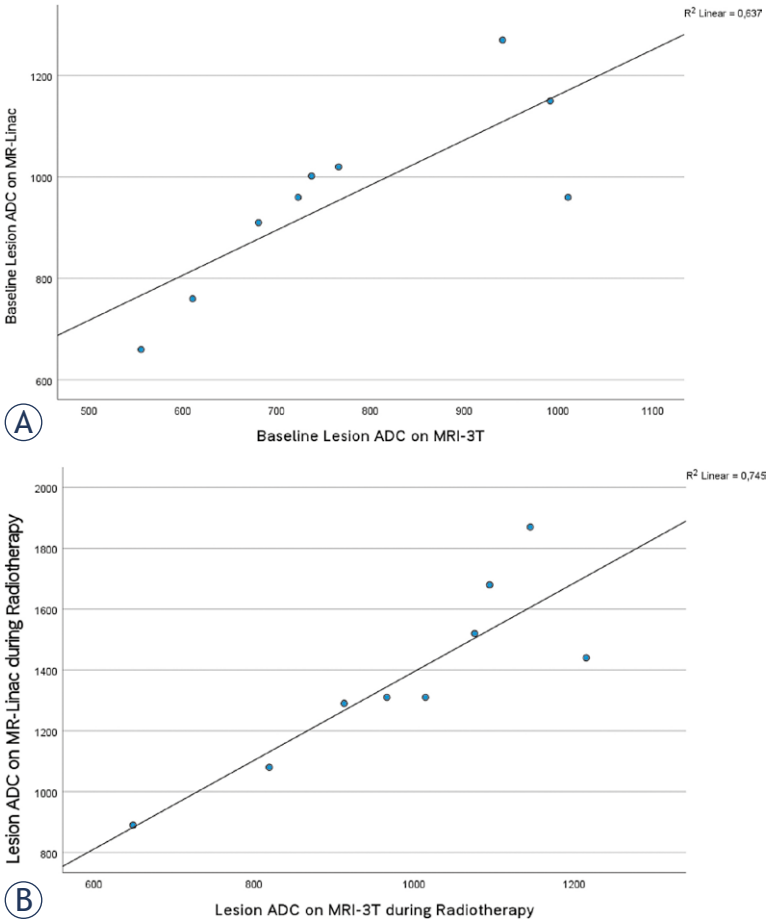

FIGURE 3. Scatter plots with a fitted line for ADC values as recorded on MR-Linac and MRI_{3T} for reader 1. **(A)** at baseline, **(B)** during radiotherapy (week 2). These plots illustrate the strong positive correlation between MRL-ADC and MRI_{3T}-ADC at both time points.

et al. reported mean ADC values of (untreated) tumor regions of 1.02 ± 0.25 x 10^{-3} mm^2/s for the peripheral zone and of 0.94 ± 0.21 x 10^{-3} mm^2/s for the transitional zone of the prostate.[13] Van Schie *et al.* reported median ADC values in the tumor scanned on a diagnostic scanner of 1.08 ± 0.39 x 10^{-3} mm^2/s (mean ± SD) prior to treatment and assessed changes of ADC prior to a hypofractionated RT and then weekly during RT in 73 patients in a similar manner as performed in our study. The group found a (non-significant) median increase of the ADC-value in the tumor of 7% for patients with concurrent ADT and a median increase of 20% for patients without ADT.[14]

ADC as biomarker for response assessment and role of MRL

Moreover, ADC values and -changes have been shown to function as biomarkers for RT response in prostate cancer patients.[6,15] Radiomics approaches seem promising in assessing response to RT, as performed by Abdollahi *et al.* prior to *vs.* after RT.[16] In all of these studies and in prostate cancer diagnostics, a 3 T MRI scanner has been established as the gold standard for mpMRI.[17] MRI_{3T} leads to optimal diagnostic images, often aided by suppression of peristalsis via intravenous application of butyl scopolamine or other agents. In contrast, on a 1.5 T MRL, the utilized sequences are optimized for fast and geometrically accurate image acquisition in an online workflow without routine administration of peristalisis suppressing medications or contrast agents. These possible limitations, in addition to technical differences of the hybrid system to diagnostic scanners[18], pose the question whether an MRL can deliver comparable functional information during RT of prostate cancer.

In principle, the hybrid system offers fertile ground for further plan adaption in prostate carcinoma patients based on mpMRT findings such as ADC values since it offers daily MR-guided plan adaptations. Treatment individualization and plan adaptation under RT are a focus of research in other tumor entities as well.[7,19,20] Longitudinal diffusion MRI on a 0.35 T hybrid system was already performed in small series for several other tumor entities with promising results (Yang *et al.*: three head and neck cancer patients and three sarcoma patients[21]; Shaverdian *et al.*: three rectal cancer patients[22]). On the 1.5 T MRL, Lawrence *et al.* report a high ADC repeatability and comparability to a diagnostic 1.5 T scanner for 59 patients with central nervous system tumors.[23] Habrich *et al.* used a test-retest approach on 11 patients with head and cancers and showed to a high repeatability of ADC measurements on the 1.5 T MRL.[24] In the context of prostate carcinoma, Habrich *et al.* also examined intravoxel incoherent motion (IVIM) and dynamic contrast enhanced (DCE) MRI changes over the course of a moderately hypofractionated RT in 20 patients, also indicating that longitudinal measurements of functional imaging parameters is feasible and could be used for response assessment in the future.[25]

However, concerning intraprostatic tumor lesions, the verification of longitudinal stability of ADC measurements on an MRL as performed in this study in a comparison to a latest generation 3 T diagnostic scanner has to the best of our knowledge not been performed yet.

In a previous study, we tested the clinical applicability based on qualitative and quantitative parameters of prostate MR images on an MRL

against a MRI_{3T} at one point of time prior to starting RT. We were able to show a promising and comparable result of T2 weighted image quality, and lesion conspicuity and we reported comparable lesion ADC measurements between MRL and MRI_{3T}.[8]

With the current work, we demonstrate longitudinal comparability and reliability between the two system during RT. This represents a necessary basis for future analyses of lesion changes over time on the MRL and confirms its potential for individualized treatment adaptations such as dose painting[26] and response assessment during treatment.

This study has limitations. Firstly, the small sample size of patients who underwent multiple prostate imaging at both devices and the fact that only one time-point during radiotherapy was used for analysis. Multiple time-points during the course of radiotherapy should be analyzed to further validate the stability and comparability of ADC measurements. However, logistic challenges hindered further validation with an MRI_{3T} at more than one time point. Secondly, treatment regimens differed in this population (either 20 x 3 Gy oder 39 x 2 Gy, additional neoadjuvant ADT in 3 patients). Thirdly, the DWI acquisition parameters did not fully conform to the published recommendations of the MR-linac consortium, which were published after we had already included the patients in our study and predefinded the technical aspects of the utilized sequences.[27]

Nonetheless, this study depicts the reality and the challenges of clinical routine and its preliminary findings could be considered novel. Indeed, further prospective studies examining mpMRI data under RT and correlating those with clinical endpoints are desirable to advance individualized radiation treatment.

In conclusion, lesion ADC as measured on MRL increased significantly during radiotherapy and lesion ADC measurements on both systems showed similar dynamics. These preliminary findings are promising but need large-scale validation. Once validated, lesion ADC on MRL might be used as a biomarker for real-time assessment of tumor response in patients with prostate cancer undergoing MR-guided radiation therapy.

Acknowledgements

This research project was partially financed through a research grant of the DFG (German Research Council, Grant MU 4603/1-1 | OT 534/3-1, Package No. 997/1). Arndt-Christian Mueller is a recipient of the IIT program (Mbase Pro 1.0 study) of the Medical Faculty of Tuebingen University (AKF 345-1-0). Haidara Almansour is a scholarship recipient of the junior clinician scientist program of the medical faculty of Tuebingen University (no. 461-0-0). The datasets used and analyzed during the current study are available from the corresponding author on reasonable request.

References

1. Mottet N, van den Bergh RCN, Briers E, van den Broeck T, Cumberbatch MG, de Santis M, et al. EAU-EANM-ESTRO-ESUR-SIOG Guidelines on Prostate Cancer-2020 Update. Part 1: screening, diagnosis, and local treatment with curative intent. *Eur Urol* 2021; **79:** 243-62. doi: 10.1016/j.eururo.2020.09.042
2. Pathmanathan AU, McNair HA, Schmidt MA, Brand DH, Delacroix L, Eccles CL, et al. Comparison of prostate delineation on multimodality imaging for MR-guided radiotherapy. *Br J Radiol* 2019; **92:** 20180948. doi: 10.1259/bjr.20180948
3. Dunlop A, Mitchell A, Tree A, Barnes H, Bower L, Chick J, et al. Daily adaptive radiotherapy for patients with prostate cancer using a high field MR-linac: initial clinical experiences and assessment of delivered doses compared to a C-arm linac. *Clin Transl Radiat Oncol* 2020; **23:** 35-42. doi: 10.1016/j.ctro.2020.04.011
4. Wegener D, Thome A, Paulsen F, Gani C, Boldt J, Butzer S, et al. First experience and prospective evaluation on feasibility and acute toxicity of online adaptive radiotherapy of the prostate bed as salvage treatment in patients with biochemically recurrent prostate cancer on a 1.5 T MR-linac. *J Clin Med* 2022; **11:** 4651. doi: 10.3390/jcm11164651
5. Grégoire V, Guckenberger M, Haustermans K, Lagendijk JJW, Ménard C, Pötter R, et al. Image-guidance in radiation therapy for better cure of cancer. *Mol Oncol* 2020; **14:** 1470-91. doi: 10.1002/1878-0261.12751
6. Decker G, Mürtz P, Gieseke J, Träber F, Block W, Sprinkart AM, et al. Intensity-modulated radiotherapy of the prostate: dynamic ADC monitoring by DWI at 3.0T. *Radiother Oncol* 2014; **113:** 115-20. doi: 10.1016/j.radonc.2014.07.016
7. Thorwarth D, Ege M, Nachbar M, Mönnich D, Gani C, Zips D, et al. Quantitative magnetic resonance imaging on hybrid magnetic resonance linear accelerators: Perspective on technical and clinical validation. *Phys Imaging Radiat Oncol* 2020; **16:** 69-73. doi: 10.1016/j.phro.2020.09.007
8. Almansour H, Afat S, Fritz V, Schick F, Nachbar M, Thorwarth D, et al. Prospective image quality and lesion assessment in the setting of MR-guided radiation therapy of prostate cancer on an MR-linac at 1.5 T: a comparison to a standard 3 T MRI. *Cancers* 2021; **13:** 1533. doi: 10.3390/cancers13071533
9. Wegener D, Zips D, Thorwarth D, Weiß J, Othman AE, Grosse U, et al. Precision of T2 TSE MRI-CT-image fusions based on gold fiducials and repetitive T2 TSE MRI-MRI-fusions for adaptive IGRT of prostate cancer by using phantom and patient data. *Acta Oncologica* 2019; **58:** 88-94. doi: 10.1080/0284186X.2018.1518594
10. Winkel D, Bol GH, Kroon PS, van Asselen B, Hackett SS, Werensteijn-Honingh AM, et al. Adaptive radiotherapy: The Elekta Unity MR-linac concept. *Clin Transl Radiat Oncol* 2019; **18:** 54-9. doi: 10.1016/j.ctro.2019.04.001
11. [*Guideline program oncology. Interdisciplinary guideline of quality S3 for early detection, diagnosis and therapy of the various stages of prostate carcinoma.*] [German]. Deutsche Krebsgesellschaft, D.K., AWMF. 2019; Long version 5.1: 345.
12. Hallgren KA. Computing inter-rater reliability for observational data: an overview and tutorial. *Tutor Quant Methods Psychol* 2012; **8:** 23-34. doi: 10.20982/tqmp.08.1.p023

13. Tamada T, Sone T, Jo Y, Toshimitsu S, Yamashita T, Yamamoto A, et al. Apparent diffusion coefficient values in peripheral and transition zones of the prostate: Comparison between normal and malignant prostatic tissues and correlation with histologic grade. *J Magn Reson Imaging* 2008; **28:** 720-6. doi: 10.1002/jmri.21503

14. van Schie MA, van Houdt PJ, Ghobadi G, Pos FJ, Walraven I, de Boer HCJ, et al. Quantitative MRI changes during weekly ultra-hypofractionated prostate cancer radiotherapy with integrated boost. *Front Oncol* 2019; **9:** 1264. doi: 10.3389/fonc.2019.01264

15. Wu S, Jiao Y, Zhang Y, Ren X, Li P, Yu Q, et al. Imaging-based individualized response prediction of carbon ion radiotherapy for prostate cancer patients. *Cancer Manag Res* 2019; **11:** 9121-31. doi: 10.2147/CMAR.S214020

16. Abdollahi H, Mofid B, Shiri I, Razzaghdoust A, Saadipoor A, Mahdavi A, et al. Machine learning-based radiomic models to predict intensity-modulated radiation therapy response, Gleason score and stage in prostate cancer. *Radiol Med* 2019; **124:** 555-67. doi: 10.1007/s11547-018-0966-4

17. Weinreb JC, Barentsz JO, Choyke PL, Cornud F, Haider MA, Macura KJ, et al. PI-RADS prostate imaging – reporting and data system: 2015, version 2. *Eur Urol* 2016; **69:** 16-40. doi: 10.1016/j.eururo.2015.08.052

18. Thorwarth D, Low DA. Technical challenges of real-time adaptive MR-guided radiotherapy. *Front Oncol* 2021; **11:** 634507. doi: 10.3389/fonc.2021.634507

19. Boeke S, Mönnich D, van Timmeren JE, Balermpas P. MR-guided radiotherapy for head and neck cancer: current developments, perspectives, and challenges. *Front Oncol* 2021; **11:** 616156. doi: 10.3389/fonc.2021.616156

20. Boldrini L, Intven M, Bassetti M, Valentini V, Gani C. MR-guided radiotherapy for rectal cancer: current perspective on organ preservation. *Front Oncol* 2021; **11:** 619852. doi: 10.3389/fonc.2021.619852

21. Yang Y, Cao M, Sheng K, Gao Y, Chen A, Kamrava M, et al. Longitudinal diffusion MRI for treatment response assessment: preliminary experience using an MRI-guided tri-cobalt 60 radiotherapy system. *Med Phys* 2016; **43:** 1369-73. doi: 10.1118/1.4942381

22. Shaverdian N, Yang Y, Hu P, Hart S, Sheng K, Lamb J, et al. Feasibility evaluation of diffusion-weighted imaging using an integrated MRI-radiotherapy system for response assessment to neoadjuvant therapy in rectal cancer. *Br J Radiol* 2017; **90:** 20160739. doi: 10.1259/bjr.20160739

23. Lawrence LSP, Chan RW, Chen H, Keller B, Stewart J, Ruschin M, et al. Accuracy and precision of apparent diffusion coefficient measurements on a 1.5 T MR-Linac in central nervous system tumour patients. *Radiother Oncol* 2021; **164:** 155-62. doi: 10.1016/j.radonc.2021.09.020

24. Habrich J, Boeke S, Nachbar M, Nikolaou K, Schick F, Gani C, et al. Repeatability of diffusion-weighted magnetic resonance imaging in head and neck cancer at a 1.5 T MR-Linac. *Radiother Oncol* 2022; **174:** 141-8. doi: 10.1016/j.radonc.2022.07.020

25. Habrich J, Boeke S, Nachbar M, Nikolaou K, Schick F, Gani C, et al. Longitudinal correlations between intravoxel incoherent motion (IVIM) and dynamic contrast-enhanced (DCE) MRI during radiotherapy in prostate cancer patients. *Front Oncol* 2022; **12:** 897130. doi: 10.3389/fonc.2022.897130

26. van der Heide UA, Houweling AC, Groenendaal G, Beets-Tan RG, Lambin P. Functional MRI for radiotherapy dose painting. *Magn Reson Imaging* 2012; **30:** 1216-23. doi: 10.1016/j.mri.2012.04.010

27. Kooreman ES, van Houdt PJ, Keesman R, Pos FJ, van Pelt VWJ, Nowee ME, et al. ADC measurements on the Unity MR-linac - A recommendation on behalf of the Elekta Unity MR-linac consortium. *Radiother Oncol* 2020; **153:** 106-13. doi: 10.1016/j.radonc.2020.09.046

research article

Awake craniotomy for operative treatment of brain gliomas – experience from University Medical Centre Ljubljana

Tilen Zele[1], Tomaz Velnar[1], Blaz Koritnik[2], Roman Bosnjak[1], Jasmina Markovic-Bozic[3]

[1] Department of Neurosurgery, University Medical Centre Ljubljana, Ljubljana, Slovenia
[2] Department of Neurophysiology, University Medical Centre Ljubljana, Ljubljana, Slovenia
[3] Department of Anaesthesiology and Intensive Care, University Medical Centre Ljubljana, Department of Anesthesiology and Reanimation Faculty of Medicine, University of Ljubljana, Ljubljana, Slovenia

Radiol Oncol 2023; 57(2): 191-200.

Received 09 10 2022
Accepted 02 11 2022

Correspondence to: Prof. assist. Jasmina Markovič-Božič, M.D., Ph.D.; Department of Anaesthesiology and Intensive Care, University Medical Centre Ljubljana, Zaloška cesta 2, SI-Ljubljana, Slovenia. E-mail: jasmina.markovic1@kclj.si.

Disclosure: No potential conflicts of interest were disclosed.

Background. Awake craniotomy is a neurosurgical technique that allows neurophysiological testing with patient cooperation during the resection of brain tumour in regional anaesthesia. This allows identification of vital functional (i.e. eloquent) brain areas during surgery and avoidance of their injury. The aim of the study was to present clinical experience with awake craniotomy for the treatment of gliomas at the University Medical Centre Ljubljana from 2015 to 2019.

Patients and methods. Awake craniotomy was considered in patients with a gliomas near or within the language brain areas, in all cases of insular lesions and selected patients with lesions near or within primary motor brain cortex. Each patient was assessed before and after surgery.

Results. During the 5-year period, 24 awake craniotomies were performed (18 male and 6 female patients; average age 41). The patient's cooperation, discomfort and perceived pain assessed during the awake craniotomy were in majority of the cases excellent, slight, and moderate, respectively. After surgery, mild neurological worsening was observed in 13% (3/24) of patients. Gross total resection, in cases of malignant gliomas, was feasible in 60% (6/10) and in cases of low-grade gliomas in 29% (4/14). The surgery did not have important negative impact on functional status or quality of life as assessed by Karnofsky score and Short-Form 36 health survey, respectively ($p > 0.05$).

Conclusions. The results suggest that awake craniotomy for treatment of gliomas is feasible and safe neurosurgical technique. The proper selection of patients, preoperative preparation with planning, and cooperation of medical team members are necessary for best treatment outcome.

Key words: awake craniotomy; surgery of gliomas; intraoperative neurophysiological testing; primary brain tumours; clinical experiences

Introduction

Gliomas are one of the most common primary brain tumours and represent 75% of all malignant primary brain tumours in adults.[1] The primary treatment consists of surgical resection, followed by radiotherapy and chemotherapy. Despite the modern treatment, gliomas remain incurable lesions.

Glial tumours are classically divided into low-grade gliomas (LGG, WHO grade II) and malignant gliomas (WHO grades III and IV).[1,2] LGGs are a heterogeneous group, histologically classified into low-grade astrocytoma, oligodendroglioma or mixed oligoastrocytoma. The average age at presentation is 35 years, and they typically occur in the frontal lobes. In 50 to 80% of patients, the first symptom is an epileptic seizure.[2] On T1-weighted magnetic

resonance images (MRI), LGGs appear as hypo- to isointense lesions, whereas on T2-weighted images they are hyperintensive.[2] Although LGGs are more indolent than their high-grade counterparts, they inevitably progress towards malignancy. This malignant transformation is present in 13 to 86% of cases in LGG recurrences.[2,3] With treatment, the median overall survival time is about six to eight years.[3,4] On the other hand, malignant gliomas are more sinister. They are histologically classified into anaplastic astrocytomas (AA, WHO grade III) and glioblastomas (GBM, WHO grade IV).[1] For AAs, the average age at presentation is 40, and for GBMs 53 years. They typically present with progressive headaches and neurological deficits. On MRI high grade gliomas usually appear as contrast enhancing lesions with central necrosis and surrounding brain oedema. They have a predilection for cerebral hemispheres. With treatment, the median overall survival time for AAs is two to five years and for GBMs less than two years.[5,6]

For patients with gliomas, overall survival was demonstrated to be related to the histological and molecular subtype of the tumour, the patient's age, the presence of neurological deficit, the Karnofsky Performance Status (KPS) score, and the size of the tumour at presentation.[7,8] In addition, several studies have also clearly demonstrated that the extent of resection (EOR) during surgery has a significant impact on survival.[9,10] Namely, in cases of LGGs the resection of more than 90% and less than 90% of the tumour resulted in an 8-year overall survival rate of 91% and 60%, respectively.[9] Similarly, in cases of AAs, gross total resection (GTR) and subtotal resection (STR) resulted in a median survival of 58 and 34 months, respectively.[10] And in cases of GBM, GTR and STR resulted in a median survival of 13 and 8 months, respectively.[10]

Gliomas are infiltrative lesions and can arise within or near the functionally the most important brain regions, such as language areas, motor cortex, etc. Over extensive resection in those vital (i.e. eloquent) areas, that directly control function, would inevitably result in permanent neurological deficit and significant postoperative morbidity, with a negative impact on the patient's quality of life. In addition, such significant postoperative neurological worsening also independently reduces the overall survival of those patients.[7,8,10,11] Therefore, the goal of the surgical treatment of gliomas is, in addition to maximal, also safe resection - i.e. removal of as much tumour as possible, without causing neurological deficits ("maximal safe resection").

To achieve the goal of maximal safe resection, the intraoperative neurophysiological testing and monitoring is mandatory to identify the precise location of individual brain functions and thus eloquent brain areas during surgery. In cases in which neurophysiological techniques cannot adequately assess brain functions under general anaesthesia and the cooperation of the patient during intraoperative testing is needed an awake craniotomy should be used.[12,13] Awake craniotomy is a neurosurgical technique that allows removal of brain tumour under regional anaesthesia while the patient is awake. It thus allows cooperation of the patient during intraoperative testing and monitoring in order to avoid the injury of eloquent brain areas. For awake craniotomy a variety of anaesthetic methods are used: local anaesthesia (scalp block, infiltration of dura), monitored anaesthesia care (awake-awake-awake technique; scalp block and sedation) or asleep-awake-asleep technique (general anaesthesia and awakening during testing).

In the present article, we presented our protocol, technique and experience with awake craniotomy for glioma surgery at the Department of Neurosurgery, Ljubljana University Medical Centre, from years 2015 to 2019.

Patients and methods

Patients

We included all consecutive patients who underwent surgery by awake craniotomy due to gliomas from years 2015 to 2019 at the Department of Neurosurgery of Ljubljana University Medical Centre. The study was approved by the National Medical Ethics Committee of the Republic of Slovenia. All the procedures were performed in accordance with the Declaration of Helsinki. Awake craniotomy was considered in selected patients with the following preoperative morphological images: I) a tumour near or within the language brain areas (Broca's and Wernicke's areas, angular gyrus), II) all cases of insular tumours and III) selected patients with lesions near or within primary motor cortex or corticospinal tract.

Each patient was assessed preoperatively by the anaesthesiologist, neuropsychologist, and neurosurgeon. A collective decision was made whether the patient was suitable for awake craniotomy. The inclusion criteria encompassed a good clinical, physical, and affective condition. The contraindications for awake craniotomy were a

non-compliant patient (e.g., due to old age or unfavourable psychosocial factors), the potential for breathing problems during surgery (e.g., known sleep apnoea, significant obesity), and important preoperative dysphasia (i.e., the patient names less than 80% of objects presented at four- second intervals). Informed consent was obtained from all study participants.

Preoperative planning and evaluation

The preoperative planning consisted of the acquisition and analysis of preoperative morphological and functional images, the selection of surgical approach and trajectory to the lesion, and the planning of the extent of the resection. MRI was performed using a 3-Tesla clinical scanner (Siemens Trio, Siemens). The diagnostic imaging included T1- and T2-weighted sequences. For 3D-imaging, we used a post-contrast T1-weighted 3D-fast spoiled gradient recalled (FSPGR) sequence (a series of 124 images, 1.4 mm thick with a matrix up to 512x512 of 240mm field of view). A fMRI was used to define the primary motor and speech areas in all patients. We used single shot echo planar imaging in a transverse plane (TR 3000/TE 40, a series of 43 images, 3 mm thick with a 64x64 matrix with 200 mm field of view) during which the patient performed a motor task (a self-paced sequential tapping of the thumb against each finger) or a speech task (verbal fluency and verb generation). A general model-based statistical analysis (SPM 12) was used to measure the extent of cortical activation.

To plan the surgical procedure, we used computer assisted 3D-visualization by neuronavigational software (Stealth Station S7 Surgical Navigation System, Medtronic) and 3D-Slicer software (http://www.slicer.org).[14] The 3D-visualization of the medical images allowed us to perform preoperative 3D-planning, i.e., to interactively present relevant anatomic structures as 3D-objects in virtual space on the computer screen, to define surgical targets, to perform quantitative measurements, and finally to select the most suitable surgical approach or trajectory to the lesion.[15] Interactive 3D-preoperative planning started with defining the tumour model characteristics (size, volume, extension) and their relationship to the models of the cortical surface and functional data. Based on the available data, we planned the position and size of the trepanation opening, the sites of intraoperative electrophysiological testing, and the preliminary EOR.

Anaesthetic method

We used awake-awake-awake technique of awake craniotomy - i.e. procedural sedation and analgesia with dexmedetomidine in combination with scalp block. Initially deksmedetomidine infusion (200 μg in 50 ml of 0.9% NaCl; rate 0.2–1.5 4 μg/kg/h) was started to sedate the patient followed by scalp block. Scalp block was performed by local infiltration of the scalp nerves (i.e. n. supratrochlearis, n. supraorbitalis, n. auriculotemporalis, n. zygomaticotemporalis, n. occipitalis minor and major, n. auricularis major) to enabled effective analgesia for skin incision and craniotomy.[16] For local infiltration of the nerves we used 1–3 ml of the mixture of levobupivacaine (Chirocaine 5 mg/ml solution, Abbvie Pharmacy) and xylocaine with adrenaline (Xylanaest 2% with epinephrin 1: 200000 solution, Kemofarmacija d.d.). Adrenaline causes vasoconstriction and thereby delays absorption of local anaesthetics, increases duration of anaesthesia and prevents local bleeding after skin incision.

In addition, we introduced therapeutic communication with medical hypnosis leaving patients less sedated, more competent during the entire surgical procedure without stress.[17] Hypnosis session was usually carried out 1 to 3 days before surgery, to gain patients approval and confidence and to teach the patient how to construct an imaginary place where they can feel safe and protected.

Anaesthesia was conducted by two senior anaesthesiologists. The standard intraoperative monitoring was used. All patients had dedicated intravenous and arterial lines, a Foley catheter, and a nasal oxygen catheter. Hypothermia was prevented with use of warming blankets. Cefazolin 2g was used intravenously for perioperative antibiotic prophylaxis.

The patients lay supine with their head rotated approximately 45 degrees to the side. They were encouraged to find the most comfortable position and were generously padded as necessary. The head was fixed in a Mayfield clamp under a scalp block combined with dexmedetomidine. Additional local anaesthesia was applied along the skin incision line and between the dural sheets before the skin and dura incision. Sedation during the procedure was maintained with dexmedetomidine, and painful phases were treated with boluses of remifentanil. Bispectral Index Scale (BIS) was used for sedation monitoring. After the surgical procedure, all patients were transferred to the intensive care unit for overnight observation.

The operative procedure and neurophysiological testing

Tumour removal was performed in accordance with classical microsurgical techniques. In all cases, microsurgical microscope was employed. During the surgical procedure, frameless neuronavigation, intraoperative neurophysiological testing and augmented malignant tumour visualization with 5-aminolevulinic acid (5-ALA) were used.

For precise intraoperative localization of the tumour, we used neuronavigation with a Stealth Station S7 (Medtronic) navigation station, thus defining the size and position of the trepanation opening and the morphological tumour boundaries on the cortical surface. During tumour removal, neuronavigation was used for approximate depth orientation, and as a help to assess the EOR intraoperatively.

Injury to the eloquent regions was avoided after they had been identified by intraoperative neurophysiological testing. For cortical stimulation, a bipolar electrode was used with biphasic electrical current (50 Hz, 0.5 ms, 4 to 10 mA). For subcortical simulation, a monopolar electrode on the tip of aspirator was used, with a train of five pulses in row (a train of five pulses at 200 Hz, 0.5 ms, from 2 to maximum 20 mA). The patient's speech was monitored by an examiner, who talked to the patient and detected potential speech difficulties. During the stimulation of the cortical surface, the patient named objects on pictures or repeated words after the examiner. When stimulating the speech area, the speech changed or ceased. The stimulation of the primary motor area on the cortical surface resulted in motor evoked potentials (MEPs) detected in the corresponding muscles of the patient's body, and discomfort and/or movements, as reported by the patient. Subcortical stimulation was performed to define the distance from the corticospinal tract in patients where the tumour was in its vicinity. During tumour removal, the subcortical white matter was continuously stimulated with a monopolar electrode, and MEPs were monitored. At the beginning of the resection, the stimulation current was set at 20 mA. When MEPs were detected during the progression of the resection, the stimulation current was gradually reduced. When the MEP response was already induced by a 3–5 mA current, the resection in that direction was stopped, due to the proximity of the corticospinal tract.[18]

In cases where the preoperative diagnostic images showed the characteristics of malignant tumours, 5-ALA was used. The fluorescence of the tumour tissue was observed under the operating microscope (OPMI Pentero 900 Microscope, Carl Zeiss).

Assessment

The demographic data of the patients were collected before surgery. According to the American Society of Anaesthesiologists, their physical status classification system ASA score was noted and KPS was assessed in all patients. In 12 patients, health-related quality of life (HRQoL) was assessed by 36-Item Short Form (SF-36) health survey.[19,20]

During the surgery, we measured duration of anaesthesia, duration of the operative procedure and duration of the neurophysiological testing. Patient cooperation during surgery was assessed by a neurosurgeon and neurophysiologist and graded on scale from 0 to 10 (modified 11-point numerical rating scale, where 0 represented poor cooperation and 10 excellent cooperation). Patient comfort and pain were assessed by the anaesthesiologist. Pain was assessed by visual analogue scale (VAS) from 0–10 (0 meaning no pain, 10 meaning intolerable pain). Comfort was assessed by modified VAS scale from 0–10 (0 being the least and 10 being the most comfortable). Intraoperative complications were recorded.

After surgery, we monitored postoperative neurological status and noted non-neurological complications. The level of effort needed for the whole procedure, as reported by the patients, was assessed by anaesthesiologist 2–5 days after surgery, by modified VAS scale from 0–10 (0 being the least and 10 being the most difficult). KPS was assessed 1 week after surgery and the patients were asked to describe what was the worst experience during the awake craniotomy. A contrast enhanced brain MRI scan was performed the day following the surgery to assess EOR in all patients. In cases of malignant gliomas (AA, GBM) EOR was assessed on T1 weighted contrast enhanced MRI images. In those cases, gross total resection (GTR) was defined as no residual enhancement on postoperative images, near total resection (NTR) was defined as rim enhancement of the resection cavity, and subtotal resection (STR) was defined as residual nodular enhancement. In cases of LGG, EOR was assessed on T2 and FLAIR weighted postoperative MRI images. In those cases, GTR was defined as no hyperintense signal changes on postoperative images, STR was defined as persistence of hyperintense signal around resection cavity, and biopsy

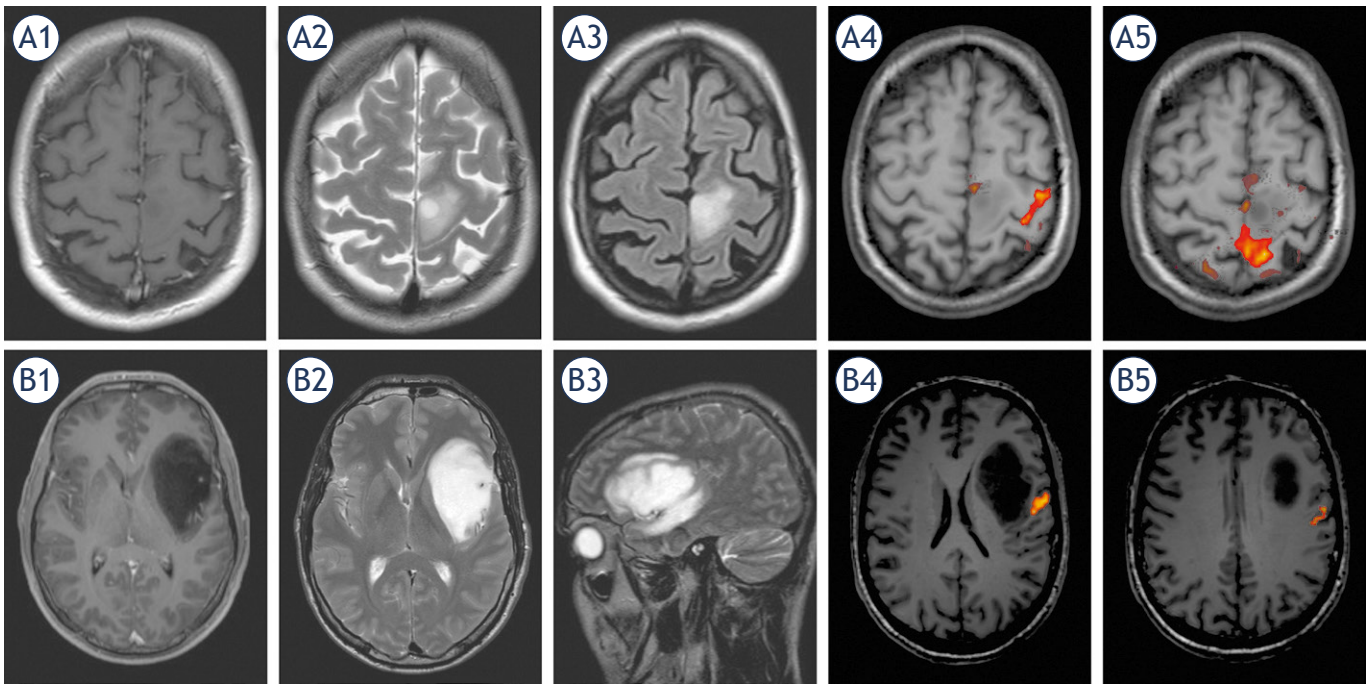

FIGURE 1. Preoperative magnetic resonance images (MRI) of low-grade glioma located in primary motor cortex **(A)** and anaplastic astrocytoma located in anterior speech area (Broca area) **(B)**. Preoperative imaging included T1 weighted contrast enhanced **(A1, B1)**, T2 weighted **(A2, B2)**, FLAIR **(A3, B3)** and functional magnetic resonance (fMRI); **(A4, A5, B4, B5)** images. The fMRI demonstrated the hand activation area (yellow/red colour) lateral (A4) and leg activation area behind **(A5)** the lesion in primary motor cortex. In second case fMRI demonstrated speech activation areas posterior to the lesion on the left side **(B4, B5).**

resection (BR) when approximately more than 50% of hyperintense signal remained on postoperative images. Length of hospital stay (LOS) was noted.

Three months after the surgery, the KPS score was assessed in all patients and the HRQoL was assessed by SF-36 health survey in the same 12 patients as before surgery. All patients were asked, if they would be willing to undergo awake craniotomy again if necessary and their answers were noted.

Statistical analysis

The means or ranges of continuous variables are presented, and categorical data are summarized as counts. The differences between the KPS scores before, after and 3 months after surgery were evaluated using One Way ANOVA. The differences between the SF-36 health survey subscales before and 3 months after surgery were evaluated using Wilcoxon test. A p-value of less than 0.05 was considered statistically significant. Data were ana-

TABLE 1. Demographics and preoperative data

No. of patients	24
Age (years)	41 ± 11
Weight (kg)	81 ± 12
Height (cm)	176 ± 8
Gender (M/F)	18/6
ASA (I/II/III)	9/15/0
First operation/reoperation	22/2
Tumour size (cm^3)	46 ± 27
Tumour location (side):	
Insular (left/right)	4/3
Frontal Central-PMC (left/right)	2/2
Frontal- Broca area (left/right)	6/1
Temporo-frontal (left/right)	3/0
Temporal-Wernicke area (left/right)	3/0

The results are expressed as mean ± SD or number of patients.

ASA = American Society of Anaesthesiologist; F = female; M = male; PMC = primary motor cortex

TABLE 2. Intraoperative and early postoperative outcomes

INTRAOPERATIVE DATA	
Duration of anaesthesia (minutes)	278 ± 47
Duration of procedure (minutes)	215 ± 48
Duration of testing (minutes)	73 ± 26
Comfort score (0- least; 10- most)	8 ± 2 (5–10)
Pain score (0- no pain; 10- intolerable)	4 ± 2 (0–5)
Cooperation score (0- poor; 10- excellent)	10 ± 1 (9–10)
Complications (none/seizure/incomplete testing)	13/8/3
EARLY POSTOPERATIVE DATA	
Pain score after procedure (0- no pain; 10- intolerable)	2 ± 1 (0–3)
Pain score ICU (0- no pain; 10- intolerable)	2 ± 1 (0–3)
Level of effort (0- least; 10- most difficult)	3 ± 2 (0–6)
Non-neurological complications	
Wound infection	1
Pulmonary embolism	1
Nausea	2
Pain	2
Neurological complications	
Walking disability	1
POCD and dysphasia	1
Mild hemiparesis, POCD, seizures	1
Tumour histology	
LGG	14
AA	7
GBM	3
Extent of resection	
LGG (GTR/STR/BR)	4/7/3
AA or GBM (GTR/NTR/STR)	6/3/1
Length of stay (days)	6 ± 5

The results are expressed as mean ± SD (range in brackets) or number of patients.

AA = anaplastic astrocytoma; BR = biopsy resection; GBM = glioblastoma; GTR = gross total resection; ICU = intensive care unit; LGG = low grade glioma; NTR = near total resection; POCD = postoperative cognitive decline; STR = subtotal resection

lysed by SPSS 13.0 software package (IBM Corp., Armonk, NY, USA).

Results

Patients and preoperative data

The demographic and preoperative data are showed in Table 1. During the 5-year study period, we performed awake craniotomies in 24 patients with glial brain tumours. They were 22 to 60 years old. In all cases, the main presenting symptom was epileptic seizure. In addition, in two patients, a mild dysphasia, and in one a disorientation was present. The main comorbidities in patients were well controlled diabetes and arterial hypertension. Four more patients were considered for awake craniotomy but were later found to be unsuitable and underwent surgery under general anaesthesia, one due to anxiety, one due to morbid obesity, one due to asthma and one due to psychosis.

The preoperative fMRI was successful in all patients and revealed speech dominance on the left side in all but one case in which it was bilateral. In 4 cases with tumour in frontal-central region (i.e., near or within primary motor region) the fMRI was used also to define primary motor regions (Figure 1).

Intraoperative and early postoperative results

Intraoperative and early postoperative outcomes are presented in Table 2. The longest surgical procedure lasted 5 hours and 20 minutes. Patient cooperation during surgery was in majority of the cases excellent. Discomfort during surgery reported by the patients was generally described as just a little uneasy and/or just starting to bother. Pain perceived during surgery was regarded as moderate. In two patients, however, we observed significant fatigue during surgery that started about 2.5 hours after the start of the procedure, and it was so intense that further neurophysiologic testing was not feasible. During cortical stimulation, we observed epileptic seizure activity in 8 out of 24 patients (33% of the patients). In one of these patients, further testing was not possible, due to limited compliance after the seizure. Neurophysiological testing by cortical stimulation was therefore successful in identifying the cortical language areas or primary motor cortex in all but three cases. Subcortical stimulation was performed in cases with insular and frontocentral located tumours. The corticospinal tract upon stimulation with a 20 mA current or less was detected in 8 out of 11 tested patients (72% of the patients).

After the surgery, the neurological worsening was observed in 3 out of 24 patients (13% of the patients) and the other postoperative complications were present in 6 out of 24 patients (25% of the patients) (Table 2). Postoperative pain was mild in almost all cases. Level of the effort during surgery

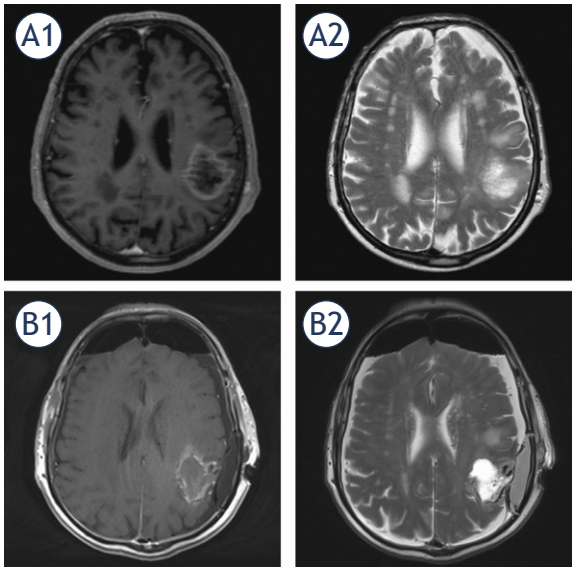

FIGURE 2. Preoperative **(A)** and postoperative **(B)** T1 weighted contrast enhanced (A1, B1) and T2 weighted (A2, B2) magnetic resonance images (MRI) of glioblastoma located in supramarginal gyrus near Wernicke area. Preoperative images **(A)** demonstrate rim enhancing central necrotic oval lesion surrounded by oedema. Postoperative images **(B)** demonstrate post-resection cavity filled with partially haemorrhagic fluid and mild irregular contrast enhancing of resection edge – i.e. near total resection.

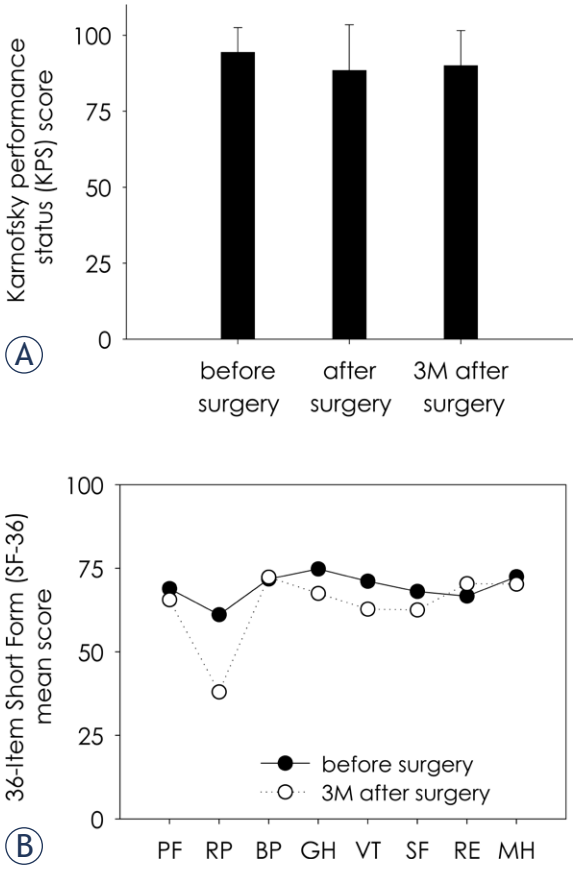

FIGURE 3. The Karnowski Performance Scale (KPS) scores **(A)** and 36-Item Short Form (SF-36) health survey subscale scores **(B)** before surgery, after surgery and 3 months after surgery. The differences between the KPS scores and SF-36 subscale scores before and after surgery were not statistically significantly different ($p > 0.05$; $n = 24$ for KPS; $n = 12$ for SF-36).

BP = bodily pain; GH = general health; PF = physical function; MH = mental health; RE = role limitations due to emotional problems; RP – role limitations due to physical problems; SF = social functioning; VT = vitality; 3M = three months

experienced by the patients was assessed and reported to be mild to moderate. When asked "what was the worst experience during the awake craniotomy", 15 patients said "nothing", four patients said, "bone cutting", two patients said, "Mayfield clamp placement", and the remaining three patients said, "scalp block", "craniofix bone flap fixation" or "waiting for the end of surgery". GTR was achieved in 29% (4 out of 14 cases) in cases of LGG, and in 60% (6 out of 10 cases) in cases of GBM and AA (Figure 2).

All patents were discharged home. The time of postoperative hospital stay was from 3 to 9 days for most of the patients, and 23 days for one patient.

Late postoperative results

Three months after surgery all patients were under postoperative oncological treatment with radiotherapy and/or chemotherapy. All patients were still on a sick leave, and none yet returned to work. The average KPS scores after surgery and 3 months after surgery were slightly lower and are shown in Figure 3A. However, the differences between the KPS scores before, after and 3 months after surgery were not significantly different ($p = 0.14$). Patient HRQoL was assessed by SF-36 health survey before surgery and 3 months after surgery, the results for each SF-36 subscale are shown in Figure 3B. We found some increase in patient perceived problems with work or other daily activities because of physical health (i.e., "role limitations due to physical problems" SF-36 subscale) three months after surgery in comparison to before surgery, however, the difference was not statistically significant ($p = 0.07$). The scores in other SF-36 subscales (i.e., physical functioning, bodily pain, general health, vitality, social functioning, role limitations due to emotional problems, mental health) were very similar before and after surgery, and

not significantly different ($p > 0.1$). Therefore, the surgery did not have important negative impact on functional status or quality of life as assessed by KPS and SF-36 health survey, respectively. Three months after surgery, the patients were asked, "if they would be willing to undergo awake craniotomy again if needed". One patient answered "no", one answered, "only if absolutely necessary" and the other 22 patients answered "yes".

Discussion

At our institution, awake craniotomy for surgical treatment of gliomas was performed in 24 patients in the last 5 years. Our experiences with awake craniotomy are good and suggest that awake craniotomy can be safely performed with low risk of complications or failure rate.

The goal of an awake craniotomy is to provide the surgeon with optimal functional monitoring during the removal of as much of the tumour as possible and thus avoiding damage to critical brain structures. Awake craniotomy is mandatory in patients where neurophysiological testing and monitoring cannot adequately assess function under general anaesthesia, and when the cooperation of the patient during testing is needed. The functions typically monitored during awake craniotomy are mainly higher mental functions, especially speech. Such monitoring allows safer tumour removal, resulting in improved treatment outcome, even for tumours in eloquent brain regions.[12,13,18,21,22]

On the other hand, awake craniotomy is a technically demanding procedure, with more potential intraoperative complications in comparison to the same procedure performed under general anaesthesia.[21] Namely, patient intolerance or non-cooperation can result in too early termination of the surgery, and incomplete or suboptimal resection.[21] Therefore, it is very important to properly select patients for the procedure. In our series, all the patients performed well, and the selection protocol for the patients was shown to be good. During preoperative evaluation, four potential candidates were found to be unsuitable for awake craniotomy. In addition to obesity, potential breathing problems and dysphasia, also patient immaturity, hypertension and alcohol abuse are also some of the risk factors for sedation failure, which may worsen the surgery and postoperative recovery.[23] Anxiety and other psychological problems may also negatively influence the patient's cooperation.[24] The selection of patients should therefore be individualized, and the decision-making process should involve all team members.

A variety of anaesthetic methods are used for awake intracranial procedures. In our institution, we combine scalp block and procedural sedation and analgesia with dexmedetomidine – i.e. awake-awake-awake protocol. This technique proved to be very safe in experienced hands, allows more control with the patient, the anaesthesiologist is by the patients side all the time and can react promptly if something goes wrong, and it usually results in better patient cooperation.[25,26] All patients are well-educated regarding all the steps of the surgical procedure to facilitate the intraoperative testing and to decrease their anxiety. In our, and also other studies, the most painful and unpleasant part of the procedure, as reported by the patients, is the placement of the cranial fixation device and trepanation.[27,28] It is important to note that because of inadequate analgesia during cranial fixation, or later due to positioning, the surgical outcome may be compromised.[29] The patient's communication with the surgical team and addressing the patient's discomfort are therefore crucial. In the case of the awake-awake-awake protocol, as used in our cases, the duration of the surgery proved important. The cooperation of two of our patients became inadequate after approximately 2.5 hours from the beginning of the surgery. To overcome this problem, we recommend early functional testing and analysis of the functions for which patent's cooperation is needed. In addition, we recommend good preoperative planning and preparation to reduce operation time.

In our study, the patient's perception of awake craniotomy was generally good. Hypnosis was well accepted in our study. Also, it was previously shown that it prolongs the time of patient cooperation during the neurophysiological testing.[30] The main challenges for patients undergoing awake craniotomies include anxiety and fears, terrifying noises and surroundings, immobility, loss of control, the feeling of helplessness and being left alone. In such situations, psychological support might be very helpful and motivates patients to have a sense of control by active participation during surgery instead of being lost in anxiety.[31,32]

The rate of occurrence of epileptic seizures during surgery in our study of 33% was higher compared to other reports, which reported a seizure rate of from 15 to 16.7%.[21,28] At the beginning of the operation, cortical stimulation, especially when used in excess during neuromonitoring, may sometimes provoke epileptic seizures.[21,28]

Reported treatment was the iced Ringer solution, which was also successfully used in our patients to stop the seizure. We believe that the higher rate in our series could be attributable to more extensive testing in selected patients. In this regard, it was observed that less stimulation is generally used with increased experience.[28]

The neurological worsening observed postoperatively in 13% of our patients is comparable to the meta-analysis data, which report rates of about 30% for early and 7% for late deficits of all severities after intraoperative stimulation mapping.[33] GTR in our study was higher in cases of GBM or AA in comparison to LGG (29% vs. 60%). The comparable GTR rates are also reported in the literature for awake craniotomy glioma surgery.[34,35] In this regard, it is important to note, that although 5-ALA and neuronavigation help to delineate the borders of the tumour tissue, the final edge of the resection is defined by the functional borders, as defined by intraoperative neurophysiological testing. Consequently, in several cases of awake craniotomy total resection of the glioma cannot be achieved due to tumour infiltration of eloquent regions. Based on intraoperative neurophysiological testing, we believe that further resection in our patients could result in significant postoperative functional deficit.

One of the goals of surgical treatment of gliomas is, in addition to maximal resection, preservation of the neurocognitive profile and quality of life.[19,20] Namely, gliomas are currently surgically incurable lesions and potential postoperative neurological deficits further reduce survival time and quality of life of those patients. In our study, the HRQoL assessed three months after surgery was not significantly impaired. We did however observe noticeable patient reported problems with work and daily activities three months after surgery. The later could be related to ongoing postoperative oncological treatment. Also, none of the patients at 3 months after the surgery was yet allowed to return to work, which probably also influenced their perception and the results.

To conclude, our experience suggests that awake craniotomy using our protocol is a feasible and safe surgical procedure. To achieve the best treatment outcome, proper selection of the patients, preoperative preparation with planning, and cooperation of the medical team are necessary.

Acknowledgments

We are thankful to all colleagues, surgeons, anaesthesiologists, nurses and technicians at the Department of Neurosurgery, Department of Anaesthesiology and Surgical Therapy and Department of Neurophysiology who in any way helped in this work. We are also thankful to all the patients who cooperated in the study.

References

1. Lapointe S, Perry A, Butowski NA. Primary brain tumours in adults. *Lancet* 2018; **392:** 432-46. doi: 10.1016/S0140-6736(18)30990-5
2. McCormack BM, Miller DC, Budzilovich GN, Voorhees GJ, Ransohoff J. Treatment and survival of low-grade astrocytoma in adults 1977-1988. *Neurosurgery* 1992; **31:** 636-42. doi: 10.1227/00006123-199210000-00004
3. Bauman G, Lote K, Larson D, Stalpers L, Leighton C, Fisher B, et al. Pretreatment factors predict overall survival for patients with low-grade glioma: recursive partitioning analysis. *Int J Radiat Oncol Biol Phys* 1999; **45:** 923-9. doi: 10.1016/s0360-3016(99)00284-9
4. Johannesen TB, Langmark F, Lote K. Progress in long-term survival in adult patients with supratentorial low-grade gliomas: a population-based study of 993 patients in whom tumours were diagnosed between 1970 and 1993. *J Neurosurg* 2003; **99:** 854-62. doi: 10.3171/jns.2003.99.5.0854
5. 5.DeAngelis LM. Brain tumours. *N Engl J Med* 2001; **344**: 114-23. doi: 10.1056/NEJM200101113440207
6. Wen PY, Kesari S. Malignant gliomas in adults. *N Engl J Med* 2008; **359**: 492-507. doi: 10.1056/NEJMra0708126
7. Berger MS, Deliganis AV, Dobbins J, Keles GE. The effect of extent of resection on recurrence in patients with low grade cerebral hemisphere gliomas. *Cancer* 1994; **74:** 1784-91. doi: 10.1016/s0090-3019(99)00103-2
8. Chang EF, Clark A, Smith JS, Polley MY, Chang SM, Barbaro NM, et al. Functional mapping-guided resection of low-grade gliomas in eloquent areas of the brain: improvement of long-term survival. *J Neurosurg* 2011; **114**: 566-73. doi: 10.3171/2010.6.JNS091246
9. Smith JS, Chang EF, Lamborn KR, Chang SM, Prados MD, Cha S, et al. Role of extent of resection in the long-term outcome of low-grade hemispheric gliomas. *J Clin Oncol* 2008; **26**: 1338-45. doi: 10.1200/JCO.2007.13.9337
10. McGirt MJ, Chaichana KL, Gathinji M, Attenello FJ, Than K, Olivi A, et al. Independent association of extent of resection with survival in patients with malignant brain astrocytoma. *J Neurosurg* 2009; **110:** 156-62. doi: 10.3171/2008.4.17536
11. Liang J, Lv X, Lu C, Ye X, Chen X, Fu J, et al. Prognostic factors of patients with gliomas - An analysis on 335 patients with glioblastoma and other forms of gliomas. *BMC Cancer* 2020; **20:** 35. doi: 10.1186/s12885-019-6511-6
12. Sanai N, Berger MS. Intraoperative stimulation techniques for functional pathway preservation and glioma resection. *Neurosurg Focus* 2010; **28:** E1. doi: 10.3171/2009.12.FOCUS09266
13. Hervey-Jumper SL, Li J, Lau D, Molinaro AM, Perry DW, Meng L, Berger MS. Awake craniotomy to maximize glioma resection: methods and technical nuances over a 27-year period. *J Neurosurg* 2015; **123:** 325-39. doi: 10.3171/2014.10.JNS141520
14. Fedorov A, Beichel R, Kalpathy-Cramer J, Finet J, Fillion-Robin JC, Pujol S, et al. 3D Slicer as an image computing platform for the quantitative imaging network. *Magn Reson Imaging* 2012; **30:** 1323-41. doi: 10.1016/j.mri.2012.05.001
15. Žele T, Matos B, Knific J, Bajrović FF, Prestor B. Use of 3D visualisation of medical images for planning and intraoperative localisation of superficial brain tumours: our experience. *Br J Neurosurg* 2010; **24:** 555-60. doi:10.3109/02688697.2010.496876

16. Osborn I, Sebeo J. "Scalp block" during craniotomy: a classic technique revisited. *J Neurosurg Anesthesiol* 2010; **22:** 187-94. doi: 10.1097/ANA.0b013e3181d48846

17. Frati A, Pesce A, Palmieri M, Iasanzaniro M, Familiari P, Angelini A, Salvati M, Rocco M, Raco A. Hypnosis-aided awake surgery for the management of intrinsic brain tumors versus standard awake-asleep-awake protocol: a preliminary, promising experience. *World Neurosurg* 2019; **121:** e882-e891. doi: 10.1016/j.wneu.2018.10.004

18. Raabe A, Beck J, Schucht P, Seidel K. Continuous dynamic mapping of the cortico- spinal tract during surgery of motor eloquent brain tumours: evaluation of a new method. *J Neurosurg* 2014; **120:** 1015-24. doi: 10.3171/2014.1.JNS13909

19. Bunevicius A. Reliability and validity of the SF-36 Health survey questionnaire in patients with brain tumours: a cross-sectional study. *Halth Qual Life Outcomes* 2017; **15:** 92. doi: 10.1186/s12955-017-0665-1

20. Ware JE, Jr. Cathy Donald Sherbourne CD. The MOS 36-item short-form health survey (SF-36): I. Conceptual framework and item selection**.** *Medical Care* 1992; **30:** 473-83. PMID: 1593914

21. Trimble G, McStravick C, Farling P, Megaw K, McKinstry S, Smyth G, et al. Awake craniotomy for glioma resection: technical aspects and initial results in a single institution. *Br J Neurosurg* 2015; **29:** 836-42. doi: 10.3109/02688697.2015.1054354

22. Saito T, Muragaki Y, Tamura M, Maruyama T, Nitta M, Tsuzuki S, et al. Awake craniotomy with transcortical motor evoked potential monitoring for resection of gliomas in the precentral gyrus: utility for predicting motor function. *J Neurosurg* 2019; **132:** 987-97. doi: 10.3171/2018.11.JNS182609

23. Senel FC, Buchanan JM Jr, Senel AC, Obeid G. Evaluation of sedation failure in the outpatient oral and maxillofacial surgery clinic. *J Oral Maxillofac Surg* 2007; **65:** 645-50. doi: 10.1016/j.joms.2006.06.252

24. Palese A, Skrap M, Fachin M, Visioli S, Zannini L. The experience of patients undergoing awake craniotomy: in the patients' own words. A qualitative study. *Cancer N*urs 2008; **31:** 166-72. doi: 10.1097/01.NCC.0000305699.97625.dc

25. Kulikov A, Lubnin A. Anesthesia for awake craniotomy. *Curr Opin Anaesthesiol* 2018; **31:** 506-10. doi: 10.1097/ACO.0000000000000625

26. Suero Molina E, Schipmann S, Mueller I, Wölfer J, Ewelt C, Maas M, et al. Conscious sedation with dexmedetomidine compared with asleep-awake-asleep craniotomies in glioma surgery: an analysis of 180 patients. *J Neurosurg* 2018; **129:** 1223-30. doi: 10.3171/2017.7.JNS171312. PMID: 29328000

27. Khu KJ, Doglietto F, Radovanovic I, Taleb F, Mendelsohn D, Zadeh G, et al. Patients' perceptions of awake and outpatient craniotomy for brain tumour: a qualitative study. *J Neurosurg* 2010; **112:** 1056-60. doi: 10.3171/2009.6.JNS09716

28. Joswig H, Bratelj D, Brunner T, Jacomet A, Hildebrandt G, Surbeck W. Awake craniotomy: first-year experiences and patient perception. *World Neurosurg* 2016; **90:** 588-96. doi: 10.1016/j.wneu.2016.02.051

29. Whittle IR, Midgley S, Georges H, Pringle AM, Taylor R. Patient perceptions of "awake" brain tumour surgery. *Acta Neurochir* 2005; **147:** 275-7. doi: 10.1007/s00701-004-0445-7

30. Pesce A, Palmieri M, Cofano F, Iasanzaniro M, Angelini A, D'Andrea G, et al. Standard awake surgery versus hypnosis aided awake surgery for the management of high grade gliomas: A non-randomized cohort comparison-controlled trial. *Clinneurosci* 2020; **77:** 41-8. doi: 10.1016/j.jocn.2020.05.047

31. Hansen E, Seemann M, Zech N, Doenitz C, Luerding R, Brawanski A. Awake craniotomies without any sedation: the awake-awake-awake technique. *Acta Neurochir* 2013; **155:** 1417-24. doi: 10.1007/s00701-013-1801-2

32. Zemmoura I, Fournier E, El-Hage W, Jolly V, Destrieux C and Velut S. Hypnosis for awake surgery of low-grade gliomas: description of the method and psychological assessment. *Neurosurgery* 2016; **78:** 53-61. doi: 10.1227/NEU.0000000000000993

33. De Witt Hamer PC, Robles SG, Zwinderman AH, Duffau H, Berger MS. Impact of intraoperative stimulation brain mapping on glioma surgery outcome: a meta-analysis. *J Clin Oncol* 2012; **30:** 2559-65. doi: 10.1200/JCO.2011.38.4818

34. Ahmadi R, Dictus C, Hartmann C, Zürn O, Edler L, Hartmann M, et al. Long-term outcome, and survival of surgically treated supratentorial low-grade glioma in adult patients. *Acta Neurochir* 2009; **151:** 1359-65. doi: 10.1007/s00701-009-0435-x

35. Motomura K, Chalise L, Ohka F, Aoki K, Tanahashi K, Hirano M, et al. Impact of the extent of resection on the survival of patients with grade II and III gliomas using awake brain mapping. *J Neurooncol* 2021; **153:** 361-72.doi: 10.1007/s11060-021-03776-w

research article

Cognitive functioning in a cohort of high-grade glioma patients

Andreja Cirila Skufca Smrdel[1,2], Anja Podlesek[2], Marija Skoblar Vidmar[3,4], Jana Markovic[1], Jana Jereb[1], Manja Kuzma Okorn[5], Uros Smrdel[3,4]

[1] Department of Psycho-Oncology, Institute of Oncology Ljubljana, Ljubljana, Slovenia
[2] Department of Psychology, Faculty of Arts, University of Ljubljana, Slovenia
[3] Division of Radiotherapy, Institute of Oncology Ljubljana, Ljubljana, Slovenia
[4] Faculty of Medicine, University of Ljubljana, Slovenia
[5] University Medical Centre Ljubljana, Slovenia

Radiol Oncol 2023; 57(2): 201-210.

Received 29 November 2022
Accepted 31 December 2022

Correspondence to: Assist. Prof. Uroš Smrdel, M.D., Ph.D., Division of Radiotherapy, Institute of Oncology Ljubljana, Zaloška 2, SI-1000 Ljubljana, Slovenia. E-mail: usmrdel@onko-i.si

Disclosure: No potential conflicts of interest were disclosed.

Background. High grade gliomas are associated with cognitive problems. The aim of the study was to investigate cognitive functioning in a cohort of patients with high grade glioma, according to isocitrate dehydrogenase (IDH) and methyl guanine methyl transferase (MGMT) status and other clinical characteristics.

Patients and methods. The patients with the high-grade glioma treated in Slovenia in given period of time were included in study. Postoperatively they completed neuropsychological assessment consisting of Slovenian Verbal Learning Test, Slovenian Controlled Oral Word Association Test, Trail Making Test Part A and B and self-evaluation questionnaire. We analysed results (z-scores and dichotomized results) also according to IDH mutation and MGMT methylation. We examined differences between groups using T-test, Mann-Whitney U, $\chi 2$ and Kendall's Tau tests.

Results. Out of 275 patients in the cohort, we included 90. Forty-six percent of patients were unable to participate due to poor performance status and other conditions related to tumour. Patients with the IDH mutation were younger, with better performance status, larger proportions of grade III tumours and MGMT methylation. In this group cognitive functioning is significantly better in the domains of immediate recall, short delayed recall and delayed recall, and in the fields of executive functioning and recognition. There were no differences in cognitive functioning in regard to MGMT status. Grade III tumours were associated with more frequent MGMT methylation. Self-assessment proved week tool, associated only with immediate recall.

Conclusions. We found no differences in cognitive functioning according to MGMT status, but cognition was better when IDH mutation was present. In a cohort study of patients with high-grade glioma, almost half were unable to participate in a study, which points to an overrepresentation of patients with better cognitive functioning in the research.

Key words: cognition; high grade glioma; IDH1 mutation; MGMT methylation

Introduction

Malignant gliomas are group of aggressive brain tumours, comprising anaplastic astrocytoma (Grade III), anaplastic oligodendrogliomas (Grade III), anaplastic astrocytoma (Grade IV) and glioblastomas (Grade IV).[1] Anaplastic gliomas are still some of the most challenging tumours for patient and caregivers, but also for the therapist. Although there are some cautious advances in this field, there is still a grim outlook for the patients. As a number of patients is ill responding to treatment there are efforts for identifying those who respond well and those who would benefit from a change in treatment strategy.

Genetic and epigenetic markers like isocitrate dehydrogenase (IDH) mutations, loss of heterozygosity of 1p/19q(LoH 1p/19q), and methyl guanine methyl transferase (MGMT) promoter methylation have recently helped to stratify patients, removing the mixed histology like anaplastic oligoastrocytoma and introducing Grade IV astrocytoma. In IDH1 mutated patients' survival was markedly longer, as is in anaplastic oligodendrogliomas (with LoH 1p/19q). Prior to widespread genetic testing, it was already clear that patients harbouring methylation of MGMT gene promoter fare better comparing to those without.[2-4]

Brain tumours are also associated with impaired cognitive functioning, due to tumour alone but also due to treatment. Cognitive impairment can manifest already at the time of diagnosis; the prevalence of cognitive deficits varies from 60 to 85% in different studies.[5] The most common are in the fields of verbal memory, executive functioning, psycho-motor speed, but also attention and language.[6-9]

Cognitive functioning is also one of the prognostic factors for survival. Early findings suggested that cognitive decline is preceding radiological progression, which was not confirmed by all studies.[10-12] Further studies confirmed cognitive impairment as independent prognostic factor in newly diagnosed patients, both at baseline and in the period after surgery.[13-16]

It was shown that IDH1 mutation (IDH1-mut) is not only an important prognostic factor, but it is also associated with better cognitive functioning. Many studies have shown that cognitive functioning is better in IDH1-mut patients when compared with IDH1-wildtype (IDH1-wt) patients.[17-19]

Among possible causes of the better cognitive functioning of patients with IDH1-mut is brain plasticity which could be affected negatively by the greater tumour growth rate in IDH1-wt tumours, while remaining intact in less invasive IDH1-mut tumours. Preserved cognitive functioning might also be related to the tumour microenvironment, with more pronounced lymphocyte infiltration and programmed death-ligand 1 (PD-L1) expression in IDH1-wt tumours, or even to differences at the synaptic level.[20]

The effect and possible role of the MGMT methylation status in patients' cognitive functioning is even less clear. Most clinical studies focus on investigating patients with MGMT promoter methylation (MGMT-met), with cognitive function as a secondary outcome.[21] According to one study, the absence of MGMT promoter methylation (MGMT-unmet) predicts greater cognitive deficit when patients are treated with radiochemotherapy.[22] The MGMT-met therefore can be considered a predictive marker for development of cognitive impairment, but further research about its role in cognitive functioning as well as the prognosis needed. Here the challenge is the frequent overlap of MGMT promoter methylation with the IDH1 mutation, which, in conjunction with relatively small number of patients in the high-grade glioma studies, presents difficulties in statistical analysis.

In our study, we examined how the expression of IDH1 mutation and MGMT promoter methylation are linked to the cognitive functioning following the operative treatment in the cohort of all Slovene Grade III and Grade IV glioma patients.

Patients and methods

Patients

We analysed the cohort of patients with high grade glioma, treated between March 2019 and December 2021. Their diagnoses (anaplastic astrocytoma, anaplastic oligodendroglioma or glioblastoma) were histological confirmed. Patients were operated in either of the two neurosurgical departments in Slovenia, then they were referred to Institute of Oncology Ljubljana for evaluation regarding the initiation of radiochemotherapy.

At the referral, they consented to be enrolled in the study. Exclusion criteria were histology other than gliomas WHO III/IV, Karnoffsky performance status less than 70% and inability to undergo evaluation (e.g., marked dysphasia). To be included in the study, they had to be 18 years old or older.

The following data were obtained from the medical documentation: age, sex, date of diagnosis, localization of the tumour, type of surgery, extent of surgery, radiotherapy parameters, systemic therapy, use of corticosteroids, histological, genetic and epigenetic characteristics of tumours. All patients also had a molecular and genetic analysis of the tumour tissue performed, so the IDH1 mutations and MGMT promoter methylation status were determined.

Cognitive functioning

To asses cognitive functioning, we used psychometric tests in the domains of verbal memory (Slovenian Verbal Learning Test – TBU, measuring immediate recall, short recall, delayed recall and recognition of distracters)[23], verbal fluency

(Slovenian Controlled Oral Word Association Test –SCOWA)[24], psycho-motor speed (Trail Making Test, Part A – TMT A), executive functions (Trail Making Test, Part B – TMT B)[25], in accordance with the recommendations for use in the studies concerning cognitive functioning of cancer patients.[26] The patients also self-evaluated their cognitive functioning on a 0–10 scale (0 = without problems, 10 = extremely intensive problems present).

Statistical analysis and ethical consideration

We used descriptive statistics with the means values and standard deviation for the demographic data. The correlation between variables was tested with Pearson's t test or Spearman's rho test.

For each cognitive test, the test scores were analysed either as standardized (z-scores) or as a dichotomized variable: no impairment present (z > –1.5 below the mean of the control group) *vs*. impairment observed (the patient had a z-score lower than –1.5 or was unable to perform the test at all). At the individual level, we analysed the percentage of impaired patient`s results.

We next compared groups of patients with different IDH1 statuses and MGMT methylation, using either a t-test or Mann-Whitney U-test (in case that Kolmogorov-Smirnov test of normality showed statistically significant departure from normality) for interval variables, a $\chi 2$ test for categorical variables and ordinal variables with Kendall's Tau test. All hypotheses were tested at a 5-percent alpha error rate.

We used the statistical program SPSS, to calculate the power of the test we used G*Power 3.1.9.7.

Written informed consent was obtained from all the patients before the inclusion in the clinical trial. The study was approved by the Institutional Review Board of the Institute of Oncology Ljubljana and by The National Medical Ethics Committee of the Republic of Slovenia (Approval number 0120-393/2018/10, date 12/12/2018) and was carried out according to the Declaration of Helsinki.

Results

Demographics and tumour characteristics

At the time the research was performed, 275 patients were diagnosed with glial tumour. Of those, 90 patients were recruited into the study, representing 33% of all patients. Figure 1 shows reasons

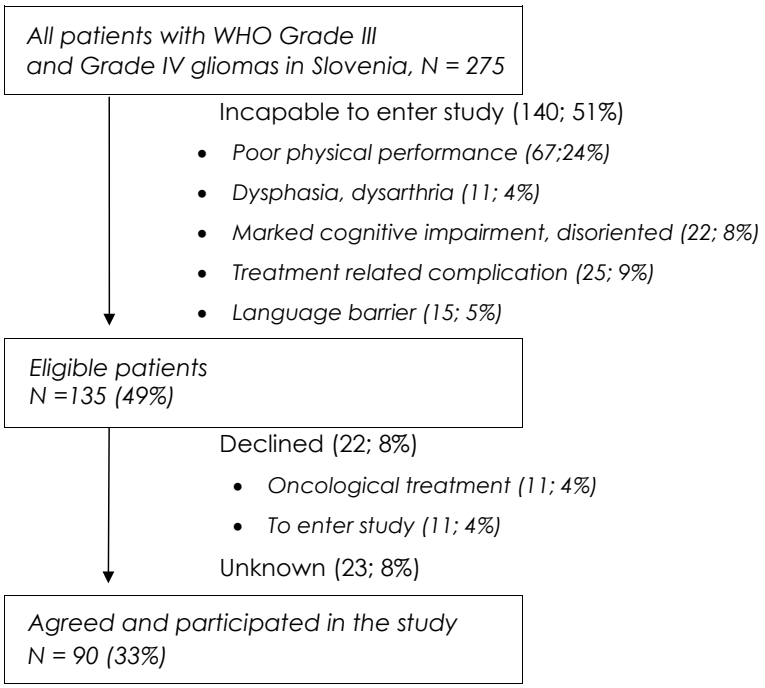

FIGURE 1. Recruitment protocol, N = 275

for patients entering and not entering the study as recorded by oncologists at the time of the first consultation. Of the 51% of patients incapable of participating, in the study the major reason was poor performance status, followed by other tumour and treatment related impairments, representing 46% of ineligible patients, the other common issue was language barrier.

Participating patients were 30 to 84-year-old (median [M] = 58.78 years, standard deviation [SD] = 11.31 years). There were more males than females (57 *vs*. 33). On average, female patients were older (M = 57.67 years, SD = 9.35 years, 39–74 years) than male patients (M = 59.42 years, SD = 12.33 years, 30–84 years), but the age difference was not statistically significant (p = 0.481).

Of all 90 patients, 78 had Grade IV tumour (all classified as glioblastoma), 8 had anaplastic astrocytoma, and 4 had anaplastic oligodendroglioma. Fifteen patients had IDH1 mutation (7 anaplastic oligodendroglioma, 4 anaplastic astrocytoma, and 4 glioblastoma). MGMT promoter was methylated in 36 patients (4 anaplastic oligodendroglioma, 5 anaplastic astrocytoma, and 27 glioblastoma), whereas in 1 glioblastoma, 2 anaplastic astrocytomas and 1 anaplastic oligodendroglioma we couldn't determine the methylation status.

Patients with Grade III tumours had a statistically better performance status – the Karnoffsky

TABLE 1. Demographic and medical data

Variable	Levels	f (%)	Descriptive statistics
Gender	Male	57 (63%)	
	Female	33 (37%)	
Age	< 50 years	17 (19%)	M = 58.78, SD = 11.31
	50–70years	60 (67%)	min = 30, max = 84
	> 70 years	13 (14%)	
Education	≤ 9 years	14 (16%)	
	10–13 years	48 (53%)	
	14–19 years	26 (29%)	
	≥ 20 years	2 (2%)	
Tumour grade	Grade III	12 (13%)	
	Grade IV	78 (87%)	
Tumour location	Frontal	34 (38%)	
	Parietal	21 (23%)	
	Temporal	26 (29%)	
	Occipital	4 (4%)	
	central	3 (3%)	
	Diffuse	2 (2%)	
Hemisphere	Right	38 (42%)	
	Left	44 (49%)	
	Both	8 (9%)	
Surgery type	Biopsy	11 (12%)	
	Reduction	49 (54%)	
	Gross tumour resection	30 (33%)	
Karnoffsky performance status	70	32 (36%)	
	80	37 (41%)	
	90	18 (20%)	
	100	3 (3%)	
Corticosteroids (Yes/no, mg)	Yes	66 (73%)	M = 5.55, SD = 4.73
	No	24 (27%)	min 0, max 24
Radio-chemotherapy (intention to treat)	Yes	90 (100%)	
	No	0 (0%)	
Time to beginning of adjuvant treatment (in weeks)	≤ 6 weeks	60 (67%)	M = 5.98, SD = 2.25
	≥ 7 weeks	30 (33%)	min 3, max 15
Epilepsy	Yes	27 (30%)	
	No	63 (70%)	
IDH1 mutation	IDH1 mutation	15 (17%)	
	IDH1 wild type	75 (83%)	
MGMT methylation*	Yes	36 (42%)	
	No	50 (58%)	

IDH1 = isocitrate dehydrogenase 1; M = median; MGMT = methyl guanine methyl transferase; SD = standard deviation

performance status was 70 in 2 (17%) patients, 80 in 2 (17%) patients, 90 in 8 (67%) patients with Grade III tumours – when compared with patients with Grade IV tumours (in these group, the Karnoffsky performance status was 70 in 30 patients, 80 in 35 patients, 90 in 10 patients, and 100 in 3 patients; U = 251.000, z = -2.75, p = 0.006). Compared to the group of patients with Grade III tumours, the group with Grade IV tumours had a statistically significantly higher percentage of IDH1-mut tumours (73% *vs.* 5%, $\chi 2(1) = 56.077$, $p < 0.001$, $V = 0.789$, $1–b = 0.987$) and MGMT promoter methylations (60% *vs.* 36%, $\chi 2(1) = 7.067$, $p = 0.008$, $V = 0.280$, $1–b = 0.756$).

Table 2 shows the structure of the sample according to the expression of IDH1 mutation and MGMT methylation. Five patients had both genetic markers expressed, two thirds of patients with IDH1-mut also had MGMT-met expressed, and among patients with expressed methylation, IDH1-mut tumours were present in 27% of pa-

tients. The difference in the proportion of MGMT methylation in the IDH1-mut and IDH1-wt groups was statistically significant, $\chi 2(1) = 5.333$, $p = 0.021$, $V = 0.243$, $1–b = 0,82$).

Cognitive functioning

The overview of cognitive evaluation is presented in Table 3. The achievements were impaired (z <–1.5) in a large proportion of the patients, especially in the field of short recall, executive functions and psycho-motor speed. The impairment was least frequent in the field of recognition and verbal fluency. The results remained similar, regardless of accounting only those who were capable of completing a specific test or the sample as whole – the biggest difference between these two analysis methods is on the TMT A and TMT B tests.

We examined on how many out of 7 tests the patients had an impaired test score (z < –1.5 or unable to finish the test) and found that 11 patients (12%) had 0–1 impaired test score, 26 (29%) patients had 2–4 impaired test scores, and 53 (60%) patients had more than 5 impaired test scores.

On the 10-point self-evaluation scale of cognitive functioning the mean rating was 3.66, SD = 2.81, min = 0, max = 10; 48 (53%) patients selected rating 0–3, 23 (26%) selected rating 4–6, and 19 (21%) selected a rating higher than 7. Correlations between self-assessment and individual tests of cognitive functioning show that self-assessment is weakly but statistically significantly related only to immediate recall ($r = -0.280$, $df = 79$, $t = 2,57$, $p = 0.012$).

The cognitive functioning in any of the measured fields was not statistically significantly affected by sex, surgery type and the presence or absence of seizures. The test scores did, however, differ with regard to age, education, and performance status. Age was statistically significantly related to participant's results in the field of verbal fluency ($r = -0.278$, $t = -2.55$, $df = 79$, $p = 0.012$), immediate recall ($r = -0.409$, $t = -3.96$, $df = 79$, $p < 0.001$), short delayed recall ($r = -0.388$, $t = 3.72$, $df = 79$, $p < 0.001$) and delayed recall ($r = -0.333$, $t = 3.12$, $df = 79$, $p = 0.003$).

Education was significantly related to results in the fields of verbal fluency ($r_s = 0.381$, $t = 3.66$, $df = 79$, $p < 0.001$), immediate recall ($r_s = 0.334$, $t = 3.13$, $df = 79$, $p = 0.002$), short delayed recall ($r_s = 0.285$, $t = 2.63$, $df = 79$, $p = 0.010$), delayed recall ($r_s = 0.265$, $t = 2.42$, $df = 80$, $p = 0.017$) and recognition ($r_s = 0.264$, $t = 2.42$, $df = 79$, $p = 0.018$).

Performance status was significantly related to immediate recall ($r_s = 0.280$, $t = 2.57$, $df = 79$, $p = 0.012$) and delayed recall ($r_s = 0.296$, $t = 2.74$, $df = 79$, $p = 0.008$).

We analysed the disease and demographic data and the results of psychological tests with regard to IDH1 mutation. Compared to IDH1-wt patients, patients with tumours harbouring IDH1-mut were statistically significantly younger, had better performance status and were more likely to have Grade III tumour and MGMT promoter methylation (Table 4). They functioned better in the field of verbal memory (had a better performance in immediate recall, short delayed recall and delayed recall, measured either with z-scores or as dichotomised test scores) and in the field of executive

TABLE 2. Number of patients with different combinations of IDH1 mutation expression and methyl guanine methyl transferase (MGMT) methylation

	MGMT-met	MGMT -unmet	Total
IDH1-mut	5	10	15
IDH1-wt	49	26	75
Total	54	36	90

IDH1-mut = isocitrate dehydrogenase 1 mutation; IDH1-wt = isocitrate dehydrogenase 1 wildtype; MGMT-met = methyl guanine methyl transferase promoter methylation; MGMT-unmet = methyl guanine methyl transferase absence of promoter methylation

TABLE 3. Descriptive statistics for standardized test scores (z–values) and proportion of impaired patients in psychological cognitive functioning tests

Domain	Test	% impaired / all	N	% impaired / capable	Mean z score	SD of z scores
Visual – motor speed	TMT A	68	68	57	2.89	3.57
Executive function	TMT B	78	46	59	2.80	2.94
Verbal fluency	SCOWA	47	81	41	–1.21	0.88
Memory						
immediate recall	SVLT-ir	64	80	60	–1.83	1.11
short delayed recall	SVLT-sr	79		76	–2.05	1.31
delayed recall	SVLT-dr	63		58	–1.92	1.35
recognition	SVLT-recog	60		52	–2.73	3.36

SCOWA = Slovenian Controlled Oral Word Association Test; SVLT = Shiraz Verbal LearningTest; TMT A = Trail Making Test, Part A; TMT B = Trail Making Test, Part B

TABLE 4. Patient characteristics, regarding isocitrate dehydrogenase 1 (IDH1) mutation

	IDH1-wt (N = 75)	IDH1-mut (N=15)	Result of the statistical test and effect size
Age mean (min/max/SD)	61.50 (31 / 84 / 9.21)	38.75 (30 / 67 / 3.86)	t = -5.97, df = 88, p< 0.001
Sex (female / male)	29 / 46	4 / 11	$\chi2(1)$ = 0.775, f = -0.93, p = 0.379
Education level (≤ 9 years /10–13 years / 14–19 years / ≥ 20 years)	11 / 40 / 22 / 2	3 / 8 / 4 / 0	$\tau b(3)$ = -0.06, z = -0.83, p = 0.547
KPS (70/80/90/100)	31 / 34 / 7 / 3	1 / 3 / 11 / 0	$\tau b(3)$ = 0.403, z = 18.95, p < 0.001
WHO grade (III / IV)	1 /74	11 /4	$\chi2(1)$ = 56.08, f = -0.789, p < 0.001
Corticosteroids mg (min/max/SD)	2 (0 / 16 / 6)	5 (0 / 24 / 4.5)	t = -1.16, df = 88, p = 0.251
biopsy/reduction/gross tumour resection	9 / 44 / 22	2 / 5 / 8	$\chi2(2)$ = 3.65, V = 0.210, p = 0.161
Tumour location (frontal / temporal / parietal / occipital / diffuse / central)	26 / 20 / 21 / 4 / 2 / 2	8 / 1 / 5 / 0 / 1 / 0	NA
Hemisphere (right / left / both)	21 / 27 / 6	17 / 17 / 2	$\chi2(2)$ = 1.14, V = 0.113, p = 0.566
MGMT (yes / no)	10 / 5	26 /49	$\chi2(1)$ = 5.33,f = 0.24, p = 0.021

IDH1-mut = isocitrate dehydrogenase 1 mutation; IDH1-wt = isocitrate dehydrogenase 1 wild type; KPS = Karnoffsky performance status; MGMT = methyl guanine methyl transferase; NA = not available; SD = standard deviation

TABLE 5. Cognitive functioning regarding to isocitrate dehydrogenase 1 (IDH1) mutation

	IDH1–wt		IDH-mut		Result of the statistical test	IDH1–wt	IDH1-mut	Result of the statistical test
	N	Mean Z score (SD)	N	Mean Z score (SD)		% of impaired	% of impaired	
TMT A	53	3.12[1] (3.84)	15	2.06 (2.23)	U = 345.000, z = -0.77, df = 66, p= 0.437	72	46	$\chi2(1)$ = 3.67, V = 0.20, p = 0.055
TMT B	33	2.82[1] (3.11)	13	2.76 (2.57)	U = 221.500, z = -0.17, df = 66, p = 0.864	82	60	$\chi2(1)$ = 3.87, V = 0.21, p = 0.050
SCOWA	66	-1.28 (0.87)	15	-0.86 (0.84)	t = -1.69, df = 79, p = 0.095	51	27	$\chi2(1)$ = 2.89, V = 0.18, p = 0.089
SVLT-ir	65	-1.98 (1.06)	15	-1.15 (1.12)	t = -2.729, df = 78, p = 0.008	71	33	$\chi2(1)$ = 7.60, V = 0.29, p = 0.006
SVLT-sr	65	-2.20 (1.29)	15	-1.37 (1.22)	t = -2.25, df = 78, p = 0.027	84	53	$\chi2(1)$ = 7.06, V = 0.28, p = 0.008
SVLT-dr	65	-2.14 (1.27)	15	-0.98 (1.34)	t = -3.13, df = 78, p =0.002	69	33	$\chi2(1)$ = 6.98, V = 0.28, p = 0.008
SVLT-recog	65	-3.06[1] (3.54)	15	-1.24 (1.91)	U = 611.000, z = -2.25, df = 78, p = 0.023	29	26	$\chi2(1)$ = 3.00, V = 0.18, p = 0.083

[1] the distribution is significantly non-normal

IDH1-mut = isocitrate dehydrogenase 1 mutation; IDH1-wt = isocitrate dehydrogenase 1 wildtype;SCOWA = Slovenian Controlled Oral Word Association Test; SD = standard deviation; SVLT = Shiraz Verbal Learning Test; SVLT-dr = SVLT delayed recall; SVLT-ir = SVLT immediate recall; SVLT-recog = SVLT recognition; SVLT-sr = SVLT short delayed recall; TMT A = Trail Making Test, Part A; TMT B = Trail Making Test, Part B

functioning (measured with dichotomised test scores) (Table 5).

Patients with IDH1-mut had on average a statistically significantly lower number of impaired tests results than patients with IDH1-wt (M = 2.93, SD = 2.25*vs.* M = 4.93, SD = 1.99; U = 286.000, z = -3.04, p = 0.002). 5 (33%) patients with IDH1-mut tumours and 6 (8%) patients without IDH1-mut had at most one impaired result on cognitive tests; impaired results on 2–4 tests had 5 (33%) *vs.* 21 (28%). Impaired scores on more than 5 tests had 5 (33%) *vs.* 48 (64%).

TABLE 6. Patient characteristics regarding methyl guanine methyl transferase (MGMT) methylation

	MGMT-unmet (N=54)	MGMT-met (N = 36)	Result of the statistical test and effect size
Age mean (min/max/SD)	58.94 (31 / 84 / 10.42) 1	58,53 (30 / 78 / 12.67)	t = -0.17, df = 88, p = 0.86
Sex (female / male)	19 / 35	14 / 22	$\chi2(1)$ = 0.13, f = 0.04, p = 0.721
Education level (≤9 years /10–13 years / 14–19 years / ≥ 20 years)	8 / 19 / 11 / 0	9 / 29 / 15 / 2	τb (3) = -0.03, z = -1.41, p = 0.776
KPS (70/80/90/100)	20 / 23 / 9 / 2	12 / 14 / 9 /1	τb (3) =0.06, z = 2.82, p = 0.541
WHO grade (III / IV)	3 / 51	9 / 27	$\chi2(1)$ = 7.07, f= -0.28, p = 0.008
Corticosteroids mg (min/max/SD)	5.67 (0 /24 / 5,04)	5.48 (0 / 16 / 4.22)	t = 0.18, df = 88, p = 0.857
Biopsy/reduction/gross tumour resection	9 / 31 / 14	2 / 18 / 16	$\chi2(2)$ = 4.62, V = 0.23, p = 0.099
Tumour location (frontal / temporal / parietal / occipital / diffuse / central)	26 / 20 / 21 / 4 / 2 / 2	8 / 1 / 5 / 0 / 1 / 0	NA
Hemisphere (right / left / both)	28 / 40 / 7	10 / 4 / 1	$\chi2(2)$ = 4.46, V = 0.223, p = 0.107
IDH1 (yes / no)	5 / 49	10 / 26	$\chi2(1)$ = 5.33, f = 0.24, p = 0.021

IDH1 = isocitrate dehydrogenase 1; MGMT-met = methyl guanine methyl transferase promoter methylation; MGMT-unmet = methyl guanine methyl transferase absence of promoter methylation; KPS = Karnoffsky performance status; SD = standard deviation

We found no differences between groups with regard to self-evaluation of cognitive functioning problems; the mean rating was 3.60,SD = 2.81, in patients with IDH1-mut tumours *vs*. 3.67, *SD* = 2.95 in patients with IDH1-wt (U = 579.000, z = 0.18, p = 0.857); 40 (53%) patients with IDH1-wt tumour gave a self-assessment of 0–3 *vs*. 8 (53%) patients with IDH1-mut, score 4–6 was given by 18 (24%) *vs*. 5 (33%) patients and a score above 7 17 (23%) *vs*. 2 patients (13%).

We also compared demographic characteristics in patients with and without MGMT promoter

TABLE 7. Cognitive functioning regarding methyl guanine methyl transferase (MGMT) methylation

	MGMT-met		MGMT-unmet		Result of the statistical test	MGMT-met	MGMT –unmet	Result of the statistical test
	N	Mean Z score (SD)	N	Mean Z score (SD)		% of impaired	% of impaired	
TMT A	26	2.67 (3.01)	42	3.03[1] (3.90)	U = 530.000, z = -0.20, df = 67, p = 0.840	69	66	$\chi2(1)$ = 0.08, V = 0.03, p = 0.782
TMT B	20	3.22 (2.30)	26	2.48[1] (3.37)	U = 334.000, z = 1.64, df = 45, p = 0.101	86	74	$\chi2(1)$ = 1.88, V = 0.14, p = 0.170
SCOWA	33	-1.25 (0.87)	48	-1.18[1] (0.89)	U = 756.000, z = -0.35, df = 70, p = 0.729	50	44	$\chi2(1)$ = 0.27, V = 0.05, p = .605
SVLT-ir	32	-1.85 (1.27)	48	-1.82[1] (1.01)	U = 771.000, z = 0.03, df = 78, p = 0.975	64	67	$\chi2(1)$ = 0.01, V = 0.01, p = 0.928
SVLT-sr	32	-2.03 (1.32)	48	-2.06 (1.32)	t = 0.09, df = 78, p = 0.926	75	81	$\chi2(1)$ = 0.54, V = 0.08, p = 0.460
SVLT-dr	32	-1.98 (1.52)	48	-1.89 (1.25)	t = -0.30, df = 78, p = 0.763	66	61	$\chi2(1)$ = 0.29, V = 0.06, p = 0.592
SVLT- recog	32	-2.731 (4.24)	48	-2.72[1] (2.71)	U = 784.000, z = 0.828, df = 78, p = 0.407	58	61	$\chi2(1)$ = 0.07, V = 0.03, p = 0.792

[1]the distribution is significantly non-normal

MGMT-met = methyl guanine methyl transferase promoter methylation; MGMT-unmet = methyl guanine methyl transferase absence of promoter methylation; SD = standard deviation; SVLT = Shiraz Verbal Learning Test; SVLT-dr = SVLT delayed recall; SVLT-ir = SVLT immediate recall; SVLT-recog = SVLT recognition; SVLT-sr = SVLT short delayed recall; TMT A = Trail Making Test, Part A; TMT B = Trail Making Test, Part B

methylation. The patients differed in the tumour grade. Despite the predominance of Grade IV tumours in our sample, the methylated phenotype was more prevalent in Grade III patients (25% *vs*. 5%, $\chi 2(1) = 7.067$, $V = 0.28$, $1 - \beta = 0.757$, $p = 0.008$). In all other demographic characteristics, the groups were comparable.

In the cognitive functioning, there were no differences in mean z-scores or dichotomized test scores between patients with methylated and unmethylated promoter MGMT (Table 7).

There were no statistically significant differences in self-evaluation of cognitive functioning problems; the mean number of impaired results were 4.50 ($SD = 1.90$) in patients with MGMT un-methylated tumours *vs*. 4.29 ($SD = 1.75$), $U = 1100.000$, $z = 1.51$, $p = 0.251$.

There were also no differences in the number of tests in which patients achieved an impaired result ($U = 1052.500$, $z = 0.67$, $p = 0.501$). With the mean 4.69 ($SD = 2.31$) and 4.54 ($SD = 2.07$) had 5 (14%) patients with MGMT methylated tumours and 6 (11%) patients MGMT unmethylated tumours at most one impaired result, 2–4 impaired results had 9 (25%) *vs*. 17 (31%) patients, and on more than 5 tests the results were impaired in 22 (61%) *vs*. 31 (57%) patients.

Discussion

High-grade glioma patients are experiencing a number of cognitive functioning problems. In our study we focused on the period following the surgical treatment and before commencement of systemic treatment.

The majority of cognitive problems we found were in the fields of executive functions, visual-motor speed and verbal memory, especially immediate and short delayed recall, as well delayed recall. There were the least problems in the field of verbal fluency, but even here more than 40% of patients had an impaired result. Among participating patients, only 12% had an impaired result in up to one measured field, while 60% had impaired results in the majority of the measured domains.

The analysis of cognitive test scores expressed as z-values gave conclusions comparable to the ones obtained with the analysis of dichotomized scores. The use of dichotomized scores enabled us to also include in the analyses the results of patients who were unable to complete some tests and so avoiding the overrepresentation of patients with better cognitive functioning in the analyses.

These results are in accordance with other studies examining cognitive functions in high-grade glioma patients, but it is noticeable that in our study the proportion of patients presenting with the "impaired" result is higher, possibly due to the fact that our study included the entire cohort of high-grade glioma patients. When comparing the results of different studies, it is necessary to consider the use of different criteria for impairment, with the otherwise dominant criterion $z < -1.5$.[5]

In comparison with IDH1-wt patients, patients with IDH1-mut (17%), were significantly younger, had better performance status and more often they had Grade III tumour. This is in line with previous studies.[27]

Additionally, the cognitive functioning of patients with IDH1-mut was statistical significantly better in verbal memory and executive functions. Immediate recall, short-delayed and long-delayed recall differ statistically significantly in the analysis of interval variables as well as in the analysis of dichotomized variables. Executive functions measured with the TMT B test only in the analysis of dichotomized variables, which may be the result of the fact that a larger proportion of patients were unable to complete this test, therefore, they are not included in the analysis of interval variables. Patients with IDH1-mut tumours achieved impaired results on significantly lower number of tests. These findings are in line with findings of the previous studies.[8,19]

According to the MGMT promoter methylation status, the groups did not differ statistically significantly in demographic data. A statistically significant difference was found in the expression of MGMT methylation according to the grade of the tumour (75% patients with grade III *vs*. 34% with grade IV).[28] We did not find differences in any of the analysed fields of cognitive functioning and also not in the number of tests in which patients achieved an impaired result.

We intended to include all patients with the diagnosis of high-grade glioma in the observed period in Slovenia. Given that, after surgery in one of the two centres in Slovenia, all newly diagnosed patients with gliomas are referred to our institution for evaluation regarding further treatment; it gives us an insight into the entire population of patients with glioma. Data collected on the entire cohort of patients revealed that a large proportion of high-grade glioma patients is unable to participate in the studies of cognitive functioning. In our case 46% of patients were unable to participate due to poor performance status or other somatic factors.

The finding that a large proportion of patients are unable at all to participate in cognitive functioning studies additionally indicates an over-representation of patients with better cognitive functioning in research. From this point of view the cohort study design corresponds better to the everyday clinical practice with the patients with high grade glioma.

Patients' self-assessments on a 1–10 scale did not correlate with the results of the tests used and probably should not be used for any assessment of cognitive functioning; we only found a weak correlation between self-assessment on a 10-point scale and objective assessment. With otherwise different methodology, foreign studies also came to similar results - there is no or weak correlation between subjective assessment and psychological tests.[29]

The limitation of our study is lack of data on cognitive functioning prior to surgical treatment. Thus, in the study we did not include eventual differences between patients with IDH1 mutated and wildtype tumours, which may be present even before surgery[19,30], which would also be important in the light of research findings regarding the different dynamics of cognitive decline after surgery.[31]

Another point worth mentioning is that several papers showed that epilepsy and the use of antiepileptics is an important factor of neurocognitive functioning. But in our sample, the use of antiepileptics could not be analysed as virtually every patient has received them following surgery even those without history of seizures; though in these cases they were weaned from antiepileptics at the beginning of oncological treatment.

Our study took place during the coronavirus pandemics. Despite this, oncological treatment was not interrupted nor delayed, but in our study, it was connected with the increase of patients refusing to participate and with longer time from surgery to the start of treatment due to infections.

It is worth to mention that targeting this population is beyond single institution capabilities. While the cohort study corresponds better to the clinical practice, on the other hand the low number of the mutations, especially in IDH1, is hampering the statistical analysis. When conducting our study, we noted a distinctive lack of prospective data regarding patients in suboptimal performance status, thus overestimating cognitive functioning of high-grade glioma patients. Even as we observed the patients in WHO performance status of 2 the number of cognitive patients rose markedly.

It is true that the single centre study is limited in its power to demonstrate effect the genetic and molecular changes exert on cognitive functioning in real life scenarios, the reason being rightly, that outside the trials where cognitive functioning is one of secondary outcomes to survival and time to progression where treatment compliance effectively excludes patients with more pronounced impairments and in reality the cognitive impairment is more widespread in our patients than reported previously, which should be taken into account in designing further studies.

Our study has finished recruiting, but the longitudinal part of the follow up is continuing, thus giving us the chance to determine the impact of genetic and epigenetic changes on cognitive functioning in patients surviving longer and maybe even determining if cognition can be used as predictive marker for progression.

References

1. Louis DN, Ohgaki H, Wiestler OD, Cavenee WK, Burger PC, Jouvet A, et al. The 2007 WHO classification of tumours of the central nervous system. *Acta Neuropathol* 2007;**114:** 97-109. doi: 10.1007/s00401-007-0243-4
2. Smrdel U, Popovic M, Zwitter M, Bostjancic E, Zupan A, Kovac V, et al. Long-term survival in glioblastoma: methyl guanine methyl transferase (MGMT) promoter methylation as independent favourable prognostic factor. *Radiol Oncol* 2015; **50:** 394-401. doi: 10.1515/raon-2015-0041
3. Millward CP, Brodbelt AR, Haylock B, Zakaria R, Baborie A, Crooks D, et al. The impact of MGMT methylation and IDH-1 mutation on long-term outcome for glioblastoma treated with chemoradiotherapy. *Acta Neurochir* 2016; **158:** 1943-53. doi: 10.1007/s00701-016-2928-8
4. Kurdi M, Shafique Butt N, Baeesa S, Alghamdi B, Maghrabi Y, Bardeesi A, et al. The impact of IDH1 mutation and MGMT promoter methylation on recurrence-free interval in glioblastoma patients treated with radiotherapy and chemotherapeutic agents. *Pathol Oncol Res* 2021; **27:** 1609778. doi: 10.3389/pore.2021.1609778
5. Sinha R, Stephenson JM, Price SJ. A systematic review of cognitive function in patients with glioblastoma undergoing surgery. *Neuro-oncology Pract* 2020; **7:** 131-42. doi: 10.1093/nop/npz018
6. Van Kessel E, Emons MAC, Wajer IH, Van Baarsen KM, Broekman ML, Robe PA, et al. Tumor-related neurocognitive dysfunction in patients with diffuse glioma: a retrospective cohort study prior to antitumor treatment. *Neuro-Oncology Pract* 2019; **6:** 463. doi: 10.1093/nop/npz008
7. Taphoorn MJB, Klein M. Cognitive deficits in adult patients with brain tumours. *Lancet Neurology* 2004; **3:** 159-68. doi: 10.1016/S1474-4422(04)00680-5
8. Jütten K, Mainz V, Gauggel S, Patel HJ, Binkofski F, Wiesmann M, et al. Diffusion tensor imaging reveals microstructural heterogeneity of normal-appearing white matter and related cognitive dysfunction in glioma patients. *Front Oncol* 2019; **9:** 536. doi: 10.3389/fonc.2019.00536
9. Van Kessel E, Snijders TJ, Anniek ·, Baumfalk E, Ruis C, Van Baarsen KM, et al. Neurocognitive changes after awake surgery in glioma patients: a retrospective cohort study. *J Neurooncol* 2020; **146:** 97-109. doi: 10.1007/s11060-019-03341-6
10. Meyers CA, Hess KR. Neuro-oncology multifaceted end points in brain tumor clinical trials: cognitive deterioration precedes MRI progression. *Neuro-Oncology*2003; **5:** 89-95. doi: 10.1093/neuonc/5.2.89
11. Armstrong CL, Goldstein B, Shera D, Ledakis GE, Tallent EM. The predictive value of longitudinal neuropsychologic assessment in the early detection of brain tumor recurrence. *Cancer* 2003; **97:** 649-56. doi: 10.1002/cncr.11099

12. Flechl B, Sax C, Ackerl M, Crevenna R, Woehrer A, Hainfellner J, et al. The course of quality of life and neurocognition in newly diagnosed patients with glioblastoma. *Radiother Oncol* 2017; **125:** 228-33. doi: 10.1016/j.radonc.2017.07.027

13. Johnson DR, Sawyer AM, Meyers CA, Patrick B, Neill O', Wefel JS. Early measures of cognitive function predict survival in patients with newly diagnosed glioblastoma. *Neuro Oncol* 2012; **14:** 808-16. doi: 10.1093/neuonc/nos082

14. Meyers CA, Hess KR, Yung WKA, Levin VA. Cognitive function as a predictor of survival in patients with recurrent malignant glioma. *J Clin Oncol* 2000; **18:** 646-50. doi: 10.1200/JCO.2000.18.3.646

15. Lee ST, Park CK, Kim JW, Park MJ, Lee H, Lim JA, et al. Early cognitive function tests predict early progression in glioblastoma. *Neuro-oncology Pract* 2015; **2:** 137-43. doi: 10.1093/nop/npv007

16. Butterbrod E, Synhaeve N, Rutten GJ, Schwabe I, Gehring K, Sitskoorn M. Cognitive impairment three months after surgery is an independent predictor of survival time in glioblastoma patients. *J Neurooncol* 2020; **149:** 103-11. doi: 10.1007/s11060-020-03577-7

17. Derks J, Kulik S, Wesseling P, Numan T, Hillebrand A, van Dellen E, et al. Understanding cognitive functioning in glioma patients: the relevance of IDH-mutation status and functional connectivity. *Brain Behav* 2019; **9:** e01204.doi: 10.1002/brb3.1204

18. van Kessel E, Snijders TJ, Baumfalk AE, Ruis C, van Baarsen KM, Broekman ML, et al. Neurocognitive changes after awake surgery in glioma patients: a retrospective cohort study. *J Neurooncol* 2020; **146:** 97-109. doi: 10.1007/s11060-019-03341-6

19. Wefel JS, Noll KR, Rao G, Cahill DP. Neurocognitive function varies by IDH1 genetic mutation status in patients with malignant glioma prior to surgical resection. *Neuro Oncol* 2016; **18:** 1656-63. doi: 10.1093/neuonc/now165

20. Bunevicius A, Miller J, Parsons M. Isocitrate dehydrogenase, patient-reported outcomes, and cognitive functioning of glioma patients: a systematic review. *Curr Oncol Rep* 2020; **22:** 120. doi: 10.1007/s11912-020-00978-9

21. Weller J, Tzaridis T, Mack F, Steinbach JP, Schlegel U, Hau P, et al. Health-related quality of life and neurocognitive functioning with lomustine-temozolomide versus temozolomide in patients with newly diagnosed, MGMT-methylated glioblastoma (CeTeG/NOA-09): a randomised, multicentre, open-label, phase 3 trial. *Lancet Oncol* 2019; **20:** 1444-53. doi: 10.1016/S1470-2045(19)30502-9

22. Wang Q, Xiao F, Qi F, Song X, Yu Y. Risk factors for cognitive impairment in high-grade glioma patients treated with postoperative radiochemotherapy. *Cancer Res Treat* 2020; **52:** 586-93. doi: 10.4143/crt.2019.242

23. Herzog A. [Validity and reliability of the new Slovenian Test of Word Learning]. [Slovenian]. [graduation thesis]. Ljubljana: Universty of Ljubljana; 2015.

24. Remšak T. [Development of the Spelling Fluency Test]. [Slovenian]. [graduation thesis]. Ljubljana: Universty of Ljubljana; 2013.

25. Sánchez-Cubillo I, Periáñez JA, Adrover-Roig D, Rodríguez-Sánchez JM, Ríos-Lago M, Tirapu J, et al. Construct validity of the Trail Making Test: role of task-switching, working memory, inhibition/interference control, and visuomotor abilities. *J Int Neuropsychol Soc* 2009; **15:** 438-50. doi: 10.1017/S1355617709090626

26. Wefel JS, Vardy J, Ahles T, Schagen SB. International Cognition and Cancer Task Force recommendations to harmonise studies of cognitive function in patients with cancer. *Lancet Oncol* 2011; **12:** 703-8. doi: 10.1016/S1470-2045(10)70294-1

27. Iorgulescu JB, Sun C, Neff C, Cioffi G, Gutierrez C, Kruchko C, et al. Molecular biomarker-defined brain tumors: epidemiology, validity, and completeness in the United States. *Neuro Oncol* 2022; **24:** 1989-2000. doi: 10.1093/neuonc/noac113

28. Capper D, Mittelbronn M, Meyermann R, Schittenhelm J. Pitfalls in the assessment of MGMT expression and in its correlation with survival in diffuse astrocytomas: proposal of a feasible immunohistochemical approach. *Acta Neuropathol* 2008; **115:** 249-59. doi: 10.1007/s00401-007-0310-x

29. Tucha O, Smely C, Preier M, Lange KW. Cognitive deficits before treatment among patients with brain tumors. *Neurosurgery* 2000; **47:** 324-33. doi: 10.1097/00006123-200008000-00011

30. Kesler SR, Noll K, Cahill DP, Rao G, Wefel JS. The effect of IDH1 mutation on the structural connectome in malignant astrocytoma. *J Neurooncol* 2017; **131:** 565-74. doi: 10.1007/s11060-016-2328-1

31. Van Kessel E, Snijders TJ, Anniek·, Baumfalk E, Ruis C, Van Baarsen KM, et al. Neurocognitive changes after awake surgery in glioma patients: a retrospective cohort study. *J Neurooncol* 2020; **146:** 97-109. doi: 10.1007/s11060-019-03341-6

research article

Changes in the quality of life of early breast cancer patients and comparison with the normative Slovenian population

Cvetka Grasic Kuhar[1,2], Tjasa Gortnar Cepeda[3], Christian Kurzeder[4], Marcus Vetter[5]

[1] Institute of Oncology Ljubljana, Department Medical Oncology, Ljubljana, Slovenia
[2] Faculty of Medicine, University of Ljubljana, Ljubljana, Slovenia
[3] Jesenice General Hospital, Jesenice, Slovenia
[4] Breast Center, University Hospital Basel, Basel, Switzerland
[5] Cancer Center Baselland, Cantonal Hospital Baselland, Liestal, Switzerland

Radiol Oncol 2023; 57(2): 211-219.

Received 27 November 2022
Accepted 26 December 2022

Correspondence to: Assist. Prof. Cvetka Grašič Kuhar, M.D., Ph.D., Institute of Oncology Ljubljana, 1000 Ljubljana, Slovenia.
E-mail: cgrasic@onko-i.si

Disclosure: No potential conflicts of interest were disclosed.

Background. We aimed to identify changes in quality of life after breast cancer treatment and compare them with the normative population data for the Slovenian population.

Patients and methods. A prospective, single-group, cohort design was used. A total of 102 early breast cancer patients treated with chemotherapy at the Institute of Oncology Ljubljana were included. Of those, 71% returned the questionnaires after one-year post-chemotherapy. The Slovenian versions of the European Organisation for Research and Treatment of Cancer (EORTC) QLQ C30 and BR23 questionnaires were used. Primary outcomes were a comparison of global health status/quality of life (GHS) and C30 Summary Score (C30-SumSc) at baseline and one-year post-chemotherapy with the normative Slovenian population. The exploratory analysis evaluated the differences in symptoms and functional scales of QLQ C-30 and QLQ BR-23 between baseline and one-year post-chemotherapy.

Results. At baseline and one-year post-chemotherapy, C30-SumSc of patients was lower than the predicted C30-SumSc from the normative Slovenian population by 2.6 points ($p = 0.04$) and 6.5 points ($p < 0.001$), resp. On the contrary, GHS was not statistically different from predicted either at baseline or after one year. Exploratory analysis revealed that one-year post-chemotherapy compared to the beginning of chemotherapy, patients had statistically significantly and clinically meaningful lower scores in body image and cognitive functioning, and increased symptom scores for pain, fatigue, and arm symptoms.

Conclusions. The C30-SumSc is reduced one- year post-chemotherapy. Early interventions should be directed toward the prevention of the decline of cognitive functioning and body image, and to alleviate fatigue, pain, and arm symptoms.

Key words: breast cancer; chemotherapy; quality of life; cognitive dysfunction; fatigue

Introduction

Global cancer statistics for 2020 estimated 2,261,419 new cases of breast cancer worldwide, which represents 11.7% of all cancers. It became the most common cancer in humans, surpassing lung cancer incidence.[1] Breast cancer survivors represent a large group of long-term cancer survivors with different health issues during and after treatment. According to Slovenian Cancer Registry data in 2019, breast cancer survivors (19.455), represent 14.3% of all cancer survivors (136.500).[2] Half of the

Slovenian breast cancer cases are diagnosed in women in the 20–65 age group, which means they are active in their professional careers and family life.

Patients with early breast cancer receive multimodal cancer treatment (surgical and/or systemic treatment including chemotherapy, targeted therapy, and endocrine therapy, and/or radiotherapy). The treatment they receive greatly affects their quality of life (QoL). For example, surgery and radiation therapy could cause local side effects, like breast and arm pain, and arm lymphoedema, however, systemic therapy could have numerous acute or long-lasting systemic side effects (nausea, neuropathy, cardiotoxicity, fatigue, cognitive dysfunction etc.). Thus, comprehensive cancer therapy affects many functional or symptom scales of QoL. However, families and employers expect patients to recover fully in a short time.

Nowadays, QoL becomes also more and more important in terms of drug development. With the validated quality of life questionnaires (QLQ), specifically the European Organisation for Research and Treatment of Cancer (EORTC) core questionnaire (QLQ C30) and breast module (QLQ BR23)[3,4], we can monitor the impact of treatment on patient-reported outcomes (PROs), like global health status/QoL and summary score, and compare different modules and symptoms over time.[5] What is the QoL at the transition from treatment to survivorship where a woman is expected to be back to work? Arm symptoms and fatigue, as well as cognitive and physical dysfunction and work-related variables (e.g., physical demands at work), interfered with the ability to perform work. Schmidt *et al*. found associations between depressive symptoms, arm symptoms, lower education, and younger age with an impaired return to work after one year.[6] Self-reported reasons that hinder the return to work were fatigue and cognitive problems.[6,7] Additionally, social and personal factors influence the functioning and working ability of individuals.

Identifying dysfunctions that disable patients after breast cancer treatment and comparing QoL of patients with the normative population data[8,9] could help caregivers provide survivors with more optimal care. They may benefit from specific interventions.

The aim of our study was to prospectively evaluate PROs in the cohort of early breast cancer patients at the start of chemotherapy and one year after the end of chemotherapy and to compare them with normative data for the Slovenian population. In our explorative analysis, we aimed to determine which functional and symptom scales appeared different one year after chemotherapy.

Patients and methods

Participants

Our current study cohort consisted of early breast cancer patients including all subtypes who had taken part in our previous prospective non-randomized cohort study evaluating the impact of mobile app use for symptom management on PROs during chemotherapy treatment. The inclusion criteria in the aforementioned study were patients with early breast cancer, treated with chemotherapy, possessing an Android-based smartphone for symptom reporting, and willing to fill in paper and pencil questionnaires reporting their quality of life while receiving treatment.[10]

In the current prospective study, we included 102 patients who had signed informed consent for the former study and were willing to fill in the additional QLQ C30, QLQ BR23, and socioeconomic questionnaires one year after the end of chemotherapy. Our first aim was to evaluate and compare pre-treatment and post-treatment PROs with normative data for the Slovenian population.[11] This reference data on QLQ-C30 dimensions was obtained on 1231 healthy Slovenian individuals. Our second aim was to compare the post-treatment health-related quality of life (HRQoL) with the pre-treatment one. This data has not been reported yet.

Study design

A prospective, single-group, cohort design was used combining data from a former two-arm trial with new follow-up data collected one year after the end of chemotherapy.[10] Patients who were admitted for treatment with chemotherapy at the Institute of Oncology Ljubljana between December 2017 and September 2018 were eligible (Figure 1). Inclusion criteria were breast cancer stage I-III, treatment with neoadjuvant or adjuvant chemotherapy, and proficiency in using an Android-based smartphone. Exclusion criteria were stage IV breast cancer, a lack of mobile device proficiency or using non-Android-based smartphones, and not understanding Slovenian. In addition to chemotherapy treatment, patients were treated with anti-HER2 therapy (in case of HER2 positivity), surgery, endocrine therapy in case of hormone-receptor-

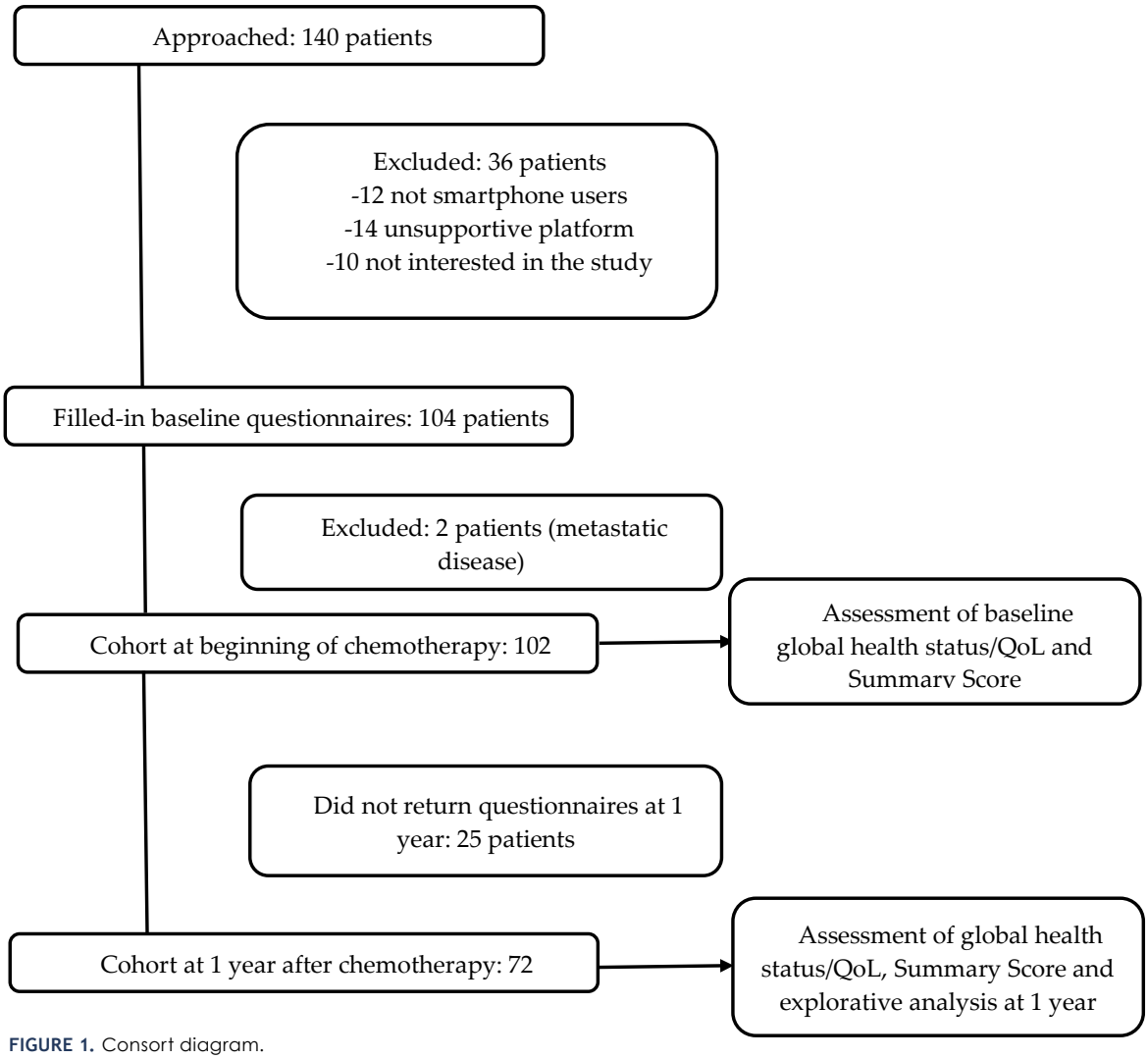

FIGURE 1. Consort diagram.

positive disease, according to ESMO guidelines, and radiation therapy, if indicated.[12] The patient's demographic characteristics and type of treatment were collected from patient charts. Ethical approval for this study had been obtained from the Ethics Committee of the Institute of Oncology Ljubljana (ERID-EK-43 and ERID-EK-0080/2019). All patients had given their written informed consent.

Instruments

We used the Slovenian version of EORTC QLQ C30 and QLQ BR23 questionnaires. QLQ C30 is a core questionnaire which includes 30 items, consisting of 5 functional scales (cognitive, emotional, physical, social and role functioning), 9 symptom scales, and two questions which include the patient's assessment of global health status/quality of life (GHS). QLQ BR23 has 23 questions comprising four functional scales (body image, sexual functioning, sexual enjoyment, future perspectives) and symptoms regarding the treatment of breast cancer (systemic therapy side effects, arm and breast symptoms and others). Socio-economic questionnaires, used routinely for surveys at the Slovenian Cancer Registry, included questions about age, gender, social class, employment, marital status, education, and place of residence.

Outcome measures

Our primary outcomes were GHS and C30 Summary Score (C30-SumSc), derived from EORTC QLQ C30. Symptoms and functional scales of QLQ C30 and QLQ BR23 were used in the exploratory analysis only. The EORTC Quality of Life

TABLE 1. Clinical characteristics of participants at beginning of the study and after one-year post-chemotherapy

Characteristic	At inclusion-before chemotherapy (n = 102) n (%)	One year after end of chemotherapy (n = 71) n (%)
Tumour stage		
T1	6 (45.1)	32 (44.4)
T2	43 (42.2)	33 (45.8)
T3	13 (12.7)	7 (9.7)
Lymph node stage		
N0	43 (42.2)	31 (43.1)
N1	38 (37.3)	30 (41.7)
N2	12 (11.8)	9 (12.5)
N3	9 (8.8)	2 (2.8)
Tumour subtype		
Luminal A-like	12 (11.8)	7 (9.7)
Luminal B-like	47 (46.1)	35 (48.6)
Luminal B HER2 positive	19 (18.6)	14 (19.4)
HER2 positive	8 (7.8)	6 (8.3)
Triple-negative	16 (15.7)	10 (13.9)
Type of surgery		
Breast-conserving surgery + Sentinel node biopsy	37 (36.3)	28 (38.9)
Breast-conserving surgery + Axillary dissection	14 (13.7)	11 (15.3)
Mastectomy + Sentinel node biopsy	23 (22.5)	15 (20.8)
Mastectomy + Axillary dissection	28 (27.5)	18 (25.0)
Breast reconstruction		
None	78 (76.5)	55 (76.4)
Deep inferior flap	13 (12.7)	10 (13.9)
Tissue expander, followed by silicone implant	11 (10.8)	7 (9.7)
Chemotherapy type		
Anthracyclines and taxanes	70 (68.7)	51 (70.8)
Anthracyclines only	19 (18.6)	13 (18.1)
Taxanes only	10 (9.8)	6 (8.3)
CMF	3 (2.9)	2 (2.8)
Anti-HER2 therapy	27 (26.4)	20 (27.8)
Adjuvant endocrine therapy	78 (76.5)	57 (79.2)
Radiotherapy	81 (79.4)	59 (81.9)

CMF = cyclophosphamide, methotrexate, fluorouracil; HER2 = human epidermal growth factor receptor 2

Scoring Manual was followed.[13] All scales had values from 0 to 100, where 100 represented the best GHS, the best functioning, or the worst symptoms. The C30-SumSc, which ranged from 0 (worst) to 100 (best), was calculated from 13 out of 15 EORTC QLQ C30 scales (the GHS and financial difficulties scale were excluded) in accordance with Giesinger *et al*. and instructions from the EORTC.[5,14] The patient's assessment of the clinical significance of changes in QLQ C30 and QLQ BR23 scores were interpreted as "slight" change either for better or for worse when the mean change in scores was about 5 to 10 points; "moderate" change for about 10 to 20 points; and "severe" change greater than 20 points. An established threshold for a clinically meaningful difference in QoL was previously set to 10 points.[15]

Data for GHS and C30-SumSc data for the normative Slovenian population were obtained from recently published work by Velenik *et al*.[11] We computed each patient's predicted normative values for C30-SumSc and GHS (co-primary outcomes) according to this external reference.[11] Using the patient's age (categorized as 18–39, 49–59, 60+) and self-rated social class (lower, middle, higher), the predicted normative value represented the patient's scores if she had not had cancer.

Statistical analysis

Categorical variables were summarized with frequencies and percentages. Numerical variables were described with means and standard deviations (or medians and interquartile ranges if distributions were asymmetric).

We compared the mean C30-SumSc and GHS of our patients with the normative general Slovenian population.[11] The mean C30-SumSc and GHS at the start of chemotherapy and one-year post-chemotherapy were compared with the corresponding mean of the normative values using two-tailed one-sample t-tests as the variability for the normative values could not be considered (the normative values were computed from the estimates from the article,[11] standard errors of the estimates were not reported).

As a part of the exploratory analysis, we performed a comparison of the GHS, C30-SumSc and QLQ C30 and QLQ BR23 scales between inclusion (start of chemotherapy) and after one year in a smaller group (72 patients) that had available data on both times. For statistical comparison of scales based on at least two questions, we calculated the average difference and 95% confidence intervals ([After 1 year] – [At inclusion]) with two-tailed paired t-tests and 95% confidence intervals (CIs). For scales based on one question, we performed Wilcoxon's test of predicted ranks.

For all scales but C30-SumSc and GHS (primary outcomes), the corresponding p-values were adjusted using the Holm method to control the family-wise error rate as so many hypotheses were tested. Corrected p-values allow a conclusion per population, but uncorrected ones do not.

An (adjusted) p-value smaller than 0.05 was considered statistically significant. Analyses were performed using R statistical software (version 3.6.3)[16] and SPSS v.24.0 (IBM Corporation).

TABLE 2. Patient-reported outcomes presented by EORTC C30 Summary Score (C-30 SumSc) and global health status/quality of life (GHS) at inclusion (beginning of chemotherapy), one-year post-chemotherapy, and the difference among both times

		Predicted	At inclusion		At 1 year		[1 year] - [At inclusion]	
	n	mean	Mean (95% CI)	p	Mean (95% CI)	p	Mean (95% CI)	p
C-30 SumSc	70	90.9	88.5 (86.1, 90.8)	0.04	82 (78.4, 85.5)	< 0.001	-6.5 (-9.6, -3.4)	< 0.001
GHS	71	72.7	71.1 (66.7, 75.6)	0.50	69.6 (65, 74.2)	0.19	-1.5 (-6.6, 3.5)	0.55

EORTC = European Organisation for Research and Treatment of Cancer

Results

Participants

At the beginning of chemotherapy, we included 102 patients (Table 1, left column). These patients were compared with the normative Slovenian population regarding baseline GHS and C30-SumSc. Seventy-two patients (71%) returned questionnaires at one-year post-chemotherapy (Table 1, right column). The median age of this cohort was 51.5 years. 44% of patients were T1 and 43% were node-negative. Regarding subtype, 49% were luminal B-like, 19% luminal HER2+, 8% HER2+ non-luminal, 14% were triple negative and 10% were luminal A-like. The most common type of surgery was breast-conserving surgery with sentinel node biopsy (39%). All patients were treated with chemotherapy (adjuvant (69%) or neoadjuvant (31%)), 28% had anti-HER2 treatment, and 79% had adjuvant endocrine therapy. 82% of patients received adjuvant radiation therapy. Patients' socioeconomic characteristics are available in Supplementary Table 1. For the calculation of predicted normative values of GHS and C30-SumSc, gender, age, and social class were used, according to Velenik *et al*.[11] Their model was based on 1231 persons, of them 612 (49.7%) were females. The age distribution of females was: 30.7% in cohort 18-39 years, 42.8% in cohort 40-59 years, and 26.5% in cohort 60-90 years. Self-rated social status of females was: 30.9% belonged to the lower, 57.4% to the middle, and 11.8% to the upper social class.[11]

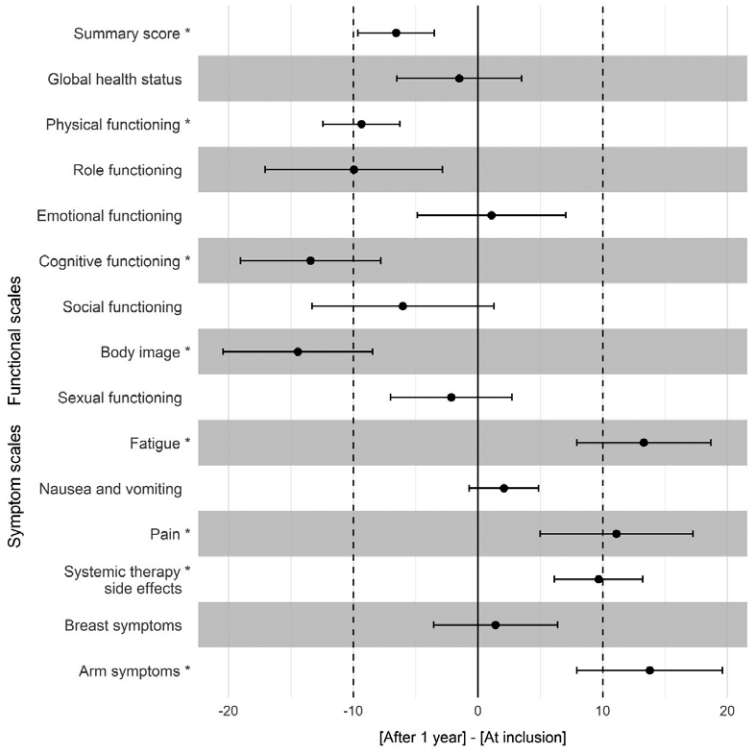

BR-23 = breast module 23 questionnaire; EORTC: European Organisation for Research and Treatment of Cancer

*Modules whose p-value is statistically significant (p < 0.05);

FIGURE 2. Difference of the global health status/quality of life (GHS), C-30 Summary Score (C-30 SumSc), and functional and symptoms scales of EORTC C-30 and BR-23 questionnaires.

Primary outcomes

At inclusion (before the start of chemotherapy), C30-SumSc of our patients was statistically significantly lower than the predicted C30-SumSc in the general Slovenian population, namely by 2.6 points (p = 0.04). After one year, compared to the start of chemotherapy, patients' mean C30-SumSc decreased by 6.5 points, which was statistically significant (p < 0.001), from the patient perspective as a slight change for worse, but not clinically meaningful change (Table 2, Figure 2 - first line). On the contrary, GHS was not statistically or clinically significantly different from predicted either at inclusion or after 1 year (Table 2, Figure 2 - second line).

Exploratory analysis

The exploratory analysis (Figure 2) revealed that patients had significantly lower functioning one year after chemotherapy compared to the beginning of chemotherapy in 3 functional scales: in body image and cognitive functioning, the difference in our sample was > 10 points (clinically meaningful change), and in physical functioning under 10 points (clinically not meaningful). Similarly, pain, fatigue, and arm symptoms score significantly increased by more than 10 points (clinically meaningful), and systemic therapy side effects increased by less than 10 points (clinically not meaningful).

Discussion

At the start of chemotherapy, early breast cancer patients had the same mean GHS as predicted from the general Slovenian population. C30-SumSc was statistically significantly lower, although this was not clinically significant since the difference was less than 10 points.

GHS in breast cancer patients one year after the end of chemotherapy was on average as good as before the beginning of chemotherapy. C30-SumSc was statistically significantly worse, from the patient's perspective as a slight change for worse, although deterioration of 6.5 points is not considered clinically important. In the exploratory analysis, we found significant deterioration in some functional scales and increased symptoms in breast cancer patients one-year post-chemotherapy compared to the pre-chemotherapy state. Cognitive functioning, body image, and physical functioning significantly deteriorated. Among symptoms, increased arm symptoms, pain, fatigue, and systemic therapy side effects were self-reported (Figure 2).

Patients in our study did not perceive deterioration of GHS by a cancer diagnosis or cancer treatment. That means that patients perceived good overall well-being, as they had not been ill. A similar finding for GHS in patients 1–15 years post-diagnosis was found by others.[7-9,17] On the other hand, our patients reported a slight deterioration of C30-SumCs one-year post-chemotherapy, probably due to the toxicities of multimodality treatment. Ferreira *et al*. noted similar persistent deterioration of C30-SumSc after two years in premenopausal patients treated with chemotherapy and postmenopausal patients treated with endocrine therapy.[18] Deterioration of C30-SumSc is not only due to treatment but could be also due to the progression of cancer. C30 Sum-Sc has recently been shown as an independent prognostic factor for overall survival in several cancers.[19]

In our explorative analysis, we found a detrimental effect of cancer treatments (either chemotherapy, endocrine therapy, surgery, or radiotherapy) on specific functional and symptom scales, evaluated with QLQ C30 and QLQ BR23. Patients reported clinically meaningful deterioration in cognitive functioning and body image from baseline to one-year post-chemotherapy. Deficits in cognitive, role, social, and emotional functioning, particularly in young patients, were also reported by others 1–10 years after surgery.[8,20,21] Compared to the general population, researchers found significantly lower mean scores for cognitive and social functioning, role functioning and emotional functioning, physical functioning and body image, and future perspective between 5–15 years post-therapy.[7,9,17,22] That means that the consequences of treatment could be life-long. Interestingly, some serum markers of systemic inflammation were found to be statistically significantly higher in cancer survivors treated with chemotherapy even 20 years after chemotherapy and were associated with lower cognitive performance.[23] Breast reconstruction, however, improved physical functioning and body image compared to breast-conserving surgery; the same applies to social functioning and future perspective.[24,25]

In addition to detrimental effects on functional scales, our exploratory analysis showed significantly increased symptom scores after one year compared to baseline: fatigue, arm symptoms, pain, and, to a lesser degree, the systemic therapy side effects. In addition to these symptoms, other researchers reported insomnia or sleep disturbances, breast symptoms and financial difficulties, dyspnoea, hot flashes, sexual problems, and polyneuropathy.[7-9,17,20] Some differences in symptoms, however, were described only as trivial, with small clinical relevance.[17]

We suppose that pain and arm symptoms are related to higher nodal burden and consequently performed axillary dissection and irradiation. However, perceived fatigue, pain, and arm symptoms could also reflect less personal engagement in avoiding or managing these symptoms. Sixty-nine percent of our patients had primary surgery, followed by adjuvant chemotherapy, and 31% had the opposite sequence of treatment. In view of this information, we would expect that arm symptoms (from the BR-23 questionnaire) will be greater

at the beginning (at inclusion in the study) than 1-year post-chemotherapy. But it turned out the opposite. We can explain this finding by the fact that arm symptoms are scores from three items, namely pain (not only pain in the arm, but also pain in the shoulder), swelling of the arm, and difficulties in the mobility of the arm. The swelling of the arm usually occurs with a delay. Swelling is more common when axillary dissection is performed (in our case 35.3% of patients) than when removing only sentinel lymph nodes. Radiotherapy, which was delivered to 81.9% of our patients, could contribute to swelling and pain as well.

Symptom pain of the C30 questionnaire is about pain anywhere and is made up of two questions, whether the pain is present and the question if it affects every day functioning. Generally, chemotherapy, especially taxanes, received by 79.1% of our patients, also contributes to the pain. Sensory polyneuropathy, not only hurts but often impedes normal functioning (walking, fine motoric). Additional pain could be contributed to adjuvant endocrine therapy (tamoxifen mainly affects large joints, and aromatase inhibitors affect small joints). Yoon *et al*. found variation in symptom reporting influenced by race/ethnicity and other sociodemographic characteristics, and several comorbid conditions.[26]

Returning to work is a significant milestone for breast cancer survivors.[7] Von Ah *et al*. found that everyday cognition correlates with work engagement. What do these findings mean for cancer survivors in the setting of clinical practice? Cognitive dysfunction and fatigue are the most important issues for patients, especially if they are employed.

Cognitive dysfunction after chemotherapy ("chemo brain") is described as the impairment of memory, attention, executive functions, and processing speed.[27,28] Recently it has also been reported for hormonal therapy (tamoxifen and nonsteroid aromatase inhibitors), targeted therapy, immunotherapy, and due to cancer itself, combined in terminus "cancer-related cognitive dysfunction".[28] Subjective cognitive problems were reported by half of breast cancer patients after chemotherapy, but only 15–25% had an objective cognitive decline.[28] Despite the mild-to-moderate severity of cognitive dysfunction, it represents an important issue for patients.[27] It is especially true for patients who are employed.[7,8,26] Impaired cognitive functioning in our patients one-year post-chemotherapy could be related to treatment with chemotherapy and surgery (general anesthesia) as well as adjuvant endocrine treatment (85% of patients).

Among symptoms, fatigue is reported most regularly in all studies. Fatigue is a subjective feeling of lack of energy, of physical, emotional, and/or cognitive tiredness or exhaustion related to cancer and/or cancer treatment, and interferes with usual functioning.[29] It is a multidimensional symptom that accompanies patients while receiving chemotherapy and can last many years after chemotherapy.[27] As with cognitive dysfunction, it could be associated with the type of treatment (surgery, chemotherapy, endocrine therapy, targeted therapy, or radiotherapy).

The rehabilitation of cancer survivors should be diverse, according to the needs of the individual patient. For example, physical functioning and fatigue could be improved with regular exercise.[30] Arm symptoms could be managed with physical rehabilitation and more specifically lymphoedema treatment, elastic compressive gloves, and painkillers. Pain (in the breast, arm, joints, peripheral polyneuropathy) should be appropriately managed by a pain specialist. Cognitive rehabilitation could include cognitive rehabilitation programs, physical activity, or relaxation programs.[27] Hot flashes and sexual issues could be managed by a gynecologist. With fewer symptoms and better symptom scales patients would probably have better cognitive and role functioning and a better body image. In order to improve the QoL of cancer survivors, a pilot study on the comprehensive rehabilitation of breast cancer patients is underway at our institute. Identifying problems early probably allows an earlier targeted approach, thus leading to better patient functioning, an earlier return to work, and less absenteeism in the workplace. Evaluation of the results of comprehensive rehabilitation on improving functional and symptom scales is eagerly awaited.

Strengths of the study

Firstly, this is a prospective cohort study of health-related quality of life, using validated questionnaires and tools, such as GHS and C30-SumSc, recommended by the EORTC. Many studies perform only cross-sectional data analysis. Secondly, we performed a comparison with our normative population to obtain information about what patients' scores would be without cancer.

Limitations of the study

The first limitation is the small sample size and that we did not have a baseline value of items in

the questionnaires before any cancer treatment. Secondly, we included only patients that were proficient in using smartphones, and thus probably inadvertently chose a subset of the population that is highly motivated, healthier, and with middle social status. However, those patients were supported by a mobile app for coping with symptoms, which would probably be even heavier without the app. Thirdly, we included only Android-based smartphone users, which represented 80% of smartphones in Slovenia at that time. However, the app for IOS had not yet been made available. An additional weakness of our study is that the aspects of depression and anxiety, which affect cognitive functioning and fatigue, were not involved. Comorbidities were also not assessed – these are also significant predictors of symptoms, especially amongst those receiving chemotherapy.

Conclusions

Patients with early breast cancer had similar GHS before chemotherapy as the normative Slovenian population, and it did not deteriorate with treatment. One year after chemotherapy, C30-SumSc deteriorated compared to that before chemotherapy. Early interventions should be directed toward the prevention of the decline of cognitive functioning and body image, and to alleviate fatigue, pain, and arm symptoms.

Acknowledgments

We thank Nina Ružić Gorenjec, who performed a statistical analysis but could not contribute as a co-author of the manuscript.

This research was partly supported by the Slovenian Research Agency (Prognostic and predictive factors for response in the treatment of breast cancer and other cancers, P3-0321).

References

1. Sung H, Ferlay J, Siegel RL, Laversanne M, Soerjomataram I, Jemal A, et al. Global Cancer Statistics 2020: GLOBOCAN estimates of incidence and mortality worldwide for 36 cancers in 185 countries. *CA Cancer J Clin* 2021; **71:** 209-249. doi: 10.3322/caac.21660
2. Institute of Oncology Ljubljana. *Cancer registry*. [Internet]. [cited 2023 Jan 22]. Available at: http://www.slora.si/en/stevilo-zivih-bolnikov
3. Aaronson NK, Ahmedzai S, Bergman B, Bullinger M, Cull A, Duez NJ, et al. The European Organization for Research and Treatment of Cancer QLQ-C30: a quality-of-life instrument for use in international clinical trials in oncology. *J Natl Cancer Inst* 1993; **85:** 365-76. doi: 10.1093/jnci/85.5.365
4. Michels FAS, Latorre MDRDDO, Maciel MDS. Validity, reliability and understanding of the EORTC-C30 and EORTC-BR23, quality of life questionnaires specific for breast cancer. *Rev Bras Epidemiol* 2013; **16:** 352-363. doi: 10.1590/S1415-790X2013000200011
5. Giesinger JM, Kieffer JM, Fayers PM, Groenvold M, Petersen MA, Scott NW. EORTC Quality of Life Group Replication and validation of higher order models demonstrated that a summary score for the EORTC QLQ-C30 is robust. *J Clin Epidemiol* 2016; **69:** 79-88. doi: 10.1016/j.jclinepi.2015.08.007
6. Schmidt ME, Scherer S, Wiskemann J, Steindorf K. Return to work after breast cancer: the role of treatment-related side effects and potential impact on quality of life. *Eur J Cancer Care* 2019; **28:** e13051. doi: 10.1111/ecc.13051
7. von Ah D, Crouch A. Relationship of perceived everyday cognitive function and work engagement in breast cancer survivors. *Support Care Cancer* 2021; **29:** 303-4309. doi: 10.1007/s00520-020-05950-8
8. Arndt V, Merx H, Stürmer T, Stegmaier C, Ziegler H, Brenner H. Age-specific detriments to quality of life among breast cancer patients one year after diagnosis. *Eur J Cancer* 2004; **40:** 673-80. doi: 10.1016/j.ejca.2003.12.007
9. Ahn SH, Park BW, Noh DY, Nam SJ, Lee ES, Lee MK, et al. Health-related quality of life in disease-free survivors of breast cancer with the general population. *Ann Oncol* 2007; **18:** 173-82. doi: 10.1093/annonc/mdl333. Erratum in: *Ann Oncol* 2009; **20:** 1753-4.
10. Grašič Kuhar C, Gortnar Cepeda T, Kovač T, Kukar M, Ružić Gorenjec N. Mobile app for symptom management and associated quality of life during systemic treatment in early stage breast cancer: nonrandomized controlled prospective cohort study. *JMIR Mhealth Uhealth* 2020; **8:** e17408. doi: 10.2196/17408
11. Velenik V, Secerov-Ermenc A, But-Hadzic J, Zadnik V. Health-related quality of life assessed by the EORTC QLQ-C30 Questionnaire in the general Slovenian population. *Radiol Oncol* 2017; **51:** 342-50. doi: 10.1515/raon-2017-0021
12. Senkus E, Kyriakides S, Penault-Llorca F, Poortmans P, Thompson A, Zackrisson S, et al; ESMO Guidelines Working Group. Primary breast cancer: ESMO Clinical Practice Guidelines for diagnosis, treatment and follow-up. *Ann Oncol* 2013; **24(Suppl 6):** vi7-23. doi: 10.1093/annonc/mdt284
13. Fayers P, Bjordal K, Groenvold M, Curran D, Bottomley A. *EORTC QLQ-C30 scoring manual*. 3rd edition. Brussels: EORTC Brussels; 2001. [Internet]. [cited 2020 Jun 22]. Available at: https://www.eortc.org/app/uploads/sites/2/2018/02/SCmanual.pdf
14. Scoring of the QLQ-C30 Summary Score. [Internet]. [cited 2022 Nov 26]. Available at: https://qol.eortc.org/app/uploads/sites/2/2018/02/scoring_of_the_qlq-c30_summary_score.pdf
15. Osoba D, Rodrigues G, Myles J, Zee B, Pater J. Interpreting the significance of changes in health-related quality-of-life scores. *J Clin Oncol* 1998; **16:** 139-44. doi: 10.1200/JCO.1998.16.1.139
16. R Core Team. R: A language and environment for statistical computing. *R Foundation for Statistical Computing*, Vienna, Austria; 2020. [Internet]. [cited 2021 Jun 6]. Available at: https://www.R-project.org/
17. Doege D, Thong MS, Koch-Gallenkamp L, Bertram H, Eberle A, Holleczek B, et al. Health-related quality of life in long-term disease-free breast cancer survivors versus female population controls in Germany. *Breast Cancer Res Treat* 2019; **175:** 499-510. doi: 10.1007/s10549-019-05188-x
18. Ferreira AR, Di Meglio A, Pistilli B, Gbenou AS, El-Mouhebb M, Dauchy S, et al. Differential impact of endocrine therapy and chemotherapy on quality of life of breast cancer survivors: a prospective patient-reported outcomes analysis. *Ann Oncol* 2019; **30:** 1784-95. doi: 10.1093/annonc/mdz298
19. Husson O, de Rooij BH, Kieffer J, Oerlemans S, Mols F, Aaronson NK, et al. The EORTC QLQ-C30 Summary Score as prognostic factor for survival of patients with cancer in the "real-world": Results from the Population-Based PROFILES Registry. *Oncologist* 2020; **25:** e722-e32. doi: 10.1634/theoncologist.2019-0348
20. Arndt V, Merx H, Stegmaier C, Ziegler H, Brenner H. Persistence of restrictions in quality of life from the first to the third year after diagnosis in women with breast cancer. *J Clin Oncol* 2005; **23:** 4945-53. doi: 10.1200/JCO.2005.03.475.
21. Harrington CB, Hansen JA, Moskowitz M, Todd BL, Feuerstein M. It's not over when it's over: long-term symptoms in cancer survivors – a systematic review. *Int J Psychiatry Med* 2010; **40:** 163-181. doi:10.2190/PM.40.2.c

22. de Ligt KM, Heins M, Verloop J, Ezendam NPM, Smorenburg CH, Korevaar JC, et al. The impact of health symptoms on health-related quality of life in early-stage breast cancer survivors. *Breast Cancer Res Treat* 2019; **178:** 703-11. doi: 10.1007/s10549-019-05433-3

23. van der Willik KD, Koppelmans V, Hauptmann M, Compter A, Ikram MA, Schagen SB. Inflammation markers and cognitive performance in breast cancer survivors 20 years after completion of chemotherapy: a cohort study. *Breast Cancer Res* 2018; **20:** 135. doi: 10.1186/s13058-018-1062-3

24. Zehra S, Doyle F, Barry M, Walsh S, Kell MR. Health-related quality of life following breast reconstruction compared to total mastectomy and breast-conserving surgery among breast cancer survivors: a systematic review and meta-analysis. *Breast Cancer* 2020; **27:** 534-66. doi: 10.1007/s12282-020-01076-1

25. Yfantis A, Sarafis P, Moisoglou I, Tolia M, Intas G, Tiniakou I, et al. How breast cancer treatments affect the quality of life of women with non-metastatic breast cancer one year after surgical treatment: a cross-sectional study in Greece. *BMC Surg* 2020; **20:** 210. doi: 10.1186/s12893-020-00871-z

26. Yoon J, Malin JL, Tao ML, Tisnado DM, Adams JL, Timmer MJ, et al. Symptoms after breast cancer treatment: are they influenced by patient characteristics? *Breast Cancer Res Treat* 2008; **108:** 153-165. doi: 10.1007/s10549-007-9599-3

27. Joly F, Lange M, Dos Santos M, Vaz-Luis I, Di Meglio A. Long-term fatigue and cognitive disorders in breast cancer survivors. *Cancers* 2019; **11:** 1896. doi: 10.3390/cancers11121896

28. Lange M, Joly F, Vardy J, Ahles T, Dubois M, Tron L, et al. Cancer-related cognitive impairment: an update on state of the art, detection, and management strategies in cancer survivors. *Ann Oncol* 2019; **30:** 1925-40. doi: 10.1093/annonc/mdz410

29. National Comprehensive Cancer Networ. NCCN guidelines for supportive care. [Internet]. [cited 2021 Jun 6]. Available at: https://www.nccn.org/professionals/physician_gls/pdf/fatigue.pdf

30. Puetz TW, Herring MP. Differential effects of exercise on cancer-related fatigue during and following treatment: a meta-analysis. *Am J Prev Med* 2012; **43:** e1-24. doi: 10.1016/j.amepre.2012.04.027

research article

Association between *PIK3CA* activating mutations and outcomes in early-stage invasive lobular breast carcinoma treated with adjuvant systemic therapy

Domen Ribnikar[1,2], Valentina Jeric Horvat[1], Ivica Ratosa[2,3], Zachary W Veitch[4], Biljana Grcar Kuzmanov[5], Srdjan Novakovic[6], Erik Langerholc[7], Eitan Amir[8], Bostjan Seruga[1,2]

[1] Department of Medical Oncology, Institute of Oncology Ljubljana, Ljubljana, Slovenia
[2] Faculty of Medicine Ljubljana, University of Ljubljana, Ljubljana, Slovenia
[3] Department of Radiation Oncology, Institute of Oncology Ljubljana, Ljubljana, Slovenia
[4] Division of Medical Oncology and Hematology, Royal Victoria Hospital, Bariie, Ontario, USA
[5] Department of Pathology, Institute of Oncology Ljubljana, Ljubljana, Slovenia
[6] Department of Molecular Diagnostics, Institute of Oncology Ljubljana, Ljubljana, Slovenia
[7] Institute of Biostatistics and informatics, Faculty of Medicine Ljubljana, University of Ljubljana, Ljubljana, Slovenia
[8] Division of Medical Oncology and Hematology, University of Toronto and Princess Margaret Cancer Centre, Toronto, Canada

Radiol Oncol 2023; 57(2): 220-228.

Received 13 February 2023
Accepted 18 May 2023

Correspondence to: Assoc. Prof. Boštjan Šeruga, M.D., Ph.D., Department of Medical Oncology, Institute of Oncology Ljubljana, Zaloška cesta 2, SI-1000 Ljubljana, Slovenia. E-mail: bseruga@onko-i.si

Disclosure: No potential conflicts of interest were disclosed.

Background. The aim of the study was to evaluate the independent prognostic role of *PIK3CA* activating mutations and an association between *PIK3CA* activating mutations and efficacy of adjuvant endocrine therapy (ET) in patients with operable invasive lobular carcinoma (ILC).

Patients and methods. A single institution study of patients with early-stage ILC treated between 2003 and 2008 was performed. Clinicopathological parameters, systemic therapy exposure and outcomes (distant metastasis-free survival [DMFS] and overall survival [OS]) were collected based on presence or absence of PIK3CA activating mutation in the primary tumor determined using a quantitative polymerase chain reaction (PCR)-based assay. An association between PIK3CA mutation status and prognosis in all patient cohort was analyzed by Kaplan-Meier survival analysis, whereas an association between PIK3CA mutation and ET was analyzed in estrogen receptors (ER) and/or progesterone receptors (PR)-positive group of our patients by the Cox proportional hazards model.

Results. Median age at diagnosis of all patients was 62.8 years and median follow-up time was 10.8 years. Among 365 patients, PIK3CA activating mutations were identified in 45%. PIK3CA activating mutations were not associated with differential DMFS and OS ($p = 0.36$ and $p = 0.42$, respectively). In patients with PIK3CA mutation each year of tamoxifen (TAM) or aromatase inhibitor (AI) decreased the risk of death by 27% and 21% in comparison to no ET, respectively. The type and duration of ET did not have significant impact on DMFS, however longer duration of ET had a favourable impact on OS.

Conclusions. PIK3CA activating mutations are not associated with an impact on DMFS and OS in early-stage ILC. Patients with PIK3CA mutation had a statistically significantly decreased risk of death irrespective of whether they received TAM or an AI.

Key words: invasive lobular carcinoma; PIK3CA mutation; endocrine therapy; genomics of invasive lobular carcinoma

Introduction

Breast cancer represents a spectrum of heterogeneous diseases with different clinical behaviour and response to specific systemic therapy. Invasive lobular carcinoma (ILC) is the second most frequent subtype of breast cancer, representing around 10% of all breast cancer cases.[1]

It has been demonstrated that ILC is a special disease entity that differs from the more common invasive breast carcinomas such as invasive ductal carcinoma (IDC). These differences include risk factors, histological and clinical characteristics, transcriptional signatures and genomic profiles.[2-4] ILCs usually arise in postmenopausal women, are larger in size at the time of diagnosis due to insidious nature of its growth, but are typically of lower histological grade. The majority of ILC tumors express hormone receptors such as estrogen receptors (ER), progesterone receptors (PR) but they less commonly exhibit human epidermal growth factor receptor-2 (HER-2) overexpression or amplification.[5] Data about prognosis of ILC vary substantially; studies have demonstrated better[6,7], the same[8], and worse long-term overall survival (OS) in comparison to unselected invasive breast cancers.[9]

Additionally, it has been reported that ILC is less responsive to chemotherapy (ChT).[10-12] However, these tumors respond well to endocrine therapy (ET) given their biological profile.[13] Results of an important retrospective study clearly showed an OS benefit of adjuvant ET for patients with ILC.[14]

Desmedt *et al.* conducted the largest genomic study of ILC and found that mutations in *PIK3CA* (phosphatidylinositol, catalytic unit), *HER* and *ESR1* (estrogen receptor 1) genes are more frequently present in ILC tumors that in other invasive breast cancers. Furthermore, in their study, approximately 50% of ILC tumors harboured PIK3CA-PTEN-AKT1 signaling alterations. Of note, *PIK3CA* mutation was associated with lower histological grade and lower Ki-67 (proliferating) index.[15] Mutations of *PIK3CA* gene are the most common somatic genetic alterations in ER-positive breast cancer and are associated with favorable breast cancer characteristics such as smaller tumor size, lower grade, ER positivity and increasing age.[16]

Investigators of the BIG 1-98 study which compared letrozole monotherapy and letrozole switching strategy to tamoxifen (TAM) monotherapy reported that postmenopausal patient population with ILC may derive greater benefit from letrozole (AIs) than patients with IBC, NOS (invasive breast carcinoma, no otherwise specified).[17] Furthermore, additional post-hoc analysis of the BIG 1-98 study showed that irrespective of the histological subtype of breast cancer tumors with *PIK3CA* mutation derive greater benefit from letrozole than from tamoxifen.[18] There are no data about the exact number of ILC patients with present *PIK3CA* mutation in the BIG 1-98 study; however in the large meta-analysis by Zardavas *et al.* there were 366 out of 951 (39%) patients who had *PIK3CA* mutated ILC.[16]

In this study, we aimed to evaluate the independent prognostic role of *PIK3CA* activating mutations and an association between *PIK3CA* activating mutations and efficacy of ET in patients with operable ILC. We hypothesized that the presence of *PIK3CA* activating mutations in primary ILC is associated with longer distant metastasis-free survival and overall survival and greater benefit of AIs and extended ET as compared to standard 5-year treatment with tamoxifen.

Patients and methods

Patients

After obtaining approval from the institutional review committee and ethical approval of the Ministry of Health of the Slovenian Republic (#0120-323/2019), we performed a retrospective analysis of a cohort of patients with early-stage ILC identified from a pathology database at the Institute of Oncology Ljubljana. Eligible patients were treated between January 1st 2003 and December 31st 2008, thereby allowing at least 10 years of follow-up at the time of data analysis.

Clinicopathological characteristics and determination of the *PIK3CA* mutation

Formalin-fixed and paraffin embedded (FFPE) and hematoxylin and eosin stained tumor slides of all included patients were reviewed by an experienced breast pathologist (BGK) to ensure that the diagnosis of ILC and its subtype(s) were correct. We collected the following clinicopathological parameters from each patient's from the existing pathology reports: age at diagnosis, subtype of ILC, tumor size, nodal status, grade, mitotic count, ER and PR expression, HER-2 overexpression or amplification, lymphovascular invasion (LVI) and perineural invasion (PNVI). Ki-67 labeling index and tumor infiltrating lymphocytes (TILs) were additionally determined retrospectively by a sin-

TABLE 1. Characteristics of the included patients and their tumors

Characteristic	All patients (n = 365; 100%)	*PIK3CA* mutated (n = 164; 45%)	*PIK3CA* non-mutated (n = 201; 55%)
Median age (range) (yrs)	62.8 (33–90)	63.1	62.4
Median tumor size (mm)	21	19	21
Nodal status			
N0	209 (57)	100 (61)	109 (54)
N1	84 (23)	37 (22)	47 (23)
N2	26 (7)	1 (7)	15 (8)
N3	46 (13)	16 (10)	30 (15)
Tumor grade			
G1	52 (14)	20 (12)	32 (16)
G2	270 (74)	134 (82)	136 (68)
G3	43 (12)	10 (6)	33 (16)
IHC* subtype			
ER+/PR+/HER2-	299 (82)	136 (46)	159 (54)
ER+/PR-/HER2-	39 (11)	14 (36)	25 (64)
HER2 +	20 (6)	9 (45)	11 (55)
ER-/PR-/HER2-	7 (2)	2 (29)	5 (71)
Median Ki-67 (range) (%)	3 (1–50)	2.5 (1–50)	3 (1–40)
Mitotic score			
M1	284 (78)	138 (84)	146 (73)
M2	55 (15)	19 (12)	36 (18)
M3	26 (7)	7 (4)	19 (9)
Presence of LVI	24 (7)	4 (2)	20 (10)
Median TILs (range) (%)	3 (1–50)	3	3
Median follow-up time (range) (yrs)	10.8 (0.1–18.6)	10.8	10.7

ER = estrogen receptor; HER = 2–human epidermal growth factor receptor-2; *IHC = immunohistochemically defined subtype; PR = progesterone receptor; LVI = lymphovascular invasion; TILs = tumor-infiltrating lymphocytes

78 patients had PIK3CA mutation on exon 9, 76 patients on exon 20; five patients had dual PIK3CA mutation on exon 9 and five patients had both, exon 9 and exon 20 PIK3CA mutations

gle breast cancer pathologist as these biomarkers were not assessed routinely in years of the cohort inception. Tumor grading was classified according to the Bloom-Richardson-Elston classification.[19] ER and PR expression and HER-2 status were determined using the American Society of Clinical Oncology/College of American Pathologists guidelines.[20,21] Proliferation index Ki-67 was estimated with DAKO, Glostrup antibody MIB1 according to recommendations from the International Ki-67 in Breast Cancer Working Group.[22] For the evaluation of TILs the recommendations of the 2014 International TILs Working Group were followed.[23] *PIK3CA* status (wild-type or mutated) was determined for each patient. DNA isolation from the FFPE tumor samples was performed by macrodissection of tumor tissue from tumor slices containing at least 70% tumor cells. Isolation was performed using the MagMAX FFPE DNA/RNA Ultra Kit (Applied Biosystems, Thermo Fisher

TABLE 2. Distribution of systemic therapy in all patients and according to PIK3CA mutation status

Systemic therapy	All pts N (%)	*PIK3CA* mutated pts N (%)	*PIK3CA* non-mutated pts N (%)
None	12 (3)	5 (3)	7 (3)
ET only	249 (68)	115 (70)	134 (67)
ChT only	13 (4)	5 (3)	8 (4)
ET and ChT	91 (25)	39 (24)	52 (26)
None ET	25 (7)	10 (6)	15 (7)
ET with TAM	106 (29)	45 (27)	61 (30)
ET with AIs	127 (35)	54 (33)	73 (37)
Sequence TAM-AI	107 (29)	55 (34)	52 (26)
Median duration (range) of ET	5 (0.2–16.7)	5 (0.4–16.7)	5 (0.2–11.2)

AIs = aromatase inhibitors; ChT = chemotherapy; ET = endocrine therapy; pts = patients, TAM = tamoxifen (TAM)

Scientific, Austin, Tx, USA) according to the manufacturer's instructions. Isolated DNA was used to identify five common mutations in the *PIK3CA* gene using the PIK3CA Mutation Analysis Kit (EntroGen, Inc. Woodland Hills, CA, USA) according to the manufacturer's protocol. This is a quantitative polymerase chain reaction (PCR) based assay that detects five hot spot mutations in the *PIK3CA* gene (NM_006218.2): c.1624G > A p.(Glu542Lys), c.1633G > A p.(Glu545Lys), c.1633G > C p.(Glu545Gln), c.3140A > G p.(His1047Arg) and c.3140A > T p.(His1047Leu). These five hot spot mutations represent around 80% of all *PIK3CA* mutations.[24]

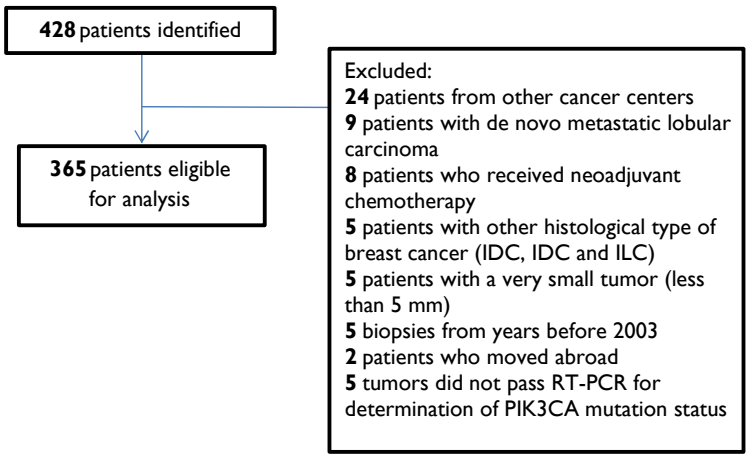

FIGURE 1. Consort diagram.

Systemic treatment

We collected all data about systemic therapy for each patient included into the study such as whether the patient received ChT, ET and HER-2-targeted therapy. We also collected data about the type of ChT (cyclophosphamide – metotrexate-5-fluorouracil regimen (CMF), anthracycline-based chemotherapy, anthracyclines and taxanes, taxanes without anthracyclines), type of ET (tamoxifen monotherapy, AI monotherapy or a switching approach [TAM-AI]) and duration of ET (up to 5 years or more than 5 years).

Statistical analysis

The outcomes of interest were distant metastasis-free survival (DMFS) and overall survival (OS) defined as time from diagnosis (date of surgery) to distant relapse or death (whichever occurred first) and as time from diagnosis to death from any cause, respectively. The last date of a follow-up was October 31st 2021. Data were analyzed using R version 4.1.2 (Vienna, Austria). Descriptive statistics were used to describe patient characteristics. Age and duration of therapy were measured in years, tumor size was measured in millimeters, Ki-67 index was measured as a proportion of positive tumor cells and logarithmised and for the number of positive axillary lymph nodes the square root was taken of in order to normalize the distribution of the variables and improve model fit. DMFS and OS were estimated using Kaplan-Meier analysis. Log-rank tests were performed to compare the survival of *PIK3CA* mutated and *PIK3CA* non-mutated cohorts of patients. Four Cox proportional hazard models were used to assess the impact of ET on survival of ER and/or PR-positive *PIK3CA* mutated patients: a simple and an advanced model for each of DMFS and OS. The simple Cox model regressed on only three variables; age at diagnosis, prior duration of tamoxifen and prior duration of AI therapy. The advanced model regressed on additional variables which are considered known or possible prognostic factors: tumor size, nodal status, histological grade, Ki-67 index, PR expression and location of *PIK3CA* mutation (exon 9 or exon 20), respectively. To avoid immortal time bias, any prior duration of tamoxifen and any prior duration of AI therapy were considered as time-dependent variables, while all other variables were known at a patients' entry in the study (at the time of surgery). Finally, adjustment for multiple significance testing was performed using Holm's method. An adjusted p-value ≤ 0.05 was considered statistically significant.

Results

Patients and their tumors

Among an initial cohort of 428 patients, we excluded 24 patients who were treated in other cancer centers in Slovenia, nine patients who had de novo metastatic lobular cancer, eight patients who received neoadjuvant ChT, five patients with other histological subtypes of breast cancer (IBC, NOS, ILC and IBC, NOS), five patients with very small tumors (less than 5 mm in size) and five patients whose biopsies were from years before 2003. Two patients were lost very early in the follow up as they moved out of country, so they were excluded from the analysis. *PIK3CA* mutation status could

FIGURE 2. Kaplan-Meier graph showing association between PIK3CA mutation and overall survival.

not be determined in five cases due to technical issues with the samples. This resulted in an analytic cohort of 365 patients (Figure 1; Consort diagram, for patient selection schema). Characteristics of included patients and their tumors are presented in Table 1. Among all patients, 164 (45%) patients had *PIK3CA* mutated ILC. Of these 78 (48%) patients had *PIK3CA* mutations in the helical domain (exon 9) and 76 (46%) patients had the mutation present in the kinase domain (exon 20). Five patients (1%) had dual *PIK3CA* mutations on exon 9 and five patients (1%) had *PIK3CA* mutations on both, exon 9 and 20. As shown in Table 1, *PIK3CA* mutated and *PIK3CA* non-mutated cohort of patients were well balanced according to prognostic tumor characteristics.

Systemic therapy exposure of all included patients is shown in Table 2. As expected, the majority of patients received ET with either TAM (106, 29%), AIs (127, 35%) or a switch approach TAM-AI (107, 29%). Ninety-one (25%) patients received ChT and ET and only 13 (4%) patients received ChT alone. Among 25 patients who did not receive any ET, 10 patients were *PIK3CA* mutated. ET agents were well balanced between *PIK3CA* mutated and *PIK3CA* non-mutated patients as shown in Table 2. Median duration of ET was 5 years in both groups of patients. 191 (52%) patients had extended ET and the longest duration of extended ET was 16.7 years.

An association between *PIK3CA* mutation status and disease outcome

Median OS was 15.7 years for patients with *PIK3CA* mutation and 14.6 years for patients without *PIK3CA* mutation. Furthermore, median DMFS for *PIK3CA* mutated and for *PIK3CA* non-mutated ILC patients was 15.6 and 13.4 years, respectively. The presence of *PIK3CA* mutation in early-stage ILC patients was not associated with differential OS (p = 0.42, Figure 2) or DMFS (p = 0.36, Figure 3). Overall, 81 (22%) patients developed distant metastases, of these 48 (24%) were *PIK3CA* non-mutated and 33 (16%) were *PIK3CA* mutated. Twenty (26%) patients of those who developed distant metastases had *PIK3CA* mutation on exon 20, 12 (15%) had *PIK3CA* mutation on exon 9 and only one (5%) patient had both, exon 9 and 20 *PIK3CA* mutation.

TABLE 3. Simple Cox proportional hazards model for DMFS in the PIK3CA mutated patient cohort

Characteristic	HR	95% CI	Adj p
Age	0.99	0.96–1.02	1.0
Duration of TAM	0.92	0.75–1.14	1.0
Duration of AIs	1.07	0.90–1.28	1.0

Adj p = adjusted p value; AIs = aromatase inhibitors; CI = confidence interval, HR = hazard ratio; TAM = tamoxifen,

An association between type and duration of ET and disease outcome in patients with *PIK3CA* mutation

The effect of the type of systemic ET and its duration on DMFS

Patients who received AIs in comparison to those who received tamoxifen were on average 10 years older at the time of diagnosis, therefore a Cox proportional hazards model was used for adjustment. In a simple model, neither type of ET nor its duration and patient age at the time of diagnosis were associated with the risk of relapse (Table 3). In advanced Cox proportional hazards model only a higher number of positive axillary lymph nodes increased the risk of distant relapse (HR 1.64, adj.p < 0.001; see Table 4).

The effect of the type of systemic ET and its duration on OS

We found that each year of aging increased the risk of death by 5%. Each year of treatment with tamoxifen decreased the risk of death by 27% in comparison to no ET for a patient of the same age (Table 5). Similarly, each year of treatment with AIs decreased the risk of death by 21% compared to no ET for a patient of the same age (Table 5).

In the advanced Cox proportional hazards model age at the time of diagnosis, grade 3 and higher number of positive axillary lymph nodes were all associated with higher risk of death (HR 1.05, *adj.* p = 0.014, HR 5.5, *adj.* p = 0.040 and HR 1.58, *adj.* p < 0.001, respectively). We also found that longer duration of ET with either tamoxifen or an AI had a favorable impact on OS (p = 0.010 for tamoxifen and p = 0.010 for an AI, respectively). In a time-dependent Cox analysis each year of prior treatment with tamoxifen decreased the risk of death by 32% in comparison to no prior ET for a patient with the same characteristics. Similarly, to tamoxifen, each year of prior AI therapy decreased the risk of death by 27% compared to no prior ET for a patient with the same characteristics (Table 6).

TABLE 4. Advanced Cox proportional hazards model for DMFS in the PIK3CA mutated patient cohort

Characteristic	HR	95% CI	Adj p
Age	1.01	0.97–1.05	1.0
Tumor size	0.99	0.57–1.71	1.0
Grade			
G1	Ref		
G2	0.91	0.26–3.22	1.0
G3	1.03	0.16–6.83	1.0
Ki-67	1.35	0.93–1.95	1.0
PR	1	0.99–1.02	1.0
***PIK3CA* status**			
Other than exon 20	Ref		
Only exon 20	2.19	1.01–4.80	0.582
No. of positive axillary LNs	1.64	1.30–2.06	< 0.001
Duration of TAM	1.02	0.81–1.29	1.0
Duration of AIs	1.06	0.87–1.28	1.0

Adj p = adjusted p value; AIs = aromatase inhibitors; CI = confidence interval; HR = hazard ratio; LNs = lymph nodes; No. = number; PR = progesterone receptor; TAM = tamoxifen

Discussion

ILC of the breast is a distinct entity with unique clinical, histological and molecular characteristics that differ from more common invasive breast cancer subtypes. The majority of older studies demonstrated that the outcome of ILC patients was better, however more recent data have suggested ILC has worse outcome compared to invasive ductal carcinoma, especially in the long term. It seems that delay and difficulty in early diagnosis, acquired resistance to conventional therapy and risk of late relapse pose challenges in management of patients with ILC.[25]

In this retrospective study our main goal was to evaluate the association between the *PIK3CA* mutational status and prognosis in patients with operable ILC. We found that *PIK3CA* mutation status has no association with either DMFS or OS. The median OS was 15.7 years for patients with *PIK3CA* mutation and 14.6 years for patients with *PIK3CA* wild type ILC.

PIK3CA mutations are the most frequent somatic genetic alterations in ER+/HER-2– breast cancer.[18] Prior data in early-stage disease have demonstrated a favorable disease outcome in patients harboring *PIK3CA* mutations.[16] At least to some extent this could be explained by a relative mutual exclusion of other somatic genetic alterations which are associated with higher proliferation and increased risk of distant relapse such as *TP53* mutations and amplifications of *MYC* (MYC proto - oncogene) gene.[18] Furthermore, recent work has shown that ultra-low risk breast cancers have higher expression scores for the *PIK3CA*-mutation-associated genes.[26]

Previous data exploring the prognostic effect of specific somatic mutations in ER+/HER-2– early-stage breast cancer have shown that *PIK3CA* and *MAP3K1* (mitogen-activated protein kinase 1) mutations co-associate and patients with tumors harboring both mutations have a more favorable clinical course than those with only one gene mutation or without any of these two mutations.[27] This may suggest that *PIK3CA* mutation alone is not prognostic in general breast cancer patient population, nor is it in ILC specifically.

The majority of first- and second-generation gene-expression profiles that have been used for molecular prognostication in early-stage breast cancer were developed initially in invasive ductal carcinomas and therefore their use in ILC is uncertain. However recent data have shown they could also be informative for prognostication in ILC patients. ILC tumors are quite homogenous clinically

TABLE 5. Simple Cox proportional hazards model for OS in the PIK3CA mutated patient cohort

Characteristic	HR	95% CI	Adj p
Age	1.05	1.02–1.07	< 0.001
Duration of TAM	0.73	0.61–0.88	0.002
Duration of AIs	0.79	0.67–0.93	0.005

Adj p = adjusted p value; AIs = aromatase inhibitors; CI = confidence interval; HR = hazard ratio; TAM = tamoxifen

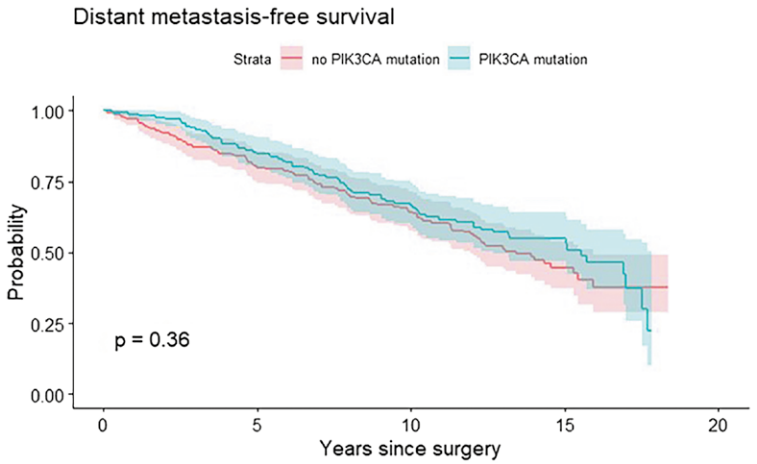

FIGURE 3. Kaplan-Meier graph showing association between PIK3CA mutation and distant metastasis-free survival

especially relating to classical prognostic features. The majority are grade 2, ER and PR positive, HER-2 negative and have a relatively low proliferative activity.[28] In contrast, it has been shown recently that a 194-gene signature called LobSig may be the best in prognosticating ILC tumors. LobSig outperformed Nottingham Prognostic Index (NPI), Prosigna ROR, Oncotype Dx and Genomic Grade Index (GGI) in a multivariate Cox proportional hazards model, especially in grade 2 ILC moderate NPI cases.[29] The authors reported that ILCs that were associated with a high-risk score were enriched for mutations in *HER-2, HER-3, TP53* (TP53 tumor suppressor gene), *ROS1* (ROS proto-oncogene 1, receptor tyrosine kinase) and *AKT1* (AKT serin - threonin protein kinase 1) genes. In contrast, those ILCs that had a good outcome (a low-risk score) had relatively few genomic alterations and interestingly, *PIK3CA* mutations were more common in the latter group than in the high risk ILC group. Based on all data discussed above it seems that *PIK3CA* mutation alone may not be an optimal genetic alteration to stratify ILC patients into better and worse prognostic group but rather an integration of several concurrent genetic alterations might outperform *PIK3CA* mutation in an individual tumor.

We also aimed to explore the predictive effect of *PIK3CA* mutation on benefit from ET. Efficacy of AIs as compared to tamoxifen have previously been explored and reported.[18] In the analysis from the randomized BIG 1-98 trial, the authors demonstrated a greater magnitude of benefit with an AI letrozole in comparison to tamoxifen for patients with *PIK3CA* mutated early-stage breast cancer (HR 0.18; 95% CI 0.06 – 0.50). Additionally, the same study demonstrated that letrozole was associated with a significantly reduced risk of disease - free survival event (DFS) in patients with luminal A and luminal B ILC concluding the magnitude of benefit from AI was greater in patients with ILC versus invasive ductal carcinomas.[30] In our study we did not find any substantial differences between the effect of tamoxifen and AIs in *PIK3CA* mutated early-stage ILC patients when compared to patients who did not receive any adjuvant therapy. We found that each year of treatment with tamoxifen decreased the risk of death by 27% in comparison to no ET for a patient of the same age. Similarly, each year of AI therapy decreased the risk of death by 21% compared to no ET for a patient of the same age. In addition, in an advanced Cox model we found similar results. The duration of any ET, either with tamoxifen or an AI, was statistically significantly associated with OS. In patients with *PIK3CA* mutation each year of tamoxifen and AIs treatment decreased the risk of death by 32% and 27% in comparison to a patient with the same tumor characteristics who did not receive any ET, respectively. However, we did not find any associations between type and duration of ET and DMFS. Only a higher number of positive axillary lymph nodes increased the risk of distant relapse of ILC in our cohort.

An interesting study evaluating the relationship of *PIK3CA* mutations and response to short-term neoadjuvant AI therapy demonstrated that the presence of *PIK3CA* mutation did not pre-

TABLE 6. Advanced Cox proportional hazards model for OS in the PIK3CA mutated patient cohort

Characteristic	HR	95% CI	Adj p
Age	1.05	1.02–1.08	0.014
Tumor size	1.38	0.90–2.10	0.84
Grade			
G1	Ref		
G2	1.41	0.59–3.38	1.0
G3	5.52	1.67–18.18	0.04
Ki-67	0.94	0.72–1.22	1.0
PR	1	0.99–1.01	1.0
***PIK3CA* status**			
Other than exon 20	Ref		
Only exon 20	1.32	0.79–2.21	1.0
No. of positive axillary LNs	1.58	1.32–1.88	< 0.001
Duration of TAM	0.68	0.55–0.86	0.01
Duration of AI	0.73	0.60–0.88	0.01

Adj p = adjusted p value; AIs = aromatase inhibitors; CI = confidence interval; HR = hazard ratio; No. = number; PR = progesterone receptor; TAM = tamoxifen

clude a response to AIs. In this study suppression of Ki-67 proliferating index, which is a validated intermediate endpoint biomarker for endocrine sensitivity was used as a surrogate marker of response.[31] Furthermore, another study showed that patients with *PIK3CA* mutated early-stage breast cancer either treated with tamoxifen or untreated had improved outcome in comparison to *PIK3CA* non-mutated patients.[32] These data were concordant with previous findings from in vitro study showing that *PIK3CA* mutated cell lines were more sensitive to tamoxifen compared to *PIK3CA* wild type cell lines.[33]

Our study has several limitations. First, due to the retrospective nature of this study our findings need to be interpreted with caution and possibly validated in the prospective setting. Second, our cohort of ILC patients is very likely molecularly heterogeneous which limits the generalizability of our findings. Third, longer duration of ET in this study is associated with significantly improved OS but not DMFS. This indicates that the impact of immortal time bias may persist despite the use of time-dependent Cox model in our analysis. Fourth, we used a PCR based assay which detects five hot spot mutations in the *PIK3CA* gene representing about 80% of all *PIK3CA* activating mutations. Results could be different if we used an alternative method for determination of all *PIK3CA* mutations such as next generation sequencing (NGS). Finally, the biggest limitation of our study is that despite the use of Cox models confounding by indication for treatment might still have an impact on our results.

In conclusion, the presence of *PIK3CA* mutation was not associated with differential DMFS or OS in patients with operable ILC. Adjuvant ET with either tamoxifen or an AI significantly decreased the risk of death in *PIK3CA* mutated ILC cohort. Furthermore, there was no significant difference in efficacy between the two classes of endocrine agents. Longer duration of ET with either tamoxifen or AIs decreases the risk of death in ILC patients with *PIK3CA* mutation. Future prospective studies based on molecular analyses will hopefully give us more exact answer about optimal endocrine agent for specific subpopulations of patients with early-stage ILC.

Acknowledgment

The authors acknowledge the financial support from the Slovenian Research agency (research core funding No P3-0321) and unrestricted donation to the Institute of Oncology Ljubljana for research.

References

1. Martinez V, Azzopardi JG. Invasive lobular carcinoma of the breast: incidence and variants. *Histopathology* 1979; **3**: 467-88. doi: 10.1111/j.1365-2559.1979.tb03029.x
2. Yoder BJ, Wilkinson EJ, Massoli NA. Molecular and morphologic distinctions between infiltrating ductal and lobular carcinoma of the breast. *Breast J* 2007; **13:** 172-79. doi: 10.1111/j.1524-4741.2007.00393.x
3. Korkola JE, DeVries S, Fridlyand J, Hwang ES, Estep AL, Chen YY, et al. Differentiation of lobular versus ductal breast carcinomas by expression microarray analysis. *Cancer Res* 2003; **63:** 7167-75. PMID: 14612510
4. Cleton-Jansen AM. E-cadherin and loss of heterozygosity at chromosome 16 in breast carcinogenesis: different genetic pathways in ductal and lobular breast cancer? *Breast Cancer Res* 2002; **4:** 5-8. doi: 10.1186/bcr416
5. Coradini D, Pellizzaro C, Veneroni S, Ventura L, Daidone MG. Infiltrating ductal and lobular breast carcinomas are characterised by different interrelationships among markers related to angiogenesis and hormone dependence. *Br J Cancer* 2002; **87:** 1105-11. doi: 10.1038/sj.bjc.6600556
6. Toikkanen S, Pylkkanen L, Joensuu H. Invasive lobular carcinoma of the breast has better short- and long-term survival than invasive ductal carcinoma. *Br J Cancer* 1997; **76:** 1234-40. doi: 10.1038/bjc.1997.540
7. Silverstein MJ, Lewinsky BS, Waisman JR, Gierson ED, Colburn WJ, Senofsky GM, et al. Infiltrating lobular carcinoma. Is it different from infiltrating duct carcinoma? *Cancer* 1994; **73:** 1673-7. doi: 10.1002/1097-0142(19940315)73:6<1673::aid-cncr2820730620>3.0.co
8. Molland JG, Donnellan M, Janu NC, Carmalt HL, Kennedy CW, Gillet DJ. Infiltrating lobular carcinoma – a comparison of diagnosis, management and outcome with infiltrating duct carcinoma. *Breast* 2004; **13:** 389-96. doi: 10.1016/j.breast.2004.03.004
9. Ashikari R, Huvos AG, Urban JA, Robbins GF. Infiltrating lobular carcinoma of the breast. *Cancer* 1973; **31:** 110-6. doi: 10.1002/1097-0142(197301)31:1<110::aid-cncr2820310115>3.0.co;2-v
10. Tubiana-Hulin M, Stevens D, Lasry S, Guinebretiere JM, Bouita L, Cohen-Solal C, et al. Response to neoadjuvant chemotherapy in lobular and ductal breast carcinomas: a retrospective study on 860 patients from one institution. *Ann Oncology 2006;* **17:** 1228-33. doi: 10.1093/annonc/mdl114
11. Cristofanilli M, Gonzales-Angulo A, Sneige N, Kau S-W, Broglio K, Theriault RL, et al. Invasive lobular carcinoma classic type: response to primary chemotherapy and survival outcomes. *J Clin Oncol* 2005; **23:** 41-8. doi: 10.1200/JCO.2005.03.111
12. Mathieu MC, Rouzier R, Llombart-Cussac A, Sideris L, Koscielny S, Travagli JP, et al. The poor responsiveness of infiltrating lobular breast carcinomas to neoadjuvant chemotherapy can be explained by their biological profile. *Eur J Cancer* 2004; **40:** 342-51. doi: 10.1016/j.ejca.2003.08.015
13. Du Toit RS, Locker AP, Ellis IO, Elston CW, Nicholson RI, Robertson JF, et al. An evaluation of differences in prognosis, recurrence patterns and receptor status between invasive lobular and other invasive carcinomas of the breast. *Eur J Surg Oncol* 1991; **17:** 251-7. PMID: 1646127
14. Rakha EA, EL-Sayed ME, Powe DG, Green AR, Habashy H, Grainge MJ, et al. Invasive lobular carcinoma of the breast: response to hormonal therapy and outcomes. *Eur J Cancer* 2008; **44:** 73-83. doi: 10.1016/j.ejca.2007.10.009
15. Desmedt C, Zoppoli G, Gundem G, Pruneri G, Larsimont D, Fornili M, et al. Genomic characterization of primary invasive lobular breast cancer. *J Clinical Oncol* 2016; **34:** 1872-81. doi: 10.1200/JCO.2015.64.0334
16. Zardavas D, Te Marvelde L, Milne RL, Fumagalli D, Fountzilas G, Kotoula V, et al. Tumor *PIK3CA* genotype and prognosis in early-stage breast cancer: a pooled analysis of individual patient data. *J Clin Oncol* 2018; **36:** 981-90. doi: 10.1200/JCO.2017.74.830
17. Metzger Filho O, Giobbie-Hurder A, Mallon E, Gusterson B, Viale G, Winer EP, et al. Relative effectiveness of letrozole compared with tamoxifen for patients with lobular carcinoma in the BIG 1-98 trial. *J Clin Oncol* 2015; **33:** 2772-9. doi: 10.1200/JCO.2015.60.8133

18. Luen SJ, Asher R, Lee CK, Savas P, Kammler R, Dell"Orto P, et al. Association of somatic driver alterations with prognosis in postmenopausal, hormone receptor-positive, HER2-negative early breast cancer: a secondary analysis of the BIG 1-98 randomized clinical trial. *JAMA Oncol* 2018; **4:** 1335-43. doi: 10.1001/jamaoncol.2018.1778

19. Elston CW, Ellis IO. Pathological prognostic factors in breast cancer. I. The value of histopathological grade in breast cancer: experience from a large study with long-term follow up. *Histopathology* 1991; **19:** 403-10. doi: 10.1111/j.1365-2559.1991.tb00229.x

20. Hammond ME, Hayes DF, Dowsett M, Allred DC, Hagerty KL, Badve S, et al. American Society of Clinical Oncology/College of American Pathologists guideline recommendations for immunohistochemical testing of estrogen and progesterone receptors in breast cancer. *Arch Pathol Lab Med* 2010; **134:** e48-72. doi: 10.1200/JCO.2009.25.6529

21. Wolff AC, Hammond ME, Hicks DG, Dowsett M, McShane LM, Allison KH, et al. Recommendations for human epidermal growth factor receptor-2 testing in breast cancer: American Society of Clinical Oncology/College of American Pathologists clinical practice guideline update. *J Clin Oncol* 2013; **31:** 3997-4013. doi: 10.1200/JCO.2013.50.9984

22. Dowsett M, O Nielsen T, A"Hern R, BartletT J, Coombes RC, Cuzick J, et al. Assessment of Ki-67 in breast cancer: recommendations from the International Ki-67 in Breast Cancer Working Group. *J Natl Cancer Inst* 2011; **103:** 1656-64. doi: 10.1093/jnci/djr393

23. Salgado R, Denkert C, Demaria S, Sirtaine N, Klauschen F, Pruneri G, et al. The evaluation of tumor-infiltrating lymphocytes (TILs) in breast cancer: recommendations by an International TILs Working Group 2014. *Ann Oncol 2015;* **26:** 259-71. doi: 10.1093/annonc/mdu450

24. Samuels Y, Wang Z, Bardeli A, Silliman N, Ptak J, Szabo S, et al. High frequency of mutation of the *PIK3CA* gene in human cancers. *Science* 2004; **304:** 554. doi: 10.1126/science.1096502

25. Pramod N, Nigam A, Basree M, Mawalkar R, Mehra S, Shinde N, et al. Comprehensive review of molecular mechanisms and clinical features of invasive lobular cancer. *Oncologist* 2021; **26:** e943-53. doi: 10.1002/onco.13734

26. Johansson A, Yu NY, Iftimi A, Tobin NP, vant Veer L, Nordenskjold B, et al. Clinical and molecular characteristics of estrogen receptor-positive ultralow risk breast cancer tumors identified by the 70-gene signature. *Int J Cancer* 2022; **150:** 2072-82. doi: 10.1002/ijc.33969

27. Griffith OL, Spies NC, Anurag M, Griffith M, Luo J, Tu D, et al. The prognostic effects of somatic mutations in ER-positive breast cancer. *Nat Commun* 2018; **9:** 3476. doi: 10.1038/s41467-018-05914-x

28. McCart Reed AE, Kalinowski L, Simpson PT, Lakhani SR. Invasive lobular carcinoma of the breast: the increasing importance of this special subtype. *Breast Cancer Res* 2021; **23:** 6. doi: 10.1186/s13058-020-01384-6

29. McCart Reed AE, Lal S, Kutasovic JR, Wockner L, Robertson A, de Luca XM, et al. LobSig is a multigene predictor of outcome in invasive lobular carcinoma. *NPJ Breast Cancer* 2019; **5:** 18. doi: 10.1038/s41523-019-0113-y

30. Metzger FO, Giobbie-Hurder A, Mallon E, Gusterson B, Viale G, Winer EP, et al. Relative effectiveness of letrozole compared with tamoxifen for patients with lobular carcinoma in the BIG 1-98 trial. *J Clin Oncol* 2015; **33:** 2772-79. doi: 10.1200/JCO.2015.60.813

31. Lopez-Knowles E, Segal CV, Gao Q, Garcia-Murillas I, Turner NC, Smith I, et al. Relationship of *PIK3CA* mutation and pathway activity with antiproliferative response to aromatase inhibition. *Breast Cancer Res* 2014; **16:** R68. doi: 10.1186/bcr3683

32. Loi S, Haibe-Kains B, Majjaj S, Lallemand F, Durbeck V, Larsimont D, et al. *PIK3CA* mutations associated with gene signature of low mTORC1 signaling and better outcomes in estrogen receptor-positive breast cancer. *Proc Natl Acad Sci USA* 2010; **107:** 10208-13. doi: 10.1073/pnas.0907011107

33. Whyte DB, Holbeck SL. Correlation of *PIK3CA* mutations with gene expression and drug sensitivity in NCI-60 cell lines. *Biochem Biophys Res Commun* 2006; **340:** 469-75. doi: 10.1016/j.bbrc.2005.12.025

research article

Subpleural fibrotic interstitial lung abnormalities are implicated in non-small cell lung cancer radiotherapy outcomes

Makoto Ito[1], Takuma Katano[2], Hiroaki Okada[1], Ami Sakuragi[3], Yoshitaka Minami[3], Souichiro Abe[1], Sou Adachi[1], Yukihiko Oshima[1], Wataru Ohashi[4], Akihito Kubo[2], Takayuki Fukui[5], Satoru Ito[2], Kojiro Suzuki[1]

[1] Department of Radiology, Aichi Medical University, Aichi, Japan
[2] Department of Respiratory Medicine and Allergology, Aichi Medical University, Aichi, Japan
[3] Department of Central Radiology, Aichi Medical University, Aichi, Japan
[4] Department of Biostatistics, Clinical Research Center, Aichi Medical University, Aichi, Japan
[5] Division of Chest Surgery, Department of Surgery, Aichi Medical University, Aichi, Japan

Radiol Oncol 2023; 57(2): 229-238.

Received 19 February 2023
Accepted 02 April 2023

Correspondence to: Dr. Makoto Ito, Department of Radiology, Aichi Medical University, 1-1 Yazako-Karimata, Nagakute, Aichi 480-1195, Japan. E-mail: itou.makoto.292@mail.aichi-med-u.ac.jp

Disclosure: No potential conflicts of interest were disclosed.

Background. The relationship between interstitial lung abnormalities (ILAs) and the outcomes of lung cancer radiotherapy is unclear. This study investigated whether specific ILA subtypes are risk factors for radiation pneumonitis (RP).

Patients and methods. This retrospective study analysed patients with non-small cell lung cancer treated with radical-intent or salvage radiotherapy. Patients were categorised into normal (no abnormalities), ILA, and interstitial lung disease (ILD) groups. The ILA group was further subclassified into non-subpleural (NS), subpleural non-fibrotic (SNF), and subpleural fibrotic (SF) types. The Kaplan–Meier and Cox regression methods were used to determine RP and survival rates and compare these outcomes between groups, respectively.

Results. Overall, 175 patients (normal, n = 105; ILA-NS, n = 5; ILA-SNF, n = 28; ILA-SF, n = 31; ILD, n = 6) were enrolled. Grade ≥2 RP was observed in 71 (41%) patients. ILAs (hazard ratio [HR]: 2.33, p = 0.008), intensity-modulated radiotherapy (HR: 0.38, p = 0.03), and lung volume receiving 20 Gy (HR: 54.8, p = 0.03) contributed to the cumulative incidence of RP. Eight patients with grade 5 RP were in the ILA group, seven of whom had ILA-SF. Among radically treated patients, the ILA group had worse 2-year overall survival (OS) than the normal group (35.3% vs 54.6%, p = 0.005). Multivariate analysis revealed that the ILA-SF group contributed to poor OS (HR: 3.07, p =0.02).

Conclusions. ILAs, particularly ILA-SF, may be important risk factors for RP, which can worsen prognosis. These findings may aid in making decisions regarding radiotherapy.

Key words: interstitial lung abnormality; subpleural fibrosis; non-small cell lung cancer; radiotherapy; radiation pneumonitis; survival analysis

Introduction

Lung cancer is one of the most common and deadliest cancers worldwide, with non-small cell lung cancer (NSCLC) accounting for approximately 85% of all cases.[1,2] Radiotherapy is a typical non-surgical curative treatment for localised NSCLC.[3] Recently, the integration of immunotherapy with chemoradiation has revolutionised the treatment of locally advanced NSCLC. For instance, the PACIFIC trial reported a 5-year overall survival (OS) rate of 42.9% and progression-free survival (PFS) rate of

33.1% among individuals who received treatment with durvalumab, an anti-programmed cell death-ligand 1 antibody, after chemoradiotherapy for stage III NSCLC.[4] However, radiation pneumonitis (RP) is a major concern with this treatment strategy. Patients with grade ≥ 2 RP (according to the Common Terminology Criteria for Adverse Events [CTCAE]) from prior chemoradiotherapy cannot use durvalumab.[5] Additionally, RP causes respiratory insufficiency that severely affects the quality of life, leading to poor prognosis and even death.[6] Risk factors should be identified before treatment to avoid grade 2 or more severe RP.

Various risk factors for RP have been reported, such as age, tumour size, and tumour location.[7] Interstitial lung disease (ILD) is a significant predisposing condition. Radiotherapy for lung cancer complicated by ILD induces a high RP rate and borders on being contraindicated.[8] In contrast, the influence of interstitial lung abnormalities (ILAs) on RP risk remains unclear. Studies investigating the relationship between ILAs and RP are limited, and their results are inconsistent; additionally, no consensus has been reached.[9,10] ILAs are specific computed tomography (CT) findings that are potentially compatible with ILD in patients without clinical indication of the disease. ILAs had been originally described as non-dependent abnormalities affecting more than 5% of any lung zone; however, they overlapped with other disease concepts.[11] In 2020, the Fleischner Society clarified the definition of ILAs and further classified them into three subtypes—namely, non-subpleural (NS), subpleural non-fibrotic (SNF), and subpleural fibrotic (SF).[12] Nevertheless, there are no reports describing lung cancer radiotherapy's effect on these newly defined ILAs.

Therefore, in this study, we retrospectively reviewed the data of patients with NSCLC who underwent radiotherapy and conducted a survival analysis to investigate how the novel ILA subtypes relate to RP risk.

Patients and methods

Patients

We retrospectively reviewed the medical records of patients with NSCLC treated with radiotherapy between January 2010 and November 2021. We included patients treated with radical-intent radiotherapy for locally advanced NSCLC or with salvage radiotherapy for locoregional recurrence postoperatively. Of the 188 consecutive patients who met these criteria, 9 who received stereotactic body radiation therapy for salvage and 4 who had a short follow-up duration (< 6 months) were excluded. We collected information from the remaining 175 patients' medical records, including age, sex, Eastern Cooperative Oncology Group performance status, smoking history, blood sampling, pulmonary function tests, pathology, and imaging data. Patients treated with radical-intent radiotherapy were staged according to the 8th edition of the Union for International Cancer Control tumour–node–metastasis classification. This study was approved by the Ethics Committee of Aichi Medical University (approval no. 2021-545) with an opt-out approach regarding the analysis before this study. All procedures involved in the study adhered to the principles of the Declaration of Helsinki. The requirement for the acquisition of informed consent from patients was waived owing to the retrospective nature of this study.

Radiotherapy

Patients were immobilised in the supine position using an external vacuum-type body mould and/or thermoplastic body mask, and a CT scan with a 2-mm slice thickness was conducted for treatment planning. Respiratory motion was confirmed by obtaining CT images in both the expiratory and inspiratory phases or during shallow breathing. Both the target volume and normal organ structures were contoured using treatment planning systems (CMS XiO, Elekta, St Louis, MO, USA; Eclipse, Varian Medical Systems, Palo Alto, CA, USA; or Maestro, MIM Software, Inc., Cleveland, OH, USA). The clinical target volume (CTV) was defined as a 0–5-mm expansion of the primary tumour and metastatic lymph nodes. To account for respiratory migration, a 5–15-mm margin was added to the CTV to define the planning target volume (PTV). Radiotherapy was delivered by 6- or 10-MV x-rays from linear accelerators (Clinac iX or TrueBeam STx, Varian Medical Systems, Palo Alto, CA, USA). Overall, 60 Gy in 30 fractions was delivered to the PTV, and 119 (68%) patients received prophylactic elective nodal irradiation of 40 Gy in 20 fractions to the lymph node area. In exceptional cases, 11 (6%) patients received dose escalation up to 64–70 Gy.

Additionally, six (3%) patients underwent hypofractionated radiotherapy of up to 2.7–3 Gy per fraction to shorten the duration of treatment. The irradiation methods used were three-dimensional conformal or intensity-modulated radiotherapy

TABLE 1. Patient characteristics

Characteristic	Normal (*n* = 105)	ILA (*n* = 64)	ILD (*n* = 6)	*p*
Age (years)	71 (41–90)	72 (60–86)	74 (63–86)	0.01
Sex (men)	82 (78%)	52 (81%)	6 (100%)	0.70
Performance status	–	–	–	0.42
0	53 (50%)	37 (58%)	4 (66%)	–
1	41 (39%)	19 (30%)	1 (17%)	–
2	7 (7%)	7 (11%)	1 (17%)	–
3	4 (4%)	1 (1%)	0 (0%)	–
Pack year	45 (0–171)	47 (0–122)	48.5 (20–84)	0.98
Pulmonary function test				
%VC (%)	99.1 (41.8–144.2)	103.0 (41.8–147.5)	86.9 (55.7–98.8)	0.08
FEV1 (L)	1.9 (0.6–3.6)	2.2 (0.9–3.5)	2.0 (1.5–2.1)	0.12
FEV1/FVC (%)	69.2 (34.1–98.1)	69.8 (36.0–85.0)	74.8 (62.2–86.8)	0.36
KL-6 (U/mL)	282 (151–3957)	370 (172–896)	393 (204–859)	0.65
Pathology	–	–	–	0.01
Adenocarcinoma	59 (56%)	21 (33%)	2 (33%)	–
Squamous cell carcinoma	40 (38%)	38 (59%)	4 (67%)	–
Others	6 (6%)	5 (8%)	0 (0%)	–
Lower-lobe primary lesion (radical-intent)	19 (22%)	14 (33%)	3 (75%)	0.20
TNM classification (radical-intent)				
T classification	–	–	–	0.53
1	13 (15%)	3 (7%)	0 (0%)	–
2	23 (26%)	12 (28%)	2 (50%)	–
3	19 (22%)	13 (30%)	0 (0%)	–
4	32 (37%)	15 (35%)	2 (50%)	–
N classification	–	–	–	0.32
0	7 (9%)	8 (19%)	0 (0%)	–
1	16 (18%)	8 (19%)	1 (25%)	–
2	42 (48%)	16 (37%)	2 (50%)	–
3	22 (25%)	11 (26%)	1 (25%)	–
Stage	–	–	–	0.40
II A	3 (3%)	1 (2%)	0 (0%)	–
II B	5 (6%)	6 (14%)	0 (0%)	–
III A	34 (39%)	15 (35%)	3 (75%)	–
III B	36 (41%)	14 (33%)	0 (0%)	–
III C	9 (11%)	7 (16%)	1 (25%)	–
Concurrent chemotherapy	65 (62%)	33 (52%)	2 (33%)	0.20
Carboplatin + paclitaxel	30 (46%)	18 (55%)	2 (100%)	–
Cisplatin + docetaxel	22 (34%)	8 (24%)	0 (0%)	–
Cisplatin + vinorelbine	13 (20%)	7 (21%)	0 (0%)	–
Durvalumab	17 (16%)	9 (14%)	0 (0%)	0.83
PD-L1 (positive)	36 (34%)	23 (36%)	0 (0%)	0.99
Mutation	–	–	–	0.99
EGFR	8 (7%)	5 (8%)	1 (17%)	–
ALK	6 (6%)	2 (3%)	1 (17%)	–
None/unknown	91 (87%)	57 (89%)	4 (66%)	–
Radiotherapy method	–	–	–	0.08
3DCRT	80 (76%)	40 (63%)	5 (83%)	–
IMRT	25 (24%)	24 (37%)	1 (17%)	–
ENI	77 (73%)	38 (59%)	4 (67%)	0.06
Hypofractionated radiotherapy	3 (3%)	3 (5%)	0 (0%)	0.67
Dose escalation	6 (6%)	5 (8%)	0 (0%)	0.75
Lung dose				
V5 (%)	34.5 (4.3–90.8)	40.3 (5.8–95.7)	34.6 (10.6–66.8)	0.18
V10 (%)	27.1 (2.7–67.7)	32.4 (3.7–81.4)	27.8 (8.8–49.9)	0.19
V20 (%)	19.8 (1.1–44.8)	22.0 (1.0–48.0)	22.6 (7.3–33.0)	0.59
Mean (Gy)	10.8 (1.7–23.5)	11.8 (2.0–19.6)	12.3 (3.8–18.0)	0.53
Median follow-up (years)	1.8 (0.1–12.1)	1.3 (0.1–9.9)	0.9 (2.1–3.9)	0.06
Median follow-up: survivors (years)	2.9 (0.6–12.1)	1.9 (0.6–9.9)	0.9 (0.9–0.9)	0.51

Data are presented as median (range) or number (%). The *p*-values represent comparisons between the normal and ILA groups.

ALK = anaplastic lymphoma kinase; EGFR = epidermal growth factor receptor; ENI = elective nodal irradiation; FEV1 = forced expiratory volume in 1 second; FEV1/FVC = forced expiratory volume % in 1 second; ILAs = interstitial lung abnormalities; ILD = interstitial lung disease; IMRT = intensity-modulated radiotherapy; KL-6 = Krebs von den Lungen-6; *n* = total number of patients; PD-L1 = programmed cell death-ligand 1; TNM = tumour–node–metastasis; VC = vital capacity percentage; Vx = percentage of lung volume receiving > x Gy; 3DCRT = three-dimensional conformal radiotherapy%

TABLE 2. Clinical details of eight patients with grade 5 radiation pneumonitis

Case	Age	ILA subcategory	Radiotherapy method	Concurrent chemotherapy	Durvalumab	Lung V20 (%)	Mean lung dose (Gy)	Days to death
1	64	SF	IMRT	Yes	No	19.2	12.8	104
2	73	SF	3DCRT	Yes	No	21.4	13.9	210
3	73	SF	IMRT	No	No	30.6	15.7	123
4	76	SF	IMRT	Yes	Yes	34.1	17.9	155
5	77	SNF	3DCRT	No	No	33.2	16.5	155
6	79	SF	IMRT	Yes	No	31.5	17.3	160
7	79	SF	3DCRT	No	No	19.4	9.7	40
8	80	SF	3DCRT	No	No	27.6	15.2	99

ILAs = interstitial lung abnormalities; IMRT = intensity-modulated radiotherapy; SF = subpleural fibrotic; SNF = subpleural non-fibrotic; V20 = percentage of lung volume receiving > 20 Gy; 3DCRT = three-dimensional conformal radiotherapy

(IMRT). Two-step IMRT was used for the entire period or only as boost irradiation of 20 Gy in 10 fractions.

The dose constraints were as follows: the goals for the global and spinal maximum doses were < 107% (< 125% allowed) and < 50 Gy (< 52 Gy allowed), respectively, whereas the goals for the lung volumes were 5 Gy (V5) < 60%, V20 < 25%, and mean lung dose < 12 Gy. Vx refers to the percentage of the lung volume receiving > x Gy. The goal for the mean heart dose was < 20 Gy. Allowance values for lung and heart doses were not set; however, every effort was made to reduce them as much as possible.

Chemotherapy and immunotherapy

Patient age, general condition, and organ function determined the appropriateness of concurrent chemotherapy and its regimen. The most commonly used regimen was weekly carboplatin/paclitaxel, and cisplatin/docetaxel or cisplatin/vinorelbine was also administered. Durvalumab has been available to patients at our institution since October 2018. We performed CT after concurrent chemoradiation therapy was completed to ensure that there was no disease progression or grade ≥ 2 RP before administration. Durvalumab was intravenously administered at a dose of 10 mg/kg every 2 weeks for 1 year. If grade 2 RP appeared, the administration was suspended until the patient recovered to grade 1. We stopped administration in cases of serious adverse events, such as grade ≥ 3 RP or confirmed disease progression.

ILA classification and treatment outcomes

ILAs were defined according to the Fleischner Society classification.[12] The grouping was primarily performed by two physicians: a chest physician engaged in ILDs and a diagnostic radiologist engaged in chest radiology. They reviewed medical records including past history, family history, and reasons for imaging studies before reviewing CT images. Next, they used diagnostic chest CT images taken before treatment for grouping. All patients were classified into the following three groups: normal (no abnormalities), ILA, and ILD. The ILA group was further subdivided into NS, SNF, and SF groups. This process was performed independently by a chest physician and a diagnostic radiologist without discussion and was later collated. Grouping of any discrepant cases was finalized by consultation among the two, with another radiologist acting as an intermediary. Details of the CT protocols used for grouping are as follows. SOMATOM Definition AS/AS+/Flash (Siemens Healthcare, München, Germany) and Light Speed VCT VISION (General Electric Healthcare, Milwaukee, Wisconsin, USA) CT scanners were used. Slice thickness was 2–2.5-mm. Tube voltage was 120 kVp. Tube current was auto exposure control. Scan mode was helical acquisition. Pitch factor was 0.8–1.5. Rotation time was 0.3–0.5.

We measured the time to the event from the date of radiotherapy commencement. Toxicity was graded according to the CTCAE version 5.0. Grade 2 RP was considered an event with steroid administration for chest symptoms; administration

TABLE 3. Univariate and multivariate analyses of the cumulative incidence of grade ≥ 2 radiation pneumonitis

Parameter	Univariate analysis		Multivariate analysis	
	HR (95% CI)	*p*	HR (95% CI)	*p*
ILA	2.95 (1.81–4.82)	<0.001	2.33 (1.18–4.61)	0.01
Age (years)	1.02 (0.99–1.05)	0.14	0.99 (0.95–1.03)	0.78
Sex (men)	1.02 (0.57–1.84)	0.94	–	–
Performance status (0,1 *vs.* 2,3)	1.17 (0.56–2.44)	0.68	–	–
Pack year	1.01 (0.99–1.01)	0.27	–	–
%VC (%)	0.99 (0.98–1.01)	0.96	–	–
FEV1 (L)	1.01 (0.64–1.55)	0.99	–	–
FEV1/FVC (%)	0.99 (0.97–1.01)	0.67	–	–
KL-6 (U/mL)	1.00 (0.99–1.01)	0.09	1.00 (0.99–1.01)	0.13
Pathology (adenocarcinoma)	0.58 (0.35–0.96)	0.04	0.85 (0.42–1.72)	0.65
Lower-lobe primary lesion	1.22 (0.69–2.12)	0.49	–	–
T classification (T4 *vs.* others)	0.81 (0.47–1.39)	0.44	–	–
N classification (positive)	1.18 (0.51–2.72)	0.70	–	–
Concurrent chemotherapy	1.17 (0.72–1.88)	0.53	–	–
Durvalumab	1.32 (0.72–2.40)	0.37	–	–
PD-L1	1.11 (0.54–2.25)	0.78	–	–
Mutation	1.24 (0.62–2.49)	0.54	–	–
Radiotherapy method (IMRT)	0.69 (0.39–1.19)	0.18	0.38 (0.16–0.91)	0.03
ENI	1.06 (0.65–1.75)	0.81	–	–
Lung dose				
V5 (%)	2.14 (0.67–6.82)	0.19	*	*
V10 (%)	3.93 (0.85–18.2)	0.08	*	*
V20 (%)	34.8 (3.05–396.4)	0.004	54.8 (1.52–1977.0)	0.03
Mean (Gy)	1.10 (1.04–1.17)	<0.001	*	*

CI = confidence interval; ENI = elective nodal irradiation; FEV1 = forced expiratory volume in 1 second; FEV1/FVC = forced expiratory volume % in 1 second; HR = hazard ratio; ILAs = interstitial lung abnormalities; IMRT = intensity-modulated radiotherapy; KL-6 = Krebs von den Lungen-6; N = node; PD-L1 = programmed cell death-ligand 1; RP = radiation pneumonitis; T = tumour; %VC = vital capacity percentage; Vx = percentage of lung volume receiving > x Gy; *vs.* = versus

* Variables with high multicollinearity were excluded.

of general cough suppressants was not included. Survival analysis was performed for patients under radical treatment.

Statistical analyses

All statistical analyses were performed using EZR version 1.55 (Saitama Medical Center, Jichi Medical University, Saitama, Japan) based on R and R commanders.[13] Patient characteristics were compared using Fisher's exact test for categorical variables and Student's t-test or the Mann–Whitney U test for continuous variables. Additionally, the Kaplan–Meier method was employed to estimate the cumulative incidence of RP and survival rates, and comparisons were performed using Gray's or log-rank test with post-hoc Bonferroni analyses for multiple comparisons. Finally, a Cox proportional hazards model was used for univariate and multivariate (stepwise elimination) analyses to determine factors contributing to RP and survival rates. Statistical significance was set at $p < 0.05$. Factors demonstrating $p < 0.2$ in the univariate analysis were included in the multivariate analysis. Receiver operating characteristic (ROC) curves were used to evaluate the relationship between RP and lung V20. The cut-off point was determined based on the Youden index, and well-balanced sensitivity and specificity values were obtained.[14]

TABLE 4. Characteristics of patients treated with radical-intent radiotherapy

Characteristic	Normal (*n* = 87)	ILA-SF (*n* = 24)	*p*
Age (years)	69 (41–90)	73 (60–82)	0.09
Performance status	–	–	0.39
0	41 (47%)	12 (50%)	–
1	36 (41%)	8 (33%)	–
2	6 (7%)	4 (17%)	–
3	4 (5%)	0 (0%)	–
Pack year	45 (0–171)	53 (0–122)	0.38
KL-6 (U/mL)	294 (151–1607)	399 (208–705)	0.91
Pathology	–	–	0.09
Adenocarcinoma	46 (53%)	7 (29%)	–
Squamous cell carcinoma	35 (40%)	14 (58%)	–
Others	6 (7%)	3 (13%)	–
Lower-lobe primary lesion	19 (22%)	6 (25%)	0.79
T classification	–	–	0.36
1	13 (15%)	1 (4%)	–
2	23 (26%)	10 (42%)	–
3	19 (22%)	5 (21%)	–
4	32 (37%)	8 (33%)	–
Concurrent chemotherapy	58 (67%)	13 (54%)	0.33
Durvalumab	15 (17%)	1 (4%)	0.19
Mutation	8 (13%)	3 (18%)	0.70
Median follow-up: survivors (years)	2.8 (0.6–12.1)	1.5 (0.7–6.0)	0.46

Data are presented as median (range) or number (%).

ILA-SF = subpleural fibrotic interstitial lung abnormalities; KL-6 = Krebs von den Lungen-6; *n* = total number of patients

Results

Patient characteristics

The final analysis included 175 patients, with the normal, ILA, and ILD groups comprising 105, 64, and 6 patients, respectively. Table 1 summarises patient characteristics.

The p-values represent comparisons between the normal and ILA groups. The normal group was younger and had more patients with adenocarcinomas than the ILA group. The median follow-up period of the 70 surviving patients was 2.5 (range, 0.6–12.1) years. The 64 patients with ILA were subcategorised into NS, SNF, and SF subtypes comprising 5, 28, and 31 patients, respectively. Examples of the ILA subcategories are shown in Figure 1. The two specialists (a chest physician and a diagnostic radiologist) matched on 125 of the 175 patient classifications (72%), and the remaining cases were grouped by discussion among the three physicians.

Radiation pneumonitis

Grade ≥ 2 RP was identified in 71 (41%) patients. Of the 105 patients in the normal group, 21 (20%), 8 (8%), and 1 (1%) exhibited grades 2, 3, and 4, respectively. Of the 64 patients in the ILA group, grades 2, 3, 4, and 5 were observed in 19 (30%), 8 (13%), 2 (3%), and 8 (13%) individuals, respectively. Of the six patients in the ILD group, 2 (33%) and 3 (50%) showed grades 2 and 3, respectively. Seven of the eight patients with grade 5 RP were in the ILA-SF group, and one was in the ILA-SNF group (details shown in Table 2).

Figure 2 shows the cumulative incidence of grade ≥ 2 RP by group or subgroup. The incidence of RP was significantly higher in the ILA group than in the normal group ($p < 0.001$), particularly between the SNF ($p = 0.014$) and SF groups ($p < 0.001$) and the normal group. Table 3 presents the results of the univariate and multivariate analyses.

ILAs (hazard ratio [HR]: 2.33, $p = 0.01$), IMRT (HR: 0.38, $p = 0.03$), and lung V20 (HR: 54.8, $p = 0.03$) were significantly associated with the cumulative incidence of grade ≥ 2 RP in the multivariate analyses.

ROC analysis using V20 showed intermediate grade ≥ 2 RP predictive accuracy in the normal group; the area under the curve (AUC) was 0.72 (95% confidence interval [CI]: 0.60–0.83). The sensitivity and specificity for a cut-off value of 21% for V20 were 76% and 67%, respectively. Conversely, the predictive accuracy in the ILA group was low, with an AUC of 0.59 (95% CI: 0.45–0.75); furthermore, the sensitivity and specificity for a cut-off value of 19% were 76% and 56%, respectively. During follow-up after radiotherapy, five patients received molecular-targeted therapies, and two had grade ≥ 2 RP. However, it was not until 2 years and 10 years after radiotherapy that the two patients, respectively, began receiving molecular-targeted therapies, which had already cured their RP.

Survival

The 2-year OS and PFS rates for the 134 radically treated patients were 47.8% (95% CI: 38.5–56.4%) and 21.2% (95% CI: 14.4–28.9%), respectively. Patients in the ILA group had worse 2-year OS than those in the normal group (35.3% *vs.* 54.6%, $p = 0.005$); however, the multivariate analysis showed

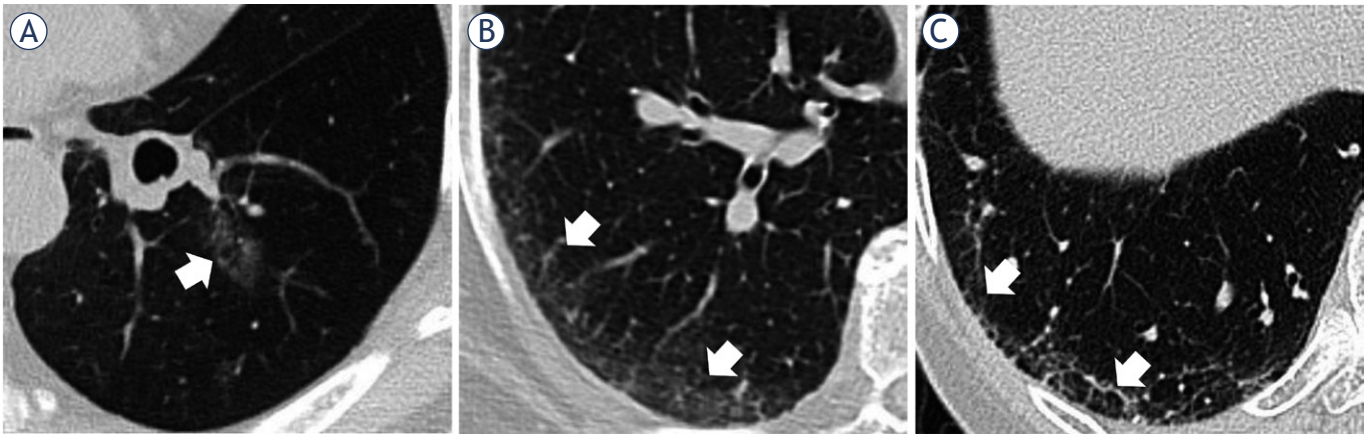

FIGURE 1. Examples of interstitial lung abnormality subcategories. **(A)** non-subpleural, **(B)** subpleural non-fibrotic, and **(C)** subpleural fibrotic. White arrows point to lesions.

no significant difference. No significant difference was found in the 2-year PFS between the ILA and normal groups (17.3% vs 24.1%, p = 0.26).

The characteristics of the patients treated with radical-intent radiotherapy are summarised in Table 4. The parameters to be entered into the multivariate analysis are listed separately for the normal and ILA-SF groups.

No significant bias was found between the two groups; however, only one patient in the ILA-SF group received durvalumab. Patients in the ILA-SF group had significantly worse 2-year OS (29.2% vs 54.6%, p < 0.001) and PFS (9.7% vs 24.1%, p = 0.009) rates than those in the normal group. Table 5 shows the results of the univariate and multivariate analyses for the OS and PFS rates.

The multivariate analysis revealed that ILA-SF was the only independent adverse factor for OS (HR: 3.07, 95% CI: 1.17–8.10, $p = 0.02$) and that it also tended to influence PFS (HR: 1.95, 95% CI: 0.91–4.14, $p = 0.08$). In contrast, younger age, adenocarcinoma, concurrent chemotherapy, and durvalumab treatment contributed to the prolongation of OS and/or PFS.

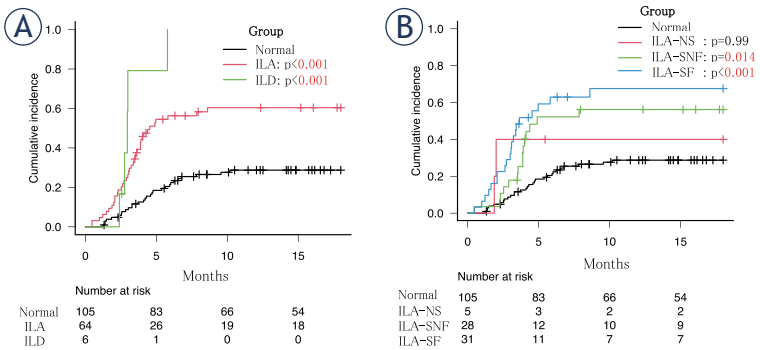

FIGURE 2. Cumulative incidence of grade ≥ 2 radiation pneumonitis by group **(A)** and subgroup **(B)**.

ILAs = interstitial lung abnormalities; ILD = interstitial lung disease; NS = non-subpleural; SF = subpleural fibrotic; SNF = subpleural non-fibrotic

Discussion

To the best of our knowledge, this is the first study to classify patients with NSCLC according to the Fleischner Society ILA subtypes and to demonstrate subtype-associated risk with respect to radiotherapy outcomes. In our analysis, ILAs were considered risk factors for grade ≥ 2 RP. Among radically treated patients, the ILA group showed significantly worse 2-year OS than the normal group. This was particularly true for the ILA-SF group, which also independently contributed to OS in the multivariate analysis.

To date, only a few studies have examined the relationship between ILAs and RP. A previous study retrospectively analysed the association between RP and original ILA scores in 145 patients with NSCLC.[9] The ILA scores were rated as follows: 0, no interstitial lung change; 1, ILAs without honeycombing (ground-glass attenuation, fine reticular opacity, and microcysts); and 2, honeycombing. They concluded that abnormalities, with or without honeycombing, were predictors of RP. Several reports indicate that ILA is a risk factor for RP in patients with small -cell lung cancer.[15,16] Conversely, another study concluded that ILAs did not independently contribute to RP.[10] This discrepancy may be due to the ambiguous previous definition of ILAs. Moreover, previous studies have

TABLE 5. Univariate and multivariate analyses for overall and progression-free survival rates

Parameter	Overall survival				Progression-free survival			
	Univariate		Multivariate		Univariate		Multivariate	
	HR (95% CI)	*P*	HR (95% CI)	*p*	HR (95% CI)	*p*	HR (95% CI)	*p*
ILA-SF	2.59 (1.51–4.43)	<0.001	3.07 (1.17–8.10)	0.02	1.88 (1.16–3.05)	0.01	1.95 (0.91–4.14)	0.08
Age (years)	1.02 (0.99–1.04)	0.09	0.95 (0.91–0.99)	0.04	1.01 (0.98–1.03)	0.59	–	–
Sex (men)	1.21 (0.70–2.10)	0.49	–	–	0.91 (0.58–1.45)	0.71	–	–
Performance status (0,1 vs. 2,3)	1.90 (1.07–3.39)	0.03	0.82 (0.19–3.38)	0.78	2.81 (1.66–4.78)	<0.001	1.35 (0.46–3.93)	0.59
Pack year	1.01 (1.00–1.01)	0.04	1.01 (0.99–1.02)	0.14	1.00 (0.99–1.01)	0.67	–	–
%VC (%)	0.99 (0.98–1.01)	0.56	–	–	0.99 (0.98–1.01)	0.51	–	–
FEV1 (L)	0.84 (0.55–1.29)	0.43	–	–	0.92 (0.62–1.36)	0.68	–	–
FEV1/FVC (%)	0.99 (0.97–1.02)	0.92	–	–	1.01 (0.98–1.02)	0.75	–	–
KL-6 (U/mL)	1.00 (0.99–1.01)	0.11	1.00 (0.99–1.01)	0.34	1.01 (1.00–1.02)	0.03	1.00 (0.99–1.01)	0.40
Pathology (adenocarcinoma)	0.46 (0.31–0.69)	<0.001	0.18 (0.08–0.44)	<0.001	0.54 (0.36–0.79)	0.002	0.34 (0.18–0.65)	0.001
Lower-lobe primary lesion	1.60 (1.02–2.53)	0.04	1.03 (0.39–2.68)	0.95	1.09 (0.72–1.65)	0.69	–	–
T classification (T4 vs. others)	1.15 (0.74–1.79)	0.53	–	–	1.47 (0.99–2.17)	0.05	1.53 (0.78–2.99)	0.21
N classification (positive)	1.02 (0.49–2.12)	0.95	–	–	0.88 (0.48–1.60)	0.67	–	–
Concurrent chemotherapy	0.51 (0.33–0.80)	0.004	0.19 (0.07–0.56)	0.002	0.60 (0.41–0.89)	0.01	0.65 (0.31–1.30)	0.22
Durvalumab	0.22 (0.08–0.60)	0.003	0.43 (0.11–1.69)	0.22	0.34 (0.18–0.65)	0.001	0.40 (0.17–0.93)	0.03
PD-L1 (positive)	0.77 (0.39–1.50)	0.44	–	–	1.03 (0.59–1.79)	0.92	–	–
Mutation	0.76 (0.47–1.22)	0.26	–	–	0.96 (0.64–1.42)	0.83	–	–
Radiotherapy method (IMRT)	0.75 (0.43–1.30)	0.31	–	–	0.86 (0.55–1.34)	0.50	–	–
ENI	0.83 (0.49–1.38)	0.47	–	–	0.99 (0.64–1.56)	0.99	–	–
Lung dose								
V5 (%)	0.45 (0.12–1.72)	0.24	–	–	0.56 (0.19–1.66)	0.30	–	–
V10 (%)	0.37 (0.06–2.27)	0.29	–	–	0.44 (0.10–1.92)	0.28	–	–
V20 (%)	0.36 (0.02–5.27)	0.46	–	–	0.23 (0.02–2.27)	0.21	–	–
Mean (Gy)	0.98 (0.93–1.04)	0.48	–	–	0.97 (0.93–1.02)	0.29	–	–

CI = confidence interval; ENI = elective nodal irradiation; FEV1 = forced expiratory volume in 1 second; FEV1/FVC = forced expiratory volume % in 1 second; HR = hazard ratio; ILA-SF = subpleural fibrotic interstitial lung abnormalities; IMRT = intensity-modulated radiotherapy; KL-6 = Krebs von den Lungen-6; PD-L1 = programmed cell death-ligand 1; %VC = vital capacity percentage; Vx = percentage of lung volume receiving > x Gy.

tended to confuse smoking-related centrilobular nodularity and pleuroparenchymal fibroelastosis with ILAs.[19,20] These disease concepts are explicitly excluded from the novel definition of ILAs. Awareness of the improved definition of ILAs is essential for correct diagnosis, which should be made before radiotherapy to guide treatment strategy. Grade ≥ 2 RP occurred at a rate as high as 71 (41%) patients in this study. We believe that one of the important factors was the large number of patients with ILA included, 64 (37%), as a characteristic of the institution. If the presence of ILA had been accurately recognised in advance, countermeasures could have been taken.

The leading treatment-related factor that predicts RP is lung V20.[19,20] V20 should be further reduced when radiotherapy is administered to patients with ILAs. Moreover, the use of IMRT should be considered along with techniques such as virtual lung block and end-inspiration irradiation.[21,22] However, the ROC analysis in the ILA group showed low predictive accuracy for grade ≥ 2 RP using V20 (AUC = 0.59). This finding implies that reducing the lung dose in patients with ILAs may not necessarily preclude severe RP.

ILA subtype divisions demonstrated notable differences. The ILA-SF group had the highest cumulative incidence of grade ≥ 2 RP, corroborat-

ing previous studies that have shown ILA-SF to be 6.6 times more likely to progress than other subtypes.[23] Contrarily, no difference was observed in the cumulative incidence of grade ≥ 2 RP between the ILA-NS and normal groups. The course of ILA-NS is usually non-progressive, suggesting a favourable prognosis.[21] ILA-NS may not be a risk factor for RP; nonetheless, we emphasise that there were few patients with ILA-NS in this study; therefore, we cannot mention its clinical significance. Therefore, this subtype should be investigated in more eligible patients in the future.

No consensus exists that patients with ILAs have a poor prognosis after radiotherapy. However, studies have reported that the outcomes of surgery and chemotherapy for patients with lung cancer and ILAs are poor.[24,25] In this study, all eight patients with grade 5 RP were in the ILA group, and seven of these patients were in the ILA-SF category. We believe that the severity of RP worsened the prognosis of the ILA group, particularly that of patients with the ILA-SF subtype. The advent of durvalumab has greatly improved the prognosis of NSCLC; however, it is difficult to administer in the long term, particularly in patients with ILA-SF. Death sometimes results from severe RP rather than cancer; therefore, the indication for radiotherapy should be carefully considered.

Our study had some limitations, particularly its retrospective and single-institution design. Additionally, other factors, such as emphysema, chronic obstructive pulmonary disease, and biomarkers (e.g., transforming growth factor-beta), may contribute to RP.[7] These factors, which we did not consider in this study, may be confounders. Furthermore, many of our patients were elderly and frail and were treated with radiotherapy alone. We also included several cases from the period before the emergence of durvalumab. These differ from modern standard treatments and may have implications for survival analysis. Retrospective studies on cases with durvalumab have been reported recently[26], and high-quality future prospective trials are warranted

Conclusions

The novel definition of ILAs and ILA subtypes may be important in determining risk for RP following radiotherapy in patients with NSCLC. RP symptoms can be severe, especially in patients with ILA-SF, and may worsen prognosis. This study suggests that recognising the presence of and categorising ILAs before treatment is vital and useful in clinical decision-making.

Acknowledgements

This work was partially supported by the Japan Society for the Promotion of Science KAKENHI [grant number JP20K16741]. The authors thank Editage (www.editage.com) for English language editing.

References

1. Bray F, Ferlay J, Soerjomataram I, Siegel RL, Torre LA, Jemal A. Global cancer statistics 2018: GLOBOCAN estimates of incidence and mortality worldwide for 36 cancers in 185 countries. *CA Cancer J Clin* 2018; **68:** 394-424. doi: 10.3322/caac.21492
2. Duma N, Santana-Davila R, Molina JR. Non-small cell lung cancer: epidemiology, screening, diagnosis, and treatment. *Mayo Clin Proc* 2019; **94:** 1623-40. doi: 10.1016/j.mayocp.2019.01.013
3. Brown S, Banfill K, Aznar MC, Whitehurst P, Faivre Finn C. The evolving role of radiotherapy in non-small cell lung cancer. *Br J Radiol* 2019; **92:** 20190524. doi: 10.1259/bjr.20190524
4. Spigel DR, Faivre-Finn C, Gray JE, Vicente D, Planchard D, Paz-Ares L, et al. Five-year survival outcomes from the PACIFIC trial: durvalumab after chemoradiotherapy in stage III non-small-cell lung cancer. *J Clin Oncol* 2022; **40:** 1301-11. doi: 10.1200/JCO.21.01308
5. Antonia SJ, Villegas A, Daniel D, Vicente D, Murakami S, Hui R, et al. Durvalumab after chemoradiotherapy in stage III non-small-cell lung cancer. *N Engl J Med* 2017; **377:** 1919-29. doi: 10.1056/NEJMoa1709937
6. Inoue A, Kunitoh H, Sekine I, Sumi M, Tokuuye K, Saijo N. Radiation pneumonitis in lung cancer patients: a retrospective study of risk factors and the long-term prognosis. *Int J Radiat Oncol Biol Phys* 2001; **49:** 649-55. doi: 10.1016/s0360-3016(00)00783-5
7. Arroyo-Hernández M, Maldonado F, Lozano-Ruiz F, Muñoz-Montaño W, Nuñez-Baez M, Arrieta O. Radiation-induced lung injury: current evidence. *BMC Pulm Med* 2021; **21:** 9. doi: 10.1186/s12890-020-01376-4
8. Hagiwara Y, Nakayama Y, Kudo S, Hayakawa T, Nakamura N, Kitamoto Y, et al. Nationwide survey of radiation therapy in Japan for lung cancer complicated with interstitial lung disease. *J Radiat Res* 2020; **61:** 563-74. doi: 10.1093/jrr/rraa018
9. Kashihara T, Nakayama Y, Ito K, Kubo Y, Okuma K, Shima S, et al. Usefulness of simple original interstitial lung abnormality scores for predicting radiation pneumonitis requiring steroidal treatment after definitive radiation therapy for patients with locally advanced non-small cell lung cancer. *Adv Radiat Oncol* 2021; **6**: 100606. doi: 10.1016/j.adro.2020.10.019
10. Higo H, Kubo T, Makimoto S, Makimoto G, Ihara H, Masaoka Y, et al. Chemoradiotherapy for locally advanced lung cancer patients with interstitial lung abnormalities. *Jpn J Clin Oncol* 2019; **49:** 458-64. doi: 10.1093/jjco/hyz016
11. Washko GR, Lynch DA, Matsuoka S, Ross JC, Umeoka S, Diaz A, et al. Identification of early interstitial lung disease in smokers from the COPDGene Study. *Acad Radiol* 2010; **17:** 48-53. doi: 10.1016/j.acra.2009.07.016
12. Hatabu H, Hunninghake GM, Richeldi L, Brown KK, Wells AU, Remy-Jardin M, et al. Interstitial lung abnormalities detected incidentally on CT: a Position Paper from the Fleischner Society. *Lancet Respir Med* 2020; **8:** 726-37. doi: 10.1016/S2213-2600(20)30168-5
13. Kanda Y. Investigation of the freely available easy-to-use software 'EZR' for medical statistics. *Bone Marrow Transplant* 2013; **48:** 452-8. doi: 10.1038/bmt.2012.244

14. Akobeng AK. Understanding diagnostic tests 3: receiver operating characteristic curves. *Acta Paediatr* 2007; **96:** 644-7. doi: 10.1111/j.1651-2227.2006.00178.x

15. Li F, Zhou Z, Wu A, Cai Y, Wu H, Chen M, et al. Preexisting radiological interstitial lung abnormalities are a risk factor for severe radiation pneumonitis in patients with small-cell lung cancer after thoracic radiation therapy. *Radiat Oncol* 2018; **13:** 82. doi: 10.1186/s13014-018-1030-1

16. Kobayashi H, Wakuda K, Naito T, Mamesaya N, Omori S, Ono A, et al. Chemoradiotherapy for limited-stage small-cell lung cancer and interstitial lung abnormalities. *Radiat Oncol* 2021; **16:** 52. doi: 10.1186/s13014-021-01780-y

17. Washko GR, Hunninghake GM, Fernandez IE, Nishino M, Okajima Y, Yamashiro T, et al. Lung volumes and emphysema in smokers with interstitial lung abnormalities. *N Engl J Med* 2011; **364:** 897-906. doi: 10.1056/NEJMoa1007285

18. Chua F, Desai SR, Nicholson AG, Devaraj A, Renzoni E, Rice A, et al. Pleuroparenchymal fibroelastosis. A review of clinical, radiological, and pathological characteristics. *Ann Am Thorac Soc* 2019; **16:** 1351-59. doi: 10.1513/AnnalsATS.201902-181CME

19. Oshiro Y, Mizumoto M, Sekino Y, Maruo K, Ishida T, Sumiya T, et al. Risk factor of pneumonitis on dose-volume relationship for chemoradiotherapy with durvalumab: multi-institutional research in Japan. *Clin Transl Radiat Oncol* 2021; **29:** 54-59. doi: 10.1016/j.ctro.2021.05.009

20. Palma DA, Senan S, Tsujino K, Barriger RB, Rengan R, Moreno M, et al. Predicting radiation pneumonitis after chemoradiation therapy for lung cancer: an international individual patient data meta-analysis. *Int J Radiat Oncol Biol Phys* 2013; **85:** 444-50. doi: 10.1016/j.ijrobp.2012.04.043

21. Ito M, Shimizu H, Aoyama T, Tachibana H, Tomita N, Makita C, et al. Efficacy of virtual block objects in reducing the lung dose in helical tomotherapy planning for cervical oesophageal cancer: a planning study. *Radiat Oncol* 2018; **13:** 62. doi: 10.1186/s13014-018-1012-3

22. Wu WC, Chan CL, Wong YW, Cuijpers JP. A study on the influence of breathing phases in intensity-modulated radiotherapy of lung tumours using four-dimensional CT. *Br J Radiol* 2010; **83:** 252-6. doi: 10.1259/bjr/33094251

23. Putman RK, Gudmundsson G, Axelsson GT, Hida T, Honda O, Araki T, et al. Imaging patterns are associated with interstitial lung abnormality progression and mortality. *Am J Respir Crit Care Med* 2019; **200:** 175-83. doi: 10.1164/rccm.201809-1652OC

24. Iwasawa T, Okudela K, Takemura T, Fukuda T, Matsushita S, Baba T, et al. Computer-aided quantification of pulmonary fibrosis in patients with lung cancer: Relationship to disease-free survival. *Radiology* 2019; **292:** 489-98. doi: 10.1148/radiol.2019182466

25. Araki T, Dahlberg SE, Hida T, Lydon CA, Rabin MS, Hatabu H, et al. Interstitial lung abnormality in stage IV non-small cell lung cancer: a validation study for the association with poor clinical outcome. *Eur J Radiol Open* 2019; **6:** 128-31. doi: 10.1016/j.ejro.2019.03.003

26. Kashihara T, Nakayama Y, Okuma K, Takahashi A, Kaneda T, Katagiri M, et al. Impact of interstitial lung abnormality on survival after adjuvant durvalumab with chemoradiotherapy for locally advanced non-small cell lung cancer. *Radiother Oncol* 2023; **180:** 109454. doi: 10.1016/j.radonc.2022.109454

research article

The influence of BCL2, BAX, and ABCB1 gene expression on prognosis of adult de novo acute myeloid leukemia with normal karyotype patients

Zlatko Pravdic[1], Nada Suvajdzic Vukovic[1,2], Vladimir Gasic[3], Irena Marjanovic[3], Teodora Karan-Djurasevic[3], Sonja Pavlovic[3], Natasa Tosic[3]

[1] Clinic of Hematology, Clinical Center of Serbia, Belgrade, Serbia
[2] School of Medicine, University of Belgrade, Serbia
[3] Institute of Molecular Genetics and Genetic Engineering, University of Belgrade, Serbia

Radiol Oncol 2023; 57(2): 239-248.

Received 12 January 2023
Accepted 30 March 2023

Correspondence to: Prof. Nataša Tosić, Ph.D., Laboratory for Molecular Biomedicine, Institute of Molecular Genetics and Genetic Engineering, University of Belgrade, Vojvode Stepe 444a, 11042 Belgrade 152, Serbia. E-mail: natasa.tosic@imgge.bg.ac.rs

Disclosure: No potential conflicts of interest were disclosed.

Background. Deregulation of the apoptotic process underlies the pathogenesis of many cancers, including leukemia, but is also very important for the success of chemotherapy treatment. Therefore, the gene expression profile of main apoptotic factors, such as anti-apoptotic *BCL2* (B-cell lymphoma protein 2) and pro-apoptotic *BAX* (BCL2-associated X), as well as genes involved in the multi-drug resistance (*ABCB1*), could have significant impact on the prognosis and could be used as targets for specific therapy.

Patients and methods. We analyzed the expression of *BCL2*, *BAX,* and *ABCB1* in bone-marrow samples collected at diagnosis from 51 adult patients with acute myeloid leukemia with normal karyotype (AML-NK) using real-time polymerase chain reaction method, and examined their prognostic potential.

Results. Increased expression of *BCL2* (*BCL2*$^{+}$) was associated with the presence of chemoresistance ($p = 0.024$), while patients with low *BAX* expression were more prone to relapse ($p = 0.047$). Analysis of the combined effect of *BCL2* and *BAX* expression showed that 87% of patients with *BAX*/*BCL2*^{low} status were resistant to therapy ($p = 0.044$). High expression of *ABCB1* was associated with *BCL2*$^{+}$ status ($p < 0.001$), and with absence *FLT3-ITD* mutations ($p = 0.019$).

Conclusions. The present analysis of *BCL2*, *BAX,* and *ABCB1* gene expression profiles is the first study focusing solely on AML-NK patients. Preliminary results showed that patients with high *BCL2* expression are likely to experience resistance to chemotherapy, and may benefit from specific anti-BCL2 treatment. Further investigations conducted on a larger number of patients could elucidate actual prognostic significance of these genes in AML-NK patients.

Key words: acute myeloid leukemia with normal karyotype; *BCL2*; *BAX*; BCL2/BAX ratio; *ABCB1*; prognosis

Introduction

Acute myeloid leukemia (AML) is a malignant hematological disease that occurs as a result of differentiation arrest, uncontrolled proliferation and diminished apoptosis of myeloid progenitor cells. It is the most common acute leukemia in adults, accounting for about 80% of all cases.[1] Despite remarkable progress in uncovering the molecular-genetic changes underlying the pathogenesis of AML, a little has changed in the initial treatment of patients which is still based on the classification of patients into risk groups according to pretreatment karyotype analysis.[2] The largest karyotype based risk group is AML with normal karyotype (AML-NK), representing almost 50% of *de novo*

adult AML cases. AML-NK is a highly heterogeneous group with respect to genetic abnormalities and clinical outcome of the patients, but the whole group is still stratified into intermediate risk group. Some of molecular markers such as mutations in fms-related tyrosine kinase-3 (*FLT3*), nucleophosmin (*NPM1*), CCAAT/enhancer binding protein alpha (*CEBPA*) and runt-related transcription factor 1 (RUNX1) gene have made an impact on prognosis of AML-NK patients, and have already been included into the revised World Health Organization (WHO) classification of myeloid neoplasms and acute leukemia, and European LeukemiaNet (ELN).[2,3] However, there is a constant need for the introduction of new molecular markers that have significant impact on the prognosis of patients.

Since diminished apoptosis is one of the hallmark traits of leukemic cells, research focused on the analysis of the expression profile of the main participants in the apoptotic process can be of great importance in the detection of new prognostic-relevant molecular markers of AML. Also, since the mechanism of action of cytotoxic drugs used in the treatment of AML involves activation of apoptotic process, the expression pattern of apoptotic factors could have an impact on the occurrence of resistance. Namely, multi drug resistance (MDR) is a main clinical obstacle to successful cancer treatment. Resistance to chemotherapy treatment in AML is still a major cause for initial treatment failure and relapse of the disease, and it is caused by multifactorial mechanisms involving genetic factors.[4,5] Two main mechanisms of MDR are: pump (transport) resistance, associated with increased expression of proteins involved in drug efflux, and non-pump (apoptotic) resistance, associated with increased activity of anti-apoptotic system.[6] Gene expression of the ATP-binding cassette (ABC) superfamily of membrane transporters (*ABCB1* formerly known as *MDR1* gene) is a marker of pump-resistance, while markers of non-pump resistance are levels of expression of *BCL2* and *BAX* genes.[7-9] These markers could be considered as pharmacotranscriptomics markers and their analysis in AML patients could be a basis for the assessment of their role in tumor resistance to several groups of drugs. The inhibitors of these markers might effectively reverse MDR in AML patients.[10]

The process of apoptosis is under the control of two distinct but interconnected pathways, intrinsic and extrinsic. Activation of intrinsic pathway is under the control of the BCL family of proteins. B-cell lymphoma 2 (BCL2) family of proteins include both pro-apoptotic (BAX, BAK) and anti-apoptotic members (BCL2, BCL-XL, MCL1).[11] BCL2 is the best-known member of BCL2-familly, with an anti-apoptotic function. Its high expression has been reported throughout the evolution of AML, at presentation, relapse and also during treatment resistance. Moreover, increased BCL2 correlated with failure to achieve complete remission (CR) and with shorter overall survival (OS) of AML patients, making it an important therapeutic target.[12,13] Indeed, these findings led to the design of potent and selective BCL2-inhibitor, venetoclax. This modern BCL2-inhibitor is used in combination with classical therapy improving outcome in patients that are ineligible for intensive chemotherapy.[14]

BCL2-associated X (BAX) is a pro-apoptotic protein, transcriptionally activated by the tumor suppressor p53. BAX is essential in the final stages of apoptotic process and its activation leads to release of cytochrome c from mitochondria and direct cell death.[15] Some studies found that high expression of BAX is good prognostic marker in AML, while others failed to prove its prognostic significance.[16-20]

Because of the existing inconsistencies in assessment of the individual impact of BCL2 and BAX expression level on AML prognosis, researchers have resorted to BAX/BCL2 ratio analysis.[9,19] Namely, BAX and BCL2 regulate apoptotic process by binding to each other and thus forming heterodimers. The BAX/BCL2 ratio determines the cell fate after apoptotic stimuli has been received.

The overexpression of *ABCB1* gene is considered to be independent factor for the occurrence of multi-drug resistance in AML. *ABCB1* gene is located at chromosome 7q21.31, and it encodes 120 kb permeability glycoprotein (P-gp), a member of ATP-binding cassette (ABC) superfamily of transporter proteins, also called adenosine triphosphate binding cassette transporter B1 (ABCB1). P-gp is an efflux pump, transporting toxic substances out of the cell.[21,22] By decreasing intracellular concentrations of drugs P-gp confers resistance to a large number of therapeutics used in clinical oncology. Also, P-gp has a drug-independent role in AML causing the inhibition of apoptosis in AML blast cells via modulation of a sphingomyelin-ceramide pathway.[23]

In order to show how the expression level of main apoptotic factors, such as *BCL2* and *BAX*, can influence the occurrence of resistance, and whether their influence is independent from the impact of multi drug resistance (*ABCB1*) gene expression

level, in this study we investigated the expression pattern of these genes, and examined the possibility of their mutual influence on the prognosis in AML-NK patients. In doing so, the expression level of these genes was analyzed in the context of other already established prognostic molecular markers. In this way, we aimed to determine how the expression pattern of these genes can be used for a more precise stratification of AML-NK patients into risk groups.

Patients and methods

Patients and therapy protocol

Bone marrow (BM) samples from the 51 newly diagnosed AML-NK patients (25 females, 26 males; median age 51 years, range 23–62 years) were collected at Clinic of Hematology, Clinical Center of Serbia. Research was conducted in accordance with the ethical standards of the World Medical Association's Declaration of Helsinki. The study was approved by the Ethics Commit-tee of the Clinical Center of Serbia (No. 110/11), and written informed consent was obtained for all patients.

Diagnostic procedures comprised cytomorphology, cytogenetics, and immunophenotyping of BM. Morphologic diagnosis was made according to the French-American-British (FAB) classification.[24] Conventional G-band karyotyping was employed for cytogenetic analysis.[25] Immunophenotyping by flow cytometry (FACS Calibur, BD Biosciences, USA) was carried out systematically in the whole group of patients according to standard protocols based on European LeukemiaNet (ELN), Work Package 10 (WP10) criteria.[26]

All patients received induction and consolidation chemotherapy with daunorubicin and cytarabine according to the protocol 3 + 7, followed by three consolidation cycles of high/intermediate doses of cytarabine.[2] Patients aged ≤ 55 years underwent allogeneic stem cell transplantation (SCT), in total 15 (25.42%) patients. Definitions of CR, overall survival (OS), disease free survival (DFS) and resistance were established by proposed criteria.[27]

Gene expression and mutational analyses

Bone marrow mononuclear cells (BMMCs) from AML-NK patients and from 14 healthy controls (BM donors, 8 males and 6 females, median age 31 years), were purified on *Ficoll-Paque*™ Plus (GE Healthcare, Buckinghamshire, UK) density gradient, suspended in TRI Reagent (Ambion, Thermo Fisher Scientific, Waltham, MA, USA) and total RNA was extracted according to manufacturer's instructions. In brief, mononuclear cells where first homogenized in TRI Reagent, and then separation phase was initiated by adding chloroform and subsequent certification. Total RNA was precipitated from the aqueous phase using isopropyl alcohol, pelleted and washed in 70%–75% ethanol. One microgram of total RNA was used for the cDNA synthesis using RevertAid Reverse Transcriptase (Invitrogen, Thermo Fisher Scientific, Waltham, MA, USA). Real time-PCR was performed on 7900HT Fast Real-Time PCR System (Applied Biosystems). For expression analysis of *ABCB1 SYBR*®Green chemistry was used and PCR reaction (10 μl) consisted of 1μl of cDNA (50 ng RNA equivalent) *SYBR*™ Green PCR Master Mix (Applied Biosystems, Foster City, CA, USA), primers in final concentration 400 nM (*ABCB1* forward 5`-GTC TAC AGT TCG TAA TGC TGA CGT and *ABCB1* reverse 5`-TGT GAT CCA CGG ACA CTC CTA C). In the case of *BCL2* and *BAX*, expression analysis was done as previously described.[28] For all target genes *GAPDH* gene was used as endogenous control, and all reactions were run in duplicate. Relative quantification analysis was performed using comparative ddCt method, using healthy controls as calibrator.[29,30]

Detection of *FLT3-ITD* and *NPM1* mutations were analyzed as previously described.[31,32]

Statistical analysis

Data are presented as medians with range, means ± SD, or as absolute numbers with percentages. Differences in continuous variables were analyzed using Mann-Whitney *U* test for distribution between 2 groups. Analyses of frequencies were performed using Fisher exact test. Survival probabilities were estimated by the Kaplan-Meier method, and differences in survival distributions were evaluated using the LogRank test.

The statistical analyses were performed using the SPSS computer software 21.0 (IBM). For all analyses, the P values were 2-tailed, and $P < 0.05$ was considered statistically significant.

Results

In the study, we analyzed the expression of *BCL2*, *BAX* and *ABCB1* gene, in a cohort of 51 newly diagnosed patients with AML-NK. Clinical and bio-

TABLE 1. Clinical characteristics for *de novo* acute myeloid leukemia with normal karyotype (AML-NK) patients stratified by the level of *BCL2*, *BAX* gene expression and *BAX/BCL2* ratio

Parameter	BCL2				*BAX*			*BAX/BCL2*		
	Total n=51	*BCL2+* n=25	*BCL2-* n=26	P	*BAX+* n=25	*BAX-* n=26	P	*BAX/BCL2high* n=25	*BAX/BCL2^{low}* n=26	P
Sex										
Male (%)	26 (51)	10 (38)	16 (62)	0.165	16 (62)	10 (38)	0.095	16 (62)	10 (38)	0.095
Female (%)	25 (49)	15 (60)	10 (40)		9 (36)	16 (64)		9 (36)	16 (64)	
Age* (years)	51 (23-62)	53 (27-62)	49 (23-62)	0.137	49 (27-62)	52.5 (23-62)	0.597	48 (23-62)	54 (27-62)	0.111
WBC count* (x10^9/L)	22 (1-349)	7 (1-184)	22.5 (2-349)	0.159	22 (1-184)	22 (0.2-349)	0.808	29 (1-349)	6 (1-184)	**0.041**
HB* (g/L)	99 (66-131)	103 (82-131)	98 (66-128)		97 (66-131)	105 (78-128)		98 (66-128)	103 (82-131)	
> 80 (g/L)	45 (88)	25 (56)	20 (44)	**0.023**	22 (49)	23 (51)	1.000	19 (53)	26 (47)	
< 80 (g/L)	6 (12)	0	6 (100)		3 (50)	3 (50)		0	6 (100)	**0.010**
Plts* (x10^9/L)	55 (8-422)	60 (8-422)	53.5 (8-169)	0.528	55 (17-169)	54.5 (8-422)	0.497	52 (8-169)	60 (8-422)	0.685
LDH *(U/L)	321 (1-2904)	175 (153-1992)	590.5 (1-2904)	**0.010**	386 (153-1992)	306.5 (1-2904)	0.816	605 (1-2904)	75 (153-1992)	**0.002**
PB blast* (%)	14 (0-98)	15 (0-98)	11 (0-97)	0.737	11 (0-92)	16 (0-98)	0.623	11 (0-97)	15 (0-98)	0.865
BM blasts* (%)	62 (30-97)	57 (30-90)	66.5 (32-90)	0.531	63 (30-97)	61 (31-90)	0.756	70 (30-90)	57 (31-97)	0.341
CD34 (%)				0.095			0.404			**0.050**
present	24 (47)	15 (63)	9 (38)		10 (42)	14 (58)		8 (33)	16 (67)	
absent	27 (53)	10 (37)	17 (363)		15 (56)	12 (44)		17 (63)	10 (37)	
FAB (%)				**0.006**			0.239			**0.002**
M0	4 (8)	4 (100)	0		1 (25)	3 (75)		0	4 (100)	
M1	5 (10)	4 (80)	1 (20)		3 (60)	2 (40)		1 (20)	4 (80)	
M2	18 (35)	10 (56)	8 (44)		7 (39)	11 (62)		6 (33)	12 (67)	
M4	17 (33)	3 (18)	14 (82)		8 (47)	9 (53)		14 (82)	3 (18)	
M5	7 (14)	4 (57)	3 (43)		6 (86)	1 (14)		4 (57)	3 (43)	
CR (%)				0.404			0.264			0.577
success	28(55)	12 (43)	16 (57)		16 (57)	12 (43)		15 (54)	13 (46)	
failure	23(45)	13 (57)	10 (43)		9 (39)	14 (61)		10 (43)	13 (57)	
Resistance (%)				**0.024**			0.703			**0.044**
yes	8 (16)	7 (88)	1 (12)		3 (38)	5 (62)		1 (13)	7 (87)	
no	43 (84)	18 (42)	25 (58)		22 (51)	21 (49)		24 (56)	19 (44)	
Relapse (%)				1.000			0.047			0.137
yes	17 (61)	7 (41)	10 (59)		7 (41)	10 (59)		7 (41)	10 (59)	
no	11 (39)	5 (45)	6 (55)		9 (82)	2 (18)		8 (73)	3 (27)	
***FLT3-ITD*mutations** (%)				0.324			1.000			0.199
present	12 (24)	4 (33)	8 (67)		6 (50)	6(50)		8 (67)	4 (33)	
absent	39 (76)	21 (54)	18 (46)		19 (49)	20 (51)		17 (44)	22 (56)	
***NPM1* mutations** (%)				0.237			0.144			0.144
present	17 (33)	6 (35)	11 (65)		11 (65)	6 (35)		11 (65)	6 (35)	
absent	34 (67)	19 (56)	15 (44)		14 (41)	20 (59)		14 (41)	20 (59)	

BM = bone marrow; CR = complete remission; HB = hemoglobin; FAB = French-American-British classification; PB = peripheral blood; Plts = platelets; WBC = white blood cell count

*median (range)

logical characteristics of the patients are shown in Table 1.

BCL2 expression

Median expression level of *BCL2* in cohort of 51 AML-NK patients at diagnosis was 1.22 (range 0.13–8.97), which was not significantly different compared to healthy controls (median 1.00, range 0.21–1.59) (P = 0.148). When *BCL2* median expression level detected among AML-NK patients (1.22) was applied as a cut-off value, 49% of patients exhibited high *BCL2* expression, and were marked as *BCL2*$^+$ (Table 1).

Examining the association of BCL2 expression level with clinical characteristics of the patients, we have found that BCL2$^+$ patients had lower LDH levels (P = 0.010) and higher hemoglobin level (P = 0.023) (Table 1.). Also, BCL2$^+$ patients primarily belonged to the M0/M1 FAB group of patients (P = 0.006). The presence of *BCL2*$^+$ status was not associated with mutations in *FLT3-ITD* and *NPM1* gene (P = 0.324 and P = 0.237, respectively).

When we analyzed the prognostic impact of high *BCL2* expression in our cohort of AML-NK patients we have found that *BCL2*$^+$ status was associated with the presence of resistant disease, since 88% of resistant patient had elevated *BCL2* expression (P = 0.024). The CR rate among our group of patients was 55%. Among *BCL2*$^+$-positive patients CR rate was lower (48%), but this was not significantly different compared to *BCL2*$^-$ group (62%) (P = 0.404). Survival analysis indicated that *BCL2*$^+$ patients had longer duration of CR compared to *BCL2*$^-$ patients (11 months *vs.* 9.3 months), but this difference showed no statistical significance after survival analysis was performed (LogRank = 0.46, P = 0.831). A similar result was obtained when analyzing the impact of *BLC2* status on OS (*BCL2*$^+$, 6 months *vs.* *BCL2*$^-$, 8 months; LogRank = 2.030, P = 0.154).

BAX expression

Median expression level of pro-apoptotic *BAX* gene in our cohort of AML-NK patients was 0.92 (range 0.27–2.64), which was not significantly different compared to healthy controls (median 1.09, range 0.41–1.55) (P = 0.704). Based on the *BAX* median expression level the patients were divided into *BAX*$^+$ and *BAX*$^-$ group. There were no significant associations between *BAX* expression level and clinical and molecular characteristics of the patients.

Analysis of the potential prognostic impact of *BAX* status showed that *BAX*$^-$ patients had lower CR rate compared to *BAX*$^+$ group, but without statistical significance (P = 0.264) (Table 1). The negative impact of low *BAX* expression was also reflected in the fact that *BAX*$^-$ patients were more prone to relapse (P = 0.047). Also, *BAX*$^-$ patients had lower DFS (*BAX*$^-$, 8 months *vs.* *BAX*$^+$, 11 months; LogRank = 0.020, P = 0.889), and lower OS (*BAX*$^-$, 5 months *vs.* *BAX*$^+$, 7 months; LogRank = 0.020, P = 0.888) but it was not statistically significant.

Combined BCL2 and BAX expression (BAX/BCL2 ratio)

The possible cumulative effect of both *BCL2* and *BAX* gene expression level was also analyzed using *BAX*/*BCL2* ratio. In AML-NK group median *BAX*/*BCL2* ratio was 0.62 (range 0.11–7.77), while in healthy samples it was 0.91 (range 0.59–3.69). We haven't found significant difference between *BAX*/*BCL2* values among patient and healthy control group (P = 0.185). When median *BAX*/*BCL2* value detected in AML-NK patients (0.62) was applied as a cut-off value for discriminating *BAX*/*BCL2* ^{high} and *BAX*/*BCL2* ^{low} group, 49% of patients had *BAX*/*BCL2*^{high} status.

Regarding the clinical characteristics of the patients, *BAX*/*BCL2* ^{high} status was associated with higher number of WBC (P = 0.041), hemoglobin levels lower than 80 g/L (P = 0.010), higher LDH level (P = 0.002), with M4 FAB group (P = 0.002), and with absence of CD34 (P = 0.050). *BAX*/*BCL2* ^{high} status was not significantly associated with mutations in *FLT3-ITD* and *NPM1* gene (P = 0.199 and P = 0.144) (Table 1).

The prognostic significance of *BAX*/*BCL2* ratio was evident only in terms of the presence of primary resistance, where *BAX*/*BCL2*^{low} status patients were in 87% resistant to therapy (P = 0.044). Survival analysis didn't show any significant difference in DFS and OS duration between *BAX*/*BCL2*^{high} and *BAX*/*BCL2*^{low} groups of patients (LogRank = 0.139, P = 0.710 and LogRank = -0.004, P = 0.951, respectively).

ABCB1 expression

In our cohort of AML-NK patients median expression level of *ABCB1* gene was significantly lower compared to healthy controls (0.16, range 0.00–13.74 *vs.* 1.02, range 0.29–5.27, respectively) (P = 0.025). According to median *ABCB1* expression level, we have divided patients into *ABCB1*$^+$ (25

TABLE 2. Clinical characteristics for *de novo* acute myeloid leukemia with normal karyotype (AML-NK) patients stratified by the level of *MDR1* gene expression

Parameter	Total n=51	MDR1+ n=26	MDR1- n=25	P
Sex				**0.051**
Male (%)	26 (51)	17 (65)	9 (35)	
Female (%)	25 (49)	9 (36)	16 (64)	
Age* (years)	51 (23-62)	53 (23-62)	49 (23-62)	0.396
WBC count* (x10⁹/L)	22 (1-349)	7 (1-184)	26 (0-349)	0.071
Hemoglobin* (g/L)	99 (66-131)	106 (78-124)	96 (66-131)	0.191
> 80 (g/L)	45 (88)	24 (53)	21 (47)	
< 80 (g/L)	6 (12)	1 (17)	5 (83)	
Platelets* (x10⁹/L)	55 (8-422)	42 (8-422)	69.5 (16-169)	0.129
LDH *(U/L)	321 (1-2904)	175 (1-2904)	553.5 (175-1992)	**0.028**
PB blast* (%)	14 (0-98)	14 (0-98)	13.5 (0-87)	0.900
BM blasts* (%)	62 (30-97)	57 (30-90)	65 (33-97)	0.565
CD34 (%)				**0.025**
present	24 (47)	16 (67)	8 (33)	
absent	27 (53)	9 (33)	18 (67)	
FAB (%)				**<0.001**
M0	4 (8)	4 (100)	0	
M1	5 (10)	5 (100)	0	
M2	18 (35)	11 (61)	7 (39)	
M4	17 (33)	3 (18)	14 (82)	
M5	7 (14)	2 (29)	5 (71)	
Complete remission (%)				0.781
success	28(55)	13 (46)	15 (54)	
failure	23(45)	12 (52)	11 (48)	
Resistance (%)				1.000
yes	8 (16)	4 (50)	4 (50)	
no	43 (84)	21 (49)	22 (51)	
Relapse (%)				0.460
yes	17 (61)	9 (53)	8 (47)	
no	11 (39)	4 (36)	7 (64)	
***FLT3-ITD* mutations** (%)				**0.019**
present	12 (24)	2 (17)	10 (83)	
absent	39 (76)	23 (59)	16 (41)	
***NPM1* mutations** (%)				0.075
present	17 (33)	5 (29)	12 (71)	
absent	34 (67)	20 (59)	14 (41)	
***BCL2*⁺**	25 (49)	20 (80)	5 (20)	**<0.001**
***BCL2*⁻**	26 (51)	5 (24)	21 (76)	
***BAX/BCL2*^{high}**	25(49)	5 (20)	20 (80)	
***BAX/BCL2*^{low}**	26 (51)	20 (77)	6 (23)	**<0.001**

BM = bone marrow; FAB = French-American-British classification; PB = peripheral blood; WBC = white blood cell count

*median (range)

patients) and *ABCB1*⁻ group (26 patients). We have found that *ABCB1*⁺ patients had lower LDH levels (P = 0.028), and were predominantly found in M0/M1 FAB group (P<0.001). Furthermore, *ABCB1*⁺ status was associated with the absence of *FLT3-ITD* (P = 0.019), as well as, with the presence of CD34 antigen (P = 0.050) (Table 2).

Interestingly, *ABCB1* status was not associated with the occurrence of resistance (P = 1.000), nor did it affect the CR rate (P = 0.781). Also, expression level of *ABCB1* did not affect DFS and OS duration (LogRank = 0.037, P = 0.848 and LogRank = 0.951, P = 0.329, respectively).

In addition, patients with high expression of *ABCB1* predominantly had high expression of *BCL2*, and therefore were frequently found in *BAX/BCL2* ^{low} group (P < 0.001).

When we performed substratification of AML-NK patients based on the presence of *FLT3-ITD* and *NPM1* mutations into 3 risk groups (favorable *NPM1*⁺-11 patients, poor *FLT3-ITD*⁺-12 patients, and intermediate *FLT3-ITD*⁻/*NPM1*⁻ -28 patients), we have found that *ABCB1*⁺ status was predominant in the *FLT3-ITD*⁻/*NPM1*⁻ group, because 71% of *FLT3-ITD*⁻/*NPM1*⁻patients had high *ABCB1* expression (P = 0.001). Analyzing the potential prognostic significance of *ABCB1* expression in this group of 28 patients, prominent impact was observed only in survival analysis for OS where *ABCB1*⁺ patients had shorter survival of 5 months, compared to *ABCB1*⁻ patients with 10 months (LogRank = 3.447, P = 0.063).

Discussion

Loss of control in the process of programmed cell death is one of the basic events in the malignant transformation and the development of various types of tumors, including AML. For this reason, many of the participants in apoptosis are recognized as targets for the design and application of therapeutics. Aberrant expression of genes that control apoptosis, like BCL2-familly members, represent a recurrent feature of leukemic cells that can lead to increased cell survival and chemotherapy resistance.[11,33,34] In this study we analyzed the expression pattern of two BCL2-family member genes, *BCL2* and *BAX*, as well as *BAX/BCL2* ratio in order to elucidate their influence on prognosis of AML-NK patients.

We have found that the expression level of *BCL2* among *de novo* AML patients was not different compared to healthy controls, and showed

extremely heterogeneous pattern, with wide range of detected values. Similar finding was reported by others.[11,35] Also, consistent with some other previously published findings, in our study *BCL2*$^+$ status was not a predictor for reduced CR rate, and did not influence DFS and OS.[9,36-38] However, in our cohort of patients a statistically significant association between *BCL2*$^+$ status and the existence of resistance was shown. We believe that this finding might be important because *BCL2*$^+$ patients may benefit from specific anti-BCL2 therapy. Bilbao-Sieyro *et al*.[38] came to the same conclusion after they reported that increased *BCL2* expression found in CR and relapsed samples (but not in diagnosis samples) was associated with poor DFS and OS.

Furthermore, we have found that high expression of *BCL2* was detected among patients with FAB M0/M1 subtypes. This is not surprising, given the fact that the expression of BCL2 is differentiation stage specific, being at its highest in immature myeloid progenitors, and decreasing at the final stages of differentiation.[35] This finding is very important when anti-BCL2 therapy (venetoclax) is used in the treatment of AML. Namely, it was shown that AML patients belonging to FAB M4/M5 subtype can exhibit resistance to this specific therapy. It is assumed that the cause of this resistance lies in the lack of therapeutic target i.e. BCL2, since leukemic cells belonging to these AML subtypes originate from more differentiated hematopoietic cells, having lower, or non-existent BCL2 expression.[39,40]

Our study showed significant association between decreased *BAX* expression level and higher relapse rate. This finding is similar with already published data, but it has to be said that the influence of *BAX* expression level on prognosis in AML was predominantly studied through its association with other apoptotic genes, like *BCL2* (*BAX*/*BCL2* ratio).[9,17,19,20,41,42] In our study, *BAX*/*BCL2*^{low} ratio was significantly associated with the presence of the resistance. Other studies showed that increased BAX/BCL2 ratio was associated with increased CR rate,[18,41] while patients with low *BAX*/*BCL2* had shorter OS.[18] Following the example of Del Poeta *et al*.[41] we also tried to prove the association of *BAX*/*BCL2*^{high} ratio with *NPM1*$^-$/*FLT3-ITD*$^+$ mutational status, but without any success since the presence of these mutations were not associated with *BCL2* and *BAX* expression level when analyzed individually.

Of note is that the methodology used in the referenced studies was different ranging from flow-cytometry, western-blot, to RT-PCR and RNA-seq, therefore their results cannot be entirely comparable. Also, the analysis focusing on only two apoptotic factors, *BCL2* and *BAX*, represents only a simplification of the real situation, where other pro- and anti-apoptotic members of the BCL2-familly interact with each other and determine the final fate of the leukemic cell.

When we analyzed expression pattern of *ABCB1* gene known to be involved in the chemoresistance, we observed some similarity with the results obtained through *BCL2* and *BAX* expression analysis. Thus, similar to *BCL2* expression, *ABCB1* expression analysis showed that *ABCB1*$^+$ status was preferably found in M0/M1 FAB subgroup of patients. This was not surprising considering the fact that ABCB1 expression is dependent on the differentiation stage, i.e. that the highest ABCB expression was observed among cells with immature immunophenotype.[43] In line with this was the finding that *ABCB1*$^+$ status was associated with CD34$^+$ status. This is also due to the fact that CD34 expression is present in pluripotent hematopoietic cells, and it's down-regulated during differentiation process, as it is the case with ABCB1 expression.[44-46]

In our study, we observed mutual exclusion between *FLT3-ITD*$^+$ and *NPM1*$^+$ status, and high expression of *ABCB1*. Similar finding was reported by others, and in the case of *FLT3-ITD*$^+$ patients it is assumed to be a consequence of a loss of *ABCB1* expression under increased proliferative activity caused by the presence of a *FLT3-ITD* mutation.[47-50]

In our study overexpression of *ABCB1* was not associated with occurrence of chemoresistance, CR rate, and the duration of DFS and OS. This can be explained by the presence of age-dependent association between high expression of *ABCB1* and adverse prognosis. Namely, the clinical relevance of *ABCB1* expression is diminished or completely lost among young adult AML patients, and particularly in pediatric AML patients.[45,51-53] In our study median age of AM-NK patients was 51 years, and 61% of older patients (> 51 years) were *ABCB1*^{high}. Based on this, we can say that our cohort of patients is represented by younger adults, in whom the association between *ABCB1* expression and chemoresistance/adverse outcome, is not so evident. However, it may be that the analysis of a larger number of patients could provide a more accurate statistical power for significance.

Also, in addition to the expression of *ABCB1*, the resistance in AML can be influenced by other members of the ABC-transporter family, or even by the expression pattern of some other prognostically

significant genes.[55-57] Some studies have shown that contribution to the resistance, and to the overall prognosis is defined by co-expression patterns of many different ABC-transporters, and not by their individual influence.[54,55,58] It is assumed that some of the ABC transporters have overlapping specificity to a range of substrates, and that their co-expression is responsible for chemoresistance. This is particularly evident in the study by Marzac C *et al*.[54] where resistant disease among AML patients increased from 21% to a 100% depending of number of overexpressed ABC transporter genes (0 to 3).

In conclusion, our study showed that occurrence of resistance was associated with increased expression of *BCL2,* while patients with low *BAX* expression were more prone to relapse. Combined impact of these two genes analyzed through *BAX*/*BCL2* ratio showed that AML-NK patients with *BAX*/*BCL2*^{low} status were resistant to chemotherapy. Also, in our cohort of patients *ABCB1* expression level was not a predictor of resistant disease, but we have found association between *ABCB1*$^{+}$ status and the absence of *NPM1* and *FLT3-ITD* mutations, molecular markers with an already established prognostic significance in AML-NK. However, we were unable to demonstrate that *ABCB1* expression could contribute to a more accurate risk stratification in these patients.

This is the first study in which the expression of *BCL2, BAX, BAX*/*BCL2* ratio and *ABCB1* was examined solely in AML-NK group of patients in which the prognostic influence of cytogenetic aberration, either unfavorable or favorable, could be excluded. This cytogenetically homogenous group of patients are extremely heterogeneous regarding their outcome, and that is why it would be of great importance if expression pattern of some of these genes should prove to be significant for prognosis and response to therapy. Since the research on pharmacotranscriptomics markers in AML is deficient, this study which includes the gene expression analysis involved in both mechanisms of multidrug resistance (apoptotic-dependent and efflux pump-dependent) has provided new data on these potential components of algorithm for individualized, personalized treatment of AML patients.

Acknowledgments

This work has been funded by grant from the Ministry of Education, Science and Technological Development, Republic of Serbia (Grant No. 451-03-68/2022-14/200042).

References

1. Shallis RM, Wang R, Davidoff A, Ma X, Zeidan AM. Epidemiology of acute myeloid leukemia: recent progress and enduring challenges. *Blood Rev* 2019, **36:** 70-87. doi: 10.1016/j.blre.2019.04.005
2. Döhner H, Wei AH, Appelbaum FR, Craddock C, DiNardo CD, Dombret H, et al. Diagnosis and management of AML in adults: 2022 recommendations from an international expert panel on behalf of the ELN. *Blood* 2022, **140:** 1345-77. doi: 10.1182/blood.2022016867
3. Arber DA, Orazi A, Hasserjian R, Thiele J, Borowitz MJ, Le Beau MM, et al. The 2016 revision to the World Health Organization classification of myeloid neoplasms and acute leukemia. *Blood* 2016, **127:** 2391-405. doi: 10.1182/blood-2016-03-643544
4. Fleischmann M, Schnetzke U, Hochhaus A, Scholl S. Management of acute myeloid leukemia: current treatment options and future perspectives. *Cancers*, 2021, **13:** 5722. doi: 10.3390/cancers13225722
5. Shaffer BC, Gillet JP, Patel C, Baer MR, Bates SE, Gottesman MM. Drug resistance: still a daunting challenge to the successful treatment of AML. *Drug Resist Updat* 2012, **15:** 62-9. doi: 10.1016/j.drup.2012.02.001
6. Wang X, Wang C, Qin YW, Yan SK, Gao YR. Simultaneous suppression of multidrug resistance and antiapoptotic cellular defense induces apoptosis in chemoresistant human acute myeloid leukemia cells. *Leuk Res* 2007, **31:** 989-94. doi: 10.1016/j.leukres.2006.09.001
7. Svirnovski AI, Shman TV, Serhiyenka TF, Savitski VP, Smolnikova VV, Fedasenka UU. ABCB1 and ABCG2 proteins, their functional activity and gene expression in concert with drug sensitivity of leukemia cells. *Hematology* 2009, **14:** 204-12. doi: 10.1179/102453309X426218
8. Robey RW, Pluchino KM, Hall MD, Fojo AT, Bates SE, Gottesman MM. Revisiting the role of ABC transporters in multidrug-resistant cancer. *Nat Rev Cancer* 2018; **18:** 452-64. doi: 10.1038/s41568-018-0005-8
9. Kulsoom B, Shamsi TS, Afsar NA, Memon Z, Ahmed N, Hasnain SN. Bax, Bcl-2, and Bax/Bcl-2 as prognostic markers in acute myeloid leukemia: are we ready for Bcl-2-directed therapy? *Cancer Manag Res* 2018, **10:** 403-16. doi: 10.2147/CMAR.S154608
10. Wu H, Medeiros LJ, Young KH. Apoptosis signaling and BCL-2 pathways provide opportunities for novel targeted therapeutic strategies in hematologic malignances. *Blood Rev* 2018, **32:** 8-28. doi: 10.1016/j.blre.2017.08.004
11. Handschuh L, Wojciechowski P, Kazmierczak M, Lewandowski K. Transcript-level dysregulation of BCL2 family genes in acute myeloblastic leukemia. *Cancers* 2021, **13:** 3175. doi: 10.3390/cancers13133175
12. Zhou JD, Zhang TJ, Xu ZJ, Gu Y, Ma JC, Li XX, et al. BCL2 overexpression: clinical implication and biological insights in acute myeloid leukemia. *Diagn Pathol* 2019, **14:** 68. doi: 10.1186/s13000-019-0841-1.
13. Tiribelli M, Michelutti A, Cavallin M, Di Giusto S, Simeone E, Fanin R, et al. BCL-2 expression in AML patients over 65 years: impact on outcomes across different therapeutic strategies. *J Clin Med* 2021, **10:** 5096. doi: 10.3390/jcm10215096
14. Richard-Carpentier G, DiNardo CD. Venetoclax for the treatment of newly diagnosed acute myeloid leukemia in patients who are ineligible for intensive chemotherapy. *Ther Adv Hematol* 2019, **10:** 2040620719882822. doi: 10.1177/2040620719882822
15. Korsmeyer SJ. BCL-2 gene family and the regulation of programmed cell death. *Cancer Res* 1999, **59:** 1693s-700s. PMID: 10197582
16. Ong YL, McMullin MF, Bailie KE, Lappin TR, Jones FG, Irvine AE. High bax expression is a good prognostic indicator in acute myeloid leukaemia. *Br J Haematol* 2000, **111:** 182-9. doi: 10.1046/j.1365-2141.2000.02315.x
17. Kornblau SM, Vu HT, Ruvolo P, Estrov Z, O'Brien S, Cortes J, et al. BAX and PKCa modulate the prognostic impact of BCL2 expression in acute myelogenous leukemia. *Clin Cancer Res* 2000, **6:** 1401-9. PMID: 10778970
18. Kohler T, Schill C, Deininger MW, Krahl R, Borchert S, Hasenclever D, et al. High Bad and BAX mRNA expression correlate with negative outcome in acute myeloid leukemia (AML). *Leukemia* 2002, **16:** 22-9. doi: 10.1038/sj.leu.2402340
19. Del Poeta G, Venditti A, Del Principe MI, Maurillo L, Buccisano F, Tamburini A, et al. Amount of spontaneous apoptosis detected by BAX/BCL2 ratio predicts outcome in acute myeloid leukemia (AML). *Blood* 2003, **101:** 2125-31. doi: 10.1182/blood-2002-06-1714

20. Vazanova A, Jurecekova J, Balharek T, Marcinek J, Stasko J, Dzian A, et al. Differential mRNA expression of the main apoptotic proteins in normal and malignant cells and its relation to in vitro resistance. *Cancer Cell Int* 2018, **18:** 33. doi: 10.1186/s12935-018-0528-9.

21. Chen CJ, Clark D, Ueda K, Pastan I, Gottesman MM, Roninson IB. Genomic organization of the human multidrug resistance (MDR1) gene and origin of P-glycoproteins. *J Biol Chem* 1990, **265:** 506-14. PMID: 1967175

22. Gerlach JH, Endicott JA, Juranka PF, Henderson G, Sarangi F, Deuchars KL, et al. Homology between P-glycoprotein and a bacterial haemolysin transport protein suggests a model for multidrug resistance. *Nature* 1986, **324:** 485-9. doi: 10.1038/324485a0

23. Pallis M, Turzanski J, Higashi Y, Russell N. P-glycoprotein in acute myeloid leukaemia: therapeutic implications of its association with both a multidrug-resistant and an apoptosis-resistant phenotype. *Leuk Lymphoma* 2002, **43:** 1221-8. doi: 10.1080/10428190290026277

24. Bennett JM, Catovsky D, Daniel MT, Flandrin G, Galton DA, Gralnick HR, et al. Proposed revised criteria for the classification of acute myeloid leukemia. A report of the French-American-British Cooperative Group. *Ann Intern Med* 1985; **103:** 620-5. doi: 10.7326/0003-4819-103-4-620

25. McGowan-Jordan J, Simons A, Schmid M. ISCN 2016 An International System for Human Cytogenomic Nomenclature. Basel: Karger; 2016. doi: 10.1159/isbn.978-3-318-06861-0

26. Béné MC, Nebe T, Bettelheim P, Buldini B, Bumbea H, Kern W, et al. Immunophenotyping of acute leukemia and lymphoproliferative disorders: a consensus proposal of the European LeukemiaNet Work Package 10. *Leukemia* 2011; **25:** 567-74. doi: 10.1038/leu.2010.312

27. Cheson BD, Bennett JM, Kopecky KJ, Büchner T, Willman CL, Estey EH, et al. Revised recommendations of the international working group for diagnosis, standardization of response criteria, treatment outcomes, and reporting standards for therapeutic trials in acute myeloid leukemia. *J Clin Oncol* 2003; **21:** 4642-9. doi: 10.1200/JCO.2003.04.036

28. Vucicevic K, Jakovljevic V, Colovic N, Tosic N, Kostic T, Glumac I, et al. Association of Bax expression and Bcl2/Bax ratio with clinical and molecular prognostic markers in chronic lymphocytic leukemia. *J Med Biochem* 2016, **35:** 150-7. doi: 10.1515/jomb-2015-0017

29. Livak KJ, Schmittgen TD. Analysis of relative gene expression data using real-time quantitative PCR and the 2(-Delta Delta C(T)) Method. *Methods* 2001; **25:** 402-8. doi: 10.1006/meth.2001.1262

30. Schmittgen TD, Livak KJ. Analyzing real-time PCR data by the comparative C(T) method. *Nat Protoc* 2008; **3:** 1101-8. doi: 10.1038/nprot.2008.73

31. Mitrovic M, Kostic T, Virijevic M, Karan-Djurasevic T, Suvajdzic Vukovic N, Pavlovic S, et al. The influence of Wilms' tumor 1 gene expression level on prognosis and risk stratification of acute promyelocytic leukemia patients. *Int J Lab Hematol* 2020, **42:** 82-7. doi: 10.1111/ijlh.13144

32. Kuzmanovic M, Tosic N, Colovic N, Karan-Djurasevic T, Spasovski V, Radmilovic M, et al. Prognostic impact of NPM1 mutations in Serbian adult patients with acute myeloid leukemia. *Acta Haematol* 2012, **128:** 203-12. doi: 10.1159/000339506

33. Dabrowska M, Pietruczuk M, Kostecka I, Suchowierska M, Kloczko J, Nasilowska B, et al. The rate of apoptosis and expression of Bcl-2 and Bax in leukocytes of acute myeloblastic leukemia patients. *Neoplasma* 2003, **50:** 339-44. PMID: 14628086

34. Tzifi F, Economopoulou C, Gourgiotis D, Ardavanis A, Papageorgiou S, Scorilas A. The role of BCL2 family of apoptosis regulator proteins in acute and chronic leukemias. *Adv Hematol* 2012, **2012:** 524308. doi: 10.1155/2012/524308

35. Haes I, Dendooven A, Mercier ML, Puylaert P, Vermeulen K, Kockx M, et al. Absence of BCL-2 expression identifies a subgroup of AML with distinct phenotypic, molecular, and clinical characteristics. *J Clin Med* 2020, **9:** 3090. doi: 10.3390/jcm9103090

36. Andreeff M, Jiang S, Zhang X, Konopleva M, Estrov Z, Snell VE, et al. Expression of Bcl-2-related genes in normal and AML progenitors: changes induced by chemotherapy and retinoic acid. *Leukemia* 1999, **13:** 1881-92. doi: 10.1038/sj.leu.2401573

37. Zhou JD, Zhang TJ, Xu ZJ, Gu Y, Ma JC, Li XX, et al. BCL2 overexpression: clinical implication and biological insights in acute myeloid leukemia. *Diagn Pathol* 2019, **14:** 68. doi: 10.1186/s13000-019-0841-1

38. Bilbao-Sieyro C, Rodríguez-Medina C, Florido Y, Stuckey R, Sáez MN, Sánchez-Sosa S, et al. BCL2 expression at post-induction and complete remission impact outcome in acute myeloid leukemia. *Diagnostics* 2020, **10:** 1048. doi: 10.3390/diagnostics10121048

39. Pei S, Pollyea DA, Gustafson A, Stevens BM, Minhajuddin M, Fu R, et al. Monocytic subclones confer resistance to venetoclax-based therapy in acute myeloid leukemia patients. *Cancer Discov* 2020, **10:** 536-51. doi: 10.1158/2159-8290.CD-19-0710

40. Kuusanmäki H, Leppä AM, Pölönen P, Kontro M, Dufva O, Deb D, et al. Phenotype-based drug screening reveals association between venetoclax response and differentiation stage in acute myeloid leukemia. *Haematologica* 2020, **105:** 708-20. doi: 10.3324/haematol.2018.214882

41. Del Poeta G, Ammatuna E, Lavorgna S, Capelli G, Zaza S, Luciano F, et al. The genotype nucleophosmin mutated and FLT3-ITD negative is characterized by high bax/bcl-2 ratio and favourable outcome in acute myeloid leukaemia. *Br J Haematol* 2010, **149:** 383-7. doi: 10.1111/j.1365-2141.2010.08098.x

42. Sharawat SK, Bakhshi R, Vishnubhatla S, Gupta R, Bakhshi S. BAX/BCL2 RMFI ratio predicts better induction response in pediatric patients with acute myeloid leukemia. *Pediatr Blood Cancer* 2013, **60:** E63-6. doi: 10.1002/pbc.24518

43. Huls M, Russel FG, Masereeuw R. The role of ATP binding cassette transporters in tissue defense and organ regeneration. *J Pharmacol Exp Ther* 2009, **328:** 3-9. doi: 10.1124/jpet.107.132225

44. Schaich M, Soucek S, Thiede C, Ehninger G, Illmer T; SHG AML96 Study Group. MDR1 and MRP1 gene expression are independent predictors for treatment outcome in adult acute myeloid leukaemia. *Br J Haematol* 2005, **128:** 324-32. doi: 10.1111/j.1365-2141.2004.05319.x

45. van den Heuvel-Eibrink MM, van der Holt B, Burnett AK, Knauf WU, Fey MF, Verhoef GE, et al. CD34-related coexpression of MDR1 and BCRP indicates a clinically resistant phenotype in patients with acute myeloid leukemia (AML) of older age. *Ann Hematol* 2007, **86:** 329-37. doi: 10.1007/s00277-007-0269-7

46. Shman TV, Fedasenka UU, Savitski VP, Aleinikova OV. $CD34^+$ leukemic subpopulation predominantly displays lower spontaneous apoptosis and has higher expression levels of Bcl-2 and MDR1 genes than CD34- cells in childhood AML. *Ann Hematol* 2008, **87:** 353-60. doi: 10.1007/s00277-008-0439-2

47. Varatharajan S, Abraham A, Karathedath S, Ganesan S, Lakshmi KM, Arthur N, et al. ATP-binding cassette transporter expression in acute myeloid leukemia: association with in vitro cytotoxicity and prognostic markers. *Pharmacogenomics* 2017, **18:** 235-44. doi: 10.2217/pgs-2016-0150

48. Hirsch P, Tang R, Marzac C, Perrot JY, Fava F, Bernard C, et al. Prognostic impact of high ABC transporter activity in 111 adult acute myeloid leukemia patients with normal cytogenetics when compared to FLT3, NPM1, CEBPA and BAALC. *Haematologica* 2012, **97:** 241-5. doi: 10.3324/haematol.2010.034447

49. Marzac C, Teyssandier I, Calendini O, Perrot JY, Faussat AM, Tang R, et al. Flt3 internal tandem duplication and P-glycoprotein functionality in 171 patients with acute myeloid leukemia. *Clin Cancer Res* 2006, **12:** 7018-24. doi: 10.1158/1078-0432.CCR-06-0641

50. Smeets ME, Raymakers RA, Vierwinden G, Pennings AH, Wessels H, de Witte T. Triggering noncycling hematopoietic progenitors and leukemic blasts to proliferate increases anthracycline retention and toxicity by down-regulating multidrug resistance. *Blood* 1999, **94:** 2414-23. doi: 10.1182/blood.V94.7.2414.417k01_2414_2423

51. Leith CP, Kopecky KJ, Godwin J, McConnell T, Slovak ML, Chen IM, et al. Acute myeloid leukemia in the elderly: assessment of multidrug resistance (MDR1) and cytogenetics distinguishes biologic subgroups with remarkably distinct responses to standard chemotherapy. A Southwest Oncology Group study. *Blood* 1997 **89:** 3323-9. doi: 10.1182/blood.V89.9.3323

52. Leith CP, Kopecky KJ, Chen IM, Eijdems L, Slovak ML, McConnell TS, et al. Frequency and clinical significance of the expression of the multidrug resistance proteins MDR1/P-glycoprotein, MRP1, and LRP in acute myeloid leukemia: a Southwest Oncology Group Study. *Blood* 1999, **94:** 1086-99. doi: 10.1182/blood.V94.3.1086.415k32_1086_1099

53. Steinbach D, Furchtbar S, Sell W, Lengemann J, Hermann J, Zintl F, et al. Contrary to adult patients, expression of the multidrug resistance gene (MDR1) fails to define a poor prognostic group in childhood AML. *Leukemia* 2003, **17:** 470-1. doi: 10.1038/sj.leu.2402806

54. Marzac C, Garrido E, Tang R, Fava F, Hirsch P, De Benedictis C, et al. ATP binding cassette transporters associated with chemoresistance: transcriptional profiling in extreme cohorts and their prognostic impact in a cohort of 281 acute myeloid leukemia patients. *Haematologica* 2011, **96:** 1293-301. doi: 10.3324/haematol.2010.031823

55. Bartholomae S, Gruhn B, Debatin KM, Zimmermann M, Creutzig U, Reinhardt D, et al. Coexpression of multiple ABC-transporters is strongly associated with treatment response in childhood acute myeloid leukemia. *Pediatr Blood Cancer* 2016, **63:** 242-7. doi: 10.1002/pbc.25785

56. Galimberti S, Guerrini F, Carulli G, Fazzi R, Palumbo GA, Morabito F, et al. Significant co-expression of WT1 and MDR1 genes in acute myeloid leukemia patients at diagnosis. *Eur J Haematol* 2004, **72:** 45-51. doi: 10.1046/j.0902-4441.2003.00185.x

57. Guo X, Shi P, Chen F, Zha J, Liu B, Li R, et al. Low MDR1 and BAALC expression identifies a new subgroup of intermediate cytogenetic risk acute myeloid leukemia with a favorable outcome. *Blood Cells Mol Dis* 2014, **53:** 144-8. doi: 10.1016/j.bcmd.2014.05.001

58. Liu B, Li LJ, Gong X, Zhang W, Zhang H, Zhao L. Co-expression of ATP binding cassette transporters is associated with poor prognosis in acute myeloid leukemia. *Oncol Lett* 2018, **15:** 6671-7. doi: 10.3892/ol.2018.8095

research article

CD56-positive diffuse large B-cell lymphoma: comprehensive analysis of clinical, pathological, and molecular characteristics with literature review

Gorana Gasljevic, Lucka Boltezar, Srdjan Novakovic, Vita Setrajcic-Dragos, Barbara Jezersek-Novakovic, Veronika Kloboves-Prevodnik

Institute of Oncology Ljubljana, Ljubljana, Slovenia

Radiol Oncol 2023; 57(2): 249-256.

Received 9 January 2023
Accepted 19 February 2023

Correspondence to: Assoc. prof. Veronika Kloboves-Prevodnik, M.D., Ph.D., Institute of Oncology Ljubljana, Zaloška 2, SI-1000 Ljubljana, Slovenia. E-mail: vkloboves@onko-i.si

Disclosure: No potential conflicts of interest were disclosed.

Background. Diffuse large B-cell lymphoma (DLBCL) is the most common non-Hodgkin lymphoma. The expression of CD56 in DLBCL is highly unusual. Little is known about its incidence and clinical importance. So far, no genetic profiling was performed in CD56 positive DLBCL.

Patients and methods. Tissue microarrays have been constructed, sectioned, and stained by H&E and immunohistochemistry for 229 patients with DLBCL diagnosed 2008–2017. For CD56 positive cases, clinical data was collected including age at diagnosis, stage of the disease, International Prognostic Index (IPI) score, treatment scheme and number of chemotherapy cycles, radiation therapy, treatment outcome, and possible relapse of the disease. Overall survival (OS) and progression-free survival (PFS) were calculated. For four patients, RNA was extracted and targeted RNA (cDNA) sequencing of 125 genes was performed with the Archer FusionPlex Lymphoma kit.

Results. CD56 expression was found in 7 cases (3%). The intensity of expression varied from weak to moderate focal, to very intensive and diffuse. All patients had *de novo* DLBCL. The median age at the time of diagnosis was 54.5 years. Five of them were women and 2 males. According to the Hans algorithm, 6 patients had the germinal centre B cells (GBC) type and one non-GBC (activated B-cell [ABC]) type, double expressor. Genetic profiling of four patients according to Schmitz's classification showed that 1 case was of the BN2 subtype, 1 of EZB subtype, 2 were unclassified. The six treated patients reached a complete response and did not experience progression of the disease during the median follow-up period of 80.5 months.

Conclusions. We report on one of the largest series of CD56+DLBCL with detailed clinicopathological data and for the first time described genetical findings in a limited number of patients. Our results show that CD56 expression is rare, but seems to be present in prognostic favourable subtypes of DLBCL not otherwise specified (NOS) as tested by immunohistochemical or genetic profiling.

Key words: diffuse large B-cell lymphoma not otherwise specified; CD56; immunohistochemistry; genetic profiling; prognosis

Introduction

CD56, also known as the neural cell adhesion molecule (NCAM), is a member of the immunoglobulin superfamily that plays important functional roles during nervous system development, differentiation, and immune surveillance. In addition to neurons and glial cells, CD56 is normally also

expressed in neuroendocrine tissues and some cells of the hematopoietic system like NK cells and activated T lymphocytes.[1] In the hematopathology service, it is mainly used as a marker of NK cells and their neoplastic counterparts. Its aberrant expression is useful as a proof of clonal plasma cell proliferation, while it can also be used as prognostic marker in plasmacytoma, as well as in acute myeloid leukemia (AML) and acute lymphoblastic leukaemia (ALL).[2-5]

Diffuse large B-cell lymphoma (DLBCL) is the most common lymphoma, representing approximately one third of all non-Hodgkin lymphomas.[2] Cases of DLBCL that do not fit the distinctive clinical presentation, tissue morphology, neoplastic cell phenotype, and/or pathogen-associated criteria of other subtypes of DLBCL are termed "DLBCL not otherwise specified (DLBCL NOS)' and represent 80–85% of all DLBCL cases.[2] The WHO 2016 classification of hematopoietic neoplasms[2] requires that the neoplastic cells in DLBCL NOS be further defined based on whether they are derived from germinal centre B cells or activated B-cells as identified by gene expression profiling (GEP) or are germinal centre B cells (GBC) or non-GBC as identified by immunohistochemical (IHC) analyses. In general, DLBCL NOS is an aggressive disease with an overall long-term survival rate in patients treated with standard chemotherapy regimens of ~60%.[7,8] Patients with activated B-cell (ABC) DLBCL and non-GBC variants have significantly worse prognoses than patients with the GBC variant.[6] Expression of markers in DLBCL NOS neoplastic cells that have clinical significance as prognostic or predictive factors include CD5, MYC, BCL2, BCL6, CD20, CD19, CD22, CD30, PD-L1, and PD-L2.[2,6] For example, 5–10% of DLBCL NOS cases express CD5 and have a very poor prognosis that is not improved by even aggressive treatment regimens, while the expression of CD30 represents a favourable prognostic indicator.[2]

Very little is known about the incidence and clinical importance of CD56 expression in DLBCL. In the last 30 years, the literature has only a few case reports or small series of CD56+ DLBCL with conflicting results on its importance.[10-18] It could have a prognostic value; however, since new target drugs are becoming available and among them is also anti-CD56 antibody, CD56 could serve as a potential target for the treatment of patients who do not respond to standard therapeutic schemes.

The purpose of this study was to evaluate CD56 expression in DLBCL in our series, to estimate its relationship to epidemiological factors, to roughly estimate its value as a prognostic marker, and to describe, for the first time the molecular findings in a subset of cases.

Patients and methods

Specimens

Data bases of the Department of Pathology Institute of Oncology Ljubljana (IOL) have been searched for all cases of DLBCL diagnosed between 2008 and 2017. Only the cases in which appropriate amount of material was present that could allow the construction of tissue microarrays (229) have been chosen for the study. Tissue microarrays have been constructed, sectioned, and stained by H&E and immunohistochemistry for the Hans algorithm as previously described.[19] Also, for the cases that were CD56 positive, flow cytometric and/or immunocytochemical staining results and data were retrieved and re-analysed from the database of the Department of Cytopathology.

Patients

For selected patients, clinical data was collected including age at diagnosis, stage of the disease, IPI score, treatment scheme and number of cycles, potential radiation therapy, outcome and possible relapse of the disease were also noted. Overall survival (OS) and progression-free survival (PFS) were calculated. Subjects were censored at their last visit to the IOL and for those who finished follow-up at IOL, a vital status from the Cancer Registry of the Republic of Slovenia. All procedures followed in this evaluation were in accordance with the ethical standards of the responsible committee on human experimentation (Ethical Committee of Institute of Oncology Ljubljana, approval number: ERID-KESOPKR-23 and the Ethical Committee of the Republic of Slovenia, approval number: 58/02/15) and the Helsinki Declaration of 1975, as revised in 2000.

Immunohistochemistry

3–4 μm thick, formalin-fixed paraffin-embedded sections of constructed TMAs were used for immunohistochemical staining with the monoclonal antibody CD56. Staining was performed on the Ventana Benchmark platform using the MRQ 42 clone (Cell Marque) in dilution 1:200.

Flow cytometric analysis and immunocytochemistry

The preparation of FNAB (fine needle aspiration biopsy) lymph node sample, cell counting, sample preparations for flow cytometric immunophenotyping, acquisition of cells with flow cytometer and measurement result analysis were performed as previously described.[20] Monoclonal antibodies against CD45, CD19, CD20, CD3, CD10, CD5, CD23, FMC7, κ and λ LCs (BD Biosciences, New Jersey, U.S.) were used. The samples were acquired using a four-colour flow cytometer FACSCalibur (BD Biosciences, New Jersey, U.S.), a six-colour flow cytometer FACSCanto II (BD Biosciences, New Jersey, U.S.) or a ten-colour FACSCanto X (BD Biosciences, New Jersey, U.S.). The measurement results were analysed using CellQuest (BD Biosciences, New Jersey, U.S.) or BD FACSDiva software (BD Biosciences, New Jersey, U.S.). For immunocytochemical staining, methanol and Delaunay-fixed cytospines were prepared. Stainings were carried out on the Ventana Benchmark Ultra platform using antibodies against CD56, CK AE1/AE3, CK18 (DAKO), CD20 (Cell Marque, Rocklin, California, U.S.), synaptophysin (Termo Scientific, Waltham, Massachusetts, U.S.), CD3 and TTF-1 (Leica Biosystems, Nussloch, Germany).

Molecular analysis - NGS sequencing

RNA was extracted from 4 paraffin-embedded tissue samples was extracted using the MagMAX™ FFPE DNA/RNA Ultra Kit (ThermoFisher, Waltham, MA, USA). Samples were treated with DNase, during the extraction process. Targeted RNA (cDNA) sequencing of 125 genes was performed with the Archer FusionPlex Lymphoma kit (InvitaeArcherDX, San Francisco, CA, USA). The final NGS library was quantified using the KAPA Library Quantification Kit (KAPA Biosystems, Merck, Ljubljana, Slovenia) and pair-end sequenced on a MiSeqDx system (Illumina, San Diego, CA, USA). The trimmed FASTQ file was uploaded to Archer Analysis software Version 6.0.3.2, which performed variant and fusion calls along with the determination of cell of origin (ABC or GCB). Variants were considered true positive if the frequency of the variant allele was above 10%, with minimum coverage of 100x.[20] All variants reported in GnomAD were excluded. Fusions were considered true positive if the fusion event was covered with a minimum of 5 unique reads and the percentage of reads supporting the event was above 10%.[21,22]

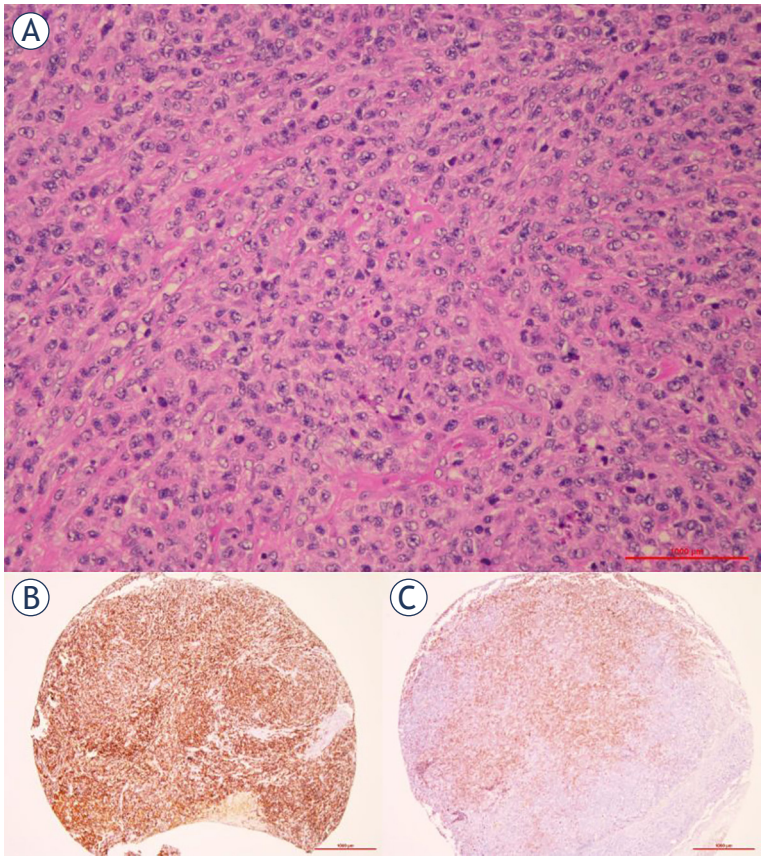

FIGURE 1. (A) Morphology of diffuse large B-cell lymphoma (DLBCL), CD56+; H&E, 20x; **(B)** Strong expression of CD56 in DLBCL not otherwise specified (NOS) (tissue microarray), 4x; **(C)** weak to moderate CD56 expression in DLBCL NOS (tissue microarray), 4x.

Statistical analysis

For numeric and demographic variables descriptive statistics were used (median, range, standard deviation, percentage). Overall survival and progression-free survival were calculated using the Kaplan-Meier method. Statistical analyses were performed using IBM SPSS Statistics, version 26.

Results

Among 229 DLBCL, NOS cases included in the study, CD56 expression was found in 7 cases (3%). The intensity of CD56 expression varied from moderate focal to very intensive and diffuse positive reaction (Figure 1). Reanalysis of the five cases in which fine needle aspiration biopsy (FNAB) of the lymph node was performed prior to surgical biopsy and histological examination showed that CD56 was not included in routine flow-cytometry

TABLE 1. Clinicopathological characteristics of patients with CD56 positive diffuse large B-cell lymphoma (DLBCL), review of the literature with our series

Publication	Coun	No of pat	Case No	Sex Age	GC type**	Non-GC type	LN	Extranodal disease and site	Clinical stage	IPI	LDH	Surg	CT and No. of cycles	RT	Response	FU
Kern 1993[23]	USA	1	1	NA	NA	NA	NA	NA	NA	NA	NA	NA	NA	NA	NA	NA
Muroi 1998[17]	Jap	2	1	M,49	Yes		Yes	Liver, Spleen,	NA	NA	NA	No	CHOP, NAx	No	PR?	NA
			2	F,62		Yes	Yes	Pericard. Ef. Liver	NA	NA	NA	No	CHOP, NAx	No	PR?	NA
Sekita 1999[18]	Jap	1	1	M,16	Yes		Yes		I	NA	NA	No	CHOP, 6x	No	CR	10 m
Hammer 1998[15]	USA	4	1	M,51	NA	NA	Yes	Stomach	NA	NA	NA		NA	NA	NA	NA
			2	M,69	NA	NA	No		NA	NA	NA		NA	NA	NA	NA
			3	M,76	NA	NA	Yes		NA	NA	NA		NA	NA	NA	NA
			4	M,54	NA	NA	Yes		NA	NA	NA		NA	NA	NA	NA
Otsuka 2004[14]	Jap	2	1	NA	Yes		NA	NA	NA	NA	NA	NA	NA	NA	NA	NA
			2	NA	Yes		NA	NA	NA	NA	NA	NA	NA	NA	NA	NA
Weisberger *2006[11]	USA	10	1	M,41	Yes	Yes	No	Ileocecal valve	NA	NA	NA	NA	NA	NA	NA	NA
			2	M,52	Yes		Yes	SpineAbdomen Brain	NA	NA	NA	NA	NA	NA	NA	NA
			3	M,54	Yes		Yes		NA	NA	NA	NA	NA	NA	NA	NA
			4	M,83	Yes		No		NA	NA	NA	NA	NA	NA	NA	NA
			5	M,49	Yes		Yes		NA	NA	NA	NA	NA	NA	NA	NA
			6	F,57	Yes		No		NA	NA	NA	NA	NA	NA	NA	NA
			7	F,69	Yes		Yes		NA	NA	NA	NA	NA	NA	NA	NA
			8	M,77	Yes		Yes		NA	NA	NA	NA	NA	NA	NA	NA
			9	M,84	Yes		Yes		NA	NA	NA	NA	NA	NA	NA	NA
			10	M,77			No		NA	NA	NA	NA	NA	NA	NA	NA
Isobe 2007[13]	Jap	3	1	M,80	Yes		Yes	Ascites	NA	NA	NA	No	THP-COP, 3x	No	NR	DOD
			2	F,87	Yes		No	Ileum	NA	NA	NA	Yes	No	No	CR	22 m
			3	M,73	Yes		Yes	Ileum	NA	NA	NA	Yes	R-CHOP, 6x	No	CR	22 m
Chen 2010[16]	Ch	1	1	NA	NA	NA	NA	NA	NA		NA	NA	NA	NA	NA	NA
Gomyo 2010[9]	Jap	7	1	M,29		Yes	Yes	Spleen	IIIB	HI	↑	No	R-CHOP, aPBSCT	No	CR	A, 24 m
			2	F,60		Yes	Yes	WR	IIA	L	N	No	R-CHOP 3x	Yes	CR	A, 50 m
			3	F,22	Yes		No	WR	IA	L	N	No	CHOP 3x	Yes	CR	A, 57 m
			4	M,64		Yes	Yes	Pl. Ef, Adr. gl, Submand. gl	IIIA	H	↑	No	CHOP 5x	No	CR	D, 4 m
			5	M,63	Yes		No	Nasal cavity	IA	L	N	No	RCHOP 3x	Yes	CR	(pneumonia)
			6	M,50	Yes		No	Intra-extradural mass	IA	L	N	No	Res+CHOP 4x	Ye	RCR	A, 43 m
			7	F,45	Yes		No	Subcutis	IVA	HI	↑	No	R-CHOP 8x	sNo		A, 70 mA, 5 m
Stacchini 2012[12]	It	5	1	M,72	Yes		Yes	Spleen, Stomach,Pancr.	NA	NA	NA	NA	NA	NA	NA	NA
			2	M,15	Yes		Yes	Stomach, Liver	NA	NA	NA	NA	NA	NA	NA	NA
			3	M,71	Yes		No	Nasopharynx	NA	NA	NA	NA	NA	NA	NA	NA
			4	M,60					NA	NA	NA	NA	NA	NA	NA	NA
			5	M,21	Yes	Yes	No		NA	NA	NA	NA	NA	NA	NA	AWD 12m
Gu 2013[10]	SK	1	1	F,5		Yes		WR	I		N	Yes	COPAD, 6x	No	CR	NA
Liu 2020[8]	Ch	1	1	M,14	Yes, DH		Yes	Nasopharynx	IV	NA	↑	No	CTX+CP R-Hyper-CVAD AB R-DA-EPOCH, 6x IT DM+CTB,4x	No	CR	NA
Gasljevic 2022	Slo	7	1	F,56	Yes		Yes	Skeletal muscle	IA	0	N	Yes	R-CHOP, 3x	No	CR	A ,63 m
			2	F,51	Yes		Yes	Small bowel	IA	0	N	No	R-CHOP, 3x	No	CR	A, 73 m
			3	M,57	Yes				IIA	0	↑	No	R-CHOP, 6x	No	CR	A, 55 m
			4	M,56		Yes, DE		Spleen, Liver, Adrenal	IVB	0	↑	No	R-EPOCH,6x +IT,2x	No	CR	A, 40 m
			5	F,53	Yes		Yes	gland	IIA	3	N	Yes	CHOP, 3x	Yes	CR	A, 62 m
			6	F,30		Yes	Yes		IVB	3	↑	No	R-CHOP,8x	Yes	CR	A, 182 m
			7	F,79	NA	NA	Yes		IVB	5	↑	No	No	No	NA	DOD

A = alive; aPBSCT = autologous peripheral blood stem cell transplantation; AWD = alive with disease; Ch = China; CHOP = cyclophosphamide, doxorubicin hydrocloride, vincristine sulfat, prednisone; Coun = country; CP = prednisone; CR = complete response; CT = chemotherapy; CTX = cyclophosphamide; D = dead; DA-EPOCH = etoposide, doxorubicin, vindesine, dexamethasone, cyclophosphamide; DE = double expressor; DOD = dead of disease; F = female; FU = follow-up; Gl = gland; Hyper-CVAD AB = A: cyclophosphamide, vindesine, liposomal doxorubicin, dexamethason, B: methotrexate, cytarabine; IPI = International Prognostic Index; It = Italy; IT = intratechal; Jap = Japan; LN = lymph nodes; M = male; m = months; N = normal; NA = not available; NR = no response; Pancr = pancreas; Pl. E = pleural effusion; PR = partial response; R = rituximab; res = resection; RT = radiotherapy; SK = South Korea; Slo = Slovenia; Submand = submandibular; THP-COP = pirarubicin, cyclophosphamide, vincristine sulfat, prednisone; WR = Waldeyers ring

* only histologically proven cases are considered

** on the basis of the CD10 positivity

work-out. There was only one case[23] (case 1 in Table 1) in which immunocytochemistry for CD56 was stained since tumour cells showed co-expression of cytokeratin and the diagnosis of metastatic neuroendocrine carcinoma has been made.

All patients had *de novo* DLBCL. The median age at the time of diagnosis was 54.5 years (range 30–57). Five of them were women and 2 males. Five patients were diagnosed with DLBCL, GC type, 2 with DLBCL non-GC (ABC) type, one being a dou-

TABLE 2. Genetic profile of CD56 positive diffuse large B-cell lymphoma (DLBCL) samples

Case number in Table 2	COO IHC	COO AFPL	fusion	variants			VAF (%)	variant classiification	Schmitz et al., 2018[32] classification
				gene	nucleotide change	amino acid change			
1	GCB	GCB	ND	RANBP1	NM_002882.3:c.23A>G	NP_002873.1:p.(His8Arg)	13,7	Uncertain significance	unclassified
2	GCB	GCB	ND	ND	ND	ND	ND	ND	unclassified
3	GCB	GCB	ND	CD79B	NM_000626.2:c.587A>T	NP_000617.1:p.(Tyr196Phe)	49,0	Pathogenic	EZB
				CD79B	NM_000626.2:c.568A>G	NP_000617.1:p.(Met190Val)	50,1	Uncertain significance	
				EZH2	NM_001203247.1:c.1922A>G	NP_001190176.1:p.(Tyr641Cys)	53,7	Pathogenic	
				MYD88	NM_001172567.1:c.656C>G	NP_001166038.1:p.(Ser219Cys)	37,7	Uncertain significance	
				SH3BP5	NM_004844.4:c.460G>A	NP_004835.2:p.(Ala154Thr)	19,3	Uncertain significance	
4	ABC	ABC	IGH-BCL6	CD79B	NM_000626.2:c.587A>C	NP_000617.1:p.(Tyr196Ser)	25,9	Pathogenic	BN2
				SH3BP5	NM_004844.4:c.460G>A	NP_004835.2:p.(Ala154Thr)	12,6	Uncertain significance	

AFPL = Archer SusionPlex lymphoma; COO= cell of origin; IHC = immunohistochemical analyses; ND = not detected; VAF = variant allele freqency;

ble expressor (DE). One patient refused staging and treatment and died shortly after being diagnosed and was therefore excluded from survival analysis.

Among the six patients who received treatment, three patients were in clinical stage 1, one in stage 2 while two were in clinical stage 4. Only patients in clinical stage 4 had constitutional symptoms. Four patients had disease localised in the lymph nodes while two of them also had extranodal infiltrates – one in the pectoral muscles and the other in the renal fascia and small bowel. Three patients had elevated LDH levels, in fact, both patients in clinical stage 4B and one in stage 2A. Those patients in stage 4 had the IPI score 3 and others had the IPI score 0.

Three patients underwent surgical procedure and were later treated with adjuvant 3 cycles of CHOP (cyclophosphamide, doxorubicin, vincristine, prednisone) and R-CHOP (rituximab, cyclophosphamide, doxorubicin, vincristine, prednisone). Other 3 patients were treated with 6 or 8 cycles of R-CHOP. Two patients were also treated with adjuvant radiotherapy after completion of systemic treatment. The patient with non-GC type DE of DLBCL was treated with 6 cycles of R-EPOCH (rituximab, etoposide, cyclophosphamide, doxorubicin, vincristine, prednisone) together with 2 doses of intrathecally administered methotrexate and cytosine arabinoside for central nervous system prophylaxis.

The 6 treated patients reached a complete response and did not experience progression of the disease during the follow-up period, meaning that 5-year PFS and OS are 100%. Median follow-up was 80.5 months (range 42–197).

The clinicopathological characteristics of our cohort together with all cases reported in the literature are shown in Table 1. Genetic profiling of 4 patients was performed as described in *Patients and methods*, and the results are presented in Table 2.

Discussion

CD56 expression in DLBCL NOS is very rare. Its incidence is reported to be 0.5 to 7% of DLBCLs, but is actually unknown since CD56 is generally not included in the immunohistochemical or flow cytometric panel for the diagnosis of DLBCL.[10-18] In our series of patients with DLBCL NOS expression of CD56 was present in 3% of patients and varied in intensity from weak to very strong and diffuse. In one of those cases, that phenomenon resulted in an incorrect diagnosis of lymph node metastasis of the neuroendocrine tumour. In fact, in the general pathology service the main use of CD56 is to prove neuroblastoma and neuroendocrine differentiation in tumours of different origin while in hematopathology service it is used as a marker of NK cells, as a proof of clonal plasma cell proliferation, and as a prognostic marker in plasmacytoma, acute myeloid leukemia (AML), and acute lymphoblastic leukemia (ALL).[2-5] Since neuroendocrine carcinomas could be unevenly and weakly positive or even negative for cytokeratins[24], it is of the greatest importance for the pathologist to be aware that strong expression of CD56 could be present al-

so in some entities that are by definition not CD56 positive.

Throughout the papers published so far, there has been much speculation about this phenomenon with regard to its expression in special clinicopathological settings and its possible prognostic value. From an epidemiological point of view, some authors[9] suggested that it could be related to racial and/or geographical factors since, at the time of the publication of the paper, almost 50% of all reported cases were reported from Japan. Thorough analysis of all the cases with available information shows that 18 out of 45 cases (40%) have arisen in the population of far east (Japan, Korea, China; Table 1), while 27 (60%) were reported in the western population, Caucasians mainly (USA, Italy, Slovenia; Table 1). These results suggest that CD56+DLBCL is not related to racial / ethnic factors opposite to some other CD56 positive lymphoproliferative diseases such as NK/T cell lymphoma, nasal type.[2] The age distribution is very wide with cases described in paediatric/adolescent population as well as in the older patient most of the patients being in 6–7th decade of life. In our series, the vast majority of patients were middle aged, in the beginning of the sixth decade. The distribution of gender showed that among the far east patients, somewhat higher number of men are reported (6 female *vs.* 9 males; for 3 cases there is no information about gender) while in the western world there is a predominance of males (7 females *vs.* 19 males; 26% *vs.* 74%). However, our series shows contradictory results in which most patients (70%) are women, so it can be assumed that the higher incidence reported in males so far could be only a mere coincidence.

There are two main biologically distinct molecular subtypes of DLBCL: GCB and ABC. ABC DLBCL is associated with substantially worse outcomes when treated with standard chemoimmunotherapy. Based on gene expression studies, Hans *et al*.[25] developed an algorithm to discriminate GBC from non-GBC types in regard to immunohistochemical expression of CD10, bcl6 and MUM1 with cutoff of 30%. In addition to GCB and ABC subtypes, double-hit lymphomas and double-expressor lymphomas, which overexpress myc and bcl2 protein, are aggressive DLBCLs and are also associated with a poor prognosis. On the basis of immunohistochemical results, a few authors[9,11-13] found a relation of CD56 expression to DLBCL of GBC origin. Of the 45 summarized cases, for 8 cases there was no information about immunophenotype. Twenty-eight out of 36 (76%) were of GBC type and the remaining 24% were of non-GBC (ABC) type. One reported case[8] was double hit lymphoma with translocations of *MYC* and *bcl-6*, while in our series one DLBCL of non-GC (ABC) type DLBCL showed so-called double expressor profile with expression of bcl2 and myc protein expression being > 30%. Somewhat lower percentage of GBC types are reported in Eastern patients compared to the Western (10/15 and 17/21 or 75% *vs.* 81%). This finding could be related to the previously recognized and reported lower frequency of the DLBCL GBC subtype in Asian countries.[26]

In addition, it has been suggested that CD56 expression in DLBCL could be related to a more frequent extranodal presentation associated to the adhesive properties of CD56.[9,11] In neural cells, it mediates cell-to-cell adhesion by CD56 molecules of adjacent cells binding together.[27] It may be involved in homophilic adhesion for NK and T cells due to the C2-set Ig regions and fibronectin regions within its extracellular domain.[28] However, its function with respect to B-cell ontogeny is unclear. The expression of CD56 has been detected in a human pluripotent stem cell.[28] A subset of very early precursor B cells has the innate capacity for CD56 expression that is down-regulated and extinguished later in differentiation. It has been shown that lymphomagenesis is a stepwise process progression of which is enabled by accumulation of genetic events.[8] In follicular or mantle cell lymphoma, for example[30], first events such as t(14,18) and t(11,14) namely, do occur in progenitor B cells. Drawing parallels to this, we could assume that CD56+ DLBCL could arise from the precursor B-cell that, for whatever reason, did not down-regulate CD56 expression and then collected additional mutations that resulted in lymphoma development. Some authors[9,11-13] underlined frequent extranodal infiltrates in CD56+DLBCL with spleen, stomach, ileum, and nasal cavity being most frequently involved. Of 40 cases with available information, 16 (40%) presented with isolated lymphadenopathy while 24 (60%) had extranodal infiltrates with or without lymphadenopathy (14 *vs.* 10). Four of our patients presented with isolated lymphadenopathy while two had extranodal disease, which is concordant with majority of our patients having limited stage disease and were therefore treated adjuvantly after surgery.

The expression of CD 56 can be used as a prognostic marker in certain hematopathological entities; it can predict the occurrence of brain infiltration in ALL[5], the aggressiveness of multiple myeloma[3], and relapsed AML.[4] So far, its prognostic

importance in DLBCL has not been confirmed. All of our patients achieved complete remission, and remained in remission which can be at least partially attributed to low IPI scores and low clinical stages; however, two patients with clinical stage 4 also achieved and maintained complete remission. None of our patients had a high IPI score of 4 or 5 which are known to have the lowest survival.[31] In most of them, DLBCL was of GCB subtype, which also carry a better prognosis.[24]

Schmitz *et al*.[32] classified DLBCL cases according to genetic findings into 4 categories, namely MCD (based on the cooccurrence of *MYD88*^{L265P} and *CD79B* mutations), BN2 (based on *bcl6* fusions and *NOTCH2* mutations), N1 (based on *NOTCH1* mutations) and the EZB group (based on *EZH2* mutations and *bcl2* translocations). These subtypes differed phenotypically and in response to immunochemotherapy, with favourable survival in the BN2 and EZB groups. Genetic profiling of four patients from our series according to Schmitz classification[32], showed that 1 case was of BN2 subtype, one belongs to the EZB group, while two were unclassified. Although data are limited and demand testing in larger cohorts of patients, so far it can be concluded that CD56 expression is more often present in cases of DLBCL NOS with prognostically favourable genetical findings.

CD56 is expressed in some aggressive tumour types such as small lung cell carcinoma and neuroblastoma. To date, it has been used as a target molecule for antibody-based immunotherapy in phase I and II clinical trials for small cell lung carcinoma[33]; a favourable safety profile has been demonstrated. That led to the development of CAR-T therapy directed against CD56 in neuroblastoma. In the xenograft neuroblastoma model, anti-CD56 therapy led to the tumour burden control but had only modest effect on survival.[34] More studies are needed in regard to neuroblastoma therapy and other CD56 positive tumours but CD56 could eventually serve as a potential target for the treatment of CD56+ DLBCL patients who do not respond to the standard therapeutic schemes.

In conclusion, here we report one of the largest series of CD56+DLBCL with detailed clinicopathological data and for the first time described genetic findings in a limited number of patients. Our results show that CD56 expression is rare but seems to be present in prognostic favourable subtypes of DLBCL NOS as tested by immunohistochemical or genetic profiling.

Acknowledgement

The publication of this article was financed by the Slovenian Research Agency (ARRS), grant No. P3-0289. The funder had no role in study design, data collection and analysis, decision to publish, or preparation of the manuscript.

Authors' contributions: GG and VKP conceived the idea, designed the study, collected the data, and wrote the initial draught of the article. LB and BJN collected and analysed the data and revised the manuscript. SN and VŠD performed the molecular testing, interpreted the data, and revised the manuscript.

References

1. Van Acker H, Capsomidis A, Smits EL, Van Tendeloo VF. CD56 in the immune system: more than a marker for cytotoxicity? *Front Immunol* 2017; **8:** 892-90. doi: 10.3389/fimmu.2017.00892
2. Swerdlow SH, Campo E, Harris NL, Jaffe ES, Pileri SA, Stein H, et al. *WHO classification of tumours of hematopoietic and lymphoid tissues*. 4th edition. Lyon: IARC; 2017.
3. Chang H, Samiee S, Yi QL. Prognostic relevance of CD56 expression in multiple myeloma: a study including 107 cases treated with high-dose melphalan-based hemotherapy and autologous stem cell transplant. *Leuk Lymphoma* 2006; **47:** 43-7. doi: 10.1080/10428190500272549
4. Chaudhri NA, Almhareb F, Walter CU, Nounou R, Khalil S, Bakshi N, et al. Expression of CD56 in acute myeloid leukemia (AML) is associated with poor outcome when patients treated with stem cell transplant in second remission but not in the first remission. *Blood* 2011; **118:** 4880-86. doi: 10.1182/blood.V118.21.4880.4880
5. Ravandi F, Cortes J, Estrov Z, Thomas D. CD56 expression predicts occurrence of CNS disease in acute lymphoblastic leukaemia. *Leuk Res* 2002; **26:** 643-49. doi: 10.1016/s0145-2126(01)00188-6
6. Grimma KE, O'Malley DP. Aggressive B cell lymphomas in the 2017 revised WHO classification of tumors of hematopoietic and lymphoid tissues. *Ann Diagn Pathol* 2019; **38:** 6-10. doi: 10.1016/j.anndiagpath.2018.09.014
7. Feugier P, Van Hoof A, Sebban C, Solal-Celigny P, Bouabdallah R, Fermé C, et al. Long-term results of the R-CHOP study in the treatment of elderly patients with diffuse large B-cell lymphoma: a study by the group d'Etude des Lymphomes de l'Adulte. *J Clin Oncol* 2005; **23:** 4117-26. doi: 10.1200/JCO.2005.09.131
8. Liu Y, Barta SK. Diffuse large B-cell lymphoma: 2019 update on diagnosis, risk stratification and treatment. *Am J Hematol* 2019; **94:** 604-16. doi: 10.1002/ajh.25460
9. Gomyo H, Kajimoto K, Miyata Y, Maeda A, Mizuno I, Yamamoto K, et al. CD56-positive diffuse large B-cell lymphoma: possible association with extranodal involvement and bcl-6 expression. *Hematology* 2010; **15:** 157-61. doi: 10.1179/102453309X12583347113573
10. Gu MJ, Ha JO. CD56 positive diffuse large B-cell lymphoma: a case report and literature review. *Int J Clin Exp Pathol* 2013; **6:** 3023-25.
11. Weisberger J, Gorczyca W, Kinney MC. CD56-Positive Large B-cell Lymphoma. *App Imm Mol Morphol* 2007; **14:** 369-74. doi: 10.1097/01.pai.0000208279.66189.43
12. Stacchini A, Barreca A, Demurtas A, Aliberti S, di Celle PF, Novero D. Flow cytometric detection and quantification of CD56 (neural cell adhesion molecule, NCAM) expression in diffuse large B cell lymphomas and review of the literature. *Histopathology* 2012; **60:** 452-59. doi: 10.1111/j.1365-2559.2011.04098.x
13. Isobe Y, Sugimoto K, Takeuchi K, Ando J, Masuda A, Mori T, et al. Neural cell adhesion molecule (CD56)-positive B-cell lymphoma. *Eur J Haematol* 2007; **79:** 166-9. doi: 10.1111/j.1600-0609.2007.00893.x

14. Otsuka M, Yakushijin Y, Hamada M, Hato T, Yasukawa M, Fujita S. Role of CD21 antigen in diffuse largeB-cell lymphoma and its clinical significance. *Br J Hematol* 2004; **127:** 416-24. doi: 10.1111/j.1365-2141.2004.05226.x

15. Hammer RD, Vnencak-Jones CL, Manning B, Glick AD, Kinney MC. Microvillus lymphomas are B-cell neoplasms that frequently express CD56. *Mod Pathol* 1998; **11:** 239-46. PMID: 9521469

16. Chen B, Sun WY, Zhang G. [CD56 positive diffuse large B-cell lymphoma: report of a case]. [Chinese]. *Zhonghua Bing Li Xue Za Zhi* 2010; **39:** 343-4. PMID: 20654160

17. Muroi K, Omine K, Kuribara R, Uchida M, Izumi T, Hatake K, et al. CD56 expression in B-cell lymphoma. *Leuk Res* 1998; **22:** 201-2. doi: 10.1016/s0145-2126(97)00153-7

18. Sekita T, Tamaru J, Isobe K, Harigaya K, Masuoka S, Katayama T, et al. Diffuse large B-cell lymphoma expressing the natural killer cell marker CD56. *Pathol Int* 1999; **49:** 752-8. doi: 10.1046/j.1440-1827.1999.00929.x

19. Boltezar L, Kloboves-Prevodnik V, Pohar-Perme M, Gasljevic G, Jezersek-Novakovic B. Comparison of the algorithms classifying the ABC and GCB subtypes in diffuse large B-cell lymphoma. *Oncol Lett* 2018; **15:** 6903-12. doi: 10.3892/ol.2018.8243

20. Brozic A, Pohar Marinsek Z, Novakovic S, Kloboves-Prevodnik V. Inconclusive flow cytometric surface light chain results; can cytoplasmic light chains, Bcl-2 expression and PCR clonality analysis improve accuracy of cytological diagnoses in B-cell lymphomas? *Diagn Pathol* 2015; **10:** 191-6. doi: 10.1186/s13000-015-0427-5

21. Crotty R, Hu K, Stevenson K, Pontius MY, Sohani AR, Ryan RJH, et al. Simultaneous identification of cell of origin, translocations, and hotspot mutations in diffuse large B-cell lymphoma using a single RNA-sequencing assay. *Am J Clin Pathol* 2021; **155:** 748-54. doi: 10.1093/ajcp/aqaa185

22. Mokánszki A, Bicskó R, Gergely L, Méhes G. Cell-free total nucleic acid-based genotyping of aggressive lymphoma: Comprehensive analysis of gene fusions and nucleotide variants by next-generation sequencing. *Cancers* 2021; **13:** 3032. doi: 10.3390/cancers13123032

23. Kern WF, Spier CM, Miller TP, Grogan TM. NCAM (CD56)-positive malignant lymphoma. *Leuk Lymphoma* 1993; **12:** 1-10. doi: 10.3109/10428199309059565

24. Kirpatrik D, Swalling A, Kasmeridis H, Farshid G. Metastatic neuroendocrine carcinoma negative for cytokeratin immunohistochemistry. *Pathology* 2017; **S1:** S140-S141. doi: 10.1016/j.pathol.2016.09.057

25. Hans CP, Weisenburger DD, Greiner TC, Gascoyne RD, Delabie J, Ott G, et al. Confirmation of the molecular classification of diffuse large B-cell lymphoma by immunohistochemistry using a tissue microarray. *Blood* 2004; **103:** 275-82. doi: 10.1182/blood-2003-05-1545

26. Shiozawa E, Yamochi-Onizuka T, Takimoto M, Ota H. The GCB subtype of diffuse large B-cell lymphoma is less frequent in Asian countries. *Leuk Res* 2007; **31:** 1579-83. doi: 10.1016/j.leukres.2007.03.017

27. Rutishauer U, Acheson A, Hall AK, Mann DM, Sunshine J. The neural adhesion molecule (NCAM) as a regulator of cell-cell interactions. *Science* 1988; **240:** 53-7. doi: 10.1126/science.3281256

28. Lanier LL, Chang C, Azuma M, Ruitenberg JJ, Hemperly JJ, Phillips JH. Molecular and functional analysis of human natural killer cell-associated neural cell adhesion molecule (N-CMCD56). *J Immunol* 1991; **146:** 4421-26.

29. Young HE, Steele TA, Bray RA, Detmer K, Blake LW, Lucas PW, et al. Human pluripotent and progenitor cells display cell surface cluster differentiation markers CD10, CD13, CD56, and MHC class-I. *Proc Soc Exp Biol Med* 1999; **221:** 63-71. doi: 10.1046/j.1525-1373.1999.d01-55.x

30. Navarrete M, Oppezzo P. The pathogenesis of follicular lymphoma beyond apoptosis resistance. *Trans Canc Res* 2017; **6:** S529-S532. doi: 10.21037/tcr.201

31. Ziepert M, Hasenclever D, Kuhnt E, Glass B, Schmitz N, Pfreundschuh M, et al. Standard International prognostic index remains a valid predictor of outcome for patients with aggressive CD20+ B-cell lymphoma in the rituximab era. *J Clin Oncol* 2010; **28:** 2373-80. doi: 10.1200/JCO.2009.26.2493

32. Schmitz R, Wright GW, Huang DW, Johnson CA, Phelan JD, Wang JQ, et al. Genetics and pathogenesis of diffuse large B-cell lymphoma. *NEJM* 2018; **378:** 1396-407. doi: 10.1056/NEJMoa1801445.

33. Shah MH, Lorigan P, O'Brien MER, Fossella FV, Moore KN, Bhatia S, et al. Phase I study of IMGN901, a CD56-targeting antibody- drug conjugate, in patients with CD56-positive solid tumours. *Invest New Drugs* 2016; **34:** 290-99. doi: 10.1007/s10637-016-0336-9.

34. Crossland DL, Denning WL, Ang S, Olivares S, Mi T, Switzer K, et al. Antitumor activity of CD56-chimeric antigen receptor T cells in neuroblastoma and SLCL models. *Oncogene* 2018; **37:** 3686-97. doi:10.1038/s41388-018-0187-2

research article

Quantitative dynamic contrast-enhanced parameters and intravoxel incoherent motion facilitate the prediction of TP53 status and risk stratification of early-stage endometrial carcinoma

Hongxia Wang[1], Ruifang Yan[1], Zhong Li[1], Beiran Wang[1], Xingxing Jin[1], Zhenfang Guo[2], Wangyi Liu[1], Meng Zhang[1], Kaiyu Wang[3], Jinxia Guo[3], Dongming Han[1]

[1] Department of MR, the First Affiliated Hospital of Xinxiang Medical University, Weihui, China
[2] Department of Neurology, the First Affiliated Hospital of Xinxiang Medical University, Weihui, China
[3] MR Research China, GE Healthcare, Beijing, China

Radiol Oncol 2023; 57(2): 257-269.

Received 9 February 2023
Accepted 6 April 2023

Correspondence to: Dr. Dongming Han, 88 Jiankang Road, Weihui 453100, PR China. E-mail: 625492590@qq.com

Disclosure: Kaiyu Wang and Jinxia Guo, who are employees of GE Healthcare, gave guidance to this paper in terms of technical parameters and language embellishment. The remaining authors declare no relationships with any companies whose products or services may be related to the subject matter of the article.

Background. The aim of the study was to investigate the value of dynamic contrast-enhanced magnetic resonance imaging (DCE-MRI) and intravoxel incoherent motion (IVIM) in differentiating TP53-mutant from wild type, low-risk from non-low-risk early-stage endometrial carcinoma (EC).

Patients and methods. A total of 74 EC patients underwent pelvic MRI. Parameters volume transfer constant (K^{trans}), rate transfer constant (K_{ep}), the volume of extravascular extracellular space per unit volume of tissue (V_e), true diffusion coefficient (D), pseudo-diffusion coefficient (D*), and microvascular volume fraction (f) were compared. The combination of parameters was investigated by logistic regression and evaluated by bootstrap (1000 samples), receiver operating characteristic (ROC) curves, calibration curves, and decision curve analysis (DCA).

Results. In the TP53-mutant group, K^{trans} and K_{ep} were higher and D was lower than in the TP53-wild group; K^{trans}, V_e, f, and D were lower in the non-low-risk group than in the low-risk group (all $P < 0.05$). In the identification of TP53-mutant and TP53-wild early-stage EC, K^{trans} and D were independent predictors, and the combination of them had an optimal diagnostic efficacy (AUC, 0.867; sensitivity, 92.00%; specificity, 80.95%), which was significantly better than D ($Z = 2.169$, $P = 0.030$) and K^{trans} ($Z = 2.572$, $P = 0.010$). In the identification of low-risk and non-low-risk early-stage EC, K^{trans}, V_e, and f were independent predictors, and the combination of them had an optimal diagnostic efficacy (AUC, 0.947; sensitivity, 83.33%; specificity, 93.18%), which was significantly better than D ($Z = 3.113$, $P = 0.002$), f ($Z = 4.317$, $P < 0.001$), K^{trans} ($Z = 2.713$, $P = 0.007$), and V_e ($Z = 3.175$, $P = 0.002$). The calibration curves showed that the above two combinations of independent predictors, both have good consistency, and DCA showed that these combinations were reliable clinical prediction tools.

Conclusions. Both DCE-MRI and IVIM facilitate the prediction of TP53 status and risk stratification in early-stage EC. Compare with each single parameter, the combination of independent predictors provided better predictive power and may serve as a superior imaging marker.

Key words: early-stage endometrial carcinoma; dynamic contrast-enhanced MRI; intravoxel incoherent motion; p53 status; risk stratification

TABLE 1. Imaging protocol parameters

Parameters	T1WI	T2WI	DWI	IVIM	DCE-MRI
Sequence	2D-FSE	2D-FSE	2D-SS-EPI	2D-SS-EPI	3D-LAVA
Orientation	Oblique Axial	Oblique Axial	Oblique Axial	Oblique Axial	Oblique Axial
TR/TE (ms)	659/12.3	6000/95	3708/74.3	2000/80.7	3.5/1.7
FOV (cm^2)	40 × 40	40 × 40	40 × 40	40 × 40	36 × 36
Matrix	288 × 192	320 × 320	96 × 128	128 × 192	288 × 192
Flip angle (°)	160	160	90	90	15
Slice thickness (mm)	6	6	6	6	6
No. of sections	20	20	20	Based on lesion's size	26
NEX	1	1	1, 4	1, 1, 1, 1, 1, 1, 2, 4, 4, 6	0.73
Fat suppression	/	STIR	STIR	STIR	FLEX
b-values (s/mm^2)	/	/	0, 800	0, 20, 40, 80, 160, 200, 400, 600, 800, 1000	/
Respiratory compensation	Free	Free	Free	Free	Free
Scan time	1 min 56 s	48 s	1 min 04 s	3~6min	6 min 08 s (40 phases)

DCE-MRI = dynamic contrast-enhanced magnetic resonance imaging; DWI = diffusion-weighted imaging; FOV = field of view; FLEX = FLEXible; FSE = fast spin echo; IVIM = intravoxel incoherent motion; LAVA = liver acquistion with volume assessmeNT; NEX = number of excitations; SS-EPI = single shot echo planar imaging; STIR = short-inversion time(TI) recovery; TR/TE = repetition time/echo time; T1WI = T1-weighted imaging; T2WI = T2-weighted imaging

Introduction

Endometrial carcinoma (EC) is a common malignant tumor of the female reproductive system worldwide, and approximately 80% of newly diagnosed EC patients are in the early stage (International Federation of Gynecology and Obstetrics (FIGO) stage IA, IB).[1] The TP53 is an important suppressor gene that is deeply involved in tumorigenesis and can control cell growth, apoptosis and regulate angiogenesis. Several studies have shown that high expression of TP53 is closely associated with poor prognosis in EC patients.[2,3] Risk stratification based on the histologic subtype, grade, FIGO stage, and lymphovascular space invasion (LVSI) is the primary basis for determining treatment strategies for early-stage EC.[4] For non-low-risk (intermediate-, high-intermediate-, and high-risk) patients, lymphadenectomy (LND) is required in addition to the standard treatment of total hysterectomy with bilateral salpingo-oophorectomy, since it can significantly improve patient benefit. But for low-risk patients, LND is not recommended as it is likely to lead to complications and increased care costs.[5] Currently, preoperative biopsy and routine magnetic resonance imaging (MRI) are the primary means of obtaining the TP53 status and risk stratification information of EC, respectively.[6] However, biopsy may not be sufficient for a reliable diagnosis due to shortcomings such as unstable sampling depending on operator experience, inadequate sampling, and invasiveness.[7,8] At the same time, conventional T1-weighted imaging (T1WI) and T2-weighted imaging (T2WI) not only fail to reflect the TP53 status, histological subtype, and grade information of the lesion but also likely to have a poor to moderate pooled sensitivity in detecting high-risk factors, including deep myometrial invasion and cervical stromal infiltration, due to the presence of adenomyosis and leiomyomas and the loss of the junctional zone.[9,10] Therefore, finding a noninvasive and effective means to assess the TP53 status and risk stratification in early-stage EC is of great benefit to patients.

Dynamic contrast-enhanced MRI (DCE-MRI) is a promising quantitative MRI sequence that can detect blood supply in biological tissues by analyzing the dynamic distribution of contrast agents through pharmacokinetic models.[11,12] Intravoxel incoherent motion (IVIM) can also be used to reflect blood perfusion, and compared to DCE-MRI, it not only eliminates the need for contrast agents but also provides additional information on the diffusion of water molecules within the lesion.[13-16] Recently, some authors have used IVIM and DCE-MRI for EC-related studies. For example, Satta *et al.* and Fu *et al.* applied IVIM and DCE-MRI to assess the grade, stage, and other histopathological fea-

tures of EC and showed that some of the derived parameters helped to identify the histopathological features of EC.[17,18] Zhang *et al*. and Meng *et al*. used IVIM[19,20], while Ye *et al*.[12] used DCE-MRI for the preoperative risk assessment of EC, and their results showed that some parameters of DCE-MRI or IVIM could play a positive role in the risk stratification prediction of EC. However, not only did none of these studies address TP53 status but also risk stratification was assessed either by applying only one of the IVIM or DCE-MRI techniques or the subjects were not early-stage EC.

The purpose of this study was to investigate the contributory value of quantitative parameters derived from DCE-MRI and IVIM in differentiating TP53-mutant from TP53-wild, low-risk from non-low-risk early-stage EC, offering a potential reference for the clinical management of early-stage EC.

Patients and methods

Study patients

This prospective study was complied with ethical committee standards and approved by the ethics committee of the First Affiliated Hospital of Xinxiang Medical University (NO. EC-022-002) and informed consent was taken from all individual participants. From January 2021 to April 2022, 114 female patients underwent pelvic MRI due to suspected EC by clinical examination, ultrasound (US), or computed tomography (CT). Forty participants were excluded during this study: 1) 7 patients were diagnosed with an endometrial polyp, atypical hyperplasia, or other non-EC diseases; 2) 16 patients had FIGO stage ≥ II; 3) 4 patients received radiotherapy or neoadjuvant chemotherapy; 4) 3 patients had claustrophobia or other diseases that prevented them from completing all the sequences; 5) 6 patients had inadequate DCE-MRI or IVIM imaging quality for analysis due to severe artifacts, and 6) 4 patients decided to perform histological analysis and treatment in other institutes. Ultimately, 74 patients were enrolled in the study (Figure 1).

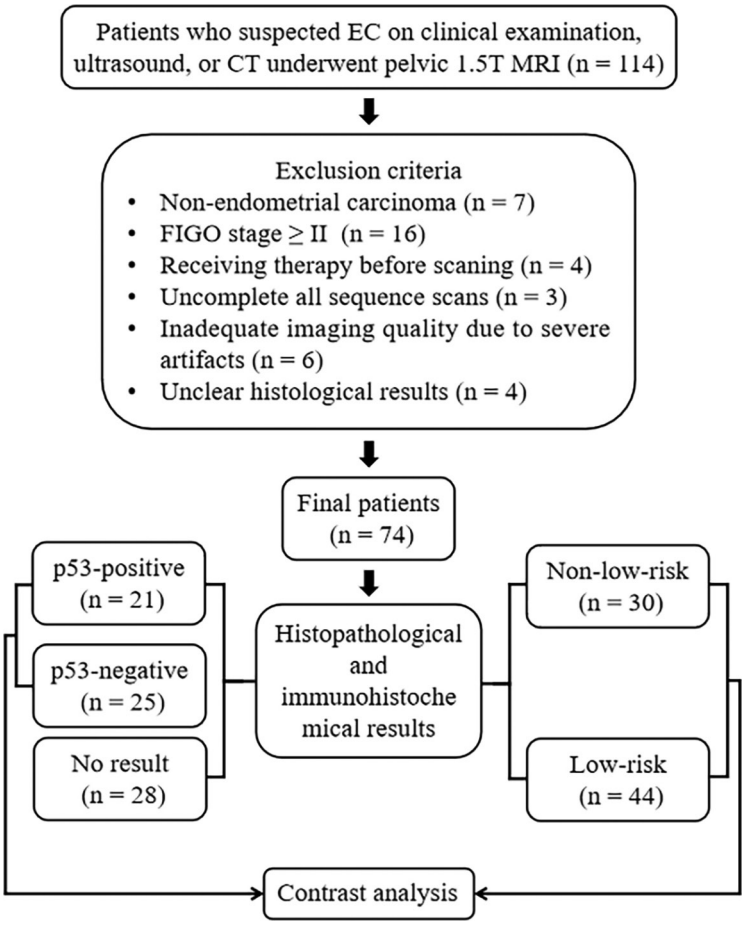

FIGURE 1. Flowchart of the present study.

EC = endometrial carcinoma

MRI protocols

A 1.5 T MR system (Optima MR360, Waukesha, WI, USA) with a 12-channel phased-array body coil was used in this study. The imaging protocol included oblique axial (perpendicular to the long axis of the uterus) T1WI, T2WI, DWI, IVIM, and DCE-MRI. For DWI and DCE-MRI sequences, the scans covered the anterior superior iliac spine to the symphysis pubis. For IVIM (b = 0, 20, 40, 80, 160, 200, 400, 600, 800, and 1000 s/mm^2), to minimize scan time, the scan was limited to the lesion area (determined by an experienced radiologist from the DWI images), and its location, layer thickness, and layer spacing were consistent with the corresponding layer of DWI.[18] DCE-MRI was performed by a three-dimensional liver acquisition with volume acceleration (3D-LAVA) sequence with 40 phases (time resolution, 9s), and gadopentetate dimeglumine (Gd-DTPA, Bayer Pharmaceutical, Berlin, Germany) was injected intravenously with an automatic injector (0.2 mL/kg, 3.0 mL/s). The protocol details are provided in Table 1.

Image postprocessing

All images were transferred to the Advantage Workstation (version 4.7), and the IVIM and DCE-MRI images were analyzed within the workstation

TABLE 2. Clinicopathologic features of the patients

Variable	Data
Age (mean ± SD) (years)	54.00 ± 7.91
Maximum diameter (mean ± SD) (mm)	25.10 (13.76, 42.58)
FIGO stage n (%)	
IA	44 (59.46)
IB	30 (40.54)
Histologic subtype n (%)	
Adenocarcinoma	67 (90.54)
Non-adenocarcinoma	7 (9.46)
Clear-cell	3 (4.06)
Undifferentiated carcinoma	2 (2.70)
Carcinosarcoma	2 (2.70)
Lymphovascular space invasion n (%)	
Positive	10 (6.76)
Negative	64 (93.24)
Histologic grade n (%)	
Grade 1	54 (72.98)
Grade 2	10 (13.51)
Grade 3	10 (13.51)
Risk stratification n (%)	
Low	44 (59.46)
Intermediate	20 (27.03)
High-intermediate	0 (0.00)
High	10 (13.51)
TP53 expression	
Mutant	21 (28.38)
Wild	25 (33.78)
No result	28 (37.84)

FIGO = International Federation of Gynecology and Obstetrics; SD = standard deviation

using vendor-provided software named MADC and GenIQ, respectively. The IVIM parameters were calculated by the following formula:

$$S_b/S_0 = (1 - f) \times \exp(-b \times D) + f \times \exp(-b \times D^*) \quad [1]$$

where S_0 was the signal intensity at the b value of 0; S_b was the signal intensity at the b value denoted by the subscript; D was the true diffusion coefficient of a water molecule; D* was the pseudo-diffusion coefficient due to microcirculation; and f was the microvascular volume fraction, indicating the fraction of diffusion related to microcirculation.[11] The DCE-MRI perfusion parameters were quantitatively calculated based on the Tofts model. The arterial input function (AIF) was obtained from the internal iliac artery. The imaging parameter K^{trans}, known as the volume transfer constant, represents the diffusion of contrast medium from the vessel to the extravascular extracellular space (EES); K_{ep}, known as the rate transfer constant, represents the diffusion of contrast medium from the EES to the vessel; and V_e represents the volume of EES per unit volume of tissue [13]; thus, $K_{ep} = K^{trans}/V_e$.

For regions of interest (ROI), first, images of DCE-MRI and IVIM were co-registered, and then on the DCE-MRI images of the phase with the clearest lesion display[21], ROIs were delineated layer by layer for all slices containing the tumor, and these ROIs were manually drawn along the inside margin of the primary tumor, avoiding areas with cystic degeneration, necrosis, apparent signs and hemorrhage artifacts, and blood vessels. Subsequently, all completed ROIs were automatically copied to the pseudo-color maps of the DCE-MRI and IVIM-derived parameters to calculate the mean values based on the volume of interest (VOI). All of these procedures were completed independently by two radiologists with 7 and 15 years of experience who were blinded to each other's results and the patient's clinicopathological data.

Histopathologic analysis

All lesion specimens were obtained surgically, and the median interval from pelvic MRI examination to surgery was 12 days (1-25 days). The specimens were processed by an experienced pathologist. The histological subtype, grade, and LVSI were confirmed by hematoxylin/eosin (HE) staining. The stage was estimated with the FIGO staging system.[22] According to the European Society for Medical Oncology (ESMO) clinical practice guidelines, low-risk patients were classified into the low-risk group, while intermediate-risk, high-intermediate-risk, and high-risk patients were classified into the non-low-risk group.[4] The TP53 status was evaluated by immunohistochemical (IHC) staining, where non-staining was viewed as the wild group, and faint, moderate, and strong staining was viewed as the mutant group. Ultimately, risk stratification was evaluated in all 74 patients, and TP53 status was evaluated in 46 patients (28 patients declined IHC for financial or other reasons).

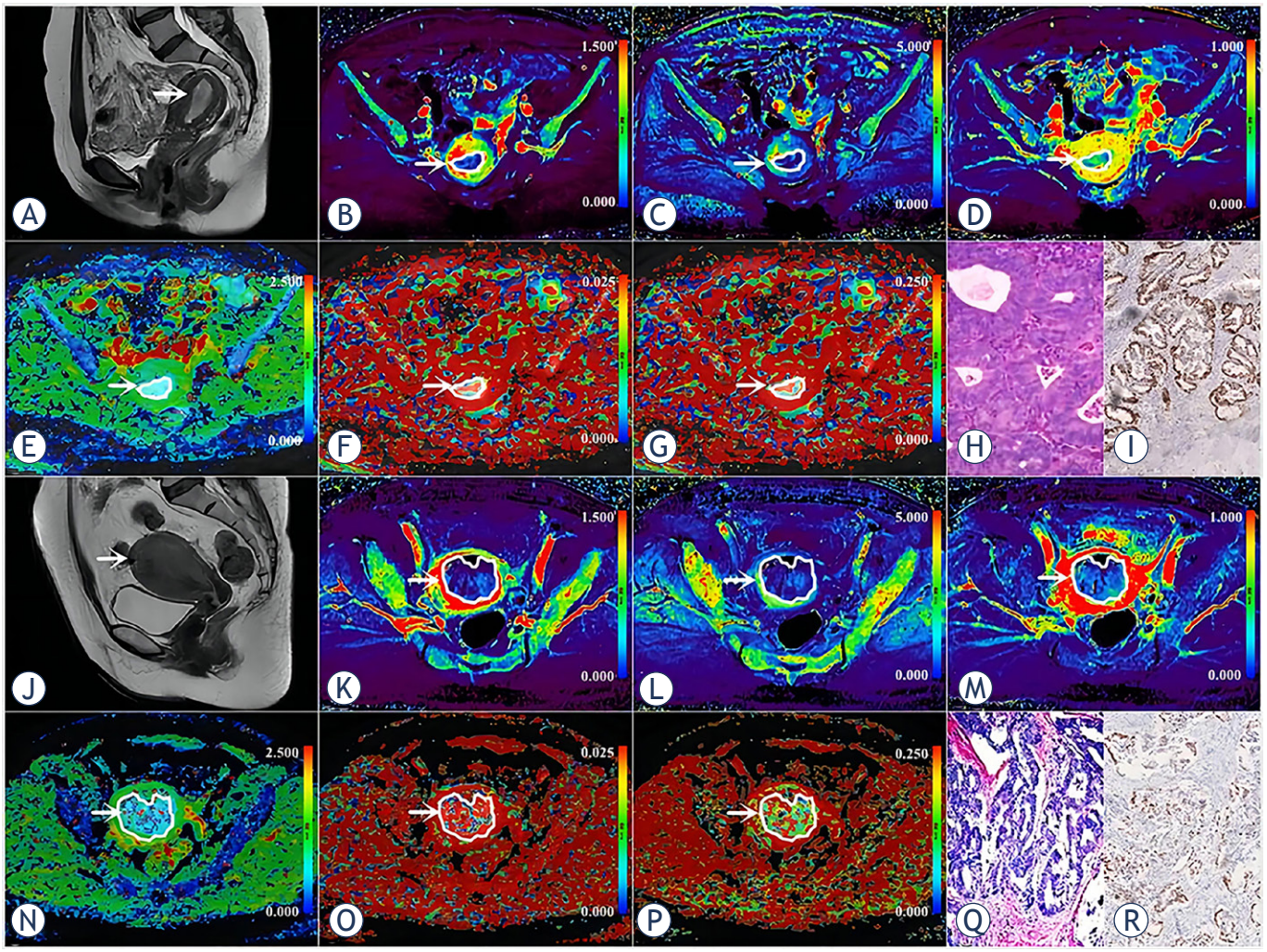

FIGURE 2. (A-I) A 53-year-old woman with low-risk endometrial carcinoma (EC) (arrowheads, endometrioid type, grade 2, stage IA, lymphovascular space invasion (LVSI) negative, and TP53-wild). **(J-R)** A 56-year-old woman with non-low-risk (intermediate) EC (arrowheads, endometrioid type, grade 1, stage IB, LVSI negative, and TP53-mutant). **(A, J)** Sagittal T2-weighted imaging maps; **(B, K)** Oblique axial pseudo colored maps of volume transfer constant (K^{trans}); **(C, L)** Oblique axial pseudo colored maps of rate transfer constant (K_{ep}); **(D, M)** Oblique axial pseudo colored maps of the volume of extravascular extracellular space per unit volume of tissue (V_e); **(E, N)** Oblique axial colored maps of true diffusion coefficient (D); **(F, O)** Oblique axial colored maps of pseudo-diffusion coefficient (D*); **(G, P)** Oblique axial colored maps of microvascular volume fraction (f), and **(H, Q)** Histopathological images (magnification = 100), and **(I, R)** Immunohistochemical image (magnification = 200).

Statistical analysis

All data were analyzed with Stata version 16.0 (Stata Corp) and MedCalc version 15.0 (MedCalc Software). $P < 0.05$ was considered statistically significant. The interobserver consistency of two radiologists was classified using the intraclass correlation coefficient (ICC) as poor (ICC < 0.40), fair ($0.40 \leq ICC < 0.60$), good ($0.60 \leq r < 0.75$), or excellent (ICC ≥ 0.75).[23] The Shapiro–Wilk test was employed to check the normality of the data. The Mann–Whitney U test and the independent samples t-test were used for nonnormally distributed data (median and interquartile range) and normally distributed data (mean ± standard deviation), respectively. The area under the receiver operating characteristic (ROC) curve (AUC) was employed to quantify the diagnostic efficacy of different parameters, and the differences were assessed using DeLong analysis. The combination of parameters was investigated by logistic regression, evaluated by bootstrap (random number set 123, repeated sampling 1000 times, backward strategy, bounded by a value of 0.1), calibration curves, and decision curve analysis (DCA).[24]

TABLE 3. Comparison of different parameters

Parameters	D ($\times10^{-3}mm^2/s$)	D* ($\times10^{-3}mm^2/s$)	f (%)	K^{trans} (min^{-1})	V_e	K_{ep} (min^{-1})
Risk stratification						
High-risk (n = 10)	0.63 (0.40, 0.73)	58.40 (40.10, 88.73)	1.64 ± 0.60	0.35 (0.15, 0.43)	0.30 ± 0.07	1.23 (0.48, 1.54)
High-intermediate-risk (n = 0)	/	/	/	/	/	/
Intermediate-risk (n = 20)	0.55 (0.40, 0.81)	52.00 (26.88, 74.33)	1.74 ± 0.96	0.37 (0.29, 0.47)	0.33 ± 0.14	1.24 (0.82, 1.98)
Low-risk (n = 44)	0.86 (0.64, 1.16)	44.35 (21.93, 95.33)	2.43 ± 1.08	0.61 (0.43, 1.14)	0.58 ± 0.25	1.53 (0.79, 2.21)
P-value	**0.033** [a]	0.464 [a]	**0.012** [a]	**< 0.001** [a]	**< 0.001** [a]	0.191 [a]
P-value (High *vs* Intermediate)	0.880 [b]	0.248 [b]	0.735 [c]	0.397 [b]	0.532 [c]	0.307 [b]
P-value (High vs Low)	**0.009** [b]	0.238 [b]	**0.004** [c]	**< 0.001** [b]	**0.001** [c]	0.099 [b]
P-value (Intermediate vs Low)	**0.001** [b]	0.937 [b]	**0.014** [c]	**< 0.001** [b]	**< 0.001** [c]	0.582
Low-risk (n = 44)	0.86 (0.64, 1.16)	44.35 (21.93, 95.33)	2.43 ± 1.08	0.61 (0.43, 1.14)	0.58 ± 0.25	1.53 (0.79, 2.21)
Non-low-risk (High + Intermediate, n = 30)	0.58 (0.40, 0.77)	55.25 (34.63, 72.78)	1.71 ± 0.84	0.37 (0.28, 0.45)	0.32 ± 0.12	1.23 (0.82, 1.87)
z/t value	- 3.793	-0.523	3.234	-5.109	5.304	-1.233
P-value	**< 0.001** [b]	0.601 [b]	**0.002** [c]	**< 0.001** [b]	**< 0.001** [c]	0.218 [b]
TP53 expression						
Mutant (n = 21)	0.72 ± 0.31	43.70 (16.30, 90.75)	2.30 ± 1.09	0.67 (0.41, 1.14)	0.32 (0.25, 0.91)	1.67 (1.17, 2.09)
Wild (n = 25)	0.91 ± 0.29	50.60 (26.90, 82.75)	2.20 ± 1.02	0.43 (0.37, 0.49)	0.49 (0.36, 0.76)	0.90 (0.58, 1.55)
Z/t value	-2.155	-0.518	0.321	-2.073	-0.783	-3.165
P-value	**0.037** [c]	0.604 [b]	0.750 [c]	**0.038** [b]	0.434 [b]	**0.002** [b]

The bold typeface in the table indicates the comparison with statistical significance.

[a] Comparisons were performed by *Analysis* of variance (ANOVA) test; [b] comparisons were performed by Mann–Whitney U test; [c] comparisons were performed by independent t test.

Results

Basic information

The clinicopathological and imaging characteristics are shown in Table 2 and Figure 2, respectively.

Interobserver consistency

The D, D*, f, K^{trans}, V_e, and K_{ep} measured by 2 radiologists had excellent consistency, and the ICCs were 0.864 (95% CI: 0.788 - 0.913), 0.799 (95% CI: 0.696 - 0.867), 0.855 (95% CI: 0.729 - 0.918), 0.868 (95% CI: 0.799 - 0.915), 0.834 (95% CI: 0.748 - 0.892), and 0.828 (95% CI: 0.739 - 0.888), respectively. The average results were used for the ultimate analysis.

Differences in parameters

The K^{trans} and K_{ep} were higher and D was lower in the TP53-mutant group than in the TP53-wild group (P = 0.038, 0.002, and 0.037, respectively), f, D*, and V_e were not significantly different between the two groups (P = 0.750, 0.604, and 0.434, respectively). The K^{trans}, V_e, f, and D values were lower in the non-low-risk group than in the low-risk group (P < 0.001, < 0.001, 0.002, and < 0.001, respectively), K_{ep} and D* were not significantly different between the two groups (P = 0.218 and 0.601) (Table 3, Figure 3).

Regression analyses

In the identification of TP53-mutant and TP53-wild early-stage EC, the potential related factors such as age, tumor size, risk stratification, FIGO stage, subtype, grade, LVSI, D, D*, f, K^{trans}, V_e, and K_{ep} were all enrolled in regression analysis. Univariate analysis demonstrated that grade, D, K^{trans}, and K_{ep} were all risk predictors (P all < 0.1), while multivariate analysis showed that only D and K^{trans} were independent predictors (P = 0.003, 0.016).

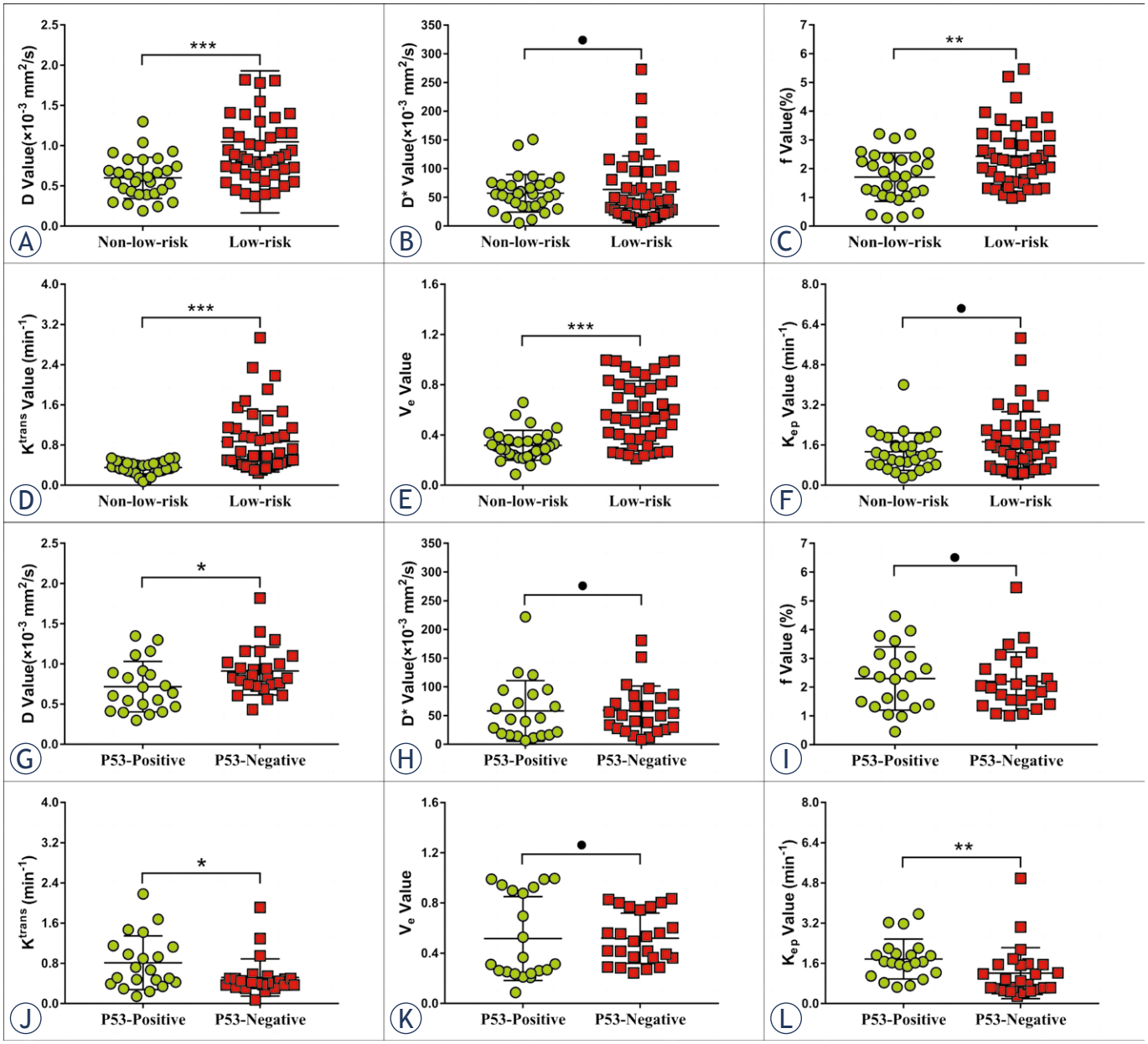

FIGURE 3. Plots show individual data points, averages, and standard deviations of true diffusion coefficient (D) **(A, G)**, pseudo-diffusion coefficient (D*) **(B, H)**, microvascular volume fraction (f) **(C, I)**, volume transfer constant (K^{trans}) **(D, J)**, the volume of extravascular extracellular space per unit volume of tissue (V_e) **(E, K)**, and rate transfer constant (K_{ep}) **(F, L)** in low-risk and non-low-risk groups **(A-F)**, TP53-mutant and TP53-wild groups **(G-L)**. Individual points are averages of values calculated by 2 readers. *P < 0.05, **P < 0.01, ***P < 0.001, and • P > 0.005.

In the identification of non-low-risk and low-risk early-stage EC, potential risk-related factors such as age, tumor size, TP53 status, D, D*, f, K^{trans}, V_e, and K_{ep} were all enrolled in regression analysis. Univariate analysis demonstrated that tumor size, D, f, K^{trans}, and V_e were all risk predictors (P all < 0.1), while multivariate analysis showed that only f, K^{trans}, and V_e were independent predictors (P = 0.036, 0.003, and 0.024, respectively) (Table 4).

Diagnostic performance of different parameters

In the differentiation of TP53-mutant and TP53-wild early-stage EC, the combination of independent predictors (K^{trans} and D) showed the optimal diagnostic efficacy (AUC = 0.867; sensitivity, 92.00%; specificity, 80.95%; P < 0.001), which was significantly better than D (AUC = 0.694, Z = 2.169,

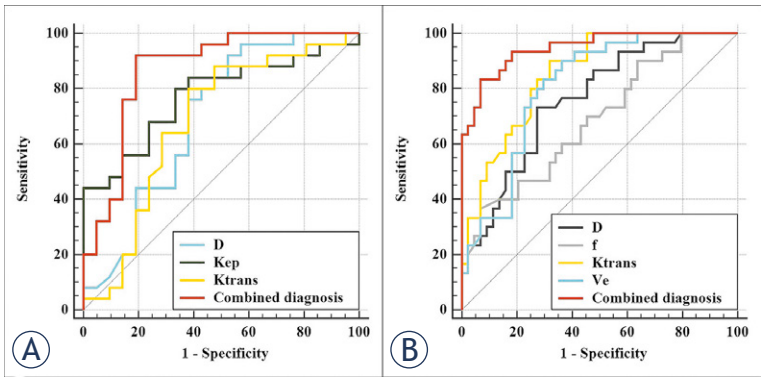

FIGURE 4. Receiver operating characteristic (ROC) curves, **(A)** shows each parameter and the combination of independent predictors for differentiation of TP53-mutant and TP53-wild early-stage endometrial carcinoma (EC); **(B)** shows each parameter and the combination of independent predictors for differentiation of low-risk and non-low-risk early-stage EC.

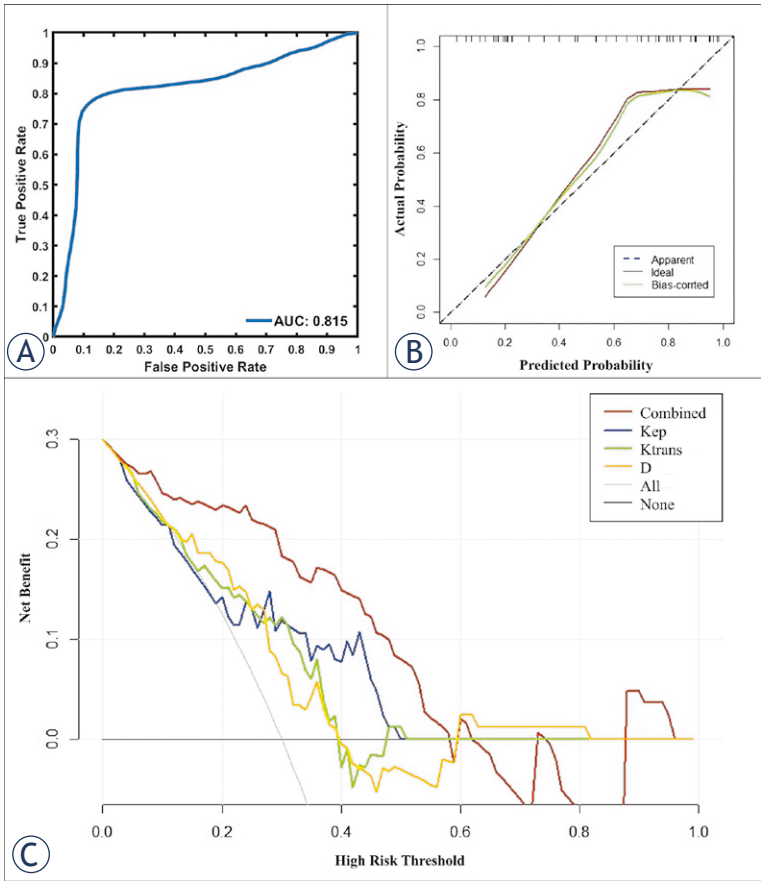

FIGURE 5. In the prediction of TP53 status, receiver operating characteristic curves **(A)**, calibration curves **(B)**, and decision curve analysis **(C)** of the validation model.

P = 0.030), and K^{trans} (AUC = 0.679, Z = 2.572, P = 0.010). However, the difference between the combination of independent predictors and K_{ep} (AUC = 0.773) was not significant (AUC = 0.773, Z = 1.272, P = 0.203) (Figure 4A, Table 5).

In the differentiation of low-risk and non-low-risk early-stage EC, the combination of independent predictors (f, K^{trans}, and V_e) showed the optimal diagnostic efficacy (AUC = 0.947; sensitivity, 83.33%; specificity, 93.18%; P < 0.001), which was significantly better than D (AUC = 0.761, Z = 3.113, P = 0.002), f (AUC = 0.688, Z = 4.317, P < 0.001), K^{trans} (AUC = 0.852, Z = 2.713, P = 0.007), and V_e (AUC = 0.808, Z = 3.175, P = 0.002) (Figure 4B, Table 5).

Validation

Bootstrapped samples were used to validate the combination of independent predictors. The ROC and the calibration curve indicated that the validation models not only had high accuracy in identifying TP53-mutant and TP53-wild early-stage EC (AUC, 0.815; 95% CI, 0.782 - 0.846, Figure 5A), and low-risk and risk early-stage EC (AUC, 0.922; 95% CI, 0.895 - 0.940, Figure 6A), but also highly had good consistency (Figure 5B, 6B). Also, DCA showed that the above combinations of independent predictors were both reliable clinical decision tools (Figure 5C, Figure 6C).

Discussion

Prediction of TP53 status and risk stratification of early-stage EC by IVIM

The parameter D of IVIM can reflect the diffusion movement of water molecules in the tissue, and usually, the more obvious the restriction of water molecule diffusion, the smaller the D value.[13] In this study, the D value of the TP53-mutant group was significantly lower than that of the TP53-wild group, which was similar to the results of Wang *et al.* in the field of epithelial ovarian cancer[25], suggesting that D values can be used to predict TP53 status of early-stage EC. Presumably, the reason was that TP53-mutant has a faster rate of cell proliferation than TP53-wild, which easily impedes the diffusion of water molecules, resulting in a lower D value.[26] In addition, D could also be used to assess the risk stratification of early-stage EC in the present study, which was consistent with previous studies.[17,19] The reason may be that there were differences in histological grade, FIGO stage, and lymph node metastasis between the low-risk

and non-low-risk early-stage EC, resulting in different degrees of influence on the diffusion of water molecules and ultimately leading to significant differences in D values between the two groups.[18,20]

D* was a perfusion parameter of IVIM that is mainly correlated with the velocity of blood flow within the microcirculation.[13] Previous publications have demonstrated that D* values with poor stability and repeatability could not effectively evaluate histopathological information of early-stage EC due to the influence of the scanning parameters, the ROI determination method, the signal-to-noise ratio (SNR), and other factors.[17-20] In this study, there was no statistically significant difference in D* between the TP53-mutant and TP53-wild groups, and the low-risk and the non-low-risk groups, which was consistent with the above research, further proving that the D* value was unable to play a role in the assessment of TP53 status and risk stratification in early-stage EC.

As another perfusion parameter derived from IVIM, f was mainly related to the microvascular density of the tissue.[13,27] A study by Zhang *et al*. involving 53 participants showed that although high-risk early-stage EC is metabolically active and rich in neovascularization, due to the dense tissue structure and more necrotic tissue, its overall internal microvascular density is instead reduced compared to that of low-risk early-stage EC, so the f value decreases.[20] This trial was conducted on a larger sample size of patients (n = 74) and obtained results consistent with those of Zhang *et al*.[19] Further analysis also identified the f value as an independent predictor for discriminating between low-risk and non-low-risk early-stage EC. However, there were also studies that have shown conflicting results of f values in the assessment of lesions. For example, the study by Meng *et al*. showed that high-risk early-stage EC had higher f values than low-risk early-stage EC.[20] Similarly, in the assessment of gliomas, the study of Bai *et al*. showed that low-grade gliomas had higher f values than high-grade gliomas[14], while Shen *et al*. concluded that high-grade gliomas have greater f values.[16] We speculate that the above phenomenon may be caused by the variations in scanning equipment and b-value settings[28], as well as the shortcoming that the f value itself is susceptible to T2 contribution and relaxation effects.[29] In addition, the results of this study also showed that the f was similar to D* and could not differentiate TP53-mutant from TP53-wild early-stage EC, which to some extent suggests that the use of IVIM perfusion parameters to assess the TP53 status of early-stage EC may still need further exploration.

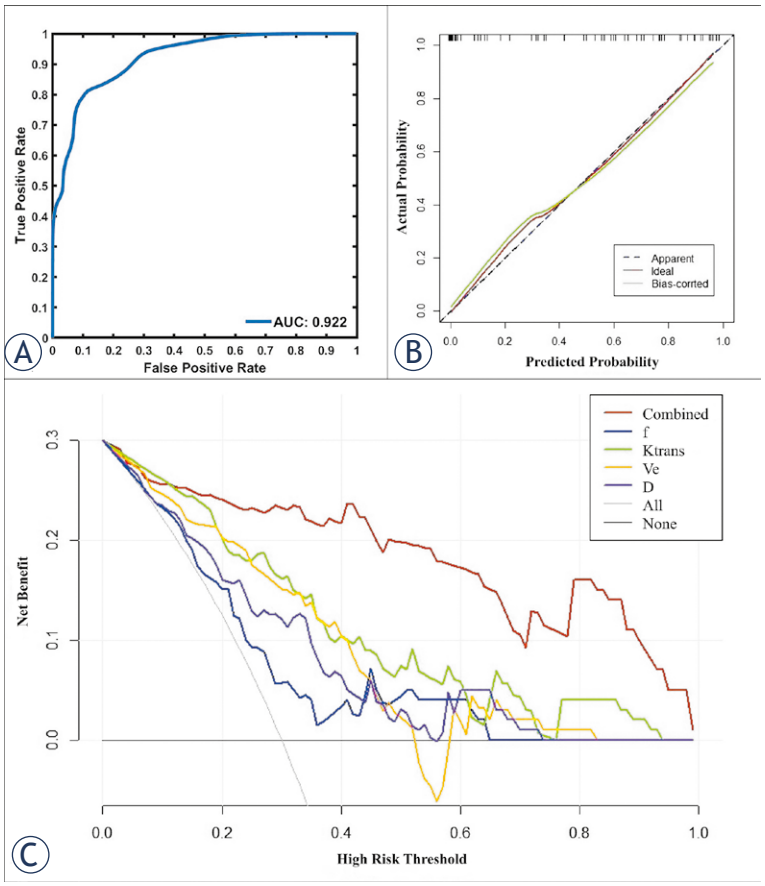

FIGURE 6. In the prediction of risk stratification, receiver operating characteristic curves **(A)**, calibration curves **(B)**, and decision curve analysis **(C)** of the validation model.

Prediction of TP53 status and risk stratification of early-stage EC by DCE-MRI

K^{trans} is the most significant perfusion-related parameter in DCE-MRI, mainly reflecting the transfer rate of the contrast agent from the vessel to the EES.[30] Previous studies have shown that the more neovascularization in the tissue and the greater the permeability, the greater the K^{trans} value.[31] In terms of TP53 status assessment, the present study found a significantly higher K^{trans} value in the TP53-mutant group compared with the TP53-wild group, which we suggest may be related to the ability of TP53 gene overexpression to promote angiogenesis.[2,3] In terms of risk stratification assessment, several studies have shown that EC with aggressive characteristics, such as grade 3,

TABLE 4. Logistic regression analyses

Parameters	Univariate Analyses OR for 1 SD (95% CI)	*P*-value	Multivariate Analyses OR for 1 SD (95% CI)	*P*-value
Low vs non-low risk				
Age (year)	1.462 (0.894–2.388)	0.130	/	/
Tumor size (mm)	1.055 (1.003–1.110)	**0.038**	1.083 (0.979–1.197)	0.123
TP53 mutant	1.506 (0.407–5.578)	0.540	/	/
D ($\times10^{-3}mm^2/s$)	0.089 (0.021–0.373)	**0.001**	0.144 (0.015–1.334)	0.088
D* ($\times10^{-3}mm^2/s$)	0.867 (0.533–1.412)	0.567	/	/
f (%)	0.419 (0.226–0.776)	**0.006**	0.292 (0.093–0.921)	**0.036**
K^{trans} (min^{-1})	0.009 (0.001–0.153)	**0.001**	0.001 (0.000–0.089)	**0.003**
V_e	0.173 (0.069–0.432)	**< 0.001**	0.130 (0.022–0.766)	**0.024**
K_{ep} (min^{-1})	0.642 (0.367–1.126)	0.122	/	/
TP53 mutant vs wild				
Age (year)	0.855 (0.465–1.548)	0.605	/	/
Tumor size (mm)	1.175 (0.649–2.127)	0.594	/	/
Subtype	77.708 (0.001–100.5)	0.999	/	/
Grade	2.099 (0.957–4.602)	**0.064**	1.961 (0.816–4.717)	0.132
Risk stratification	1.506 (0.407–5.578)	0.540	/	/
FIGO stage	1.360 (0.739–2.505)	0.323	/	/
LVSI	802.578 (0.001–1150.5)	0.999	/	/
D ($\times10^{-3}mm^2/s$)	2.063 (1.016–4.191)	**0.045**	8.274 (2.066–33.136)	**0.003**
D* ($\times10^{-3}mm^2/s$)	1.020 (0.567–1.835)	0.948	/	/
f (%)	0.906 (0.504–1.629)	0.742	/	/
K^{trans} (min^{-1})	0.487 (0.236–1.003)	**0.051**	0.155 (0.034–0.710)	**0.016**
V_e	1.008 (0.560–1.812)	0.979	/	/
K_{ep} (min^{-1})	0.501 (0.244–1.032)	**0.061**	1.172 (0.425–3.234)	0.759

D = true diffusion coefficient; D* = pseudo-diffusion coefficient; f = microvascular volume fraction; FIGO = international federation of gynecology and obstetrics; CI = confidence interval; K_{ep} = rate transfer constant; K^{trans} = volume transfer constant; LVSI = lymphovascular space invasion; OR = odds ratio;. SD = standard deviation; V_e = volume of extravascular extracellular space per unit volume of tissue

The bold typeface in the table indicates the logistic regression analyses with statistical significance.

In the analysis of the high- and low-risk group, the TP53 mutant data were analysed only for these patients who had the p53 gene test. The remaining parameters, such as diameter, were analysed for all 74 patients.

advanced FIGO stage, and non-endometrioid subtype, grows quickly without sufficient neoangiogenesis (i.e., blood support), resulting in tissue hypoxia. Hypoxia will lead to tissue necrosis and the formation of hypoperfused areas, thus eventually causing a decrease in overall tumor perfusion and a decrease in K^{trans} values.[12,17,32,33] In this work, the K^{trans} value was significantly lower in the non-low-risk group than in the low-risk group, which was consistent with the above findings and further demonstrates that the K^{trans} value can play a role in the risk stratification of early-stage EC.

K_{ep} was designed to reflect the transfer rate of the contrast agent from the EES into vessels, so similar to K^{trans}, its size was closely related to the number of new vessels and vascular permeability.[29] In this study, since TP53 overexpression can promote angiogenesis[2,3], the K_{ep} value of the TP53-mutant group was significantly higher than those of the TP53-wild group, and the diagnostic efficacy was 0.773. However, the K_{ep} value did not show significant value in the identification of different risk stratifications, which was not consistent with the study of Ye *et al.*[12] We speculated that this may be because the study by Ye *et al.* included both early-stage (stage I) and advanced-stage (stage II, III, and IV) EC, whereas the present study population included only early-stage EC, which reduced the differences

TABLE 5. Predictive performance of different parameters

Parameters	AUC (95% CI)	P-value	Cutoff	Sensitivity	Specificity	Comparison with combined diagnosis
Low vs non-low risk						
D ($\times10^{-3}mm^2/s$)	0.761 (0.648–0.853)	< 0.001	0.691	73.33%	72.73%	Z = 3.113, P = 0.002
D* ($\times10^{-3}mm^2/s$)	0.536 (0.416–0.653)	0.598	/	/	/	/
f (%)	0.688 (0.569–0.790)	0.003	1.240	36.67%	93.18%	Z = 4.317, P < 0.001
K^{trans} (min^{-1})	0.852 (0.750–0.924)	< 0.001	0.487	90.00%	68.18%	Z = 2.713, P = 0.007
V_e	0.808 (0.700–0.890)	< 0.001	0.401	83.33%	70.45%	Z = 3.175, P = 0.002
K_{ep} (min^{-1})	0.585 (0.652–0.849)	0.204	/	/	/	/
Combined diagnosis 1	0.947 (0.869–0.986)	< 0.001	/	83.33%	93.18%	/
TP53 mutant vs wild						
D ($\times10^{-3}mm^2/s$)	0.694 (0.541–0.821)	0.019	0.605	92.00%	47.62%	Z = 2.169, P = 0.030
D* ($\times10^{-3}mm^2/s$)	0.545 (0.391–0.692)	0.498	/	/	/	/
f (%)	0.535 (0.382–0.648)	0.388	/	/	/	/
K^{trans} (min^{-1})	0.679 (0.525–0.809)	0.036	0.499	80.00%	61.90%	Z = 2.572, P = 0.010
V_e	0.568 (0.413–0.713)	0.675	/	/	/	/
K_{ep} (min^{-1})	0.773 (0.626–0.884)	< 0.001	1.557	80.00%	66.67%	Z = 1.272, P = 0.203
Combined diagnosis 2	0.867 (0.734–0.949)	< 0.001	/	92.00%	80.95%	/

AUC = *area* under the receiver operating characteristic (ROC) curve; D = true diffusion coefficient; D* = pseudo-diffusion coefficient; f = microvascular volume fraction; K_{ep} = rate transfer constant; K^{trans} = volume transfer constant; V_e = volume of extravascular extracellular space per unit volume of tissue

The combined diagnosis 1 represents f + K^{trans} + V_e; the combined diagnosis 2 represents D + V_e

in patients between the different groups and ultimately resulted in nonfunctional K_{ep} values.

V_e is a parameter in DCE-MRI that can reflect the volume of EES. In the present study, there was no significant difference in V_e between the TP53-mutant and TP53-wild groups, which may be related to the fact that TP53 overexpression promotes both cell proliferation and angiogenesis, resulting in difficulty in significant changes in EES.[2,3] In terms of risk stratification assessment, V_e values in the non-low-risk group were significantly smaller than those in the low-risk group, which was similar to the results of previous studies[17,34], and we speculated that the reason for this result may lie in the fact that the non-low-risk group had greater invasiveness and therefore greater cell density, tighter tissue structure, and smaller EEC compared with the low-risk group. However, some studies have also concluded that V_e was difficult to use in the evaluation of diseases such as EC and breast cancer.[12,35] This may be related to the fact that V_e is less stable and susceptible to factors such as lesion edema and microcystic changes.[36] In a follow-up study, we will expand the sample size and further explore the role of V_e in EC assessment to obtain more convincing results.

Diagnostic performance comparison

The diagnostic efficacy of the combination of independent predictors and each individual parameter was compared in this study, and the results showed that the diagnostic efficacy of the former was significantly higher than that of the latter, which may be because the combination of independent predictors concentrates the advantages of different parameters and therefore can reflect the lesion characteristics more comprehensively and accurately. Therefore, we suggest that the combined application of IVIM and DCE-MRI in clinical routine may provide a more reliable basis for the TP53 status and risk stratification prediction of early-stage EC when conditions permit.

Correlation of risk stratification with TP53 mutation

In this study, TP53 mutation and risk stratification in early-stage EC were included in each other's regression analysis, and the results showed that neither was a predictor of the other. Although the small sample size may have affected the reliability of the above results to a certain extent, it indicates

to some extent that the TP53 status in early-stage EC is not significantly correlated with risk stratification. In the future, as the sample size increases, we will conduct more in-depth studies on the relationship between the two, with a view to obtaining more accurate results.

This study has several limitations. First, our study was designed at a single institution with a relatively small number of patients, especially since some patients forgo immunohistochemical testing for financial reasons, which may have led to selection bias. Second, due to the small sample size, this study did not set up a separate validation set but used the bootstrap (1000 samples) method to validate the combination of independent predictors, which may have reduced the reliability of the experimental results. Third, areas of cystic degeneration, necrosis, apparent signs and hemorrhage artifacts, or vessels were avoided in the delineation of the ROI, which may influence the determination of some parameters. Finally, the machine used in this study was a 1.5 T MRI, and its imaging quality and parameter reliability may be inferior to those of a 3.0 T MRI.

Conclusions

Both DCE-MRI and IVIM facilitate the prediction of TP53 status and risk stratification in early-stage EC. Comparison with each single parameter, the combination of independent predictors provided better predictive power and may serve as a superior imaging marker.

Acknowledgement

This work was supported by the Roentgen Imaging Research Project (HN-20201017-002), the Key Project of Henan Province Medical Science and Technology Project (LHGJ20200519). The datasets and analyses during the current study are available from the corresponding author on reasonable request.

References

1. Miller KD, Ortiz AP, Pinheiro PS, Bandi P, Minihan A, Fuchs HE, et al. Cancer statistics for the US Hispanic/Latino population, 2021. *CA Cancer J Clin* 2021; **71:** 466-87. doi: 10.3322/caac.21695
2. Nakamura M, Obata T, Daikoku T, Fujiwara H. The association and significance of p53 in gynecologic cancers: the potential of targeted therapy. *Int J Mol Sci* 2019; **20:** 5482. doi: 10.3390/ijms20215482
3. Jamieson A, Thompson EF, Huvila J, Gilks CB, McAlpine JN. p53abn endometrial cancer: understanding the most aggressive endometrial cancers in the era of molecular classification. *Int J Gynecol Cancer* 2021; **31:** 907-13. doi: 10.1136/ijgc-2020-002256
4. Colombo N, Creutzberg C, Amant F, Bosse T, González-Martín A, Ledermann J, et al. ESMO-ESGO-ESTRO Consensus Conference on Endometrial Cancer: diagnosis, treatment and follow-up. *Ann Oncol* 2016; **27:** 16-41. doi: 10.1093/annonc/mdv484
5. Brooks RA, Fleming GF, Lastra RR, Lee NK, Moroney JW, Son CH, et al. Current recommendations and recent progress in endometrial cancer. *CA Cancer J Clin* 2019; **69:** 258-79. doi: 10.3322/caac.21561
6. Makker V, MacKay H, Ray-Coquard I, Levine DA, Westin SN, Aoki D, et al. Endometrial cancer. *Nat Rev Dis Primers* 2021; **7:** 88. doi: 10.1038/s41572-021-00324-8
7. Visser NCM, Reijnen C, Massuger LFAG, Nagtegaal ID, Bulten J, Pijnenborg JMA. Accuracy of endometrial sampling in endometrial carcinoma: a systematic review and meta-analysis. *Obstet Gynecol* 2017; **130:** 803-13. doi: 10.1097/AOG.0000000000002261
8. Garcia TS, Appel M, Rivero R, Kliemann L, Wender MC. Agreement between preoperative endometrial sampling and surgical specimen findings in endometrial carcinoma. *Int J Gynecol Cancer* 2017; **27:** 473-8. doi: 10.1097/IGC.0000000000000922
9. Sala E, Rockall AG, Freeman SJ, Mitchell DG, Reinhold C. The added role of MR imaging in treatment stratification of patients with gynecologic malignancies: what the radiologist needs to know. *Radiology* 2013; **266:** 717-40. doi: 10.1148/radiol.12120315
10. Luomaranta A, Leminen A, Loukovaara M. Magnetic resonance imaging in the assessment of high-risk features of endometrial carcinoma: a meta-analysis. *Int J Gynecol Cancer* 2015; **25:** 837-42. doi: 10.1097/IGC.0000000000000194
11. Khalifa F, Soliman A, El-Baz A, Abou El-Ghar M, El-Diasty T, Gimel'farb G, et al. Models and methods for analyzing DCE-MRI: a review. *Med Phys* 2014; **41:** 124301. doi: 10.1118/1.4898202
12. Ye Z, Ning G, Li X, Koh TS, Chen H, Bai W, et al. Endometrial carcinoma: use of tracer kinetic modeling of dynamic contrast-enhanced MRI for preoperative risk assessment. *Cancer Imaging* 2022; **22:** 14. doi: 10.1186/s40644-022-00452-8.
13. Le Bihan D, Breton E, Lallemand D, Aubin ML, Vignaud J, Laval-Jeantet M. Separation of diffusion and perfusion in intravoxel incoherent motion MR imaging. *Radiology* 1988; **168:** 497-505. doi: 10.1148/radiology.168.2.3393671
14. Bai Y, Lin Y, Tian J, Shi D, Cheng J, Haacke EM, et al. Grading of gliomas by using monoexponential, biexponential, and stretched exponential diffusion-weighted MR imaging and diffusion kurtosis MR imaging. *Radiology* 2016; **278:** 496-504. doi: 10.1148/radiol.20151 42173
15. Liu C, Wang K, Chan Q, Liu Z, Zhang J, He H, et al. Intravoxel incoherent motion MR imaging for breast lesions: comparison and correlation with pharmacokinetic evaluation from dynamic contrast-enhanced MR imaging. *Eur Radiol* 2016; **26:** 3888-98. doi: 10.1007/s003 3 0-016-4241-6
16. Shen N, Zhao L, Jiang J, Jiang R, Su C, Zhang S, et al. Intravoxel incoherent motion diffusion-weighted imaging analysis of diffusion and microperfusion in grading gliomas and comparison with arterial spin labeling for evaluation of tumor perfusion. *J Magn Reson Imaging* 2016; **44:** 620-32. doi: 10.1002/jmri.25191
17. Satta S, Dolciami M, Celli V, Di Stadio F, Perniola G, Palaia I, et al. Quantitative diffusion and perfusion MRI in the evaluation of endometrial cancer: validation with histopathological parameters. *Br J Radiol* 2021; **94:** 20210054. doi: 10.1259/bjr.20210054
18. Fu F, Meng N, Huang Z, Sun J, Wang X, Shang J, et al. Identification of histological features of endometrioid adenocarcinoma based on amide proton transfer-weighted imaging and multimodel diffusion-weighted imaging. *Quant Imaging Med Surg* 2022; **12:** 1311-23. doi: 10.21037/qims-21-189
19. Zhang Q, Yu X, Lin M, Xie L, Zhang M, Ouyang H, et al. Multi-b-value diffusion weighted imaging for preoperative evaluation of risk stratification in early-stage endometrial cancer. *Eur J Radiol* 2019; **119:** 108637. doi: 10.1016/j.ejrad.2019.08.006

20. Meng N, Fang T, Feng P, Huang Z, Sun J, Wang X, et al. Amide proton transfer-weighted imaging and multiple models diffusion-weighted imaging facilitates preoperative risk stratification of early-stage endometrial carcinoma. *J Magn Reson Imaging* 2021; **54:** 1200-11. doi: 10.1002/jmri.27684

21. Romeo V, Cavaliere C, Imbriaco M, Verde F, Petretta M, Franzese M, et al. Tumor segmentation analysis at different post-contrast time points: a possible source of variability of quantitative DCE-MRI parameters in locally advanced breast cancer. *Eur J Radiol* 2020; **126:** 108907. doi: 10.1016/j.ejrad.2020.108907

22. Pecorelli S. Revised FIGO staging for carcinoma of the vulva, cervix, and endometrium. *Int J Gynaecol Obstet* 2009; **105:** 103-4. doi: 10.1016/j.ijgo.2009.02.012

23. Shieh G. Choosing the best index for the average score intraclass correlation coefficient. *Behav Res Methods* 2016; **48:** 994-1003. doi: 10.3758/s13428-015-0623-y

24. Xu C, Yu Y, Li X, Sun H. Value of integrated PET-IVIM MRI in predicting lymphovascular space invasion in cervical cancer without lymphatic metastasis. *Eur J Nucl Med Mol Imaging* 2021; **48:** 2990-3000. doi: 10.1007/s00259-021-05208-3

25. Wang F, Wang Y, Zhou Y, Liu C, Liang D, Xie L, et al. Apparent diffusion coefficient histogram analysis for assessing tumor staging and detection of lymph node metastasis in epithelial ovarian cancer: correlation with p53 and Ki-67 expression. *Mol Imaging Biol* 2019; **21:** 731-39. doi: 10.1007/s11307-018-1295-7

26. Wang Y, Bai G, Zhang X, Shan W, Xu L, Chen W. Correlation analysis of apparent diffusion coefficient value and P53 and Ki-67 expression in esophageal squamous cell carcinoma. *Magn Reson Imaging* 2020; **68:** 183-9. doi: 10.1016/j.mri.2020.01.011

27. Shi C, Liu D, Xiao Z, Zhang D, Liu G, Liu G, et al. Monitoring tumor response to antivascular therapy using non-contrast intravoxel incoherent motion diffusion-weighted MRI. *Cancer Res* 2017; **77:** 3491-501. doi: 10.1158/0008-5472.CAN-16-2499

28. Pang Y, Turkbey B, Bernardo M, Kruecker J, Kadoury S, Merino MJ, et al. Intravoxel incoherent motion MR imaging for prostate cancer: an evaluation of perfusion fraction and diffusion coefficient derived from different b-value combinations. *Magn Reson Med* 2013; **69:** 553-62. doi: 10.1002/mrm.24277

29. Sumi M, Van Cauteren M, Sumi T, Obara M, Ichikawa Y, Nakamura T. Salivary gland tumors: use of intravoxel incoherent motion MR imaging for assessment of diffusion and perfusion for the differentiation of benign from malignant tumors. *Radiology* 2012; **263:** 770-7. doi: 10.1148/radiol.12111248

30. Ang T, Juniat V, Patel S, Selva D. Evaluation of orbital lesions with DCE-MRI: a literature review. *Orbit* 2022 Nov 27; 1-9. [Ahead of print]. doi: 10.1080/01676830.2022.2149819

31. Mazaheri Y, Akin O, Hricak H. Dynamic contrast-enhanced magnetic resonance imaging of prostate cancer: a review of current methods and applications. *World J Radiol* 2017; **9:** 416-25. doi: 10.4329/wjr.v9.i12.416

32. Bredholt G, Mannelqvist M, Stefansson IM, Birkeland E, Bø TH, Øyan AM, et al. Tumor necrosis is an important hallmark of aggressive endometrial cancer and associates with hypoxia, angiogenesis and inflammation responses. *Oncotarget* 2015; **6:** 39676-91. doi: 10. 18632/oncotarget.5344

33. Vaupel P, Mayer A. Hypoxia in tumors: pathogenesis-related classification, characterization of hypoxia subtypes, and associated biological and clinical implications. *Adv Exp Med Biol* 2014; **812:** 19-24. doi: 10.1007/978-1-4939-0620-8_3

34. Haris M, Gupta RK, Singh A, Husain N, Husain M, Pandey CM, et al. Differentiation of infective from neoplastic brain lesions by dynamic contrast-enhanced MRI. *Neuroradiology* 2008; **50:** 531-40. doi: 10.1007/s00234-008-0378-6

35. Liu C, Wang K, Chan Q, Liu Z, Zhang J, He H, et al. Intravoxel incoherent motion MR imaging for breast lesions: comparison and correlation with pharmacokinetic evaluation from dynamic contrast-enhanced MR imaging. *Eur Radiol* 2016; **26:** 3888-98. doi: 10.1007/s 00330-016-4241-6

36. Cho N, Im SA, Park IA, Lee KH, Li M, Han W, et al. Breast cancer: early prediction of response to neoadjuvant chemotherapy using parametric response maps for MR imaging. *Radiology* 2014; **272:** 385-96. doi: 10.1148/radiol.14131332

research article

Two-stage hepatectomy in resection of colorectal liver metastases – a single-institution experience with case-control matching and review of the literature

Spela Turk[1,2], Irena Plahuta[1,2], Tomislav Magdalenic[1], Tajda Spanring[1,2], Kevin Laufer[1,2], Zan Mavc[1], Stojan Potrc[1,2], Arpad Ivanecz[1,2]

[1] Clinical Department of Abdominal and General Surgery, University Medical Centre Maribor, Maribor, Slovenia
[2] Department of Surgery, Faculty of Medicine, University of Maribor, Maribor, Slovenia

Radiol Oncol 2023; 57(2): 270-278.

Received 18 March 2023
Accepted 15 May 2023

Correspondence to: Assist. Prof. Arpad Ivanecz, M.D., Ph.D., Clinical Department of Abdominal and General Surgery, University Medical Centre Maribor, Ljubljanska ulica 5, SI-2000 Maribor, Slovenia. E-mail: arpad.ivanecz@ukc-mb.si

Spela Turk and Irena Plahuta contributed equally to this work.

Disclosure: No potential conflicts of interest were disclosed. The abstract was accepted for presentation at the 15th Biennial Congress of the European Hepato-Pancreato-Biliary Association in June 2023 in Lyon, France.

Background. Two-stage hepatectomy (TSH) has been proposed for patients with bilateral liver tumours who have a high risk of posthepatectomy liver failure after one-stage hepatectomy (OSH). This study aimed to determine the outcomes of TSH for extensive bilateral colorectal liver metastases.

Patients and methods. A retrospective review of a prospectively maintained database of liver resections for colorectal liver metastases was conducted. The TSH group was compared to the OSH group in terms of perioperative outcomes and survival. Case-control matching was performed.

Results. A total of 632 consecutive liver resections for colorectal liver metastases were performed between 2000 and 2020. The study group (TSH group) consisted of 15 patients who completed TSH. The control group included 151 patients who underwent OSH. The case-control matching-OSH group consisted of 14 patients. The major morbidity and 90-day mortality rates were 40% and 13.3% in the TSH group, 20.5% and 4.6% in the OSH group and 28.6% and 7.1% in the case-control matching-OSH group, respectively. The recurrence-free survival, median overall survival, and 3- and 5-year survival rates were 5 months, 21 months, 33% and 13% in the TSH group; 11 months, 35 months, 49% and 27% in the OSH group; and 8 months, 23 months, 36% and 21%, respectively, in the case-control matching-OSH group, respectively.

Conclusions. TSH used to be a favourable therapeutic choice in a select population of patients. Now, OSH should be preferred whenever feasible because it has lower morbidity and equivalent oncological outcomes to those of completed TSH.

Key words: colorectal cancer; liver metastases; hepatectomy; future liver remnant; posthepatectomy liver failure; survival analysis

Introduction

Colorectal cancer is the third most diagnosed cancer worldwide.[1] At diagnosis, the disease has spread to the liver in 15% to 25% of patients, and another 25% develop colorectal liver metastases metachronously.[2] Liver resection remains the only potentially curative treatment option for these patients.[2] Despite the ability of the liver to regenerate after significant tissue loss, a future liver

remnant, which contributes 25–30% of the total liver volume, has been the minimal requirement in patients with a noncirrhotic liver.[2] Therefore, major hepatectomies are associated with a high risk of posthepatectomy liver failure.[3] Innovative approaches have been developed to improve colorectal liver metastases resectability, i.e., two-stage hepatectomy (TSH).[2,4] Their initial phase can be portal vein embolization or intraoperative selective portal vein ligation. The novelist approach is the associating liver partition and portal vein ligation for staged hepatectomy (ALPPS) procedure.[2]

This study aimed to determine the feasibility and safety of TSH for patients with extensive bilateral colorectal liver metastases by comparing perioperative and long-term outcomes between TSH and one-stage hepatectomy (OSH) groups.

Patients and methods

Study population

A retrospective review of a prospectively obtained database of 632 consecutive liver procedures for colorectal liver metastases at the Clinical Department of Abdominal and General Surgery of the University Medical Centre Maribor in Slovenia was performed. This department is a specialised referral centre for hepato-pancreato-biliary surgery. The study period was from 1 January 2000 until 31 December 2020.

Before the surgery, patients consented to their anonymous data being used for research. Therefore, their records were anonymised and deidentified before analysis. Ethical approval for this study was obtained from the National Medical Ethics Committee of the Republic of Slovenia (0120-455/2020/3). All methods were performed following the relevant guidelines and regulations.

Inclusion and exclusion criteria

The inclusion criteria were patients with bilateral colorectal liver metastases who:

- completed TSH or
- underwent their first OSH for colorectal liver metastases,
- the TSH group was formed from patients who underwent portal vein embolization or portal vein ligation, as proposed by Regimbeau.[5]

The exclusion criteria were as follows:

- explorative laparotomies without liver resections,
- repeated liver resections,
- patients with unilateral colorectal liver metastases,
- radiofrequency ablation (RFA) or its combinations with liver resections.

Definitions

Routinely available clinical characteristics were analysed, including patient demographics, performance status defined according to the American Society of Anaesthesiologists Classification (ASA classification)[6], application of neoadjuvant chemotherapy, preoperative carcinoembryonic antigen (CEA) level, and presence of extrahepatic disease. Primary colorectal tumour variables included the tumour location and nodal invasion. Liver metastasis variables included synchronous/metachronous metastases and the number and size of metastases.

Patients were presented at the multidisciplinary team meeting.[2] Bilateral colorectal liver metastases were resected in a single procedure when both the volume and function of the future liver remnant were considered sufficient. The parenchyma-sparing principle of liver surgery for colorectal liver metastases was applied.[7] The types of liver resections were classified according to the Brisbane terminology.[8] Major liver resections involved three or more adjacent liver segments, including conventional major resections (left/extended left hepatectomies, right/extended right hepatectomies, central hepatectomies).[8] The analysis of future liver remnant consisted of computed tomography (CT) volumetry, laboratory liver tests (prothrombin time and albumins), and the indocyanine green clearance test.[2]

Specimens were analysed by a gastrointestinal histopathologist who assessed the resection margin. The histological surgical margins for malignant lesions were defined as microscopically negative (R0) or positive (<1 mm, R1).[7] In addition, the Clinical Risk Score devised by Fong *et al*. was applied.[9]

Two-stage hepatectomy

Portal vein embolization, intraoperative selective portal vein ligation, or the ALPPS procedure were performed when the analysis suggested an insufficient future liver remnant.[2] Portal vein embolization was followed by atrophy of the embolized hemiliver and hypertrophy of the other hemiliver.[2] TSH with portal vein ligation was performed when the intraoperative findings were unfavourable.[4] In the first stage, the metastasectomy of one hemiliver

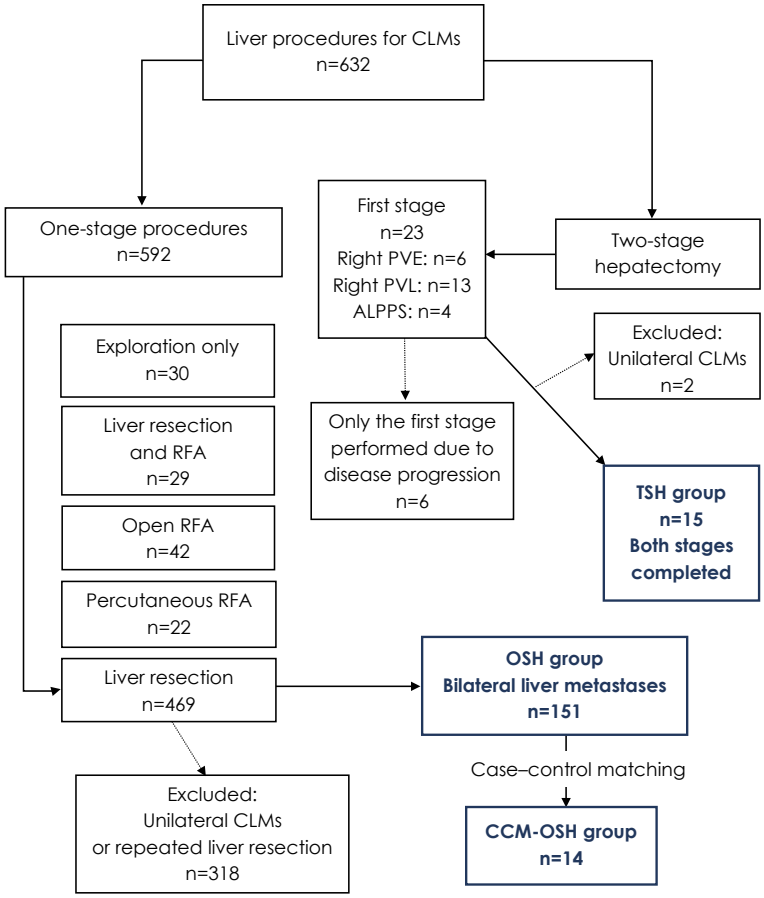

FIGURE 1. The study flowchart. The study period covers 1 January 2000 to 31 December 2020.

ALPPS = associating liver partition and portal vein ligation for staged hepatectomy; CCM-OSH = case-control matching one-stage hepatectomy; CLMs = colorectal liver metastases; OSH = one-stage hepatectomy; PVE = portal vein embolization; PVL = portal vein ligation; RFA = radiofrequency ablation; TSH = two-stage hepatectomy

was performed along with portal vein ligation for the other hemiliver.[4] The effect was similar to that of preoperative portal vein embolization.[10] The second stage followed a few weeks later and consisted of a major hepatectomy.[2,4] ALPPS was performed with the same rationale; the difference was the addition of liver parenchyma transection in the first stage.[11]

RFA has been applied where radical liver resection has been infeasible due to the proximity of large vessels.[2] Therefore, RFA has been applied intraoperatively as an independent procedure or adjunct to liver resection.[2] RFA has also been used as a percutaneous procedure. However, these patients were excluded from the analyses.

Follow-up

Patients were followed-up at the outpatient clinic at periodic intervals. The follow-up protocol consisted of a CEA level, a chest radiograph or CT, an abdominal ultrasound, CT, or magnetic resonance imaging every three months for the first two years and every six months afterwards.[2]

Study endpoints

Primary outcomes – overall survival and recurrence-free survival

The primary outcome was overall survival (OS). It was defined as the interval between the date of liver resection (the second stage in the TSH group) of colorectal liver metastases and the date of death or the last follow-up in surviving patients.

The second primary outcome was recurrence-free survival (RFS). It was calculated from the date of liver resection (the second stage in the TSH group) to the date of any detected recurrence or the last follow-up in patients without recurrence.

Secondary outcomes – morbidity and mortality

Morbidity was reported according to the Clavien-Dindo (CD) classification.[12] Major morbidity was defined as CD ≥ 3a. Mortality rates were reported as the number of patients who died within 90 post-operative days.

Posthepatectomy haemorrhage, bile leakage, and liver failure were graded according to the International Study Group of Liver Surgery (ISGLS).[13-15]

Statistical analysis

IBM SPSS for Windows Version 28.0 (IBM Corp., Armonk, NY, USA) was used for the statistical analysis. Percentages are reported to one decimal place. A P value ≤ 0.05 was considered statistically significant.

Categorical variables are displayed as numbers with percentages. The differences between categorical variables were tested using the chi-square or Fisher-Freeman Halton test when more than two categories were present. Continuous variables were expressed as medians (minimum-maximum, interquartile range) and analysed with the Mann-Whitney test since the distribution analysis showed the non-normal distribution of data.

Survival data for median OS and RFS are presented as Kaplan-Meier curves, and groups were compared by a log-rank test. The results are expressed in months as the median (95% confidence interval (95% CI)). Survival tables were used for 3- and 5-year OS and RFS, given in percentages.

TABLE 1. Clinical characteristics and perioperative outcomes of the 166 patients

Clinical characteristics	OSH (n=151)	TSH (n=15)	P value
Male sex [a]	109 (72.2%)	13 (86.7%)	0.365
Age (years) [b]	62 (34–84; 14)	64 (45–75; 12)	0.819
ASA score ≥ 3 [a]	32 (21.2%)	2 (13.3%)	0.701
Primary tumour location [c]			
Right colon	27 (17.9%)	1 (6.7%)	0.166
Left colon	61 (40.4%)	6 (40.0%)	
Rectum	61 (40.4%)	7 (46.7%)	
> 1 primary tumour	2 (1.3%)	1 (6.7%)	
Primary tumour nodal invasion [a]	99 (66.0%)	10 (66.7%)	1.000
Synchronous liver metastases [a]	81 (53.6%)	11 (73.3%)	0.179
Number of liver metastases [b]	3 (1–19; 3)	5 (2–12; 6)	**0.001**
Size of liver metastases (cm) [b]	4 (0.6–20; 3)	5 (1.5–11; 5.5)	0.183
Neoadjuvant chemotherapy [a]	79 (52.3%)	13 (86.7%)	**0.013**
Preoperative CEA level (ng/mL) [b]	14 (1–1359; 47.5)	12 (2–1312; 60)	0.464
Extrahepatic disease [a]	27 (17.9%)	3 (20.0%)	1.000
Clinical risk score 3–5 [a]	92 (60.9%)	10 (66.7%)	0.875
Major liver resection [a]	**58 (38.4%)**	**15 (100%)**	**<0.001**
Atypical resection	29 (19.2%)	0 (0.0%)	/
Segmentectomy/segmentectomy & atypical resection	3 (2.0%)/14 (9.3%)	0 (0.0%)	/
Bisegmentectomy/bisegmentectomy & atypical resection	10 (6.6%)/37 (24.5%)	0 (0.0%)	/
Right/extended right hepatectomy	28 (18.5%)/6 (4.0%)	13 (86.7%)/2 (13.3%)	/
Left/extended left hepatectomy	6 (4.0%)/3 (2.0%)	0 (0.0%)	/
Trisegmentectomy	6 (4.0%)	0 (0.0%)	/
Trisegmentectomy & atypical resection	5 (3.3%)	0 (0.0%)	/
Central resection	4 (2.6%)	0 (0.0%)	/
R0 resection [a]	118 (78.1%)	10 (66.7%)	0.492
CD ≥ 3a [a]	31 (20.5%)	6 (40.0%)	0.161
90-day mortality [a]	7 (4.6%)	2 (13.3%)	0.189
ISGLS haemorrhage grade C [a]	2 (1.3%)	0 (0.0%)	1.000
ISGLS bile leakage grade C [a]	5 (3.3%)	1 (6.7%)	1.000
ISGLS liver failure – any grade [a]	40 (26.5%)	12 (80.0%)	**<0.001**
Grade A [a]	16 (10.6%)	5 (33.3%)	**0.034**
Grade B [a]	19 (12.6%)	6 (40.0%)	**0.014**
Grade C [a]	5 (3.3%)	1 (6.7%)	1.000
Hospital stay (days) [b]	10 (5–63; 7)	14 (8–158; 11)	**0.028**

[a] Categorical variable reported as n (%), chi-square test; [b] continuous variable, non-normal distribution, reported as median (minimum-maximum, interquartile range), Mann-Whitney test; [c] categorical variable with more than two groups, reported as n (%), Fisher-Freeman-Halton test;

ASA = American Society of Anaesthesiologists; CEA = carcinoembryonic antigen; CD = Clavien-Dindo classification; ISGLS = International Study Group of Liver Surgery; OSH = one-stage hepatectomy; TSH = two-stage hepatectomy

Case-control matching was performed for 15 patients from the TSH group.[16] Patients from the OSH group (controls) were selected based on the variables that were statistically significant in a bivariate analysis. The sampling was performed without replacement and with maximising execu-

TABLE 2. Clinical characteristics of the matched groups

Clinical characteristics	CCM-OSH (n = 14)	TSH (n = 15)	P value
Male sex [a]	11(78.6%)	13(86.7%)	1.000
Age (years) [b]	60 (53–78; 13)	64 (45–75; 12)	0.463
ASA score ≥ 3 [a]	2 (14.3%)	2 (13.3%)	1.000
Primary tumour in right colon [a]	2 (14.3%)	1 (6.7%)	1.000
Primary tumour in left colon [a]	10 (71.4%)	6 (40%)	0.125
Primary tumour in rectum [a]	2 (14.3%)	7 (46.7%)	0.063
> 1 primary tumour [a]	0 (0.0%)	1 (6.7%)	1.000
Primary tumour nodal invasion [a]	10 (71.4%)	10 (66.7%)	1.000
Synchronous liver metastases [a]	11(78.6%)	11(73.3%)	1.000
Number of liver metastases [b]	5 (2–12; 6)	5 (2–12; 6)	0.317
Size of liver metastases (cm) [b]	4.6 (1–20; 7)	5 (1.5–11; 5.5)	0.463
Neoadjuvant chemotherapy [a]	13 (92.9%)	13 (86.7%)	1.000
Preoperative CEA level (ng/mL) [b]	9 (1–261; 76)	12 (2–1312; 60)	0.975
Extrahepatic disease [a]	1 (7.1%)	3 (20.0%)	1.000
Clinical risk score 3–5 [a]	13 (92.9%)	10 (66.7%)	0.250
Major hepatectomy [a]	14(100%)	15 (100%)	1.000
Right/extended right hepatectomy	8 (57.1%)/2 (14.3%)	13 (86.7%)/2 (13%)	/
Left hemihepatectomy	1 (7.1%)	0 (0.0%)	/
Trisegmentectomy & atypical resection	3 (21.4%)	0 (0.0%)	/
R0 resection [a]	8 (57.1%)	10 (66.7%)	1.000
CD ≥ 3a [a]	4 (28.6%)	6 (40.0%)	0.688
90-day mortality [a]	1 (7.1%)	2 (13.3%)	1.000
ISGLS haemorrhage grade C [a]	0 (0.0%)	0 (0.0%)	1.000
ISGLS bile leakage grade C [a]	1 (7.1%)	1 (6.7%)	1.000
ISGLS liver failure – any grade [a]	10 (71.4%)	12 (80%)	1.000
Grade A [a]	4 (28.6%)	5 (33.3%)	1.000
Grade B [a]	5 (35,7%)	6 (40.0%)	1.000
Grade C [a]	1 (7.1%)	1 (6.7%)	1.000
Hospital stay (days) [b]	16 (6–63; 13)	14 (8–158; 11)	0.406

[a] Categorical variable reported as n (%), McNemar test; [b] continuous variable, nonnormal distribution, reported as the median (minimum-maximum, interquartile range), Wilcoxon signed ranks test

ASA = American Society of Anaesthesiologists; CCM-OSH = case-control matching one-stage hepatectomy; CEA = carcinoembryonic antigen; CD = Clavien-Dindo classification; ISGLS = International Study Group of Liver Surgery; TSH = two-stage hepatectomy

tion performance modality. Matched patients were assigned to the case-control matching-OSH group. The statistical analysis of continuous variables was performed with the Wilcoxon signed ranks test. The analysis of categorical variables was performed with the McNemar test.[16] Survival was estimated as described previously.

Results

The study population was stratified into two groups. The study group TSH consisted of 15 patients who completed TSH. The control group OSH included 151 patients. The study flowchart is shown in Figure 1.

TABLE 3. Survival analysis

	Overall	OSH (n = 151)	TSH (n = 15)	P value
Median OS (months) [95% CI]	35 [30–40]	35 [31–39]	21 [17–25]	0.063
3-year OS	48%	49%	33%	0.107
5-year OS	26%	27%	13%	0.107
RFS (months) [95% CI]	11 [8–14]	11 [9–13]	5 [2–8]	0.138
3-year RFS	14%	15%	13%	0.070
5-year RFS	10%	10%	7%	0.070
After case-control matching				
	Overall	**CCM-OSH (N=14)**	**TSH (N=15)**	**P value**
Median OS (months) [95% CI]	23 [19–27]	23 [5–41]	21 [17.0–25.0]	0.575
3-year OS	34%	36%	33%	0.743
5-year OS	17%	21%	13%	0.743
RFS (months) [95% CI]	7 [4–10]	8 [1–15]	5 [2–8]	0.888
3-year RFS	14%	14%	13%	0.498
5-year RFS	3%	0%	7%	0.498

CI = confidence interval; CCM = case-control matching; OS = overall survival; OSH = one-stage hepatectomy; RFS = recurrence-free survival; TSH = two-stage hepatectomy

Clinical characteristics of patients

This study included 166 patients: 151 in the OSH group and 15 in the TSH group. Their clinical characteristics and perioperative outcomes are summarised in Table 1.

Case-control matching

To reduce the bias and equilibrate the number of group members, case-control matching was conducted. Patients from the OSH group (controls) were selected based on the predictors that were statistically significant in bivariate analysis (Table 1): number of liver metastases, neoadjuvant chemotherapy, and extent of liver resection.

Case-control matching returned 14 controls among the OSH group, annotated as case-control matching-OSH. All three variables were statistically significant in the case-control matching model ($P < 0.001$). The Wilcoxon signed ranks test for the median of differences between before and after matching was insignificant ($P = 0.317$).

Analyses after case-control matching

After case-control matching, the TSH and OSH groups were compared (Table 2).

Morbidity and mortality

Perioperative morbidity and 90-day mortality rates are provided in Table 1 and Table 2.

In the OSH group, seven (4.6%) patients died postoperatively. The causes of death were sepsis

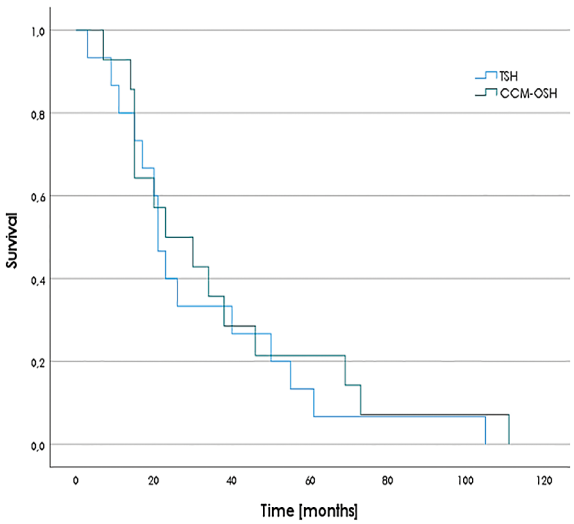

FIGURE 2. Overall survival after case-control matching (TSH *vs.* case-control matching-OSH groups), P = 0.575.

CCM-OSH = case-control matching one-stage hepatectomy; TSH = two-stage hepatectomy

TABLE 4. Literature review of surgical outcomes and survival after two-stage hepatectomy for colorectal liver metastases

Authors	Year	Study period	N of patients	Major liver resection (%)	R0 resection (%)	Morbidity (%)	Mortality (%)	Median follow-up (months)	Median RFS (months)	3-y RFS (%)	5-y RFS (%)	Median OS (months)	3-y OS (%)	5-y OS (%)
Adam *et al.*, France[4]	2000	1992–1999	13	62	NR	45	15	22	NR	31	31	44	35	NR
Tanaka *et al.*, Japan[17]	2007	1992–2004	22	67	87	23	0	NR	NR	6	NR	NR	33	NR
Wicherts *et al.*, France[24]	2008	1992–2007	41	76	NR	59	7	24	NR	26	13	39	60	42
Narita *et al.*, France[25]	2011	1996–2009	61	95	NR	54	0	30	NR	15	8	40	59	32
Turrini *et al.*, France[26]	2012	2000–2010	34	91	100	20	6	41	NR	24	14	44	59	35
Omichi *et al.*, Japan[27]	2022	2013–2019	32	NR	78	22	0	17	6	NR	NR	41	61	NR
The present study, Slovenia	2023	2000–2020	15	100	67	40	13	174	7	13	7	21	33	13
Multicentre studies														
Tsai *et al.*, USA and Portugal[28]	2010	1994–2008	35	80	NR	26	5	NR	NR	NR	NR	16	58	NR
Regimbeau *et al.* LiverMetSurvey registry[5]	2017	2000–2014	625	NR	58	25	9	84[a]	41[a]	43	23	40a	45	23
Petrowsky *et al.* ALPPS registry[29]	2020	2009–2019	510	100	73	21	5	38	11	19	12	37	52	27
Chavez *et al.* Five centres in the USA[22]	2021	2000–2016	196	76	92	23	5	28	NR	19	18	50	64	44

[a] = mean

ALPPS = associating liver partition and portal vein ligation for staged hepatectomy; N = number; NR = not reported; OS = overall survival; RFS = recurrence-free survival; USA = United States of America

(n = 1), cardiorespiratory failure (n = 1), multiorgan failure (n = 3), and posthepatectomy liver failure (n = 2). In the TSH group, two (13.3%) patients died postoperatively. One patient suffered from colonic perforation, was reoperated on several times, and died of multiorgan failure. The second patient died of cardiorespiratory failure after acute myocardial infarction. In the case-control matching-OSH group, the patient (7.1%) died of posthepatectomy liver failure.

Survival analysis

Patients were followed until their death or until 31 December 2022. The median follow-up was 174 (95% CI 113–235) months. A summary of the survival analysis is provided in Table 3 and Figure 2.

The RFS, median OS, and 3- and 5-year survival rates were 5 months, 21 months, 33% and 13% in the TSH group; 11 months, 35 months, 49% and 27% in the OSH group; and 8 months, 23 months, 36% and 21% in the case-control matching-OSH group, respectively.

Discussion

The main finding of our research is that the TSH group had a similar survival to that of the case-control matching-OSH group (median OS: 21 *vs.* 23 months), while the major morbidity rate was lower in the case-control matching-OSH group (40% *vs.* 28.6%).

The first TSH was performed on the proposition that a liver resection where some tumour tissue remains in place could be justified if it could be removed by second liver resection.[4] The time during surgeries was intended for liver hypertrophy, which was enhanced by portal vein embolization or portal vein ligation.[4,17]

Our first TSH was performed in 2005, and 23 patients with the most difficult patterns of colorectal liver metastases were allocated for this demanding treatment (Figure 1).[18-20] Only 15 patients who finished both stages were eligible for this study. This figure is among the lowest, especially compared to the most recent multicentre studies, but close to those in earlier studies.[2] Regimbeau *et al.*

and Chavez *et al*. published large multicentre studies.[5,22] Their study periods overlap with previous analyses from included centres, as shown in some reviews (Table 4).[21,23]

The diversity of first-step procedures challenges further analysis.[30] Nevertheless, this research adheres to the criteria by Regimbeau *et al*.[5] except for one case of completed ALPPS.

The clinical characteristics of patients in the OSH and TSH groups differed only in the median number of colorectal liver metastases (3 *vs*. 5) and the rate of chemotherapy treatment (52.3% *vs*. 86.7%). Both characteristics denote an extensive tumour burden in the TSH group.[27]

The concept of parenchyma-sparing liver surgery for colorectal liver metastases was established approximately 30 years ago.[7] This explains the large group of one-stage hepatectomies (n = 151), even in the case of bilateral colorectal liver metastases, and the lower rate of major hepatectomies in this group (38.4%) (Tables 1 and 2). In the TSH group, the rate of major hepatectomies was 100%, and the difference from the OSH group was statistically significant. The reported rates of major liver resections are given in Table 4.

There was a significant difference in posthepatectomy liver failure when comparing the TSH (80%) and OSH groups (26.5%) (P < 0.001) (Table 1). However, this difference disappeared after case-control matching because the matched group was selected based on neoadjuvant chemotherapy, the extent of liver resection and the number of liver metastases. In the case-control matching-OSH group, 71% of patients had any grade of posthepatectomy liver failure (Table 2), and one patient died of it. However, the reported rates of posthepatectomy liver failure are from 2.6 to 16%.[5,25,27-28] This wide range may also be due to several definitions of it.[31] The most commonly used definitions were the following: peak bilirubin > 7 mg/dL[32], the "50-50" criteria (50% of normal for the prothrombin index and 50 μmol/L for bilirubin on postoperative day 5)[33], and the definition by the ISGLS used in this study.[14]

The high rate of major morbidity (40% in the TSH group) reflects the burden of demanding two-stage procedures. On the other hand, 4 (28.6%) patients suffered from major morbidity in the case-control matching-OSH group, and the difference between these two groups was statistically insignificant (P = 0.688). The 90-day mortality in our TSH group (13%) did not exceed the reported 15% (Table 4).

TSH aims to improve the survival of patients by resecting all tumoral tissue and enabling sufficient future liver remnant. Our last TSH was performed in 2016, a year before Torzilli *et al*. published results of enhanced OSH as a safe alternative to TSH for multiple bilateral deep-located colorectal liver metastases.[34]

The prognosis was thought to depend on the size and number of colorectal liver metastases.[2] Whether the resection of colorectal liver metastases could achieve R0, survival was the same regardless of the number of lesions.[2] However, Fong *et al*. showed that the prognosis depends on the combination of survival factors, i.e., Clinical Risk Score.[9]

There was no significant difference (P = 0.063) in the median OS between the OSH (35 months) and TSH groups (21 months). The rate of R0 resections and the high Clinical Risk Score did not differ. After case-control matching, the OS in the case-control matching-OSH group was 23 months. However, the median OS in recent reports is longer (37–50 months) (Table 4).

Our study showed an insignificant difference in the 3-year RFS between the TSH group (13%) and the case-control matching-OSH group (14%). The 3-year RFS in our study was similar to that reported by Narita *et al*. and Chavez *et al*., but much shorter than the 43% reported by Regimbeau *et al*. (Table 4).[5,22,25]

Limitations of our study could explain these differences in survival. First, this was a single-institution, retrospective study covering a wide period. We had a small group of patients who underwent TSH. Furthermore, the operative technique and use of portal vein embolization have changed over time; thus, it is difficult to apply this study to other modern scenarios. In addition, the interpretation of data and their comparison to other reports was difficult because the TSH group consisted of various first-stage procedures.

To conclude, parenchyma-sparing surgery is a principle of liver surgery for colorectal liver metastases. TSH used to be a safe and favourable therapeutic choice in a select population of patients because it could prevent posthepatectomy liver failure and enable good oncological results. Now, OSH should be preferred whenever feasible because it has lower morbidity and equivalent oncological outcomes as completed TSH.

Acknowledgements

The University Medical Centre Maribor funded this study but had no role in its design, practice, or analysis.

References

1. Morgan E, Arnold M, Gini A, Lorenzoni V, Cabasag CJ, Laversanne M, et al. Global burden of colorectal cancer in 2020 and 2040: incidence and mortality estimates from GLOBOCAN. *Gut* 2023; **72:** 338-44. doi: 10.1136/gutjnl-2022-327736
2. Kow AWC. Hepatic metastasis from colorectal cancer. *J Gastrointest Oncol* 2019; **10:** 1274-98. doi: 10.21037/jgo.2019.08.06
3. Müller PC, Linecker M, Kirimker EO, Oberkofler CE, Clavien PA, Balci D, et al. Induction of liver hypertrophy for extended liver surgery and partial liver transplantation: state of the art of parenchyma augmentation-assisted liver surgery. *Langenbecks Arch Surg* 2021; **406:** 2201-15. doi: 10.1007/s00423-021-02148-2
4. Adam R, Laurent A, Azoulay D, Castaing D, Bismuth H. Two-stage hepatectomy: a planned strategy to treat irresectable liver tumors. *Ann Surg* 2000; **232:** 777-85. doi: 10.1097/00000658-200012000-00006
5. Regimbeau JM, Cosse C, Kaiser G, Hubert C, Laurent C, Lapointe R, et al. Feasibility, safety and efficacy of two-stage hepatectomy for bilobar liver metastases of colorectal cancer: a LiverMetSurvey analysis. *HPB* 2017; **19:** 396-405. doi: 10.1016/j.hpb.2017.01.008
6. Doyle DJ, Hendrix JM, Garmon EH. *American Society of Anesthesiologists Classification*. 2022. In: StatPearls [Internet]. Treasure Island (FL): StatPearls Publishing LLC. [cited 2923 Feb 15]. PMID: 28722969. Available at: https://www.ncbi.nlm.nih.gov/books/NBK441940/
7. Torzilli G, Vigano L, Gatti A, Costa G, Cimino M, Procopio F, et al. Twelve-year experience of "radical but conservative" liver surgery for colorectal metastases: impact on surgical practice and oncologic efficacy. *HPB (Oxford)* 2017; **19:** 775-84. doi: 10.1016/j.hpb.2017.05.006
8. Strasberg SM, Belghiti J, Clavien PA, Gadzijev E, Garden JO, Lau WY, et al. The Brisbane 2000 terminology of liver anatomy and resections. *HPB (Oxford)* 2000; **2:** 333-39. doi: 10.1016/s1365-182x(17)30755-4
9. Fong Y, Fortner J, Sun RL, Brennan MF, Blumgart LH. Clinical score for predicting recurrence after hepatic resection for metastatic colorectal cancer: analysis of 1001 consecutive cases. *Ann Surg* 1999; **230:** 309-18; discussion 18-21. doi: 10.1097/00000658-199909000-00004
10. Broering DC, Hillert C, Krupski G, Fischer L, Mueller L, Achilles EG, et al. Portal vein embolization vs. portal vein ligation for induction of hypertrophy of the future liver remnant. *J Gastrointest Surg* 2002; **6:** 905-13; discussion 13. doi: 10.1016/s1091-255x(02)00122-1
11. Schnitzbauer AA, Lang SA, Goessmann H, Nadalin S, Baumgart J, Farkas SA, et al. Right portal vein ligation combined with in situ splitting induces rapid left lateral liver lobe hypertrophy enabling 2-staged extended right hepatic resection in small-for-size settings. *Ann Surg* 2012; **255:** 405-14. doi: 10.1097/SLA.0b013e31824856f5
12. Clavien PA, Barkun J, de Oliveira ML, Vauthey JN, Dindo D, Schulick RD, et al. The Clavien-Dindo classification of surgical complications: five-year experience. *Ann Surg* 2009; **250:** 187-96. doi: 10.1097/SLA.0b013e3181b13ca2
13. Rahbari NN, Garden OJ, Padbury R, Maddern G, Koch M, Hugh TJ, et al. Post-hepatectomy haemorrhage: a definition and grading by the International Study Group of Liver Surgery (ISGLS). *HPB (Oxford)* 2011; **13:** 528-35. doi: 10.1111/j.1477-2574.2011.00319.x
14. Rahbari NN, Garden OJ, Padbury R, Brooke-Smith M, Crawford M, Adam R, et al. Posthepatectomy liver failure: a definition and grading by the International Study Group of Liver Surgery (ISGLS). *Surgery* 2011; **149:** 713-24. doi: 10.1016/j.surg.2010.10.001
15. Koch M, Garden OJ, Padbury R, Rahbari NN, Adam R, Capussotti L, et al. Bile leakage after hepatobiliary and pancreatic surgery: a definition and grading of severity by the International Study Group of Liver Surgery. *Surgery* 2011; **149:** 680-8. doi: 10.1016/j.surg.2010.12.002
16. Pearce N. Analysis of matched case-control studies. *BMJ* 2016; **352:** i969. doi: 10.1136/bmj.i969
17. Tanaka K, Shimada H, Matsuo K, Ueda M, Endo I, Togo S. Remnant liver regeneration after two-stage hepatectomy for multiple bilobar colorectal metastases. *Eur J Surg Oncol* 2007; **33:** 329-35. doi: 10.1016/j.ejso.2006.10.038
18. Plahuta I, Magdalenić T, Turk Š, Potrč S, Ivanecz A. Achievements in surgical treatment for colorectal liver metastases from 2000 until 2020. *AMB Acta Medico-Biotechnica* 2022; **15:** 41-53. doi: 10.18690/actabiomed.231
19. Turk Š, Plahuta I, Magdalenić T, Mavc Ž, Ivanecz A. [How can we prevent liver failure after extensive resections of colorectal liver metastases]? [Slovenian]. [Internet]. *Gastroenterolog* 2022; **26:** 37-47. [cited 2023 Feb 16]. Available at: https://dk.um.si/IzpisGradiva.php?lang=slv&id=83727
20. Ivanecz A, Krebs B, Stozer A, Jagric T, Plahuta I, Potrc S. Simultaneous pure laparoscopic resection of primary colorectal cancer and synchronous liver metastases: a single institution experience with propensity score matching analysis. *Radiol Oncol* 2018; **52:** 42-53. doi: 10.1515/raon-2017-0047
21. Lam VW, Laurence JM, Johnston E, Hollands MJ, Pleass HC, Richardson AJ. A systematic review of two-stage hepatectomy in patients with initially unresectable colorectal liver metastases. *HPB (Oxford)* 2013; **15:** 483-91. doi: 10.1111/j.1477-2574.2012.00607.x
22. Chavez MI, Gholami S, Kim BJ, Margonis GA, Ethun CG, Tsai S, et al. Two-stage hepatectomy for bilateral colorectal liver metastases: a multi-institutional analysis. *Ann Surg Oncol* 2021; **28:** 1457-65. doi: 10.1245/s10434-020-09459-6
23. Vauthey JN, Kawaguchi Y, Adam R. *Colorectal liver metastasis*. 1st edition. Cham (CH): Springer; 2022.
24. Wicherts DA, Miller R, de Haas RJ, Bitsakou G, Vibert E, Veilhan LA, et al. Long-term results of two-stage hepatectomy for irresectable colorectal cancer liver metastases. *Ann Surg* 2008; **248:** 994-1005. doi: 10.1097/SLA.0b013e3181907fd9
25. Narita M, Oussoultzoglou E, Jaeck D, Fuchschuber P, Rosso E, Pessaux P, et al. Two-stage hepatectomy for multiple bilobar colorectal liver metastases. *Br J Surg* 2011; **98:** 1463-75. doi: 10.1002/bjs.7580
26. Turrini O, Ewald J, Viret F, Sarran A, Goncalves A, Delpero JR. Two-stage hepatectomy: who will not jump over the second hurdle? *Eur J Surg Oncol* 2012; **38:** 266-73. doi: 10.1016/j.ejso.2011.12.009
27. Omichi K, Inoue Y, Mise Y, Oba A, Ono Y, Sato T, et al. Hepatectomy with perioperative chemotherapy for multiple colorectal liver metastases is the available option for prolonged survival. *Ann Surg Oncol* 2022; **29:** 3567-76. doi: 10.1245/s10434-022-11345-2.
28. Tsai S, Marques HP, de Jong MC, Mira P, Ribeiro V, Choti MA, et al. Two-stage strategy for patients with extensive bilateral colorectal liver metastases. *HPB (Oxford)* 2010; **12:** 262-9. doi: 10.1111/j.1477-2574.2010.00161.x
29. Petrowsky H, Linecker M, Raptis DA, Kuemmerli C, Fritsch R, Kirimker OE, et al. First long-term oncologic results of the ALPPS procedure in a large cohort of patients with colorectal liver metastases. *Ann Surg* 2020; **272:** 793-800. doi: 10.1097/sla.0000000000004330
30. Baumgart J, Jungmann F, Bartsch F, Kloth M, Mittler J, Heinrich S, et al. Two-stage hepatectomy and ALPPS for advanced bilateral liver metastases: a tailored approach balancing risk and outcome. *J Gastrointest Surg* 2019; **23:** 2391-400. doi: 10.1007/s11605-019-04145-9
31. Joechle K, Goumard C, Vega EA, Okuno M, Chun YS, Tzeng CD, et al. Long-term survival after post-hepatectomy liver failure for colorectal liver metastases. *HPB (Oxford)* 2019; **21:** 361-69. doi: 10.1016/j.hpb.2018.07.019
32. Mullen JT, Ribero D, Reddy SK, Donadon M, Zorzi D, Gautam S, et al. Hepatic insufficiency and mortality in 1,059 noncirrhotic patients undergoing major hepatectomy. *J Am Coll Surg* 2007; **204:** 854-62; discussion 62-4. doi: 10.1016/j.jamcollsurg.2006.12.032
33. Balzan S, Belghiti J, Farges O, Ogata S, Sauvanet A, Delefosse D, et al. The "50-50 criteria" on postoperative day 5: an accurate predictor of liver failure and death after hepatectomy. *Ann Surg* 2005; **242:** 824-8, discussion 28-9. doi: 10.1097/01.sla.0000189131.90876.9e
34. Torzilli G, Viganò L, Cimino M, Imai K, Vibert E, Donadon M, et al. Is Enhanced one-stage hepatectomy a safe and feasible alternative to the two-stage hepatectomy in the setting of multiple bilobar colorectal liver metastases? A comparative analysis between two pioneering centers. *Dig Surg* 2018; **35:** 323-32. doi: 10.1159/000486210

Radiol Oncol 2023; 57(2): 141-149.
doi: 10.2478/raon-2023-0029

Elektrosklerotherapija z bleomicinom (BEST) za zdravljenje žilnih malformacij. Poročilo študijske skupine Mednarodne mreže za izmenjavo praks o elektrokemoterapiji (InspECT)

Muir T, Bertino G, Groselj A, Ratnam L, Kis E, Odili J, McCafferty I, Wohlgemuth WA, Cemazar M, Krt A, Bosnjak M, Zanasi A, Battista M, de Terlizzi F, Campana LG, Sersa G

Izhodišča. Biomedicinske aplikacije elektroporacije širimo s področja onkologije na področja cepljenja, zdravljenja aritmij in tudi na zdravljenja žilnih malformacij. Bleomicin široko uporabljamo kot sklerotizirajoče sredstvo pri zdravljenju različnih žilnih malformacij. Uporaba električnih pulzov ob hkratni uporabi bleomicina poveča učinkovitost zdravila, kar dokazuje elektrokemoterapija z bleomicinom pri zdravljenju tumorjev. Enak princip upoštevamo pri elektrosklerotherapiji z bleomicinom (*angl. bleomycin electrosclerotherapy*, BEST). Zdi se, da ta način omogoča učinkovito zdravljenje žilnih malformacij z nizkim pretokom (venskim in limfnim) in morda celo malformacij z visokim pretokom (arteriovenskim). Čeprav je bilo do zdaj objavljenih le nekaj poročil, se kirurška stroka zanj zanima in vse več centrov uporablja metodo BEST pri zdravljenju žilnih malformacij. V okviru konzorcija Mednarodne mreže za izmenjavo praks o elektrokemoterapiji (*angl. International Network for Sharing Practices on Electrochemotherapy,* InspECT) je bila ustanovljena posebna delovna skupina za razvoj standardnih operativnih postopkov za BEST in spodbujanje kliničnih preizkušanj.

Zaključki. S standardizacijo zdravljenja in uspešnim zaključkom kliničnih preskušanj, ki dokazujejo učinkovitost in varnost pristopa, je mogoče doseči kakovostnejše rezultate in klinični izhod bolezni.

Radiol Oncol 2023; 57(2): 150-157.
doi: 10.2478/raon-2023-0021

Korelacija srednjega difuzijskega koeficienta (ADC) in vrednost maksimalnega standardiziranega privzema (SUVmax) pri difuzijsko obteženem magnetno resonančnem slikanju (MRI) in 18F-FDG-PET/CT pri otrocih z Hodgkinovim limfomom. Raziskava izvedljivosti

Rosbach N, Fischer S, Koch V, Vogl TJ, Bochennek K, Lehrnbecher T, Mahmoudi S, Grünewald L, Grünwald F, Bernatz S

Izhodišča. Želeli smo ugotoviti, ali lahko slikanje z magnetno resonanco (MRI) deluje kot nadomestna diagnostična metoda, pri kateri bolnik ni izpostavljen sevanju. glede na (18)F-fluorodeoksiglukozo (FDG) pozitronsko emisijsko tomografijo/računalniško tomografijo (PET/CT) pri otrocih s histološko potrjenim Hodgkinovim limfomom (HL) pred zdravljenjem. Analizirali smo potencialno korelacijo med difuzijskim koeficientom (*angl. apparent diffusion coefficient*, ADC) pri MRI in največjo standardizirano vrednostjo privzema (SUVmax) pri FDG-PET/CT.

Bolniki in metode. Retrospektivno smo analizirali 17 bolnikov s histološko potrjenim HL (6 žensk, 11 moških; srednja starost 16 let, razpon: 12–20 let). Bolnikom smo pred začetkom zdravljenja naredili preiskavi s MRI in PET/CT z (18)F-FDG. Zbrali smo podatke slikanja z F-FDG PET/CT in korelacijske zemljevide ADC pri MRI. Za vsako HL-lezijo sta dva neodvisna ocenjevalca določila vrednost SUVmax in korelacijsko povprečje ADC.

Rezultati. Pri 17 bolnikih smo ugotovili skupno 72 lezij HL in med moškimi in ženskami ni bilo pomembne razlike v številu lezij (srednja vrednost pri moških 15, razpon 12–19 let; pri ženskah 17, razpon: 12–18 let; p = 0,021). Povprečen razmik med MRI in PET/CT preiskavo je bil 5,9 ± 5,3 dni. Ujemanje med ocenjevalci, ocenjeno s korelacijskim koeficientom znotraj razreda (*angl. intraclass correlation coefficient*, ICC), je bilo odlično (ICC = 0,98; 95 % interval zaupanja [CI]: 0,97–0,99). Korelirani SUVmax in srednji ADC vseh 17 bolnikov (ROI n = 72) sta pokazala močno negativno korelacijo -0,75 (95 % CI: -0,84, -0,63; p = 0,001). Analiza je pokazala razliko v korelaciji ocenjevanih področij. Korelirani SUVmax in srednji ADC sta pokazala močno korelacijo pri pregledih vratu in prsnega koša (vrat: -0,83, 95 % CI: -0,93, – -0,63; p < 0,0001; prsni koš: -0,82, 95 % CI: -0,91, – -0,64 , p < 0,0001) in dobro korelacijo pri abdominalnih pregledih -0,62 (95 % CI: -0,83, -0,28; p = 0,001).

Zaključki. SUVmax in srednji ADC sta pokazala močno negativno korelacijo pri pediatričnih lezijah HL. Ocena lezij se je zdela trdna. Rezultati kažejo, da lahko zemljevidi ADC in srednji ADC nadomestijo PET/CT pri analizi aktivnosti bolezni pri pediatričnih bolnikih s HL. To bi lahko zmanjšalo število preiskav PET/CT in zmanjšalo izpostavljenost otrok sevanju.

Radiol Oncol 2023; 57(2): 158-167.
doi: 10.2478/raon-2023-0024

Biopsija neopredeljenih sumljivih intrahepatičnih lezij z računalniškotomografskim vodenjem. Označevanje z lipiodolom pred posegom izboljša uspešnost biopsije

Langenbach MC, Vogl TJ, Buchinger A, Eichler K, Scholtz JE, Hammerstingl R, Gruber-Rouh T

Izhodišča. Jetrne biopsije, vodene z računalniško tomografijo (CT), običajno izvajamo brez uporabe kontrastnega sredstva (KS). Uporaba KS pa je koristna predvsem pri zahtevnih vbodnih poteh in zahtevnih lokacijah lezij. Namen raziskave je bil oceniti natančnost CT vodenih biopsij jetrnih lezij brez uporabe KS, z uporabo intravenskega KS ali pa z označenjem lezij z intraarterijsko aplikacijo lipiodola.

Bolniki in metode. Retrospektivno smo ovrednotili 607 bolnikov (358 moških [59,0 %]; povprečna starost 61 let; standardna deviacija [SD] ± 12,04) s suspektnimi jetrnimi lezijami, pri katerih smo izvedli CT vodeno biopsijo. Uspešne biopsije so bile tiste, pri katerih histološko nismo videli tipičnega jetrnega tkiva ali pa nespecifičnih jetrnih sprememb. Glede na način izvedbe CT vodene biopsije, smo bolnike razdelili v tri skupine in jih med seboj primerjali: skupina brez KS, skupina z lipiodolom in skupina z intravenskim KS. Ugotavljali smo tehnično uspešnost in tudi dejavnike, ki bi lahko vplivali na uspešnost biopsije ter zaplete. Rezultate smo analizirali z uporabo Wilcoxon-Man-Whitneyjevega t-testa, hi-kvadrat testa in testa Spearman-Rho.

Rezultati. Celokupni delež uspešnih biopsij je bil 73,1 %, Uspešnost pa je bila značilno pri lezijah, označenih z lipiodolom (79,3 %), v primerjavi s skupino brez KS (73,8 %) in skupino z intravenskem KS (65,2 %) ($p = 0,037$). Pri manjših lezijah (premer < 20 mm) je označevanje z lipiodolom še v večji meri izboljšalo uspešnost biopsij (71,2%) v primerjavi s skupino brez KS (65,5 %) in skupino z intravenskim KS (47,7 %) ($p = 0,021$). Jetrna ciroza ($p = 0,94$) in etiologija lezij ($p = 0,78$) nista vplivala na stopnjo uspešnosti biopsij med skupinami. Med posegi ni prišlo do pomembnejših zapletov.

Zaključki. Označevanje sumljivih jetrnih lezij z lipiodolom pred biopsijo znatno poveča uspešnost biopsij in je še posebej koristno za biopsije manjših lezij s premerom manj kot 20 mm. Dodatno, pri lezijah, ki jih ne vidimo s CT-jem brez uporabe kontrasta, je označevanje z lipiodolom boljše kot uporaba intravenskega kontrasta. Entiteta tarčne lezije ne vpliva na stopnjo uspešnih biopsij.

Radiol Oncol 2023; 57(2): 168-177.
doi: 10.2478/raon-2023-0025

Radiološka ocena indeksa skeletne mišičnine in miosteatoze ter njun vpliv na pooperativne zaplete po presaditvi jeter

Petrič M, Jordan T, Karteek P, Ličen S, Trotovšek B, Tomažič A

Izhodišča. Presaditev jeter pri bolnikih z akutno ali kronično jetrno odpovedjo predstavlja možnost ozdravitve in izboljša kvaliteto življenja. Vpliv prehranskega status na pooperativni potek po presaditvi jeter še ni jasno določen. Z raziskavo smo skušali ugotoviti napovedno vrednost indeksov skeletne mišičnine in miosteatoze na rezultate zdravljenja s presaditvijo jeter.

Bolniki in metode. Retrospektivno smo zbrali podatke 138 polnoletnih bolnikov, ki so imeli prvo ortotopno presaditev jeter. Z analizo slik računalniške tomografije na nivoju tretjega ledvenega vretenca smo izračunali indeks skeletne mišičnine in miosteatoze. Analizirali smo njun vpliv na pooperativni potek po presaditvi jeter.

Rezultati. Nizke vrednosti indeksa skeletne mišičnine so bile prisotne pri 63 % moških in 28,9 % ženskih prejemnikov jeter. Miosteatoza je bila prisotna pri 45 (32,6 %) bolnikih. Moški prejemniki z visokim indeksom skeletne mišičnine so imeli daljšo ležalno dobo v enoti intenzivne terapije ($P < 0.025$) v primerjavi z nizkim indeksom. Indeks skeletne mišičnine pri ženskah pa ni imel vpliva na ležalno dobo v enoti intenzivne terapije ($P = 0,544$), prav tako ne prisotnost miosteatoze ne glede na spol ($P = 0,161$). Indeksa skeletne mišičnine in miosteatoza nista vplivala na čas hospitalizacije (moški, $P > 0,05$ ter ženske, $P = 0,843$), stopnjo pooperativnih zapletov (moški, $P = 0,883$ ter ženske, $P = 0,113$), okužb (moški, $P = 0,293$ ter ženske, $P = 0,285$; $P = 0,173$) in zavrnitve presadka (moški, $P = 0,875$ ter ženske, $P = 0,135$).

Zaključki. V pričujoči raziskavi indeksa skeletne mišičnine in miosteatoza nista imela vpliva na pooperativne zaplete po presaditvi jeter. Uporaba CT analize sestave telesa ter določitev specifičnih parametrov so ključni za pridobitev verodostojnih podatkov v prihodnosti.

Radiol Oncol 2023; 57(2): 178-183.
doi: 10.2478/raon-2023-0022

Vrednost koeficienta ADC kot biološkega označevalca zorenja možganovine ploda

Kobal L, Šurlan Popović K, Avsenik J, Vipotnik Vesnaver T

Izhodišča. Pri razvoju plodovih možganov ima pomembno vlogo mielinizacija, ki poteka v točno določenem zaporedju. Količina vode v možganih je sorazmerna z mielinizacijo – bolj kot so možgani mielinizirani, manjša je vsebnost vode v njih. Difuzijo vodnih molekul lahko kvantitativno ocenimo s pomočjo difuzijskega koeficienta (angl. apparent diffusion coefficient, ADC). Zanimalo nas je, ali lahko z določanjem vrednosti ADC kvantitativno ocenimo razvoj možganovine ploda.

Bolniki in metode. V retrospektivno raziskavo smo vključili 42 plodov gestacijske starosti med 25 in 35 tedni. Na sekvencah difuzijsko poudarjenega magnetnoresonančnega slikanja smo ročno izbrali 13 področij, v katerih smo izmerili vrednosti ADC. Statistično značilne razlike med vrednostmi ADC smo preverili s pomočjo enosmerne analize variance in Tukeyevim post hoc testom. Povezavo med vrednostmi ADC možganskih področij in gestacijsko starostjo plodov smo nato ocenili s pomočjo linearne regresije.

Rezultati. Povprečna gestacijska starost plodov je bila 29,8 ± 2,4 tednov. Vrednosti ADC v talamusih, ponsu in malih možganih so se statistično značilno razlikovale med seboj ter od vrednosti ADC v vseh preostalih možganskih področjih. V talamusih, ponsu in malih možganih je linearna regresija pokazala statistično značilen upad vrednosti ADC z naraščajočo gestacijsko starostjo. V raziskavi smo upoštevali stopnjo značilnosti $p = 0,05$.

Zaključki. Vrednosti ADC se z naraščanjem gestacijske starosti ploda spreminjajo, razlikujejo se tudi med različnimi možganskimi področji. V ponsu, malih možganih in talamusih je koeficient ADC uporaben biološki označevalec zorenja možganovine ploda, saj se vrednosti ADC z naraščanjem gestacijske starosti linearno znižujejo.

Radiol Oncol 2023; 57(2): 184-190.
doi: 10.2478/raon-2023-0020

Longitudinalno spremljanje difuzijskega koeficienta (ADC) pri bolnikih z rakom prostate, ki jih zdravimo z magnetnoresonančno vodeno radioterapijo na napravi MR-Linac z 1,5 T. Prospektivna raziskava izvedljivosti

Almansour H, Schick F, Nachbar M, Afat S, Fritz V, Thorwarth D, Zips D, Bertram F, Müller AC, Nikolaou K, Othman AE, Wegener D

Izhodišča. Hibridni magnetnoresonančni (MR) linearni pospeševalniki (*angl. linear accelerator,* MR-Linak) bi lahko omogočili individualno neposredno prilagajanje radioterapije (RT) z uporabo kvantitativnih sekvenc MR, kot je difuzijsko tehtano slikanje. Namen raziskave je bil proučiti dinamiko difuzijskega koeficienta (*angl. apparent diffusion coefficient*, ADC) lezij pri bolnikih z rakom prostate, pri katerih smo z 1,5 T obteženim MR-Linakom izvajali RT z MR vodenjem. Kot referenčni standard smo uporabili vrednosti ADC na diagnostičnem MR s 3T.

Bolniki in metode. V prospektivno raziskavo smo vključili bolnike z biopsijsko potrjenim rakom prostate, ki smo jim opravili preiskavo s 3 T obteženem MR, (MR3T), in preiskavo na 1,5 T obteženem MR-Linak (MRL) pred in med RT. Vrednosti ADC lezij sta izmerila radiolog in radioterapevt na rezini z največjo lezijo. Vrednosti ADC na obeh sistemih smo primerjali s pomočjo parnih t-testov. Izračunali smo Pearsonov korelacijski koeficient in soglasje med odčitovalcema.

Rezultati. Vključili smo 9 bolnikov, starih 67 ± 6 let (razpon od 60 do 67 let). Pri 7 bolnikih je bila rakava sprememba v perifernem območju, pri 2 bolnikih pa v prehodnem območju. Zanesljivost med odčitovalcema glede merjenja ADC lezije je bila odlična, s koeficientom znotraj razreda (*angl. intraclass correlation coefficient*, ICC) > 0,90 pred in med RT, tako navajamo rezultati prvega odčitovalca. Pri obeh sistemih je prišlo do statistično značilnega zvišanja ADC lezij med RT (povprečno MRL-ADC pred RT 0,97 ± 0,18 x 10–3 mm^2/s v primerjavi s MRL-ADC med RT 1,38 ± 0,3 x 10–3 mm^2/s, kar pomeni povprečno zvišanje ADC lezij za 0,41 ± 0,20 x 10–3 mm^2/s; p < 0,001). Povprečna vrednost MR3T-ADC pred RT je bila 0,78 ± 0,165 x 10–3 mm^2/s v primerjavi s povprečno vrednostjo MR3T-ADC med RT 0,99 ± 0,175 x 10–3 mm^2/s, kar pomeni povprečno povišanje ADC lezije za 0,21 ± 0,96 x 10–3 mm^2/s,;p < 0,001). Absolutne vrednosti ADC iz MRL so bile pred in med RT stalno pomembno višje od vrednosti iz MR3T (p < = 0,001). Kljub temu je bila med MRL-ADC in MR3T-ADC pred (r = 0,798, p = 0,01) in med RT (r = 0,863, p = 0,003) močna pozitivna korelacija.

Zaključki. ADC lezij, izmerjen na MRL, se je med RT znatno povečal, meritve ADC lezij na obeh sistemih pa so pokazale podobno dinamiko. To kaže, da bi ADC lezij, izmerjen na MRL, lahko uporabljali kot biološki označevalec za oceno odziva na zdravljenje. Nasprotno pa so absolutne vrednosti ADC, izračunane z algoritmom proizvajalca MRL, pokazale sistematična odstopanja od vrednosti, pridobljenih na diagnostičnem sistemu MR3T. Pričujoče preliminarne ugotovitve so obetavne, vendar jih je potrebno potrditi z večjo raziskavo. Po potrditvi, bi lahko ADC lezij na MRL uporabljali za oceno tumorskega odziva v realnem času pri bolnikih z rakom prostate, ki jih zdravimo z MR vodenim obsevanjem.

Radiol Oncol 2023; 57(2): 191-200.
doi: 10.2478/raon-2022-0052

Kraniotomija pri budnem bolniku med operativnim zdravljenjem možganskih gliomov. Izkušnje iz Univerzitetnega kliničnega centra Ljubljana

Žele T, Velnar T , Koritnik B, Bošnjak R, Markovič-Božič J

Izhodišča. Kraniotomija pri budnem bolniku (*ang. awake craniotomy*) je nevrokirurška tehnika, ki omogoča intraoperativno nevrofiziološko testiranje s sodelovanjem bolnika med odstranjevanjem možganskega tumorja v regionalni anesteziji. To omogoči prepoznavanje vitalno najpomembnejših (*i.e.* elokventnih) možganskih področij pri operaciji in zmanjša možnost njihove poškodbe. Namen raziskave je bil predstaviti izkušnje s kraniotomijo pri budnem bolniku med operativnim zdravljenjem gliomov v Univerzitetnem kliničnem centru Ljubljana od 2015 do 2019.

Bolniki in metode. Kandidati za kraniotomijo v budnem stanju so bili bolniki z glialnim tumorjem znotraj ali v bližini govornih možganskih področji, tumorjem v področju inzule in tumorjem znotraj ali v bližini primarne motorične skorje. Bolnike smo klinično ocenili pred in po operaciji.

Rezultati. V 5-letnem obdobju smo opravili 24 kraniotomij pri budnem bolniku (18 moških in 6 ženskih; povprečna starost 41 let). Njihovo sodelovanje med operacijo smo pri večini bolnikov ocenili kot »odlično«, stopnjo neugodja kot »blažje neugodje« in bolečino kot »zmerno«. Po operaciji smo opažali blago nevrološko poslabšanje pri 13 % bolnikov (3/24). Popolno resekcijo smo lahko naredili pri malignih gliomih v 60 % (6/10) pri nizkomalignih gliomih pa v 29 % (4/14). Primerjava predoperativnega in pooperativnega funkcionalnega stanja bolnika z lestvico po Karnovskem in kvalitete življenja z anketnim vprašalnikom kratke oblike 36 (*angl. Short-Form 36 health survey,* SF-36) je pokazala, da operacija ni pomembno negativno vplivala na telesno zmogljivost ali kakovost življenja bolnikov ($p > 0,05$).

Zaključki. Izkušnjah iz terciarnega centra kažejo, da je kraniotomija pri budnem pacientu izvedljiva in varna nevrokirurška tehnika. Izbira ustreznih bolnikov, natančno načrtovanje in predoperativna priprava ter timski pristop so ključni pri doseganju najboljšega poteka operacije in uspeha tovrstnega zdravljenja.

Radiol Oncol 2023; 57(2): 201-210.
doi: 10.2478/raon-2023-0009

Kognitivno funkcioniranje v kohorti bolnikov z visokomalignimi gliomi

Škufca Smrdel AC, Podlesek A, Skoblar Vidmar M, Markovič J, Jereb J, Kuzma Okorn M, Smrdel U

Izhodišča. Visoko maligni gliomi so povezani s kognitivnimi motnjami. V raziskavi smo želeli preučiti kognitivno funkcioniranje v kohorti bolnikov z malignimi gliomi, glede na stanje izocitratdehidrogenaze (IDH) in metil gvanin metil transferaze (MGMT) ter druge klinične značilnosti.

Bolniki in metode. V raziskavo smo vključili bolnike z visoko malignimi gliomi, zdravljenimi v opazovanem času. Pooperativno smo naredili nevropsihološko oceno in pri tem uporabili Slovenski test verbalnega učenja, Slovenski test črkovne fluentnosti, Test psihomotorične hitrosti (*angl. Trail Making Test, Part A and B*) ter samoocenjevalni vprašalnik. Rezultate smo analizirali kot vrednost 'z' (*angl. z-score*) in dihotomizirano glede na stanje IDH in MGMT. Razlike med skupinami smo proučevali z uporabo T-testa ter testov Mann-Whitney U, $\chi 2$ in Kendall's Tau.

Rezultati. Od 275 bolnikov v kohorti smo jih lahko vključili 90. Med njimi 46 % bolnikov ni bilo sposobnih sodelovati zaradi slabega stanja zmogljivosti ali dejavnikov, povezanih z boleznijo. Bolniki, kjer je bila prisotna mutacija IDH, so bili mlajši in bolj zmogljivi, imeli so več tumorjev gradusa III in več metilacij MGMT. V tej skupini je bilo kognitivno funkcioniranje statistično značilno boljše na področjih neposrednega verbalnega priklica, kratkoodloženega in dolgoodloženega priklica, kot tudi na področjih izvršilnih funkcij ter prepoznavanja. Glede na stanje MGMT pa razlik nismo našli. Tumorji gradusa III so bili povezani s pogostejšo metilacijo. Samoocena se je pokazala kot šibko orodje, povezano le z neposrednim priklicom.

Zaključki. Glede na stanje MGMT nismo našli razlik v kognitivnem funkcioniranju, je pa bilo boljše ob prisotnosti IDH mutacije. V naši kohorti bolnikov z visokomalignimi gliomi jih skoraj polovica ni bila sposobna sodelovanja in jih nismo vključili v raziskavo, kar kaže na veliko zastopanost prognostično ugodnejših bolnikov v raziskavah.

Radiol Oncol 2023; 57(2): 211-219.
doi: 10.2478/raon-2023-0019

Spremembe v kakovosti življenja pri bolnicah z zgodnjim rakom dojk in primerjava z normativno slovensko populacijo

Grašič Kuhar C, Gortnar Cepeda T, Kurzeder C, Vetter M

Izhodišča. Želeli smo proučiti spremembe v kakovosti življenja bolnic, zdravljenih zaradi raka dojk, in primerjati njihovo kakovost življenja z normativnimi podatki slovenske populacije.

Bolniki in metode. Izvedli smo prospektivno kohortno raziskavo. Vključili smo 102 bolnici z zgodnjim rakom dojk, ki smo jih zdravili na Onkološkem inštitutu Ljubljana s kemoterapijo. Eno leto po zaključeni kemoterapiji je izpolnilo vprašalnike 71 % vseh bolnic. Uporabili smo slovensko različico vprašalnikov EORTC QLQ C30 in BR23. Primarni cilj je bila primerjava globalnega zdravstvenega stanja/kakovosti življenja in skupnega rezultata C30 (*angl. C30-Summary Score*, C30-SumSc) pred kemoterapijo in eno leto po zaključeni kemoterapiji z normativno slovensko populacijo. V eksplorativni analizi smo proučili razlike v simptomih in funkcionalnih lestvicah QLQ C-30 in QLQ BR-23 med izhodiščnim stanjem in stanjem eno leto po koncu kemoterapije.

Rezultati. Izhodiščni C30-SumSc bolnic je bil za 2,6 točke (p = 0,04) nižji od predvidenega C30-SumSc populacije, po enem letu po zaključku kemoterapije je bil za 6,5 točke (p <0,001) nižji od predvidenega C30-SumSc populacije. Nasprotno pa se globalno zdravstveno stanje bolnic ni statistično razlikovalo od napovedi iz populacije niti izhodiščno niti po enem letu. Eksploratorna analiza je pokazala, da so imele bolnice eno leto po kemoterapiji v primerjavi z začetkom kemoterapije statistično značilne in klinično pomembne nižje ocene pri telesni podobi in kognitivnem funkcioniranju ter višje ocene simptomov za bolečino, utrujenost in simptome roke.

Zaključki. C30-SumSc je po enem letu po kemoterapiji znižan. Zgodnje intervencije je potrebno usmeriti v preprečevanje kognitivnega upada in telesne podobe ter v zmanjšanje utrujenosti, bolečine in simptomov roke.

Radiol Oncol 2023; 57(2): 220-228.
doi: 10.2478/raon-2023-0028

Pomen *PIK3CA* aktivirajočih mutacij za izhod bolezni in sistemsko zdravljenje operabilnega invazivnega lobularnega karcinoma dojke

Ribnikar D, Jerič Horvat V, Ratoša I, Veitch ZW, Grčar Kuzmanov B, Novaković S, Langerholc E, Amir E, Šeruga B

Izhodišča. Namen raziskave je bil ovrednotiti vpliv PIK3CA aktivirajočih mutacij za izhod bolezni in učinkovitost doponilnega endokrinega zdravljenja pri bolnicah z operabilnim invazivnim lobularnim karcinomom.

Bolniki in metode. V raziskavo smo vključili bolnice z zgodnjim invazivnim lobularnim karcinomom dojke, ki smo jih na Onkološkem inštitutu Ljubljana zdravili med leti 2003 in 2008. S pomočjo metode Kaplan-Meier smo izračunali čas do prvega oddaljenega razsoja bolezni in celokupno preživetje v celotni skupini bolnic z ozirom na mutacijski status *PIK3CA* v primarnem tumorju dojke. Povezanost med *PIK3CA* aktivirajočo mutacijo in učinkovitostjo dopolnilnega endokrinega zdravljenja pa smo analizirali s pomočjo Coxovih modelov v skupini bolnic, ki so imele v tumorju pozitivne estrogenske in progesteronske receptorje.

Rezultati. Srednja starost vseh bolnic ob diagnozi je bila 62,8 let in srednji čas opazovanja 10,8 let. Med 365 bolnicami, ki smo jih vključili v raziskavo, smo odkrili *PIK3CA* aktivirajočo mutacijo pri 45 %. Ugotovili smo, da prisotnost *PIK3CA* mutacije v primarnem ILC dojke ne vpliva na čas do prvega oddaljenega razsoja bolezni (p = 0,36) in ne na celokupno preživetje (p = 0,42). Pri bolnicah s prisotno aktivirajočo *PIK3CA* mutacijo je vsako leto zdravljenja s tamoksifenom zmanjšalo tveganje za smrt za 27 %, pri bolnicah zdravljenih z zaviralci aromataze pa za 21 % v primerjavi z bolnicami, ki niso prejele endokrinega zdravljenja. Vrsta in trajanje endokrinega zdravljenja nista imela vpliva na čas do prvega oddaljenega razsoja bolezni, je pa podaljšano endokrino zdravljenje imelo ugoden vpliv na celokupno preživetje.

Zaključki. Prisotnost aktivirajoče mutacije *PIK3CA* v primarnem operabilnem ILC dojke ne vpliva na čas do prvega oddaljenega razsoja bolezni in tudi ne na celokupno preživetje. Bolnice s prisotno *PIK3CA* aktivirajočo mutacijo so imele statistično pomembno zmanjšanje tveganja smrti ne glede na to, ali so v dopolnilnem hormonskem zdravljenju prejele tamoksifen ali zaviralce aromataze.

Radiol Oncol 2023; 57(2): 229-238.
doi: 10.2478/raon-2023-0018

Subplevralne fibrozne intersticijske nepravilnosti v pljučih vplivajo na izid radioterapije nedrobnoceličnega pljučnega raka

Ito M, Katano T, Okada H, Sakuragi A, Minami Y, Abe S, Adachi S, Oshima Y, Ohashi W, Kubo A, Fukui T, Ito S, Suzuki K

Izhodišča. Povezava med intersticijskimi pljučnimi nepravilnostmi in rezultati zdravljenja pljučnega raka z radioterapijo je nejasna. Namen raziskave je bil ugotoviti, ali so specifični podtipi intersticijskih pljučnih nepravilnosti dejavniki tveganja za radiacijski pnevmonitis.

Bolniki in metode. V retrospektivni raziskavi smo analizirali bolnike z nedrobnoceličnim pljučnim rakom, ki smo jih zdravili z radikalno ali rešilno radioterapijo. Bolnike smo razdelili v skupino normalnih (brez nepravilnosti), skupino z intersticijskimi pljučnimi nepravilnostmi in skupino z intersticijsko pljučno boleznijo. Skupino z intersticijskimi pljučnimi nepravilnostmi smo nadalje razdelili na nesubpleuralno, subpleuralno nefibrotično in subpleuralno fibrotično skupino. Za določitev radiacijskega pnevmonitisa in preživetja ter primerjavo teh rezultatov med skupinami smo uporabili Kaplan-Meierjevo in Coxovo regresijsko metodo.

Rezultati. V raziskavo smo vključili 175 bolnikov: normalni, n = 105; intersticijske pljučne nepravilnosti--nesubpleuralno, n = 5; intersticijske pljučne nepravilnosti-subpleuralno nefibrotično, n = 28; intersticijske pljučne nepravilnosti-subpleuralno fibrotično, n = 31; intersticijska pljučna bolezen, n = 6. Radiacijski pnevmonitis stopnje ≥ 2 smo opazili pri 71 bolnikih (41 %). Intersticijske pljučne nepravilnosti (razmerje tveganj [HR]: 2,33; p = 0,008), radioterapija z modulirano intenzivnostjo (HR: 0,38; p = 0,03) in prostornina pljuč, ki je prejela 20 Gy (HR: 54,8; p = 0,03), so prispevali h kumulativni pojavnosti radiacijskega pnevmonitisa. V skupini intersticijske pljučne nepravilnosti je bilo 8 bolnikov z radiacijskim pnevmonitisom 5. stopnje, od tega jih je imelo 7 subpleuralno fibrotično obliko. Med radikalno zdravljenimi bolniki je imela skupina intersticijske pljučne nepravilnosti slabše 2-letno celokupno preživetje kot normalna skupina (35,3 % proti 54,6 %; p = 0,005). Multivariatna analiza je pokazala, da je skupina z intersticijskimi pljučnimi nepravilnostmi-subpleuralno fibrotičnimi prispevala k slabšemu celokupnemu preživetju (HR: 3,07; p = 0,02).

Zaključki. Intersticijske pljučne nepravilnosti, zlasti subpleuralne fibrotične, so lahko pomembni dejavniki tveganja za radiacijski pnevmonitis, ki lahko poslabšajo napoved poteka bolezni. Te ugotovitve lahko pomagajo pri odločanju glede radioterapije.

Radiol Oncol 2023; 57(2): 239-248.
doi: 10.2478/raon-2023-0017

Vpliv izražanja genov *BCL2*, *BAX* in *ABCB1* na napoved poteka bolezni pri odraslih bolnikih z *de novo* akutno mieloično levkemijo z normalnim kariotipom

Pravdić Z, Suvajdžić Vuković N, Gasić V, Marjanović I, Karan-Djurašević T, Pavlović S, Tosić N

Izhodišča. Deregulacija apoptotičnega procesa je v ozadju patogeneze številnih vrst raka, vključno z levkemijo, in je zelo pomembna tudi za uspeh kemoterapevtskega zdravljenja. Zato bi lahko profil izražanja genov glavnih apoptotičnih dejavnikov, kot sta antiapoptotični *BCL2* (protein 2 limfoma celic B) in proapoptotični *BAX* (BCL2-associated X), ter genov, vključenih v odpornost na več zdravil (*ABCB1*), pomembno vplival na napoved poteka bolezni. Uporabili bi ga lahko tudi kot tarčo za specifično zdravljenje.

Bolniki in metode. Z metodo verižne reakcije s polimerazo v realnem času smo analizirali izražanje *BCL2, BAX* in *ABCB1* v vzorcih kostnega mozga, ki smo jih zbrali ob diagnozi pri 51 odraslih bolnikih z akutno mieloično levkemijo z normalnim kariotipom (AML-NK), in preučili njihovo napovedno moč.

Rezultati. Povečano izražanje *BCL2* (*BCL2*$^{+}$) je bilo povezano s kemorezistenco (p = 0,024), medtem ko so bili bolniki z nizkim izražanjem *BAX (BAX*^{nizko}*)* bolj nagnjeni k ponovitvi bolezni (p = 0,047). Analiza skupnega učinka izražanja *BCL2* in *BAX* je pokazala, da je bilo 87 % bolnikov s statusom *BAX*/*BCL2*^{nizko} odpornih na zdravljenje (p = 0,044). Visoko izražanje *ABCB1* je bilo povezano s statusom *BCL2*$^{+}$ (p < 0,001) in odsotnostjo mutacij *FLT3-ITD* (p = 0,019).

Zaključki. Pričujoča analiza profilov izražanja genov *BCL2*, *BAX* in *ABCB1* je prva raziskava, ki obravnava izključno bolnike z AML-NK. Preliminarni rezultati so pokazali, da so bolniki z visokim izražanjem *BCL2* v večji meri odporni na kemoterapijo in bi jim lahko koristilo specifično zdravljenje proti *BCL2*. Z nadaljnjimi raziskavami na večjem številu bolnikov bi lahko pojasnili dejanski napovedni pomen teh genov pri bolnikih z AML-NK.

Radiol Oncol 2023; 57(2): 249-256.
doi: 10.2478/raon-2023-0016

CD56-pozitivni difuzni velikocelični limfom B. Celovita analiza kliničnih, patoloških in molekularnih značilnosti s pregledom literature

Gašljević G, Boltežar L, Novaković S, Šetrajčič-Dragoš V, Jezeršek-Novaković B, Kloboves-Prevodnik V

Izhodišča. Difuzni velikocelični limfom B (*angl. diffuse large B-cell lymphoma,* DLBCL) brez dodatnih oznak (*angl. not otherwise specified*, NOS) je najpogostejši ne-Hodgkinov limfom. Izražanje CD56 na celicah DLBCL-NOS, je zelo neobičajno. O pojavnosti izražanja in njegovem kliničnem pomenu pri DLBCL je malo znanega. Pri takšnih primerih še niso naredili genetskega profila.

Bolniki in metode. V raziskavo smo vključili 229 bolnikov s histološko potrjenim DLBCL-NOS, ki so bili diagnosticirani na Onkološkem inštitutu Ljubljana v obdobju 2008–2017. Iz tkivnih blokov vseh bolnikov smo izdelali tkivne mreže in naredili tkivne rezine za barvanje s hematoksilin eozinom in imunohistokemična barvanja. Za vse primere DLBCL-NOS, kjer smo na limfomskih celicah imunohistokemično dokazali izražanje CD56, smo pridobili klinične podatke, vključno s starostjo ob diagnozi, stadijem bolezni, mednarodnim napovednim indeksom (*angl. International Prognostic Index*, IPI), shemo zdravljenja in številom krogov kemoterapije, zdravljenjem z radioterapijo, izidom zdravljenja in morebitno ponovitvijo bolezni. Izračunali smo celokupno preživetje in preživetje brez napredovanja. Pri štirih bolnikih s CD56 pozitivnim DLBCL-NOS smo izolirali RNA in opravili ciljno sekvenciranje RNA (cDNA) 125 genov s kompletom *Archer FusionPlex Lymphoma*.

Rezultati. Izražanje CD56 smo ugotovili v 7 od 229 primerov (3%). Stopnja izražanja je bila zmerna žariščna do zelo intenzivna in difuzna. Vsi bolniki so imeli na novo nastal DLBCL-NOS. Srednja starost bolnikov ob diagnozi je bila 54,5 let, med njimi je bilo pet žensk in 2 moška. Po Hansovem algoritmu je imelo 6 bolnikov podtip GBC in en podtip ne-GBC (ABC), dvojni ekspresor. Genetski profil štirih bolnikov, določen po Schmitzovi klasifikaciji, je pokazal, da je bil en primer podtipa BN2, en podtipa EZB, dva pa sta bila nerazvrščena. Pri vseh 6 zdravljenih bolnikih smo dosegli popoln odgovor na zdravljenje in nismo ugotovili napredovanja bolezni v srednjem obdobju spremljanja 80,5 mesecev.

Zaključki. Naša serija CD56 pozitivnih DLBCL-NOS je ena izmed največjih do sedaj objavljenih, v kateri so podrobno opisane klinično-patološke značilnosti. Prav tako je to prva serija CD56 pozitivnih DLBCL-NOS, pri kateri smo določili genetski profil. Rezultati kažejo, da je izražanje CD56 v DLBCL-NOS redko, vendar prisotno v napovedno ugodnih imunohistokemičnih in genetskih podtipih DLBCL-NOS.

Radiol Oncol 2023; 57(2): 257-269.
doi: 10.2478/raon-2023-0023

Kvantitativni dinamični kontrastni parametri in znotrajvokselno nekoherentno gibanje omogočajo napovedovanje statusa TP53 in opredelitev tveganja pri začetnem endometrijskem karcinomu

Wang H, Yan R, Li Z, Wang B, Jin X, Guo Z, Liu W, Zhang M, Wang K, Guo J, Han D

Izhodišča. Namen raziskave je bil raziskati vrednost dinamičnega kontrastnega magnetnoresonančnega slikanja (DCE-MRI) in znotrajvokselnega inkoherentnega gibanja (IVIM) za razlikovanje med mutiranim TP53 in nemutiranim, nizkim in visokim tveganjem pri začetnem endometrijskem karcinoma.

Bolniki in metode. Pri 74 bolnikih z endometrijskim karcinomom smo naredili MRI medenice. Primerjali smo parametre: konstanta volumskega prenosa (Ktrans), konstanta hitrosti prenosa (Kep), volumen ekstravaskularnega zunajceličnega prostora na enoto volumna tkiva (Ve), pravi difuzijski koeficient (D), psevdodifuzijski koeficient (D*) in mikrovaskularni volumski delež (f). Kombinacijo parametrov smo analizirali z logistično regresijo in ovrednotili z metodo zagonskega traku (*angl. bootstrap*) (1000 vzorcev), ROC krivuljami, kalibracijskimi krivuljami in analizo krivulje odločanja (DCA).

Rezultati. V skupini z mutiranim TP53 sta bila Ktrans in Kep višja, D pa nižji kot v skupini z divjim tipom TP53; Ktrans, Ve, f in D so bili nižji v skupini z visokim tveganjem kot v skupini z nizkim tveganjem (vsi P < 0,05). Pri prepoznavanju začetnega endometrijskega karcinoma z mutiranim TP53 in nemutiranim TP53 sta bila Ktrans in D neodvisna napovedna dejavnika, njuna kombinacija pa je imela optimalno diagnostično učinkovitost (AUC 0,867; občutljivost 92 %; specifičnost 80,95 %), kar je bilo pomembno boljše od D (Z = 2,169; P = 0,030) in Ktrans (Z = 2,572, P = 0,010). Pri prepoznavanju začetnega endometrijskega karcinoma z nizkim in visokim tveganjem so bili neodvisni napovedni kazalci Ktrans, Ve in f, njihova kombinacija pa je imela optimalno diagnostično učinkovitost (AUC 0,947; občutljivost 83,33 %; specifičnost 93,18 %), kar je bilo bistveno boljše od D (Z = 3,113; P = 0,002), f (Z = 4,317; P < 0,001), Ktrans (Z = 2,713; P = 0,007) in Ve (Z = 3,175; P = 0,002). Umeritvene krivulje so pokazale, da imata obe zgornji kombinaciji neodvisnih napovednih dejavnikov dobro skladnost, DCA pa je pokazala, da sta ti kombinaciji zanesljivi klinični napovedni orodji.

Zaključki. Tako DCE-MRI kot IVIM olajšata napoved statusa TP53 in opredelitev tveganja pri začetnem endometrialnem karcinomu. V primerjavi s posameznimi parametri je imela kombinacija neodvisnih napovednih dejavnikov boljšo napovedno moč in lahko služi kot boljši slikovni označevalec.

Radiol Oncol 2023; 57(2): 270-278.
doi: 10.2478/raon-2023-0026

Dvostopenjska hepatektomija pri resekciji jetrnih metastaz raka debelega črevesa in danke. Izkušnje terciarne ustanove s primerjavo primerov in kontrol ter pregled literature

Turk S, Plahuta I, Magdalenič T, Španring T, Laufer K, Mavc Ž, Potrč S, Ivanecz A

Izhodišča. Dvostopenjsko hepatektomijo so uvedli pri bolnikih z bilateralnimi jetrnimi tumorji, ki imajo visoko tveganje za jetrno odpoved po enostopenjski hepatektomiji. Namen raziskave je bil analizirati dvostopenjske hepatektomije pri obsežnih obojestranskih jetrnih zasevkih raka debelega črevesa in danke.

Bolniki in metode. Retrospektivno smo pregledali prospektivno vodene podatkovne baze jetrnih resekcij zaradi zasevkov raka debelega črevesa in danke. Skupino dvostopenjskih hepatektomij smo primerjali s skupino enostopenjskih hepatektomij glede pooperativnih izidov in preživetja. Izvedli smo ujemanje primerov in kontrol (*angl. case-control matching*).

Rezultati. Med leti 2000 in 2020 smo naredili 632 jetrnih resekcij zaradi zasevkov raka debelega črevesa in danke. Skupina z dvostopenjsko hepatektomijo je obsegala 15 bolnikov, kontrolna skupina z enostopenjskih hepatektomijo pa je vključeval 151 bolnikov. Skupina enostopenjskih hepatektomij, kjer smo izvedli ujemanje primerov je vsebovala 14 bolnikov. Huda obolevnost in 90-dnevna smrtnost sta bili v skupini z dvostopenjsko hepatektomijo 40 % in 13,3 %; v skupini z enostopenjsko hepatektomijo pa 20,5 % in 4,6 % ter v skupini z enostopenjsko hepatektomijo in hkratno ujemanje primerov 28,6 % oziroma 7,1 %. Preživetje brez bolezni, srednje celokupno preživetje ter 3- in 5-letni preživetji so v skupini dvostopenjskih hepatektomij bili 5 mesecev, 21 mesecev, 33 % in 13 %; v skupini enostopenjskih hepatektomij pa 11 mesecev, 35 mesecev, 49 % in 27 % ter v skupini z enostopenjsko hepatektomijo in hkratno ujemanje primerov 8 mesecev, 23 mesecev, 36 % in 21 %.

Zaključki. Dvostopenjska hepatektomija je bila dokaj varen in učinkovit postopek zdravljenja. Prednost enostopenjske hepatektomije pa je, da z njo lahko dosegamo ob enakovrednih onkoloških rezultatih nižjo hudo obolevnost po operaciji.

Fundacija "Docent dr. J. Cholewa"
je neprofitno, neinstitucionalno in nestrankarsko
združenje posameznikov, ustanov in organizacij, ki želijo
materialno spodbujati in poglabljati raziskovalno
dejavnost v onkologiji.

Dunajska 106
1000 Ljubljana
IBAN: SI56 0203 3001 7879 431

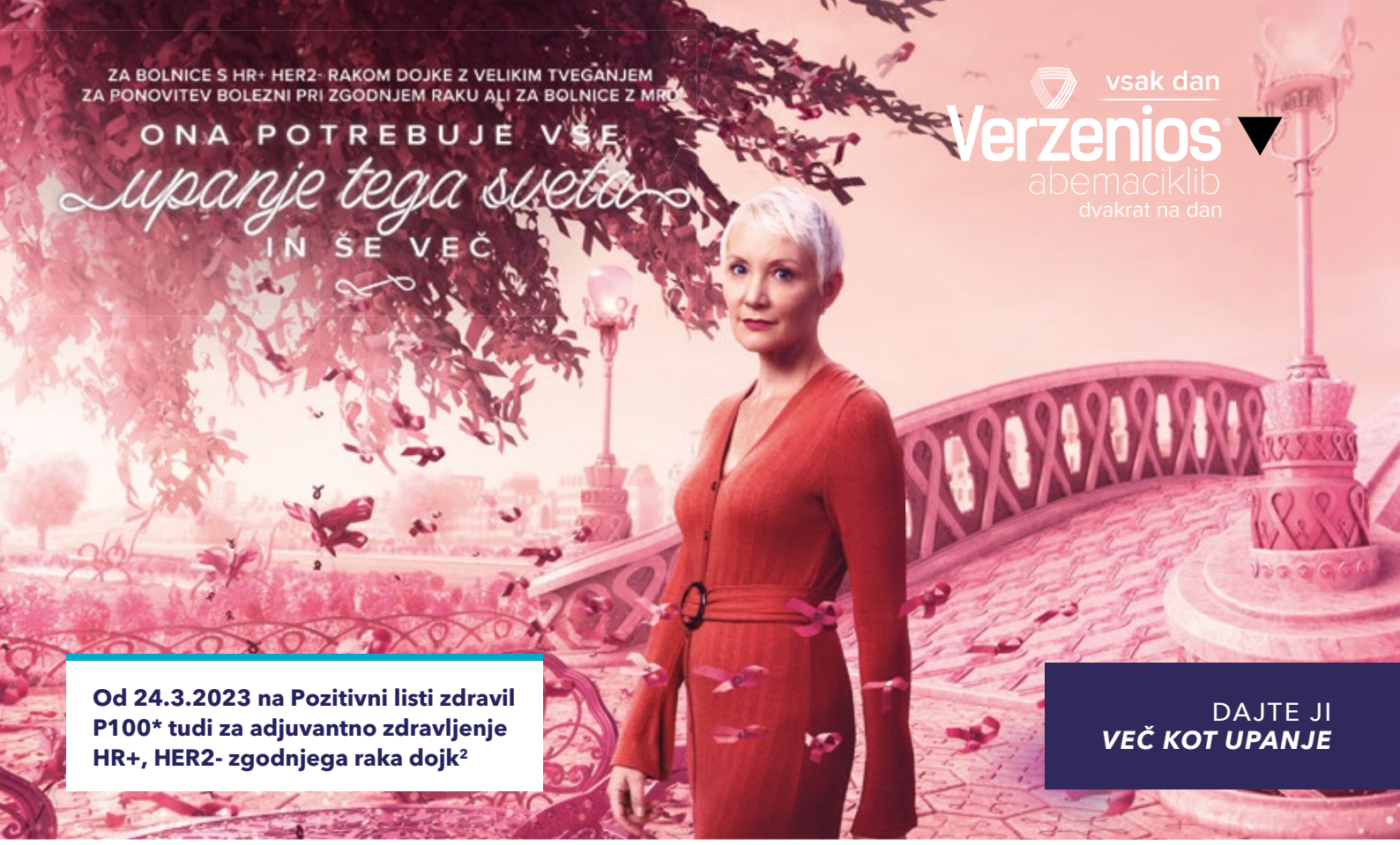

SKRAJŠAN POVZETEK GLAVNIH ZNAČILNOSTI ZDRAVILA

Za to zdravilo se izvaja dodatno spremljanje varnosti. Tako bodo hitreje na voljo nove informacije o njegovi varnosti. Zdravstvene delavce naprošamo, da poročajo o katerem koli domnevnem neželenem učinku zdravila.

IME ZDRAVILA: Verzenios 50 mg/100 mg/150 mg filmsko obložene tablete **KAKOVOSTNA IN KOLIČINSKA SESTAVA:** Ena filmsko obložena tableta vsebuje 50 mg/100 mg/150 mg abemaciklib. Ena filmsko obložena tableta vsebuje 14 mg/28 mg/42 mg laktoze (v obliki monohidrata). **Terapevtske indikacije:** Zgodnji rak dojk: Zdravilo Verzenios je v kombinaciji z endokrinim zdravljenjem indicirano za adjuvantno zdravljenje odraslih bolnikov z na hormonske receptorje (HR – Hormone Receptor) pozitivnim, na receptorje humanega epidermalnega rastnega faktorja 2 (HER2 – Human Epidermal Growth Factor Receptor 2) negativnim zgodnjim rakom dojk s pozitivnimi bezgavkami, pri katerih obstaja veliko tveganje za ponovitev. Pri ženskah v pred- ali perimenopavzi je treba endokrino zdravljenje z zaviralcem aromataze kombinirati z agonistom gonadoliberina (LHRH – Luteinizing Hormone–Releasing Hormone). Napredovali ali metastatski rak dojk: Zdravilo Verzenios je indicirano za zdravljenje žensk z lokalno napredovalim ali metastatskim, na hormonske receptorje (HR – *Hormone Receptor*) pozitivnim in na receptorje humanega epidermalnega rastnega faktorja 2 (HER2 – *Human Epidermal Growth Factor Receptor 2*) negativnim rakom dojk v kombinaciji z zaviralcem aromataze ali s fulvestrantom kot začetnim endokrinim zdravljenjem ali pri ženskah, ki so prejele predhodno endokrino zdravljenje. Pri ženskah v pred- ali perimenopavzi je treba endokrino zdravljenje kombinirati z agonistom LHRH. **Odmerjanje in način uporabe:** Zdravljenje z zdravilom Verzenios mora uvesti in nadzorovati zdravnik, ki ima izkušnje z uporabo zdravil za zdravljenje rakavih bolezni. *Zdravilo Verzenios v kombinaciji z endokrinim zdravljenjem:* Priporočeni odmerek abemaciklibа je 150 mg dvakrat na dan, kadar se uporablja v kombinaciji z endokrinim zdravljenjem. *Zgodnji rak dojk:* Zdravilo Verzenios je treba jemati neprekinjeno dve leti, ali do ponovitve bolezni ali pojava nesprejemljive toksičnosti. *Napredovali ali metastatski rak dojk:* Zdravilo Verzenios je treba jemati, dokler ima bolnica od zdravljenja klinično korist ali do pojava nesprejemljive toksičnosti. Če bolnica bruha ali izpusti odmerek zdravila Verzenios, ji je treba naročiti, da naj naslednji odmerek vzame ob predvidenem času; dodatnega odmerka ne sme vzeti. Obvladovanje nekaterih neželenih učinkov lahko zahteva prekinitev in/ali zmanjšanje odmerka. Zdravljenje z abemaciklibom prekinite v primeru povišanja vrednosti AST in/ali ALT >3 x ZMN SKUPAJ s celokupnim bilirubinom > 2,0 x ZMN v odsotnosti holestaze ter pri bolnicah z intersticijsko pljučno boleznijo (ILD)/pnevmonitis stopnje 3 ali 4. Sočasni uporabi močnih zaviralcev CYP3A4 se je treba izogibati. Če se uporabi močnih zaviralcev CYP3A4 ni mogoče izogniti, je treba odmerek abemaciklibа znižati na 100 mg dvakrat na dan. Pri bolnicah, pri katerih je bil odmerek znižan na 100 mg abemaciklibа dvakrat na dan in pri katerih se sočasnemu dajanju močnega zaviralca CYP3A4 ni mogoče izogniti, je treba odmerek abemaciklibа dodatno znižati na 50 mg dvakrat na dan. Pri bolnicah, pri katerih je bil odmerek znižan na 50 mg abemaciklibа dvakrat na dan in pri katerih se sočasnemu dajanju močnega zaviralca CYP3A4 ni mogoče izogniti, je mogoče z odmerkom abemaciklibа nadaljevati ob natančnem spremljanju znakov toksičnosti. Alternativno je mogoče odmerek abemaciklibа znižati na 50 mg enkrat na dan ali prekiniti dajanje abemaciklibа. Če je uporaba zaviralca CYP3A4 prekinjena, je treba odmerek abemaciklibа povečati na odmerek, kakršen je bil pred uvedbo zaviralca CYP3A4 (po 3–5 razpolovnih časih zaviralca CYP3A4). Prilagajanje odmerka glede na starost in pri bolnicah z blago ali zmerno ledvično okvaro ter z blago (Child Pugh A) ali zmerno (Child Pugh B) jetrno okvaro ni potrebno. Pri dajanju abemaciklibа bolnicam s hudo ledvično okvaro sta potrebna previdnost in skrbno spremljanje glede znakov toksičnosti. Način uporabe: Zdravilo Verzenios je namenjeno za peroralno uporabo. Odmerek se lahko vzame s hrano ali brez nje. Zdravilo se ne sme jemati z grenivko ali grenivkinim sokom. Bolnice naj odmerke vzamejo vsak dan ob približno istem času. Tableto je treba zaužiti celo (bolnice je pred zaužitjem ne smejo gristi, drobiti ali deliti). **Kontraindikacije:** Preobčutljivost na učinkovino ali katero koli pomožno snov. **Posebna opozorila in previdnostni ukrepi:** Pri bolnicah, ki so prejemale abemaciklib, so poročali o nevtropeniji, o večji pogostnosti okužb kot pri bolnicah, zdravljenih s placebom in endokrinim zdravljenjem, o povečanih vrednostih ALT in AST. Pri bolnicah, pri katerih se pojavi nevtropenija stopnje 3 ali 4, je priporočljivo prilagoditi odmerek. Do primerov nevtropenične sepse s smrtnim izidom je prišlo pri < 1 % bolnic z metastatskim rakom dojk. Bolnicam je treba naročiti, naj o vsaki epizodi povišane telesne temperature poročajo zdravstvenemu delavcu. Bolnice je treba spremljati za znake in simptome globoke venske tromboze (VTE) in pljučne embolije ter jih zdraviti, kot je medicinsko utemeljeno. Glede na stopnjo VTE bo morda treba spremeniti odmerek abemaciklibа. Glede na povečanje vrednosti ALT ali AST je mogoče potrebna prilagoditev odmerka. Driska je najpogostejši neželeni učinek. Bolnice je treba ob prvem znaku tekočega blata začeti zdraviti z antidiaroiki, kot je loperamid, povečati vnos peroralnih tekočin in obvestiti zdravnika. Sočasni uporabi induktorjev CYP3A4 se je treba izogibati zaradi tveganja za zmanjšano učinkovitost abemaciklibа. Bolnice z redkimi dednimi motnjami, kot so intoleranca za galaktozo, popolno pomanjkanje laktaze ali malapsorpcija glukoze/galaktoze, tega zdravila ne smejo jemati. Bolnice spremljajte glede pljučnih simptomov, ki kažejo na ILD/pnevmonitis, in jih ustrezno zdravite. Glede na stopnjo ILD/pnevmonitisa je morda potrebno prilagajanje odmerka abemaciklibа. **Medsebojno delovanje z drugimi zdravili in druge oblike interakcij:** Abemaciklib se primarno presnavlja s CYP3A4. Sočasna uporaba abemaciklibа in zaviralcev CYP3A4 lahko poveča plazemsko koncentracijo abemaciklibа. Uporabi močnih zaviralcev CYP3A4 sočasno z abemaciklibom se je treba izogibati. Če je močne zaviralce CYP3A4 treba dajati sočasno, je treba odmerek abemaciklibа zmanjšati, nato pa bolnico skrbno spremljati glede toksičnosti. Pri bolnicah, zdravljenih z zmernimi ali šibkimi zaviralci CYP3A4, ni potrebno prilagajanje odmerka, vendar jih je treba skrbno spremljati za znake toksičnosti. Sočasni uporabi močnih induktorjev CYP3A4 (vključno, vendar ne omejeno na: karbamazepin, fenitoin, rifampicin in šentjanževko) se je treba izogibati zaradi tveganja za zmanjšano učinkovitost abemaciklibа. Abemaciklib in njegovi glavni aktivni presnovki zavirajo prenašalce v ledvicah, in sicer kationski organski prenašalec 2 (OCT2) ter prenašalca MATE1. *In vivo* lahko pride do medsebojnega delovanja abemaciklibа in klinično pomembnih substratov teh prenašalcev, kot je dofelitid ali kreatinin. Trenutno ni znano, ali lahko abemaciklib zmanjša učinkovitost sistemskih hormonskih kontraceptivov, zato se ženskam, ki uporabljajo sistemske hormonske kontraceptive, svetuje, da hkrati uporabljajo tudi mehansko metodo. **Neželeni učinki:** Najpogostejši neželeni učinki so driska, okužbe, nevtropenija, levkopenija, anemija, utrujenost, navzea, bruhanje in zmanjšanje apetita. *Zelo pogosti:* okužbe, nevtropenija, levkopenija, anemija, trombocitopenija, limfopenija, zmanjšanje apetita, glavobol, disgevzija, omotica, driska, bruhanje, navzea, stomatitis, alopecija, pruritus, izpuščaj, pireksija, utrujenost, povečana vrednost alanin-aminotransferaze, povečana vrednost aspartat-aminotransferaze. *Pogosti:* povečano solzenje, venska trombembolija, ILD/pnevmonitis, dispepsija, spremembe na nohtih, suha koža, mišična šibkost. *Občasni:* febrilna nevtropenija. **Rok uporabnosti** 3 leta. **Posebna navodila za shranjevanje** Za shranjevanje zdravila niso potrebna posebna navodila. **Imetnik dovoljenja za promet z zdravilom**: Eli Lilly Nederland B.V., Papendorpseweg 83, 3528BJ, Utrecht, Nizozemska. Datum prve odobritve dovoljenja za promet: 27. september 2018. **Datum zadnje revizije besedila**: 26.1.2023. **Režim izdaje:** Rp/Spec - Predpisovanje in izdaja zdravila je le na recept zdravnika specialista ustreznega področja medicine ali od njega pooblaščenega zdravnika.

Reference: 1. Povzetek glavnih značilnosti zdravila Verzenios, zadnja odobrena verzija. **2.** ZZZS, Spremembe liste zdravil_2023_03_07

Pomembno: Predpisovanje in izdaja zdravila je le na recept zdravnika specialista ustreznega področja medicine ali od njega pooblaščenega zdravnika. Pred predpisovanjem zdravila Verzenios si preberite zadnji veljavni Povzetek glavnih značilnosti zdravil. Podrobne informacije o zdravilu so objavljene na spletni strani Evropske agencije za zdravila http://www.ema.europa.eu

Eli Lilly farmacevtska družba, d.o.o., Dunajska cesta 167, 1000 Ljubljana, telefon 01 / 580 00 10, faks 01 / 569 17 05

PP-AL-SI-0186, 9.3.2023, Samo za strokovno javnost.

PR/BSI/BEN/2022/017

TANTUM VERDE®

benzidaminijev klorid

Za lajšanje bolečine in oteklin v ustni in žrelu, ki so posledica radiomukozitisa

Bistvene informacije iz Povzetka glavnih značilnosti zdravila

Tantum Verde 1,5 mg/ml oralno pršilo, raztopina
Tantum Verde 3 mg/ml oralno pršilo, raztopina

Sestava: 1,5 mg/ml: 1 ml raztopine vsebuje 1,5 mg benzidaminijevega klorida, kar ustreza 1,34 mg benzidamina. V enem razpršku je 0,17 ml raztopine. En razpršek vsebuje 0,255 mg benzidaminijevega klorida, kar ustreza 0,2278 mg benzidamina. **Sestava 3 mg/ml:** 1 ml raztopine vsebuje 3 mg benzidaminijevega klorida, kar ustreza 2,68 mg benzidamina. V enem razpršku je 0,17 ml raztopine. En razpršek vsebuje 0,51 mg benzidaminijevega klorida, kar ustreza 0,4556 mg benzidamina. **Terapevtske indikacije:** Samozdravljenje: Lajšanje bolečine in oteklin pri vnetju v ustni votlini in žrelu, ki so lahko posledica okužb in stanj po operaciji. Po nasvetu in navodilu zdravnika: Lajšanje bolečine in oteklin v ustni votlini in žrelu, ki so posledica radiomukozitisa. **Odmerjanje in način uporabe:** Uporaba: 2- do 6-krat na dan (vsake 1,5 do 3 ure). Odmerjanje 1,5 mg/ml: Odrasli: 4 do 8 razprškov 2- do 6-krat na dan. Pediatrična populacija: Mladostniki, stari od 12 do 18 let: 4-8 razprškov 2- do 6-krat na dan. Otroci od 6 do 12 let: 4 razprški 2- do 6-krat na dan. Otroci, mlajši od 6 let: 1 razpršek na 4 kg telesne mase; do največ 4 razprške 2- do 6-krat na dan. Odmerjanje 3 mg/ml: Odrasli: 2 do 4 razprški 2- do 6-krat na dan. Pediatrična populacija: Mladostniki, stari od 12 do 18 let: 2 do 4 razprški 2- do 6-krat na dan. Otroci od 6 do 12 let: 2 razprška 2- do 6-krat na dan. Otroci, mlajši od 6 let: 1 razpršek na 8 kg telesne mase; do največ 2 razprška 2- do 6-krat na dan. Starejši bolniki, bolniki z jetrno okvaro in bolniki z ledvično okvaro: niso potrebni posebni previdnostni ukrepi. Trajanje zdravljenja ne sme biti daljše od 7 dni. Način uporabe: Za orofaringealno uporabo. Zdravilo se razprši v usta in žrelo. **Kontraindikacije:** Preobčutljivost na učinkovino ali katero koli pomožno snov. **Posebna opozorila in previdnostni ukrepi:** Pri nekaterih bolnikih lahko resne bolezni povzročijo ustne/žrelne ulceracije. Če se simptomi v treh dneh ne izboljšajo, se mora bolnik posvetovati z zdravnikom ali zobozdravnikom, kot je primerno. Uporaba benzidamina ni priporočljiva za bolnike s preobčutljivostjo na salicilno kislino ali druga nesteroidna protivnetna zdravila. Pri bolnikih, ki imajo ali so imeli bronhialno astmo, lahko pride do bronhospazma. Pri takih bolnikih je potrebna previdnost. To zdravilo vsebuje 13,6 mg alkohola (etanola) v enem razpršku (0,17 ml), kar ustreza manj kot 0,34 ml piva oziroma 0,14 ml vina. Majhna količina alkohola v zdravilu ne bo imela nobenih opaznih učinkov. To zdravilo vsebuje metilparahidroksibenzoat (E218). Lahko povzroči alergijske reakcije (lahko zapoznele). To zdravilo vsebuje manj kot 1 mmol (23 mg) natrija v enem razpršku (0,17 ml), kar v bistvu pomeni 'brez natrija'. Zdravilo vsebuje aromo poprove mete z benzilalkoholom, cinamilalkoholom, citralom, citronelolom, geraniolom, izoevgenolom, linalolom, evgenolom in D-limonen, ki lahko povzročijo alergijske reakcije. Zdravilo z jakostjo 3 mg/ml vsebuje makrogolglicerol hidroksistearat 40. Lahko povzroči želodčne težave in drisko. **Medsebojno delovanje z drugimi zdravili in druge oblike interakcij:** Študij medsebojnega delovanja niso izvedli. **Nosečnost in dojenje:** O uporabi benzidamina pri nosečnicah in doječih ženskah ni zadostnih podatkov. Uporaba zdravila med nosečnostjo in dojenjem ni priporočljiva. **Vpliv na sposobnost vožnje in upravljanja strojev:** Zdravilo v priporočenem odmerku nima vpliva na sposobnost vožnje in upravljanja strojev. **Neželeni učinki:** Neznana pogostnost (ni mogoče oceniti iz razpoložljivih podatkov): anafilaktične reakcije, preobčutljivostne reakcije, odrevenelost, laringospazem, suha usta, navzea in bruhanje, oralna hipestezija, angioedem, fotosenzitivnost, pekoč občutek v ustih. Neposredno po uporabi se lahko pojavi občutek odrevenelosti v ustih in v žrelu. Ta učinek se pojavi zaradi načina delovanja zdravila in po kratkem času izgine. **Način in režim izdaje zdravila:** BRp-Izdaja zdravila je brez recepta v lekarnah in specializiranih prodajalnah. **Imetnik dovoljenja za promet:** Aziende Chimiche Riunite Angelini Francesco – A.C.R.A.F. S.p.A., Viale Amelia 70, 00181 Rim, Italija **Datum zadnje revizije besedila:** 05. 04. 2022

Pred svetovanjem ali izdajo preberite celoten Povzetek glavnih značilnosti zdravila.

Samo za strokovno javnost.

Datum priprave informacije: april 2022

ANGELINI

Odgovoren za trženje: Bonifar d.o.o.

IMFINZI™
durvalumab
50 mg/ml koncentrat za raztopino za infundiranje

AKTIVIRA IMUNSKI SISTEM.
PREPOZNA. **REAGIRA.**

IMFINZI podaljša preživetje in obenem ohranja kvaliteto življenja bolnikov z razsejanim drobnoceličnim rakom pljuč [1,2]

Po treh letih je bilo živih 3x več bolnikov zdravljenih z zdravilom Imfinzi v kombinaciji z EP kot bolnikov zdravljenih samo z EP[1]

POSODOBLJENA ANALIZA CELOKUPNEGA PREŽIVETJA (srednji čas spremljanja 39,4 mesecev)

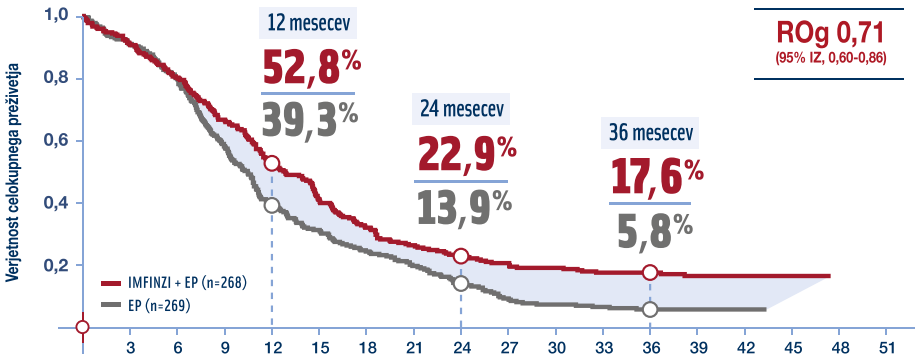

ROg 0,71
(95% IZ, 0,60-0,86)

Število bolnikov izpostavljenih tveganju

IMFINZI + EP	268	244	214	177	140	109	85	70	60	54	50	46	39	25	13	3	0	0
EP	269	243	212	156	104	82	64	51	36	24	19	17	13	10	3	0	0	0

- **3-letna analiza celokupnega preživetje je bila izvedena po 469 dogodkih, ki so se zgodili v obeh skupinah bolnikov zdravljenih s kombinacijo IMFINZI + EP ali samo z EP (86% zrelost podatkov)[1]**

SKRAJŠAN POVZETEK GLAVNIH ZNAČILNOSTI ZDRAVILA

▼ Za to zdravilo se izvaja dodatno spremljanje varnosti. Tako bodo hitreje na voljo nove informacije o njegovi varnosti. Zdravstvene delavce naprošamo, da poročajo o katerem koli domnevnem neželenem učinku zdravila.

Imfinzi 50 mg/ml koncentrat za raztopino za infundiranje

SESTAVA: 1 ml koncentrata za raztopino za infundiranje vsebuje 50 mg durvalumaba. Ena viala z 2,4 ml koncentrata vsebuje 120 mg durvalumaba. Ena viala z 10 ml koncentrata vsebuje 500 mg durvalumaba. **INDIKACIJE:** Neoperabilni nedrobnocelični rak pljuč (NSCLC) Zdravilo IMFINZI je kot samostojno zdravljenje indicirano za zdravljenje lokalno napredovalega, neoperabilnega nedrobnoceličnega raka pljuč (NSCLC – non small cell lung cancer) pri odraslih, ki imajo tumorje z ≥ 1 % izraženostjo PD L1 na tumorskih celicah in pri katerih bolezen ni napredovala po kemoradioterapiji na osnovi platine. Zdravilo IMFINZI je v kombinaciji s tremelimumabom in kemoterapijo na osnovi platine indicirano za prvo linijo zdravljenja odraslih z metastatskim NSCLC brez senzibilizirajočih mutacij EGFR ali pozitivnih mutacij ALK. Drobnocelični rak pljuč (SCLC) Zdravilo IMFINZI je v kombinaciji z etopozidom in bodisi karboplatinom bodisi cisplatinom indicirano za prvo linijo zdravljenja odraslih z razsejanim drobnoceličnim rakom pljuč (ES SCLC – extensive stage small cell lung cancer). Rak bilarnega trakta (RBT) Zdravilo IMFINZI je v kombinaciji z gemcitabinom in cisplatinom indicirano za prvo linijo zdravljenja odraslih z neoperabilnim ali metastatskim rakom bilarnega trakta (RBT).. Hepatocelularni karcinom (HCK). Zdravilo IMFINZI je v kombinaciji s tremelimumabom indicirano za prvo linijo zdravljenja odraslih z napredovalim ali neoperabilnim karcinomom jetrnih celic (hepatocelularnim karcinomom – HCK). **ODMERJANJE IN NAČIN UPORABE:** Zdravljenje mora uvesti in nadzorovati zdravnik, ki ima izkušnje na področju zdravljenja raka. Bolnike z lokalno napredovalim nedrobnoceličnim rakom pljuč je treba za zdravljenje izbrati na podlagi izraženosti PD-L1, ugotovljene z validirano testno metodo. Odmerjanje: Priporočeni odmerek zdravila Imfinzi pri samostojnem zdravljenju pri lokalno napredovalem NSCLC je 10 mg/kg na 2 tedna ali 1500 mg na 4 tedne do napredovanja bolezni, nesprejemljivih toksičnih učinkov ali največ 12 mesecev. Priporočeni odmerek zdravila Imfinzi pri kombiniranem zdravljenju pri metastatskem NSCLC je med kemoterapijo s platino: 1500 mg v kombinaciji s 75 mg tremelimumaba in kemoterapijo na osnovi platine na 3 tedne (21 dni) 4 cikle (12 tednov), po kemoterapiji s platino: 1500 mg na 4 tedne kot monoterapija za vzdrževalno zdravljenje s pemetreksedom (na podlagi histologije) na 4 tedne, peti odmerek 75 mg tremelimumaba je treba dati 16. teden skupaj z zdravilom Imfinzi, do napredovanja bolezni ali nesprejemljivih toksičnih učinkov. Pri ES-SCLC je priporočeni odmerek zdravila Imfinzi 1500 mg v kombinaciji s kemoterapijo na 3 tedne (21 dni) 4 cikluse in nato 1500 mg na 4 tedne kot samostojno zdravljenje do napredovanja bolezni ali nesprejemljivih toksičnih učinkov. Pri RBT je priporočeni odmerek zdravila Imfinzi 1500 mg v kombinaciji s kemoterapijo na 3 tedne (21 dni) do 8 ciklusov, nato po 1500 mg na 4 tedne kot samostojno zdravljenje do napredovanja bolezni ali nesprejemljivih toksičnih učinkov. Pri HCK je priporočeni odmerek 1500 mg zdravila IMFINZI v kombinaciji s 300 mg tremelimumaba v enem odmerku 1. dan 1. cikla, nato zdravilo Imfinzi kot monoterapija na 4 tedne do napredovanja bolezni ali nesprejemljivih toksičnih učinkov. Povečevanje ali zmanjševanje odmerka ni priporočljivo. Glede na individualno varnost in prenašanje je lahko potrebna odložitev zdravljenja ali trajno prenehanje uporabe zdravila. V primeru domnevnih imunsko pogojenih neželenih učinkov je treba opraviti ustrezno ovrednotenje za potrditev etiologije oziroma izključitev druge etiologije. Glede na resnost neželenega učinka je treba prenehati uporabljati zdravilo Imfinzi in/ali tremelimumab in pričeti z dajanjem kortikosteroidov. Če se stanje ne izboljša ali se poslabša, pride v poštev povečanje odmerka kortikosteroidov in/ali dodatna uporaba sistemskih imunosupresivov. Po izboljšanju na ≤ 1. stopnjo je treba začeti s postopnim zmanjševanjem kortikosteroida in ga zmanjševati v obdobju vsaj 1 meseca. Po odločitvi uporabe je mogoče zdravilo Imfinzi in/ali tremelimumab znova začeti uporabljati v času 12 tednov, če se neželeni učinki izboljšajo na ≤ 1. stopnjo in je odmerek kortikosteroida zmanjšan na ≤ 10 mg prednizona ali ekvivalenta na dan. Zdravilo Imfinzi in tremelimumab je treba dokončno ukiniti, če se imunsko pogojeni neželeni učinki 3. stopnje (močno izraženi ponavljajo in pri katerih koli imunsko pogojenih neželenih učinkih 4. stopnje (življenjsko nevarni), razen pri endokrinopatijah, ki jih nadziramo z nadomestnimi hormoni. Način uporabe: Zdravilo Imfinzi je namenjeno za intravensko uporabo. Dati ga je treba kot raztopino za intravensko infundiranje v obdobju 1 ure. Če je zdravilo Imfinzi uporabljeno v kombinaciji s kemoterapijo, je treba dati zdravilo Imfinzi pred kemoterapijo na isti dan. Če je zdravilo Imfinzi uporabljeno v kombinaciji s tremelimumabom in kemoterapijo na osnovi platine, je treba najprej dati tremelimumab, ki mu v istem dnevu sledita zdravilo Imfinzi in nato kemoterapija na osnovi platine. Če je zdravilo Imfinzi uporabljeno v kombinaciji s petim odmerkom tremelimumaba in vzdrževalnim zdravljenjem s pemetreksedom 16. teden, je treba najprej dati tremelimumab, ki mu v istem dnevu sledita zdravilo Imfinzi in potem vzdrževalno zdravljenje s pemetreksedom. Zdravilo Imfinzi, tremelimumab in kemoterapijo na osnovi platine je treba dati v ločenih intravenskih infuzijah. Dajanje zdravila Imfinzi in tremelimumaba vsako traja po 1 uro. Če je zdravilo Imfinzi uporabljeno v kombinaciji s tremelimumabom, je treba dati tremelimumab pred zdravilom Imfinzi na isti dan. Zdravilo Imfinzi in tremelimumab je treba dati v ločenih intravenskih infuzijah. **KONTRAINDIKACIJE:** Preobčutljivost na učinkovino (učinkovine) ali katero koli pomožno snov. **OPOZORILA IN PREVIDNOSTNI UKREPI:** Za izboljšanje sledljivosti bioloških zdravil je treba jasno zabeležiti lastniško ime in številko serije uporabljenega zdravila. Imunsko pogojeni pnevmonitis: Pri bolnikih, ki so prejemali zdravilo Imfinzi ali zdravilo Imfinzi v kombinaciji s tremelimumabom, sta se pojavila imunsko pogojeni pnevmonitis ali intersticijska bolezen pljuč, opredeljeno kot potreba po uporabi sistemskih kortikosteroidov in brez jasne druge etiologije. Pnevmonitis in radiacijski pnevmonitis: Pri bolnikih, zdravljenih z radioterapijo pljuč, je pogost radiacijski pnevmonitis in klinična slika pnevmonitisa in radiacijskega pnevmonitisa je zelo podobna. V študiji PACIFIC sta se pri bolnikih, ki so opravili zdravljenje z najmanj 2 cikloma sočasne kemoradioterapije od 1 do 42 dni pred začetkom preskušanja, pnevmonitis ali radiacijski pnevmonitis pojavila pri 161 (33,9 %) bolnikih v skupini z zdravilom Imfinzi in pri 58 (24,8 %) bolnikih v skupini s placebom, vključno s 3. stopnjo (3,4 % in 3,0 %) in 5. stopnjo (1,1 % in 1,7 %). Bolnike je treba spremljati glede znakov in simptomov pnevmonitisa ali radiacijskega pnevmonitisa. Imunsko pogojeni hepatitis: Pri bolnikih, ki so prejemali zdravilo Imfinzi ali zdravilo Imfinzi v kombinaciji s tremelimumabom, se je pojavil imunsko pogojeni hepatitis, opredeljen kot potreba po sistemskih kortikosteroidih in brez jasne druge etiologije. Alanin-aminotransferazo, aspartat-aminotransferazo, celokupni bilirubin in alkalno fosfatazo kontrolirajte pred začetkom zdravljenja in pred vsako naslednjo infuzijo. Dodaten nadzor pride v poštev na podlagi klinične ocene. Imunsko pogojeni kolitis: Pri bolnikih, ki so prejemali zdravilo Imfinzi ali zdravilo Imfinzi v kombinaciji s tremelimumabom, sta se pojavila imunsko pogojeni kolitis ali driska, opredeljeno kot potreba po sistemskih kortikosteroidih in brez jasne druge etiologije. Pri bolnikih, ki so prejemali zdravilo Imfinzi v kombinaciji s tremelimumabom, so poročali o neželenih učinkih perforacije črevesa in perforacije debelega črevesa. Imunsko pogojene endokrinopatije: Imunsko pogojeni hipotiroidizem, hipertiroidizem in tiroiditis: Pri bolnikih, ki so prejemali zdravilo Imfinzi ali zdravilo Imfinzi v kombinaciji s tremelimumabom, so se pojavili imunsko pogojeni hipotiroidizem, hipertiroidizem in tiroiditis; hipertiroidizmu lahko sledi hipotiroidizem. Bolnike je treba spremljati glede neonormalnih izvidov delovanje ščitnice pred zdravljenjem in redno med zdravljenjem ter kot je potrebno glede na klinično oceno. Imunsko pogojena adrenalna insuficienca: Pri bolnikih, ki so prejemali zdravilo Imfinzi ali zdravilo Imfinzi v kombinaciji s tremelimumabom, se je pojavila imunsko pogojena adrenalna insuficienca. Bolnike je treba spremljati glede kliničnih znakov in simptomov adrenalne insuficience. Imunsko pogojena sladkorna bolezen tipa 1: Pri bolnikih, ki so prejemali zdravilo Imfinzi ali zdravilo Imfinzi v kombinaciji s tremelimumabom, se je pojavila imunsko pogojena sladkorna bolezen tipa 1, ki se lahko najprej kaže kot diabetična ketoacidoza, ki je lahko smrtno nevarna, če je dovolj zgodaj ne odkrijemo. Bolnike je treba spremljati glede kliničnih znakov in simptomov sladkorne bolezni tipa 1. Imunsko pogojeni hipofizitis/hipopituitarizem: Pri bolnikih, ki so prejemali zdravilo Imfinzi ali zdravilo Imfinzi v kombinaciji s tremelimumabom, sta se pojavila imunsko pogojena hipofizitis ali hipopituitarizem. Bolnike je treba spremljati glede kliničnih znakov in simptomov hipofizitisa ali hipopituitarizma. Imunsko pogojeni nefritis: Pri bolnikih, ki so prejemali zdravilo Imfinzi v kombinaciji s tremelimumabom, se je pojavil imunsko pogojeni nefritis, opredeljen kot potreba po sistemskih kortikosteroidih in brez jasne druge etiologije. Imunsko pogojeni izpuščaj: Pri bolnikih, ki so prejemali zdravilo Imfinzi ali zdravilo Imfinzi v kombinaciji s tremelimumabom, se je pojavil imunsko pogojeni izpuščaj ali dermatitis (vključno s pemfigoidom), opredeljen kot potreba po sistemskih kortikosteroidih in brez jasne druge etiologije. Pri bolnikih, ki so bili zdravljeni z zaviralci PD-1, so poročali o pojavljanju Stevens-Johnsonovega sindroma ali toksične epidermalne nekrolize. Imunsko pogojeni miokarditis: Pri bolnikih, ki so prejemali zdravilo Imfinzi ali zdravilo Imfinzi v kombinaciji s tremelimumabom, se je pojavil imunsko pogojeni miokarditis, ki je lahko usoden. Imunsko pogojeni pankreatitis: Pri bolnikih, ki so prejemali zdravilo Imfinzi v kombinaciji s tremelimumabom in kemoterapijo, se je pojavil imunsko pogojeni pankreatitis. Drugi imunsko pogojeni neželeni učinki: Glede na mehanizem delovanja zdravila Imfinzi ali zdravila Imfinzi v kombinaciji s tremelimumabom se lahko pojavijo še drugi potencialno imunsko pogojeni učinki. Naslednji imunsko pogojeni neželeni učinki so bili opaženi pri bolnikih, ki so prejemali samostojno zdravljenje z zdravilom Imfinzi ali zdravilo Imfinzi v kombinaciji s tremelimumabom: miastenija gravis, transverzni mielitis, miozitis, polimiozitis, meningitis, encefalitis, Guillain Barréjev sindrom, imunska trombocitopenija, neinfektivni cistitis. Z infundiranjem povezane reakcije: Bolnike je treba spremljati glede znakov in simptomov z infundiranjem povezanih reakcij. Pri bolnikih, ki so prejemali zdravilo Imfinzi ali zdravilo Imfinzi v kombinaciji s tremelimumabom, so bile opisane hude z infundiranjem povezane reakcije. Za bolezen specifični previdnostni ukrepi (RBT): Holangitis in okužbe bilarnega trakta pri bolnikih z napredovalim RBT niso redke. V študiji TOPAZ-1 so o primerih holangitisa poročali v obeh terapevtskih skupinah (14,5 % v skupini z zdravilom Imfinzi + kemoterapijo, 6,2 % v skupini s placebom + kemoterapijo); ti primeri so bili večinoma povezani z biliarnimi opornicami in niso imeli imunsko posredovane etiologije. Bolnike z RBT (zlasti tiste z biliarno opornico) je treba natančno nadzorovati glede holangitisa ali okužb biliarnega trakta tako pred uvedbo zdravljenja kot redno med zdravljenjem. Metastatski NSCLC: Podatkov o starejših bolnikih (≥ 75 let), zdravljenih z zdravilom Imfinzi v kombinaciji s tremelimumabom in kemoterapijo na osnovi platine, je malo. Morebitno korist/tveganje te sheme je priporočljivo skrbno pretehtati za vsakega bolnika posebej. Bolniki, ki niso bili vključeni v klinična preizkušanja: V klinična preskušanja niso bili vključeni bolniki z naslednjimi značilnostmi: izhodiščno oceno zmogljivosti ECOG ≥ 2; aktivno ali predhodno dokumentirano avtoimunsko boleznijo v 2 letih pred začetkom študije; anamnezo imunske pomanjkljivosti; anamnezo hudih imunsko pogojenih neželenih učinkov; boleznimi, ki so zahtevale sistemsko imunosupresijo, razen fiziološkega odmerka sistemskih kortikosteroidov (≤ 10 mg na dan prednizona ali ekvivalenta); neobvladanimi sočasnimi boleznimi; aktivno tuberkulozo ali okužbo s hepatitisom B ali C ali HIV; bolniki, ki so prejeli živo oslabljeno cepivo v 30 dneh pred začetkom zdravljenja z zdravilom Imfinzi ali v 30 dneh po začetku. Dokler takšnih podatkov ni, je treba durvalumab v teh skupinah bolnikov uporabljati previdno ter po skrbnem individualnem pretehtanju možnih koristi in tveganj za posameznega bolnika. Varnost sočasnega profilaktičnega kranialnega obsevanja obenem z zdravilom Imfinzi pri bolnikih z ES SCLC ni znana. **MEDSEBOJNO DELOVANJE Z DRUGIMI ZDRAVILI:** Razen fizioloških odmerkov sistemskih kortikosteroidov (≤ 10 mg na dan prednizona ali ekvivalenta) pred uvedbo durvalumaba ni priporočljivo uporabljati sistemskih kortikosteroidov ali imunosupresivov, ker lahko vplivajo na farmakodinamično aktivnost in učinkovitost durvalumaba. Vendar pa je mogoče kortikosteroide ali druge imunosupresive uporabiti po začetku zdravljenja z durvalumabom za zdravljenje imunsko pogojenih neželenih učinkov. Z durvalumabom niso izvedli formalnih farmakokinetičnih (PK) študij medsebojnega delovanja zdravil. Primarni poti odstranjevanja durvalumaba sta katabolizem beljakovin preko retikuloendotelijskega sistema oziroma tarčno posredovano odstranjevanje, zato ni pričakovati presenovnih medsebojnih delovanj med zdravili. Farmakokinetična medsebojna delovanja med durvalumabom in kemoterapijo so ocenjevali v študiji CASPIAN; izkazalo se je, da sočasno zdravljenje z durvalumabom ne vpliva na farmakokinetiko etopozida, karboplatina ali cisplatina. Poleg tega populacijska farmakokinetična analiza kaže, da sočasno zdravljenje s kemoterapijo ne vpliva pomembno na farmakokinetiko durvalumaba. Farmakokinetična medsebojna delovanja med durvalumabom v kombinaciji s tremelimumabom in kemoterapijo na osnovi platine so ocenili v študiji POSEIDON. Izkazalo se je, da med sočasnim zdravljenjem ni bilo klinično pomembnih farmakokinetičnih medsebojnih delovanj med tremelimumabom, durvalumabom, nab-paklitakselom, gemcitabinom, pemetreksedom, karboplatinom ali cisplatinom. **PLODNOST, NOSEČNOST IN DOJENJE:** Ženske v rodni dobi morajo med zdravljenjem z durvalumabom in vsaj še 3 mesece po zadnjem odmerku durvalumaba uporabljati učinkovito kontracepcijo. Podatkov o uporabi durvalumaba pri nosečnicah ni. Glede na mehanizem delovanja durvalumab lahko vpliva na vzdrževanje nosečnosti; v alogenskem modelu nosečnosti pri miših je bilo ugotovljeno, da moteno signaliziranje PD-L1 poveča izgubo plodov. Pri nosečnici uporabljeni durvalumab lahko škoduje plodu in ga ni priporočljivo uporabljati med nosečnostjo in pri ženskah v rodni dobi, ki ne uporabljajo učinkovite kontracepcije med zdravljenjem in vsaj še 3 mesece po zadnjem odmerku. Ni znano, ali se durvalumab pri človeku izloča v materinem mleku. Pri človeku protitelesa lahko prehajajo v materino mleko, a možnost absorpcije in škode za novorojenčka ni znana. Toda možnega tveganja za dojenega otroka ni mogoče izključiti. Odločiti se je treba, ali naj ženska prekine z dojenjem ali naj prekine zdravljenje z durvalumabom oziroma sploh ne začne zdravljenja z njim, pri čemer je treba upoštevati koristi dojenja za otroka in koristi zdravljenja za žensko. Podatkov o možnih vplivih durvalumaba na plodnost pri človeku ali živalih ni. **NEŽELENI UČINKI:** Ugotovitve o varnosti zdravila Imfinzi pri samostojnem zdravljenju temeljijo na kumulativnih podatkih 3006 bolnikov z več vrstami tumorjev. Zdravilo Imfinzi so uporabljali v odmerku 10 mg/kg na 2 tedna ali v odmerku 20 mg/kg na 4 tedne. Najpogostejši neželeni učinki (> 10 %) so bili kašelj/produktiven kašelj (21,5 %), driska (16,3 %), izpuščaj (16,0 %), zvišana telesna temperatura (13,8 %), okužbe zgornjih dihal (13,5 %), bolečine v trebuhu (12,7 %), srbenje (10,8 %) in hipotiroidizem (10,1 %). Podatki o varnosti zdravila Imfinzi v kombinaciji s kemoterapijo temeljijo na kumulativnih podatkih 685 bolnikov iz 2 študij (TOPAZ-1 in CASPIAN). Najpogostejši (> 10 %) neželeni učinki so bili nevtropenija (53,1 %), anemija (43,8 %), navzea (37,5 %), utrujenost (36,8 %), trombocitopenija (28,0 %), zaprtje (25,4 %), zmanjšan apetit (22,6 %), bolečine v trebuhu (18,4 %), alopecija (18,4 %), levkopenija (17,2 %), bruhanje (16,9 %), zvišana telesna temperatura (15,1 %), izpuščaj (14,8 %), driska (13,8 %), zvišana aspartat-aminotransferaza ali zvišana alanin-aminotransferaza (10,9 %), kašelj/produktiven kašelj (10,8 %) in srbenje (10,4 %). Izsledki o varnosti zdravila Imfinzi v kombinaciji s 75 mg tremelimumaba in kemoterapijo temeljijo na podatkih 330 bolnikov z metastatskim NSCLC. Najpogostejši (> 20 %) neželeni učinki so bili anemija (49,7 %), navzea (41,5 %), nevtropenija (41,2 %), utrujenost (36,1 %), izpuščaj (25,8 %), trombocitopenija (24,5 %) in driska (21,5 %). Izsledki o varnosti zdravila Imfinzi v kombinaciji z enkratnim odmerkom 300 mg tremelimumaba temeljijo na združenih podatkih 462 bolnikov s HCK iz študije HIMALAYA in še ene študije pri bolnikih s HCK, študija 22. Najpogostejši neželeni učinki (> 10 %) so bili izpuščaj (32,5 %), srbenje (25,5 %), driska (25,3 %), bolečine v trebuhu (19,7 %), zvišana aspartat aminotransferaza/zvišana alanin aminotransferaza (18,0 %), zvišana telesna temperatura (13,9 %), hipotiroidizem (13,0 %), kašelj/produktiven kašelj (10,8 %), periferni edemi (10,4 %) in zvišana lipaza (10,0 %). **VRSTA IN VSEBINA OVOJNINE:** 2,4 ml (skupno 120 mg durvalumaba) koncentrata v stekleni viali iz stekla tipa 1 z elastomernim zamaškom in sivo snemno aluminijsko zaporo. Pakiranje vsebuje 1 vialo. 10 ml (skupno 500 mg durvalumaba) koncentrata v stekleni viali iz stekla tipa 1 z elastomernim zamaškom in belo snemno aluminijsko zaporo. Pakiranje vsebuje 1 vialo. **NAČIN IZDAJANJA ZDRAVILA:** H - Predpisovanje in izdaja zdravila je le na recept. **DATUM REVIZIJA BESEDILA:** 30.1.2023 (SI-2851) **IMETNIK DOVOLJENJA ZA PROMET:** AstraZeneca AB, S-151 85, Södertälje, Švedska **Pred predpisovanjem, prosimo, preberite celoten povzetek glavnih značilnosti zdravila.** Dodatne informacije so na voljo pri družbi AstraZeneca UK Limited, Podružnica v Sloveniji, Verovškova 55, Ljubljana, telefon +386 1 51 35 600. Samo za strokovno javnost. Informacija pripravljena aprila 2023.

1. Paz-Ares L, Chen Y, Reinmuth N, et al. Durvalumab ± tremelimumab + platinum-etoposide in first-line extensive-stage SCLC (ES-SCLC): 3-year overall survival update from the phase 3 CASPIAN study; ESMO Open. 2022 Apr;7(2):100408. 2. Goldman JW, Garassino MC, Chen Y, et al. Patient-reported outcomes with first-line durvalumab plus platinum-etoposide versus platinum-etoposide in extensive-stage small-cell lung cancer (CASPIAN): a randomized, controlled, open-label, phase III study. Lung Cancer. 2020;149:46-52.

AstraZeneca

SI-2964

SKRAJŠAN POVZETEK GLAVNIH ZNAČILNOSTI ZDRAVILA

▼Za to zdravilo se izvaja dodatno spremljanje varnosti. Tako bodo hitreje na voljo nove informacije o njegovi varnosti. Zdravstvene delavce naprošamo, da poročajo o katerem koli domnevnem neželenem učinku zdravila.

Calquence 100 mg trde kapsule
Calquence 100 mg filmsko obložene tablete

SESTAVA: Ena trda kapsula vsebuje 100 mg akalabrutiniba. Ena filmsko obložena tableta vsebuje 100 mg akalabrutiniba (v obliki akalabrutinibijevega maleata). Akalabrutinib je selektiven zaviralec Brutonove tirozin-kinaze. **INDIKACIJE:** Zdravilo Calquence je kot monoterapija ali v kombinaciji z obinutuzumabom indicirano za zdravljenje odraslih bolnikov s predhodno nezdravljeno kronično limfocitno levkemijo. In kot monoterapija za zdravljenje odraslih bolnikov s kronično limfocitno levkemijo, ki so predhodno prejemali vsaj eno zdravljenje. **ODMERJANJE IN NAČIN UPORABE:** Zdravljenje s tem zdravilom mora uvesti in nadzorovati zdravnik, ki ima izkušnje z uporabo zdravil za zdravljenje raka. Priporočeni odmerek je 100 mg akalabrutiniba dvakrat na dan. Zdravljenje je treba nadaljevati do napredovanja bolezni ali nesprejemljive toksičnosti. Informacija o priporočenih prilagoditve odmerka zdravila Calquence v primeru neželenih učinkov ≥ 3. stopnje in pri uporabi z zaviralci ali induktorji CYP3A in zdravili za zmanjšanje izločanja želodčne kisline najdete v povzetku glavnih značilnosti zdravila. Starejšim bolnikom odmerka ni treba prilagoditi. Kliničnih študij pri bolnikih z okvaro ledvic niso izvedli. Bolnike z blago ali zmerno okvaro ledvic so zdravili v kliničnih študijah zdravila Calquence. Bolnikom z blago ali zmerno okvaro odmerka ni treba prilagoditi. Pri bolnikih s hudo okvaro ledvic se zdravilo Calquence lahko uporabi le, če koristi odtehtajo tveganje; te bolnike je treba skrbno spremljati glede znakov toksičnosti. Podatkov o bolnikih s hudo okvaro ledvic in bolnikih na dializi ni. Bolnikom z blago ali zmerno okvaro jeter odmerka ni treba prilagoditi. Vendar je treba bolnike z zmerno okvaro jeter natančno nadzorovati glede znakov toksičnosti. Zdravila Calquence ni priporočljivo uporabljati pri bolnikih s hudo okvaro jeter. Bolniki s hudimi srčno-žilnimi boleznimi niso bili vključeni v klinične študije zdravila Calquence. Varnost in učinkovitost zdravila Calquence pri otrocih in mladostnikih v starosti od 0 do 18 let nista bili dokazani. Zdravilo Calquence je namenjeno za peroralno uporabo. Kapsule ali tablete je treba zaužiti cele z vodo, vsak dan ob približno istem času, s hrano ali brez nje. Kapsul ali tablet se ne sme gristi, raztapljati ali odpirati. **KONTRAINDIKACIJE:** Preobčutljivost za zdravilno učinkovino ali katerokoli pomožno snov. **OPOZORILA IN PREVIDNOSTNI UKREPI:** Krvavitve: Pri bolnikih s hematološkimi malignomi, ki so bili zdravljeni z zdravilom Calquence v monoterapiji ali v kombinaciji z obinutuzumabom, so se pojavile večje krvavitve, vključno s krvavitvami v osrednjem živčevju in gastrointestinalnimi krvavitvami, v nekaterih primerih s smrtnim izidom. Ti dogodki so se pojavili tako pri bolnikih s trombocitopenijo kot tudi pri tistih brez nje. Na splošno pa so bile krvavitve manj hudi dogodki, ki so vključevali podplutbe in petehije. Bolniki, ki prejemajo antitrombotična zdravila, imajo večje tveganje za krvavitve. Varfarina ali drugih antagonistov vitamina K se ne sme uporabljati sočasno z zdravilom Calquence. Razmislite o koristih in tveganjih zadržanja zdravila Calquence vsaj 3 dni pred kirurškim posegom in po njem. Okužbe: Pri bolnikih s hematološkimi malignomi, ki so bili zdravljeni z zdravilom Calquence v monoterapiji ali v kombinaciji z obinutuzumabom, so se pojavile resne okužbe (bakterijske, virusne ali glivične), vključno s smrtnimi primeri. Te okužbe so se večinoma pojavile brez nevtropenije 3. ali 4. stopnje. Reaktivacija virusov: Pri bolnikih, ki so prejemali zdravilo Calquence, so poročali o primerih reaktivacije hepatitisa B. Med uporabo zdravila Calquence v okviru predhodnega ali sočasnega imunosupresivnega zdravljenja so poročali o primerih progresivne multifokalne levkoencefalopatije (PML), vključno s primeri s smrtnim izidom. Zdravniki morajo PML upoštevati v diferencialni diagnostiki pri bolnikih, ki imajo nove nevrološke, kognitivne ali vedenjske znake ali simptome, oziroma se jim ti znaki ali simptomi poslabšajo. V primeru suma na PML je treba zdravljenje z zdravilom Calquence prekiniti, dokler PML ni izključena. Citopenije: Pri bolnikih s hematološkimi malignomi, ki so bili zdravljeni z zdravilom Calquence v monoterapiji ali v kombinaciji z obinutuzumabom, so se med zdravljenjem pojavile citopenije 3. ali 4. stopnje, vključno z nevtropenijo, anemijo in trombocitopenijo. Drugi primarni malignomi: Pri bolnikih s hematološkimi malignomi, ki so bili zdravljeni z zdravilom Calquence v monoterapiji ali v kombinaciji z obinutuzumabom, so se pojavili drugi primarni malignomi, vključno s kožnim in nekožnim rakom. O kožnem raku so poročali pogosto. Atrijska fibrilacija: Pri bolnikih s hematološkimi malignomi, ki so bili zdravljeni z zdravilom Calquence v monoterapiji ali v kombinaciji z obinutuzumabom, se je pojavila atrijska fibrilacija/undulacija. **MEDSEBOJNO DELOVANJE Z DRUGIMI ZDRAVILI:** Sočasna uporaba močnih zaviralcev CYP3A in zdravila Calquence lahko poveča izpostavljenost akalabrutinibu in tako poveča tveganje za toksične učinke. Nasprotno pa lahko sočasna uporaba induktorjev CYP3A zmanjša izpostavljenost akalabrutinibu in tako pomeni tveganje za nezadostno učinkovitost. Sočasni uporabi z močnimi zaviralci CYP3A se je treba izogniti. Če bo uporaba teh zaviralcev kratkotrajna (npr. antiinfektivna zdravila do sedem dni), je treba zdravljenje z zdravilom Calquence prekiniti. V primeru uporabe zmernega zaviralca CYP3A je treba bolnike skrbno nadzorovati glede znakov toksičnosti. Sočasni uporabi z močnimi induktorji CYP3A4 se je treba izogibati zaradi tveganja za nezadostno učinkovitost. Tablete akalabrutiniba je mogoče jemati sočasno z zdravili za zmanjšanje izločanja želodčne kisline (zaviralci protonske črpalke, antagonisti receptorjev H2, antacidi), za razliko od kapsul akalabrutiniba, pri katerih je privzem z zdravili za zmanjšanje izločanja kisline moten. Ker zaviralci protonske črpalke učinkujejo dolgo časa, je mogoče, da časovna ločitev odmerkov zaviralcev protonske črpalke ne odpravi medsebojnega delovanja, zato se je treba sočasni uporabi s kapsulami akalabrutiniba izogniti. **NEŽELENI UČINKI:** Med bolniki, ki so prejemali zdravilo Calquence v monoterapiji, so bili najpogosteje poročani neželeni učinki katere koli stopnje okužba, glavobol, driska, podplutbe, mišično-skeletne bolečine, navzea, utrujenost, kašelj in izpuščaj. Najpogosteje poročani neželeni učinki ≥ 3. stopnje so bili okužba, levkopenija, nevtropenija in anemija. Med bolniki, ki so prejemali zdravilo Calquence v okviru kombiniranega zdravljenja, so bili najpogosteje poročani neželeni učinki katere koli stopnje okužba, mišično-skeletne bolečine, driska, glavobol, levkopenija, nevtropenija, kašelj, utrujenost, artralgija, navzea, omotica in zaprtje. Najpogosteje poročani neželeni učinki ≥ 3. stopnje so bili levkopenija, nevtropenija, okužba, trombocitopenija in anemija. Med bolniki, zdravljenimi z monoterapijo zdravila Calquence, so o prenehanju zdravljenja zaradi neželenih učinkih poročali pri 9,3 % bolnikov. Ti glavni neželeni učinki so vključevali pljučnico, trombocitopenijo in drisko. O zmanjšanju odmerka zaradi neželenih učinkov so poročali pri 4,2 % bolnikov. Ti glavni neželeni učinki so vključevali reaktivacijo hepatitisa B, sepso in drisko. Med bolniki, zdravljenimi z zdravilom Calquence v obliki kombiniranega zdravljenja, so o prenehanju zdravljenja zaradi neželenih učinkov poročali pri 10,8 % bolnikov. Ti glavni neželeni učinki so vključevali pljučnico, trombocitopenijo in drisko. O zmanjšanju odmerka zaradi neželenih učinkov so poročali pri 6,7 % bolnikov. Ti glavni neželeni učinki so vključevali nevtropenijo, drisko in bruhanje. **POSEBNA NAVODILA ZA SHRANJEVANJE:** Posebna navodila za shranjevanje niso potrebna. **VRSTA IN VSEBINA OVOJNINE:** Calquence 100 mg trde kapsule: Aluminij/aluminijski pretisni omoti s simboli sonca/lune, vsebujejo 6 ali 8 trdih kapsul. Škatle s 56 ali 60 kapsulami. Calquence 100 mg filmsko obložene tablete: Aluminij/aluminijska pakiranja pretisnih omotov s simboli sonca/lune, vsebujejo 8 ali 10 filmsko obloženih tablet. Škatle s 56 ali 60 tabletami. Na trgu morda ni vseh navedenih pakiranj. **NAČIN IZDAJANJA ZDRAVILA:** Rp/Spec - Predpisovanje in izdaja zdravila je le na recept s posebnim režimom. **DATUM REVIZIJE BESEDILA:** februar 2023 (SI-2882) **IMETNIK DOVOLJENJA ZA PROMET:** AstraZeneca AB, S-151 85, Sodertalje, Švedska **Pred predpisovanjem, prosimo, preberite celoten povzetek glavnih značilnosti zdravila.** Dodatne informacije so na voljo pri družbi AstraZeneca UK Limited, Podružnica v Sloveniji, Verovškova 55, Ljubljana.

Reference: 1. Barf, T. et al. (2017). Acalabrutinib (ACP-196): a covalent Bruton tyrosine kinase inhibitor with a differentiated selectivity and in vivo potency profile. Journal of Pharmacology and Experimental Therapeutics, 363(2), 240-252. **2.** Byrd, J. C., Hillmen, P., Ghia, P., Kater, A. P., Chanan-Khan, A., Furman, R. R., ... & Jurczak, W. (2021, July). Acalabrutinib versus ibrutinib in previously treated chronic lymphocytic leukemia: results of the first randomized phase III trial. American Society of Clinical Oncology (ASCO).

BTK = Brutonova tirozin-kinaza; **KLL =** kronična limfocitna levkemija

AstraZeneca

Dodatne informacije so na voljo pri družbi Astrazeneca UK Limited, Podružnica v Sloveniji, Verovškova 55, Ljubljana. Tel. (01) 51 35 600

Samo za strokovno javnost.
Datum priprave besedila: april 2023
SI-3038

CALQUENCE™
(akalabrutinib) 100 mg kapsule

ODOBRENO PO VSAJ ENI PREDHODNI TERAPIJI NA PODLAGI ANTI-HER2[1]

ENHERTU®
trastuzumab derukstekan

NEPRIMERLJIVO PREŽIVETJE*
POSTAVLJA NOVE STANDARDE ZDRAVLJENJA RAZSEJANEGA HER2+ RAKA DOJK[2]

Terapija prvega izbora za 2L v smernicah ESMO in NCCN[4,5]

Zdravilo ENHERTU se uporablja v monoterapiji in je v raziskavi DESTINY-Breast03 dokazalo neprimerljivo podaljšanje PFS v primerjavi s trenutnim standardom zdravljenja (T-DM1). Poročali so o primerih intersticijske pljučne bolezni (ILD) in pnevmonitisa. Za diagnozo je ključno prepoznavanje simptomov, zato je bolnike treba spremljati in pričeti z zdravljenjem ob prvih znakih ILD.[1,2]

SKRAJŠAN POVZETEK GLAVNIH ZNAČILNOSTI ZDRAVILA

▼Za to zdravilo se izvaja dodatno spremljanje varnosti. Tako bodo hitreje na voljo nove informacije o njegovi varnosti. Zdravstvene delavce naprošamo, da poročajo o katerem koli domnevnem neželenem učinku zdravila.

ENHERTU 100 mg prašek za koncentrat za raztopino za infundiranje

SESTAVA: Ena viala praška za koncentrat za raztopino za infundiranje vsebuje 100 mg trastuzumab derukstekana. Po rekonstituciji ena viala s 5 ml raztopine vsebuje 20 mg/ml trastuzumab derukstekana. Trastuzumab derukstekan je konjugat protitelesa in zdravila, ki vsebuje humanizirano monoklonsko protitelo IgG1 proti HER2 z istim zaporedjem aminokislin, kot ga ima trastuzumab. Proizvajajo ga sesalske celice (ovarij kitajskega hrčka) in je prek razcepljivega veznika na tetrapeptidni bazi kovalentno vezan na DXd, ki je derivat eksatekana in zaviralec topoizomeraze I. Na vsako molekulo protitelesa je vezanih približno 8 molekul derukstekana. *Pomožne snovi:* L-histidin, L-histidinijev klorid monohidrat, saharoza, polisorbat 80. **TERAPEVTSKE INDIKACIJE:** ***Rak dojk:*** *HER2-pozitiven rak dojk:* Zdravilo Enhertu kot monoterapija je indicirano za zdravljenje odraslih bolnikov z neresektabilnim ali metastatskim HER2-pozitivnim rakom dojk, ki so pred tem že prejeli eno ali več shem zdravljenja na podlagi anti-HER2. *Rak dojk z nizkim statusom HER2:* Zdravilo Enhertu kot monoterapija je indicirano za zdravljenje odraslih bolnikov z neresektabilnim ali metastatskim rakom dojk z nizkim statusom HER2, ki so pred tem že prejeli kemoterapijo v prisotnosti metastaz ali pa se je pri njih bolezen ponovila med adjuvantno kemoterapijo ali znotraj 6 mesecev po njenem zaključku. ***Rak želodca:*** Zdravilo Enhertu v obliki monoterapije je indicirano za zdravljenje odraslih bolnikov z napredovalim HER2-pozitivnim adenokarcinomom želodca ali gastroezofagealnega prehoda, ki so pred tem že prejeli shemo na podlagi trastuzumaba. **ODMERJANJE IN NAČIN UPORABE:** Zdravilo Enhertu mora predpisati zdravnik in njegovo dajanje nadzorovati zdravstveni delavec, ki sta izkušena v uporabi zdravil proti raku. Za preprečitev napak, povezanih z zdravili, je pomembno, da preverite nalepke na vialah in se prepričate, da je zdravilo, ki se pripravlja in daje, res zdravilo Enhertu (trastuzumab derukstekan), in ne trastuzumab ali trastuzumab emtanzin. Zdravilo Enhertu se ne sme zamenjati s trastuzumabom ali trastuzumab emtanzinom. Bolniki, ki se zdravijo s trastuzumab derukstekanom zaradi *HER2-pozitivnega raka dojk, raka želodca ali gastroezofagealnega prehoda*, morajo imeti dokumentiran HER2-pozitiven status tumorja, ki je opredeljen kot ocena 3 + na podlagi imunohistokemije (IHC) ali razmerje ≥ 2,0 na podlagi *in situ* hibridizacije (ISH) ali fluorescenčne *in situ* hibridizacije (FISH), ocenjeno z *in vitro* diagnostičnim (IVD) medicinskim pripomočkom z oznako CE. Bolniki, ki se zdravijo s trastuzumab derukstekanom zaradi *raka dojk z nizkim statusom HER2*, morajo imeti dokumentiran nizek status HER2 tumorja, ki je opredeljen kot ocena IHC 1+ ali IHC 2+/ISH-, ocenjeno z IVD z oznako CE. Če IVD z oznako CE ni na voljo, je treba status HER2 oceniti z drugim potrjenim testom Odmerjanje: *Rak dojk:* Priporočeni odmerek zdravila Enhertu je 5,4 mg/kg, ki se daje z intravensko infuzijo enkrat vsake 3 tedne (21-dnevni cikel) do napredovanja bolezni ali nesprejemljive toksičnosti. *Rak želodca:* Priporočeni odmerek zdravila Enhertu je 6,4 mg/kg, ki se daje z intravensko infuzijo enkrat vsake 3 tedne (21-dnevni cikel) do napredovanja bolezni ali nesprejemljive toksičnosti. Začetni odmerek je treba dati z 90-minutno intravensko infuzijo. Če bolnik prejšnjo infuzijo dobro prenaša, se lahko naslednji odmerki zdravila Enhertu dajejo kot 30-minutne infuzije. Hitrost infundiranja zdravila Enhertu je treba zmanjšati ali infundiranje prekiniti, če se pri bolniku razvijejo simptomi, povezani z infuzijo. V primeru hudih reakcij na infuzijo je treba zdravilo Enhertu trajno ukiniti. Premedikacija: Zdravilo Enhertu je emetogeno, kar vključuje zapoznelo navzeo in/ali bruhanje. Pred vsakim odmerkom zdravila Enhertu je treba bolnike premedicirati s kombiniranim režimom dveh ali treh zdravil (npr. deksametazon z antagonistom receptorjev 5-HT3 in/ali antagonistom receptorjev NK1 ter drugimi zdravili, kot je indicirano) za preprečevanje navzee in bruhanja zaradi kemoterapije. Prilagajanje odmerka: Obvladovanje neželenih učinkov lahko zajema začasno prekinitev uporabe, zmanjšanje odmerka ali ukinitev zdravljenja z zdravilom Enhertu, skladno s smernicami, podanimi v povzetku glavnih značilnosti zdravila (preglednici 1 in 2). Po zmanjšanju odmerka zdravila Enhertu se odmerek ne sme več ponovno povečati. Načrt zmanjševanja odmerka: Priporočeni začetni odmerek je 5,4 mg/kg pri raku dojk oz. 6,4 mg/kg pri raku želodca; prvo zmanjšanje odmerka (4,4 mg/kg oz. 5,4 mg/kg), drugo zmanjšanje odmerka (3,2 mg/kg oz. 4,4 mg/kg), pri potrebi po nadaljnjem zmanjšanju odmerka ukinite zdravljenje. *Prosimo, glejte celoten povzetek glavnih značilnosti zdravila Enhertu za prilagajanje odmerka zaradi neželenih učinkov: intersticijska pljučna bolezen (IPB)/pnevmonitis* (asimptomatska IPB/asimptomatski pnevmonitis (stopnja 1), simptomatska IPB/simptomatski pnevmonitis (stopnja 2 ali višja)), *nevtropenija* (stopnja 3 (manj kot 1,0-0,5 × 10^9/l), stopnja 4 (manj kot 0,5 × 10^9/l)), *febrilna nevtropenija* (absolutno število nevtrofilcev manj kot 1,0 × 10^9/l in telesna temperatura, višja od 38,3 °C, ali telesna temperatura 38 °C ali višja, ki vztraja več kot eno uro), *zmanjšan iztisni delež levega prekata* (LVEF) (LVEF več kot 45 % in absolutno zmanjšanje glede na izhodiščno vrednost za 10 % do 20 %; LVEF 40 % do 45 %; LVEF manj kot 40 % ali absolutno zmanjšanje glede na izhodiščno vrednost za več kot 20 %; simptomatično kongestivno srčno popuščanje). Zakasnjen ali izpuščen odmerek: Če se načrtovani odmerek zakasni ali izpusti, ga je treba dati takoj, ko je mogoče, brez čakanja na naslednji načrtovani cikel. Časovni načrt dajanja je treba prilagoditi, da se ohrani 3-tedenski razmik med odmerki. Infuzijo je treba dati s hitrostjo in odmerkom, ki ga je bolnik prenašal pri zadnji infuziji. Posebne populacije: *Starejši:* Pri bolnikih, starih 65 let ali starejših, prilagajanje odmerka zdravila Enhertu ni potrebno. Podatki pri bolnikih, starih ≥ 75 let, so omejeni. *Okvara ledvic:* Prilagajanje odmerka pri bolnikih z blago (očistek kreatinina [CLcr] ≥ 60 in < 90 ml/min) ali zmerno (CLcr ≥ 30 in < 60 ml/min) okvaro ledvic ni potrebno. Morebitne potrebe po prilagajanju odmerka pri bolnikih s hudo okvaro ledvic ali končno ledvično odpovedjo ni mogoče opredeliti, ker je bila huda okvara ledvic v kliničnih študijah izključitveni kriterij. Pri bolnikih z zmerno okvaro ledvic so opazili višjo pogostnost IPB stopnje 1 in 2/pnevmonitisa, ki sta vodila do zvečanja števila prekinitev zdravljenja. Pri bolnikih z zmerno okvaro ledvic v izhodišču, ki so prejemali zdravilo Enhertu 6,4 mg/kg, so ugotovili večjo pogostnost resnih neželenih učinkov kot pri tistih z normalnim delovanjem ledvic. Bolnike z zmerno ali hudo okvaro ledvic je treba natančno spremljati glede neželenih učinkov, vključno z IPB/pnevmonitisom. *Okvara jeter:* Pri bolnikih, ki imajo celokupni bilirubin ≤ 1,5-kratnik zgornje meje normalnih vrednosti (ZMN), ne glede na vrednost aspartat transaminaze (AST), odmerka ni treba prilagajati. Morebitne potrebe po prilagajanju odmerka pri bolnikih, ki imajo celokupni bilirubin > 1,5-kratnik ZMN, ne glede na vrednost AST, ni mogoče opredeliti zaradi pomanjkanja podatkov. Zato je treba te bolnike natančno spremljati. Način uporabe: Zdravilo Enhertu je za intravensko uporabo. Zdravstveni delavec ga mora rekonstituirati in razredčiti. Treba ga je dati z intravenskim infundiranjem. Zdravilo Enhertu se ne sme dati kot hitro intravensko injekcijo ali bolus. **KONTRAINDIKACIJE:** Preobčutljivost na učinkovino ali katero koli pomožno snov. **POSEBNA OPOZORILA IN PREVIDNOSTNI UKREPI:** Intersticijska pljučna bolezen/pnevmonitis: Pri zdravilu Enhertu so poročali o primerih intersticijske pljučne bolezni (IPB) in/ali pnevmonitisa. Nekateri primeri so bili smrtni. Bolnikom je treba naročiti, naj takoj poročajo o kašlju, dispneji, zvišani telesni temperaturi in/ali katerih koli novih dihalnih simptomih ali poslabšanju obstoječih. Bolnike je treba spremljati glede znakov in simptomov IPB/pnevmonitisa. Dokaze za IPB/pnevmonitis je treba takoj proučiti. Bolnike s sumom na IPB/pnevmonitis je treba oceniti z radiografskimi posnetki, najbolje z računalniško tomografijo (CT). Treba je razmisliti o posvetu s pulmologom. Nevtropenija: V kliničnih študijah z zdravilom Enhertu so poročali o primerih nevtropenije, vključno s primeri febrilne nevtropenije s smrtnim izidom. Pred uvedbo zdravila Enhertu in pred vsakim odmerkom ter vsakič, ko je klinično indicirano, je treba preveriti celotno krvno sliko. Morda bo treba začasno prekiniti dajanje zdravila Enhertu ali zmanjšati odmerek, odvisno od tega, kako huda je nevtropenija. Zmanjšanje iztisnega deleža levega prekata: Pri zdravljenjih anti-HER2 so poročali o zmanjšanem iztisnem deležu levega prekata (LVEF). Pred uvedbo zdravljenja z zdravilom Enhertu in v rednih intervalih med njim (v skladu s kliničnimi indikacijami) je treba izvesti standardne preiskave delovanja srca (ehokardiografija ali slikanje MUGA) za oceno LVEF. Zmanjšanje LVEF je treba obvladovati s prekinitvami zdravljenja. Zdravljenje z zdravilom Enhertu je treba trajno ukiniti, če se potrdi LVEF manj kot 40 % ali absolutno zmanjšanje glede na izhodiščno vrednost za več kot 20 %. Zdravilo Enhertu je treba trajno ukiniti pri bolnikih s simptomatskim kongestivnim srčnim popuščanjem. Embrio-fetalna toksičnost: Zdravilo Enhertu lahko ima škodljiv vpliv na plod, če se da nositi. Pri ženskah v rodni dobi je treba pred uvedbo zdravljenja z zdravilom Enhertu preveriti status nosečnosti. Bolnice je treba sezanaiti z možnimi tveganji za plod. Ženskam v rodni dobi je treba svetovati, da uporabljajo učinkovito kontracepcijo med zdravljenjem in še vsaj 7 mesecev po zadnjem odmerku zdravila Enhertu. Moškim bolnikom s partnerkami v rodni dobi je treba svetovati, da uporabljajo učinkovito kontracepcijo med zdravljenjem z zdravilom Enhertu in še vsaj 4 mesece po zadnjem odmerku zdravila Enhertu. Bolniki z zmerno ali hudo okvaro jeter: Zdravilo Enhertu je treba pri bolnikih z zmerno in hudo okvaro jeter dajati previdno. **MEDSEBOJNO DELOVANJE Z DRUGIMI ZDRAVILI IN DRUGE OBLIKE INTERAKCIJ:** Pri sočasnem dajanju trastuzumab derukstekana z zdravili, ki so zaviralci CYP3A ali OATP1B ali prenašalcev P-gp, odmerka ni treba prilagajati. **PLODNOST, NOSEČNOST IN DOJENJE:** Nosečnost: Dajanje zdravila Enhertu nosečnicam se ne priporoča. Bolnice je treba seznaniti z možnimi tveganji za plod, preden zanosijo. Ženske, ki zanosijo, se morajo takoj obrniti na zdravnika. Če ženska zanosi med zdravljenjem z zdravilom Enhertu ali v obdobju 7 mesecev po zadnjem odmerku zdravila Enhertu, se priporoča natančno spremljanje. Dojenje: Ni znano, ali se trastuzumab derukstekan izloča v materino mleko. Humani IgG se izloča v materino mleko in potencial za absorpcijo in resne neželene učinke na dojenčka ni znan. Zato ženske ne smejo dojiti med zdravljenjem z zdravilom Enhertu in še 7 mesecev po zadnjem odmerku. Odločiti se je treba med prenehanjem dojenja in prenehanjem zdravljenja z zdravilom Enhertu, pri čemer je treba pretehtati prednosti dojenja za otroka in prednosti zdravljenja za mater. Plodnost: Namenskih študij plodnosti s trastuzumab derukstekanom niso izvedli. Ni znano, ali so trastuzumab derukstekan ali njegovi presnovki prisotni v semenski tekočini. Pred začetkom zdravljenja je treba moškim bolnikom svetovati, da se posvetujejo o možnosti shranjevanja semena. Moški bolniki v celotnem obdobju zdravljenja in še najmanj 4 mesece po zadnjem odmerku zdravila Enhertu ne smejo zamrzniti ali darovati semena. **NEŽELENI UČINKI:** *Zdravilo Enhertu 5,4 mg/kg:* Združeno varnostno populacijo so ocenili pri bolnikih, ki so v kliničnih študijah dobili vsaj en odmerek 5,4 mg/kg zdravila Enhertu (N = 944) zaradi različnih vrst tumorjev. Mediani čas trajanja zdravljenja v tej združeni populaciji je bil 39,6 meseca (razpon: 0,2-37,9 meseca). *Zelo pogosti:* okužba zgornjih dihal, anemija, nevtropenija, trombocitopenija, levkopenija, zmanjšan apetit, hipokaliemija, glavobol, omotica, intersticijska pljučna bolezen, kašelj, dispneja, epistaksa, navzea, bruhanje, driska, zaprtje, bolečina v trebuhu, stomatitis, dispepsija, zvišane transaminaze, alopecija, izpuščaj, mišično-skeletna bolečina, utrujenost, pireksija, zmanjšanje telesne mase, zmanjšan iztisni delež. *Pogosti:* pljučnica, limfopenija, febrilna nevtropenija, dehidracija, disgevzija, zameglјen vid, abdominalna distenzija, flatulenca, gastritis, pruritus, hiperpigmentacija kože, perifermni edem, zvišana alkalna fosfataza v krvi, zvišan bilirubin v krvi, zvišan kreatinin v krvi, reakcije povezane z infuzijo. *Zdravilo Enhertu 6,4 mg/kg:* Združeno varnostno populacijo so ocenili za bolnike, ki so v kliničnih študijah dobili vsaj en odmerek 6,4 mg/kg zdravila Enhertu (N = 619) zaradi različnih vrst tumorjev. Mediani čas trajanja zdravljenja v tej združeni populaciji je bil 5,6 meseca (razpon: 0,7-41,0 meseca). *Zelo pogosti:* okužba zgornjih dihal, pljučnica, anemija, nevtropenija, trombocitopenija, levkopenija, limfopenija, zmanjšan apetit, hipokaliemija, glavobol, disgevzija, intersticijska pljučna bolezen, kašelj, navzea, bruhanje, driska, zaprtje, bolečina v trebuhu, stomatitis, zvišane transaminaze, alopecija, mišično-skeletna bolečina, utrujenost, pireksija, perifermni edem, zmanjšanje telesne mase, zmanjšan iztisni delež. *Pogosti:* febrilna nevtropenija, dehidracija, omotica, zameglјen vid, dispneja, epistaksa, dispepsija, izpuščaj, pruritus, hiperpigmentacija kože, zvišana alkalna fosfataza v krvi, zvišan bilirubin v krvi, zvišan kreatinin v krvi, reakcije povezane z infuzijo. **IMETNIK DOVOLJENJA ZA PROMET Z ZDRAVILOM:** Daiichi Sankyo Europe GmbH, Zielstattstrasse 48, 81379 München, Nemčija **DATUM ZADNJE REVIZIJE BESEDILA:** 23. 1. 2023 (SI-2799) **REŽIM PREDPISOVANJA IN IZDAJE:** H **Prosimo, da pred predpisovanjem preberete celoten povzetek glavnih značilnosti zdravila.** Dodatne informacije so na voljo pri podjetju AstraZeneca UK Limited, Podružnica v Sloveniji, Verovškova 55, 1000 Ljubljana, telefon: 01/51 35 600.

* zmanjšanje tveganja za napredovanje bolezni ali smrti (PFS)

** tveganje za napredovanje bolezni ob zdravljenju z zdravilom ENHERTU v primerjavi s T-DM1 (HR: 0,33; 95 % IZ: 0,26-0,43; p<0,000001, ključni opazovani dogodek raziskave: PFS glede na BICR). Mediani PFS je znašal **28,8 mesecev** pri bolnikih, ki so prejemali ENHERTU, v primerjavi s **6,8 mesecev** pri bolnikih zdravljenih s T-DM1[3]

PFS - preživetje brez napredovanja bolezni, **mPFS** - mediano preživetje brez napredovanja bolezni, **T-DM1** - trastuzumab emtanzin, **BICR** - ocena slepega neodvisnega centralnega pregleda, **IZ** - interval zaupanja, **HR** - razmerje ogroženosti

Literatura: 1. Povzetek glavnih značilnosti zdravila ENHERTU, 23. 1. 2023, **2.** Cortes J et al; Trastuzumab Deruxtecan versus Trastuzumab Emtansine for Breast Cancer; NEJM 2022;386(12):1143-1154, **3.** Hurvitz SA et al, Presented at SABCS 2022, 6-10.12.2022 in San Antonio. Presentation ID: GS2-02, **4.** Gennari A et al: Ann Oncol 2021;32(12): 1475-1495 **5.** NCCN guidelines Breast Cancer, v2.2023, https://www.nccn.org/guidelines/category_1, dostopano 10.3.2023.

Daiichi-Sankyo | AstraZeneca

Datum priprave materiala: maj 2023. Samo za strokovno javnost. SI-3059

5 NA NOVO razvrščenih indikacij:[1]

KEYTRUDA®
(pembrolizumab, MSD)

- **MELANOM,** adjuvantno zdravljenje melanoma v stadiju IIB/IIC[2]
- **RAK LEDVIČNIH CELIC,** adjuvantno zdravljenje po nefrektomiji[2]
- **KOLOREKTALNI RAK,** z MSI-H ali dMMR, metastatski, samostojno zdravljenje v 1L[2]
- **TROJNO NEGATIVNI RAK DOJK:**
  – v kombinaciji s kemoterapijo za neoadjuvantno, v nadaljevanju samostojno adjuvantno zdravljenje lokalno napredovalega TNRD ali TNRD v zgodnjem stadiju z visokim tveganjem za ponovitev bolezni[2]
  – v kombinaciji s kemoterapijo za zdravljenje lokalno ponovljenega neoperabilnega ali metastatskega TNRD z PD-L1 CPS ≥ 10[2]

Okrajšave: MSI-H - visoka mikrosatelitska nestabilnost; dMMR - pomankljivo popravljanje neujemanja pri podvojevanju DNA; 1L - prva linija zdravljenja; TNRD - trojno negativni rak dojk

Referenci: 1. www.zzzs.si; https://www.zzzs.si/zzzs-api/e-gradiva/vsa-gradiva/?vrsta=BR3A2Q326 (22.12.2022) 2. KEYTRUDA SPC

Ime zdravila: KEYTRUDA 25 mg/ml koncentrat za raztopino za infundiranje vsebuje pembrolizumab. Terapevtske indikacije: Zdravilo KEYTRUDA je kot samostojno zdravljenje indicirano za zdravljenje: odraslih in mladostnikov, starih 12 let ali več, z napredovalim (neoperabilnim ali metastatskim) melanomom; za adjuvantno zdravljenje odraslih in mladostnikov, starih 12 let ali več, z melanomom v stadiju IIB, IIC ali III, in sicer po popolni kirurški odstranitvi; metastatskega nedrobnoceličnega pljučnega raka (NSCLC) v prvi liniji zdravljenja pri odraslih, ki imajo tumorje z ≥ 50 % izraženostjo PD-L1 (TPS) in brez pozitivnih tumorskih mutacij EGFR ali ALK; lokalno napredovalega ali metastatskega NSCLC pri odraslih, ki imajo tumorje z ≥ 1 % izraženostjo PD-L1 (TPS) in so bili predhodno zdravljeni z vsaj eno shemo kemoterapije, bolniki s pozitivnimi tumorskimi mutacijami EGFR ali ALK so pred prejemom zdravila KEYTRUDA morali prejeti tudi tarčno zdravljenje; odraslih in pediatričnih bolnikov, starih 3 leta ali več, s ponovljenim ali neodzivnim klasičnim Hodgkinovim limfomom (cHL), pri katerih avtologna presaditev matičnih celic (ASCT) ni bila uspešna, ali po najmanj dveh predhodnih zdravljenjih kadar ASCT ne pride v poštev kot možnost zdravljenja; lokalno napredovalega ali metastatskega urotelijskega raka pri odraslih, predhodno zdravljenih s kemoterapijo, ki je vključevala platino; lokalno napredovalega ali metastatskega urotelijskega raka pri odraslih, ki niso primerni za zdravljenje s kemoterapijo, ki vsebuje cisplatin in imajo tumorje z izraženostjo PD-L1 ≥ 10, ocenjeno s kombinirano pozitivno oceno (CPS); ponovljenega ali metastatskega ploščatoceličnega raka glave in vratu (HNSCC) pri odraslih, ki imajo tumorje z ≥ 50 % izraženostjo PD-L1 (TPS), in pri katerih je bolezen napredovala med zdravljenjem ali po zdravljenju s kemoterapijo, ki je vključevala platino; za adjuvantno zdravljenje odraslih z rakom ledvičnih celic s povišanim tveganjem za ponovitev bolezni po nefrektomiji, ali po nefrektomiji in kirurški odstranitvi metastatskih lezij, za zdravljenje odraslih z MSI-H (microsatellite instability-high) ali dMMR (mismatch repair deficient) kolorektalnim rakom v naslednjih terapevtskih okoliščinah: prva linija zdravljenja metastatskega kolorektalnega raka; zdravljenje neoperabilnega ali metastatskega kolorektalnega raka po predhodnem kombiniranem zdravljenju, ki je temeljilo na fluoropirimidinu; in za zdravljenje MSI-H ali dMMR tumorjev pri odraslih z: napredovalim ali ponovljenim rakom endometrija, pri katerih je bolezen napredovala med ali po predhodnem zdravljenju, ki je vključevalo platino, v katerih koli terapevtskih okoliščinah, in ki niso kandidati za kurativno operacijo ali obsevanje; neoperabilnim ali metastatskim rakom želodca, tankega črevesa ali žolčnika in žolčnih vodov, pri katerih je bolezen napredovala med ali po vsaj enem predhodnem zdravljenju. Zdravilo KEYTRUDA je kot samostojno zdravljenje ali v kombinaciji s kemoterapijo s platino in 5-fluorouracilom (5-FU) indicirano za prvo linijo zdravljenja metastatskega ali neoperabilnega ponovljenega ploščatoceličnega raka glave in vratu pri odraslih, ki imajo tumorje z izraženostjo PD-L1 s CPS ≥ 1. Zdravilo KEYTRUDA je v kombinaciji s pemetreksedom in kemoterapijo na osnovi platine indicirano za prvo linijo zdravljenja metastatskega neploščatoceličnega NSCLC pri odraslih, pri katerih tumorji nimajo pozitivnih mutacij EGFR ali ALK; v kombinaciji s karboplatinom in bodisi paklitakselom bodisi nab-paklitakselom je indicirano za prvo linijo zdravljenja metastatskega ploščatoceličnega NSCLC pri odraslih; v kombinaciji z aksitinibom ali v kombinaciji z lenvatinibom je indicirano za prvo linijo zdravljenja napredovalega raka ledvičnih celic (RCC) pri odraslih; v kombinaciji s kemoterapijo s platino in fluoropirimidinom je indicirano za prvo linijo zdravljenja lokalno napredovalega neoperabilnega ali metastatskega raka požiralnika ali HER-2 negativnega adenokarcinoma gastroezofagealnega prehoda pri odraslih, ki imajo tumorje z izraženostjo PD-L1 s CPS ≥ 10; v kombinaciji s kemoterapijo za neoadjuvantno zdravljenje, in v nadaljevanju kot samostojno adjuvantno zdravljenje po kirurškem posegu, je indicirano za zdravljenje odraslih z lokalno napredovalim trojno negativnim rakom dojk ali trojno negativnim rakom dojk v zgodnjem stadiju z visokim tveganjem za ponovitev bolezni; v kombinaciji s kemoterapijo je indicirano za zdravljenje lokalno ponovljenega neoperabilnega ali metastatskega trojno negativnega raka dojk pri odraslih, ki imajo tumorje z izraženostjo PD-L1 s CPS ≥ 10 in predhodno niso prejeli kemoterapije za metastatsko bolezen; v kombinaciji z lenvatinibom je indicirano za zdravljenje napredovalega ali ponovljenega raka endometrija (EC) pri odraslih z napredovalo boleznijo med ali po predhodnem zdravljenju s kemoterapijo, ki je vključevala platino, v katerih koli terapevtskih okoliščinah, in ki niso kandidati za kurativno operacijo ali obsevanje; v kombinaciji s kemoterapijo, z bevacizumabom ali brez njega, je indicirano za zdravljenje persistentnega, ponovljenega ali metastatskega raka maternične vratu pri odraslih bolnicah, ki imajo tumorje z izraženostjo PD-L1 s CPS ≥ 1. **Odmerjanje in način uporabe:** Testiranje PD-L1: Če je navedeno v indikaciji, je treba izbiro bolnika za zdravljenje z zdravilom KEYTRUDA na podlagi izraženosti PD-L1 tumorja potrditi z validirano preiskavo. Testiranje MSI/MMR: Če je navedeno v indikaciji, je treba izbiro bolnika za zdravljenje z zdravilom KEYTRUDA na podlagi MSI-H/dMMR statusa tumorja potrditi z validirano preiskavo. Odmerjanje: Priporočeni odmerek zdravila KEYTRUDA pri odraslih je bodisi 200 mg na 3 tedne ali 400 mg na 6 tednov, apliciran z intravensko infuzijo v 30 minutah. Priporočeni odmerek zdravila KEYTRUDA za samostojno zdravljenje pri pediatričnih bolnikih s cHL, starih 3 leta ali več, ali bolnikih z melanomom, starih 12 let ali več, je 2 mg/kg telesne mase (do največ 200 mg) na 3 tedne, apliciran z intravensko infuzijo v 30 minutah. Za uporabo v kombinaciji glejte povzetke glavnih značilnosti zdravil sočasno uporabljenih zdravil. Če se uporablja kot del kombiniranega zdravljenja skupaj z intravensko kemoterapijo, je treba zdravilo KEYTRUDA aplicirati prvo. Bolnike je treba zdraviti do napredovanja bolezni ali nesprejemljivih toksičnih učinkov (in do maksimalnega trajanja zdravljenja, če je le to določeno za indikacijo). Pri adjuvantnem zdravljenju melanoma ali RCC je treba zdravilo uporabljati do ponovitve bolezni, pojava nesprejemljivih toksičnih učinkov oziroma mora zdravljenje trajati do enega leta. Za neoadjuvantno in adjuvantno zdravljenje TNBC morajo bolniki neoadjuvantno prejeti zdravilo KEYTRUDA v kombinaciji s kemoterapijo, in sicer 8 odmerkov po 200 mg na 3 tedne ali 4 odmerke po 400 mg na 6 tednov, ali do napredovanja bolezni, ki izključuje definitivni kirurški poseg, ali do pojava nesprejemljivih toksičnih učinkov, čemur sledi adjuvantno zdravljenje z zdravilom KEYTRUDA kot samostojnim zdravljenjem, in sicer 9 odmerkov po 200 mg na 3 tedne ali 5 odmerkov po 400 mg na 6 tednov ali do ponovitve bolezni ali pojava nesprejemljivih toksičnih učinkov. Bolniki, pri katerih pride do napredovanja bolezni, ki izključuje definitivni kirurški poseg, ali do nesprejemljivih toksičnih učinkov povezanih z zdravilom KEYTRUDA kot neoadjuvantnim zdravljenjem v kombinaciji s kemoterapijo, ne smejo prejeti zdravila KEYTRUDA kot samostojnega zdravljenja za adjuvantno zdravljenje. Če je aksitinib uporabljen v kombinaciji s pembrolizumabom, se lahko razmisli o povečanju odmerka aksitiniba nad začetnih 5 mg v presledkih šest tednov ali več. V primeru uporabe v kombinaciji z lenvatinibom je treba zdravljenje z enim ali obema zdraviloma prekiniti, kot je primerno. Uporabo lenvatiniba je treba zadržati, odmerek zmanjšati ali prenehati z uporabo, v skladu z navodili v povzetku glavnih značilnosti zdravila za lenvatinib, in sicer za kombinacijo s pembrolizumabom. Pri bolnikih starih ≥ 65 let, bolnikih z blago do zmerno okvaro ledvic, bolnikih z blago ali zmerno okvaro jeter prilagoditev odmerka ni potrebna. Odložitev odmerka ali ukinitev zdravljenja: Zmanjšanje odmerka zdravila KEYTRUDA ni priporočljivo. Za obvladovanje neželenih učinkov je treba uporabo zdravila KEYTRUDA zadržati ali ukiniti, prosimo, glejte celoten Povzetek glavnih značilnosti zdravila. **Kontraindikacije:** Preobčutljivost na učinkovino ali katero koli pomožno snov. **Povzetek posebnih opozoril, previdnostnih ukrepov, interakcij in neželenih učinkov:** Imunsko pogojeni neželeni učinki (pnevmonitis, kolitis, hepatitis, nefritis, endokrinopatije, neželeni učinki na kožo in drugi): Pri bolnikih, ki so prejemali pembrolizumab, so se pojavili imunsko pogojeni neželeni učinki, vključno s hudimi in smrtnimi primeri. Večina imunsko pogojenih neželenih učinkov, ki so se pojavili med zdravljenjem s pembrolizumabom, je bila reverzibilnih in so jih obvladali s prekinitvami uporabe pembrolizumaba, uporabo kortikosteroidov in/ali podporno oskrbo. Pojavijo se lahko tudi po zadnjem odmerku pembrolizumaba in hkrati prizadanejo več organskih sistemov. V primeru suma na imunsko pogojene neželene učinke je treba poskrbeti za ustrezno oceno za potrditev etiologije oziroma izključitev drugih vzrokov. Glede na izrazitost neželenega učinka je treba zadržati uporabo pembrolizumaba in uporabiti kortikosteroide – za natančna navodila, prosimo, glejte Povzetek glavnih značilnosti zdravila Keytruda. Zdravljenje s pembrolizumabom lahko poveča tveganje za zavrnitev pri prejemnikih presadkov čvrstih organov. Pri bolnikih, ki so prejemali pembrolizumab, so poročali o hudih z infuzijo povezanih reakcijah, vključno s preobčutljivostjo in anafilaksijo. Pembrolizumab se iz obtoka odstrani s katabolizmom, zato presnovnih medsebojnih delovanj zdravil ni pričakovati. Uporabi sistemskih kortikosteroidov ali imunosupresivov pred uvedbo pembrolizumaba se je treba izogibati, ker lahko vplivajo na farmakodinamično aktivnost in učinkovitost pembrolizumaba. Vendar pa je kortikosteroide ali druge imunosupresive mogoče uporabiti za zdravljenje imunsko pogojenih neželenih učinkov. Kortikosteroide je mogoče uporabiti tudi kot premedikacijo, če je pembrolizumab uporabljen v kombinaciji s kemoterapijo, kot antiemetično profilakso in/ali za ublažitev neželenih učinkov, povezanih s kemoterapijo. Ženske v rodni dobi morajo med zdravljenjem s pembrolizumabom in vsaj še 4 mesece po zadnjem odmerku pembrolizumaba uporabljati učinkovito kontracepcijo, med nosečnostjo in dojenjem se ga ne sme uporabljati. Varnost pembrolizumaba pri samostojnem zdravljenju so v kliničnih študijah ocenili pri 7.631 bolnikih, ki so imeli različne vrste raka, s štirimi odmerki (2 mg/kg telesne mase na 3 tedne, 200 mg na 3 tedne in 10 mg/kg telesne mase na 2 ali 3 tedne). V tej populaciji bolnikov je mediani čas opazovanja znašal 8,5 meseca (v razponu od 1 dneva do 39 mesecev), najpogostejši neželeni učinki zdravljenja s pembrolizumabom pa so bili utrujenost (31 %), diareja (22 %) in navzea (20 %). Večina poročanih neželenih učinkov pri samostojnem zdravljenju je bila po izrazitosti 1. ali 2. stopnje. Najresnejši neželeni učinki so bili imunsko pogojeni neželeni učinki in hude z infuzijo povezane reakcije. Pojavnost imunsko pogojenih neželenih učinkov pri uporabi pembrolizumaba samega za adjuvantno zdravljenje (n = 1.480) je znašala 36,1 % za vse stopnje in 8,9 % od 3. do 5. stopnje, pri metastatski bolezni (n = 5.375) pa 24,2 % za vse stopnje in 6,4 % od 3. do 5. stopnje. Pri adjuvantnem zdravljenju niso zaznali nobenih novih imunsko pogojenih neželenih učinkov. Varnost pembrolizumaba pri kombiniranem zdravljenju s kemoterapijo so ocenili pri 3.123 bolnikih z različnimi vrstami raka, ki so v kliničnih študijah prejemali pembrolizumab v odmerkih 200 mg, 2 mg/kg telesne mase ali 10 mg/kg telesne mase na vsake 3 tedne. V tej populaciji bolnikov so bili najpogostejši neželeni učinki naslednji: anemija (55 %), navzea (54 %), utrujenost (38 %), nevtropenija (36 %), zaprtost (35 %), alopecija (35 %), diareja (34 %), bruhanje (28 %) in zmanjšanje apetita (27 %). Pojavnost neželenih učinkov 3. do 5. stopnje je pri bolnikih z NSCLC pri kombiniranem zdravljenju s pembrolizumabom znašala 67 % in pri zdravljenju samo s kemoterapijo 66 %, pri bolnikih s HNSCC pri kombiniranem zdravljenju s pembrolizumabom 85 % in pri zdravljenju s kemoterapijo v kombinaciji s cetuksimabom 84 %, pri bolnikih z rakom požiralnika pri kombiniranem zdravljenju s pembrolizumabom 86 % in pri zdravljenju samo s kemoterapijo 83 %, pri bolnikih s TNBC pri kombiniranem zdravljenju s pembrolizumabom 80 % in pri zdravljenju samo s kemoterapijo 77 % in pri bolnicah z rakom materničnega vratu pri kombiniranem zdravljenju s pembrolizumabom 82 % in pri zdravljenju samo s kemoterapijo 75 %. Varnost pembrolizumaba v kombinaciji z aksitinibom ali lenvatinibom pri napredovalem RCC in v kombinaciji z lenvatinibom pri napredovalem EC so ocenili pri skupno 1.456 bolnikih z napredovalim RCC ali napredovalim EC, ki so v kliničnih študijah prejemali 200 mg pembrolizumaba na 3 tedne skupaj s 5 mg aksitiniba dvakrat na dan ali z 20 mg lenvatiniba enkrat na dan, kot je bilo ustrezno. V teh populacijah bolnikov so bili najpogostejši neželeni učinki diareja (58 %), hipertenzija (54 %), hipotiroidizem (46 %), utrujenost (41 %), zmanjšan apetit (40 %), navzea (40 %), artralgija (30 %), bruhanje (28 %), zmanjšanje telesne mase (28 %), disfonija (28 %), bolečine v trebuhu (28 %), proteinurija (27 %), sindrom palmarno-plantarne eritrodizestezije (26 %), izpuščaj (26 %), stomatitis (25 %), zaprtost (25 %), mišično-skeletna bolečina (23 %), glavobol (23 %) in kašelj (21 %). Neželenih učinkov od 3. do 5. stopnje je bilo pri bolnikih z RCC med uporabo pembrolizumaba v kombinaciji z aksitinibom ali lenvatinibom 80 % in med uporabo sunitiniba samega 71 %. Pri bolnicah z EC je bilo neželenih učinkov od 3. do 5. stopnje med uporabo pembrolizumaba v kombinaciji z lenvatinibom 89 % in med uporabo kemoterapije same 73 %. Za celoten seznam neželenih učinkov, prosimo, glejte celoten Povzetek glavnih značilnosti zdravila. Za dodatne informacije o varnosti v primeru uporabe pembrolizumaba v kombinaciji glejte povzetke glavnih značilnosti zdravila za posamezne komponente kombiniranega zdravljenja. **Način in režim izdaje zdravila:** H – Predpisovanje in izdaja zdravila je le na recept, zdravilo se uporablja samo v bolnišnicah. **Imetnik dovoljenja za promet z zdravilom:** Merck Sharp & Dohme B.V. , Waarderweg 39, 2031 BN Haarlem, Nizozemska.

MSD
Merck Sharp & Dohme inovativna zdravila d.o.o.,
Ameriška ulica 2, 1000 Ljubljana, tel: +386 1/ 520 42 01, fax: +386 1/ 520 43 50;
Pripravljeno v Sloveniji, 01/2023; SI-KEY-00501 EXP: 01/2025

Samo za strokovno javnost.

H - Predpisovanje in izdaja zdravila je le na recept, zdravilo pa se uporablja samo v bolnišnicah. Pred predpisovanjem, prosimo, preberite celoten Povzetek glavnih značilnosti zdravila Keytruda, ki je na voljo pri naših strokovnih sodelavcih ali na lokalnem sedežu družbe.

ZDRAVILO ZA ZDRAVLJENJE DIFUZNEGA VELIKOCELIČNEGA LIMFOMA B V PRVI LINIJI[1]

Klinična korist

%

manjše tveganje za napredovanje bolezni, ponovitev bolezni ali smrt v primerjavi s kombinacijo R-CHOP.[1]

Indikacija

POLIVY (polatuzumab vedotin) je v kombinaciji z rituksimabom, ciklofosfamidom, doksorubicinom in prednizonom indiciran za zdravljenje odraslih bolnikov s predhodno nezdravljenim difuznim velikoceličnim limfomom B (DVCLB).

POLIVY® ▼
polatuzumab vedotin

DVCLB = difuzni velikocelični limfom B; R-CHOP = rituksimab + ciklofosfamid + doksorubicin + vinkristin + prednizon.

Reference: 1. Povzetek glavnih značilnosti zdravila POLIVY. Dostopano (19.12.2022) na https://www.ema.europa.eu/en/documents/product-information/polivy-epar-product-information_sl.pdf

SKRAJŠAN POVZETEK GLAVNIH ZNAČILNOSTI ZDRAVILA POLIVY

▼ Za to zdravilo se izvaja dodatno spremljanje varnosti. Tako bodo hitreje na voljo nove informacije o njegovi varnosti. Zdravstvene delavce naprošamo, da poročajo o katerem koli domnevnem neželenem učinku zdravila. Kako poročati o neželenih učinkih, si poglejte skrajšani povzetek glavnih značilnosti zdravila pod „Poročanje o domnevnih neželenih učinkih".

Ime zdravila: Polivy 30 mg prašek za koncentrat za raztopino za infundiranje in Polivy 140 mg prašek za koncentrat za raztopino za infundiranje
Kakovostna in količinska sestava: Polivy 30 mg: Ena viala s praškom za koncentrat za raztopino za infundiranje vsebuje 30 mg polatuzumaba vedotina. Po rekonstituciji en mililiter vsebuje 20 mg polatuzumaba vedotina. Polivy 140 mg: Ena viala s praškom za koncentrat za raztopino za infundiranje vsebuje 140 mg polatuzumaba vedotina. Po rekonstituciji en mililiter vsebuje 20 mg polatuzumaba vedotina. Polatuzumab vedotin je konjugat protitelesa in zdravila, sestavljen iz antimitotičnega sredstva monometil-avristatina E (MMAE), kovalentno konjugiranega na monoklonsko protitelo, ki je usmerjeno proti CD79b. **Terapevtske indikacije:** Zdravilo Polivy je v kombinaciji z rituksimabom, ciklofosfamidom, doksorubicinom in prednizonom (R-CHP) indicirano za zdravljenje odraslih bolnikov s predhodno nezdravljenim difuznim velikoceličnim limfomom B (DVCLB). Zdravilo Polivy je v kombinaciji z bendamustinom in rituksimabom indicirano za zdravljenje odraslih bolnikov z difuznim velikoceličnim limfomom B (DVCLB), ki se na prejšnje zdravljenje niso odzvali ali pa se je bolezen pri njih ponovila in niso primerni za presaditev krvotvornih matičnih celic. **Odmerjanje in način uporabe:** Odmerjanje: **Difuzni velikocelični limfom B** *Predhodno nezdravljeni bolniki:* Priporočeni odmerek zdravila Polivy je 1,8 mg/kg v intravenski infuziji na 21 dni v kombinaciji z rituksimabom, ciklofosfamidom, doksorubicinom in prednizonom (R-CHP) v obdobju 6 ciklov. *Bolniki s ponovljeno boleznijo ali bolniki, neodzivni na zdravljenje:* Priporočeni odmerek zdravila Polivy je 1,8 mg/kg v intravenski infuziji na 21 dni v kombinaciji z bendamustinom in rituksimabom v trajanju 6 ciklov. Način uporabe: Zdravilo Polivy je namenjeno intravenski uporabi. Začetni odmerek zdravila Polivy je treba dati v 90-minutni intravenski infuziji. Bolnike je treba med infundiranjem in vsaj še 90 minut po končani infuziji začetnega odmerka nadzorovati glede reakcij, povezanih z infundiranjem in preobčutljivostnih reakcij. Če je bolnik prejšnje infundiranje dobro prenesel, je mogoče nadaljnje odmerke zdravila Polivy dati v 30-minutni infuziji, bolnika pa je treba nadzirati med infundiranjem in vsaj še 30 minut po končani infuziji. Zdravilo Polivy je treba rekonstituirati in razredčiti z upoštevanjem aseptičnega postopka in pod nadzorom zdravstvenega delavca. Treba ga je aplicirati v intravenski infuziji po namenski infuzijski liniji, opremljeni s sterilnim nepirogenim filtrom, ki malo veže beljakovine in s katetrom. Zdravila Polivy se ne sme aplicirati kot hiter intravenski odmerek ali bolus. *Previdnostni ukrepi, potrebni pred ravnanjem z zdravilom ali dajanjem zdravila:* Zdravilo Polivy vsebuje citotoksično komponento, ki je kovalentno vezana na monoklonsko protitelo. Upoštevajte ustrezen postopek za ravnanje in odstranjevanje. **Kontraindikacije:** Preobčutljivost na učinkovino ali katero koli pomožno snov. **Posebna opozorila in previdnostni ukrepi:** Sledljivost: Z namenom izboljšanja sledljivosti bioloških zdravil je treba jasno zabeležiti ime in številko serije uporabljenega zdravila. Mielosupresija: Pri bolnikih, zdravljenih z zdravilom Polivy, so poročali o resni in hudi nevtropeniji in febrilni nevtropeniji že v prvem ciklu zdravljenja. Treba je razmisliti o profilaktični uporabi granulocitnega rastnega dejavnika (G-CSF), saj je bila med kliničnim razvojem zdravila potrebna njegova uporaba. Med uporabo zdravila Polivy se lahko pojavi tudi trombocitopenija ali anemija 3. ali 4. stopnje. Pred vsakim odmerkom zdravila Polivy je treba kontrolirati celotno krvno sliko. Pri bolnikih z nevtropenijo in/ali trombocitopenijo 3. ali 4. stopnje je treba pretehtati opravljanje pogostejših laboratorijskih kontrol in/ali odložitev ali ukinitev uporabe zdravila Polivy. Periferna nevropatija: Pri bolnikih, zdravljenih z zdravilom Polivy, so poročali o periferni nevropatiji že v prvem ciklu zdravljenja; tveganje se povečuje z zaporednimi odmerki. Bolnikom z že obstoječo periferno nevropatijo se nevropatija lahko poslabša. Bolnike je treba nadzorovati glede simptomov periferne nevropatije. Bolnikom, pri katerih se pojavi novonastala periferna nevropatija ali se poslabša obstoječa periferna nevropatija, bo morda treba odmerek zdravila Polivy odložiti, zmanjšati ali uporabo zdravila Polivy ukiniti. Okužbe: Pri bolnikih, zdravljenih z zdravilom Polivy, so poročali o resnih, življenje ogrožajočih ali smrtnih okužbah, vključno z oportunističnimi okužbami. Poročali so tudi o ponovni aktivaciji latentnih okužb. Bolnike je treba med zdravljenjem skrbno nadzorovati glede znakov bakterijskih, glivnih ali virusnih okužb; če se pojavijo znaki in simptomi okužbe, mora bolnik poiskati zdravniško pomoč. Razmisliti je treba o profilaksi z zdravili proti okužbam v celotnem obdobju zdravljenja z zdravilom Polivy. Zdravila Polivy se ob prisotnosti aktivne hude okužbe ne sme aplicirati. Pri bolnikih, pri katerih se pojavijo resne okužbe, je treba ukiniti zdravilo Polivy in sočasno kemoterapijo. Imunizacija: Sočasno z zdravljenjem se bolnikom ne sme dajati živih in živih oslabljenih cepiv. Progresivna multifokalna levkoencefalopatija (PML): Med zdravljenjem z zdravilom Polivy so poročali o pojavu PML. Bolnike je treba skrbno nadzorovati glede novonastalih nevroloških, kognitivnih ali vedenjskih sprememb, ki nakazujejo na PML, oziroma glede poslabšanja takšnih sprememb. V primeru suma na PML je treba uporabo zdravila Polivy in morebitne sočasne kemoterapije odložiti, v primeru potrjene diagnoze pa ukiniti. Sindrom razpada tumorja: Bolniki z velikim tumorskim bremenom in hitro proliferirajočim tumorjem imajo lahko večje tveganje za sindrom razpada tumorja. Pred zdravljenjem z zdravilom Polivy je treba uporabiti ustrezne profilaktične ukrepe v skladu z lokalnimi smernicami. Bolnike je treba med zdravljenjem z zdravilom Polivy skrbno spremljati glede pojava sindroma razpada tumorja. Reakcije, povezane z infundiranjem: Zdravilo Polivy lahko povzroči reakcije, povezane z infundiranjem, vključno s hudimi primeri. Zapoznele reakcije, povezane z infundiranjem, so se pojavile tudi 24 ur po prejetju zdravila Polivy. Pred zdravilom Polivy je treba aplicirati antihistaminik in antipiretik in skrbno spremljati bolnike ves čas infundiranja. Če se pojavi reakcija, povezana z infundiranjem, infundiranje prekinite in ustrezno ravnajte oziroma zdravite. Embrio-fetalna toksičnost: Glede ne mehanizem delovanja in rezultate predkliničnih študij lahko pri nosečnici uporabljeno zdravilo Polivy škoduje plodu. Nosečnicam je treba svetovati glede tveganja za plod. Ženskam v rodni dobi je treba svetovati, naj uporabljajo učinkovito kontracepcijo med zdravljenjem z zdravilom Polivy in še vsaj 9 mesecev po zadnjem odmerku. Moškim, ki imajo partnerke v rodni dobi, je treba svetovati, naj uporabljajo učinkovito kontracepcijo med zdravljenjem z zdravilom Polivy in še vsaj 6 mesecev po zadnjem odmerku. Plodnost: Za moške, ki se bodo zdravili z zdravilom Polivy, je priporočljivo pred zdravljenjem shraniti seme. Starejši bolniki: Klinične študije z zdravilom Polivy niso vključevale zadostnega števila bolnikov, starih 65 let ali več, da bi lahko določili, ali se odzovejo drugače od mlajših bolnikov. Hepatotoksičnost: Pri bolnikih, zdravljenih z zdravilom Polivy, so se pojavili resni primeri hepatotoksičnosti. Predhodna bolezen jeter, izhodiščno zvišani jetrni encimi in uporaba sočasnih zdravil lahko tveganje povečajo. Kontrolirati je treba raven jetrnih encimov in bilirubina. **Medsebojno delovanje z drugimi zdravili in druge oblike interakcij:** Namenskih kliničnih študij medsebojnega delovanja zdravil s polatuzumabom vedotinom pri človeku niso izvedli. Pri sočasnem zdravljenju z zaviralcem CYP3A4 je potrebna previdnost. Bolnike, ki sočasno prejemajo močne zaviralce CYP3A4, je treba skrbneje nadzorovati glede znakov toksičnosti. Močni induktorji CYP3A4 lahko zmanjšajo izpostavljenost nekonjugiranemu MMAE. Sočasna uporaba polatuzumaba vedotina ne vpliva na farmakokinetiko rituksimaba, bendamustina, ciklofosfamida in doksorubicina. **Neželeni učinki:** Seznam neželenih učinkov pri bolnikih, zdravljenih z zdravilom Polivy v kliničnih preskušanjih: Zelo pogosti: pljučnica, okužba zgornjih dihal, febrilna nevtropenija, nevtropenija, trombocitopenija, anemija, levkopenija, hipokaliemija, zmanjšan apetit, periferna nevropatija, kašelj, diareja, navzea, zaprtost, bruhanje, mukozitis, bolečine v trebuhu, alopecija, zvišana telesna temperatura, utrujenost, astenija, zmanjšanje telesne mase in z infundiranjem povezana reakcija. Pogosti: sepsa, okužba s herpesvirusom, okužba s citomegalovirusom, okužba sečil, limfopenija, pancitopenija, hipokalciemija, hipoalbuminemija, omotica, pnevmonitis, dispneja, srbenje, okužbe kože, izpuščaj, suha koža, artralgija, mialgija, periferni edem, mrzlica, zvišanje transaminaz, zvišanje lipaze in hipofosfatemija. Poročanje o domnevnih neželenih učinkih: Poročanje o domnevnih neželenih učinkih zdravila po izdaji dovoljenja za promet je pomembno. Omogoča namreč stalno spremljanje razmerja med koristmi in tveganji zdravila. Od zdravstvenih delavcev se zahteva, da poročajo o katerem koli domnevnem neželenem učinku zdravila na: Javna agencija Republike Slovenije za zdravila in medicinske pripomočke, Sektor za farmakovigilanco, Nacionalni center za farmakovigilanco, Slovenčeva ulica 22, SI-1000 Ljubljana, Tel: +386 (0)8 2000 500, Faks: +386 (0)8 2000 510, e-pošta: h-farmakovigilanca@jazmp.si, spletna stran: www.jazmp.si. Za zagotavljanje sledljivosti zdravila je pomembno, da pri izpolnjevanju obrazca o domnevnih neželenih učinkihzdravila navedete številko serije biološkega zdravila. **Režim izdaje zdravila:** ℍ. **Imetnik dovoljenja za promet:** Roche Registration GmbH, Emil-Barell-Strasse 1, 79639 Grenzach-Wyhlen, Nemčija. **Verzija: 1.0/22**

DODATNE INFORMACIJE SO NA VOLJO PRI: Roche farmacevtska družba d.o.o., Stegne 13G, 1000 Ljubljana

Samo za strokovno javnost

M-SI-00000784(v1.0) Pripravljeno: februar 2023

Zdravilo Lonsurf je indicirano v monoterapiji za zdravljenje odraslih bolnikov z metastatskim kolorektalnim rakom (KRR), ki so bili predhodno že zdravljeni ali niso primerni za zdravljenja, ki so na voljo. Ta vključujejo kemoterapijo na osnovi fluoropirimidina, oksaliplatina in irinotekana, zdravljenje z zaviralci žilnega endotelijskega rastnega dejavnika (VEGF – Vascular Endothelial Growth Factor) in zaviralci receptorjev za epidermalni rastni dejavnik (EGFR – Epidermal Growth Factor Receptor).[1]

Zdravilo Lonsurf je indicirano v monoterapiji za zdravljenje odraslih bolnikov z metastatskim rakom želodca vključno z adenokarcinomom gastro-ezofagealnega prehoda, ki so bili predhodno že zdravljeni z najmanj dvema sistemskima režimoma zdravljenja za napredovalo bolezen.[1]

VEČ ČASA

za več trenutkov, ki štejejo

Podaljša celokupno preživetje
v 3. liniji zdravljenja bolnikov z mCRC in mGC[2,3]

Literatura: 1. Povzetek glavnih značilnosti zdravila Lonsurf, december 2020.
2. Mayer R et al. N Engl J Med. 2015;372:1909-19. 3. Shitara K et al.
Lancet Oncol. 2018;19:1437-1448.
Družba Servier ima licenco družbe Taiho za zdravilo Lonsurf®.
Pri globalnem razvoju zdravila sodelujeta obe družbi
in ga tržita na svojih določenih področjih.

Lonsurf®
trifluridin/tipiracil

Skrajšan povzetek glavnih značilnosti zdravila: Lonsurf 15 mg/6,14 mg filmsko obložene tablete in Lonsurf 20 mg/8,19 mg filmsko obložene tablete
SESTAVA*: Lonsurf 15 mg/6,14 mg: Ena filmsko obložena tableta vsebuje 15 mg trifluridina in 6,14 mg tipiracila (v obliki klorida). **Lonsurf 20 mg/8,19 mg**: Ena filmsko obložena tableta vsebuje 20 mg trifluridina in 8,19 mg tipiracila (v obliki klorida). **TERAPEVTSKE INDIKACIJE*:** Kolorektalni rak - v monoterapiji za zdravljenje odraslih bolnikov z metastatskim kolorektalnim rakom, ki so bili predhodno že zdravljeni ali niso primerni za zdravljenja, ki so na voljo. Ta vključujejo kemoterapijo na osnovi fluoropirimidina, oksaliplatina in irinotekana, zdravljenje z zaviralci žilnega endotelijskega rastnega dejavnika (VEGF - Vascular Endothelial Growth Factor) in zaviralci receptorjev za epidermalni rastni dejavnik (EGFR - Epidermal Growth Factor Receptor). Rak želodca - v monoterapiji za zdravljenje odraslih bolnikov z metastatskim rakom želodca vključno z adenokarcinomom gastro-ezofagealnega prehoda, ki so bili predhodno že zdravljeni z najmanj dvema sistemskima režimoma zdravljenja za napredovalo bolezen. **ODMERJANJE IN NAČIN UPORABE*:** Priporočeni začetni odmerek zdravila Lonsurf pri odraslih je 35 mg/m^2/odmerek peroralno dvakrat dnevno na 1. do 5. dan in 8. do 12. dan vsakega 28-dnevnega cikla zdravljenja, najpozneje 1 uro po zaključku jutranjega in večernega obroka (20 mg/m^2/odmerek dvakrat dnevno pri bolnikih s hudo ledvično okvaro). Odmerek, izračunan glede na telesno površino, ne sme preseči 80 mg/odmerek. Možne prilagoditve odmerka glede na varnost in prenašanje zdravila: dovoljena so zmanjšanja odmerka na najmanjši odmerek 20 mg/m^2 dvakrat dnevno (oz. 15 mg/m^2 dvakrat dnevno pri bolnikih s hudo ledvično okvaro). Potem ko je bil odmerek zmanjšan, povečanje ni dovoljeno. **KONTRAINDIKACIJE*:** Preobčutljivost na učinkovini ali katero koli pomožno snov. **OPOZORILA IN PREVIDNOSTNI UKREPI*:** Supresija kostnega mozga: Pred uvedbo zdravljenja in po potrebi za spremljanje toksičnosti zdravila, najmanj pred vsakim ciklom zdravljenja, je treba pregledati celotno krvno sliko. Zdravljenja ne smete začeti, če je absolutno število nevtrofilcev < 1,5 x 10^9/l, če je število trombocitov < 75 x 10^9/l ali če se je pri bolniku zaradi predhodnih zdravljenj pojavila klinično pomembna nehematološka toksičnost 3. ali 4. stopnje, ki še traja. Bolnike je treba skrbno spremljati zaradi morebitnih okužb, uvesti je treba ustrezne ukrepe, kot je klinično indicirano. Toksičnost za prebavila: Potrebna je uporaba antiemetikov, antidiarikov ter drugih ukrepov, kot je klinično indicirano. Če je potrebno, prilagodite odmerke. Ledvična okvara: Uporaba zdravila ni priporočljiva pri bolnikih s končno stopnjo ledvične okvare. Bolnike z ledvično okvaro je potrebno med zdravljenjem skrbno spremljati; bolnike z zmerno ali hudo ledvično okvaro je treba zaradi hematološke toksičnosti bolj pogosto spremljati. Jetrna okvara: Uporaba zdravila Lonsurf pri bolnikih z obstoječo zmerno ali hudo jetrno okvaro ni priporočljiva. Proteinurija: Pred začetkom zdravljenja in med njim je priporočljivo spremljanje proteinurije z urinskimi testnimi lističi. Pomožne snovi: Zdravilo vsebuje laktozo. **INTERAKCIJE*:** Previdnost: Zdravila, ki medsebojno delujejo z nukleozidnimi prenašalci CNT1, ENT1 in ENT2, zaviralci OCT2 ali MATE1, substrati humane timidin-kinaze (npr. zidovudin), hormonski kontraceptivi. **PLODNOST*. NOSEČNOST IN DOJENJE*:** Ni priporočljivo. **KONTRACEPCIJA*:** Ženske in moški morajo uporabljati zelo učinkovite metode kontracepcije med zdravljenjem in do 6 mesecev po zaključku zdravljenja. **VPLIV NA SPOSOBNOST VOŽNJE IN UPRAVLJANJA STROJEV*:** Med zdravljenjem se lahko pojavijo utrujenost, omotica ali splošno slabo počutje. **NEŽELENI UČINKI*:** *Zelo pogosti:* nevtropenija, levkopenija, anemija, trombocitopenija, zmanjšan apetit, diareja, navzea, bruhanje, utrujenost. *Pogosti:* okužba spodnjih dihal, febrilna nevtropenija, limfopenija, hipoalbuminemija, disgevzija, periferna nevropatija, dispneja, bolečina v trebuhu, zaprtje, stomatitis, bolezni ustne votline, hiperbilirubinemija, sindrom palmarne plantarne eritrodisestezije, izpuščaj, alopecija, pruritus, suha koža, proteinurija, pireksija, edem, vnetje sluznice, splošno slabo počutje, zvišanje jetrnih encimov, zvišanje alkalne fosfataze v krvi, zmanjšanje telesne mase. *Občasni:* septični šok, infekcijski enteritis, pljučnica, okužba žolčevoda, gripa, okužba sečil, gingivitis, herpes zoster, tinea pedis, okužba s kandido, bakterijska okužba, okužba, nevtropenična sepsa, okužba zgornjih dihal, konjunktivitis, bolečina zaradi raka, pancitopenija, granulocitopenija, monocitopenija, eritropenija, levkocitoza, monocitoza, dehidracija, hiperglikemija, hiperkaliemija, hipokaliemija, hipofosfatemija, hipernatriemija, hiponatriemija, hipokalciemija, protin, anksioznost, nespečnost, nevrotoksičnost, disestezija, hiperestezija, hipoestezija, sinkopa, parestezija, pekoč občutek, letargija, omotica, glavobol, zmanjšana ostrina vida, zamegljen vid, diplopija, katarakta, suho oko, vrtoglavica, neugodje v ušesu, angina pektoris, aritmija, palpitacije, embolija, hipertenzija, hipotenzija, vročinski oblivi, pljučna embolija, plevralni izliv, izcedek iz nosu, disfonija, orofaringealna bolečina, epistaksa, kašelj, hemoragični enterokolitis, krvavitev v prebavilih, akutni pankreatitis, ascites, ileus, subileus, kolitis, gastritis, refluksni gastritis, ezofagitis, moteno praznjenje želodca, abdominalna distenzija, analno vnetje, razjede v ustih, dispepsija, gastroezofagealna refluksna bolezen, proktalgija, bukalni polip, krvavitev dlesni, glositis, parodontalna bolezen, bolezen zob, siljenje na bruhanje, flatulenca, slab zadah, hepatotoksičnost, razširitev žolčnih vodov, luščenje kože, urtikarija, preobčutljivostne reakcije na svetlobo, eritem, akne, hiperhidroza, žulj, bolezni nohtov, otekanje sklepov, artralgija, bolečina v kosteh, mialgija, mišično-skeletna bolečina, mišična oslabelost, mišični krči, bolečina v okončinah, ledvična odpoved, neinfektivni cistitis, motnje mikcije, hematurija, levkociturija, motnje menstruacije, poslabšanje splošnega zdravstvenega stanja, bolečina, občutek spremembe telesne temperature, kseroza, nelagodje, zvišanje kreatinina v krvi, podaljšanje intervala QT na elektrokardiogramu, povečanje mednarodnega umerjenega razmerja (INR), podaljšanje aktiviranega parcialnega tromboplastinskega časa (aPTČ), zvišanje sečnine v krvi, zvišanje laktatne dehidrogenaze v krvi, znižanje celokupnih proteinov, zvišanje C-reaktivnega proteina, zmanjšan hematokrit. *Post-marketinške izkušnje:* intersticijska bolezen pljuč. **PREVELIKO ODMERJANJE*:** Neželeni učinki, o katerih so poročali v povezavi s prevelikim odmerjanjem, so bili v skladu z uveljavljenim varnostnim profilom. Glavni pričakovani zaplet prevelikega odmerjanja je supresija kostnega mozga. **FARMAKODINAMIČNE LASTNOSTI*:** *Farmakoterapevtska skupina:* zdravila z delovanjem na novotvorbe, antimetaboliti, oznaka ATC: L01BC59. Zdravilo Lonsurf sestavljata antineoplastični timidinski nukleozidni analog, trifluridin, in zaviralec timidin-fosforilaze (TPaze), tipiracilijev klorid. Po privzemu v rakave celice timidin-kinaza fosforilira trifluridin. Ta se v celicah nato presnovi v substrat deoksiribonukleinske kisline (DNA), ki se vgradi neposredno v DNA ter tako preprečuje celično proliferacijo. TPaza hitro razgradi trifluridin in njegova presnova po peroralni uporabi je hitra zaradi učinka prvega prehoda, zato je v zdravilo vključen zaviralec TPaze, tipiracilijev klorid. **PAKIRANJE*:** 20 filmsko obloženih tablet. **NAČIN PREDPISOVANJA IN IZDAJE ZDRAVILA:** Rp/Spec. **Imetnik dovoljenja za promet:** Les Laboratoires Servier, 50, rue Carnot, 92284 Suresnes cedex, Francija. Številka dovoljenja za promet z zdravilom: EU/1/16/1096/001 (Lonsurf 15 mg/6,14 mg), EU/1/16/1096/004 (Lonsurf 20 mg/8,19 mg). **Datum zadnje revizije besedila: december 2020. *Pred predpisovanjem preberite celoten povzetek glavnih značilnosti zdravila. Celoten povzetek glavnih značilnosti zdravila in podrobnejše informacije so na voljo pri: Servier Pharma d.o.o., Podmilščakova ulica 24, 1000 Ljubljana, tel: 01 563 48 11, www.servier.si.**

LON AD1 C1 2022-23. Samo za strokovno javnost.
Datum priprave informacije: oktober 2022.

SERVIER
moved by you

Instructions for authors

The editorial policy

Radiology and Oncology is a multidisciplinary journal devoted to the publishing original and high-quality scientific papers and review articles, pertinent to oncologic imaging, interventional radiology, nuclear medicine, radiotherapy, clinical and experimental oncology, radiobiology, medical physics, and radiation protection. Papers on more general aspects of interest to the radiologists and oncologists are also published (no case reports).

The Editorial Board requires that the paper has not been published or submitted for publication elsewhere; the authors are responsible for all statements in their papers. Accepted cannot be published elsewhere without the written permission of the editors.

Submission of the manuscript

The manuscript written in English should be submitted to the journal via online submission system Editorial Manager available for this journal at: **www.radioloncol.com**.

In case of problems, please contact Sašo Trupej at **saso.trupej@computing.si** or the Editor of this journal at **gsersa@onko-i.si**

All articles are subjected to the editorial review and when the articles are appropriated they are reviewed by independent referees. In the cover letter, which must accompany the article, the authors are requested to suggest 3-4 researchers, competent to review their manuscript. However, please note that this will be treated only as a suggestion; the final selection of reviewers is exclusively the Editor's decision. The authors' names are revealed to the referees, but not vice versa.

Manuscripts which do not comply with the technical requirements stated herein will be returned to the authors for the correction before peer-review. The editorial board reserves the right to ask authors to make appropriate changes of the contents as well as grammatical and stylistic corrections when necessary. Page charges will be charged for manuscripts exceeding the recommended length, as well as additional editorial work and requests for printed reprints.

Articles are published printed and on-line as the open access: (**https://content.sciendo.com/raon**).

All articles are subject to 1200 EUR + VAT publication fee. Exceptionally, waiver of payment may be negotiated with editorial office, at the time of article submission.

Manuscripts submitted under multiple authorship are reviewed on the assumption that all listed authors concur in the submission and are responsible for its content; they must have agreed to its publication and have given the corresponding author the authority to act on their behalf in all matters pertaining to publication. The corresponding author is responsible for informing the coauthors of the manuscript status throughout the submission, review, and production process.

Preparation of manuscripts

Radiology and Oncology will consider manuscripts prepared according to the Uniform Requirements for Manuscripts Submitted to Biomedical Journals by International Committee of Medical Journal Editors (www.icmje.org). The manuscript should be written in grammatically and stylistically correct language. Abbreviations should be avoided. If their use is necessary, they should be explained at the first time mentioned. The technical data should conform to the SI system. The manuscript, excluding the references, tables, figures and figure legends, must not exceed 5000 words, and the number of figures and tables is limited to 8. Organize the text so that it includes: Introduction, Materials and methods, Results and Discussion. Exceptionally, the results and discussion can be combined in a single section. Start each section on a new page, and number each page consecutively with Arabic numerals. For ease of review, manuscripts should be submitted as a single column, double-spaced text.

The Title page should include a concise and informative title, followed by the full name(s) of the author(s); the institutional affiliation of each author; the name and address of the corresponding author (including telephone, fax and E-mail), and an abbreviated title (not exceeding 60 characters). This should be followed by the abstract page, summarizing in less than 250 words the reasons for the study, experimental approach, the major findings (with specific data if possible), and the principal conclusions, and providing 3-6 key words for indexing purposes. Structured abstracts are required. Slovene authors are requested to provide title and the abstract in Slovene language in a separate file. The text of the research article should then proceed as follows:

Introduction should summarize the rationale for the study or observation, citing only the essential references and stating the aim of the study.

Materials and methods should provide enough information to enable experiments to be repeated. New methods should be described in details.

Results should be presented clearly and concisely without repeating the data in the figures and tables. Emphasis should be on clear and precise presentation of results and their significance in relation to the aim of the investigation.

Discussion should explain the results rather than simply repeating them and interpret their significance and draw conclusions. It should discuss the results of the study in the light of previously published work.

Charts, Illustrations, Images and Tables

Charts, Illustrations, Images and Tables must be numbered and referred to in the text, with the appropriate location indicated. Charts, Illustrations and Images, provided electronically, should be of appropriate quality for good reproduction. Illustrations and charts must be vector image, created in CMYK color space, preferred font "Century Gothic", and saved as .AI, .EPS or .PDF format. Color charts, illustrations and Images are encouraged, and are published without additional charge. Image size must be 2.000 pixels on the longer side and saved as .JPG (maximum quality) format. In Images, mask the identities of the patients. Tables should be typed double-spaced, with a descriptive title and, if appropriate, units of numerical measurements included in the column heading. The files with the figures and tables can be uploaded as separate files.

References

References must be numbered in the order in which they appear in the text and their corresponding numbers quoted in the text. Authors are responsible for the accuracy of their references. References to the Abstracts and Letters to the Editor must be identified as such. Citation of papers in preparation or submitted for publication, unpublished observations, and personal communications should not be included in the reference list. If essential, such material may be incorporated in the appropriate place in the text. References follow the style of Index Medicus, DOI number (if exists) should be included.

All authors should be listed when their number does not exceed six; when there are seven or more authors, the first six listed are followed by "et al.". The following are some examples of references from articles, books and book chapters:

Dent RAG, Cole P. In vitro maturation of monocytes in squamous carcinoma of the lung. *Br J Cancer* 1981; **43:** 486-95. doi: 10.1038/bjc.1981.71

Chapman S, Nakielny R. *A guide to radiological procedures*. London: Bailliere Tindall; 1986.

Evans R, Alexander P. Mechanisms of extracellular killing of nucleated mammalian cells by macrophages. In: Nelson DS, editor. *Immunobiology of macrophage.* New York: Academic Press; 1976. p. 45-74.

Authorization for the use of human subjects or experimental animals

When reporting experiments on human subjects, authors should state whether the procedures followed the Helsinki Declaration. Patients have the right to privacy; therefore, the identifying information (patient's names, hospital unit numbers) should not be published unless it is essential. In such cases the patient's informed consent for publication is needed, and should appear as an appropriate statement in the article. Institutional approval and Clinical Trial registration number is required. Retrospective clinical studies must be approved by the accredited Institutional Review Board/Committee for Medical Ethics or other equivalent body. These statements should appear in the Materials and methods section.

The research using animal subjects should be conducted according to the EU Directive 2010/63/EU and following the Guidelines for the welfare and use of animals in cancer research (Br J Cancer 2010; 102: 1555 – 77). Authors must state the committee approving the experiments, and must confirm that all experiments were performed in accordance with relevant regulations.

These statements should appear in the Materials and methods section (or for contributions without this section, within the main text or in the captions of relevant figures or tables).

Transfer of copyright agreement

For the publication of accepted articles, authors are required to send the License to Publish to the publisher on the address of the editorial office. A properly completed License to Publish, signed by the Corresponding Author on behalf of all the authors, must be provided for each submitted manuscript.

Conflict of interest

When the manuscript is submitted for publication, the authors are expected to disclose any relationship that might pose real, apparent or potential conflict of interest with respect to the results reported in that manuscript. Potential conflicts of interest include not only financial relationships but also other, non-financial relationships. In the Acknowledgement section the source of funding support should be mentioned. The Editors will make effort to ensure that conflicts of interest will not compromise the evaluation process of the submitted manuscripts; potential editors and reviewers will exempt themselves from review process when such conflict of interest exists. The statement of disclosure must be in the Cover letter accompanying the manuscript or submitted on the form available on **www.icmje.org/coi_disclosure.pdf**

Page proofs

Page proofs will be sent by E-mail to the corresponding author. It is their responsibility to check the proofs carefully and return a list of essential corrections to the editorial office within three days of receipt. Only grammatical corrections are acceptable at that time.

Open access

Papers are published electronically as open access on **https://content.sciendo.com/raon**, also papers accepted for publication as E-ahead of print.

Zdravilo IBRANCE že več kot 8 let pomaga do trenutkov, kot so ti.[2-5] Zdravilo IBRANCE, ki ga podpirajo obširne izkušnje iz klinične in vsakodnevne dejanske prakse ter dokazana klinična učinkovitost in dobro prenašanje,[1,4,6-35] vašim bolnicam pomaga, da najbolje izkoristijo vsak dan.[4,5,36,37]

HR+/HER2- = pozitiven na estrogenske receptorje in negativen na receptorje humanega epidermalnega rastnega faktorja 2; **mRD** = metastatski rak dojke

BISTVENI PODATKI IZ POVZETKA GLAVNIH ZNAČILNOSTI ZDRAVILA

IBRANCE 75 mg, 100 mg, 125 mg trde kapsule[(1)]
IBRANCE 75 mg, 100 mg, 125 mg filmsko obložene tablete[(2)]
Sestava in oblika zdravila: (1) Ena trda kapsula vsebuje 75 mg, 100 mg ali 125 mg palbocikliba in 56 mg, 74 mg ali 93 mg laktoze (v obliki monohidrata). (2) Ena filmsko obložena tableta vsebuje 75 mg, 100 mg ali 125 mg palbocikliba. **Indikacije:** Zdravljenje lokalno napredovalega ali metastatskega na hormonske receptorje (HR – *Hormone Receptors*) pozitivnega in na receptorje humanega epidermalnega rastnega faktorja 2 (HER2 – *Human Epidermal growth factor Receptor 2*) negativnega raka dojk: v kombinaciji z zaviralcem aromataze ali v kombinaciji s fulvestrantom pri ženskah, ki so prejele predhodno endokrino zdravljenje. Pri ženskah v pred- in perimenopavzi je treba endokrino zdravljenje kombinirati z agonistom gonadoliberina. **Odmerjanje in način uporabe:** Zdravljenje mora uvesti in nadzorovati zdravnik, ki ima izkušnje z uporabo zdravil za zdravljenje rakavih bolezni. Priporočeni odmerek je 125 mg enkrat na dan 21 zaporednih dni, sledi 7 dni brez zdravljenja (shema 3/1), celotni cikel traja 28 dni. Zdravljenje je treba nadaljevati, dokler ima bolnik od zdravljenja klinično korist ali dokler se ne pojavi nesprejemljiva toksičnost. Pri sočasnem dajanju s palbociklibom je treba zaviralec aromataze dajati v skladu s shemo odmerjanja, ki je navedena v Povzetku glavnih značilnosti zdravila (PGZZ). Pri sočasnem dajanju s palbociklibom je priporočeni odmerek fulvestranta 500 mg intramuskularno 1., 15. in 29. dan ter nato enkrat na mesec, glejte PGZZ za fulvestrant. Prilagajanja odmerkov: Za prilagajanja odmerkov zaradi hematološke toksičnosti glejte preglednico 2, zaradi nehematološke toksičnosti pa preglednico 3 v PGZZju. Pri bolnikih s hudo intersticijsko boleznijo pljuč (ILD)/pnevmonitisom je treba zdravljenje trajno prekiniti. Posebne skupine bolnikov: *Starejši:* Prilagajanje odmerka ni potrebno. *Okvara jeter ali ledvic*: Pri bolnikih z blago ali zmerno okvaro jeter ali blago, zmerno ali hudo okvaro ledvic prilagajanje odmerka ni potrebno. Pri bolnikih s hudo okvaro jeter je priporočeni odmerek 75 mg enkrat na dan po shemi 3/1. *Pediatrična populacija*: Varnost in učinkovitost pri otrocih in mladostnikih, starih < 18 let, nista bili dokazani. Način uporabe: Peroralna uporaba. (1) Jemanje s hrano, priporočljivo z obrokom. (2) Tablete se lahko jemlje s hrano ali brez nje. (1, 2) Ne smemo jemati z grenivko ali grenivkinim sokom. Kapsule oz. tablete zdravila je treba pogoltniti cele. **Kontraindikacije:** Preobčutljivost na učinkovino ali katerokoli pomožno snov. Uporaba pripravkov s šentjanževko. **Posebna opozorila in previdnostni ukrepi:** Ženske v pred- in perimenopavzi: Kadar zdravilo uporabljamo v kombinaciji z zaviralcem aromataze je obvezna ovarijska ablacija ali supresija z agonistom gonadoliberina. Hematološke bolezni: Pri nevtropeniji stopnje 3 ali 4 je priporočljiva prekinitev odmerjanja, zmanjšanje odmerka ali odložitev začetka ciklov zdravljenja, bolnike pa je treba ustrezno spremljati. ILD/pnevmonitis: Pri bolnikih se lahko pojavita huda, življenjsko ogrožajoča ali smrtna ILD in/ali pnevmonitis, kadar zdravilo jemljejo v kombinaciji z endokrinim zdravljenjem. Bolnike je treba spremljati glede pljučnih simptomov, ki kažejo na ILD/pnevmonitis (npr. hipoksija, kašelj, dispneja), in pri pojavu novih ali poslabšanju respiratornih simptomov oz. sumu na ILD/pnevmonitis zdravljenje prekiniti. Okužbe: Zdravilo lahko poveča nagnjenost k okužbam, zato je bolnike treba spremljati glede znakov in simptomov okužbe ter jih ustrezno zdraviti. Okvara jeter ali ledvic: Pri bolnikih z zmerno ali hudo okvaro jeter ali ledvic je treba zdravilo uporabljati previdno in skrbno spremljati znake toksičnosti. (1) Laktoza: Vsebuje laktozo. Bolniki z redko dedno intoleranco za galaktozo, odsotnostjo encima laktaze ali malabsorpcijo glukoze-galaktoze ne smejo jemati tega zdravila. **Medsebojno delovanje z drugimi zdravili in druge oblike interakcij:** Učinki drugih zdravil na farmakokinetiko palbocikliba: *Zaviralci CYP3A:* Sočasni uporabi močnih zaviralcev CYP3A, med drugim klaritromicina, indinavirja, itrakonazola, ketokonazola, lopinavirja/ritonavirja, nefazodona, nelfinavirja, posakonazola, sakvinavirja, telaprevirja, telitromicina, vorikonazola in grenivke ali grenivkinega soka, se je treba izogibati. *Induktorji CYP3A:* Sočasni uporabi močnih induktorjev CYP3A, med drugim karbamazepina, enzalutamida, fenitoina, rifampicina in šentjanževke, se je treba izogibati. Učinek zdravil za zmanjševanje kisline: (1) Če palbociklib zaužijemo s hrano, klinično pomembnega učinka na izpostavljenost palbociklibu ni pričakovati. (2) Klinično pomembnega učinka na izpostavljenost palbociklibu ni pričakovati. Učinki palbocikliba na farmakokinetiko drugih zdravil: Pri sočasni uporabi bo morda treba zmanjšati odmerek občutljivih substratov CYP3A z ozkim terapevtskim indeksom (npr. alfentanil, ciklosporin, dihidroergotamin, ergotamin, everolimus, fentanil, pimozid, kinidin, sirolimus in takrolimus), saj IBRANCE lahko poveča izpostavljenost tem zdravilom. Študije *in vitro* s prenašalci: Palbociklib lahko zavira prenos, posredovan s P-gp v prebavilih in beljakovino odpornosti pri raku dojk (BCRP). Uporaba palbocikliba z zdravili, ki so substrati P-gp (npr. digoksin, dabigatran, kolhicin) ali BCRP (npr. pravastatin, rosuvastatin, sulfasalazin) lahko poveča njihov terapevtski učinek in neželene učinke. Palbociklib lahko zavira privzemni prenašalec organskih kationov OCT1. **Plodnost, nosečnost in dojenje:** Med zdravljenjem in vsaj 3 tedne (ženske) oziroma 14 tednov (moški) po koncu zdravljenja je treba uporabljati ustrezne kontracepcijske metode. Zdravila ne uporabljajte pri nosečnicah in ženskah v rodni dobi, ki ne uporabljajo kontracepcije. Bolnice, ki prejemajo palbociklib, ne smejo dojiti. Zdravljenje s palbociklibom lahko ogrozi plodnost pri moških. Pred začetkom zdravljenja naj moški zato razmislijo o hrambi sperme. **Vpliv na sposobnost vožnje in upravljanja s stroji:** Ima blag vpliv na sposobnost vožnje in upravljanja strojev. Potrebna je previdnost. **Neželeni učinki:** Zelo pogosti: okužbe, nevtropenija, levkopenija, anemija, trombocitopenija, pomanjkanje teka, stomatitis, navzea, diareja, bruhanje, izpuščaj, alopecija, suha koža, utrujenost, astenija, pireksija, povečane vrednosti ALT/AST. **Način in režim izdaje:** Rp/Spec - Predpisovanje in izdaja zdravila je le na recept zdravnika specialista ustreznega področja medicine ali od njega pooblaščenega zdravnika. **Imetnik dovoljenja za promet:** Pfizer Europe MA EEIG, Boulevard de la Plaine 17, 1050 Bruxelles, Belgija. **Datum zadnje revizije besedila:** 30.03.2023
Pred predpisovanjem se seznanite s celotnim povzetkom glavnih značilnosti zdravila.

Literatura: 1. Povzetek glavnih značilnosti zdravila Ibrance, 30.3.2023. **2.** Beaver JA, et al. Clin Cancer Res. 2015;21(21):4760-4766. **3.** George MA, et al. Front Oncol. 2021;11:693104. **4.** Rugo H, et al. Breast Cancer Res Treat. 2019;174(3):719-729. **5.** Rugo HS, et al. Ann Oncol. 2018;29:888-894. **6.** Cristofanilli M, et al. Clin Cancer Res. 2022;28(16):3433-3442. **7.** Xu B, et al. Eur J Cancer. 2022;175:236-245. **8.** Finn RS, et al. N Engl J Med. 2016;375(20):1925-1936. **9.** Gelmon K, et al. Breast. 2021;59:321-326. **10.** Rugo HS, et al. Eur J Cancer. 2018;101:123-133. **11.** Turner NC, et al. Ann Oncol. 2018;29(3):669-680. **12.** Cristofanilli F, et al. Lancet Oncol. 2016;17(4):425-439. **13.** Harbeck N, et al. Future Oncol. 2021;17(16):2107-2122. **14.** Goyal RK, et al. Cancer. 2023 Feb 9. Epub ahead of print. **15.** Richardson D, et al. Breast Cancer Res Treat. 2021;187(1):113-124. **16.** De Michele A, et al. Breast Cancer Res. 2021;23:37. **17.** Rugo HS, et al. NPJ Breast Cancer. 2022;8(1):114. **18.** Taylor-Stokes G, et al. Breast. 2019;43:22-27. **19.** Waller J, et al. J Glob Oncol. 2019;5:JGO1800239. **20.** Mycock K, et al. Future Oncol. 2022;18:349-362. **21.** Mycock K, et al. Curr Oncol. 2021;28:678-688. **22.** Mycock K, et al. Cancer Treat Res Commun. 2022;32:100573. Epub 6 May 2022. **23.** Mycock K, et al. Clin Ther. 2022;44(12):1588-1601. **24.** Kraus AL, et al. Clin Pharmacol Ther. 2022;111(1):302-309. **25.** Rugo HS, et al. SABCS 2022; Abstract P3-01-15. **26.** De Laurentiis M, et al. SABCS 2019; Poster P3-11-25. **27.** Caillet P. ASCO 2021; Oral presentation 1012. **28.** Tripathy D, et al. ESMO 2022; Poster 251P. **29.** Karuturi MS, et al. ESMO BC 2022; Poster 190P. **30.** Blum J, et al. SABCS 2021; Abstract P1-18-29. **31.** Finn R, et al. ASCO 2022; Oral presentation. **32.** Finn R, et al. Oncologist. 2021;26:e749-e755. **33.** Diéras V, et al. Oncologist. 2019;24(12):1514-1525. **34.** Verma S, et al. Oncologist. 2016;21(10):1165-1175. **35.** Harbeck N, et al. Ann Oncol. 2016;27(6):1047-1054. **36.** Rocque G, et al. ESMO 2022; Poster 266P. **37.** Karuturi M, et al. SABCS 2021; Poster P1-18-25.

Pfizer Luxembourg SARL, GRAND DUCHY OF LUXEMBOURG,
51, Avenue J. F. Kennedy, L-1855
Pfizer, podružnica Ljubljana, Letališka cesta 29a, Ljubljana

PP-IBR-SVN-0011
Datum priprave: maj 2023.
Samo za strokovno javnost.

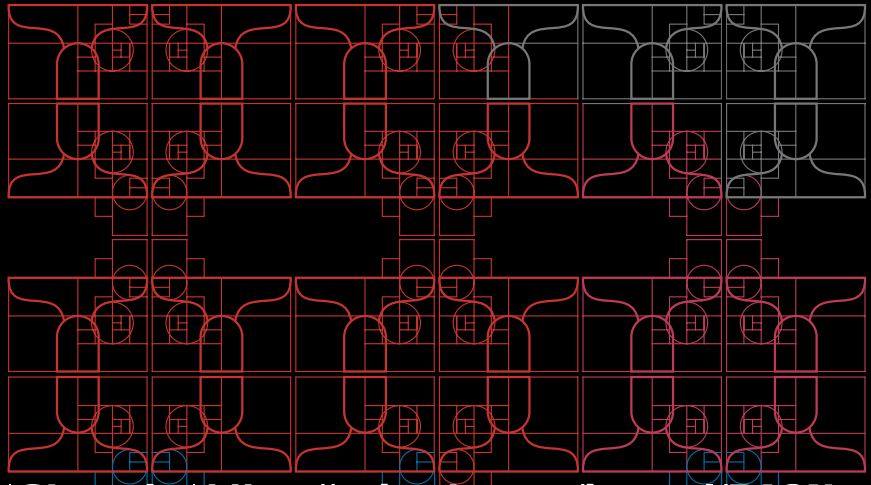

Radiology and Oncology | Ljubljana | Slovenia | https://sciendo.com/journal/RAON

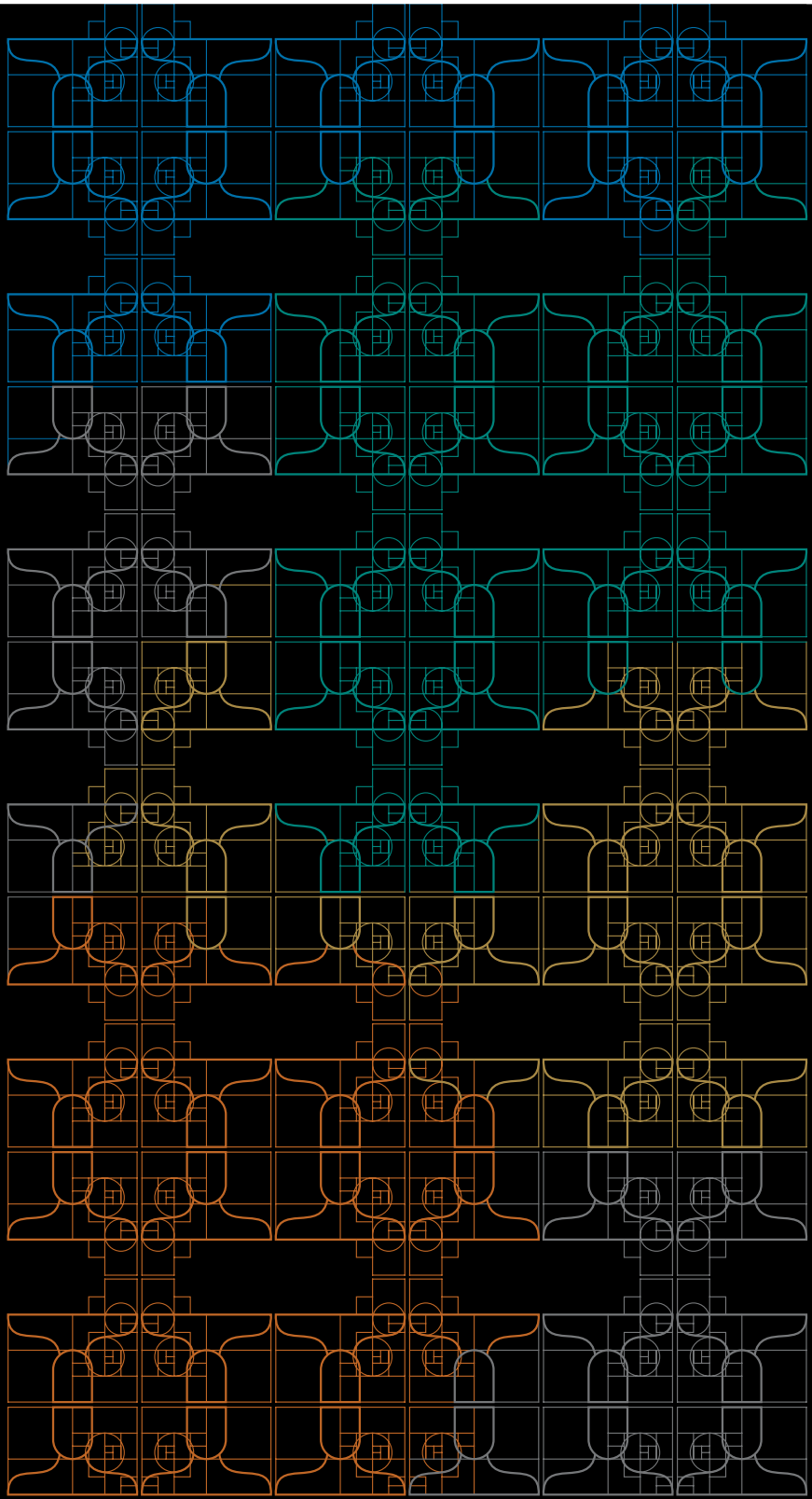

ISSN 1318 - 2099